

R
ADIOLGY
AND
O
NCOLGY

vol.54 no.4

december 2020



CABOMETYX®

(kabozantinib) tablete

60 mg | 40 mg | 20 mg

CABOMETYX® pomembno izboljša PFS, OS in drugi liniji zdravljenja napredovalega karcinoma ledvičnih celic¹

✓ PFS²

✓ OS²

✓ ORR²

ORR: objektivna stopnja odziva; OS: celokupno preživetje; PFS: preživetje brez napredovanja bolezni

Referenci: 1. Choueiri TK, Escudier B, Powles T, et al. Cabozantinib versus everolimus in advanced renal cell carcinoma (METEOR): final results from a randomised, open-label, phase 3 trial. *The Lancet Oncology*. 2016;17(7):917-27. 2. Povzetek glavnih značilnosti zdravila Cabometyx.

Skrajšan povzetek glavnih značilnosti zdravila

CABOMETYX 20 mg | 40 mg | 60 mg filmsko obložene tablete (kabozantinib)

TERAPEVTSKE INDIKACIJE Zdravljenje napredovalega karcinoma ledvičnih celic (KLC) pri predhodno nezdruženih odraslih bolnikih s srednje ugodnim ali slabim prognostičnim obetom ter pri odraslih bolnikih po predhodnem zdravljenju, usmerjenem v vaskularni endoteljski rastni faktor (VEGF). V monoterapiji zdravljenje hepatocelularnega karcinoma (HCK) pri odraslih bolnikih, ki so se predhodno že zdravili s sorafenibom. **ODMERJANJE IN NAČIN UPORABE** Pri bolnikih s KLC in HCK je priporočeni odmerek 60 mg enkrat na dan. Zdravljenje je treba nadaljevati tako dolgo, dokler bolnik več nima kliničnih koristi od terapije ali do pojavnega nesprejemljive toksičnosti. Pri sumu na neželeno reakcijo bo morda treba zdravljenje začasno prekiniti in/ali zmanjšati odmerek. Če je treba odmerek zmanjšati, se priporoča zmanjšanje na 40 mg/dan in nato na 20 mg/dan. Prekinitev odmerka se priporoča pri obravnavi toksičnosti 3. ali višje stopnje po CTCAE (*common terminology criteria for adverse events*) ali nevzdržni toksičnosti 2. stopnje. Zmanjšanje odmerka se priporoča za dogodke, ki bi lahko čez čas postali resni ali nevzdržni. Za priporočila glede prilagoditve odmerka ob pojavu neželenih učinkov glejte celoten povzetek glavnih značilnosti zdravila. Pri blagi ali zmerni ledvični okvari je treba kabozantinib uporabljati previdno. Uporaba se ne priporoča pri hudi ledvični okvari. Pri blagi okvari jeter odmerka ni treba prilagajati. Pri zmerni okvari jeter (Child Pugh B) je priporočljivo skrbno spremljanje celokupne varnosti. Pri bolnikih s hudo okvaro jeter (Child Pugh C) uporaba kabozantiniba ni priporočljiva. **Način uporabe:** Tablete je treba pogoltniti cele in jih ni dovoljeno drobiti. Bolnikom je treba naročiti, naj vsaj 2 uri pred uporabo zdravila in 1 uro po tem ničesar ne jedo. **KONTRAINDIKACIJE** Preobčutljivost na učinkovino ali katero koli pomožno snov. **POSEBNA OPOZORILA IN PREVIDNOSTNI UKREPI** Večina dogodkov se pojavi zgodaj v teku zdravljenja, zato mora zdravnik bolnika v prvih 8 tednih zdravljenja skrbno spremljati, da oceni, ali je treba odmerek prilagoditi. Dogodki, ki se običajno pojavijo zgodaj, vključujejo hipokalcemijo, hipokalemijo, trombocitopenijo, hipertenzijo, sindrom palmarno-plantarne eritrodisezesteze (PPES), proteinurijo in GI dogodke (bolečine v trebuhu, vnetje sluznice, zaprtje, driska, bruhanje). Pred uvedbo zdravljenja s kabozantinibom je priporočljivo izvesti preiskave delovanja jeter (ALT, AST in bilirubin), vrednosti skrbno spremljati med zdravljenjem in po potrebi prilagoditi odmerek. Bolnike je treba spremljati glede znakov in simptomov jetrne encefalopatije. Bolnike, ki imajo vnetno bolezen črevesja, ki imajo tumorsko infiltracijo prebavil ali so imeli pred posegom na prebavilih zaplete, je treba pred uvedbo zdravljenja skrbno oceniti, nato pa natančno spremljati za pojav simptomov GI perforacij in fistul, vključno z abscesi in sepo. Z uporabo kabozantiniba je treba pri bolnikih, pri katerih se pojavi GI perforacija ali fistula, ki je ni možno ustrezno obravnavati, prenehati. Driska, navzea/bruhanje, zmanjšanje apetita in vnetje ustne sluznice/bolečina v ustni votlini so nekateri od najpogostejših poročanih neželenih učinkov na prebavila. Nemudoma je treba ustrezne medicinske ukrepe, vključno s podpornim zdravljenjem z antiemetiki, antiidiariki ali antacidi. Če pomembni neželeni učinki na prebavila vztrajajo ali se ponavljajo, je treba presoditi o prekinitvi odmerjanja, zmanjšanju odmerka ali trajni ukinitvi zdravljenja s kabozantinibom.

▼ Za to zdravilo se izvaja dodatno spremljanje varnosti. Tako bodo hitreje na voljo nove informacije o njegovi varnosti. Zdravstvene delavce naprošamo, da poročajo o katerem koli domnevnem neželenem učinku zdravila.

Kabozantinib je treba uporabljati previdno pri bolnikih, pri katerih obstaja tveganje za pojav venske tromboembolije, vključno s pljučno embolijo, in arterijske tromboembolije ali imajo te dogodke v anamnezi. Z uporabo je treba prenehati pri bolnikih, pri katerih se razvije akutni miokardni infarkt ali drugi klinično pomembni znaki zapletov tromboembolije. Kabozantiniba se ne sme dajati bolnikom, ki hudo krvavijo ali pri katerih obstaja tveganje za hudo krvavitev. Uporaba zaviralcev poti VEGF pri bolnikih s hipertenzijo ali brez nje lahko spodbudi nastanek anevrizem in/ali disekcij arterij. Med zdravljenjem s kabozantinibom je treba spremljati vrednosti trombocitov in odmerek prilagoditi glede na resnost trombocitopenije. Vsaj 28 dni pred načrtovanim kirurškim posegom je treba zdravljenje ustaviti, če je mogoče. Kabozantinib je treba ukiniti pri bolnikih z zapleti s celjenjem rane, zaradi katerih je potrebna zdravniška pomoč. Pred uvedbo kabozantiniba je treba dobro obvladati krvni tlak. Med zdravljenjem je treba vse bolnike spremljati za pojav hipertenzije in jih po potrebi zdraviti s standardnimi antihipertenzivi. V primeru trdovratne hipertenzije, kljub uporabi antihipertenzivov, je treba odmerek kabozantiniba zmanjšati oz. prenehati z zdravljenjem. V primeru hipertenzijske krize je treba zdravljenje ukiniti. Pred uvedbo kabozantiniba je treba opraviti pregled ustne votline in le-tega v času zdravljenja periodično ponavljati. Ob pojavu osteonekroze čeljusti je treba prenehati z uporabo kabozantiniba. Pri resni PPES je treba razmisliti o prekinitvi zdravljenja. Nadaljevanje zdravljenja naj se začne z nižjim odmerkom, ko se PPES umiri do 1. stopnje. V času zdravljenja je treba redno spremljati beljakovine v urinu. Če se pri bolniku razvije nefrotični sindrom, je treba z uporabo kabozantiniba prenehati. Pri uporabi kabozantiniba so opazili sindrom posteriorne reverzibilne encefalopatije (PRES). Pri bolnikih s PRES je treba zdravljenje ukiniti. Kabozantinib je treba uporabljati previdno pri bolnikih s podaljšanjem intervala QT v anamnezi, pri bolnikih, ki jemljejo antiaritmike, in pri bolnikih z relevantno obstoječo boleznijo srca, bradikardijo ali elektrolitskimi motnjami. Uporaba kabozantiniba je bila povezana z večjo pojavnostjo elektrolitskih nepravilnosti, zato je priporočljivo spremljati biokemijske parametre in po potrebi uvesti ustrezno nadomestno zdravljenje v skladu s standardno klinično prakso. Bolniki z redko dedno intoleranco za galaktozo, laponsko obliko zmanjšane aktivnosti laktaze ali malabsorpcijo glukoze/galaktoze ne smejo jemati tega zdravila. **Plodnost, nosečnost in dojenje:** Ženskam v rodni dobi je treba svetovati, da v času zdravljenja s kabozantinibom ne smejo zanositi. Zanositev morajo preprečiti tudi ženske partnerke moških bolnikov, ki uporabljajo kabozantinib. Med zdravljenjem in še vsaj 4 mesece po končanju terapije je treba uporabljati zanesljiv način kontracepcije. Kabozantiniba se ne sme uporabljati med nosečnostjo, razen če zdravljenje ni nujno potrebno zaradi kliničnega stanja ženske. Matere med zdravljenjem in še 4 mesece po končanju terapije ne smejo dojiti. Kabozantinib lahko predstavlja tveganje za plodnost pri moških in ženskah. **INTERAKCIJE** Kabozantinib je substrat za CYP3A4. Pri sočasni uporabi močnih zaviralcev CYP3A4 (npr. ritonavirja, itrakonazola, eritromicina, klaritromicina, soka grenivke) je potrebna previdnost. Kronični sočasni uporabi močnih induktorjev CYP3A4 (npr. fenitoina, karbamazepina, rifampicina, fenobarbitala ali pripravkov zeliščnega izvora iz šentjanževke) se je treba izogibati. Razmisliti je treba o sočasni uporabi alternativnih zdravil, ki CYP3A4 ne inducirajo in ne zavirajo ali pa

inducirajo in zavirajo le neznatno. Pri sočasni uporabi zaviralcev MRP2 (npr. ciklosporina, efavirenza, emtricitabina) je potrebna previdnost, saj lahko povzročijo povečanje koncentracij kabozantiniba v plazmi. Učinka kabozantiniba na farmakokinetiko kontraceptivnih steroidov niso preučili, vendar pa se priporoča dodatna kontracepcijska metoda (pregradna metoda). Zaradi visoke stopnje vezave kabozantiniba na plazemske beljakovine je možna interakcija z varfarinom v obliki izpodrinjanja s plazemskih beljakovin, zato je treba spremljati vrednosti INR. Kabozantinib morda lahko poveča koncentracije sočasno uporabljenih substratov P-gp v plazmi. Bolnike je treba opozoriti na uporabo substratov P-gp (npr. feksofenadina, aliskirena, ambrisentana, dabigatran eteksilata, digoksina, kolhicina, maraviroka, posakonazola, ranolazina, saksagliptina, sitagliptina, talinolola, tolvaptana) sočasno s kabozantinibom. **NEŽELENI UČINKI** Za popolno informacijo o neželenih učinkih, prosimo, preberite celoten povzetek glavnih značilnosti zdravila Cabometyx. Najpogostejši resni neželeni učinki zdravila v populaciji bolnikov s KLC so bili bolečine v trebuhu, driska, navzea, hipertenzija, embolija, hiponatremija, pljučna embolija, bruhanje, dehidracija, utrujenost, astenija, zmanjšanje apetita, globoka venska tromboza, omotica, hipomagnezija in PPES. Najpogostejši resni neželeni učinki zdravila v populaciji bolnikov s HCK so bili jetrna encefalopatija, astenija, utrujenost, PPES, driska, hiponatremija, bruhanje, bolečine v trebuhu in trombocitopenija. **Zelo pogosti:** anemija, trombocitopenija, hipotiroidizem, zmanjšanje apetita, hipomagnezija, hipokalemija, hipalbuminemija, paragevzija, glavobol, omotica, hipertenzija, krvavitev, disfonija, dispneja, kašelj, driska, navzea, bruhanje, stomatitis, obstipacija, bolečine v trebuhu, dispneja, bolečina v zgornjem predelu trebuha, PPES, izpuščaji, bolečine v okončinah, utrujenost, vnetje sluznice, astenija, periferni edem, zmanjšanje telesne mase, zvišanje ALT v serumu, zvišanje AST. **Pogosti:** absces, nevropenija, limfopenija, dehidracija, hipofosfatemija, hiponatremija, hipokalcemija, hiperkalemija, hiperbilirubinemija, hiperglikemija, hipoglikemija, periferna nevropatija (vključno s senzorično), tinitus, globoka venska tromboza, venska tromboza, arterijska tromboza, pljučna embolija, GI perforacija, fistula, GERB, hemoroidi, bolečina v ustni votlini, suha usta, disfgija, glossodinija, jetrna encefalopatija, pruritus, alopecija, suha koža, akneiformni dermatitis, sprememba barve las oz. dlak, hiperkeratoza, mišični krči, artralgija, proteinurija, zvišanje ALP v krvi, GGT, kreatinina v krvi, amilaze, lipaze, holesterola v krvi, trigliceridov v krvi. **Občasni:** konvulzije, pankreatitis, holestatični hepatitis, osteonekroza čeljusti, zapleti z ranami. **Neznana pogostost:** možganska kap, miokardni infarkt, anevrizme in disekcije arterij. **Vrsta ovojnine in vsebina:** Plastenka vsebuje 30 filmsko obloženih tablet. **Režim izdaje:** Rp/Spec **Imetnik dovoljenja za promet z zdravilom:** Ipsen Pharma, 65 quai Georges Gorse, 92100 Boulogne-Billancourt, Francija. **Pred predpisovanjem, prosimo, preberite celoten povzetek glavnih značilnosti zdravila!** CAB-300420



Publisher

Association of Radiology and Oncology

Aims and Scope

Radiology and Oncology is a multidisciplinary journal devoted to the publishing original and high quality scientific papers and review articles, pertinent to diagnostic and interventional radiology, computerized tomography, magnetic resonance, ultrasound, nuclear medicine, radiotherapy, clinical and experimental oncology, radiobiology, medical physics and radiation protection. Therefore, the scope of the journal is to cover beside radiology the diagnostic and therapeutic aspects in oncology, which distinguishes it from other journals in the field.

Editor-in-Chief

Gregor Serša, Institute of Oncology Ljubljana, Department of Experimental Oncology, Ljubljana, Slovenia (Subject Area: Experimental Oncology)

Executive Editor

Viljem Kovač, Institute of Oncology Ljubljana, Department of Radiation Oncology, Ljubljana, Slovenia (Subject Areas: Clinical Oncology, Radiotherapy)

Editorial Board

Subject Areas:

Radiology and Nuclear Medicine

Sotirios Bisdas, University College London, Department of Neuroradiology, London, UK

Boris Brkljačić, University Hospital "Dubrava", Department of Diagnostic and Interventional Radiology, Zagreb, Croatia

Maria Gódnéy, National Institute of Oncology, Budapest, Hungary

Gordana Ivanac, University Hospital Dubrava, Department of Diagnostic and Interventional Radiology, Zagreb, Croatia

Luka Ležaić, University Medical Centre Ljubljana, Department for Nuclear Medicine, Ljubljana, Slovenia

Katarina Šurlan Popovič, University Medical Center Ljubljana, Clinical Institute of Radiology, Ljubljana, Slovenia

Jernej Vidmar, University Medical Center Ljubljana, Clinical Institute of Radiology, Ljubljana, Slovenia

Deputy Editors

Andrej Čör, University of Primorska, Faculty of Health Science, Izola, Slovenia (Subject Areas: Clinical Oncology, Experimental Oncology)

Božidar Casar, Institute of Oncology Ljubljana, Department for Dosimetry and Quality of Radiological Procedures, Ljubljana (Subject Area: Medical Physics)

Maja Čemažar, Institute of Oncology Ljubljana, Department of Experimental Oncology, Ljubljana, Slovenia (Subject Area: Experimental Oncology)

Subject Areas:

Clinical Oncology and Radiotherapy

Serena Bonin, University of Trieste, Department of Medical Sciences, Cattinara Hospital, Surgical Pathology Bldg, Molecular Biology Lab, Trieste, Italy

Luca Campana, Veneto Institute of Oncology (IOV-IRCCS), Padova, Italy

Christian Dittrich, Kaiser Franz Josef - Spital, Vienna, Austria

Blaž Grošelj, Institute of Oncology Ljubljana, Department of Radiation Oncology, Ljubljana

Luka Milas, UT M. D. Anderson Cancer Center, Houston, USA

Miha Oražem, Institute of Oncology Ljubljana, Department of Radiation Oncology, Ljubljana

Gaber Plavc, Institute of Oncology Ljubljana, Department of Radiation Oncology, Ljubljana

Csaba Polgar, National Institute of Oncology, Budapest, Hungary

Dirk Rades, University of Lubeck, Department of Radiation Oncology, Lubeck, Germany

Luis Souhami, McGill University, Montreal, Canada

Borut Štabuc, University Medical Center Ljubljana, Division of Internal Medicine, Department of Gastroenterology, Ljubljana, Slovenia

Andrea Veronesi, Centro di Riferimento Oncologico- Aviano, Division of Medical Oncology, Aviano, Italy

Branko Zakotnik, Institute of Oncology Ljubljana, Department of Medical Oncology, Ljubljana, Slovenia

Igor Kocijančič, University Medical Center Ljubljana, Institute of Radiology, Ljubljana, Slovenia (Subject Areas: Radiology, Nuclear Medicine)

Karmen Stanič, Institute of Oncology Ljubljana, Department of Radiation Oncology, Ljubljana, Slovenia (Subject Areas: Radiotherapy; Clinical Oncology)

Primož Strojjan, Institute of Oncology Ljubljana, Department of Radiation Oncology, Ljubljana, Slovenia (Subject Areas: Radiotherapy, Clinical Oncology)

Subject Area: Experimental Oncology

Metka Filipič, National Institute of Biology, Department of Genetic Toxicology and Cancer Biology, Ljubljana, Slovenia

Janko Kos, University of Ljubljana, Faculty of Pharmacy, Ljubljana, Slovenia

Tamara Lah Turnšek, National Institute of Biology, Ljubljana, Slovenia

Damijan Miklavčič, University of Ljubljana, Faculty of Electrical Engineering, Ljubljana, Slovenia

Justin Teissié, CNRS, IPBS, Toulouse, France

Gillian M. Tozer, University of Sheffield, Academic Unit of Surgical Oncology, Royal Hallamshire Hospital, Sheffield, UK

Subject Area: Medical Physics

Robert Jeraj, University of Wisconsin, Carbone Cancer Center, Madison, Wisconsin, USA

Mirjana Josipovic, Rigshospitalet, Department of Oncology, Section of Radiotherapy, Copenhagen, Denmark

Håkan Nyström, Skandionkliniken, Uppsala, Sweden

Ervin B. Podgoršak, McGill University, Medical Physics Unit, Montreal, Canada

Matthew Podgorsak, Roswell Park Cancer Institute, Departments of Biophysics and Radiation Medicine, Buffalo, NY, USA

Advisory Committee

Tullio Giraldi, University of Trieste, Faculty of Medicine and Psychology, Department of Life Sciences, Trieste, Italy

Vassil Hadjidekov, Medical University, Department of Diagnostic Imaging, Sofia, Bulgaria

Marko Hočevar, Institute of Oncology Ljubljana, Department of Surgical Oncology, Ljubljana, Slovenia

Miklós Kásler, National Institute of Oncology, Budapest, Hungary

Maja Osmak, Ruder Bošković Institute, Department of Molecular Biology, Zagreb, Croatia

Editorial office

Radiology and Oncology

Zaloška cesta 2

P. O. Box 2217

SI-1000 Ljubljana

Slovenia

Phone: +386 1 5879 369

Phone/Fax: +386 1 5879 434

E-mail: gsera@onko-i.si

Copyright © Radiology and Oncology. All rights reserved.

Reader for English

Vida Kološa

Secretary

Mira Klemenčič

Zvezdana Vukmirović

Design

Monika Fink-Serša, Samo Rován, Ivana Ljubanović

Layout

Matjaž Lužar

Printed by

Tiskarna Ozimek, Slovenia

Published quarterly in 400 copies

Beneficiary name: DRUŠTVO RADIOLOGIJE IN ONKOLOGIJE

Zaloška cesta 2

1000 Ljubljana

Slovenia

Beneficiary bank account number: SI56 02010-0090006751

IBAN: SI56 0201 0009 0006 751

Our bank name: Nova Ljubljanska banka, d.d.,

Ljubljana, Trg republike 2,

1520 Ljubljana; Slovenia

SWIFT: LJBASIX

Subscription fee for institutions EUR 100, individuals EUR 50

The publication of this journal is subsidized by the Slovenian Research Agency.

Indexed and abstracted by:

- Baidu Scholar
- Case
- Chemical Abstracts Service (CAS) - CAplus
- Chemical Abstracts Service (CAS) - SciFinder
- CNKI Scholar (China National Knowledge Infrastructure)
- CNPIEC - cnpLINKer
- Dimensions
- DOAJ (Directory of Open Access Journals)
- EBSCO (relevant databases)
- EBSCO Discovery Service
- Embase
- Genamics JournalSeek
- Google Scholar
- Japan Science and Technology Agency (JST)
- J-Gate
- Journal Citation Reports/Science Edition
- JournalGuide
- JournalTOCs
- KESLI-NDSL (Korean National Discovery for Science Leaders)
- Medline
- Meta
- Microsoft Academic
- Naviga (Softweco)
- Primo Central (ExLibris)
- ProQuest (relevant databases)
- Publons
- PubMed
- PubMed Central
- PubsHub
- QOAM (Quality Open Access Market)
- ReadCube
- Reaxys
- SCImago (SJR)
- SCOPUS
- Sherpa/RoMEO
- Summon (Serials Solutions/ProQuest)
- TDNet
- Ulrich's Periodicals Directory/ulrichsweb
- WanFang Data
- Web of Science - Current Contents/Clinical Medicine
- Web of Science - Science Citation Index Expanded
- WorldCat (OCLC)

This journal is printed on acid-free paper

On the web: ISSN 1581-3207

<https://content.sciendo.com/raon>

<http://www.radioloncol.com>

contents

review

- 371 **Modern treatment of vulvar cancer**
Sebastjan Merlo
- 377 **Combining radiotherapy and immunotherapy in definitive treatment of head and neck squamous cell carcinoma: review of current clinical trials**
Gaber Plavc, Primož Strojjan

radiology

- 394 **Correlations between DTI-derived metrics and MRS metabolites in tumour regions of glioblastoma: a pilot study**
Eduardo Flores-Alvarez, Edgar-Anselmo Rios-Piedra, Griselda-Adriana Cruz-Priego, Coral Durand-Muñoz, Sergio Moreno-Jimenez, Ernesto Roldan-Valadez
- 409 **Adrenal vein sampling for primary aldosteronism: a 15-year national referral center experience**
Tomaz Kocjan, Mojca Jensterle, Gaj Vidmar, Rok Vrckovnik, Pavel Berden, Milenko Stankovic
- 419 **Adnexal masses characterized on 3 tesla magnetic resonance imaging - added value of diffusion techniques**
Julia Dimova, Dora Zlatareva, Rumiana Bakalova, Ichio Aoki, George Hadjidekov

clinical oncology

- 429 **The influence of genetic variability in *IL1B* and *MIR146A* on the risk of pleural plaques and malignant mesothelioma**
Petra Piber, Neza Vavpetic, Katja Goricar, Vita Dolzan, Viljem Kovac, Alenka Franko
- 437 **Neutrophil-to-lymphocyte ratio can predict outcome in extensive-stage small cell lung cancer**
Gordana Drpa, Maja Sutic, Jurica Baranasic, Marko Jakopovic, Miroslav Samarzija, Suzana Kukulj, Jelena Knezevic
- 447 **Treatment patterns and real-world evidence for stage III non-small cell lung cancer in Central and Eastern Europe**
Milada Zemanova, Marko Jakopovic, Karmen Stanic, Małgorzata Łazar-Poniatowska, Martina Vrankar, Petronela Rusu, Tudor Ciuleanu, Davorin Radosavljevic, Krisztina Bogos, Sergiusz Nawrocki
- 455 **Treatment of rhabdomyosarcoma in children and adolescent from four low health expenditures average rates countries**
Maja Cesen Mazic, Aleksandra Bonevski, Martina Mikeskova, Emilia Mihut, Gianni Bisogno, Janez Jazbec

- 461 **Influence of concurrent capecitabine based chemoradiotherapy with bevacizumab on the survival rate, late toxicity and health-related quality of life in locally advanced rectal cancer: a prospective phase II CRAB trial**
Vaneja Velenik, Vesna Zadnik, Mirko Omejc, Jan Grosek, Mojca Tuta
- 470 **Breast size and dose to cardiac substructures in adjuvant three-dimensional conformal radiotherapy compared to tangential intensity modulated radiotherapy**
Ivica Ratoska, Aljasa Jenko, Zeljko Sljivic, Maja Pirnat, Irena Oblak
- 480 **Long-term toxicity and survival outcomes after stereotactic ablative radiotherapy for patients with centrally located thoracic tumors**
Banu Atalar, Teuta Zoto Mustafayev, Terence T. Sio, Bilgehan Sahin, Gorkem Gungor, Gokhan Aydin, Bulent Yapici, Enis Ozyar
- 488 **Does regular quality control improve the quality of surgery in Slovenian breast cancer screening program?**
Andraz Perhavec, Sara Milicevic, Barbara Peric, Janez Zgajnar

radiophysics

- 495 **Experimental validation of Monte Carlo based treatment planning system in bone density equivalent media**
Djeni Smilovic Radojicic, Bozidar Casar, David Rajlic, Manda Svabic Kolacio, Ignasi Mendez, Nevena Obajdin, Dea Dundara Debeljuh, Slaven Jurkovic
- 505 **Comparison of three film analysis softwares using EBT2 and EBT3 films in radiotherapy**
Tamás Pócza, Zsuzsánna Zongor, Barbara Melles-Bencsik, Dóra Zita Tatai-Szabó, Tibor Major, Csilla Pesznyák

slovenian abstracts

Modern treatment of vulvar cancer

Sebastjan Merlo^{1,2}

¹ Gynaecological Oncology Unit, Department of Surgery, Institute of Oncology Ljubljana, Ljubljana, Slovenia

² Faculty of Medicine, University of Ljubljana, Ljubljana, Slovenia

Radiol Oncol 2020; 54(4): 371-376.

Received 28 June 2020

Accepted 21 July 2020

Correspondence to: Assist. Sebastjan Merlo, M.D., Ph.D., Gynaecological Oncology Unit, Department of Surgery, Institute of Oncology Ljubljana, Zaloška, SI-1000 Ljubljana, Slovenia. E-mail: smerlo@onko-i.si

Disclosure: No potential conflicts of interest were disclosed.

Background. Vulvar cancer accounts for 3–5% of malignant diseases of the female genital tract. The Slovenian incidence rate is 5.5/100,000, which means 57 new cases per year. The most common histological type (90%) is squamous cell carcinoma. Based on etiology, it can be classified into the first type which correlates with human papillomavirus (HPV) infection and the second type which is not associated with HPV. The most common and long-lasting symptom of vulvar cancer is pruritus. The preferred diagnostic procedure to confirm the diagnosis is a punch or incision biopsy. Surgery in combination with radiotherapy is the standard treatment for vulvar cancer. Sentinel lymph node biopsy with lymphoscintigraphy is now a standard part of surgical treatment. Chemotherapy is a palliative treatment option.

Conclusions. Vulvar cancer is a rare disease. Because of the pathogenesis, surgery and radiotherapy are the main treatment modalities. The sentinel node biopsy (SNB) represents a contemporary approach to the vulvar cancer treatment and significantly reduces morbidity. Improvements in treatment of vulvar cancer contributed to the decrease of mortality among Slovenian women.

Key words: vulvar cancer; surgical treatment; sentinel lymph node biopsy; lymphoscintigraphy; radiotherapy

Introduction

Vulvar cancer is the fourth most common gynaecological malignancy.¹ The basic treatment for vulvar cancer is still surgery, but the radical nature of the procedure has changed or decreased over the last twenty years. Historically treatment included radical vulvectomy and a radical inguino-femoral lymphadenectomy. The procedure was associated with a high rate of postoperative complications. For this reason, a minimally invasive surgical technique was developed. This is the sentinel lymph node biopsy, which is now a standard procedure in the treatment of patients with early-stage vulvar cancer. This procedure significantly reduced morbidity and improved quality of life.²

Epidemiology

Vulvar cancer accounts for 3–5% of all gynaecological cancers in the world. This puts it in fourth

place among gynaecological malignancies. The first three places are occupied by cancer of the uterus, ovaries and cervix. Every year 27,000 women worldwide are diagnosed with vulvar cancer. The highest incidence is in Europe, North and South America, Oceania, and the lowest in Asia.¹

In 2016, 57 women were diagnosed with vulvar cancer in Slovenia with an incidence of 5.5 / 100,000. An analysis of the time trends over the last 15 years shows an increase in incidence since 2003, while mortality has remained constant. It should be noted that this coincides with the introduction of the national program for the early detection of precancerous changes in the cervix. This has led to an increased number of gynaecological examinations, including the older population. Vulvar cancer occurs most frequently in women over 80 years of age. In 2016 there were no cases of women under 30 years of age in Slovenia. According to the 2016 data, 59.6% of patients had a limited stage of the disease at diagnosis, 29.8% an advanced stage and 7% of patients had metastatic disease.³

The survival of patients with vulvar cancer improved slightly over time. According to the Slovenian Cancer Registry, the 5-year survival rate of patients with vulvar cancer was 43% between 2004 and 2009, while between 2010 and 2016 5-year survival rate was 48%. Patients diagnosed with localized disease have significantly longer overall survival than patients with locally advanced disease.^{4,5}

The international EUROCORE-5 study showed a relative 5-year survival rate for different cancers. In this study patients with vulvar and vaginal cancer were pooled. The average European relative 5-year survival rate in this study was 56% for patients between 2000 and 2007.⁶

Etiopathogenesis

More than 90% of cases of vulvar cancer are defined as squamous cell carcinoma. It can develop in two different ways. In younger women (aged 35–65 years), HPV infection plays a key role in the development of squamous cell carcinoma, especially strains 16 and 18. Risk factors include a history of genital warts and other sexually transmitted diseases, low socioeconomic status, smoking and immunodeficiency. The second type of development is independent of HPV and occurs more frequently in older patients (aged 55–85 years). It is a gradual process of development of cellular atypia leading to vulvar intraepithelial neoplasia (VIN) and then squamous cell carcinoma. The risk factor is the *lichen sclerosus*. The crossing of the two pathogenetic pathways is also possible.⁷⁻⁹

Clinical manifestation and diagnostic procedures

The most common symptom of vulvar cancer is persistent itching. Less common symptoms are bleeding from the vulvar skin, bleeding or discharge from the vagina, dysuria and pain. In advanced cases, a tumour can be seen on the vulva. The tumour may be ulcerated, leukoplactic or warty.¹

Treatment of a woman with suspected malignant disease of the vulva starts with a thorough medical history, followed by a clinical examination. It is important to accurately describe suspicious changes, their size, number, position, mobility, assessment of infiltration of deeper structures and safety margins in case of excision. A bimanual vaginal and rectal examination should always be performed to assess

vaginal and rectal involvement. Since HPV occurs in 86% of precancerous changes in the vulva and in 28.6% of vulvar cancers, the examination should also include a colposcopic examination of the vagina and cervix. Assessment of the size, mobility and consistency of the inguinal lymph nodes is mandatory. The condition of the skin above the inguinal lymph nodes should also be noted. Palpation of the supraclavicular lymph nodes is important as well. If there is already a pathology of the vulva (atrophic *lichen sclerosus*, pathological cytological smear of the vulva), vulvoscopy is also advisable.²

A targeted biopsy with histological examination of the tissue taken is necessary to make a definitive diagnosis. It is important that the sample is taken at the site of the vital tissue, so it is advisable to take a tissue sample near the edge of the alteration. Necrosis, granulation tissue, fibrin or inflammation are often found in the middle of the changes in the form of ulcers, blisters, atrophy and scarring. Such a histo-pathological pattern is neither appropriate nor representative. The size of the biopsy taken should be at least 4 mm³.² The preferred method of sampling is the punch biopsy. Excisional biopsy is not recommended as it may prevent proper further treatment. In patients with multiple vulvar lesions, a separate biopsy of all lesions should be performed and the sampling site should be indicated.²

Treatment

The treatment of vulvar cancer often involves a combination of surgery and radiotherapy. Systemic treatment is rarely used. Treatment can be long lasting and have a major impact on quality of life.^{2,9}

Surgical treatment

Primary vulvar lesion. The basic criterion for the treatment of a tumour lesion is the depth of the stromal invasion into the biopsy tissue taken. If an early stage disease is defined as T1a (≤ 1 mm of stromal invasion), a wide local excision is performed. If the disease is defined as T1b (> 1 mm stromal invasion) or T2 ≤ 4 cm and the lesion is 1 cm from the median line, wide local excision or a modified radical vulvectomy and ipsilateral sentinel node biopsy (SNB) is performed. However, in the case of a lesion in the median line, a wide local excision and a bilateral SNB is required.

If the disease is locally advanced (T2 > 4 cm and T3) and the lesion is ≥ 1 cm from the median line, a radical vulvectomy and ipsilateral dissection of

the inguino-femoral lymph nodes is performed. If the lesion is in the median line, a radical vulvectomy and bilateral dissection of the inguino-femoral lymph nodes are performed. If the lymph nodes are positive, we opt for external beam radiotherapy (EBRT) of the primary tumour, lymph nodes and pelvis. In case of negative lymph nodes, we choose EBRT of the primary tumour and/or selected inguino-femoral lymph nodes. In all cases, adjuvant treatment follows.

If the patient has metastatic disease outside the pelvis (any T, any N, M1 outside the pelvis), we do not opt for surgical treatment, but for palliative EBRT and/or symptomatic treatment.^{2,9}

Lymph nodes. The most basic method for determining the status of inguino-femoral lymph nodes is palpation, but its accuracy is only 9% preoperatively and 55% intraoperatively. The status can also be determined by ultrasound examination of the inguinal regions. The sensitivity and specificity of lymph node ultrasound examination for vulvar cancer is 76.3% and 91.3%, with positive and negative predictive values of 82.9% and 87.5%, respectively. Fine needle biopsy and cytological verification follow if lymph node involvement is suspected.^{10,11} Other imaging methods have proven to be less reliable compared to ultrasound.^{12,13}

In the absence of a reliable method for detecting inguino-femoral lymph node involvement, inguino-femoral lymphadenectomy was part of the standard treatment of vulvar cancer.¹ Metastases in the inguino-femoral lymph nodes in early stages of the disease are found in only 20–30% of patients, which means that all other patients do not benefit from a complete lymphadenectomy. The possible postoperative complications following a complete lymphadenectomy are lymphedema of the lower extremity (14–49%), lymphocyst formation (11–40%) and wound infections with dehiscence.^{14,15}

Due to the lack of non-invasive techniques to determine the status of inguino-femoral lymph nodes, the absence of lymph node metastases in most patients with early stage disease and the frequent morbidity following inguino-femoral lymphadenectomy, the minimally invasive surgical technique, SNB biopsy was developed. SNB is now part of the standard treatment of early-stage vulvar cancer. Vulvar cancer has a predictable course of the lymphatic vessels and lymphatic drainage is predictable. Therefore, SNB of inguino-femoral lymph nodes is a safe replacement for inguino-femoral lymphadenectomy. The sentinel lymph node is defined as the first lymph node in the lymphatic basin into which the lymph of the primary

tumour drains. Histological examination of the sentinel lymph node is representative for all other lymph nodes in the area, and histologically, a negative sentinel lymph node means the absence of metastases in subsequent lymph nodes.^{16–19}

The sentinel lymph node is marked in two ways, with a nanocolloid bound to 99mTc (Technetium) and with a patent blue. This method is the most reliable, as the sentinel lymph node is found in 97.7% of cases. Only by injecting patent blue the sentinel lymph node is identified in 68.7%, and only by the nanocolloid bound to technetium in 94%.^{20,21}

At the Institute of Oncology Ljubljana, the technique has changed over the years. It is crucial that patent blue is injected intradermally and not subcutaneously. The volume of the injected, undiluted dye is 2 ml. On the day of surgery, 0.5 ml of technetium-labeled nanocolloid is injected intradermally with a thin needle at four points near the outer edge of the tumour. Lymphoscintigraphy with a gamma camera follows. The first active accumulation point of the radiopharmaceutical is the sentinel lymph node, and its position is marked on the skin. Sometimes several points of high activity appear, in this case we mark them all. Immediately before the beginning of the surgical procedure, 2 ml of patent blue is injected intradermally in the same place as radiopharmaceutical. Then a 3 to 4 cm long skin incision is made at the marked site. The tissue is carefully dissected until a blue stained lymph node is found. Its activity is checked with a hand-held gamma detector and then removed.²

Women with histologically confirmed unifocal vulvar carcinoma, less than 4 cm in diameter, with an invasion depth of more than 1 mm, and in whom there are clinically no metastases in the inguino-femoral lymph nodes, are candidates for sentinel lymph node biopsy.^{2,22}

A tumour located 1 cm or more from the midline of the vulva is usually drained into the unilateral lymphatic system, so a sentinel lymph node biopsy is performed on the same side. Bilateral drainage is present in tumours that are central or less than 1 cm from the median line. In this case a biopsy of the sentinel lymph node should be performed bilaterally. If the lymph node is detected in the lymphoscintigraphy on one side only, inguino-femoral lymphadenectomy on the opposite side is recommended to avoid a false negative result.^{2,9,22}

Patients with a multifocal tumour are not suitable candidates for sentinel lymph node biopsy because they have a higher incidence of disease recurrence (10.5%) compared to patients with a unifocal tumour (2.3%).²³ Previous surgery and

excisions of the vulva that may interfere with lymphatic flow in the inguino-femoral region are relative contraindications for sentinel lymph node biopsy, but the decision in these cases is made on a patient-specific basis. Lymphadenectomy is recommended in patients with recurrent disease or in patients who have already had an inguino-femoral sentinel lymph node biopsy.^{2,20}

Radiotherapy

The purpose of postoperative radiotherapy is to reduce the likelihood of local and/or regional recurrence, prolong disease-free survival and overall survival.² Due to the low incidence of vulvar cancer, the number of randomized clinical trials and evidence-based treatment outcomes is also low. As a result, there are no standard indications and recommendations for adjuvant treatment of vulvar cancer. The data collected suggest that adjuvant treatment is not necessary in patients with early-stage cancer, negative inguino-femoral lymph node status and a favourable prognosis.²⁴

However, treatment of locally advanced disease sometimes requires adjuvant treatment following surgery. Lymph node metastases, large primary tumours, deep stromal invasion, lymphovascular invasion and close surgical margins are associated with a higher incidence of disease recurrence. The role of adjuvant therapy in these patients is still not fully understood. Radiation or radiation combined with lymph node dissection is very effective in preventing disease recurrence in the inguino-femoral lymph nodes in patients with squamous cell carcinoma of the vulva. According to the recommendations of the Gynecologic Oncology Group (GOG), adjuvant radiation is considered the standard treatment for squamous cell carcinoma of the vulva in patients with 2 or more positive lymph nodes with extracapsular spread or inguino-femoral dissection is not feasible. The benefit of adjuvant radiotherapy has been demonstrated in patients with two or more positive inguino-femoral lymph nodes, while the role of irradiation of patients with only one positive inguino-femoral lymph node remains undetermined.^{2,24,25}

Systemic treatment

Data on the role of systemic therapy in the treatment of vulvar cancer are very sparse, as they are based on small, non-randomized phase II clinical trials involving fewer than 50 patients treated with various regimens of chemotherapy. Currently,

chemotherapy is not recommended as a stand-alone preoperative (neoadjuvant) or postoperative (adjuvant) systemic treatment. Chemotherapy can only be considered as a palliative treatment for metastatic disease if other treatments are not feasible. Various cytostatic drugs (cisplatin, paclitaxel, bleomycin, navelbin, 5-fluorouracil) were used in the trials in combination or monotherapy. The response rate was 0–40%, progression-free survival 1–10 months and overall survival up to 19 months. Due to the toxicity of cisplatin, the less toxic carboplatin has been increasingly used in recent years to treat metastatic vulvar cancer. In analogy to metastatic cervical cancer, the combination of carboplatin and paclitaxel has been increasingly used in recent years for the treatment of metastatic vulvar cancer because the combination is similarly effective and less toxic than the combination of cisplatin and paclitaxel.²⁶

Chemotherapy can be used in combination with concomitant radiation (chemoradiotherapy), either as a stand-alone treatment or as preoperative (neoadjuvant) treatment in patients with locally advanced disease. Various cytostatic drugs (cisplatin, 5-fluorouracil, mitomycin-C) are used in chemoradiotherapy to improve the local effect of radiation (chemosensitization). Since concomitant treatment with chemotherapy and radiation is associated with higher toxicity, lower doses of cytostatic drugs are used during radiation, so in this case it is actually a topical rather than a systemic treatment.^{26,27}

The role of targeted therapeutics in the treatment of advanced vulvar cancer is still unknown. We have data from a small clinical trial with the targeted therapeutic erlotinib, an epidermal growth factor receptor (EGFR) inhibitor, which included 41 patients with advanced disease. Partial response was achieved in 27%, progression-free survival was short (median treatment time 3 months), and treatment was associated with many adverse events.^{28,29}

Follow-up

There is currently insufficient evidence to support a uniform follow-up pattern after radical treatment of vulvar cancer. Experts and professional associations therefore disagree on follow up schedule. Local recurrence can occur at any time, so lifelong follow-up is recommended.

Depending on the type of treatment, the European Society of Gynaecological Oncology (ESGO) suggests the following follow-up scheme.

After primary surgical treatment, the first examination is performed 6–8 weeks after the surgical procedure, then clinical examinations of the vulva and groin region are performed every 3–4 months for a period of two years. In the following three years, follow-up examinations are scheduled twice a year. After this period, it is advisable to perform annual clinical examinations. This is particularly important for patients at increased risk, such as patients diagnosed with *lichen sclerosus / planus*.

10–12 weeks after chemotherapy or radiotherapy, a computed tomography or positron emission tomography-computed tomography (PET-CT) examination is recommended to confirm remission. Later, clinical examinations of the vulva and groin region are recommended every 3–4 months for the first two years, followed by examinations twice a year for 3 years and then annual examinations.

If a local recurrence is suspected, a biopsy should be performed, and if there is a suspicion of groin region relapse of the disease or extended disease, appropriate imaging diagnostics should follow. The early detection of malignant recurrences that can still be treated surgically can significantly improve quality of life, but there is currently no firm evidence of the effects on morbidity and mortality.^{2,6,30}

Conclusions

Surgical treatment is still standard treatment of vulvar cancer. The greatest progress in this field in recent years has been the development of a minimally invasive surgical technique, sentinel lymph node biopsy, which is now standard treatment in selected cases. The replacement of inguino-femoral lymphadenectomy with this procedure significantly reduced morbidity and improved quality of life. Due to the rarity of vulvar cancer, patients should be treated in specialized centres where appropriate equipment, knowledge and experience are available.

References

- Alkatout I, Schubert M, Garbrecht N, Weigel MT, Jonat W, Mundhenke C, et al. Vulvar cancer: epidemiology, clinical presentation, and management options. *Int J Womens Health* 2015; **7**: 305-13. doi: 10.2147/IJWH.S68979
- Onk MHM, Planchamp F, Baldwin P, Bidzinski M, Brännström M, Landoni F, et al. European Society of Gynaecological Oncology Guidelines for the management of patients with vulvar cancer. *Int J Gynecol Cancer* 2017; **27**: 832-7. doi: 10.1097/IGC.0000000000000975
- Cancer Registry of Republic of Slovenia [Internet] 2016 [cited 2020 May 6]. Available from: <https://www.onko-i.si/rrs/>
- Zadnik V, Primic Zakelj M, Lokar K, Jarm K, Ivanus U, Zagar T. Cancer burden in Slovenia with the time trends analysis. *Radiol Oncol* 2017; **51**: 47-55. doi: 10.1515/raon-2017-0008
- Cancer in Slovenia 2016. Ljubljana: Cancer in Slovenia 2016. Ljubljana: Institute of Oncology Ljubljana, Epidemiology and Cancer Registry, Slovenian Cancer Registry; [internet] 2019 [cited 2020 May 12]. Available from: https://www.onko-i.si/fileadmin/onko/datoteke/dokumenti/RRS/LP_2016.pdf
- De Angelis R, Sant M, Coleman MP, Francisci S, Baili P, Pierannunzio D, et al. Cancer survival in Europe 1999-2007 by country and age: results of EURO-CARE-5-a population-based study. *Lancet Oncol* 2014; **15**: 23-34. doi: 10.1016/S1470-2045(13)70546-1
- Del Pino M, Rodriguez-Carunchio L, Ordi J. Pathways of vulvar intraepithelial neoplasia and squamous cell carcinoma. *Histopathology* 2013; **62**: 161-75. doi: 10.1111/his.12034
- Pils S, Gensthaler L, Alemany L, Horvat R, de Sanjosé S, Joura EA. HPV prevalence in vulvar cancer in Austria. *Wien Klin Wochenschr* 2017; **129**: 805-9. doi: 10.1007/s00508-017-1255-2
- Wohlmuth C, Wohlmuth-Wieser I. Vulvar malignancies: an interdisciplinary perspective. *J Dtsch Dermatol Ges* 2019; **17**: 1257-76. doi: 10.1111/ddg.13995
- Angelico G, Santoro A, Inzani F, Spadola S, Fiorentino V, Cianfrini F, et al. Ultrasound-guided FNA cytology of groin lymph nodes improves the management of squamous cell carcinoma of the vulva: results from a comparative cytohistological study. *Cancer Cytopathol* 2019; **127**: 514-20. doi: 10.1002/ncy.22154
- de Gregorio N, Ebner F, Schwentner L, Friedl TWP, Deniz M, Látó K, et al. The role of preoperative ultrasound evaluation of inguinal lymph nodes in patients with vulvar malignancy. *Gynecol Oncol* 2013; **131**: 113-7. doi: 10.1016/j.ygyno.2013.07.103
- Kataoka MY, Sala E, Baldwin P, Reinhold C, Farhadi A, Hudolin T, et al. The accuracy of magnetic resonance imaging in staging of vulvar cancer: a retrospective multi-centre study. *Gynecol Oncol* 2010; **117**: 82-7. doi: 10.1016/j.ygyno.2009.12.017
- Andersen K, Zobbe V, Thranov IR, Pedersen KD. Relevance of computerized tomography in the preoperative evaluation of patients with vulvar cancer: a prospective study. *Cancer Imaging* 2015; **15**: 8. Available from: <https://www.ncbi.nlm.nih.gov/pmc/articles/PMC4470090/>. doi: 10.1186/s40644-015-0044-2
- Cham S, Chen L, Burke WM, Hou JY, Tergas AI, Hu JC, et al. Utilization and outcomes of sentinel lymph node Biopsy for vulvar cancer. *Obstet Gynecol* 2016; **128**: 754-60. doi: 10.1097/AOG.0000000000001648
- Huang J, Yu N, Wang X, Long X. Incidence of lower limb lymphedema after vulvar cancer: a systematic review and meta-analysis. *Medicine* 2017; **96**: 8722. doi: 10.1097/MD.00000000000008722
- Slomovitz BM, Coleman RL, Onk MHM, van der Zee A, Levenback C. Update on sentinel lymph node biopsy for early-stage vulvar cancer. *Gynecol Oncol* 2015; **138**: 472-7. doi: 10.1016/j.ygyno.2015.05.017
- Onk MHM, Hollema H, van der Zee AGJ. Sentinel node biopsy in vulvar cancer: implications for staging. *Best Pract Res Clin Obstet Gynaecol* 2015; **29**: 812-21. doi: 10.1016/j.bpobgyn.2015.03.007
- Zigras T, Kupets R, Barbera L, Covens A, Liu Y, Gien LT. Uptake of sentinel lymph node procedures in women with vulvar cancer over time in a population based study. *Gynecol Oncol* 2019; **153**: 574-9. doi: 10.1016/j.ygyno.2019.03.010
- Brincat MR, Muscat Baron Y. Sentinel lymph node biopsy in the management of vulvar carcinoma: an evidence-based insight. *Int J Gynecol Cancer* 2017; **27**: 1769-73. doi: 10.1097/IGC.0000000000001075
- van Doorn HC, van Beekhuizen HJ, Gaarenstroom KN, van der Velden J, van der Zee AGJ, Onk MHM, et al. Repeat sentinel lymph node procedure in patients with recurrent vulvar squamous cell carcinoma is feasible. *Gynecol Oncol* 2016; **140**: 415-9. doi: 10.1016/j.ygyno.2016.01.013
- Verbeek FPR, Tummers QRJG, Rietbergen DDD, Peters AAW, Schaafsma BE, van de Velde CJH, et al. Sentinel lymph node biopsy in vulvar cancer using combined radioactive and fluorescence guidance. *Int J Gynecol Cancer* 2015; **25**: 1086-93. doi: 10.1097/IGC.0000000000000419
- Ghoniem K, Shazly SA, Dinoi G, Zanfagnin V, Glaser GE, Mariani A. Sentinel lymph nodes and precision surgery in gynecologic cancer. *Clin Obstet Gynecol* 2020; **63**: 12-23. doi: 10.1097/GRF.0000000000000517

23. Van der Zee AGJ, Oonk MH, De Hullu JA, Ansink AC, Vergote I, Verheijen RH, et al. Sentinel node dissection is safe in the treatment of early-stage vulvar cancer. *J Clin Oncol* 2008; **26**: 884-9. doi: 10.1200/JCO.2007.14.0566
24. Mitra S, Sharma MK, Kaur I, Khurana R, Modi KB, Narang R, et al. Vulvar carcinoma: dilemma, debates, and decisions. *Cancer Manag Res* 2018; **10**: 61-8. doi: 10.2147/CMAR.S143316
25. Swanick CW, Eifel PJ, Huo J, Meyer LA, Smith GL. Challenges to delivery and effectiveness of adjuvant radiation therapy in elderly patients with node-positive vulvar cancer. *Gynecol Oncol* 2017; **146**: 87-93. doi: 10.1016/j.ygyno.2017.05.004
26. Deppe G, Mert I, Belotte J, Winer IS. Chemotherapy of vulvar cancer: a review. *Wien Klin Wochenschr* 2013; **125**: 119-28. doi: 10.1007/s00508-013-0338-y
27. Domingues AP, Mota F, Durão M, Frutuoso C, Amaral N, de Oliveira CF. Neoadjuvant chemotherapy in advanced vulvar cancer. *Int J Gynecol Cancer* 2010; **20**: 294-8. doi: 10.1111/igc.0b013e3181c93adc
28. Inrhaoun H, Elghissassi I, Gutierrez M, Brain E, Errihani H. Long term response to erlotinib in a patient with recurrent vulvar carcinoma: case report and review of literature. *Gynecol Oncol Case Rep* 2012; **2**: 119-20. doi: 10.1016/j.ygnor.2012.07.002
29. Horowitz NS, Olawaiye AB, Borger DR, Growdon WB, Krasner CN, Matulonis UA, et al. Phase II trial of erlotinib in women with squamous cell carcinoma of the vulva. *Gynecologic Oncology* 2012; **127**: 141-6. doi: 10.1016/j.ygyno.2012.06.028
30. Schnürch HG, Ackermann S, Alt-Radtke CD, Angleitner L, Barinoff J, Beckmann MW, et al. Diagnosis, therapy and follow-up of vaginal cancer and its precursors. Guideline of the DGGG and the DKG (S2k-Level, AWMF Registry No. 032/042, October 2018). *Geburtshilfe Frauenheilk* 2019; **79**: 1060-78. doi: 10.1055/a-0919-4959

Combining radiotherapy and immunotherapy in definitive treatment of head and neck squamous cell carcinoma: review of current clinical trials

Gaber Plavc^{1,2}, Primoz Strojjan^{1,2}

¹ Department of Radiation Oncology, Institute of Oncology Ljubljana, Ljubljana, Slovenia

² Faculty of Medicine, University of Ljubljana, Ljubljana, Slovenia

Radiol Oncol 2020; 54(4): 394-408.; 54(4): 377-393.

Received 18 August 2020

Accepted 22 September 2020

Correspondence to: Assist. Gaber Plavc, M.D., Institute of Oncology Ljubljana, Department of Radiation Oncology, Zaloška cesta 2, SI-1000 Ljubljana, Slovenia. E-mail: gplavc@onko-i.si

Disclosure: No potential conflicts of interest were disclosed.

Background. Head and neck squamous cell carcinoma (HNSCC) presents as locally advanced disease in a majority of patients and is prone to relapse despite aggressive treatment. Since immune checkpoint inhibitors (ICI) have shown clinically significant efficacy in patients with recurrent/metastatic HNSCC (R/M HNSCC), a plethora of trials are investigating their role in earlier stages of disease. At the same time, preclinical data showed the synergistic role of concurrently administered radiotherapy and ICIs (immunoradiotherapy) and explained several mechanisms behind it. Therefore, this approach is prospectively tested in a neoadjuvant, definitive, or adjuvant setting in non-R/M HNSCC patients. Due to the intricate relationship between host, immunotherapy, chemotherapy, and radiotherapy, each of these approaches has its advantages and disadvantages. In this narrative review we present the biological background of immunoradiotherapy, as well as a rationale for, and possible flaws of, each treatment approach, and provide readers with a critical summary of completed and ongoing trials.

Conclusions. While immunotherapy with ICIs has already become a standard part of treatment in patients with R/M HNSCC, its efficacy in a non-R/M HNSCC setting is still the subject of extensive clinical testing. Irradiation can overcome some of the cancer's immune evasive manoeuvres and can lead to a synergistic effect with ICIs, with possible additional benefits of concurrent platinum-based chemotherapy. However, the efficacy of this combination is not robust and details in trial design and treatment delivery seem to be of unprecedented importance.

Key words: head and neck neoplasms; immunoradiotherapy; radiotherapy; immunotherapy

Introduction

Head and neck squamous cell carcinoma (HNSCC) accounts for more than 800,000 new cancer cases and over 400,000 deaths each year worldwide.¹ Despite aggressive therapeutic approaches the outcomes are still highly dependent on disease burden. Five-year disease control ranges from almost 100% in patients with T1a glottic carcinoma to below 30% in patients with locally-advanced hypopharyngeal cancer.^{2,3} More than 60% of all cases are locally-advanced at diagnosis with a 50% rate

of relapse in the first two years, despite the use of multimodal state-of-the-art treatment.⁴ Therefore, while treatment-related toxicity is now of primary concern in early stage HNSCC and low-risk human papilloma virus (HPV) mediated oropharyngeal carcinomas, with 3-year overall survival rates in excess of 90%^{5,6}, in other patients the focus of research is on treatment intensification and/or modification.

After intrinsic tumour suppressor mechanisms fail, further tumour progression is the result of an inefficient elimination phase or equilibrium phase

of the extrinsic tumour suppression by the immune system.⁷ Genetically unstable cancer cells under constant immune selection pressure evade immune recognition and destruction. Thus, they become invisible to immune cells by reducing the presentation of tumour antigens, decreasing their sensitivity to the cytotoxic effects of immune cells, and rendering their microenvironment immunosuppressive.⁷ In the fight against the latter, immune checkpoint inhibitors (ICI) targeting immune checkpoint programmed cell death protein 1 (anti-PD-1) are now considered standard care in recurrent and metastatic HNSCC (R/M HNSCC).^{8,9} Because of their proven efficacy and significantly improved toxicity profile as well as positive effect on quality of life as compared to standard chemotherapy regimens, an increasing number of trials are testing ICIs in the earlier stages of HNSCC.¹⁰⁻¹²

Besides a well-known immunosuppressive effect of radiotherapy (RT), it can also lead to positive alterations in innate and adaptive immunity.¹³ The same is true for the positive effects of the immune system on radiation efficacy, as a tumoricidal effect of RT is dependent on functional T cells, even at ablative doses.¹⁴ Furthermore, RT induces programmed death-ligand 1 (PD-L1) expression in dendritic cells (DCs) and cancer cells which contributes to acquired cancer radioresistance, which could be overcome by concurrent anti-PD-1/L1.¹⁵ These intricate interactions form the basis for combined treatment with RT and ICIs (immunoradiotherapy). This combination was shown to cause similar toxicity compared to either RT or ICI alone across different cancer types.¹⁶ Encouraging efficacy of this treatment combination has also been shown in early prospective trials in metastatic malignant melanoma and non-small cell lung cancer.¹⁷⁻²¹ The first results of trials using immunoradiotherapy in non-R/M HNSCC are now also available and many are underway. In this review we presented a biological rationale for the combination of RT and anti-PD-1/L1 and performed a systematic search for, and critical assessment of, completed and ongoing trials using a combination in non-R/M HNSCC.

Role of anti-PD-1 and radiotherapy in immune rejection of HNSCC

The efficacy of anti-PD1 therapy in HNSCC is poor with less than 20% of responding patients.^{8,22,23} These high rates of primary or acquired resistance

in R/M HNSCC to anti-PD1 agents are a result of absent antigenic proteins, defective antigen presentation, T cell exhaustion/absence, insensibility of tumours to T cells, presence of immunosuppressive cells, and/or presence of other inhibitory immune checkpoints.²⁴

For the immune system to exert its cytotoxic function, mutant peptides, also known as tumour neoantigens (TNA) or ectopically expressed antigens, must be presented to antigen-presenting cells by cancer cells on major histocompatibility complex I (MHC I).²⁵ Even though the tumour mutation burden in HNSCC is rather high with 5 mutations per million base pairs, a proper presentation is needed for them to elicit an immune response.^{26,27} A vital role of antigen processing machinery in this step is evident by the absence of CD8⁺ T cell recognition of HNSCC in the case of defective antigen processing machinery (defect present in 20–80% of HNSCCs).²⁸⁻³⁰ The next step is presentation of the TNA by MHC I. The complete loss of MHC I results in natural killer (NK) cells' activation, while aberrant expression is beneficial for cancer cells and is present in up to 60% of HNSCCs.³¹⁻³³ Up to 80% of HNSCC patients overexpress the epidermal growth factor receptor (EGFR), which also down-regulates MHC I.³⁴ Treatment with anti-PD-1 was shown to be less efficient in cancers with aberrant MHC I.^{35,36}

Yet tumour antigenicity is not enough to elicit immune response by itself. TNA presentation must be put in context by accompanying adjuvants in the form of danger-associated molecular patterns (DAMP) which are recognised by pattern recognition receptors on the cells of innate immunity. Different types of DAMPs are exposed by different modes of cell death and even by stressed cancer cells.³⁷ These include membrane-bound calreticulin, emitted ATP, and passively released nuclear high-mobility group box protein 1 (HMGB1). This leads to the recruitment and activation of dendritic (DCs) and other mononuclear cells.^{38,39} DCs cross-present antigens to naïve CD8⁺ T and by co-stimulatory signals (ligands and cytokines provided by DCs upon stimulation by DAMPs and type I interferons [IFNs]) prime these cytotoxic T lymphocytes in regional lymph nodes.⁴⁰ Type I IFN is produced by cancer cells as a result of a stimulator of interferon genes (STING) responding to DNA in the cytosol of cancer cell, which is a consequence of cancer's unstable genome.^{41,42}

To prevent unnecessary damage to surrounding tissue in their fight against viruses, CD8⁺ T lymphocytes also express inhibitory receptors, such

as PD-1, with its ligand PD-L1 on host tissue and immune cells.⁴³ The same PD-L1 expression is exploited by cancer cells to escape immune surveillance.⁴⁴ An active PD-1/PD-L1 pathway in tumour microenvironment (TME) also promotes T cell exhaustion and differentiation of regulatory T cells (Treg).⁴⁵ Primed tumour-infiltrating lymphocytes (TILs) that are suppressed due to PD-1/PD-L1 interaction are vital for anti-PD-1 efficacy, which also tips the balance from differentiation of exhausted T cells and Tregs towards generation of effector T cells.^{45,46}

Immunostimulatory effect of RT depends a great deal on inducing the above-described immunogenic cell death, with dose-dependent (from 2 to 20 Gy) increase in concentrations of DAMPs calreticulin, HMGB1, and ATP.⁴⁷ RT also produces free cytosolic DNA which is more pronounced in cancers with a loss of p53 function, as is the case in the majority of HNSCC.^{48,49} Cytosolic DNA is sensed by various pattern recognition receptors with STING being a central connecting protein. Activation of the cyclic GMP-AMP synthase-STING (cGAS-STING) pathway by free cytosolic DNA leads to type I IFN production in cancer and DCs.^{41,50} Regarding antigenicity, RT increases MHC I expression and diversifies the tumour-infiltrating T cell receptor repertoire which is a positive predictor of response to anti-PD-1/L1.⁵¹⁻⁵³ Previously silent mutated genes can be expressed by RT, thus leading to presentation of these TNAs by MHC I.^{54,55} RT also induces some constituents of antigen processing machinery by enhancing degradation of proteins into peptides.⁵¹ The positive effects of RT are also apparent in TME. By reducing tumour hypoxia and consequently reducing the expression of vascular endothelial growth factor, SBRT can inhibit mobilisation of myeloid-derived suppressor cells (MDSC).⁵⁶ Some authors also observed an enhanced recruitment of T cells into TME after RT.⁵⁷ RT-enhanced death receptor Fas expression further promotes the antitumour activity of recruited T cells.^{58,59} Furthermore, RT promotes the function and differentiation of cytotoxic T cells by inducing interleukin-1B, tumour necrosis factor- α , and interleukin-6.¹³ Considering vasculature, low dose RT increases the ratio of antitumoural macrophages type 1 and tumour-promoting macrophages type 2, which leads to vascular normalisation and T cell recruitment.⁶⁰ Besides, low dose RT also appears to decrease TME's immunosuppressive cells such as Tregs and MDSCs.⁶¹ Another beneficial vasculature-related effect of RT is induction of cell adhesion molecules, for example Intercellular Adhesion

Molecule 1 and E-selectin, that help leukocytes extravasate to TME.⁶²

Importantly, as a part of standard treatment in HNSCC, concurrent platin-based chemoradiotherapy (CRT) was also shown to induce immunogenic cell death.⁴⁷ In the *in vitro* model, antigen presentation and T cell cytotoxicity were enhanced by moderate doses of cisplatin. In the *in vivo* mouse model synergism of cisplatin and anti-PD-1 was observed.⁶³ However, cisplatin also resulted in PD-L1 upregulation on cancer cells and higher doses were immunosuppressive. Nevertheless, Luo *et al.* showed on murine cancer models that cisplatin combined with anti-PD-1 treatment enhances RT-induced abscopal effect in non-irradiated nodes.⁶⁴

It should be noted that all the above-mentioned effects of RT were observed in preclinical studies and are not universally beneficial, as was shown in clinical setting. Release of DAMPs HMGB1 and ATP, which is degraded into extracellular adenosine, can have many immunosuppressive effects.⁶⁵⁻⁷⁰ Activation of cGAS-STING can lead to increased concentrations of MDSC in TME and even increase cancer aggressiveness.^{71,72} STING activation can also lead to depletion of tryptophan in TME via upregulation of Indoleamine 2,3-dioxygenase, resulting in reduced T cell cytotoxicity and increased tumour-associated macrophages and MDSCs.^{73,74} Even sustained type I IFN signalling is detrimental as it results in increased Treg and MDSC concentrations in TME and enhanced expression of PD-1.⁷⁵ Besides, RT increases tumour growth factor beta concentration which was shown to promote tumour-promoting macrophages type 2 differentiation and inhibit DCs and cytotoxic T cells.¹³ In addition, RT was shown to even upregulate hypoxia inducible factor-1 α , leading to eventual Treg and MDSC accumulation and DC and T cell inhibition via vascular endothelial growth factor.⁷⁶⁻⁸⁰

Methods

We searched PubMed and Clinicaltrials.gov databases with search terms ((immunoradiotherapy OR radioimmunotherapy) OR ((head and neck) OR (oral cavity) OR (oropharyngeal) OR (oropharynx) OR (larynx) OR (laryngeal) OR (hypopharynx) OR (hypopharyngeal)) AND (immunotherapy OR checkpoint OR pembrolizumab OR avelumab OR atezolizumab OR camrelizumab OR durvalumab OR avelumab OR nivolumab OR toripalimab OR PD-1 OR PD-L1 OR tremelimumab OR CTLA-4)

TABLE 1. Neoadjuvant immunoradiotherapy trials

Trial, start year	Phase	N	Subsite and subtype	Basic scheme	Immunotherapy details	RT details	Main results
NIRT-HNC, NCT03247712, ⁸⁹ 2018	I	10	HPV+ resectable HNSCC stage I-III or CUP with clinical indications for adj. RT or TORS ineligible	NIVO+SBRT 5 weeks before surgery, followed by NIVO	3x NIVO neoadj. and 3x adj. NIVO starting 4 weeks postop.	SBRT to GTV+3mm; 5pts: 5x8Gy daily (A), and 5 pts: 3x8Gy (B) every other day; delivered between 1st and 2nd NIVO cycle	no surgical delays; G3 postop. toxicity higher in cohort A; pCR: 100% in cohort A, and 80% in cohort B.
	II	11, ongoing	cohort C: same as phase I, cohort D: stage III-IV HPV- resectable HNSCC	cohort C: SBRT alone 5 weeks before surgery, followed by NIVO, cohort D: same as phase I	cohort C: only adj. NIVO, same as in phase I cohort D: same as phase I	cohort C (6pts): SBRT 3 x 8 Gy cohort D (5 pts): SBRT 3 x 8 Gy	no G3-4 toxicity; major pathologic response in majority of pts
NCT03635164, ⁹¹ 2018	I	18	HPV- resectable LAHNSCC	DURVA+SBRT 3-6 weeks before surgery, followed by DURVA	DURVA neoadj. with the first SBRT fraction and up to 6x DURVA postop.	SBRT to gross disease only, starting dose of 2x6Gy (planned increase to 3x6Gy, cohort size of 3 patients) every other day, starting concurrently with DURVA	NA
NCT03618134, ⁹² 2018	I/II	82	TORS eligible HPV+ oropharyngeal HNSCC	DURVA+SBRT+/- tremelimumab 5-7 weeks before TORS, followed by DURVA	DURVA+/- tremelimumab neoadj. with the first SBRT fraction and on day 27, followed by up to 4x adj. DURVA	SBRT in 5fx, starting concurrently with DURVA+/- tremelimumab	NA

adj. = adjuvant; CUP = cancer of unknown primary; DURVA = durvalumab; fx = fraction; GTV = gross tumour volume; G3 = grade 3; HNSCC = head and neck squamous cell carcinoma; HPV- = human papilloma virus negative cancer; HPV+ = human papilloma virus associated cancer; LAHNSCC = locally advanced HNSCC; N = planned number of enrolled patients, NA = not available; neoadj. = neoadjuvantly, NIVO = nivolumab; pCR = pathological complete response; postop. = postoperatively; pts = patients; RT = radiotherapy, SBRT = stereotactic body RT; TORS = transoral robotic surgery

AND (radiotherapy OR SBRT OR RT OR SABR OR irradiation) and with the start date of the studies from 15th July 2013 to 15th July 2020. In total, 39 completed or ongoing trials were found, using concurrent (chemo)radiotherapy and ICIs in primary definitive treatment of non-R/M HNSCC (non-nasopharyngeal).

Trials using anti-PD-1/L1 and radiotherapy combination in HNSCC: different approaches

In completed and ongoing trials, concurrent anti-PD-1/L1 and RT was delivered either before or after surgery, or as a sole definitive treatment. Few delivered anti-PD-1/L1 also as an extended consolidative treatment. Taking the intricate relationship between the immune system and therapy into account, attention to the below-described caveats should help shed light on the pros and cons of these research approaches.

Neoadjuvant immunoradiotherapy

Except for the earliest stages of HNSCC, elective neck treatment either by lymphadenectomy or irradiation is part of the standard treatment.⁸¹ Lymph nodes are also one of the places where DCs cross-prime CD8⁺ T lymphocytes.⁸² Even though the immediate treatment effect of concurrent anti-PD-1 and RT depends primarily on TILs already present in the primary tumour, T cells from lymph nodes are responsible for long-lasting tumour control.^{83,84} Preclinical studies in murine cancer models clearly showed the vital role of functioning draining lymph nodes for RT efficacy with or without concurrent ICI.^{85,86} Removal of draining lymph nodes or elective nodal irradiation led to reduced tumour-specific TILs.^{85,86} Furthermore, clinical data show reduced efficacy of anti-PD-1 in previously treated patients with HNSCC.⁸⁷ This speaks strongly in favour of using an immunoradiotherapy combination before surgery as compared to its postoperative application.

Neoadjuvant RT is not considered a standard of care in HNSCC, therefore these “window of opportunity trials” serve mostly to advance our understanding of the underlying mechanisms and to lay the ground for further studies.⁸⁸ Special attention must be therefore given to patient safety. In the, so far only, immunoradiotherapy “window of opportunity” trial that reported results, no surgical delays were noted.⁸⁹ The possibility of anti-PD-1 induced hyperprogression must nevertheless be kept in mind as it was reported in up to 29% of patients with R/M HNSCC.⁹⁰

The ongoing trials are presented in detail in Table 1. Leidner *et al.* completed phase I of their phase I/II trial and already provided intriguing results.⁸⁹ In the first phase, 10 patients with stage I-III HPV associated HNSCC or cancer of unknown primary with clinical indications for adjuvant RT or who were ineligible for transoral robotic surgery were accrued. Two cohorts were formed of which five patients received neoadjuvant SBRT with 5x8 Gy (A cohort), and another five patients had SBRT with 3x8 Gy (B cohort), both with concurrent nivolumab. No grade 4 toxicity was observed, with somewhat higher grade 3 toxicity in the A cohort. Notably, grade 2 renal insufficiency was observed in 50% of patients. Both fractionation regimens were shown to be effective with 100% and 80% complete pathological responses in the A and B cohort, respectively. However, on presurgical imaging evaluated by RECIST criteria, no complete responses were found. Recently, preliminary results of their phase II cohort expansion were also presented.⁹¹ Only the SBRT fractionation of the B cohort was further pursued. In cohort C inclusion criteria were the same as in cohorts A and B, while these six patients were treated with only neoadjuvant SBRT, followed by surgery and adjuvant nivolumab. Cohort D included only patients with HPV-negative HNSCC, and these five patients were treated the same as those in cohort B (SBRT with 3x8 Gy concurrently with nivolumab). Results were so far only vaguely described: there was no limiting toxicity, but the complete pathological response rate was somewhat lower than in cohorts A and B. In-detail results are awaited.

The approach to treatment was similar in HPV-negative HNSCC patients in the NCT03635164 trial, with the difference that anti-PD-L1 agent durvalumab was used instead of nivolumab.⁹¹ The third ongoing trial (NCT03618134) with a similar approach is testing whether the addition of tremelimumab, an anti-cytotoxic T-lymphocyte-associated protein 4 (anti-CTLA-4), to durvalumab

can improve the outcome in HPV-positive HNSCC patients.⁹² These two ICIs provide complementary effects, albeit at the expense of increased toxicity.^{93,94}

Definitive immunoradiotherapy

Considering only non-cancer/TME-related factors, synergism between anti-PD-1 and RT is probably most pronounced when these two treatment modalities are delivered concurrently in previously untreated patients with intact draining lymph nodes and no lymphopenia.^{85–87,95–98} Definitive immunoradiotherapy as a sole treatment fulfils these criteria, except for nodal irradiation. If, in a neoadjuvant setting, elective nodal irradiation is not mandatory, its omission would be ill-advised in a definitive (chemo)radiotherapy setting based on our current knowledge.⁸¹ However, advancement in diagnostic imaging and treatment (e.g. sentinel lymph node biopsy) provides the basis for ongoing trials testing reduced dose and/or volume of elective nodal irradiation which would be welcomed in immunoradiotherapy as well.⁹⁹

Preclinical studies also provide rather strong support for greater efficacy of hypofractionated RT compared to conventionally fractionated RT.^{56,100,101} In contrast to all the above-listed trials with immunotherapy in the neoadjuvant setting, however, the definitive setting immunoradiotherapy trials mostly utilise conventionally fractionated RT courses as compared to hypofractionated SBRT. This could be an important outcome-defining factor.

Concurrent chemoradiotherapy with cisplatin causes severe radiomucositis (grade 3–4) in around 40% of HNSCC patients.^{102,103} Even though anti-PD-1/L1 induced oral mucositis or stomatitis occurs in less than 3% of patients and is usually mild, it can nevertheless occasionally be severe.¹⁰⁴ Special attention should be paid to this when using an approach with combined CRT and anti-PD-1/L1, despite the fact that pertinent trials have so far not reported exacerbated toxicity in oral mucosa (see below). Another important aspect of concurrent CRT and immunotherapy is the effect of chemotherapy on immunotherapy's efficacy which seems to be beneficial in low doses, whereas high-dose chemotherapy is known to cause myelosuppression and could be detrimental to the efficacy of immunotherapy.^{63,64} Several trials use ICI combined with cetuximab, an anti-EGFR agent. Cetuximab is a mouse/human chimeric monoclonal IgG1 antibody.¹⁰⁵ Besides acting through targeting EGFR and dysregulating its signaling pathway, it also stimulates NK cells anti-

tumour activity, activates DCs, and recruits cytotoxic CD8⁺ T cells.¹⁰⁵ Cetuximab's ability to prime adaptive and innate immunity is met with regulatory immunosuppressive mechanisms. Targeting these immunosuppressive mechanisms (induction of Tregs, MDSC, PD-1, PD-L1, CTLA-4) by immunotherapy such as ICI has great potential and is still being tested in several trials.¹⁰⁶ A prospective trial using anti-PD-1 combined with cetuximab in 33 patients with platinum-refractory/ineligible R/M HNSCC showed a 41% response rate. About a third of patients experienced treatment-related grade 3 toxicity.¹⁰⁷ Furthermore, retrospectively gathered data on a triple combination of cetuximab, chemotherapy and anti-PD-1 used in 15 patients with R/M HNSCC was presented in 2018 by Lin *et al.*¹⁰⁸ The combination seemed effective with 58% partial responses and acceptable toxicity.

Completed and ongoing trials treating patients with non-R/M HNSCC with a definitive immunoradiotherapy combination are presented in Table 2, while important details are presented below.

JAVELIN Head and Neck 100 (NCT02952586) is the first randomised phase III trial combining CRT with concomitant ICI in patients with LAHNSCC to be terminated due to inefficiency.¹⁰⁹ Concurrent administration of a PD-L1 inhibitor avelumab and standard CRT (70 Gy and high-dose cisplatin) followed by maintenance avelumab for 12 months was compared to a placebo arm receiving the same CRT but with placebo instead of avelumab in 697 high-risk LAHNSCC patients.¹¹⁰ A pre-planned interim analysis showed that this combination is unlikely to show a significant improvement in progression-free survival and the trial was therefore terminated. Detailed study findings are awaited.

In a GORTEC 2017-01 REACH trial (NCT02999087), two standard arms (CRT with a three-weekly high-dose cisplatin in a cohort of patients fit for high-dose cisplatin, and RT with concurrent cetuximab in a cohort of patients unfit for high-dose cisplatin) were compared to experimental arms with the same RT regimen and concurrent avelumab and cetuximab (preliminary results, Table 2).^{111,112} All patients completed RT except for one cisplatin-ineligible patient receiving RT concurrently with avelumab and cetuximab. 88% and 76% of patients received all planned doses of avelumab and cetuximab, respectively. A grade ≥ 4 adverse effect occurred in 5/41 (12%) patients in experimental arms (all in the cohort of patients ineligible for high-dose cisplatin), and in 5/41 (12%) patients in standard arms (14% in high-dose cisplatin eligible and 10% in high-dose cisplatin ineli-

gible patients) where one grade 5 toxicity was also observed. The trial continues.

In 2019, results of the lead-in phase of randomised phase II/III trial NRG-HN004 (NCT03258554) were presented. Ten out of a planned 523 cisplatin-ineligible patients received durvalumab concomitantly with RT and all completed RT as planned, while 8/10 patients received all the planned durvalumab cycles. Randomisation will continue to either RT with durvalumab or RT with cetuximab.¹¹³

The GORTEC 2015-01 PembroRad randomised phase II trial's safety-related results were presented in 2018.¹¹⁴ In 133 cisplatin ineligible patients with LAHNSCC cetuximab or pembrolizumab were added to conventional RT, which resulted in a similar completion rate of RT (86 vs. 88%) and dysphagia (34 vs. 39%). However, mucositis was more prevalent in the cetuximab arm and the same goes for dermatitis (49 vs. 17%) (Table 2). Final results are still awaited.

The results of the first 16 randomised patients of the planned 120 patients with HPV- LAHNSCC in a DURTRE-RAD trial (NCT03624231) were recently presented.¹¹⁵ Among the first six patients treated with a combination of RT, durvalumab and tremelimumab (arm A), five patients (83%) stopped treatment due to immune-related adverse effects (irAE), of which one was grade 5. This arm was terminated due to excessive toxicity. Arm B with only durvalumab added to RT, which resulted in only 1/10 patients stopping treatment due to irAE, is continuing to enrol.

Weiss *et al.* (NCT02609503) presented the results of their phase II trial after a median follow-up of 21 months.¹¹⁶ In 29 cisplatin ineligible patients with LAHNSCC pembrolizumab was given concurrently with definitive RT and for an additional three adjuvant cycles (Table 2). The estimated two-year overall and progression-free survival was 75% and 71% respectively. RT was delivered in full in 28/29 patients, and 25/29 patients received all pembrolizumab doses. Toxicities were mild with a major exception being grade 3–4 lymphopenia, which occurred in 59% of patients, however, absolute lymphopenia did not predict for progression. Further characterisation of this unexpected lymphopenia showed declines in blood concentrations of B cells and CD4⁺ T cells, whereas CD8⁺ T cells were relatively preserved.¹¹⁶

Powel *et al.* presented results from their phase I trial (NCT02586207), testing pembrolizumab with chemoradiotherapy in 59 patients with LAHNSCC.¹¹⁷ Pembrolizumab was discontinued due to irAE in 9% during CRT and for non-irAE

TABLE 2. Definitive immunoradiotherapy trials

Trial, start year	Phase	N	Subsite and subtype	Basic scheme	Immunotherapy details	RT details	Main results
NCT02586207, ¹¹⁷ 2015	I	59	LAHNSCC eligible for CRT (34 pts HPV + and 23 pts HPV-)	PEMBRO + CRT, followed by PEMBRO	PEMBRO on days -7 (before CRT), 15 and 36 (conc. with CRT), and adj. for 5 cycles	starting on day 1: CRT with IMRT 70 Gy (2Gy/tx) and LD-CDDP for 6 cycles	HPV + : 85% CR 12 weeks after CRT; HPV-: 78% CR 12 weeks after CRT; HPV + : 2-year OS 97% and PFS 93%; HPV-: 1-year OS 87% and PFS 73%
GORTEC 2015-01 "PembroRad" (NCT02707588), ¹¹⁴ 2016	II, rand.	133	LAHNSCC ineligible for CDDP	arm A: CETUX + RT; arm B: PEMBRO + RT	arm A: CETUX during RT; arm B: PEMBRO during RT	IMRT (69.99Gy/33fx)	arm A: 94% grade 3 toxicity, 57% grade 3 mucositis, 86% received full RT; arm B: 78% grade 3 toxicity, 24% grade 3 mucositis, 88% received full RT
KEYNOTE-412 (NCT03040999), ¹²⁴ 2017	III, rand.	780	LAHNSCC eligible for CRT	arm A: PEMBRO + CRT, followed by PEMBRO; arm B: placebo + CRT, followed by placebo	arm A: priming dose of PEMBRO followed by 2x PEMBRO + CRT, followed by 14x maint. PEMBRO; arm B: placebo instead of PEMBRO	CRT (70Gy/35fx) and HD-CDDP	NA
NCT02759575, ¹³¹ 2016	I/II	47	LAHNSCC of larynx	PEMBRO + CRT	PEMBRO starting 3 weeks before CRT, maximum 4x	CRT (70Gy/35fx) and HD-CDDP	NA
NCT02609503, ¹¹⁶ 2016	II	29	LAHNSCC ineligible for CDDP	PEMBRO + RT, followed by PEMBRO	PEMBRO conc. with RT and 3 adj. cycles	IMRT (70Gy/35fx)	2-year OS 75% and PFS 71%; 59% grade 3-4 lymphopenia
NCT02777385, ¹³⁰ 2016	II, rand.	90	LAHNSCC	arm A: PEMBRO + CRT; arm B: CRT followed by PEMBRO	arm A: 8x PEMBRO 1 week prior to RT; arm B: 8x PEMBRO beginning in week 10	CRT with IMRT (70Gy/35fx) and LD-CDDP	NA
NCT03532737, ¹³² 2018	II	50	LAHNSCC	PEMBRO + CRT or PEMBRO + CETUX + RT	PEMBRO starting 3 weeks before (C)RT and during CRT or during RT + CETUX	CRT with IMRT (66-70Gy/30-35fx) and HD-CDDP or conc. CETUX	NA
KEYCHAIN (NCT03383094), ¹³³ 2018	II, rand.	114	HPV + LAHNSCC	arm A: PEMBRO + RT; arm B: CRT	arm A: conc. and adj. PEMBRO for 20 cycles; arm B: CDDP-based CRT	IMRT (70Gy/33-35fx) (arm A) and HD-CDDP in arm B	NA
PEACH (NCT02819752), ¹³⁴ 2017	I	36	LAHNSCC	PEMBRO + CRT, followed by PEMBRO	pre-loading dose of PEMBRO (dose-escalation trial, 100-200mg) and conc. CRT and PEMBRO and 4x adj. PEMBRO	standard CRT	NA
NCT04369937, ¹²⁷ 2020	II	50	IR HPV + HNSCC	HPV-16 vaccination (ISA101b) + PEMBRO + CRT	3x ISA101b starting 1 week prior to PEMBRO and two weeks prior to CRT	CRT with IMRT (70Gy/35fx) and HD-CDDP	NA
RTOG 3504 (NCT02764593), ¹²⁰ 2016	I	40	IR-HR LAHNSCC	conc. and adj. NIVO added to each of 4 (C)RT cohorts	conc. NIVO starting 2 weeks before (C)RT and adj. NIVO starting 3 months after CRT	all cohorts: IMRT (70Gy/35fx); cohort 1: CRT with LD-CDDP; cohort 2: CRT with HD-CDDP; cohort 3: RT + CETUX; cohort 4: RT	adj. NIVO infeasible after HD-CDDP or in CDDP-ineligible pts; low rates of NIVO DLT
NCT03349710, ¹²⁵ 2017	III, rand.	1046	LAHNSCC	NIVO + RT vs. CETUX + RT vs. NIVO + CRT vs. CRT	Closed due to slow accrual		

Trial, start year	Phase	N	Subsite and subtype	Basic scheme	Immunotherapy details	RT details	Main results
NCT03162731, ¹²¹ 2017	I	24	HR LAHNSCC	NIVO + ipilimumab + RT	17x NIVO and 6x ipilimumab, both starting 2 weeks before RT	IMRT (70Gy/35fx)	first 12 pts: grade 3 in-RT-field toxicity in 50% of pts, 3 pts discontinued therapy >3 months post-RT, 1 grade 3 colitis, 1 grade 5 bleeding, irAE in 50% of pts
NCT03894891, ¹³⁵ 2019	II	70	LAHNSCC of larynx and hypopharynx	induction docetaxel + CDDP + NIVO, followed by NIVO + RT	standard institutional dosing	standard institutional dosing	NA
NCT03829722, ¹³⁶ 2019	II	40	HR HPV + OP cancer	NIVO + CRT, followed by adj. NIVO	4x NIVO before and conc. with CRT, followed by 4x NIVO	CRT (70Gy/35fx) and carboplatin + paclitaxel combination once per week	NA (temporarily suspended due to COVID-19)
NRG-HN005 (NCT03952585), ¹²⁶ 2019	II/III, rand.	711	early-stage HPV + OP cancer	arm A: NIVO + deescalated RT; arm B: CRT arm C: deescalated CRT	6x NIVO, starting 1 week prior to RT	IMRT, CRT with HD-CDDP	NA
NCT03799445, ¹³⁷ 2019	II	180	low-intermediate volume HPV + OP cancer	NIVO + ipilimumab + RT	NIVO on days 1, 15, 29, and ipilimumab on day 1; for 2 cycles	IMRT 50–66Gy starting on day 1 of 2. cycle of NIVO + ipilimumab	NA
GORTEC 2017-01 "REACH" (NCT02999087), ¹³⁸ 2017	III, rand.	688	LAHNSCC	Cohort 1 (fit for CDDP): CRT with CDDP (arm 1A), RT + AVEL + CETUX (arm 1B); Cohort 2 (unfit for CDDP): RT + CETUX (arm 2A), RT + AVEL + CETUX (arm 2B)	AVEL and CETUX starting 1 week prior to RT, followed by AVEL maint. for 12 months	IMRT 69.96Gy with either HD-CDDP or CETUX	first 82 pts: thresholds of the safety monitoring rule not crossed; trial continues
JAVELIN HEAD AND NECK 100 (NCT02952586), ¹¹⁰ 2016	III, rand.	697	LAHNSCC	arm A: AVEL + CRT; arm B: placebo + CRT	AVEL starting 1 week prior to CRT, followed by maint. AVEL for 12 months	CRT with IMRT (70Gy/35fx) and HD-CDDP	preplanned interim analysis: unlikely to show improvement, terminated
NCT02938273, ¹²² 2017	I	10	LAHNSCC ineligible for CDDP	AVEL + CETUX + RT	AVEL starting 1 week prior to RT, followed by maint. AVEL for 4 months; CETUX conc.	VMAT (70Gy/35fx)	tumour recurrence in 50% after a median follow up of 12months; transient and manageable irAE
DUCRO-HN (NCT03051906), ¹³⁹ 2018	I/II	69	LAHNSCC	DURVA + CETUX + RT	DURVA and CETUX, both conc. with RT, followed by adj. DURVA for 6 months	IMRT (69.9Gy/33fx)	NA
DURTRE-RAD (NCT03624231), ¹¹⁵ 2018	II, rand.	120	HPV-LAHNSCC	arm A: DURVA + TREM + RT; arm B: DURVA + RT	DURVA started 2 weeks prior to RT and TREM started with RT, followed by DURVA for up to 9 cycles	RT (70Gy/35fx)	first 16 patients: in arm A 5/6 stopped treatment due to toxicity -> terminated; in arm B 1/10 patients stopped treatment
CheckRad-CD8 (NCT03426657), ¹²³ 2018	II	120	LAHNSCC	induction DURVA + TREM + CDDP + docetaxel and in case of increased CD8 + TILs compared to pre-treatment Bx -> DURVA + TREM + RT	after induction: DURVA with RT and TREM with RT, followed by DURVA for up to 12 cycles	RT (70Gy/35fx)	first 10pts after induction (re-biopsies): pCR in 8/10pts, 2 grade 3 + toxicities

Trial, start year	Phase	N	Subsite and subtype	Basic scheme	Immunotherapy details	RT details	Main results
NRG-HN004 (NCT03258554), ¹¹³ 2017	II/III, rand.	523	LAHNSCC ineligible for CDDP	arm A: DURVA + RT; arm B: CETUX + RT	DURVA started 2 weeks prior to RT for 7 cycles; CETUX conc.	RT (70Gy/35fx)	lead-in trial, 10 pts: all received arm A treatment, all completed RT, 8/10 received all doses of DURVA
CITHARE (NCT03623646), ¹⁴⁰ 2019	II, rand.	66	early-stage HPV + OP cancer	arm A: DURVA + RT; arm B: CRT	DURVA conc. with RT	RT 70Gy with CDDP in arm B	NA
REWRITE (NCT03726775), ¹²⁹ 2018	II	73	HNSCC T1-2 or HNSCC T3-4 and not eligible for CRT/CETUX + RT	DURVA + RT, followed by additional 6 months of DURVA	DURVA conc. with RT, followed by 6 months of DURVA	RT to only primary tumour and immediately adjacent nodal level without extended neck irradiation	NA
NCT04405154, ¹⁴¹ 2020	II	32	LAHNSCC	CRT + camrelizumab	camrelizumab conc. with CRT and after for total of 8 cycles	CRT with IMRT/VMAT (66–70Gy/33–35fx) and HD-CDDP	NA

adj. = adjuvantly; AVEL = avelumab; CETUX = cetuximab; ; CDDP = cisplatin; conc. = concurrently; CR = complete response; CRT = chemoradiotherapy; DLT = dose-limiting toxicity; DURVA = durvalumab; , fx = fractions; HD-CDDP = high dose cisplatin 100 mg/m² every three weeks during RT; HR = high-risk; HPV+ = human papilloma virus associated cancer; HPV- = human papilloma virus negative cancer; IMRT = intensity modulated RT; IR = intermediate-risk; irAE = immune-related adverse effects; LAHNSCC = locally advanced head and neck squamous cell carcinoma; LD-CDDP = low dose cisplatin 40 mg/m² every week during RT; maint. = maintenance; N = planned enrolment; NA = not available; NIVO = nivolumab; OP = oropharyngeal; OS = overall survival; PEMBRO = pembrolizumab; PFS = progression-free survival; RT = radiotherapy, TILs = tumour infiltrating lymphocytes; TREM = tremelimumab; VMAT = volumetric modulated arc therapy

related causes in 12% after CRT. The goal cisplatin dose of 200 mg/m² or more was received by 88% of patients and 98% of patients received all 70 Gy of RT. 76% of patients received all eight planned pembrolizumab cycles. Grade 4 toxicities were solely hematologic and electrolyte abnormalities. Outcomes are described in Table 2.

In the RTOG 3504, a phase I trial enrolling 40 patients with intermediate risk (HPV-associated oropharyngeal HNSCC, T1-2N2b-N3/T3-4N0-3, >10 pack-years or T4N0-N3, T1-3N3 ≤10 pack-years) or high-risk LAHNSCC (oral cavity, laryngeal, hypopharyngeal, or HPV-negative oropharyngeal HNSCC, T1-2N2a-N3 or T3-4N0-3), nivolumab was added to each of four (C)RT cohorts in a concurrent and adjuvant setting.^{118–120} RT was delivered with either a weekly low-dose or three-weekly high-dose cisplatin, with cetuximab, or as monotherapy (Table 2). The addition of nivolumab concurrently to all four (C)RT regimens was found safe. Levels of dose-limiting toxicity were acceptable and after 17, 16, 10, and 6 months of median follow-up in each of the four RT cohorts there were 0/10 (RT plus weekly cisplatin), 1/9 (RT plus three-weekly cisplatin), 1/10 (RT plus cetuximab), and 3/10 (RT only) events (i.e. death or disease progression), respectively. However, adjuvant administration of nivolumab was infeasible after (C)RT in cisplatin-ineligible patients or in those who received high-dose three-weekly concurrent cisplatin.

Data from the first 12 patients (planning to enrol 24 patients) from the NCT03162731 phase I trial, adding nivolumab and ipilimumab to standard RT in high-risk LAHNSCC, were also presented.¹²¹ After a follow-up of 7.2–18.4 months, 10 of the 12 patients are alive with no evidence of disease. Major toxicities are presented in Table 2.

Elbers *et al.* recently reported results from their phase I trial (NCT02938273) in 10 cisplatin ineligible patients with LAHNSCC that received avelumab and cetuximab in conjunction with RT, followed by avelumab as a maintenance therapy for an additional four months (Table 2).¹²² After a median follow-up of 12 months disease recurred in 50% of the patients. The majority of adverse effects were related to RT and cetuximab; grade 3 irAE occurred in four patients and were successfully managed.

An innovative approach is used in the CheckRad-CD8 phase II trial (NCT03426657) in which 120 patients with LAHNSCC have a second biopsy after induction durvalumab, tremelimumab, cisplatin, and docetaxel therapy. In the case of increased CD8⁺ TILs compared to pre-treatment biopsy, patients receive concurrent durvalumab, tremelimumab, and RT. Non-responders continue with standard therapy outside of the trial. The interim analysis for the first 10 patients was presented in 2019. After induction therapy re-biopsies showed a complete pathological response in 8/10 patients with another two patients showing an in-

crease in CD8⁺ TILs. There were two cases of grade III-IV toxicity: hepatitis and infectious diarrhoea.¹²³ Further results are awaited.

There are an additional 16 ongoing trials employing a combination of RT and ICIs that have not presented their results yet. Two of these are randomized phase III studies. The first one, KEYNOTE-412, will hopefully provide robust data to clarify the role of anti-PD-1 agent pembrolizumab given concomitantly with CRT and as a maintenance therapy in patients with locally advanced HNSCC.¹²⁴ The interpretation of the results could be hindered by the inability to discern the distinct effects of the priming, concurrent, and maintenance applications of pembrolizumab. Notably, a similar international phase III trial has previously been terminated due to slow accrual, and another similar trial, JAVELIN Head and Neck 100, testing the addition of anti-PD-L1 agent to CRT in LAHNSCC was terminated due to inefficiency.^{109,125} An additional phase III trial, NRG-HN005, is a non-inferiority trial, testing treatment de-escalation in patients with early stage HPV-positive oropharyngeal carcinoma.¹²⁶ A reduced dose RT, concurrently with either cisplatin or nivolumab, will be compared to standard CRT with cisplatin. The results will add valuable information to expanding pool of knowledge from the de-escalation trials in patients with HPV-positive HNSCC.

A somewhat different approach will be examined in the NCT04369937.¹²⁷ HPV-16 E6/E7-specific therapeutic vaccination (ISA101b) will be administered to 50 patients with intermediate risk of HPV+ HNSCC one week prior to the start of pembrolizumab and two weeks prior to the start of CRT with cisplatin (Table 2). The combination of ISA101 and nivolumab was already examined in a single-arm phase II trial where 24 patients with incurable HPV-positive cancers (22 oropharyngeal and one cervical and one anal cancer) were enrolled. An overall response rate of 33% with a median duration of response of 10.3 months and a median overall survival of 17.5 months seemed promising.¹²⁸

REWRITE (NCT03726775), a phase II trial that started in 2018, follows the recommendations from preclinical studies about omitting extended elective nodal irradiation when combining RT with immunotherapy. In this trial, patients with early stage T1–2 HNSCC or those with T3–4 disease and who are ineligible for cisplatin or cetuximab concurrently with RT will simultaneously receive durvalumab and RT to the primary tumour and immediately adjacent lymph nodes only. This will be followed by six months of maintenance durvalumab.¹²⁹

NCT02777385 is a phase II trial, planning to randomise 90 patients with LAHNSCC to either concurrent CRT with cisplatin and pembrolizumab or to CRT followed by pembrolizumab (Table 2).¹³⁰ It will hopefully help to answer if concurrent application is better than sequential or vice versa.

Adjuvant (postoperative) immunoradiotherapy

Testing novel treatments in an adjuvant setting offers a unique opportunity to stratify operated patients by risk of recurrence based on a detailed histopathological report, and therefore to avoid overtreatment. However, one should be aware of the above-described disadvantages when using immunotherapy with or without concurrent radiotherapy in patients with resected draining lymph nodes or after intensive treatment.

Two trials testing the potentials of adjuvant immunoradiotherapy reported early results. Wise-Draper *et al.* presented results of the lead-in stage of their phase II trial (NCT02641093). One to three weeks before planned surgery, patients who were clinically at high risk (cT3/4 stage and/or ≥ 2 +LNs) had one priming application of pembrolizumab followed by risk adjusted administration of adjuvant pembrolizumab in combination with RT or CRT. The pathological response to priming application of pembrolizumab was seen in 47% and was correlated with increased TILs. Adjuvant combination treatment with pembrolizumab and RT/CRT has an acceptable safety profile (Table 3).¹⁴² The other trial is a phase I NRG-HN003 trial that was conducted with the aim of determining a schedule for a phase II study. The tested regimen consisted of pembrolizumab added to adjuvant RT in patients with previously resected HPV-negative HNSCC with microscopically positive margins or an extracapsular extension of nodal metastases.¹⁴³ Pembrolizumab administered every three weeks in a dose of 200 mg for eight doses, starting the week before adjuvant CRT, was declared as worth pursuing. irAE were rare and non-significant (Table 3).

Beside these, there are six more ongoing trials registered in the international databases delivering different concurrent immunoradiotherapy combinations in an adjuvant setting and three of them are randomised phase 3 trials. The experimental arm in KEYNOTE-689 (NCT03765918) is similar to the one in trial by Wise-Draper *et al.*, except that two cycles of neoadjuvant pembrolizumab will be administered and longer maintenance therapy with pembrolizumab is planned. This will be com-

TABLE 3. Trials utilizing adjuvant immunoradiotherapy

Trial, start year	Phase	N	Subsite and subtype	Basic scheme	Immunotherapy details	RT details	Main results
NCT02641093, ¹⁴² 2016	II	80	LAHNSCC	neoadj. PEMBRO followed by resection, followed by PEMBRO + (C)RT	PEMBRO 1 week prior to surgery and conc. with RT for total of 7 doses	IMRT (60–66Gy/30fx) + /- LD-CDDP (if ECE + /R1)	first 23 pts (lead-in phase): 47% pathological response, no DLT, 2 pts recurred
NRG-HN003 (NCT02775812), ¹⁴³ 2016	I	34	resected R1/ECE + HPV- HNSCC	adj. PEMBRO + CRT	3 different schedules aimed to determine phase II schedule	CRT with IMRT (60Gy/30fx) and LD-CDDP	No irAE unacceptably delayed RT, 50% got all 8 doses of PEMBRO
KEYNOTE-689 (NCT03765918), ^{144,145} 2018	III, rand.	600	resected LAHNSCC	arm A: neoadj. PEMBRO followed by resection then PEMBRO + (C)RT; arm B: resection then (C)RT	arm A: 2x neoadj. PEMBRO and PEMBRO conc. with adj. (C) RT, followed by PEMBRO for up to 15 cycles	(C)RT 60–70Gy/30–35fx + /- HD-CDDP depending on risk factors	NA
GORTEC 2018-01 "NIVOPOSTOP" (NCT03576417), ¹⁴⁶ 2018	III, rand.	680	resected R1/ECE + LAHNSCC	arm A: adj. NIVO + CRT; arm B: adj. CRT	NIVO starting 3 weeks before CRT for total of 4 doses	CRT with IMRT (66Gy/33fx) and HD-CDDP	NA
ADHERE (NCT03673735), ¹⁴⁷ 2019	III, rand.	650	resected HR HPV- HNSCC	arm A: adj. DURVA + CRT; arm B: adj. CRT	1 dose of DURVA 1 week prior to CRT and maint. DURVA for 6 doses	CRT 66Gy/33fx and HD-CDDP	NA
ADRISK (NCT03480672), ¹⁴⁹ 2018	II, rand.	240	resected LAHNSCC with >1LN/ECE + /R1	arm A: adj. PEMBRO + CRT; arm B: adj. CRT	PEMBRO conc. with RT and for up to 12 months	CRT with CDDP	NA
NCT03715946, ¹⁵⁰ 2018	II	135	resected IR-HR HPV + oropharyngeal cancer	adj. NIVO + deescalated RT	NIVO conc. with RT and for additional 6 doses after RT	RT (45–50Gy/25fx)	NA
NCT03529422, ¹⁵¹ 2019	II	33	resected IR HNSCC	adj. DURVA + RT	DURVA starting conc. with RT for total of 6 cycles	IMRT (60Gy/30fx)	NA

adj. = adjuvant; CDDP = cisplatin; conc. = concurrent; CRT = chemoradiotherapy; DLT = dose-limiting toxicity; DURVA = durvalumab; ECE+ = extracapsular extension of metastasis in lymph node; fx = fractions; HD-CDDP = high dose cisplatin 100 mg/m² every three weeks during RT; HPV+ = human papilloma virus associated cancer; HPV- = human papilloma virus negative cancer; HR = high-risk; IMRT = intensity modulated RT; IR = intermediate-risk; irAE = immune-related adverse effects; LAHNSCC = locally advanced head and neck squamous cell carcinoma; LD-CDDP = low dose cisplatin 40 mg/m² every week during RT; N = planned enrolment; neoadj. = neoadjuvant; NIVO = nivolumab; PEMBRO = pembrolizumab; RT = radiotherapy; R1 = microscopically positive resection margin, LN = lymph node; NA = not available

pared to standard adjuvant CRT in LAHNSCC patients with either more than one pathological lymph node, microscopically positive margins or an extracapsular extension of nodal metastases.^{144,145} The two other randomised phase III trials, GORTEC 2018-01 (NCT03576417, also known as NIVOPOSTOP)¹⁴⁶ and ADHERE (NCT03673735)¹⁴⁷, will both enrol patients with resected high-risk HNSCC and randomise them to either adjuvant CRT with concurrent nivolumab (NIVOPOSTOP)/durvalumab (ADHERE), or to standard of care adjuvant CRT. These three phase III trials could set ground for the new era in the setting of adjuvant treatment of a high-risk HNSCC based on pathological data (microscopically positive margins or extracapsular extension of nodal metastases). Currently, with adjuvant CRT locoregional relapse rates as well as distant metastases rates at five years are around 20% in these patients.^{102,148} Based

on the preclinical data described above, it would be reasonable to expect a synergistic locoregional activity of radioimmunotherapy. A major drawback of adding immunotherapeutics to RT in postoperative setting could be the absence of regional lymph nodes that could hinder the efficacy of this combination. Nevertheless, ICIs will be delivered in doses that were shown to be effective systemically, therefore, it is justified to expect improved distant control of the disease.^{8,10}

The other three phase I and phase II trials are presented in Table 3.

Adjuvant/maintenance therapy with immune checkpoint inhibitor

In several of the above-described trials anti-PD-1/L1 therapy is also applied as a prolonged adjuvant or maintenance therapy. Support for this approach

comes from two other tumour types. In patients with unresectable locally-advanced non-squamous cell carcinoma lung cancer (NSCLC) without progression after definitive CRT, consolidation durvalumab was shown to prolong survival.¹⁵² Also, after a complete resection of stage III melanoma, adjuvant ipilimumab prolonged overall survival compared to placebo, while adjuvant nivolumab compared head-to-head to adjuvant ipilimumab showed better relapse-free survival and less toxicity. Long-term data of the latter study are not yet available.^{153,154} Besides differences in tumour-intrinsic factors and the composition of their TME, another important aspect to consider is the different recurrence pattern of these tumours. While melanoma and NSCLC are prone to dissemination, HNSCC tends to recur more often locoregionally in previously treated tissue. After resection alone, stage III melanoma spreads to distant sites in more than 60% of cases, and stage III NSCLC relapses distantly after CRT alone in up to 50% of cases.^{154,155} On the other hand, the risk of distant metastases is around 15% in HNSCC, whereas isolated locoregional relapses are much more common.^{4,156} Whether consolidation anti-PD-1/L1 agents can decrease rates of distant metastases as well as locoregional relapses in HNSCC is still to be determined.

Another important consideration in prolonged treatment with anti-PD-1/L1 agents is toxicity. Even though the overall effect on the quality of life with anti-PD-1 agents in R/M HNSCC was found to be positive and there were fewer adverse effects compared to standard chemotherapy, irAE nevertheless occurred in around 60% of patients with 17% of them experiencing a grade 3 or higher toxic event.^{22,157} Prolonged treatment with anti-PD-1/L1 agents should therefore be approached carefully and weighted against its toxicity. It should not be ignored that there is also financial toxicity associated with these treatments. It was estimated that in CheckMate 141 the incremental cost-effectiveness ratio per quality-adjusted life year for nivolumab was around 90,000 euros.¹⁵⁸ Even if the methods used in such calculations had some flaws, the financial burden of these new drugs is obvious and therefore special attention should already be paid in trial design.¹⁵⁸ Importantly, with the above-described trials it will be hard to discern the benefit of concurrent immunoradiotherapy from the benefit of maintenance immunotherapy as none of these trials compares this extended adjuvant treatment to a comparator arm without it. In either case, careful patient selection for immunotherapy, probably biomarker driven, will help to prevent unneces-

sary additional toxicity and the financial burden of this treatment. Potential biomarkers for immunotherapy in HNSCC have recently been extensively reviewed by Gavrielatou *et al.*¹⁵⁹

Conclusions

Researchers pursue different strategies in using a RT-ICI combination in a non-R/M HNSCC setting and the first results are already available. Window of opportunity trials are most welcomed since biological mechanisms behind the synergistic effect of combined immunoradiotherapy are not fully understood and reliable criteria for patient selection are lacking. The first results of these trials that use immunoradiotherapy neoadjuvantly are encouraging. In a definitive setting results are more varied. A large phase III trial employing concurrent and maintenance avelumab for 12 months post-chemoradiotherapy was terminated because of inefficacy. Prolonged RT courses with large treatment fields and high doses of concomitant chemotherapy agents could be detrimental to the success of immunotherapy. In an adjuvant setting it is hard to overlook factors such as a changed anatomy of lymphatics and a changed microenvironment of possible remaining cancer cells due to previous surgery, which could both adversely affect the effectiveness of immunoradiotherapy. Additionally, many of these trials administer anti-PD-1/L1 agents not only concurrently with RT but also as prolonged adjuvant treatment, without a comparator arm for proper evaluation of this approach. However, immunoradiotherapy is evolving rapidly in HNSCC and final results of the herein presented ongoing trials are eagerly awaited.

Acknowledgments

This study was funded by the Slovenian Research Agency (program no. P3-0307).

References

1. Bray F, Ferlay J, Soerjomataram I, Siegel RL, Torre LA, Jemal A. Global cancer statistics 2018: GLOBOCAN estimates of incidence and mortality worldwide for 36 cancers in 185 countries. *CA Cancer J Clin* 2018; **68**: 394-424. doi: 10.3322/caac.21492
2. Petersen JF, Timmermans AJ, van Dijk BAC, Overbeek LIH, Smit LA, Hilgers FJM, et al. Trends in treatment, incidence and survival of hypopharynx cancer: a 20-year population-based study in the Netherlands. *Eur Arch Otorhino-Laryngology* 2018; **275**: 181-9. doi: 10.1007/s00405-017-4766-6

3. Goor KM, Peeters AJGE, Mahieu HF, Langendijk JA, Leemans CR, Verdonck-de Leeuw IM, et al. Cordectomy by CO2 laser or radiotherapy for small T1a glottic carcinomas: Costs, local control, survival, quality of life, and voice quality. *Head Neck* 2007; **29**: 128-36. doi: 10.1002/hed.20500
4. Argiris A, Karamouzis MV, Raben D, Ferris RL. Head and neck cancer. *Lancet* 2008; **371**: 1695-709. doi: 10.1016/S0140-6736(08)60728-X
5. Corry J, Smee R, Ferlito A, Suárez C, Rapidis AD, Strojan P, et al. Management of locally advanced HPV-related oropharyngeal squamous cell carcinoma: where are we? *Eur Arch Oto-Rhino-Laryngology* 2015; **273**: 2877-94. doi: 10.1007/s00405-015-3771-x
6. Ang KK, Harris J, Wheeler R, Weber R, Rosenthal DI, Nguyen-Tân PF, et al. Human papillomavirus and survival of patients with oropharyngeal cancer. *N Engl J Med* 2010; **363**: 24-35. doi: 10.1056/NEJMoa0912217
7. Schreiber RD, Old LJ, Smyth MJ. Cancer immunoediting: integrating immunity's roles in cancer suppression and promotion. *Science* 2011; **331**: 1565-70. doi: 10.1126/science.1203486
8. Burtneß B, Harrington KJ, Greil R, Soulières D, Tahara M, de Castro G, et al. Pembrolizumab alone or with chemotherapy versus cetuximab with chemotherapy for recurrent or metastatic squamous cell carcinoma of the head and neck (KEYNOTE-048): a randomised, open-label, phase 3 study. *Lancet* 2019; **394**: 1915-28. doi: 10.1016/S0140-6736(19)32591-7
9. Ferris RL, Blumenschein G, Fayette J, Guigay J, Colevas AD, Licitra L, et al. Nivolumab for recurrent squamous-cell carcinoma of the head and neck. *N Engl J Med* 2016; **375**: 1856-67. doi: 10.1056/NEJMoa1602252
10. Saba NF, Blumenschein G, Guigay J, Licitra L, Fayette J, Harrington KJ, et al. Nivolumab versus investigator's choice in patients with recurrent or metastatic squamous cell carcinoma of the head and neck: efficacy and safety in CheckMate 141 by age. *Oral Oncol* 2019; **96**: 7-14. doi: 10.1016/j.oraloncology.2019.06.017
11. Hanna GJ, Adkins DR, Zolkind P, Uppaluri R. Rationale for neoadjuvant immunotherapy in head and neck squamous cell carcinoma. *Oral Oncol* 2017; **73**: 65-9. doi: 10.1016/j.oraloncology.2017.08.008
12. Harrington KJ, Ferris RL, Blumenschein G, Colevas AD, Fayette J, Licitra L, et al. Nivolumab versus standard, single-agent therapy of investigator's choice in recurrent or metastatic squamous cell carcinoma of the head and neck (CheckMate 141): health-related quality-of-life results from a randomised, phase 3 trial. *Lancet Oncol* 2017; **18**: 1104-15. doi: 10.1016/S1470-2045(17)30421-7
13. Monjazeb AM, Schalper KA, Villarreal-Espindola F, Nguyen A, Shiao SL, Young K. Effects of radiation on the tumor microenvironment. *Semin Radiat Oncol* 2020; **30**: 145-57. doi: 10.1016/j.semradonc.2019.12.004
14. Lee Y, Auh SL, Wang Y, Burnette B, Wang Y, Meng Y, et al. Therapeutic effects of ablative radiation on local tumor require CD8+ T cells: changing strategies for cancer treatment. *Blood* 2009; **114**: 589-95. doi: 10.1182/blood-2009-02-206870
15. Deng L, Liang H, Burnette B, Beckett M, Darga T, Weichselbaum RR, et al. Irradiation and anti-PD-L1 treatment synergistically promote antitumor immunity in mice. *J Clin Invest* 2014; **124**: 687-95. doi: 10.1172/JCI67313
16. Sha CM, Lehrer EJ, Hwang C, Trifiletti DM, Mackley HB, Drabick JJ, et al. Toxicity in combination immune checkpoint inhibitor and radiation therapy: a systematic review and meta-analysis. *Radiother Oncol* 2020; **151**: 141-8. doi: 10.1016/j.radonc.2020.07.035
17. Hiniker SM, Reddy SA, Maecker HT, Subrahmanyam PB, Rosenberg-Hasson Y, Swetter SM, et al. A prospective clinical trial combining radiation therapy with systemic immunotherapy in metastatic melanoma. *Int J Radiat Oncol* 2016; **96**: 578-88. doi: 10.1016/j.ijrobp.2016.07.005
18. Sundahl N, De Wolf K, Kruse V, Meireson A, Reynders D, Goetghebuer E, et al. Phase 1 dose escalation trial of ipilimumab and stereotactic body radiation therapy in metastatic melanoma. *Int J Radiat Oncol* 2018; **100**: 906-15. doi: 10.1016/j.ijrobp.2017.11.029
19. Campbell AM, Cai WL, Burkhardt D, Gettinger SN, Goldberg SB, Amodio M, et al. Final results of a phase II prospective trial evaluating the combination of stereotactic body radiotherapy (SBRT) with concurrent pembrolizumab in patients with metastatic non-small cell lung cancer (NSCLC). *Int J Radiat Oncol* 2019; **105**: S36-7. doi: 10.1016/j.ijrobp.2019.06.453
20. Theelen WSME, Peulen HMU, Lalezari F, van der Noort V, de Vries JF, Aerts JGJ V, et al. Effect of pembrolizumab after stereotactic body radiotherapy vs pembrolizumab alone on tumor response in patients with advanced non-small cell lung cancer. *JAMA Oncol* 2019; **5**: 1276. doi: 10.1001/jamaoncol.2019.1478
21. Patel JD, Bestvina CM, Karrison T, Jelinek MJ, Juloori A, Pointer K, et al. Randomized phase I trial to evaluate Concurrent or Sequential Ipilimumab, Nivolumab, and stereotactic body Radiotherapy in patients with stage IV non-small cell lung cancer (COSINR Study). [abstract]. *J Clin Oncol* 2020; **38(15 Suppl)**: 9616. doi: 10.1200/JCO.2020.38.15_suppl.9616
22. Ferris RL, Licitra L, Fayette J, Even C, Blumenschein G, Harrington KJ, et al. Nivolumab in patients with recurrent or metastatic squamous cell carcinoma of the head and neck: efficacy and safety in CheckMate 141 by prior cetuximab use. *Clin Cancer Res* 2019; **25**: 5221-30. doi: 10.1158/1078-0432.CCR-18-3944
23. Cohen EEW, Soulières D, Le Tourneau C, Dinis JJ, Licitra L, Ahn MJ, et al. Pembrolizumab versus methotrexate, docetaxel, or cetuximab for recurrent or metastatic head-and-neck squamous cell carcinoma (KEYNOTE-040): a randomised, open-label, phase 3 study. *Lancet* 2019; **393**: 156-67. doi: 10.1016/S0140-6736(18)31999-8
24. Sharma P, Hu-Lieskovan S, Wargo JA, Ribas A. Primary, adaptive, and acquired resistance to cancer immunotherapy. *Cell* 2017; **168**: 707-23. doi: 10.1016/j.cell.2017.01.017
25. Jensen PE. Recent advances in antigen processing and presentation. *Nat Immunol* 2007; **8**: 1041-8. doi: 10.1038/ni1516
26. Chalmers ZR, Connelly CF, Fabrizio D, Gay L, Ali SM, Ennis R, et al. Analysis of 100,000 human cancer genomes reveals the landscape of tumor mutational burden. *Genome Med* 2017; **9**: 34. doi: 10.1186/s13073-017-0424-2
27. Schumacher TN, Schreiber RD. Neoantigens in cancer immunotherapy. *Science* 2015; **348**: 69-74. doi: 10.1126/science.aaa4971
28. López-Albaitero A, Nayak J V, Ogino T, Machandia A, Gooding W, DeLeo AB, et al. Role of antigen-processing machinery in the in vitro resistance of squamous cell carcinoma of the head and neck cells to recognition by CTL. *J Immunol* 2006; **176**: 3402-9. doi: 10.4049/jimmunol.176.6.3402
29. Meissner M, Reichert TE, Kunkel M, Gooding W, Whiteside TL, Ferrone S, et al. Defects in the human leukocyte antigen class I antigen-processing machinery in head and neck squamous cell carcinoma: association with clinical outcome. *Clin Cancer Res* 2005; **11**: 2552-60. doi: 10.1158/1078-0432.CCR-04-2146
30. Concha-Benavente F, Srivastava R, Ferrone S, Ferris RL. Immunological and clinical significance of HLA class I antigen processing machinery component defects in malignant cells. *Oral Oncol* 2016; **58**: 52-8. doi: 10.1016/j.oraloncology.2016.05.008
31. Hoglund P, Sundback J, Olsson-Alheim MY, Johansson M, Salcedo M, Ohien C, et al. Host MHC class I gene control of NK-cell specificity in the mouse. *Immunol Rev* 1997; **155**: 11-28. doi: 10.1111/j.1600-065X.1997.tb00936.x
32. Grandis JR, Falkner DM, Melhem MF, Gooding WE, Drenning SD, Morel PA. Human leukocyte antigen class I allelic and haplotype loss in squamous cell carcinoma of the head and neck: clinical and immunogenetic consequences. *Clin Cancer Res* 2000; **6**: 2794-802. PMID: 10914726
33. Ferris RL, Hunt JL, Ferrone S. Human leukocyte antigen (HLA) class I defects in head and neck cancer: molecular mechanisms and clinical significance. *Immunol Res* 2005; **33**: 113-34. doi: 10.1385/IR:33:2:113
34. Pollack BP, Sapkota B, Cartee T V. Epidermal growth factor receptor inhibition augments the expression of MHC class I and II genes. *Clin Cancer Res* 2011; **17**: 4400-13. doi: 10.1158/1078-0432.CCR-10-3283
35. Chowell D, Morris LGT, Grigg CM, Weber JK, Samstein RM, Makarov V, et al. Patient HLA class I genotype influences cancer response to checkpoint blockade immunotherapy. *Science* 2018; **359**: 582-7. doi: 10.1126/science.aaa4572
36. Chen P-L, Roh W, Reuben A, Cooper ZA, Spencer CN, Prieto PA, et al. Analysis of immune signatures in longitudinal tumor samples yields insight into biomarkers of response and mechanisms of resistance to immune checkpoint blockade. *Cancer Discov* 2016; **6**: 827-37. doi: 10.1158/2159-8290.CD-15-1545
37. Patel SA, Minn AJ. Combination cancer therapy with immune checkpoint blockade: mechanisms and strategies. *Immunity* 2018; **48**: 417-33. doi: 10.1016/j.immuni.2018.03.007

38. Zitvogel L, Kepp O, Kroemer G. Decoding cell death signals in inflammation and immunity. *Cell* 2010; **140**: 798-804. doi: 10.1016/j.cell.2010.02.015
39. Kroemer G, Galluzzi L, Kepp O, Zitvogel L. Immunogenic cell death in cancer therapy. *Annu Rev Immunol* 2013; **31**: 51-72. doi: 10.1146/annurev-immunol-032712-100008
40. Sánchez-Paulete AR, Teijeira A, Cueto FJ, Garasa S, Pérez-Gracia JL, Sánchez-Arráez A, et al. Antigen cross-presentation and T-cell cross-priming in cancer immunology and immunotherapy. *Ann Oncol* 2017; **28**: xii44-55. doi: 10.1093/annonc/mdx237
41. Zitvogel L, Galluzzi L, Kepp O, Smyth MJ, Kroemer G. Type I interferons in anticancer immunity. *Nat Rev Immunol* 2015; **15**: 405-14. doi: 10.1038/nri3845
42. Hatch EM, Fischer AH, Deerinck TJ, Hetzer MW. Catastrophic nuclear envelope collapse in cancer cell micronuclei. *Cell* 2013; **154**: 47-60. doi: 10.1016/j.cell.2013.06.007
43. Duan S, Thomas PG. Balancing immune protection and immune pathology by CD8+ T-cell responses to influenza infection. *Front Immunol* 2016; **7**: doi: 10.3389/fimmu.2016.00025
44. Freeman GJ, Long AJ, Iwai Y, Bourque K, Chernova T, Nishimura H, et al. Engagement of the PD-1 immunoinhibitory receptor by a novel B7 family member leads to negative regulation of lymphocyte activation. *J Exp Med* 2000; **192**: 1027-34. doi: 10.1084/jem.192.7.1027
45. Bardhan K, Anagnostou T, Boussiotis VA. The PD1:PD-L1/2 pathway from discovery to clinical implementation. *Front Immunol* 2016; **7**: 550. doi: 10.3389/fimmu.2016.00550
46. Tumeah PC, Harview CL, Yearley JH, Shintaku IP, Taylor EJM, Robert L, et al. PD-1 blockade induces responses by inhibiting adaptive immune resistance. *Nature* 2014; **515**: 568-71. doi: 10.1038/nature13954
47. Golden EB, Frances D, Pellicciotti I, Demaria S, Helen Barcellos-Hoff M, Formenti SC, et al. Radiation fosters dose-dependent and chemotherapy-induced immunogenic cell death. *Oncimmunology* 2014; **3**: e28518. doi: 10.4161/onci.28518
48. Lawrence MS, Sougnez C, Lichtenstein L, Cibulskis K, Lander E, Gabriel SB, et al. Comprehensive genomic characterization of head and neck squamous cell carcinomas. *Nature* 2015; **517**: 576-82. doi: 10.1038/nature14129
49. Durante M, Formenti SC. Radiation-induced chromosomal aberrations and immunotherapy: micronuclei, cytosolic DNA, and interferon-production pathway. *Front Oncol* 2018; **8**: 192. doi: 10.3389/fonc.2018.00192
50. Vanpouille-Box C, Demaria S, Formenti SC, Galluzzi L. Cytosolic DNA Sensing in organismal tumor control. *Cancer Cell* 2018; **34**: 361-78. doi: 10.1016/j.ccell.2018.05.013
51. Reits EA, Hodge JW, Herberts CA, Groothuis TA, Chakraborty M, K.Wansley E, et al. Radiation modulates the peptide repertoire, enhances MHC class I expression, and induces successful antitumor immunotherapy. *J Exp Med* 2006; **203**: 1259-71. doi: 10.1084/jem.20052494
52. Twyman-Saint Victor C, Rech AJ, Maity A, Rengan R, Pauken KE, Stelekati E, et al. Radiation and dual checkpoint blockade activate non-redundant immune mechanisms in cancer. *Nature* 2015; **520**: 373-7. doi: 10.1038/nature14292
53. Han J, Duan J, Bai H, Wang Y, Wan R, Wang X, et al. TCR repertoire diversity of peripheral PD-1 + CD8 + T cells predicts clinical outcomes after immunotherapy in patients with non-small cell lung cancer. *Cancer Immunol Res* 2020; **8**: 146-54. doi: 10.1158/2326-6066.CIR-19-0398
54. Khan S, de Giuli R, Schmidtke G, Bruns M, Buchmeier M, van den Broek M, et al. Cutting edge: neosynthesis is required for the presentation of a T cell epitope from a long-lived viral protein. *J Immunol* 2001; **167**: 4801-4. doi: 10.4049/jimmunol.167.9.4801
55. Weichselbaum RR, Hallahan D, Fuks Z, Kufe D. Radiation induction of immediate early genes: Effectors of the radiation-stress response. *Int J Radiat Oncol* 1994; **30**: 229-34. doi: 10.1016/0360-3016(94)90539-8
56. Lan J, Li R, Yin LM, Deng L, Gui J, Chen BQ, et al. Targeting myeloid-derived suppressor cells and programmed death ligand 1 confers therapeutic advantage of ablative hypofractionated radiation therapy compared with conventional fractionated radiation therapy. *Int J Radiat Oncol Biol Phys* 2018; **101**: 74-87. doi: 10.1016/j.ijrobp.2018.01.071
57. Matsumura S, Wang B, Kawashima N, Braunstein S, Badura M, Cameron TO, et al. Radiation-induced CXCL16 release by breast cancer cells attracts effector T cells. *J Immunol* 2008; **181**: 3099-107. doi: 10.4049/jimmunol.181.5.3099
58. Chakraborty M, Abrams SI, Camphausen K, Liu K, Scott T, Coleman CN, et al. Irradiation of tumor cells up-regulates Fas and enhances CTL lytic activity and CTL adoptive immunotherapy. *J Immunol* 2003; **170**: 6338-47. doi: 10.4049/jimmunol.170.12.6338
59. Chakraborty M, Abrams SI, Coleman CN, Camphausen K, Schlom J, Hodge JW. External beam radiation of tumors alters phenotype of tumor cells to render them susceptible to vaccine-mediated T-cell killing. *Cancer Res* 2004; **64**: 4328-37. doi: 10.1158/0008-5472.CAN-04-0073
60. Klug F, Prakash H, Huber PE, Seibel T, Bender N, Halama N, et al. Low-dose irradiation programs macrophage differentiation to an iNOS+/M1 phenotype that orchestrates effective T cell immunotherapy. *Cancer Cell* 2013; **24**: 589-602. doi: 10.1016/j.ccr.2013.09.014
61. Savage T, Pandey S, Guha C. Postablation modulation after single high-dose radiation therapy improves tumor control via enhanced immunomodulation. *Clin Cancer Res* 2020; **26**: 910-21. doi: 10.1158/1078-0432.CCR-18-3518
62. Hallahan D, Kuchibhotla J, Wyble C. Cell adhesion molecules mediate radiation-induced leukocyte adhesion to the vascular endothelium. *Cancer Res* 1996; **56**: 5150-5. PMID: 8912850
63. Tran L, Allen CT, Xiao R, Moore E, Davis R, Park SJ, et al. Cisplatin alters antitumor immunity and synergizes with PD-1/PD-L1 inhibition in head and neck squamous cell carcinoma. *Cancer Immunol Res* 2017; **5**: 1141-51. doi: 10.1158/2326-6066.CIR-17-0235
64. Luo R, Firat E, Gaedicke S, Guffart E, Watanabe T, Niedermann G. Cisplatin facilitates radiation-induced abscopal effects in conjunction with PD-1 checkpoint blockade through CXCR3/CXCL10-mediated T-cell recruitment. *Clin Cancer Res* 2019; **25**: 7243-55. doi: 10.1158/1078-0432.CCR-19-1344
65. Teijeira A, Garasa S, Gato M, Alfaro C, Migueliz I, Cirella A, et al. CXCR1 and CXCR2 Chemokine receptor agonists produced by tumors induce neutrophil extracellular traps that interfere with immune cytotoxicity. *Immunity* 2020; **52**: 856-71.e8. doi: 10.1016/j.immuni.2020.03.001
66. Shinde-Jadhav S, Mansure JJ, Rayes R, Ayoub M, Spicer J, Kassouf W. Abstract 3743: Neutrophil extracellular traps and their implication with radioresistance in muscle invasive bladder cancer. [abstract]. In: Proceedings AACR Annual Meeting 2019; March 29-April 3, 2019; Atlanta, GA. *Cancer Res* 2019; **79(13 Suppl)**: 3743. doi: 10.1158/1538-7445.AM2019-3743
67. Deaglio S, Robson SC. Ectonucleotidases as regulators of purinergic signaling in thrombosis, inflammation, and immunity. *Adv Pharmacol*; 2011; **61**: 301-32. doi: 10.1016/B978-0-12-385526-8.00010-2
68. Ohta A, Kini R, Ohta A, Subramanian M, Madasu M, Sitkovsky M. The development and immunosuppressive functions of CD4+ CD25+ FoxP3+ regulatory T cells are under influence of the adenosine-A2A adenosine receptor pathway. *Front Immunol* 2012; **3**: 190. doi: 10.3389/fimmu.2012.00190
69. Palmer TM, Trevethick MA. Suppression of inflammatory and immune responses by the A2A adenosine receptor: an introduction. *Br J Pharmacol* 2008; **153**: S27-34. doi: 10.1038/sj.bjpp.0707524
70. Cekic C, Day YJ, Sag D, Linden J. Myeloid expression of adenosine a2A receptor suppresses T and NK cell responses in the solid tumor microenvironment. *Cancer Res* 2014; **74**: 7250-9. doi: 10.1158/0008-5472.CAN-13-3583
71. Liang H, Deng L, Hou Y, Meng X, Huang X, Rao E, et al. Host STING-dependent MDSC mobilization drives extrinsic radiation resistance. *Nat Commun* 2017; **8**: 1736. doi: 10.1038/s41467-017-01566-5
72. Bakhoun SF, Ngo B, Laughney AM, Cavallo J-A, Murphy CJ, Ly P, et al. Chromosomal instability drives metastasis through a cytosolic DNA response. *Nature* 2018; **553**: 467-72. doi: 10.1038/nature25432
73. Lemos H, Mohamed E, Huang L, Ou R, Pacholczyk G, Arbab AS, et al. STING promotes the growth of tumors characterized by low antigenicity via IDO activation. *Cancer Res* 2016; **76**: 2076-81. doi: 10.1158/0008-5472.CAN-15-1456
74. Monjabez AM, Kent MS, Grossenbacher SK, Mall C, Zamora AE, Mirsoian A, et al. Blocking indolamine-2,3-dioxygenase rebound immune suppression boosts antitumor effects of radio-immunotherapy in murine models and spontaneous canine malignancies. *Clin Cancer Res* 2016; **22**: 4328-40. doi: 10.1158/1078-0432.CCR-15-3026

75. Jacquelot N, Yamazaki T, Roberti MP, Duong CPM, Andrews MC, Verlingue L, et al. Sustained Type I interferon signaling as a mechanism of resistance to PD-1 blockade. *Cell Res* 2019; **29**: 846-61. doi: 10.1038/s41422-019-0224-x
76. Moeller BJ, Cao Y, Li CY, Dewhirst MW. Radiation activates HIF-1 to regulate vascular radiosensitivity in tumors. *Cancer Cell* 2004; **5**: 429-41. doi: 10.1016/S1535-6108(04)00115-1
77. Corzo CA, Condamine T, Lu L, Cotter MJ, Youn J-I, Cheng P, et al. HIF-1 α regulates function and differentiation of myeloid-derived suppressor cells in the tumor microenvironment. *J Exp Med* 2010; **207**: 2439-53. doi: 10.1084/jem.20100587
78. Suzuki H, Onishi H, Wada J, Yamasaki A, Tanaka H, Nakano K, et al. VEGFR2 is selectively expressed by FOXP3high CD4+ Treg. *Eur J Immunol* 2009; **40**: 197-203. doi: 10.1002/eji.200939887
79. Gabrilovich D, Ishida T, Oyama T, Ran S, Kravtsov V, Nadaf S, et al. Vascular endothelial growth factor inhibits the development of dendritic cells and dramatically affects the differentiation of multiple hematopoietic lineages in vivo. *Blood* 1998; **92**: 4150-66. doi: 10.1182/blood.v92.11.4150.423k45_4150_4166
80. Horikawa N, Abiko K, Matsumura N, Hamanishi J, Baba T, Yamaguchi K, et al. Expression of vascular endothelial growth factor in ovarian cancer inhibits tumor immunity through the accumulation of myeloid-derived suppressor cells. *Clin Cancer Res* 2017; **23**: 587-99. doi: 10.1158/1078-0432.CCR-16-0387
81. National Comprehensive Cancer Network (NCCN). *Head and Neck Cancers, Version 2.2020*. (cited 2020 Jul 20). Available at: <https://www.nccn.org>
82. Ma Y, Adjemian S, Mattarollo SR, Yamazaki T, Aymeric L, Yang H, et al. Anticancer chemotherapy-induced intratumoral recruitment and differentiation of antigen-presenting cells. *Immunity* 2013; **38**: 729-41. doi: 10.1016/j.immuni.2013.03.003
83. Crittenden MR, Zebertavage L, Kramer G, Bambina S, Friedman D, Troesch V, et al. Tumor cure by radiation therapy and checkpoint inhibitors depends on pre-existing immunity. *Sci Rep* 2018; **8**: 1-15. doi: 10.1038/s41598-018-25482-w
84. Markovsky E, Budhu S, Samstein RM, Li H, Russell J, Zhang Z, et al. An anti-tumor immune response is evoked by partial-volume single-dose radiation in 2 murine models. *Int J Radiat Oncol* 2019; **103**: 697-708. doi: 10.1016/j.ijrobp.2018.10.009
85. Takeshima T, Chamoto K, Wakita D, Ohkuri T, Togashi Y, Shirato H, et al. Local radiation therapy inhibits tumor growth through the generation of tumor-specific CTL: its potentiation by combination with TH1 cell therapy. *Cancer Res* 2010; **70**: 2697-706. doi: 10.1158/0008-5472.CAN-09-2982
86. Marciscano AE, Ghasemzadeh A, Nirschl TR, Theodoros D, Kochel CM, Francica BJ, et al. Elective nodal irradiation attenuates the combinatorial efficacy of stereotactic radiation therapy and immunotherapy. *Clin Cancer Res* 2018; **24**: 5058-71. doi: 10.1158/1078-0432.CCR-17-3427
87. Botticelli A, Mezi S, Pomati G, Sciattella P, Cerbelli B, Roberto M, et al. The impact of locoregional treatment on response to nivolumab in advanced platinum refractory head and neck cancer: The need trial. *Vaccines* 2020; **8**: 191. doi: 10.3390/vaccines8020191
88. Zandberg DP, Ferris RL. Window studies in squamous cell carcinoma of the head and neck: values and limits. *Curr Treat Options Oncol* 2018; **19**: 68. doi: 10.1007/s11864-018-0587-0
89. Leidner R, Bell RB, Young K, Curti B, Couey M, Patel A, et al. Abstract CT182: Neoadjuvant immuno-radiotherapy (NIRT) in head and neck cancer: Phase I/lb study of combined PD-1/SBRT prior to surgical resection. [abstract]. In: Proceedings AACR Annual Meeting 2019; March 29-April 3, 2019; Atlanta, GA. *Cancer Res* 2019; **79**(13 Suppl): CT182. doi: 10.1158/1538-7445.AM2019-CT182
90. Saâda-Bouزيد E, Defaucheux C, Karabajakian A, Coloma VP, Servois V, Paoletti X, et al. Hyperprogression during anti-PD-1/PD-L1 therapy in patients with recurrent and/or metastatic head and neck squamous cell carcinoma. *Ann Oncol* 2017; **28**: 1605-11. doi: 10.1093/annonc/mdx178
91. Bell RB, Leidner R, Young KH, Curti B, Couey M, Patel A, et al. Cohort expansion study of neoadjuvant immunoradiotherapy in locoregionally advanced HPV+ and HPV- head and neck squamous cell carcinoma. *Int J Radiat Oncol* 2020; **106**: 1225-6. doi: 10.1016/j.ijrobp.2020.02.013
92. Chin R. Stereotactic body radiation therapy and Durvalumab with or without Tremelimumab before surgery in treating participants with human papillomavirus positive oropharyngeal squamous cell cancer. (cited 2020 Jul 15). Available at: <https://clinicaltrials.gov/ct2/show/NCT03618134>
93. Economopoulou P, Kotsantis I, Psyri A. The promise of immunotherapy in head and neck squamous cell carcinoma: combinatorial immunotherapy approaches. *ESMO Open* 2017; **1**: e000122. doi: 10.1136/esmopen-2016-000122
94. Barbari C, Fontaine T, Parajuli P, Lamichhane N, Jakubski S, Lamichhane P, et al. Immunotherapies and combination strategies for immuno-oncology. *Int J Mol Sci* 2020; **21**: 5009. doi: 10.3390/ijms21145009
95. Diehl A, Yarchoan M, Hopkins A, Jaffee E, Grossman SA. Relationships between lymphocyte counts and treatment-related toxicities and clinical responses in patients with solid tumors treated with PD-1 checkpoint inhibitors. *Oncotarget* 2017; **8**: 114268-80. doi: 10.18632/oncotarget.23217
96. Dovedi SJ, Adlard AL, Lipowska-Bhalla G, McKenna C, Jones S, Cheadle EJ, et al. Acquired resistance to fractionated radiotherapy can be overcome by concurrent PD-L1 blockade. *Cancer Res* 2014; **74**: 5458-68. doi: 10.1158/0008-5472.CAN-14-1258
97. Chen D, Patel RR, Verma V, Ramapriyan R, Barsoumian HB, Cortez MA, et al. Interaction between lymphopenia, radiotherapy technique, dosimetry, and survival outcomes in lung cancer patients receiving combined immunotherapy and radiotherapy. *Radiother Oncol* 2020 Aug 13; [Ahead of print]. doi: 10.1016/j.radonc.2020.05.051
98. Ho WJ, Yarchoan M, Hopkins A, Mehra R, Grossman S, Kang H. Association between pretreatment lymphocyte count and response to PD1 inhibitors in head and neck squamous cell carcinomas. *J Immunother Cancer* 2018; **6**: 84. doi: 10.1186/s40425-018-0395-x
99. Kaanders JHAM, van den Bosch S, Dijkema T, Al-Mamgani A, Raaijmakers CPJ, Vogel W V. Advances in cancer imaging require renewed radiotherapy dose and target volume concepts. *Radiother Oncol* 2020; **148**: 140-2. doi: 10.1016/j.radonc.2020.04.016
100. Grapin M, Richard C, Limagne E, Boidot R, Morgand V, Bertaut A, et al. Optimized fractionated radiotherapy with anti-PD-L1 and anti-TIGIT: a promising new combination. *J Immunother Cancer* 2019; **7**: 1-12. doi: 10.1186/s40425-019-0634-9
101. Filatenkov A, Baker J, Mueller AMS, Kenkel J, Ahn GO, Dutt S, et al. Ablative tumor radiation can change the tumor immune cell microenvironment to induce durable complete remissions. *Clin Cancer Res* 2015; **21**: 3727-39. doi: 10.1158/1078-0432.CCR-14-2824
102. Bernier J, Dommene C, Ozsahin M, Matuszewska K, Lefebvre J-L, Greiner RH, et al. Postoperative irradiation with or without concomitant chemotherapy for locally advanced head and neck cancer. *N Engl J Med* 2004; **350**: 1945-52. doi: 10.1056/NEJMoa032641
103. Forastiere AA, Goepfert H, Maor M, Pajak TF, Weber R, Morrison W, et al. Concurrent chemotherapy and radiotherapy for organ preservation in advanced laryngeal cancer. *N Engl J Med* 2003; **349**: 2091-8. doi: 10.1056/NEJMoa031317
104. Yoon S-Y, Han JJ, Baek SK, Kim HJ, Maeng CH. Pembrolizumab-induced severe oral mucositis in a patient with squamous cell carcinoma of the lung: a case study. *Lung Cancer* 2020; **147**: 21-5. doi: 10.1016/j.lungcan.2020.06.033
105. García-Foncillas J, Sunakawa Y, Aderka D, Wainberg Z, Ronga P, Witzler P, et al. Distinguishing features of Cetuximab and Panitumumab in colorectal cancer and other solid tumors. *Front Oncol* 2019; **9**: 849. doi:10.3389/fonc.2019.00849
106. Ferris RL, Lenz H-J, Trotta AM, García-Foncillas J, Schulten J, Audhuy F, et al. Rationale for combination of therapeutic antibodies targeting tumor cells and immune checkpoint receptors: harnessing innate and adaptive immunity through IgG1 isotype immune effector stimulation. *Cancer Treat Rev* 2018; **63**: 48-60. doi: 10.1016/j.ctrv.2017.11.008
107. Sacco AG, Chen R, Ghosh D, Worden F, Wong DJ, Adkins D, et al. An open-label, non-randomized, multi-arm, phase II trial evaluating pembrolizumab combined with cetuximab in patients (pts) with recurrent/metastatic (R/M) head and neck squamous cell carcinoma (HNSCC): updated results of cohort 1 analysis. *Int J Radiat Oncol* 2020; **106**: 1121-2. doi: 10.1016/j.ijrobp.2019.11.376

108. Lin Y-C, Uen W-C, Hao S-P, Hsiao C-Y, Lai H-C. Triple combination treatment of cetuximab, chemotherapy, and anti-PD1 check-point inhibitor for recurrent and/or metastatic head and neck squamous cell carcinoma: a single institute experience. *J Clin Oncol* 2018; **36**: e18001. doi: 10.1200/JCO.2018.36.15_suppl.e18001
109. EMD Serono and Pfizer provide update on phase III JAVELIN Head and Neck 100 Study. (cited 2020 Jul 15). Available at: https://www.pfizer.com/news/press-release/press-release-detail/emd_serono_and_pfizer_provide_update_on_phase_iii_javelin_head_and_neck_100_study
110. Yu Y, Lee NY. JAVELIN Head and Neck 100: a Phase III trial of avelumab and chemoradiation for locally advanced head and neck cancer. *Futur Oncol* 2019; **15**: 687-94. doi: 10.2217/fon-2018-0405
111. Tao Y, Auperin A, Sun XS, Sire C, Martin L, Bera G, et al. Avelumab-cetuximab-radiotherapy (RT) versus standards of care (SoC) in locally advanced squamous cell carcinoma of the head and neck (SCCHN): safety phase of the randomized trial GORTEC 2017-01 (REACH). *J Clin Oncol* 2018; **36**: 6076. doi: 10.1200/jco.2018.36.15_suppl.6076
112. Tao Y, Auperin A, Sun XS, Sire C, Martin L, Bera G, et al. Avelumab-cetuximab-radiotherapy versus standards of care in locally advanced squamous cell carcinoma of the head and neck: safety phase of the randomized phase III trial GORTEC 2017-01 REACH. (cited 2020 Jul 15). Available at: https://www.gortec.net/images/publi/ESMO2019_REACH_POSTER_Discussion.pdf
113. Mell LK, Torres-Saavedra PA, Wong SJ, Chang S, Kish JA, Minn A, et al. Safety of radiotherapy with concurrent and adjuvant MEDI4736 (durvalumab) in patients with locoregionally advanced head and neck cancer with a contraindication to cisplatin: NRG-HN004. *J Clin Oncol* 2019; **37**: 6065. doi: 10.1200/JCO.2019.37.15_suppl.6065
114. Sun XS, Sire C, Tao Y, Martin L, Alfonsi M, Prevost JB, et al. A phase II randomized trial of pembrolizumab versus cetuximab, concomitant with radiotherapy (RT) in locally advanced (LA) squamous cell carcinoma of the head and neck (SCCHN): first results of the GORTEC 2015-01 "PembroRad" trial. *J Clin Oncol* 2018; **36**: 6018. doi: 10.1200/jco.2018.36.15_suppl.6018
115. Klinghammer KF, Gauler TC, Stromberger C, Kofla G, de Wit M, Gollrad J, et al. DURTREERAD: a phase II open-label study evaluating feasibility and efficacy of durvalumab (D) and durvalumab and tremelimumab (DT) in combination with radiotherapy (RT) in non-resectable locally advanced HPV-negative HNSCC – results of the preplanned feasibility. *J Clin Oncol* 2020; **38**: 6574. doi: 10.1200/JCO.2020.38.15_suppl.6574
116. Weiss J, Sheth S, Deal AM, Grilley Olson JE, Patel S, Hackman TG, et al. Concurrent definitive immunoradiotherapy for patients with stage III-IV head and neck cancer and cisplatin contraindication. *Clin Cancer Res* 2020; **26**: 4260-7. doi: 10.1158/1078-0432.CCR-20-0230
117. Powell SF, Gold KA, Gitau MM, Sumey CJ, Lohr MM, McGraw SC, et al. Safety and efficacy of pembrolizumab with chemoradiotherapy in locally advanced head and neck squamous cell carcinoma: a phase IB study. *J Clin Oncol* 2020; **38**: 2427-37. doi: 10.1200/JCO.19.03156
118. Gillison M, Ferris RL, Zhang Q, Colevas AD, Mell LK, Kirsch C, et al. Safety evaluation of nivolumab concomitant with platinum-based chemoradiation therapy for intermediate and high-risk local-regionally advanced head and neck squamous cell carcinoma: RTOG foundation 3504. *Int J Radiat Oncol* 2018; **100**: 1307-8. doi: 10.1016/j.ijrobp.2017.12.022
119. Ferris RL, Gillison ML, Harris J, Colevas AD, Mell LK, Kong C, et al. Safety evaluation of nivolumab (Nivo) concomitant with cetuximab-radiotherapy for intermediate (IR) and high-risk (HR) local-regionally advanced head and neck squamous cell carcinoma (HNSCC): RTOG 3504. *J Clin Oncol* 2018; **36**: 6010. doi: 10.1200/JCO.2018.36.15_suppl.6010
120. Gillison ML, Ferris RL, Harris J, Colevas AD, Mell LK, Kong C, et al. Safety and disease control achieved with the addition of nivolumab (Nivo) to chemoradiotherapy (CRT) for intermediate (IR) and high-risk (HR) local-regionally advanced head and neck squamous cell carcinoma (HNSCC): RTOG Foundation 3504. *J Clin Oncol* 2019; **37**: 6073. doi: 10.1200/jco.2019.37.15_suppl.6073
121. Johnson JM, Bar Ad V, Lorber E, Poller D, Luginbuhl A, Curry JM, et al. Safety of nivolumab and ipilimumab in combination with radiotherapy in patients with locally advanced squamous cell carcinoma of the head and neck (LA SCCHN). *J Clin Oncol* 2019; **37**: 6070. doi: 10.1200/JCO.2019.37.15_suppl.6070
122. Elbers JBW, Al-Mamgani A, Tesseslaar MET, van den Brekel MWM, Lange CAH, van der Wal JE, et al. Immuno-radiotherapy with cetuximab and avelumab for advanced stage head and neck squamous cell carcinoma: results from a phase-I trial. *Radiother Oncol* 2020; **142**: 79-84. doi: 10.1016/j.radonc.2019.08.007
123. Hecht M, Gostian A-O, Eckstein M, Rutzner S, von der Grün J, Illmer T, et al. Single cycle induction treatment with cisplatin/docetaxel plus durvalumab/tremelimumab in stage III-IVB head and neck squamous cell cancer (CheckRad-CD8 trial). *Ann Oncol* 2019; **30**: v456-7. doi: 10.1093/annonc/mdz252.016
124. Machiels J-P, Tao Y, Burtness B, Tahara M, Licita L, Rischin D, et al. Pembrolizumab given concomitantly with chemoradiation and as maintenance therapy for locally advanced head and neck squamous cell carcinoma: KEYNOTE-412. *Futur Oncol* 2020; **16**: 1235-43. doi: 10.2217/fon-2020-0184
125. Nivolumab or nivolumab plus cisplatin, in combination with radiotherapy in patients with cisplatin-ineligible or eligible locally advanced squamous cell head and neck cancer. (cited 2020 Jul 15). Available at: <https://clinicaltrials.gov/ct2/show/NCT03349710>
126. Yom SS. De-intensified radiation therapy with chemotherapy (cisplatin) or immunotherapy (nivolumab) in treating patients with early-stage, HPV-positive, non-smoking associated oropharyngeal cancer. (cited 2020 Jul 15). Available at: <https://clinicaltrials.gov/ct2/show/NCT03952585>
127. Ferris RL. HPV-16 Vaccination and pembrolizumab plus cisplatin for "intermediate risk" HPV-16-associated head and neck squamous cell carcinoma. (cited 2020 Jul 15). Available at: <https://clinicaltrials.gov/ct2/show/NCT04369937>
128. Massarelli E, William W, Johnson F, Kies M, Ferrarotto R, Guo M, et al. Combining immune checkpoint blockade and tumor-specific vaccine for patients with incurable human papillomavirus 16-related cancer. *JAMA Oncol* 2019; **5**: 67. doi: 10.1001/jamaoncol.2018.4051
129. Trial evaluating the tolerance and safety of durvalumab - RT combination for treatment in SCCHN (REWRITE). (cited 2020 Jul 15). Available at: <https://clinicaltrials.gov/ct2/show/NCT03726775>
130. Clump D. Pembrolizumab in combination with cisplatin and intensity modulated radiotherapy (IMRT) in head and neck cancer. (cited 2020 Jul 15). Available at: <https://clinicaltrials.gov/ct2/show/NCT02777385>
131. Takiar V. A study of chemoradiation plus pembrolizumab for locally advanced laryngeal squamous cell carcinoma. (cited 2020 Jul 15). Available at: <https://clinicaltrials.gov/ct2/show/NCT02759575>
132. El-Sherify MS. Concomitant immune check point inhibitor with radiochemotherapy in head and neck cancer. (cited 2020 Jul 15). Available at: <https://clinicaltrials.gov/ct2/show/NCT03532737>
133. Mell L. Chemoradiation vs immunotherapy and radiation for head and neck cancer. (cited 2020 Jul 15). Available at: <https://clinicaltrials.gov/ct2/show/NCT03383094>
134. Harrington K. Pembrolizumab combined with chemoradiotherapy in squamous cell carcinoma of the head and neck (PEACH). (cited 2020 Jul 15). Available at: <https://clinicaltrials.gov/ct2/show/NCT02819752>
135. Haddad R. Induction TPN followed by nivolumab with radiation in locoregionally advanced laryngeal and hypopharyngeal cancer. (cited 2020 Jul 15). Available at: <https://clinicaltrials.gov/ct2/show/NCT03894891>
136. Mierzwa M. Radiotherapy, carboplatin/paclitaxel and nivolumab for high risk HPV-related head and neck cancer. (cited 2020 Jul 15). Available at: <https://clinicaltrials.gov/ct2/show/NCT03829722>
137. Gillison ML. Ipilimumab, nivolumab, and radiation therapy in treating patients with HPV positive advanced oropharyngeal squamous cell carcinoma. (cited 2020 Jul 15). Available at: <https://clinicaltrials.gov/ct2/show/NCT03799445>
138. Tao Y, Auperin A, Sun XS, Sire C, Martin L, Bera G, et al. Avelumab-cetuximab-radiotherapy versus standards of care in locally advanced squamous cell carcinoma of the head and neck: safety phase of the randomized phase III trial GORTEC 2017-01 REACH. (cited 2020 Jul 15). Available at: https://gortec.net/images/publi/ESMO2019_REACH_POSTER_Discussion.pdf

139. Bonomo P, Desideri I, Loi M, Mangoni M, Sottili M, Marrazzo L, et al. Anti PD-L1 durvalumab combined with cetuximab and radiotherapy in locally advanced squamous cell carcinoma of the head and neck: a phase I/II study (DUCRO). *Clin Transl Radiat Oncol* 2018; **9**: 42-7. doi: 10.1016/j.ctro.2018.01.005
140. Cisplatin or immunotherapy in association with definitive radiotherapy in HPV-related oropharyngeal squamous cell carcinoma: a randomized phase II trial. (CITHARE). (cited 2020 Jul 15). Available at: <https://clinicaltrials.gov/ct2/show/NCT03623646>
141. Li Y. A study of concomitant camrelizumab with chemoradiation for locally advanced head and neck cancer. (cited 2020 Jul 15). Available at: <https://clinicaltrials.gov/ct2/show/NCT04405154>
142. Wise-Draper TM, Old MO, Worden FP, O'Brien PE, Cohen EEW, Dunlap N, et al. Phase II multi-site investigation of neoadjuvant pembrolizumab and adjuvant concurrent radiation and pembrolizumab with or without cisplatin in resected head and neck squamous cell carcinoma. *J Clin Oncol* 2018; **36**: 6017. doi: 10.1200/JCO.2018.36.15_suppl.6017
143. Bauman JE, Harris J, Uppaluri R, Yao M, Ferris RL, Chen J, et al. NRG-HN003: Phase I and expansion cohort study of adjuvant cisplatin, intensity-modulated radiation therapy (IMRT), and MK-3475 (pembrolizumab) in high-risk head and neck squamous cell carcinoma (HNSCC). *J Clin Oncol* 2019; **37**: 6023. doi: 10.1200/JCO.2019.37.15_suppl.6023
144. Uppaluri R, Lee NY, Westra W, Cohen EEW, Haddad RI, Temam S, et al. KEYNOTE-689: Phase 3 study of adjuvant and neoadjuvant pembrolizumab combined with standard of care (SOC) in patients with resectable, locally advanced head and neck squamous cell carcinoma. *J Clin Oncol* 2019; **37**: TPS6090. doi: 10.1200/JCO.2019.37.15_suppl.TPS6090
145. Uppaluri R, Lee NY, Westra W, Cohen EEW, Haddad RI, Temam S, et al. KEYNOTE-689: phase 3 study of neoadjuvant and adjuvant pembrolizumab combined with standard of care in patients with resectable, locally advanced head and neck squamous cell carcinoma. (cited 2020 Jul 15). Available at: http://uppalurilab.dana-farber.org/uploads/1/2/9/7/129766176/uppaluri_kn689_asco_2019_poster_presented.pdf
146. A trial evaluating the addition of nivolumab to cisplatin-RT for treatment of cancers of the head and neck (NIVOPOSTOP). (cited 2020 Jul 15). Available at: <https://clinicaltrials.gov/ct2/show/NCT03576417>
147. Maintenance immune check-point inhibitor following post-operative chemo-radiation in subjects with HPV-negative HNSCC (ADHERE). (cited 2020 Jul 15). Available at: <https://clinicaltrials.gov/ct2/show/NCT03673735>
148. Cooper JS, Pajak TF, Forastiere AA, Jacobs J, Campbell BH, Saxman SB, et al. Postoperative concurrent radiotherapy and chemotherapy for high-risk squamous-cell carcinoma of the head and neck. *N Engl J Med* 2004; **350**: 1937-44. doi: 10.1056/NEJMoa032646
149. Dietz A. Postoperative aRCH with cisplatin versus aRCH with cisplatin and pembrolizumab in locally advanced head and neck squamous cell carcinoma. (cited 2020 Jul 14). Available at: <https://clinicaltrials.gov/ct2/show/NCT03480672>
150. Ferris R. Adjuvant de-escalated radiation + adjuvant nivolumab for intermediate-high risk P16+ oropharynx cancer. (cited 2020 Jul 15). Available at: <https://clinicaltrials.gov/ct2/show/NCT03715946>
151. Weiss J. Durvalumab with radiotherapy for adjuvant treatment of intermediate risk SCCHN. (cited 2020 Jul 16). Available at: <https://clinicaltrials.gov/ct2/show/NCT03529422>
152. Antonia SJ, Villegas A, Daniel D, Vicente D, Murakami S, Hui R, et al. Overall survival with durvalumab after chemoradiotherapy in stage III NSCLC. *N Engl J Med* 2018; **379**: 2342-50. doi: 10.1056/NEJMoa1809697
153. Weber JS, Mandalà M, Del Vecchio M, Gogas H, Arance AM, Cowey CL, et al. Adjuvant therapy with nivolumab (NIVO) versus ipilimumab (IPI) after complete resection of stage III/IV melanoma: updated results from a phase III trial (CheckMate 238). *J Clin Oncol* 2018; **36**: 9502. doi: 10.1200/JCO.2018.36.15_suppl.9502
154. Eggermont AMM, Chiarion-Sileni V, Grob J-J, Dummer R, Wolchok JD, Schmidt H, et al. Adjuvant ipilimumab versus placebo after complete resection of stage III melanoma: long-term follow-up results of the European Organisation for Research and Treatment of Cancer 18071 double-blind phase 3 randomised trial. *Eur J Cancer* 2019; **119**: 1-10. doi: 10.1016/j.ejca.2019.07.001
155. Steuer CE, Behera M, Ernani V, Higgins KA, Saba NF, Shin DM, et al. Comparison of concurrent use of thoracic radiation with either carboplatin-paclitaxel or cisplatin-etoposide for patients with stage III non-small-cell lung cancer. *JAMA Oncol* 2017; **3**: 1120. doi: 10.1001/jamaoncol.2016.4280
156. Duprez F, Berwouts D, De Neve W, Bonte K, Boterberg T, Deron P, et al. Distant metastases in head and neck cancer. *Head Neck* 2017; **39**: 1733-43. doi: 10.1002/hed.24687
157. Wang H, Mustafa A, Liu S, Liu J, Lv D, Yang H, et al. Immune checkpoint inhibitor toxicity in head and neck cancer: from identification to management. *Front Pharmacol* 2019; **10**: doi: 10.3389/fphar.2019.01254
158. Santana-Davila R, Rodriguez CP. Immunotherapy for head and neck cancer in the era of exponentially increasing health care expenditure. *Oncologist* 2018; **23**: 147-9. doi: 10.1634/theoncologist.2017-0527
159. Gavrielatou N, Doumas S, Economopoulou P, Foukas PG, Psyrris A. Biomarkers for immunotherapy response in head and neck cancer. *Cancer Treat Rev* 2020; **84**: 101977. doi: 10.1016/j.ctrv.2020.101977

Correlations between DTI-derived metrics and MRS metabolites in tumour regions of glioblastoma: a pilot study

Eduardo Flores-Alvarez¹, Edgar-Anselmo Rios-Piedra², Griselda-Adriana Cruz-Priego³, Coral Durand-Muñoz⁴, Sergio Moreno-Jimenez⁵, Ernesto Roldan-Valadez^{6,7}

¹ Department of Neurosurgery, General Hospital of Mexico, Secretariat of Health, Mexico City, Mexico

² Department of Radiology, Stanford University, CA, USA; Department of Electrical Engineering, Stanford University, CA, USA

³ Postgraduate Unit, Faculty of Medicine, National Autonomous University of Mexico, Mexico City, Mexico

⁴ Department of Internal Medicine, Medica Sur Clinic and Foundation, Mexico City, Mexico

⁵ Radioneurosurgery Unit, The National Institute of Neurology and Neurosurgery, Mexico City, Mexico

⁶ Department of Radiology, I.M. Sechenov First Moscow State Medical University (Sechenov University), Moscow, Russia

⁷ Directorate of Research, General Hospital of Mexico, Secretariat of Health, Mexico City, Mexico

Radiol Oncol 2020; 54(4): 394-408.

Received 9 July 2020

Accepted 31 July 2020

Correspondence to: Ernesto Roldan-Valadez, M.D., M.Sc., D.Sc., Department of Radiology, I.M. Sechenov First Moscow State Medical University (Sechenov University), Trubetskaya str., 8, b. 2, 119992, Moscow, Russia. Email: ernest.rolan@usa.net

Disclosure: No potential conflicts of interest were disclosed.

Introduction. Specific correlations among diffusion tensor imaging (DTI)-derived metrics and magnetic resonance spectroscopy (MRS) metabolite ratios in brains with glioblastoma are still not completely understood.

Patients and methods. We made retrospective cohort study. MRS ratios (choline-to-N-acetyl aspartate [Cho/NAA], lipids and lactate to creatine [LL/Cr], and myo-inositol/creatin [ml/Cr]) were correlated with eleven DTI biomarkers: mean diffusivity (MD), fractional anisotropy (FA), pure isotropic diffusion (p), pure anisotropic diffusion (q), the total magnitude of the diffusion tensor (L), linear tensor (Cl), planar tensor (Cp), spherical tensor (Cs), relative anisotropy (RA), axial diffusivity (AD) and radial diffusivity (RD) at the same regions: enhanced rim, peritumoral oedema and normal-appearing white matter. Correlational analyses of 546 MRS and DTI measurements used Spearman coefficient.

Results. At the enhancing rim we found four significant correlations: FA \leftrightarrow LL/Cr, $R_s = -.364$, $p = .034$; Cp \leftrightarrow LL/Cr, $R_s = .362$, $p = .035$; q \leftrightarrow LL/Cr, $R_s = -.349$, $p = .035$; RA \leftrightarrow LL/Cr, $R_s = -.357$, $p = .038$. Another ten pairs of significant correlations were found in the peritumoral edema: AD \leftrightarrow LL/Cr, AD \leftrightarrow ml/Cr, MD \leftrightarrow LL/Cr, MD \leftrightarrow ml/Cr, p \leftrightarrow LL/Cr, p \leftrightarrow ml/Cr, RD \leftrightarrow ml/Cr, RD \leftrightarrow ml/Cr, L \leftrightarrow LL/Cr, L \leftrightarrow ml/Cr.

Conclusions. DTI and MRS biomarkers answer different questions; peritumoral oedema represents the biggest challenge with at least ten significant correlations between DTI and MRS that need additional studies. The fact that DTI and MRS measures are not specific of one histologic type of tumour broadens their application to a wider variety of intracranial pathologies.

Key words: brain neoplasms; diffusion tensor imaging; magnetic resonance spectroscopy; statistics as topic; software tools

Introduction

Since the last decade, a particular interest prevails for the identification of clinical prognostic markers for glioblastoma.¹ During this time, medical imaging research has focused its attention in the

conventional magnetic resonance imaging (MRI) diagnosis of gliomas, identifying regional tumour infiltration and oedema boundaries in those qualitative patterns observed in the T₂-weighted imaging (T₂-w), fluid-attenuated inversion recovery (FLAIR), pre-contrast T₁-w weighted imaging

(T_1 -w), and post-contrast T_1 -w.² Other MRI-based quantitative morphological features that have been reported include the contrast-enhancing (CE) rim width and surface regularity³, residual tumour volume (RTV) and extent of resection (EOR).⁴ A recent meta-analysis highlighted the limitations of the current conventional MRI-based Response Assessment in Neuro-Oncology (RANO) criteria for treatment evaluation in glioblastoma.⁵

Some volumetric features of the oedema region might have a role as predictors of progression-free survival (PFS) in patients with glioblastoma.⁶

Diffusion tensor imaging (DTI) and magnetic resonance spectroscopy (MRS) biomarkers are currently reported in glioblastoma research as a consequence of their higher diagnostic accuracy than conventional MRI for the detection of tumour progression.^{7,8} A recent meta-analysis found the sensitivity and specificity of MRS were 91% and 95%, respectively.⁹ MRS found that the choline-to-N-acetyl aspartate (Cho/Naa) ratio is the most substantial survival predictor in glioblastoma with a log-hazard function of 2.672 (each unit of increase in the Cho/Naa ratio represents a 267% increase in the risk of death in glioblastoma).¹⁰ The usefulness of DTI-derived biomarkers has been proved in the differentiation of glioblastoma from brain abscesses and metastatic brain tumours¹¹ and between glioblastoma and healthy brains.¹² Up to 11 DTI-derived biomarkers have been calculated in brain MRI, each one with different diagnostic performance depending on the selected tumour region.¹³

However, despite the above technological advances in glioblastoma imaging, there is a low correlation between the conventional MR images and the gross pathologic margin of the tumour with the actual margins of the areas of neoplastic infiltration.¹⁴ Most of the advanced MRI techniques have been reported as separated diagnostic methods without a correlational assessment.⁵ For example, some studies have been published about the whole brain MRS correlations with Sox2-positive cell density⁸, but no with other advanced MRI techniques. We found only one article in the literature that studied the correlations between DTI and MRS in schizophrenic patients and healthy controls.¹⁵ Although it is known that MRS and DTI use different mechanisms to visualize abnormal pathologies, they can provide complementary imaging data on white matter changes in brain.¹⁵

The assessment of MRS and DTI biomarkers in glioblastoma is one of the leading research lines for our group. To the best of our knowledge, no previous studies have evinced a correlation among

these variables; we aimed to analyse the correlations between the three most commonly reported MRS metabolites ratios and the eleven-known DTI-derived metrics in glioblastoma. Our null hypothesis considered no correlations between MRS metabolite ratios and DTI metrics; our alternative hypothesis expects that at least one pair of significant correlations were found at each tumour region in glioblastoma.

Patients and methods

Patients

Retrospective cohort of patients with at first (suspected) diagnosis and later pathology confirmation of glioblastoma according to the WHO; inclusion criteria considered examinations between January 2010 and December 2014. Exclusion criteria applied to corticosteroid or antibiotic treatment, lesions with areas related to calcification and haemorrhage and previous brain surgery. MR examinations with other structural abnormalities were excluded. The local Institutional Review Board approved the study and the study was performed in accordance with the ethical standards laid down in the 1964 Declaration of Helsinki and its later amendments.

Brain image acquisition

MR was performed by using a 3T unit (Signa HDxt, GE Healthcare, Waukesha, WI, USA) with a high-resolution eight-channel head coil (Invivo, Gainesville, FL, USA). MR sequences included conventional axial T_2 -w, axial Fluid-Attenuated Inversion Recovery (Flair), and pre-contrast axial T_1 -w. Post-contrast axial T_1 -w used 0.1 mmol/kg of body weight of gadopentetate dimeglumine (Magnevist; Schering, Berlin, Germany). Pre-contrast axial Spoiled Gradient Echo (SPGR) that exploited the T1 shortening effects of methemoglobin allowed direct visualization of lesions with haemorrhage. Diffusion-weighted imaging (DWI) was performed using a single-shot SE EPI sequence with b-values of 1000 s/mm² and an image without diffusion weighting with b-value of 0 s/mm².

DTI was performed using a single-shot SE EPI sequence. Diffusion gradients were applied in 25 directions with b-values of 1000 s/mm² and an image without diffusion weighting with b-value of 0 s/mm². DTI sequences were acquired in the axial plane with 44 contiguous sections, 2.4 mm section thickness, no intersection gap, TR/TE of 17,000/80 ms, with parallel imaging to reduce off-resonance

artefacts (PI factor was 2); 25 x 25 cm FOV, and 128 x 128 matrix size.

Selected tumour regions

A board-certified radiologist (ERV) blinded to the clinical history of each patient, manually traced the boundaries of the tumour regions. For all parameters derived from MRS and DTI, measurements were acquired in three areas: normal-appearing white matter (NAWM), drawn in the patient's contralateral hemisphere; viable tumour region (area of the enhanced rim at T1-w post-contrast); and peritumoral oedema (arbitrarily chosen as an adjacent immediate zone with a 10-mm-wide band).

Metabolites measurements using MRS

Multi-voxel spectroscopic imaging (MV-MRS) was performed using a point-resolved spectroscopic sequence technique (PRESS). The volume of interest (VOI) size was individually adjusted positioning the voxel over the lesion and trying to minimise partial-volume effects resulting from other neighbouring tissues including bones and cerebral spinal fluid (CSF) of the ventricles. Proton spectra were recorded in the axial plane with T1-w post-contrast images via TR; 1500 ms, TE; 26 and 144 ms, FOV; 24 x 24 cm, 1–1.5 cm section thickness, 256 x 256 matrix and 24 x 24 phase encoding. Knowing that cerebral metabolites have different inherent T1 and T2 relaxation times, a TE of 24 ms allowed us to quantify metabolites that are identified only at short TE (Lipids and Myo-inositol). The intermediate TE of 144 ms let us identified the Cho and Lactate peaks, which are the primary metabolites altered in neoplasms. Because fewer metabolites were observed with longer TE values, the spectrum obtained is easier to interpret (we could quickly identify the rest of selected metabolites (NAA and Cr). Additionally, a TE of 144 ms identified the Lactate peak invert below baseline.¹⁶

The MRS data were transferred to a clinical workstation, with FDA-cleared software (GE Advantage). A short echo time allowed the acquisition of four brain spectra with metabolite signal peaks centred within a range of 0–4.35 ppm as follows: methyl protons of N-acetylaspartate (NAA) at 2.0 ppm, N-trimethyl protons of choline-containing metabolites at 3.2 ppm (Cho), creatine (Cr) at 3–3.1 ppm, a compound peak containing lipids and lactate (LL) at 0.8–1.4 ppm, and a compound peak of the protons of myo-inositol (mI) at 3.56 and 4.06 ppm.¹⁶ Automatic shimming of the linear x, y,

z channels was used to optimise field homogeneity, water resonance and water suppression pulses were optimised. Relative quantification of metabolites was performed after Gaussian curve fitting using standard spectroscopic analysis software FuncTool 9.4.04b, (GE Healthcare, Milwaukee, WI, USA). Three metabolite ratios were calculated: Cho/NAA, lipids and lactate to creatine (LL/Cr), and and myo-inositol/creatine (mI/Cr). Figure 1 A–F show examples of the MRS measurements at the enhancing rim and peritumoral oedema.

DTI-derived metrics

We used the FA maps, and T₁-post gadolinium orientation maps to draw three regions of interest (ROI) from each selected region (NAWM, enhancing rim and peritumoral oedema). For each ROI, we obtained the major (λ_1), intermediate (λ_2), and minor (λ_3) eigenvalues at the selected regions using a GE Advantage Workstation with the software FuncTool 9.4.04b (GE Medical Systems, Milwaukee, WI, USA). The three eigenvalues were applied to the eleven formulas previously published for the calculation of DTI-derived metrics: mean diffusivity (MD), fractional anisotropy (FA), pure isotropic diffusion (p), pure anisotropic diffusion (q), the total magnitude of the diffusion tensor (L), linear tensor (Cl), planar tensor (Cp), spherical tensor (Cs), relative anisotropy (RA), axial diffusivity (AD) and radial diffusivity (RD)¹³; Figure 1 G–I presents an example of FA map used to locate the ROI at the selected regions: enhancing rim, peritumoral oedema, and NAWM.

Statistical analysis

Sample size

We used the sample-size formula published by Browner *et al.* for determining whether a correlation coefficient differs from zero.¹⁷

$$N = [(Z\alpha + Z\beta) \div C]^2 + 3, \text{ for this formula:}$$

N = Total number of measurements required

Z α = the standard normal deviate for α (If the alternative hypothesis is two-sided, Z α = 1.96 when α = 0.05)

Z β = the standard normal deviate for β (Z β = 0.84 when β = 0.20)

$$C = 0.5 \times \ln [(1 + r)/(1 - r)]$$

r = expected correlation coefficient

Considering that Tang *et al.* reported a correlation coefficient between DTI and MRS biomarkers up to 33.2% in schizophrenic patients¹⁵, our alternative hypothesis was that correlation coefficients

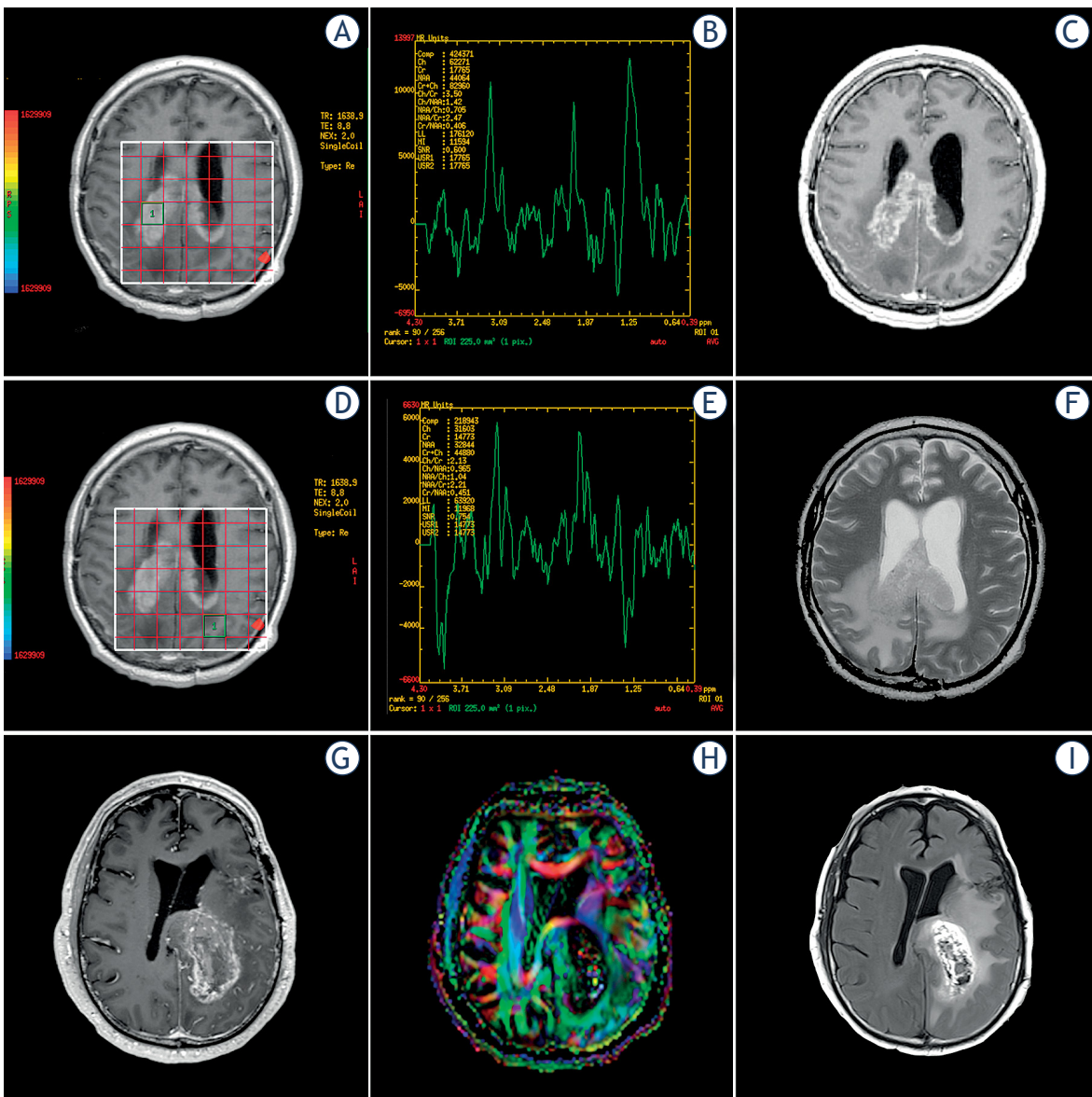


FIGURE 1. (A-F) magnetic resonance spectroscopy (MRS) measurements at the enhancing rim and peritumoral edema. (G-I) example of a FA map used to locate the ROI at the selected regions: enhancing rim, peritumoral oedema, and normal-appearing white matter (NAWM).

between DTI and MRS biomarkers would be above 50%. With this expected correlation coefficient, a two-sided alternative hypothesis, $\alpha = 0.05$, $\beta = 0.20$, and statistical power = 80%; $N = 29$. We had 33 different measurements per each DTI biomarkers.

Correlation analyses

Bivariate correlations were performed using the Spearman correlation coefficient (R_s)¹⁸ to describe the degree of the linear relationship between three metabolites ratios (Cho/Naa, LL/Cr, and ml/Cr)

and the eleven DTI-derived biomarkers (MD, FA, p, q, L, Cl, Cp, Cs, RA, AD and RD). We chose the R_s because it is a non-parametric test that can be used with variables that have a non-normal distribution.¹⁹ Each correlation coefficient was interpreted as *Very strong* (at least of 0.8), *Moderately strong* (0.6 up to 0.8), *Fair* (0.3 up to 0.6) and *Poor* (less than 0.3). Squaring R-values represented the *coefficient of determination*, the proportion of variance that each two compared variables had in common.¹⁸ We additionally tested the statistical significance of the difference between R coefficients between groups

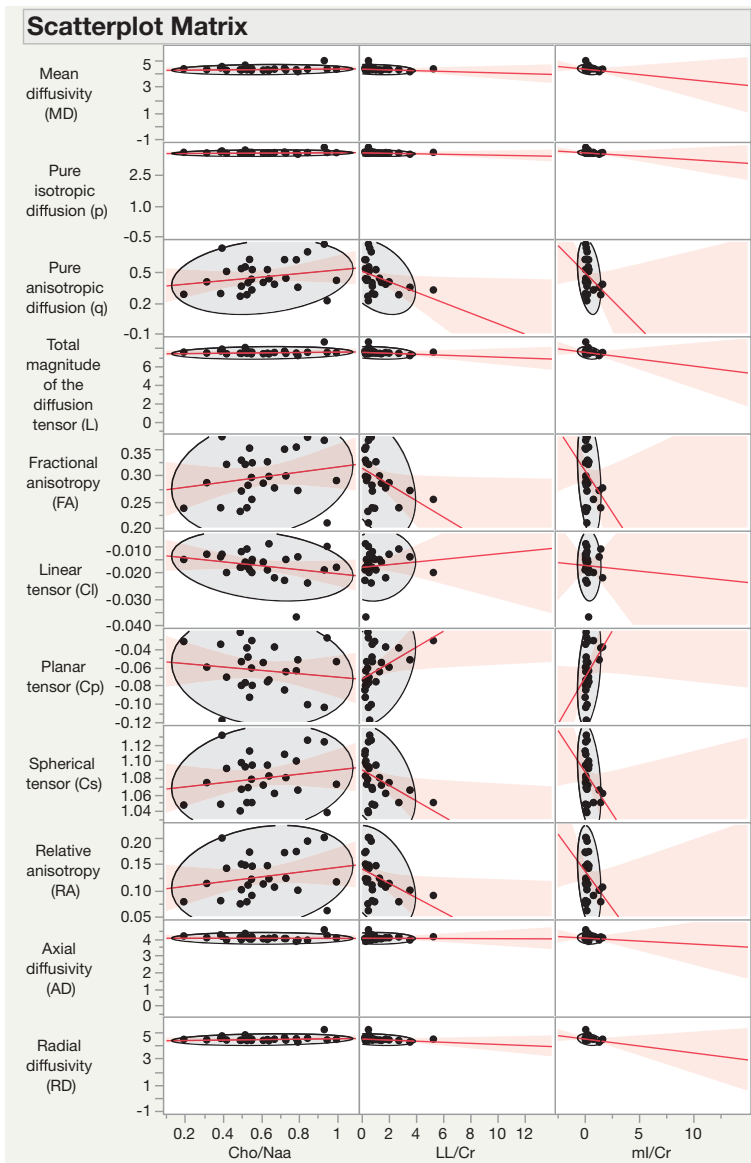


FIGURE 2. Scatter plots showing the correlation between magnetic resonance spectroscopy (MRS) metabolites and diffusion tensor imaging (DTI) metric at the normal-appearing white matter (NAWM).

by converting each pair of R values into standard z scores, then using the formula proposed by Pallant and colleagues²⁰:

$$Z_{obs} = \frac{Z_1 - Z_2}{\sqrt{\frac{1}{N_1 - 3} + \frac{1}{N_2 - 3}}}$$

Observed Z value (Z_{obs}) ≤ -1.96 or ≥ 1.96 were considered statistically significantly different.

Software

All analyses were carried out using the IBM® SPSS® Statistics software (version 26.0.0.1 IBM

Corporation; Armonk, NY, USA) and JMP® Pro software (version 14.3, SAS Institute Inc., Cary, NC, USA). Statistical significance was indicated by $p < 0.05$ (two-tailed).

Results

DTI and MRS measurements

For each patient, we recorded MRS and DTI measurements at three selected regions: NAWM, enhancing rim and oedema. The three MRS measures for each metabolite ratio (Cho/Naa, LL/Cr, and ml/Cr) were recorded at all tumour region, adding 9 MRS measurements per patient. Similarly, 11 DTI-derived metrics (MD, FA, p, q, L, Cl, Cp, Cs, RA, AD and RD) were calculated at each tumour region for each patient, with a total of 33 DTI measurements. Then, for each patient, we got 42 measurements (9 from MRS and 33 from DTI), this amount multiplied by 13 patients added 546 measurements that integrated 33 MRS-DTI parameter pairs per region. A total of 99 bivariate pairs were obtained in our correlation analyses.

DTI↔MRS correlation at the NAWM

We found five pairs of bivariate correlations showing statistical significance all of them with the same metabolite LL/Cr. Only one correlation was positive, Cp ↔ LL/Cr, $R_s = .468$, $p = .014$. The other four depicted negative R_s coefficients: FA ↔ LL/Cr, $R_s = -.475$, $p = .012$; q ↔ LL/Cr, $R_s = -.495$, $p = .009$; RA ↔ LL/Cr, $R_s = -.490$, $p = .010$; Cs ↔ LL/Cr, $R_s = -.488$, $p = .010$. Table 1 shows the correlations between DTI metrics and MRS metabolites at the NAWM region. Figure 2 depicts a scatterplot matrix of the DTI and MRS correlations at the NAWM region.

DTI↔MRS correlation at the gadolinium-enhanced tumour region

Similar to the findings in the NAWM, we found only four significant correlations between only one MRS metabolite and 4 DTI-derived metrics: FA ↔ LL/Cr, $R_s = -.364$, $p = .034$; Cp ↔ LL/Cr, $R_s = .362$, $p = .035$; q ↔ LL/Cr, $R_s = -.349$, $p = .035$; RA ↔ LL/Cr, $R_s = -.357$, $p = .038$. Table 2 depicts the correlations between DTI metrics and MRS metabolites at the tumor region. Figure 3 show a scatterplot matrix of the DTI and MRS correlations at the enhancing rim region.

TABLE 1. Correlations between diffusion tensor imaging (DTI) metrics and magnetic resonance spectroscopy (MRS) metabolites for the normal-appearing white matter (NAWM) region

DTI-derived biomarker	MRS	Spearman ρ	p-value	-0.8	-0.6	-0.4	-0.2	0	0.2	0.4	0.6	0.8
Axial diffusivity (AD)	Cho/Naa	-0.2862	0.1479									
	LL/Cr	0.1900	0.3426									
	ml/Cr	-0.1777	0.3751									
Fractional anisotropy (FA)	Cho/Naa	0.2300	0.2485									
	LL/Cr	-0.4749	0.0123*									
	ml/Cr	-0.2110	0.2907									
Linear tensor (Cl)	Cho/Naa	-0.2827	0.1530									
	LL/Cr	0.2061	0.3024									
	ml/Cr	-0.2147	0.2822									
Mean diffusivity (MD)	Cho/Naa	-0.0961	0.6336									
	LL/Cr	-0.1020	0.6126									
	ml/Cr	-0.2683	0.1761									
Planar tensor (Cp)	Cho/Naa	-0.1441	0.4732									
	LL/Cr	0.4680	0.0138*									
	ml/Cr	0.3139	0.1108									
Pure anisotropic diffusion (q)	Cho/Naa	0.2119	0.2886									
	LL/Cr	-0.4950	0.0087*									
	ml/Cr	-0.2577	0.1944									
Pure isotropic diffusion (p)	Cho/Naa	-0.0961	0.6336									
	LL/Cr	-0.1020	0.6126									
	ml/Cr	-0.2683	0.1761									
Radial diffusivity (RD)	Cho/Naa	0.0440	0.8276									
	LL/Cr	-0.2840	0.1511									
	ml/Cr	-0.2228	0.2640									
Relative anisotropy (RA)	Cho/Naa	0.2217	0.2665									
	LL/Cr	-0.4898	0.0095*									
	ml/Cr	-0.2290	0.2506									
Spherical tensor (Cs)	Cho/Naa	0.1930	0.3348									
	LL/Cr	-0.4883	0.0098*									
	ml/Cr	-0.2547	0.1998									
Total magnitude of the diffusion tensor (L)	Cho/Naa	-0.0680	0.7363									
	LL/Cr	-0.1408	0.4836									
	ml/Cr	-0.2781	0.1602									

Cho/Naa = choline-to-N-acetyl aspartate; LL/Cr = lipids and lactate to creatine; ml/Cr = and myo-inositol/creatine [ml/Cr]

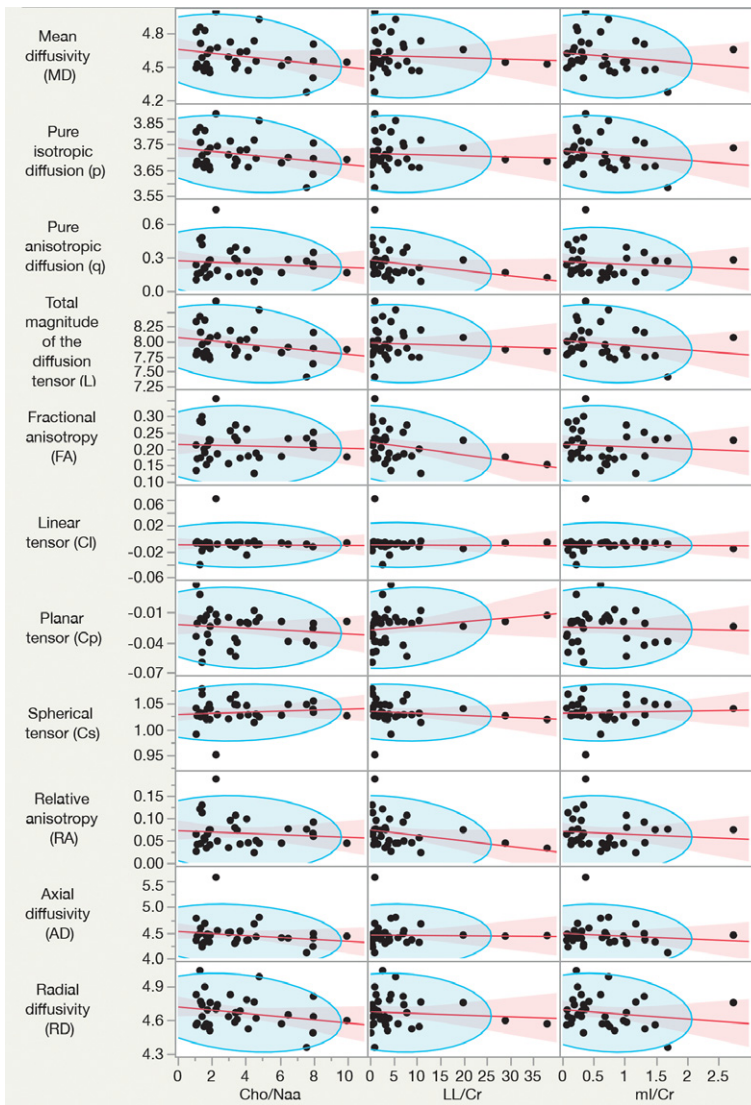


FIGURE 3. Scatter plots showing the correlation between magnetic resonance spectroscopy (MRS) metabolites and diffusion tensor imaging (DTI) metric at the enhancing rim.

DTI↔MRS correlation at the oedema region

At the edema region we found that besides the LL/Cr metabolite, the concentrations of mI/Cr also depicted statistical significance with five DTI metrics different than the observed correlations in the tumor and NAWM regions. It meant we found ten significant correlations: AD ↔ LL/Cr, $R_s = .658$, $p < .001$; AD ↔ mI/Cr, $R_s = .493$, $p = .006$; MD ↔ LL/Cr, $R_s = .685$, $p < .001$; MD ↔ mI/Cr, $R_s = .513$, $p = .004$; p ↔ LL/Cr, $R_s = .685$, $p < .001$; p ↔ mI/Cr, $R_s = .513$, $p = .004$; RD ↔ mI/Cr, $R_s = .693$, $p < .001$; RD ↔ mI/Cr, $R_s = .508$, $p = .004$; L ↔ LL/Cr, $R_s = .685$, $p < .001$; L ↔

mI/Cr, $R_s = .513$, $p = .004$. Table 3 presents the correlations between DTI metrics and MRS metabolites at the edema region. Figure 4 show a scatterplot matrix of the DTI and MRS correlations at the peritumoral edema. Figure 5 depicts a diagram showing the significant correlations observed between DTI-MRS bivariate correlations at the NAWM, tumor and edema regions.

Statistical significance between identical DTI-MRS bivariate pairs in different regions

The assessment of the statistical significance of the difference between R coefficients found only four pairs of DTI-MRS correlations that were coincidentally significant at NAWM and tumor enhanced regions (Figure 4). We did not find statistical significances between their R coefficients: Cp ↔ LL/Cr, $Z = .54$, $p = .589$; FA ↔ LL/Cr, $Z = .57$, $p = .568$; q ↔ LL/Cr, $Z = .76$, $p = .447$; RA ↔ LL/Cr, $Z = .69$, $p = .490$.

Discussion

Between 1998 and 2009, quantitative biomarkers from MRS (NAA, Cho, LL, and mI) were accepted to be measured with sufficient sensitivity in the millimoles per litre range to be used in clinical diagnosis.²¹ Recent studies have shown the importance of Cho/NAA and LL/Cr ratios in assembling significant survival models in glioblastoma.¹⁰ The use of DTI allows *diffusion directionality* to be quantified as different DTI-derived metrics²¹; it yields ultrastructural information on cellular density and properties of the extracellular matrix.²² In 2006, Pena *et al.* expressed that it was not completely understood the magnitudes and associations among DTI measurements observed in the evaluation of brain tumours.²³ Cortez-Conradis *et al.* in 2015, evaluated correlations among DTI-derived metrics in glioblastoma²⁴, but without exploring the associations with MRS metabolites in the same tumour regions.

In this study, we were able to probe the alternative hypothesis posed at the introduction and methods sections: bivariate correlations among DTI-metrics and MRS metabolite ratios are significant at selected tumour regions and above 50% of R_s value in glioblastoma (NAWM, enhancing rim and peritumoral oedema). To the best of our knowledge, there are no similar studies in the literature with whom compare our findings.

TABLE 2. Correlations between diffusion tensor imaging (DTI) metrics and magnetic resonance spectroscopy (MRS) metabolites for the tumour region

DTI-derived biomarker	MRS	Spearman ρ	p-value	-0.8	-0.6	-0.4	-0.2	0	0.2	0.4	0.6	0.8
Axial diffusivity (AD)	Cho/Naa	-0.0961	0.5886									
	LL/Cr	0.2044	0.2463									
	ml/Cr	-0.0824	0.6432									
Fractional anisotropy (FA)	Cho/Naa	0.0165	0.9262									
	LL/Cr	-0.3643	0.0342*									
	ml/Cr	-0.1238	0.4855									
Linear tensor (Cl)	Cho/Naa	0.0017	0.9924									
	LL/Cr	0.0674	0.7048									
	ml/Cr	0.0395	0.8246									
Mean diffusivity (MD)	Cho/Naa	-0.1152	0.5167									
	LL/Cr	0.0790	0.6569									
	ml/Cr	-0.1713	0.3327									
Planar tensor (Cp)	Cho/Naa	-0.1699	0.3369									
	LL/Cr	0.3629	0.0349*									
	ml/Cr	0.0604	0.7342									
Pure anisotropic diffusion (q)	Cho/Naa	0.0003	0.9986									
	LL/Cr	-0.3488	0.0432*									
	ml/Cr	-0.1394	0.4317									
Pure isotropic diffusion (p)	Cho/Naa	-0.1152	0.5167									
	LL/Cr	0.0790	0.6569									
	ml/Cr	-0.1713	0.3327									
Radial diffusivity (RD)	Cho/Naa	-0.1478	0.4040									
	LL/Cr	0.0558	0.7539									
	ml/Cr	-0.1839	0.2978									
Relative anisotropy (RA)	Cho/Naa	0.0200	0.9105									
	LL/Cr	-0.3569	0.0382*									
	ml/Cr	-0.1241	0.4843									
Spherical tensor (Cs)	Cho/Naa	0.0983	0.5804									
	LL/Cr	-0.3188	0.0661									
	ml/Cr	-0.0944	0.5953									
Total magnitude of the diffusion tensor (L)	Cho/Naa	-0.1232	0.4877									
	LL/Cr	0.0799	0.6532									
	ml/Cr	-0.1606	0.3643									

Cho/Naa = choline-to-N-acetyl aspartate; LL/Cr = lipids and lactate to creatine; ml/Cr = and myo-inositol/creatine

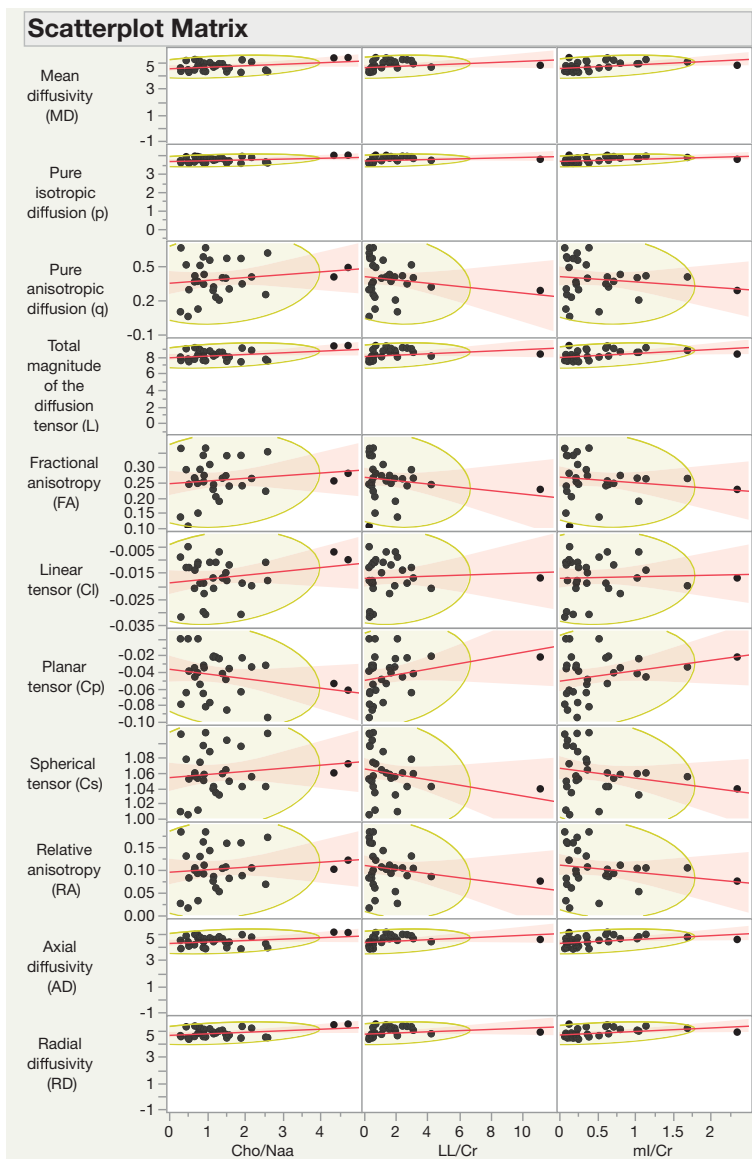


FIGURE 4. Scatter plots showing the correlation between magnetic resonance spectroscopy (MRS) metabolites and diffusion tensor imaging (DTI) metric at the peritumoral edema.

The clinical relevance of our findings is the statistical evidence that DTI and MRS depict significant associations in glioblastoma. MRS measurements represent a biochemical profile of brains with glioblastoma: decreased N-acetylaspartate (NAA) is a putative indicator of persistent axonal damage; increases of choline and myo-inositol correspond to glial proliferation, and elevated lactate has been associated with inflammation.²⁵ DTI metrics measure the amount of coherence of water diffusion, which putatively reflects the amount of myelination in axonal bundles or the coherence of fibre tracts.¹⁵ Although DTI and MRS reflect differ-

ent mechanisms of damage by glioblastoma, together they provide complementary imaging data on white matter integrity in brain. The supplementary information provided by DTI and MRS is what we consider the rationale of our study, both techniques should complement the information from conventional MRI in day-to-day practice. The clinical implications will allow researchers to combine DTI and MRS metrics to test several prediction models for tumour progression or the presence of tumour cells in peritumoral oedema and decrease the patient-to-patient prognostic variability. For example, you could combine the variables of two significant bivariate pairs with $R_s > 65\%$ in our study (for example $AD \Leftrightarrow LL/Cr$ and $RD \Leftrightarrow ml/Cr$ measured in peritumoral oedema) together with age, in a Cox's proportional-hazards regression model for prediction of survival. The results might be compared with previously published models.¹⁰

To simplify the discussion of our findings, we grouped them into four sections:

Lack of significant correlations between Cho/NAA and any of the 11 DTI biomarkers in the three selected regions

This was the first finding that caught our attention. To explain this fact, we should remember that Cho peak is the most complex, receiving contributions from a range of choline-containing compounds (acetylcholine, glycerophosphocholine, phosphocholine, free choline, phosphatidylcholine and choline-plasmalogen); its concentration is frequently taken as an empirical marker of the density and turnover of cell membranes.²⁶ Because increased Cho may be seen in diverse pathologies like infarction (from gliosis or ischemic damage to myelin) or inflammation (glial proliferation); it is considered to be nonspecific.²⁶ NAA is present in the soma of neurons, in dendrites and axons, its regional variability is likely related to differences in neural architecture, population and density. A simple linear relationship of NAA with the mass of neurons has been considered unlikely given that it also reflects reversible metabolic changes.²⁷ A high concentration of Cho has been observed in brain tumours and *in vitro* tumour proliferation markers with Cho/NAA ratio significantly more elevated in high-grade gliomas than in low-grade gliomas. However, threshold values are not well established.²⁸ glioblastoma exhibit high choline-containing compound levels, especially in the tumour regions, Cho/NAA quantifies those lipid components, and the DTI-derived metrics evaluates ultra-

TABLE 3. Correlations between diffusion tensor imaging (DTI) metrics and magnetic resonance spectroscopy (MRS) metabolites for the oedema region

DTI-derived biomarker	MRS	Spearman ρ	p-value	-0.8	-0.6	-0.4	-0.2	0	0.2	0.4	0.6	0.8
Axial diffusivity (AD)	Cho/Naa	0.0913	0.6315									
	LL/Cr	0.6575	<.0001*									
	ml/Cr	0.4926	0.0057*									
Fractional anisotropy (FA)	Cho/Naa	0.0939	0.6217									
	LL/Cr	-0.2817	0.1316									
	ml/Cr	-0.1444	0.4465									
Linear tensor (CI)	Cho/Naa	0.0571	0.7645									
	LL/Cr	0.1461	0.4412									
	ml/Cr	-0.0161	0.9329									
Mean diffusivity (MD)	Cho/Naa	0.1155	0.5435									
	LL/Cr	0.6845	<.0001*									
	ml/Cr	0.5132	0.0037*									
Planar tensor (Cp)	Cho/Naa	-0.1556	0.4115									
	LL/Cr	0.3295	0.0754									
	ml/Cr	0.2033	0.2813									
Pure anisotropic diffusion (a)	Cho/Naa	0.1357	0.4745									
	LL/Cr	-0.2034	0.2811									
	ml/Cr	-0.0926	0.6266									
Pure isotropic diffusion (p)	Cho/Naa	0.1155	0.5435									
	LL/Cr	0.6845	<.0001*									
	ml/Cr	0.5132	0.0037*									
Radial diffusivity (RD)	Cho/Naa	0.1384	0.4658									
	LL/Cr	0.6933	<.0001*									
	ml/Cr	0.5082	0.0041*									
Relative anisotropy (RA)	Cho/Naa	0.1197	0.5286									
	LL/Cr	-0.2294	0.2226									
	ml/Cr	-0.1104	0.5615									
Spherical tensor (Cs)	Cho/Naa	0.1338	0.4809									
	LL/Cr	-0.2883	0.1224									
	ml/Cr	-0.1605	0.3969									
Total magnitude of the diffusion tensor (L)	Cho/Naa	0.1155	0.5435									
	LL/Cr	0.6845	<.0001*									
	ml/Cr	0.5132	0.0037*									

Cho/Naa = choline-to-N-acetyl aspartate; LL/Cr = lipids and lactate to creatine; ml/Cr = and myo-inositol/creatine

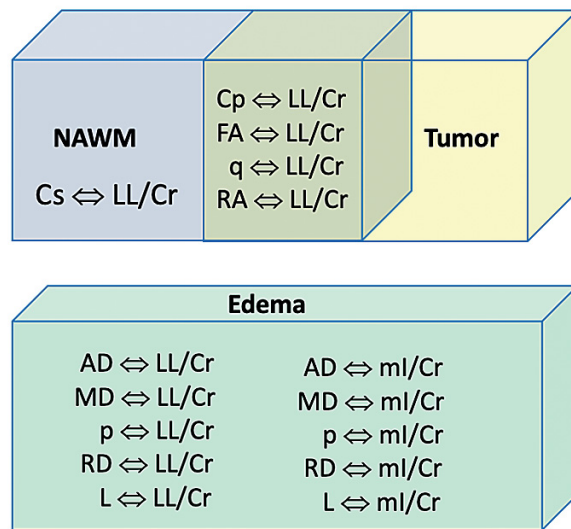


FIGURE 5. Diagram representation of the significant correlations between diffusion tensor imaging (DTI)- magnetic resonance spectroscopy (MRS) biomarkers at the selected regions: normal-appearing white matter (NAWM), enhancing rim and peritumoral edema. Notice that NAWM and the enhancing rim share four pairs of biomarkers correlations; while in peritumoral oedema ten pairs of correlations were exclusive of that region.

structural properties of water molecules and their movements, then the non-significant correlation.

Significant correlations between four DTI metrics and LL/Cr at NAWM and enhancing tumour regions

In our second group of findings, four significant correlations pairs ($Cp \Leftrightarrow LL/Cr$, $FA \Leftrightarrow LL/Cr$, $q \Leftrightarrow LL/Cr$, $RA \Leftrightarrow LL/Cr$) coincidentally appeared in the NAWM and the enhancing tumour regions. They showed some direction of correlation on both region: Three were negative (the more LL/Cr, the less concentration of FA, q and RA); and one positive (LL/Cr and Cp increase or decrease in the same direction).

To understand these relationships, we begin mentioning that creatine, Cr, is a marker of energetic systems and intracellular metabolism; it is considered a stable metabolite for its relatively constant concentration and is used as an internal reference for calculating metabolite ratios.²⁹ In the combined ratio, LL/Cr, lipid resonances frequently dominate, and lactate (that can be seen in all tumour grades) is mainly present at high levels in glioblastoma.³⁰

About the four selected DTI metrics (Cp, FA, q, and RA) that assembled significant bivariate correlations with LL/Cr; FA measures the directional-

ity of water diffusion (shape of the diffusion tensor in each voxel). FA values vary between 0 (isotropic diffusion) and 1 (infinite anisotropy).³¹ FA is decreased in glioblastoma.¹¹ Diffusion is anisotropic in white matter fibre tracts, as axonal membranes and myelin sheaths present barriers to the motion of water molecules, in directions not parallel to their orientation. Reduced FA (water diffusion parallel to axonal tracts) is indicative of axonal degeneration.³²

We found two articles in the last 15 years mentioning the q biomarker: q is the anisotropic component of the diffusion tensor, with a marked decrease of q in disrupted tracts; q-value in the low-grade tumours is slightly higher than in high-grade tumours, although this is not significantly different.³³ In 2006 Price *et al.* conclude that q may provide a complete picture of the diffusion profile of a brain tumour.³⁴

Cp is the planar, geometric representation of the diffusion tensor, and since one decade has been used in the differential diagnosis among abscesses, glioblastomas, and metastases.¹¹ Mean values of Cp have been quantified at the enhancing rim, peritumoral oedema and NAWM regions.¹³

RA is a ratio of the normalised standard deviations between the anisotropic part of the diffusion coefficient and its isotropic part³⁵; it is a function of the variance of the eigenvalues of the diffusion tensor, which is not equal to the variance of the diffusivities along with all directions.³⁶ It was not surprising to find significant correlations of RA and LL/Cr in NAWM, as it has been reported as one of the best biomarkers to characterise NAWM.¹³

$Cs \Leftrightarrow LL/Cr$, the only significant correlations exclusive of NAWM

Cs and LL/Cr depicted a negative correlation, meaning the increase or decrease in opposite directions. Cs describes the spherical, geometric properties of the diffusion tensor¹¹; after RA, Cs is the second DTI metric with the best diagnostic performance to characterise the NAWM.¹³ It is not clear for us why $Cs \Leftrightarrow LL/Cr$, was the only significant correlation observed at the NAWM, but not observed in peritumoral oedema and enhancing rim.

Significant bivariate correlations exclusive of the peritumoral region

In our fourth and last group of observations, we found ten significant bivariate correlations only observed in that region ($AD \Leftrightarrow LL/Cr$, $MD \Leftrightarrow LL/Cr$,

Cr, $p \leftrightarrow LL/Cr$, $RD \leftrightarrow LL/Cr$, $L \leftrightarrow LL/Cr$, $AD \leftrightarrow mI/Cr$, $MD \leftrightarrow mI/Cr$, $p \leftrightarrow mI/Cr$, $RD \leftrightarrow mI/Cr$, $L \leftrightarrow mI/Cr$). All correlations had a positive sign, meaning that any increase in LL/Cr or mI/Cr , will coincide with increases in AD , MD , p , RD and L .

Although scarce, there are independent publications on MRS and DTI metrics that helped us understand better these observations. Firstly, we briefly mention basic concepts of the mI/Cr metabolite ratio, after the five DTI metrics observed for this region (AD , MD , p , RD and L).

mI/Cr includes a range of compounds: phosphatidylinositol, inositol polyphosphate, inositol monophosphate, myo-inositol and, to a smaller extent, glycine; because inositol is elevated within astrocytes, its increased peak is taken as an empirical marker of glial density and proliferation.³⁷ The exact biological significance of mI/Cr , measurable only at short echo time, had been considered uncertain in gliomas.²¹

MD measures the average motion of water molecules, independent of tissue directionality³¹; it is considered a synonym of the coefficient of diffusion in different space guidelines.³⁸ Increased MD has been observed in the peritumoral region of high-grade gliomas.³⁹ The best diagnostic performance by MD in the peritumoral region¹³ is explained because it measures the magnitude of molecular motion of water. However, MD does not depend directly on the integrity of myelinated fibre tracts.³⁵

p is the isotropic component of the diffusion tensor; p values are significantly higher in the low-grade tumours, possibly reflecting the increased cellularity and restriction of water diffusion in high-grade gliomas; disrupted tracts, however, show a marked increase in p .³³ p showed one of the three best diagnostic performance to characterise peritumoral oedema.¹³ AD and RD describes microscopic water movement parallel and perpendicular to the axon tract, respectively; inconsistent changes of RD and AD appeared in axonal injury.⁴⁰⁻⁴² L represents the total magnitude of the diffusion tensor; it shows an increased mean in peritumoral oedema in glioblastoma.⁴³

DTI and MRS features of peritumoral oedema in glioblastoma

Characterisation of peritumoral oedema is one of the most challenging topics in glioblastoma. Discrimination of tumour-infiltrated oedema from vasogenic oedema using DTI metrics has demonstrated conflicting results.⁴⁴

Since last ten years, authors coincide that there is no threshold value at which a clear distinction could be made between tumour infiltration and purely vasogenic oedema; no DTI metric can, by itself, definitively distinguish between these regions.⁴³ Tumour infiltration may occur in brains that appear normal on T2-weighted images in 40% of cases.³⁴ Gliosis (measured by mI/Cr), is an astrocytic response to any central nervous system injury, which can occur in peritumoral oedema. In the relatively long-standing oedema surrounding glioblastoma, glial fibres assume a more regular arrangement, resulting in more organised water diffusion detected with DTI.¹¹

Limitations of the study

Some limitations need to be acknowledged: we did not use the single-voxel technique that it is favourite in clinical practice (widely available, usually good field homogeneity, can be readily performed at short echo times, and is relatively easy to process and interpret). However, its highest single limitation is the lack of ability to determine the spatial heterogeneity of spectral patterns and the fact that only a small number of brain regions can be covered within the time constraints of a routine clinical MR exam.⁴⁵ We did not measure metabolite relaxation rates due to scan-time limitations related to a large number of voxels under investigation. We were not able to calculate concentrations of additional metabolites such as glutamine, glutamate, alanine, amino acids, separation of lipids and lactate; they required special software packages ready to fit short-echo and long-echo spectra, such as *LCModel*⁴⁶ and *jMRUI*⁴⁷; these were not available at our institution when the MRS data for this project were acquired. We would have liked to obtain a higher number of directional motion-probing gradients (MPG) like other studies reporting up to 40- and 81- for the DTI acquisition.⁴⁸ It is known that the minimal mathematic requirement for DTI-parameters calculation is 6 independent directional MPG settings.⁴⁸ Because the amount of imaging time is limited in most clinical situations, we followed the recommendations of the MRI scanner vendor. Our choice of 25 MPG settings thus involved a trade-off between minimizing directional bias and minimizing scanning time, it also complied with the minimum of 20 unique sampling orientations necessary for a robust estimation of anisotropy.⁴⁹

Our statement that tumour infiltration coexist with vasogenic oedema in a heterogeneous pattern

in the peritumoral region was not confirmed with histopathology. The limited explanations to our findings might support the statement by Pena *et al.* "it is still not known a priori which tensor measure is the most appropriate to quantify pathological changes in brain tissue".²³

Future directions

We acknowledge the unmet need of generalising the MRI studies in glioblastoma acquiring advanced imaging techniques, including perfusion-weighted imaging, MR spectroscopy, and DTI, to assess tumour infiltration.⁵⁰ Because the MRS and DTI biomarkers have been measured in other types of tumours^{11,16}, we believe that the results of this study also apply to those tumours. However, future studies should address if similar correlations are also observed for them. To achieve a deeper understanding of the DTI and MRS interactions; multivariate analysis of DTI metrics and MRS metabolites, controlling the effect of confounders (gender, age, regional location of the tumour, infiltration patterns using MRS and DTI) might unveil unknown interactions of these biomarkers at the ultrastructural level in glioblastoma to support the speculation in our explanations.

We believe MRS and DTI will be incorporated soon in the context of the World Health Organization (WHO) updated the central nervous system (CNS) tumour classification. In the updated 2016 WHO CNS tumour classification version, some tumours were defined by a combination of microscopic morphologic and molecular and genetic factors, whereas others continue to be defined by morphology alone. Although not official, there is a role for DTI and MRS in the current evaluation of glioblastoma: IDH1 and IDH2 mutations (which are referred collectively as isocitrate dehydrogenase [IDH] mutation) have become definitional for infiltrating gliomas in adults, with 1p/19q codeletion further characterizing the type.⁵¹ Mutation in IDH1 and IDH2 alters the role of the IDHs in the citric acid cycle and leads to accumulation of the oncometabolite 2-hydroxyglutarate (2HG) within tumour cells. Although IDH mutants themselves do not present a clear radiologic signature, 2HG can be detected at MR spectroscopy.⁵² The 1p/19q codeletion is associated with the apparent diffusion coefficient value⁵³, which is equivalent to the MD²⁴, a DTI metric that had significant Rs in our study. Routine use of advanced MRI in glioblastoma has been incorporated into glioma imaging protocols at some institutions.⁵¹

Conclusions

A comprehensive understanding of appropriate DTI and MRS biomarkers for each tumour region in glioblastoma would obtain complementary metabolic and ultrastructural information necessary to preoperatively identify sites of significant tumour infiltration that appear normal on conventional MRI and in the follow-up of glioblastoma patients. DTI, in combination with MRS, are additional tools of the "biologic targeting" for radiation therapy. DTI and MRS biomarkers answer different questions; peritumoral oedema represents the biggest challenge with at least ten significant correlations between DTI and MRS that need additional studies. The fact that DTI and MRS measures are not specific of one histologic type of tumour broadens their application to a wider variety of intracranial pathologies. Correlation maps between DTI and MRS might help researchers supplement the diagnosis and treatment planning of brain tumours, decreasing the underlying empiricism in this area.

Acknowledgement

Eduardo Flores-Alvarez was supported by Consejo Nacional de Ciencia y Tecnología (CONACyT), Mexico, fellowship award. This work was submitted in partial fulfilment of the requirements for the DSc degree of Eduardo Flores-Alvarez at the Programa de Doctorado en Ciencias Médicas, Facultad de Medicina, Universidad Nacional Autónoma de México.

References

1. Tugcu B, Postalci LS, Gunaldi O, Tanriverdi O, Akdemir H. Efficacy of clinical prognostic factors on survival in patients with glioblastoma. *Turk Neurosurg* 2010; **20**: 117-25. doi: 10.5137/1019-5149.JTN.2461-09.4
2. Seidel C, Dörner N, Osswald M, Wick A, Platten M, Bendszus M, et al. Does age matter? - A MRI study on peritumoral edema in newly diagnosed primary glioblastoma. *BMC cancer* 2011; **11**: 127. doi: 10.1186/1471-2407-11-127
3. Perez-Beteta J, Molina-García D, Martínez-González A, Henares-Molina A, Amo-Salas M, Luque B, et al. Morphological MRI-based features provide pretreatment survival prediction in glioblastoma. *Eur Radiol* 2019; **29**: 1968-77. doi: 10.1007/s00330-018-5758-7
4. Blomstergren A, Rydelius A, Abul-Kasim K, Lätt J, Sundgren PC, Bengzon J. Evaluation of reproducibility in MRI quantitative volumetric assessment and its role in the prediction of overall survival and progression-free survival in glioblastoma. *Acta Radiol* 2019; **60**: 516-25. doi: 10.1177/0284185118786060
5. Abbasi AW, Westerlaan HE, Holtman GA, Aden KM, van Laar PJ, van der Hoorn A. Incidence of tumour progression and pseudoprogression in high-grade gliomas: a systematic review and meta-analysis. *Clin Neuroradiol* 2018; **28**: 401-11. doi: 10.1007/s00062-017-0584-x

6. Durand-Munoz C, Flores-Alvarez E, Moreno-Jimenez S, Roldan-Valadez E. Pre-operative apparent diffusion coefficient values and tumour region volumes as prognostic biomarkers in glioblastoma: correlation and progression-free survival analyses. *Insights Imaging* 2019; **10**: 36. doi: 10.1186/s13244-019-0724-8
7. Zikou A, Sioka C, Alexiou GA, Fotopoulos A, Voulgaris S, Argyropoulou MI. Radiation necrosis, pseudoprogression, pseudoresponse, and tumor recurrence: imaging challenges for the evaluation of treated gliomas. *Contrast Media Mol Imaging* 2018; **2018**: 6828396. doi: 10.1155/2018/6828396
8. Cordova JS, Shu HK, Liang Z, Gurbani SS, Cooper LA, Holder CA, et al. Whole-brain spectroscopic MRI biomarkers identify infiltrating margins in glioblastoma patients. *Neuro Oncol* 2016; **18**: 1180-9. doi: 10.1093/neuonc/nov036
9. van Dijken BRJ, van Laar PJ, Holtman GA, van der Hoorn A. Diagnostic accuracy of magnetic resonance imaging techniques for treatment response evaluation in patients with high-grade glioma, a systematic review and meta-analysis. *Eur Radiol* 2017; **27**: 4129-44. doi: 10.1007/s00330-017-4789-9
10. Roldan-Valadez E, Rios C, Motola-Kuba D, Matus-Santos J, Villa AR, Moreno-Jimenez S. Choline-to-N-acetyl aspartate and lipids-lactate-to-creatine ratios together with age assemble a significant Cox's proportional-hazards regression model for prediction of survival in high-grade gliomas. *Br J Radiol* 2016; **89**: 20150502. doi: 10.1259/bjr.20150502
11. Toh CH, Wei KC, Ng SH, Wan YL, Lin CP, Castillo M. Differentiation of brain abscesses from necrotic glioblastomas and cystic metastatic brain tumors with diffusion tensor imaging. *AJNR Am J Neuroradiol* 2011; **32**: 1646-51. doi: 10.3174/ajnr.A2581
12. Roldan-Valadez E, Rios C, Cortez-Conradis D, Favila R, Moreno-Jimenez S. Global diffusion tensor imaging derived metrics differentiate glioblastoma multiforme vs. normal brains by using discriminant analysis: introduction of a novel whole-brain approach. *Radiol Oncol* 2014; **48**: 127-36. doi: 10.2478/raon-2014-0004
13. Cortez-Conradis D, Favila R, Isaac-Olive K, Martinez-Lopez M, Rios C, Roldan-Valadez E. Diagnostic performance of regional DTI-derived tensor metrics in glioblastoma multiforme: simultaneous evaluation of p, q, L, Cl, Cp, Cs, RA, RD, AD, mean diffusivity and fractional anisotropy. *Eur Radiol* 2013; **23**: 1112-21. doi: 10.1007/s00330-012-2688-7
14. Rees JH, Smirniotopoulos JG, Jones RV, Wong K. Glioblastoma multiforme: radiologic-pathologic correlation. *Radiographics* 1996; **16**: 1413-38; quiz 1462-3. doi: 10.1148/radiographics.16.6.8946545
15. Tang CY, Friedman J, Shungu D, Chang L, Ernst T, Stewart D, et al. Correlations between diffusion tensor imaging (DTI) and magnetic resonance spectroscopy (1H MRS) in schizophrenic patients and normal controls. *BMC Psychiatry* 2007; **7**: 25. doi: 10.1186/1471-244X-7-25
16. Brandao LA, Domingues RC. Brain metabolites and their significance in spectral analysis. In: Brandao LA, Domingues RC, editors. *MR spectroscopy of the brain*. Philadelphia, PA: Lippincott Williams & Wilkins; 2004. p. 11-2.
17. Browner WS, Newman TB, Hulley SB. Total sample size required when using the correlation coefficient (r). Appendix 6c. In: Hulley SB, Cummings SR, Browner WS, Grady DG, Newman TB. *Designing clinical research*. Philadelphia, PA: Lippincott, Williams & Wilkins; 2013. p. 79.
18. Chan YH. Biostatistics 104: correlational analysis. *Singapore Med J* 2003; **44**: 614-9. PMID: 14770254
19. Barton B, Peat J. Correlation coefficients. Chapter 7. In: Barton B, Peat J, editors. *Medical statistics. A guide to SPSS, data analysis and critical appraisal*. West Sussex, UK: John Wiley & Sons Ltd; 2014. p. 197-204.
20. Pallant J. Testing the statistical significance of the difference between correlation coefficients. In: Pallant J, editor. *SPSS survival manual*. Crows Nest, NSW, Australia: Allen & Unwin; 2011. p. 139-41.
21. Waldman AD, Jackson A, Price SJ, Clark CA, Booth TC, Auer DP, et al. Quantitative imaging biomarkers in neuro-oncology. *Nat Rev Clin Oncol* 2009; **6**: 445-54. doi: 10.1038/nrclinonc.2009.92
22. Sadeghi N, Camby I, Goldman S, Gabius HJ, Balériaux D, Salmon I, et al. Effect of hydrophilic components of the extracellular matrix on quantifiable diffusion-weighted imaging of human gliomas: preliminary results of correlating apparent diffusion coefficient values and hyaluronan expression level. *AJR Am J Roentgenol* 2003; **181**: 235-41. doi: 10.2214/ajr.181.1.1810235
23. Peña A, Green HA, Carpenter TA, Price SJ, Pickard JD, Gillard JH. Enhanced visualization and quantification of magnetic resonance diffusion tensor imaging using the p:q tensor decomposition. *Br J Radiol* 2006; **79**: 101-9. doi: 10.1259/bjr/24908512.
24. Cortez-Conradis D, Rios C, Moreno-Jimenez S, Roldan-Valadez E. Partial correlation analyses of global diffusion tensor imaging-derived metrics in glioblastoma multiforme: Pilot study. *World J Radiol* 2015; **7**: 405-14. doi: 10.4329/wjrv.7.i11.405
25. Bitsch A, Bruhn H, Vougioukas V, Stringaris A, Lassmann H, Frahm J, et al. Inflammatory CNS demyelination: histopathologic correlation with in vivo quantitative proton MR spectroscopy. *AJNR Am J Neuroradiol* 1999; **20**: 1619-27. PMID: 10543631
26. Barker PB, Soher BJ, Blackband SJ, Chatham JC, Mathews VP, Bryan RN. Quantitation of proton NMR spectra of the human brain using tissue water as an internal concentration reference. *NMR in biomedicine* 1993; **6**: 89-94. doi: 10.1002/nbm.1940060114
27. Gasparovic C, Arfai N, Smid N, Feeney DM. Decrease and recovery of N-acetylaspartate/creatine in rat brain remote from focal injury. *J Neurotrauma* 2001; **18**: 241-6. doi: 10.1089/08977150151070856
28. Law M, Yang S, Wang H, Babb JS, Johnson G, Cha S, et al. Glioma grading: sensitivity, specificity, and predictive values of perfusion MR imaging and proton MR spectroscopic imaging compared with conventional MR imaging. *AJNR Am J Neuroradiol* 2003; **24**: 1989-98. doi: 10.1148/radiol.2382041896
29. Bertholdo D, Watcharakorn A, Castillo M. Proton magnetic resonance spectroscopy. Introduction and overview. In: Brandao LA, editor. *MR spectroscopy of the brain*. Philadelphia, PA: Elsevier Inc.; 2013. p. 359-80.
30. Stadlbauer A, Gruber S, Nimsky C, Fahlbusch R, Hammen T, Buslei R, et al. Preoperative grading of gliomas by using metabolite quantification with high-spatial-resolution proton MR spectroscopic imaging. *Radiology* 2006; **238**: 958-69. doi: 10.1148/radiol.2382041896
31. Pierpaoli C, Basser PJ. Toward a quantitative assessment of diffusion anisotropy. *Magn Reson Med* 1996; **36**: 893-906. doi: 10.1002/mrm.1910360612
32. Neil J, Miller J, Mukherjee P, Hüppi PS. Diffusion tensor imaging of normal and injured developing human brain - a technical review. *NMR in biomedicine* 2002; **15**: 543-52. doi: 10.1002/nbm.784
33. Price SJ, Peña A, Burnet NG, Jena R, Green HA, Carpenter TA, et al. Tissue signature characterisation of diffusion tensor abnormalities in cerebral gliomas. *Eur Radiol* 2004; **14**: 1909-17. doi: 10.1007/s00330-004-2381-6
34. Price SJ, Jena R, Burnet NG, Hutchinson PJ, Dean AF, Peña A, et al. Improved delineation of glioma margins and regions of infiltration with the use of diffusion tensor imaging: an image-guided biopsy study. *AJNR Am J Neuroradiol* 2006; **27**: 1969-74.
35. Le Bihan D, Mangin JF, Poupon C, Clark CA, Pappata S, Molko N, et al. Diffusion tensor imaging: concepts and applications. *J Magn Reson Imaging* 2001; **13**: 534-46. doi: 10.1002/jmri.1076
36. Ozarslan E, Vemuri BC, Mareci TH. Generalized scalar measures for diffusion MRI using trace, variance, and entropy. *Magn Reson Med* 2005; **53**: 866-76. doi: 10.1002/mrm.20411
37. Minati L, Aquino D, Bruzzone MG, Erbetta A. Quantitation of normal metabolite concentrations in six brain regions by in-vivoH-MR spectroscopy. *Med Phys* 2010; **35**: 154-63. doi: 10.4103/0971-6203.62128
38. Mori S, Barker PB. Diffusion magnetic resonance imaging: its principle and applications. *Anat Rec* 1999; **257**: 102-9. doi: 10.1002/(SICI)1097-0185(19990615)257:3<102::AID-AR7>3.0.CO;2-6
39. Lu S, Ahn D, Johnson G, Cha S. Peritumoral diffusion tensor imaging of high-grade gliomas and metastatic brain tumors. *AJNR Am J Neuroradiol* 2003; **24**: 937-41.
40. Budde MD, Xie M, Cross AH, Song SK. Axial diffusivity is the primary correlate of axonal injury in the experimental autoimmune encephalomyelitis spinal cord: a quantitative pixelwise analysis. *J Neurosci* 2009; **29**: 2805-13. doi: 10.1523/JNEUROSCI.4605-08.2009
41. Song SK, Sun SW, Ramsbottom MJ, Chang C, Russell J, Cross AH. Demyelination revealed through MRI as increased radial (but unchanged axial) diffusion of water. *Neuroimage* 2002; **17**: 1429-36. doi: 10.1006/nimg.2002.1267
42. Zhang X, Sun P, Wang J, Wang Q, Song SK. Diffusion tensor imaging detects retinal ganglion cell axon damage in the mouse model of optic nerve crush. *Invest Ophthalmol Vis Sci* 2011; **52**: 7001-6. doi: 10.1167/iovs.11-7619

43. Wang W, Steward CE, Desmond PM. Diffusion tensor imaging in glioblastoma multiforme and brain metastases: the role of p, q, L, and fractional anisotropy. *AJNR Am J Neuroradiol* 2009; **30**: 203-8. doi: ajnr.A1303 [pii]10.3174/ajnr.A1303
44. Lu S, Ahn D, Johnson G, Law M, Zagzag D, Grossman RI. Diffusion-tensor MR imaging of intracranial neoplasia and associated peritumoral edema: introduction of the tumor infiltration index. *Radiology* 2004; **232**: 221-8. doi: 10.1148/radiol.2321030653
45. Barker PB, Bizzi A, Stefano ND, Gullapalli RP, Lin DDM. *Clinical MR spectroscopy. Techniques and Applications*. Cambridge, UK: Cambridge University Press; 2010.
46. Provencher SW. Automatic quantitation of localized in vivo 1H spectra with LCModel. *NMR Biomed* 2001; **14**: 260-4. doi: 10.1002/nbm.698
47. Naressi A, Couturier C, Castang I, de Beer R, Graveron-Demilly D. Java-based graphical user interface for MRUI, a software package for quantitation of in vivo/medical magnetic resonance spectroscopy signals. *Comput Biol Med* 2001; **31**: 269-86. doi: 10.1016/s0010-4825(01)00006-3
48. Yamamoto A, Miki Y, Urayama S, Fushimi Y, Okada T, Hanakawa T, et al. Diffusion tensor fiber tractography of the optic radiation: analysis with 6-, 12-, 40-, and 81-directional motion-probing gradients, a preliminary study. *AJNR Am J Neuroradiol* 2007; **28**: 92-6.
49. Jones DK. The effect of gradient sampling schemes on measures derived from diffusion tensor MRI: a Monte Carlo study. *Magn Reson Med* 2004; **51**: 807-15. doi: 10.1002/mrm.20033
50. Bette S, Huber T, Gempt J, Boeckh-Behrens T, Wiestler B, Kehl V, et al. Local fractional anisotropy is reduced in areas with tumor recurrence in glioblastoma. *Radiology* 2017; **283**: 499-507. doi: 10.1148/radiol.2016152832
51. Johnson DR, Guerin JB, Giannini C, Morris JM, Eckel LJ, Kaufmann TJ. 2016 updates to the WHO brain tumor classification system: What the radiologist needs to know. *Radiographics* 2017; **37**: 2164-80. doi: 10.1148/rg.2017170037
52. Pope WB, Prins RM, Albert Thomas M, Nagarajan R, Yen KE, Bittinger MA, et al. Non-invasive detection of 2-hydroxyglutarate and other metabolites in IDH1 mutant glioma patients using magnetic resonance spectroscopy. *J Neurooncol* 2012; **107**: 197-205. doi: 10.1007/s11060-011-0737-8
53. Johnson DR, Diehn FE, Giannini C, Jenkins RB, Jenkins SM, Parney IF, et al. Genetically defined oligodendroglioma is characterized by indistinct tumor borders at MRI. *AJNR Am J Neuroradiol* 2017; **38**: 678-84. doi: 10.3174/ajnr.A5070

Adrenal vein sampling for primary aldosteronism: a 15-year national referral center experience

Tomaz Kocjan^{1,2}, Mojca Jensterle^{1,2}, Gaj Vidmar^{2,3,4}, Rok Vrckovnik^{1,2}, Pavel Berden^{2,5}, Milenko Stankovic^{2,5}

¹ Department of Endocrinology, Diabetes and Metabolic Diseases, University Medical Centre Ljubljana, Ljubljana, Slovenia

² Faculty of Medicine, University of Ljubljana, Ljubljana, Slovenia

³ University Rehabilitation Institute, Ljubljana, Slovenia

⁴ FAMNIT, University of Primorska, Koper, Slovenia

⁵ Clinical Institute of Radiology, University Medical Centre Ljubljana, Ljubljana, Slovenia

Radiol Oncol 2020; 54(4): 409-418.

Received 14 April 2020

Accepted 12 July 2020

Correspondence to: Prof. Tomaž Kocjan, M.D., Ph.D., Department of Endocrinology, Diabetes and Metabolic Diseases, University Medical Centre Ljubljana, Zaloška 7, SI-1525 Ljubljana, Slovenia. E-mail: tomaz.kocjan@kclj.si

Disclosure: No potential conflicts of interest were disclosed.

Background. Adrenal vein sampling (AVS) is essential for diagnostics of primary aldosteronism, distinguishing unilateral from bilateral disease and determining treatment options. We reviewed the performance of AVS for primary aldosteronism at our center during first 15 years, comparing the initial period to the period after the introduction of a dedicated radiologist. Additionally, AVS outcomes were checked against CT findings and the proportion of operated patients with proven unilateral disease was estimated.

Patients and methods. A retrospective cross-sectional study conducted at the national endocrine referral center included all patients with primary aldosteronism who underwent AVS after its introduction in 2004 until the end of 2018. AVS was performed sequentially during Synacthen infusion. When the ratio of cortisol concentrations from adrenal vein and inferior vena cava was at least 5, AVS was considered successful.

Results. Data from 235 patients were examined (168 men; age 32–73, median 56 years; BMI 18–48, median 30.4 kg/m²). Average number of annual AVS procedures increased from 7 in the 2004–2011 period to 29 in the 2012–2018 period ($p < 0.001$). AVS had to be repeated in 10% of procedures; it was successful in 77% of procedures and 86% of patients. The proportion of patients with successful AVS (92% in 2012–2018 vs. 66% in 2004–2011, $p < 0.001$) and of successful AVS procedures (82% vs. 61%, $p < 0.001$) was statistically significantly higher in the recent period.

Conclusions. Number of AVS procedures and success rate at our center increased over time. Introduction of a dedicated radiologist and technical advance expanded and improved the AVS practice.

Key words: angiography; adrenal gland; endocrine disorders; secondary hypertension

Introduction

Primary aldosteronism is the most common form of secondary hypertension, with a prevalence of 5.9% among hypertensive patients in primary care practice.¹ Autonomous and excessive secretion of aldosterone from one or both adrenal glands in patients with primary aldosteronism causes sig-

nificantly higher cardiovascular risk and more pronounced renal damage compared to equally severe essential hypertension.^{1–3} Amongst available targeted treatment, the preferred therapeutic option is unilateral laparoscopic adrenalectomy, which can normalize or decrease blood pressure in most patients with proven unilateral disease.^{4,5} Long-term medical treatment with mineralocorticoid

receptor antagonists is not only more expensive and less convenient, but it might also have worse outcomes overall.^{4,6}

Therefore, a crucial part of diagnostic workup in primary aldosteronism is to correctly determine which patients have unilateral disease and could pursue surgical cure. Adrenal computed tomography (CT) (or magnetic resonance imaging (MRI)) should be the first test in the subtype evaluation of primary aldosteronism and to exclude adrenocortical carcinoma.⁴ However, because of increasing prevalence of nonfunctioning adrenal incidentalomas, the reliability of CT in localizing unilateral disease (e.g. an aldosterone producing adenoma) declines with patient age.^{4,7} In most patients CT cannot accurately distinguish between unilateral and bilateral forms, and may even lead to inappropriate treatment of primary aldosteronism.⁸ The only exception are infrequent younger patients below 35 years of age with florid disease and a clear one-sided adrenal adenoma with normal contralateral gland.^{4,8,9}

All other surgical candidates should proceed to adrenal vein sampling (AVS), which is regarded as the gold standard to demonstrate lateralization and to avoid unnecessary or inappropriate adrenalectomy. More than 50 years after its introduction, AVS remains controversial as an invasive, expensive and a technically challenging method with successful bilateral catheterization obtained

in only about 75% of cases.^{4,10} Cannulation of the small and short right adrenal vein with direct drainage into the inferior vena cava (IVC) is often the main obstacle to a successful procedure, while the sampling from the left adrenal vein is relatively straightforward. There is substantial inconsistency in how AVS is performed and interpreted. When done by experienced radiologists, the complication rate is low at between 0.2 and 0.9%.¹¹ Only a limited number of referral centers worldwide routinely carry out the procedure.^{10,12} Recently, the introduction of cone beam CT (CBCT) and other technical developments have further improved the AVS success rate and reduced the complications.¹³⁻¹⁶

Primarily, we aimed to review the performance of AVS for primary aldosteronism at our center from its introduction in 2004 up to 2018. The initial period from 2004 to 2011 was compared to the period after the introduction of a dedicated radiologist in 2012. Our secondary objectives were to check the outcomes of AVS against CT findings and to estimate the proportion of patients with proven unilateral disease who ultimately had surgery.

Patients and methods

Study design

We conducted a retrospective cross-sectional study from AVS introduction in November 2004 to the end of 2018 at the Slovenian national tertiary endocrine referral center, which serves a country with a population of 2 million inhabitants. All the data originated from the Slovenian AVS database. The data collection and its analysis were approved by the National Medical Ethics Committee.

Patients

All patients with confirmed primary aldosteronism who underwent AVS at our center during the study period were suitable for enrollment. The diagnostic work-up for primary aldosteronism was done according to the established guidelines^{4,17}, as previously detailed elsewhere.¹⁸

Radiological imaging

One to three months before the AVS, all patients but one had adrenal imaging with a dual-source computed tomography (CT) scanner (Somatom Dual Source, Siemens, Germany). Our pre-specified adrenal CT protocol included 1 mm axial slices through the abdomen before, and if necessary also

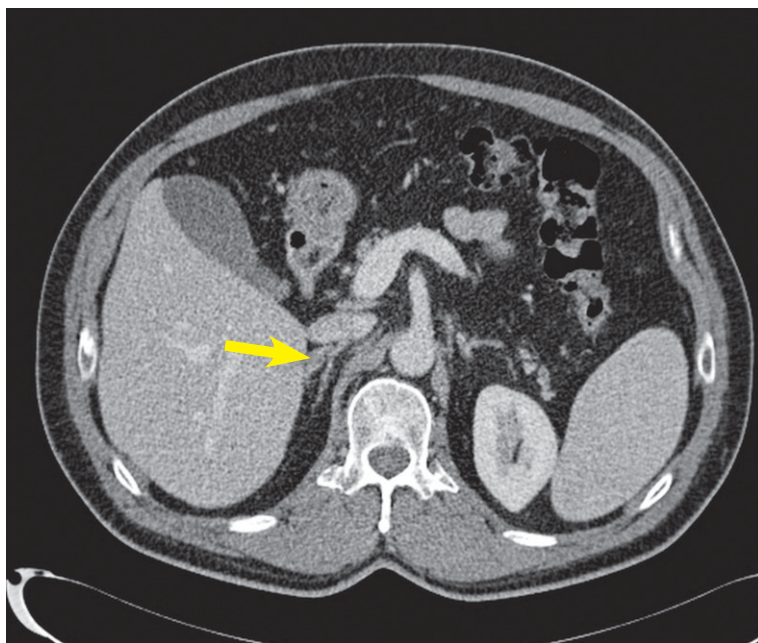


FIGURE 1. Tiny aldosterone-producing adenoma (8 mm) in lateral limb of the right adrenal gland (arrow) (CT scan).

after, the intravenous administration of 80–100 ml of iodinated contrast (370 mgJ/mL), injected at a rate of 3–4 ml/s via antecubital vein during breath-holding. Contrast-enhanced images were acquired after 60 seconds and 15 minutes. The standard scanning parameters included beam collimation of 64x0.6 mm, 16 slices and gantry rotation time of 0.5 s. Tube voltage was set at 120 kV, while the tube current was variable, optimized for body mass index and size, ranging between 160 and 210 mA. Source images of all phases were reconstructed on the axial plane at 5 mm, and on the coronal planes at 4 mm. Since 2017 a new-generation CT scanner (Somatom Force, Siemens, Germany) has been used, which allowed for more precise adaptation to the individual patient body characteristics. The scanning protocol remained essentially the same except for axial reconstructions at 2 mm. In 2014, interdisciplinary meetings dedicated to adrenal pathology were introduced where CT scans were meticulously reassessed with a radiologist, if both adrenals were described as normal. Finally, any thickening of at least 5 mm was deemed abnormal (Figure 1). The interventional radiologist also reviewed the images, in order to recognize the adrenal veins, especially on the right side.

Adrenal vein sampling

AVS was executed after an overnight fast between 8 and 9 AM. All patients were in the recumbent position for at least 1 hour before sampling. Infusion of synthetic adrenocorticotrophic hormone (ACTH) Synacthen (50 µg/h) was started 30 min before AVS and continued throughout the procedure.

During local anesthesia, a 5 Fr sheath (Avanti+ Introducer, Cordis, USA in the first period; Radiofocus Introducer II, Terumo, Japan in the recent period) was introduced into the right femoral vein. AVS was performed sequentially with the right adrenal vein always being cannulated and sampled first, using a 5 Fr Mickelson catheter (Cook Medical Inc., USA) or a 5 Fr Cobra C2 catheter with open-ended tip and two side-holes (Cordis, USA) in the first period. In the recent period a 4 Fr Mickelson catheter (Cook Medical Inc., USA) was routinely used on the right side (Figure 2). Catheterization of the left renal vein then followed with the same catheter, which was used as a guide for a 2.7 Fr Progreat microcatheter (coaxial type with catheter and guidewire; Terumo Interventional Systems, USA) to cannulate the common trunk of the left inferior phrenic vein and the left adrenal vein. The corresponding blood sample was drawn either at

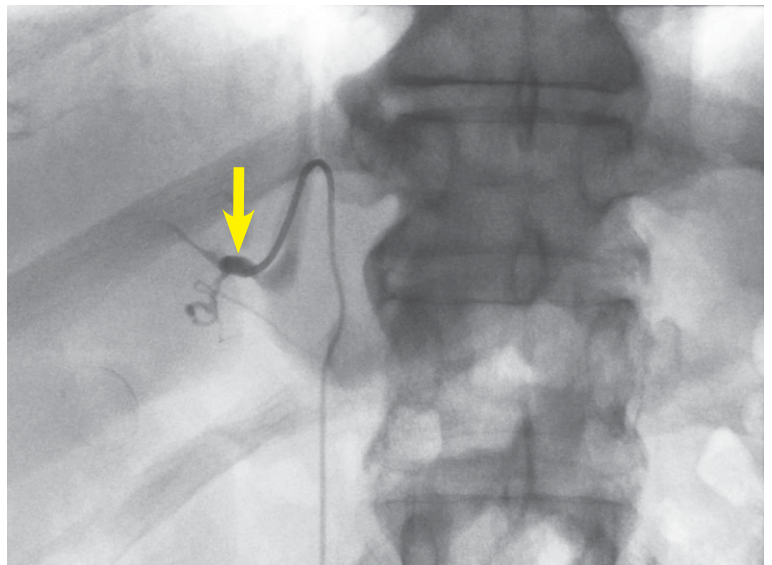


FIGURE 2. The right adrenal vein during sampling (arrow) (angiography).

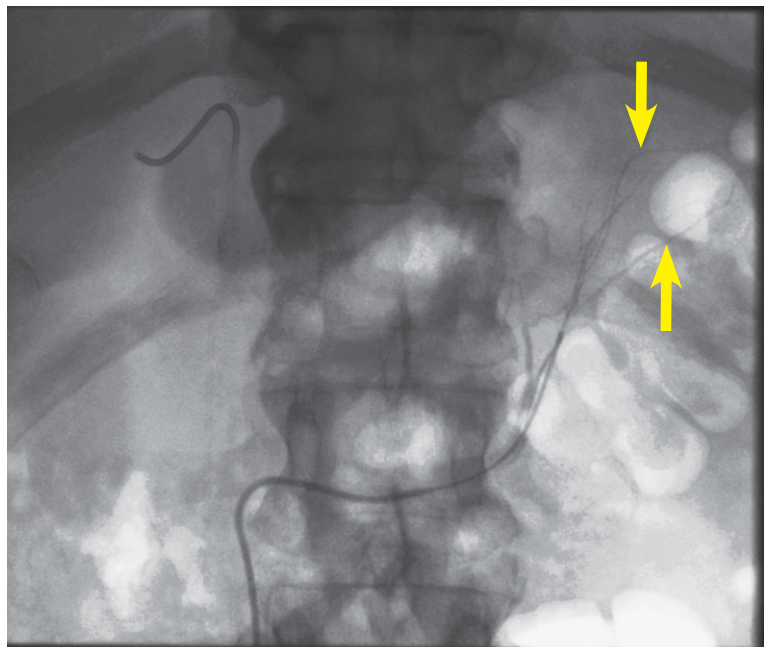


FIGURE 3. Branches of the left adrenal vein during sampling (arrows) (angiography).

the junction of these two veins or selectively from the left adrenal vein above the junction (Figure 3). Finally, a microcatheter was removed and the Mickelson catheter slightly pulled out to sample blood from the infra-renal IVC. On the other hand, a 4 Fr MPA 2 catheter with open-ended tip and two side-holes (Cordis, USA) was used on the left side in the first period. Standard 0.035-inch guidewire (J Tef Guidewire, Kimal, UK) was used in all cases. Additionally, 0.035-inch guidewire with J angled

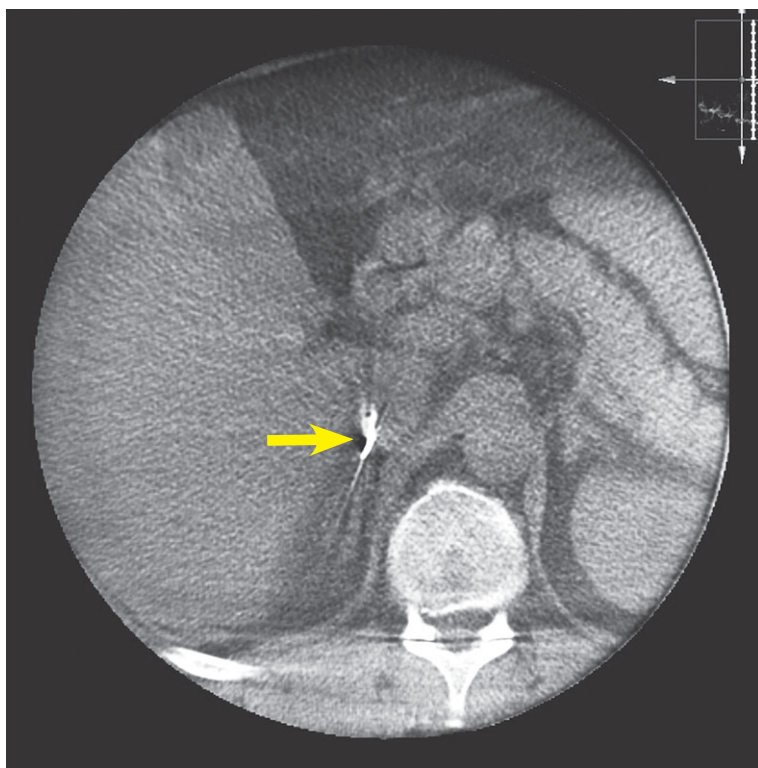


FIGURE 4. Tip of the catheter in the right adrenal vein (arrow); both limbs of the right adrenal gland are visible underneath (cone beam CT).

tip (Terumo, Japan) was used on the left side in the first period. Blood samples were drawn in 5 ml syringes and sent to laboratory for aldosterone and cortisol measurements. Hemostasis at the puncture site was ensured by manual compression.

During the initial period from 2004 to 2011 there were two interventional radiologists performing AVS; from 2012 onwards all procedures were done by a single dedicated interventional radiologist. During the first period, AVS was performed with fluoroscopic guidance by digital subtraction angiography (INTEGRIS V5000; Philips, The Netherlands), which was later changed to single-plane digital subtraction angiography (Allura Xper FD; Philips, The Netherlands). In the majority of cases, small amounts of contrast (90 ml on average per procedure in the first period and 52 ml on average per procedure in the recent period, respectively) were injected to better visualize the right adrenal vein.

High-resolution CBCT (Phillips Allura XperCT, The Netherlands) acquisition during AVS has been used since 2012 at first sporadically and then more consistently to identify the tip of the catheter accurately, in order to differentiate between the right

adrenal vein and a hepatic accessory vein or a paravertebral vein when necessary (Figure 4).

The average AVS procedure time decreased from 18.2 minutes in the first period to 16.8 minutes in the recent period.

When the selectivity index (SI), computed as the ratio of concentrations of cortisol from an adrenal vein and the infra-renal IVC, was at least 5, AVS was deemed successful. Lateralization index (LI), defined as the ratio of the higher over the lower cortisol-corrected aldosterone ratio, of more than 4 indicated unilateral aldosterone excess, while the values between 3 and 4 were assumed borderline.¹⁹ Suppressed plasma renin activity (PRA) values (< 0.6 ng/mL/h) were used as proof for unlikely stimulation of the contralateral adrenal cortex at a level adequate to confound interpretation of lateralization.^{20,21}

Assays

Serum aldosterone was measured with the Active® Aldosterone RIA (Beckman Coulter, Immunotech, Czech Republic). Serum cortisol was measured with an automated chemiluminescent immunoassay (CLIA) on the Immulite® 2000 XPi (Siemens Healthcare, Gwynedd, United Kingdom). The respective within- and between-assay coefficients of variation were below 4.5% and 9.8% for aldosterone and below 6.8% and 9.4% for cortisol. PRA measurements were performed using the Angiotensin I RIA KIT (Beckman Coulter, Immunotech, Czech Republic). The respective within- and between-assay coefficients of variation were below 11.3% and 20.9%.

Statistical analysis

Descriptive statistics were calculated. Patient characteristics and outcomes were compared between periods or groups using *t*-test, exact Mann-Whitney test and Fisher's exact test. Cohen's kappa was used to assess agreement between diagnostic methods. Statistical analyses were conducted using IBM SPSS Statistics 20 (IBM Corp., Armonk, USA, 2011).

Results

Data from 235 patients with primary aldosteronism were examined. Their clinical characteristics and laboratory parameters are presented in Table 1.

Most of them had a unilateral adrenal abnormality (62%) on CT scan, while bilateral adrenal thick-

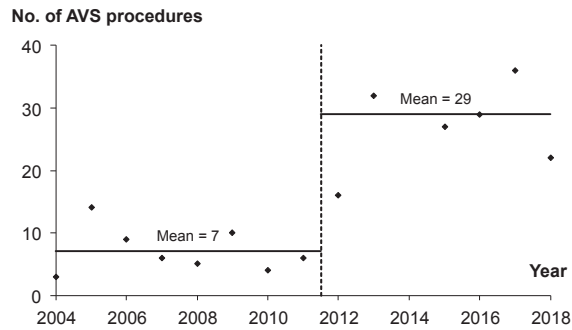
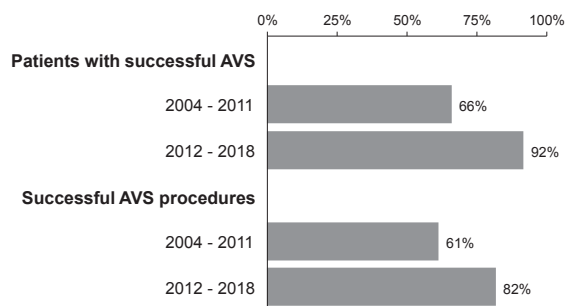
TABLE 1. Clinical characteristics and laboratory parameters of the patients

Characteristic	Descriptive statistics
n	235
Male patients	168 (71%)
Age (years)	56 (32–73)
Body Mass Index (kg/m ²)	30.4 (18.3–48.4)
Systolic BP at presentation (mm Hg)	155 (145–170)
Diastolic BP at presentation (mm Hg)	90 (80–95)
Number of antihypertensive agents	3 (2–4)
Hypokalemia	172 (73%)
eGFR (ml/min/1.73 m ²)	88 (71–102)
Baseline aldosterone (nmol/L)	0.7 (0.3–8.8)
Baseline PRA (ng/mL/h)	0.2 (0.2–0.9)
Baseline ARR	4.2 (1.1–43.8)
CT* normal / bilateral / unilateral	66 (28%) / 24 (10%) / 144 (62%)
Tumor size on CT (mm)	13 (8–19)

* = not performed in one patient; ARR = serum aldosterone-to-renin ratio; BP = blood pressure; eGFR = estimated glomerular filtration rate; PRA = plasma renin activity; Descriptive statistics are reported as median (interquartile range) for numeric variables and number (percentage) for categorical variables;

ening was present in 10% of the cases. The average adrenal nodules' size was 13 mm and left-sided lesions were more prevalent than the right-sided ones (62% vs. 38% in total). There were 28 left-sided lesions (60%) in the first period and 91 left-sided lesions (62%) in the recent period. Finally, in 28% of the cases CT scans of both adrenals were considered normal.

The average number of AVS procedures performed per year increased statistically significantly from 7 in the 2004–2011 period to 29 in the 2012–2018 period ($p < 0.001$) (Figure 5). In total, AVS had to be repeated in 10% of the procedures (9% in the first period, 10% in the recent period). AVS was successful (SI ≥ 5 in both adrenal veins) in 86% of the patients and in 77% of the procedures. The overall success rate of left adrenal vein cannulation was significantly higher than that of the right adrenal vein ($p = 0.001$). While the success rate on the left side remained unchanged over time (94% vs. 97%; $p = 0.434$), there was a statistically significant improvement on the right side after the introduction of a single dedicated interventional radiologist in 2012 (66% vs. 94%; $p < 0.001$). Consequently, the proportion of patients with successful AVS (66% vs.

**FIGURE 5.** Number of adrenal vein sampling procedures per year during the study period.**FIGURE 6.** Patients with successful adrenal vein sampling (AVS) and successful AVS procedures during the study period.

92%, $p < 0.001$) and of successful AVS procedures (61% vs. 82%, $p < 0.001$) was also significantly higher in the recent period (Figure 6). The right and left median SI values were not statistically significantly different (22.3 [interquartile range 18.2] vs. 22.4 [13.1]; $p = 0.285$). Decreasing the SI to ≥ 3 instead of ≥ 5 would not have improved the AVS performance on either side. Among previously tested clinical determinants of bilateral AVS success^{22,23}, only younger age proved to be statistically significant ($p = 0.004$) in our cohort, whereas higher BMI and male gender did not. Adrenal hemorrhage due to vein rupture occurred during two procedures (0.8% overall), one in the initial period (1 out of 57 procedures, 1.8%) and another in the recent period (1 out of 203 procedures; 0.5%), both resolved conservatively. Primary aldosteronism persisted in both cases and was treated medically. There were no other serious adverse events associated with AVS during the study.

CT and AVS results were compared in 181 patients with bilaterally successful AVS, excluding cases with borderline LI values between 3 and 4. The agreement amongst the two diagnostic meth-

	AVS bilateral	AVS left	AVS right	Total	
CT bilateral	51 (28%)	6 (3%)	14 (8%)	71	39%
CT left	32 (18%)	36 (20%)	4 (2%)	72	40%
CT right	17 (9%)	2 (1%)	19 (10%)	38	21%
Total	100 55%	44 24%	37 20%	N = 181	

FIGURE 7. Agreement between adrenal vein sampling (AVS) and CT findings depicted with a variable-width stacked column chart. Patients with normal CT scans are included in the CT bilateral category

ods was present in only 59% of cases ($\kappa = 0.36$) (Figure 7).

Among the patients with successful AVS, 44% overall ($n = 79$) had $LI > 4$ and hence proven unilateral disease. The percentage of lateralized cases did not statistically significantly differ between the two study periods ($p = 0.248$) or between younger (< 40 years) and older patients ($p = 0.470$). Adrenalectomy was recommended to all the patients with lateralized aldosterone secretion, but only 86% of them underwent surgery. All patients below 40 years of age with proven unilateral disease were operated on, but the same was true for only 84% of older subjects. The main reason for not having surgery was patient's reluctance ($n = 9$). One patient was diagnosed with liver cirrhosis and was rejected by the surgeon, two patients were lost to follow-up. The proportion of patients with unilateral disease undergoing surgery did not differ statistically significantly between the periods (89% *vs.* 85%, $p = 1.000$). Finally, additional four out of 21 patients with successful AVS and borderline LI values between 3 and 4 also opted for surgery. Three of them had clear unilateral adrenal nodule on CT, whereas the remaining patient had normal glands on imaging. All other patients were treated medically.

Discussion

The present study provides an important insight in the implementation process and continued development of AVS at the Slovenian national endocrine referral center over 15 years. The overall success rate for the AVS procedures during this period

was 77%, which is similar to the recently published large multicenter AVS registry study on 1625 patients, where 80% of cases were bilaterally selective.²⁴ Interestingly, the data from German Conn's Registry revealed that only 31% of their initial AVS studies were successful with later increase of the success rate to 61%.²⁵ On the other hand, the proportion of successful AVS procedures at our institution increased from 61% in 2004–2011 to 82% in 2012–2018. With 10% of procedures being repeated overall, the proportion of our patients with successful AVS rose concurrently from 66% to 92%, which is close to the success rate at the centers of excellence.^{19,26,27} The observed increment could be partially explained by our decision in 2012 to follow the recommendation for low-volume centers and focus the expertise on a single, dedicated interventional radiologist.^{12,28} This decision not only improved, but also expanded the AVS performance at our center (Figure 5).

The overall success rate improved due to superior cannulation of the right adrenal vein in the recent period (94% *vs.* 66%), whereas the success rate on the left side remained around 95% and unchanged over time. This was most probably not only due to the learning curve of the radiologist^{29,30} but mainly due to more regular pre-procedural review of CT images and intra-procedural use of high-resolution CBCT since 2012 to better map the adrenal venous anatomy, especially on the right side. The same approach has been recently used in other centers and allowed not only a better evaluation of the selectivity of right-sided adrenal vein cannulation, but also a significant decrease in the fluoroscopy time and quantity of iodine contrast injected in combination with unchanged or even lower radiation exposure.^{13–16}

Recently, another possibility to improve the catheterization success has been offered by using the newly developed ultra-rapid technique for semi-quantitative measurement of the cortisol level in adrenal veins in approximately 5 minutes, thus enabling the radiologist to reposition the catheter if the first result indicates an incorrect position.³¹ The rapid on-site measurement of the cortisol might be associated with a shorter procedure time and lower radiation dose than CT assisted AVS.³² However, this approach was not available at our center during the analyzed period.

Throughout the study period we strictly followed the Mayo Clinic protocol and used continuous Synacthen infusion starting 30 min before sampling and continuing throughout the procedure during sequential AVS.¹⁹ The main rationale

for ACTH-stimulated AVS is to maximize the cortisol gradient between the adrenal veins and VCI. Consequently, SI is increased and so is the proportion of diagnostic AVS procedures, which is why such a practice is particularly suitable for less experienced and low-volume centers.^{20,21} On the other hand, some authors consider the use of ACTH-stimulation as controversial because it might have the undesirable effect of masking the lateralization of aldosterone production, thus rendering some patients with unilateral primary aldosteronism apparently unsuitable for surgery.¹⁰ Fortunately, accumulated data overall suggest that surgical outcomes are similar irrespective of whether AVS is done by ACTH stimulation or not.^{5,33,34}

ACTH stimulation also minimizes stress-induced variations in aldosterone secretion during sequential sampling¹⁹⁻²¹, which might otherwise generate artificial between-sides gradients and lower its diagnostic accuracy.³⁵ Additionally, according to our protocol the right adrenal vein was always being cannulated first to lessen the time lag amid the sides.²⁸ Thereafter, a microcatheter was used to quickly cannulate the left adrenal vein³⁶ and to keep the delay between sequential sampling under 5 minutes in most of our AVS procedures.³⁷

Clearly, AVS studies that are not bilaterally successful should not be used to establish lateralization.²⁰ The choice of the correct SI is pivotal for the reported catheterization success rate, diagnostic reliability of the method and clinical outcome.^{34,38,39} According to the expert consensus the cutoff value for the SI should be ≥ 3.0 during ACTH stimulation²⁰, but we consistently applied an even more robust criterion ($SI \geq 5$) in order to minimize the chance of misdiagnosing either unilateral or bilateral primary aldosteronism.^{19,21} It is conceivable that there is a progressive decrease in success rate with increasing SI cut-offs, although the recent multicenter study showed this to be less dramatic with ACTH-stimulation.³⁴ Concordantly, decreasing the SI to ≥ 3 instead of ≥ 5 in our cohort would not improve the cannulation success rate on either side. Furthermore, the data from the same study showed post-ACTH SI cut-off of 5 to be able to clearly segregate biochemically successful and non-successful studies.³⁴ Actually, our median SI values were much higher than the advocated threshold. There was no usual distinction between higher median right-sided and lower median left-sided SI values^{7,19}, pointing to selective cannulation of the left adrenal vein in most cases with the microcatheter. Notably, blood sampling from the common trunk of the inferior phrenic vein and the

left adrenal vein might be the preferable method of AVS due to better potential diagnostic accuracy, technical ease, lower cost and lower risk of vein rupture.⁴⁰

The overall complication rate during the study was low (0.8%). Despite the almost fourfold increase of AVS procedures in the recent period, the between periods complication rates were comparable, with one adrenal hemorrhage due to vein rupture in each period (1.8% *vs.* 0.5%). The observation confirmed that the major determinant of the incidence of such events is the number of AVS performed by each radiologist.¹²

When AVS results were used as the gold standard for lateralization in a subgroup with unequivocal diagnosis of unilateral ($LI > 4$) or bilateral ($LI < 3$) disease, CT misdiagnosed the primary aldosteronism subtype in 41% of our patients despite reassessment of all normal scans at our interdisciplinary meetings. If we had relied only on imaging, 20/71 (28%) patients would have been incorrectly denied adrenalectomy and treated medically. In addition, 49/100 (49%) patients with bilateral primary aldosteronism would have been sent to unilateral adrenalectomy, and 6/77 (8%) patients with unilateral primary aldosteronism would have had removed the normal-functioning adrenal (Figure 7). By contrast, Mulatero *et al.* demonstrated much higher agreement of AVS and CT (77%) when imaging was performed by the same highly motivated radiologist.⁴¹ Nevertheless, the proportion of discordant AVS and CT results in our cohort closely resembles the findings of a systematic review of 38 diagnostic studies on 950 patients, where CT (or MRI) might have missed the type of primary aldosteronism in 37.8% of cases.⁸

Ultimately, 44% of our patients lateralized on AVS, which represents a slightly higher prevalence of unilateral disease than traditionally reported.^{4,7} Yet this finding was not unexpected, because several clinical characteristics of our cohort, *e.g.* high median number of antihypertensives, prevalent spontaneous hypokalemia and higher median aldosterone values, pointed towards more severe disease, which is consistent with unilateral primary aldosteronism. We used the most stringent LI cut-off (> 4), which is favored by the expert consensus for ACTH-stimulated AVS, in order to avoid false-positives and ensure highest possible cure rates.^{10,20,21} Only four out of 21 patients with borderline LI values (3–4) were referred to surgery. Use of contralateral gland suppression (*e.g.* lower aldosterone to cortisol ratio than the same ratio in IVC) might be potentially helpful to determine lat-

eralization in intermediate cases^{8,10,38} but was not employed during the study period. Using our conservative approach to make surgical decision, close to 100% of operated patients at our center achieved complete biochemical remission of primary aldosteronism according to the international PASO outcome consensus.⁵

Adrenalectomy was recommended to all patients who lateralized on AVS, however a substantial proportion (14%) was ultimately treated medically. Only patients older than 40 years changed their mind and decided against the operation. These outcomes stress the importance of careful selection of patients for AVS and operation.²⁸ Most appropriate candidates desire surgery and have a high probability of unilateral primary aldosteronism. On the other hand, AVS is not needed in individuals who prefer medical therapy and in those who are not suitable for surgery due to comorbidities or age.^{21,42} A simple clinical prediction criterion could probably identify some patients with bilateral primary aldosteronism who should avoid unnecessary AVS and be treated medically.¹⁸ Last but not least, the primary aldosteronism surgical outcome predictor might help finding patients who are expected to attain long-term blood pressure control after adrenalectomy to guide preoperative patient counseling and final decision for or against AVS and surgery.⁴³

There are some limitations of the present study. Primarily, the outcomes were deduced from a retrospective analysis. However, all relevant clinical and laboratory data were logged into our AVS database virtually without missing values. Furthermore, discontinuation and/or adjustment of the antihypertensive agents before and during AVS could probably have been more rigorous, especially during the early years. Still, hypokalemia was always corrected, mineralocorticoid antagonists and potassium-wasting diuretics were discontinued on time. Most patients had resistant hypertension, so we mostly followed the expert recommendation that less interfering antihypertensive medications may be used if PRA, which was routinely measured before AVS, remained suppressed.^{20,21} ACTH stimulation might have the potential to mask lateralization of aldosterone production in patients with adenomas simultaneously producing cortisol, which appears more frequently than we thought earlier.^{10,44} During the study dexamethasone suppression testing to detect this entity was recommended only in rare patients with relatively large adrenal tumors of ≥ 3 cm and not routinely.^{4,17} Consequently, another possible source of error

might have been unrecognized autonomous cortisol cosecretion in some patients. Finally, the technical advances in AVS techniques over the 15-year study period and their impact on the AVS success rate might not have been emphasized enough.

The main strength of our study is that our results were derived from a relatively large and a well-defined national cohort. Management of the patients was standardized and followed the Endocrine Society clinical guidelines whenever feasible^{4,17}, which can significantly decrease the selection bias.

Conclusions

Based on the present study, we conclude that the introduction of a dedicated radiologist with higher workload and regular use of intra-procedural CBCT since 2012 have significantly enhanced the AVS performance at our center. In the future, we aim to improve the concordance of AVS results with CT findings by revising our interdisciplinary strategy with radiologists. We will also address the protocols for the selection of appropriate candidates for AVS, since we demonstrated that a substantial number of patients with proven unilateral primary aldosteronism did not proceed to surgery.

Acknowledgements

The authors would like to thank Marjana Turk Jerovsek, M.D. and Barbara Robnik, M.D. for their work with the AVS database. We appreciate the assistance of Vlasta Hocevar and Mateja Adamlje, RNs.

References

1. Monticone S, Burrello J, Tizzani D, Bertello C, Viola A, Buffolo F, et al. Prevalence and clinical manifestations of primary aldosteronism encountered in primary care practice. *J Am Coll Cardiol* 2017; **69**: 1811-20. doi: 10.1016/j.jacc.2017.01.052
2. Savard S, Amar L, Plouin PF, Steichen O. Cardiovascular complications associated with primary aldosteronism: a controlled cross-sectional study. *Hypertension* 2013; **62**: 331-6. doi: 10.1161/HYPERTENSIONAHA.113.01060
3. Monticone S, Sconfienza E, D'Ascenzo F, Buffolo F, Satoh F, Sechi LA, et al. Renal damage in primary aldosteronism: a systematic review and meta-analysis. *J Hypertens* 2020; **38**: 3-12. doi: 10.1097/HJH.0000000000002216
4. Funder JW, Carey RM, Mantero F, Murad MH, Reincke M, Shibata H, et al. The management of primary aldosteronism: case detection, diagnosis, and treatment: an endocrine society clinical practice guideline. *J Clin Endocrinol Metab* 2016; **101**: 1889-916. doi: 10.1210/jc.2015-4061

5. Williams TA, Lenders JWM, Mulatero P, Burrello J, Rottenkolber M, Adolf C, et al. Outcomes after adrenalectomy for unilateral primary aldosteronism: an international consensus on outcome measures and analysis of remission rates in an international cohort. *Lancet Diabetes Endocrinol* 2017; **5**: 689-99. doi: 10.1016/S2213-8587(17)30135-3
6. Hundemer GL, Curhan GC, Yozamp N, Wang M, Vaidya A. Cardiometabolic outcomes and mortality in medically treated primary aldosteronism: a retrospective cohort study. *Lancet Diabetes Endocrinol* 2018; **6**: 51-9. doi: 10.1016/S2213-8587(17)30367-4
7. Young WF. Diagnosis and treatment of primary aldosteronism: practical clinical perspectives. *J Intern Med* 2019; **285**: 126-48. doi: 10.1111/joim.12831
8. Kempers MJ, Lenders JW, van Outhusden L, van der Wilt GJ, Kool LJS, Hermus AR, et al. Systematic review: diagnostic procedures to differentiate unilateral from bilateral adrenal abnormality in primary aldosteronism. *Ann Intern Med* 2009; **151**: 329-37. doi: 10.7326/0003-4819-151-5-200909010-00007
9. Lim V, Guo Q, Grant CS, Thompson GB, Richards ML, Farley DR, et al. Accuracy of adrenal imaging and adrenal venous sampling in predicting surgical cure of primary aldosteronism. *J Clin Endocrinol Metab* 2014; **99**: 2712-19. doi: 10.1210/jc.2013-4146
10. Wolley M, Thuzar M, Stowasser M. Controversies and advances in adrenal venous sampling in the diagnostic workup of primary aldosteronism. *Best Pract Res Clin Endocrinol Metab* 2020; **34**: 101400. doi: 10.1016/j.beem.2020.101400
11. Monticone S, Satoh F, Dietz AS, Goupil R, Lang K, Pizzolo F, et al. Clinical management and outcomes of adrenal hemorrhage following adrenal vein sampling in primary aldosteronism. *Hypertension* 2016; **67**: 146-52. doi: 10.1161/HYPERTENSIONAHA.115.06305
12. Rossi GP, Barisa M, Allolio B, Auchus RJ, Amar L, Cohen D, et al. The Adrenal Vein Sampling International Study (AVIS) for identifying the major subtypes of primary aldosteronism. *J Clin Endocrinol Metab* 2012; **97**: 1606-14. doi: 10.1210/jc.2011-2830
13. Busser WMH, Arntz MJ, Jenniskens SFM, Deinum J, Hoogeveen YL, de Lange F, et al. Image registration of cone-beam computer tomography and pre-procedural computer tomography aids in localization of adrenal veins and decreasing radiation dose in adrenal vein sampling. *Cardiovasc Intervent Radiol* 2015; **38**: 993-7. doi: 10.1007/s00270-014-0969-z
14. Ringe K, Wacker F, Terkamp C, Meyer B. Value of additional cone-beam CT acquisitions for adrenal vein sampling. [Abstract]. *J Vasc Interv Radiol* 2017; **28(Suppl)**: S139-40. Abstract No. 321. doi: 10.1016/j.jvir.2016.12.937
15. Maruyama K, Sofue K, Okada T, Koide Y, Ueshima E, Iguchi G, et al. Advantages of intraprocedural unenhanced ct during adrenal venous sampling to confirm accurate catheterization of the right adrenal vein. *Cardiovasc Intervent Radiol* 2019; **42**: 542-51. doi: 10.1007/s00270-018-2135-5
16. Meyrignac O, Arcis É, Delchier M-C, Mokrane F-Z, Darcourt J, Rousseau H, et al. Impact of cone beam - CT on adrenal vein sampling in primary aldosteronism. *Eur J Radiol* 2020; **124**: 108792. doi: 10.1016/j.ejrad.2019.108792
17. Funder JW, Carey RM, Fardella C, Gomez-Sanchez CE, Mantero F, Stowasser M, et al. Case detection, diagnosis, and treatment of patients with primary aldosteronism: an endocrine society clinical practice guideline. *J Clin Endocrinol Metab* 2008; **93**: 3266-81. doi: 10.1210/jc.2008-0104
18. Kocjan T, Janez A, Stankovic M, Vidmar G, Jensterle M. A new clinical prediction criterion accurately determines a subset of patients with bilateral primary aldosteronism before adrenal venous sampling. *Endocr Pract* 2016; **22**: 587-94. doi: 10.4158/EP15982.OR
19. Young WF, Stanson AW, Thompson GB, Grant CS, Farley DR, van Heerden JA. Role for adrenal venous sampling in primary aldosteronism. *Surgery* 2004; **136**: 1227-35. doi: 10.1016/j.surg.2004.06.051
20. Rossi GP, Auchus RJ, Brown M, Lenders JWM, Naruse M, Plouin PF, et al. An expert consensus statement on use of adrenal vein sampling for the subtyping of primary aldosteronism. *Hypertension* 2014; **63**: 151-60. doi: 10.1161/HYPERTENSIONAHA.113.02097
21. Monticone S, Viola A, Rossato D, Veglio F, Reincke M, Gomez-Sanchez C, et al. Adrenal vein sampling in primary aldosteronism: towards a standardised protocol. *Lancet Diabetes Endocrinol* 2015; **3**: 296-303. doi: 10.1016/S2213-8587(14)70069-5
22. Berney M, Maillard M, Doenz F, Matter M, Pechère-Bertschi A, Burnier M, et al. Clinical determinants of adrenal vein sampling success. *Cardiovasc Med* 2015; **18**: 246-51. doi: 10.4414/cvm.2015.00352
23. Chayovan T, Limumpornpetch P, Hongsakul K. Success rate of adrenal venous sampling and predictors for success: a retrospective study. *Pol J Radiol* 2019; **84**: e136-e141. doi: 10.5114/pjr.2019.84178
24. Rossi GP, Rossitto G, Amar L, Azizi M, Riestler A, Reincke M, et al. Clinical outcomes of 1625 patients with primary aldosteronism subtyped with adrenal vein sampling. *Hypertension* 2019; **74**: 800-8. doi: 10.1161/HYPERTENSIONAHA.119.13463
25. Vonend O, Ockenfels N, Gao X, Allolio B, Lang K, Mai K, et al. Adrenal venous sampling: evaluation of the German Conn's registry. *Hypertension* 2011; **57**: 990-5. doi: 10.1161/HYPERTENSIONAHA.110.168484
26. Doppman JL, Gill JR. Hyperaldosteronism: sampling the adrenal veins. *Radiology* 1996; **198**: 309-12. doi: 10.1148/radiology.198.2.8596821
27. Daunt N. Adrenal vein sampling: how to make it quick, easy, and successful. *Radiogr Rev Publ Radiol Soc N Am Inc* 2005; **25 (Suppl 1)**: S143-58. doi: 10.1148/rg.25si055514
28. Young WF, Stanson AW. What are the keys to successful adrenal venous sampling (AVS) in patients with primary aldosteronism? *Clin Endocrinol* 2009; **70**: 14-7. doi: 10.1111/j.1365-2265.2008.03450.x
29. Siracuse JJ, Gill HL, Epelboym I, Clarke NC, Kabutey N-K, Kim I-K, et al. The vascular surgeon's experience with adrenal venous sampling for the diagnosis of primary hyperaldosteronism. *Ann Vasc Surg* 2014; **28**: 1266-70. doi: 10.1016/j.avsg.2013.10.009
30. Jakobsson H, Farmaki K, Sakinis A, Ehn O, Johannsson G, Ragnarsson O. Adrenal venous sampling: the learning curve of a single interventionalist with 282 consecutive procedures. *Diagn Interv Radiol* 2018; **24**: 89-93. doi: 10.5152/dir.2018.17397
31. Yoneda T, Karashima S, Kometani M, Usukura M, Demura M, Sanada J, et al. Impact of new quick gold nanoparticle-based cortisol assay during adrenal vein sampling for primary aldosteronism. *J Clin Endocrinol Metab* 2016; **101**: 2554-61. doi: 10.1210/jc.2016-1011
32. Chang C-C, Lee B-C, Chang Y-C, Wu V-C, Huang K-H, Liu K-L, et al. Comparison of C-arm computed tomography and on-site quick cortisol assay for adrenal venous sampling: a retrospective study of 178 patients. *Eur Radiol* 2017; **27**: 5006-14. doi: 10.1007/s00330-017-4930-9
33. Laurent I, Astère M, Zheng F, Chen X, Yang J, Cheng Q, et al. Adrenal venous sampling with or without adrenocorticotrophic hormone stimulation: meta-analysis. *Clin Endocrinol Metab* 2018. [Ahead of print].; doi: 10.1210/jc.2018-01324
34. Rossitto G, Amar L, Azizi M, Riestler A, Reincke M, Degenhart C, et al. Subtyping of primary aldosteronism in the avis-2 study: assessment of selectivity and lateralization. *J Clin Endocrinol Metab* 2020; **105**: dgz017. doi: 10.1210/clinem/dgz017
35. Rossitto G, Battistel M, Barbiero G, Bisogni V, Maiolino G, Diego M, et al. The subtyping of primary aldosteronism by adrenal vein sampling: sequential blood sampling causes factitious lateralization. *J Hypertens* 2018; **36**: 335-43. doi: 10.1097/HJH.0000000000001564
36. Noda Y, Goshima S, Nagata S, Kawada H, Tanahashi Y, Kato T, et al. Utility of microcatheter in adrenal venous sampling for primary aldosteronism. *Br J Radiol* 2020; **93**: 20190636. doi: 10.1259/bjr.20190636
37. Almarzooqi M-K, Chagnon M, Soulez G, Giroux M-F, Gilbert P, Oliva VL, et al. Adrenal vein sampling in primary aldosteronism: concordance of simultaneous vs sequential sampling. *Eur J Endocrinol* 2017; **176**: 159-67. doi: 10.1530/EJE-16-0701
38. Mulatero P, Bertello C, Sukor N, Gordon R, Rossato D, Daunt N, et al. Impact of different diagnostic criteria during adrenal vein sampling on reproducibility of subtype diagnosis in patients with primary aldosteronism. *Hypertension* 2010; **55**: 667-73. doi: 10.1161/HYPERTENSIONAHA.109.146613.
39. Lethielleux G, Amar L, Raynaud A, Plouin P-F, Steichen O. Influence of diagnostic criteria on the interpretation of adrenal vein sampling. *Hypertension* 2015; **65**: 849-54. doi: 10.1161/HYPERTENSIONAHA.114.04812
40. Umakoshi H, Wada N, Ichijo T, Kamemura K, Matsuda Y, Fuji Y, et al. Optimum position of left adrenal vein sampling for subtype diagnosis in primary aldosteronism. *Clin Endocrinol (Oxf)* 2015; **83**: 768-73. doi: 10.1111/cen.12847

41. Mulatero P, Bertello C, Rossato D, Mengozzi G, Milan A, Garrone C, et al. Roles of clinical criteria, computed tomography scan, and adrenal vein sampling in differential diagnosis of primary aldosteronism subtypes. *J Clin Endocrinol Metab* 2008; **93**: 1366-71. doi: 10.1210/jc.2007-2055
42. Kocjan T. Rational approach to a patient with suspected primary aldosteronism. In: Lew JI, editor. *Clinical management of adrenal tumors*. InTech; 2017. doi: 10.5772/66965
43. Burrello J, Burrello A, Stowasser M, Nishikawa T, Quinkler M, Prejbisz A, et al. The primary aldosteronism surgical outcome score for the prediction of clinical outcomes after adrenalectomy for unilateral primary aldosteronism. *Ann Surg* 2019; [Ahead of print]. doi: 10.1097/SLA.0000000000003200
44. Arlt W, Lang K, Sitch AJ, Dietz AS, Rhayem Y, Bancos I, et al. Steroid metabolome analysis reveals prevalent glucocorticoid excess in primary aldosteronism. *JCI Insight* 2017; **2**: e93136. doi: 10.1172/jci.insight.93136

Adnexal masses characterized on 3 tesla magnetic resonance imaging - added value of diffusion techniques

Julia Dimova¹, Dora Zlatareva¹, Rumiana Bakalova^{2,3,4}, Ichio Aoki^{3,4}, George Hadjidekov^{2,5}

¹ Department of Diagnostic Imaging, Medical University, Sofia, Bulgaria

² Department of Physics, Biophysics and Radiology, Sofia University "St. Kliment Ohridski", Sofia, Bulgaria

³ Department of Molecular Imaging and Theranostics and

⁴ Group of Quantum-state Controlled MRI, National Institutes for Quantum and Radiological Science and Technology (QST/NIRS), Chiba, Japan

⁵ Department of Radiology, University Hospital "Lozenetz", Sofia, Bulgaria

Radiol Oncol 2020; 54(4): 419-428.

Received 19 June 2020

Accepted 14 September 2020

Correspondence to: Prof. George Hadjidekov, M.D., University Hospital Lozenetz, Department of Radiology, Koziak 1 str. 1407 Sofia, Bulgaria, E-mail: jordiman76@yahoo.com

Disclosure: No potential conflicts of interest were disclosed.

Background. To assess different types of adnexal masses as identified by 3T MRI and to discuss the added value of diffusion techniques compared with conventional sequences.

Patients and methods. 174 women age between 13 and 87 underwent an MRI examination of the pelvis for a period of three years. Patients were examined in two radiology departments – 135 of them on 3 Tesla MRI Siemens Verio and 39 on 3 Tesla MRI Philips Ingenia. At least one adnexal mass was diagnosed in 98 patients and they are subject to this study. Some of them were reviewed retrospectively. Data from patients' history, physical examination and laboratory tests were reviewed as well.

Results. 124 ovarian masses in 98 females' group of average age 47.2 years were detected. Following the MRI criteria, 59.2% of the cases were considered benign, 30.6% malignant and 10.2% borderline. Out of all masses 58.1% were classified as cystic, 12.9% as solid and 29% as mixed. Of histologically proven tumors 74.4% were benign and 25.6% were malignant. All of the malignant tumors had restricted diffusion. 64 out of all patients underwent contrast enhancement. (34 there were a subject of contraindications). 39 (61%) of the masses showed contrast enhancement.

Conclusions. Classifying adnexal masses is essential for the preoperative management of the patients. 3T MRI protocols, in particular diffusion techniques, increase significantly the accuracy of the diagnostic assessment.

Key words: adnexal masses; 3 Tesla MRI; diagnosis; malignancy; ovarian neoplasms; diffusion restriction

Introduction

Incidental adnexal masses are commonly detected in daily medical practice due to the frequent lack of clinical manifestation.¹ Approximately 9% to 10% of women undergoing ultrasound have ovarian lesions.² Although most commonly used, ultrasound has some limitations including the small field of view, low resolution and interference by obesity or by gaseous bowel loops.³ Ultrasound indeterminate adnexal masses vary between 5% and 25%.^{4,5}

If furthermore examined with computed tomography (CT), distant metastases, respectively the staging of the disease could be assessed. Magnetic resonance (MR) has been considered as the most useful imaging technique for characterizing adnexal formations. This modality has a key role in the preoperative evaluation and their follow-up, identifying the origin of the mass and the different types of tissue contained in with accuracy of 88% to 93%.⁶ 3 Tesla MRI is superior for examining female pelvis due to its higher resolution and the possibil-

ity of providing more detailed images.⁷⁻⁹ MRI techniques such as diffusion-weighted imaging (DWI) and apparent diffusion coefficient (ADC) are of an additional benefit differentiating malignant from benign lesions.¹⁰⁻¹²

The aim of our study is to assess different types of adnexal masses as identified by 3T MRI and to discuss the added value of diffusion and perfusion techniques compared with conventional sequences.

Patients and methods

174 women age between 13 and 87 underwent MRI examination of the pelvis for a period of three years. Indications were: sonographically detected pelvic mass; or gynecological complaints; or history of previous adnexal tumor; or family history of ovarian cancer. Six women were examined for other reasons (hips, sigma/colon or perianal abscess), nine for uterine pathology, but adnexal mass was detected and the complete gynecological MRI protocol was performed, too. At least one adnexal mass was diagnosed in 98 patients and they are subject of this study. 51% of them were reviewed retrospectively. Data from patients' history, physical examination and laboratory tests were reviewed as well.

Patients were examined in two radiology departments, 135 of them on 3 Tesla MRI Siemens Verio and the 39 on 3 Tesla MRI Philips Ingenia. The Siemens MRI protocol included: coronal (COR) T1; sagittal (SAG) T2; paracoronar and paratransversal of the uterus T2 with and without fat saturation; SAG T1; transversal T1 Vibe Dixon; DWI and ADC. The Philips MRI protocol included: COR STIR; SAG T2; COR T2; COR T1; axial (AX) T2; AX T2 with fat saturation; DWI and ADC. (Table 1)

Measurement of the ADC value was carried out for all ovarian masses in our study. For each tumor a region of interest (ROI: 1 cm²) was manually defined. In the mixed malignant formations ROIs were placed on the solid component only. The ADC values are presented as numerical value x 10⁻³ mm²/s representing quantitative metric.

Intravenous contrast administration was applied when needed and when there were no contraindications. A macrocyclic contrast agent Gadobutrol [1.0 mmol/ml] (Gadovist® 1.0, Bayerhealthcare, Berlin, Germany) was used at a dose of 0.1 mmol/kg in all contrast-enhanced studies on both MR devices. Injection rate of 0.5 mL/sec was performed in order to achieve equimolar amounts of gadolin-

ium. Saline flush (25–30 ml) at the same flow rate followed the contrast administration.

In part of our cases dynamic contrast enhanced – magnetic resonance imaging (DCE-MRI) was performed and time-signal intensity curve (TIC) was generated using the Mean Curve software package (Philips). A round region of interest (ROI: 1 cm²) was placed at target areas referring to T2W and contrast-enhanced images. Areas with hemorrhage and necrosis were avoided.

The following patterns were evaluated on MR images:

- tumor appearance (cystic, solid or mixed)
- uni- or bilateral ovaries involvement
- size of the mass
- adipose tissue presence or not
- signal intensity on T2 weighted images
- diffusion restriction
- wall thickness
- presence or not of septa
- papillary projections
- presence or not of ascites
- lymph nodes involvement and metastases

Following MR criteria of malignancy, as reported in the literature (by Jeong *et al.*¹³, Valentini *et al.*⁶ and El-Wekil *et al.*¹⁴), are used:

- lesion size more than 4 cm
- solid components with heterogeneous enhancement
- papillary projections
- septa thick more than 3 mm
- areas of necrosis and breaking down
- lymph nodes involvement sized more than 1 cm.

SPSS Statistics release 21 for Microsoft Windows was used to perform Kolmogorov-Smirnov (2-tailed) test for establishing correlations between malignancy and diffusion restriction and between malignancy and type of mass.

Approval was obtained from the Institutional Review Board of both University hospitals prior the initiation of the study. Informed written consent was obtained from each patient. Personal identity information of all patients was protected.

Results

In 98 females of average age 47.2 years, a total of 124 ovarian masses were detected. In 16 of the patients (16.3%) additional uterine pathology was found. One case considered as an ovarian cyst was histologically proven to be an inclusion peritoneal

TABLE 1. 3 Tesla Siemens and 3 Tesla Philips MRI protocols

SIEMENS VERIO 3.0T							
	FOV (mm)	Matrix (mm)	Slice thickness (mm)	TR (ms)	TE (ms)	Voxel size (mm)	TA (min)
T1 COR	300	390/320	5	500	8.7	0.9×0.9×5.0	01:36
T2 SAG	200	320/320	4	3300	133	0.6×0.6×4.0	03:44
T2 paracor	200	320/320	4	3700	140	0.6×0.6×4.0	03:24
T2 paracor +FS	200	256/256	4	3700	131	0.8×0.8×4.0	01:58
T2 paratra	200	320/320	4	3740	148	0.6×0.6×4.0	03:29
T2 paratra + FS	200	256/256	4	3700	138	0.8×0.8×4.0	02:13
T1 SAG	160	217/192	4	569	12	0.4×0.4×4.0	03:44
T1 vibe dixon AX	380	188/320	3.5	3.92	1.27	0.6×0.6×3.5	00:19
DWI AX (b50-400-800)	360	100/128	5	4700	57	1.4×1.4×5.0	02:49
POST C							
T1 vibe dixon AX	380	188/320	3.5	3.92	1.27	0.6×0.6×3.5	00:19
T1 SAG	160	217/192	4	569	12	0.4×0.4×4.0	03:44
T1 COR	300	390/320	5	500	8.7	0.9×0.9×5.0	01:36
PHILIPS INGENIA 3.0T							
COR STIR	340	228/186	5	5622	50	1.5×1.5×5.0	03:45
T2 SAG	229	208/208	3	3776	100	1.1×1.1×3.0	03:01
COR T2	315	392/297	5	4846	90	0.8×1.6×5.0	01:56
COR T1	315	392/315	5	483	8	0.8×1.2×5.0	02:11
AX T2	261	328/251	5	4805	100	0.8×1.0×5.0	02:05
AX T2 FS	261	236/208	5	4346	80	1.11×1.25×5.0	02:37
DWI 3b 0,100,800	375	124/106	4	5299	77	3.0×3.0×4.0	01:51
POST C							
MDixon AX	240	220/222	3.5	5.4	1.96	1.09×1.08×3.5	02:58
COR T1 FS	315	392/309	5	519	8	0.8×1.02×5.0	02:17

AX = axial; COR = coronal; COR STIR = coronal short tau inversion recovery; DWI = diffusion-weighted imaging; FS = fat sat; paracor = paracoronar; SAG = sagittal

cyst. The results of all ovarian masses according to their MRI features are listed in Table 2.

Following the MRI criteria, 59.2% of the cases were considered benign, 30.6% malignant and 10.2% borderline. The results of DWI sequences show a statistically significant correlation with the assessment of masses as benign/borderline/malignant. 34.3% of all malignant cases were found in the age group 61–70. Of all patients 32 were tested for CA-125 tumor marker and 12 had elevated levels. Only half of those 12 cases were histologically proven malignant.

The biggest diameter of all 124 ovarian masses was measured – the largest one was 216 mm, the smallest one was under 10 mm. 54% of all tumors had diameter larger than 4 cm.

58.1% out of all masses were classified as cystic, 12.9% as solid and 29% as mixed. In four cases both solid and cystic masses were found in the same patient. Of all ovarian tumors 37 (29.8%) had wall thickness greater than 3 mm, 16 (12.9%) had papillary projections and 41 (33%) were septated. Only 6 masses of all contained fat, 5 of them were histologically proven to be mature teratomas. Kolmogorov-Smirnov test shows a statistically significant correlation between the type of mass and the assessment of masses as benign/borderline/malignant.

Of histologically proven tumors 74.4% were benign and 25.6% were malignant. All masses classified on MRI as benign were identified correctly. Two masses, described as suspicious and malignant, turned out to be benign. All of the malignant

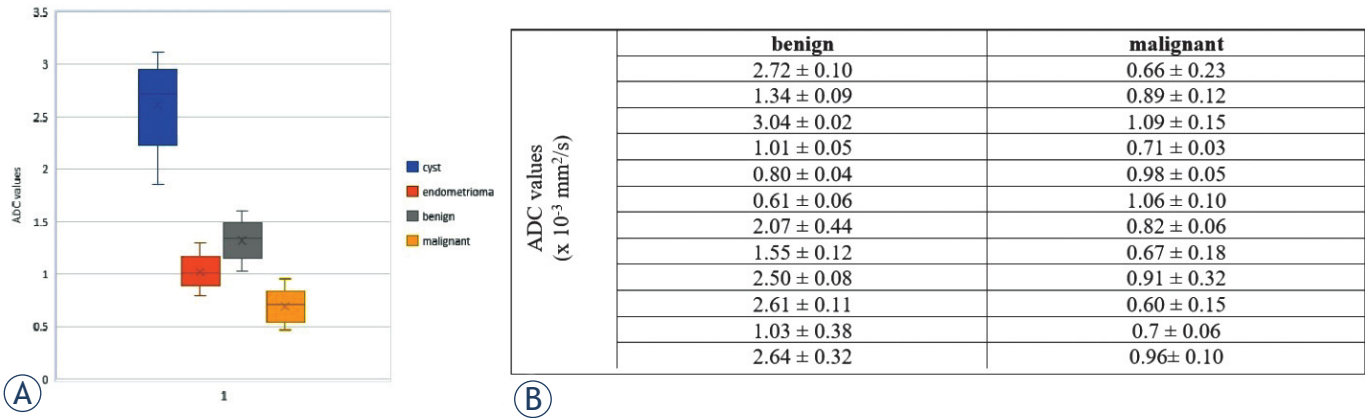


FIGURE 1. (A) Box plot presenting ADC values in four different types of adnexal tumors – highest ADC value found in a simple cyst; lowest found in a malignant tumor. **(B)** Mean apparent diffusion coefficient (ADC) values of twelve patients with histologically proven benign adnexal lesion and twelve patients with histologically proven malignant adnexal lesion. All values are expressed as mean value ± standard deviation (SD) x 10⁻³ mm²/s.

tumors had restricted diffusion. The calculated ADC values of malignant adnexal masses are significantly lower than the ADC values of benign masses. Exceptions were found for endometrioma ($1.01 \pm 0.05 \times 10^{-3} \text{ mm}^2/\text{s}$); mature teratoma ($0.80 \pm 0.04 \times 10^{-3} \text{ mm}^2/\text{s}$) and chronic abscess (0.61 ± 0.06

$\times 10^{-3} \text{ mm}^2/\text{s}$) – all of them presenting lower ADC values. (Figure 1) 72.7% of malignant neoplasms were mixed masses, 18.2% were solid and only one (9.1%) was cystic. Compared to them, 75% of benign tumors were cystic.

64 out of all 98 patients underwent contrast enhancement. 34 there were a subject of contraindications (history of previous allergic reactions to the contrast agent, elevated levels of serum creatinine or patient refusal). 39 (61%) of the masses showed enhancement. Three were classified as benign and four – as suspicious. 32 of the enhanced tumors were identified as malignant.

Ascites was found in 33 of the cases – in 15 of which is located only in the pouch of Douglas. In 15.3% of the cases, enlarged lymph nodes with diffusion restriction were found – all in patients with malignant masses and one with a proven chronic inflammatory process. In 15 cases enlarged metastatic locoregional lymph nodes were found. Eight patients had peritoneal deposits; four patients liver metastases; three patients bone metastases, two patients were with urinary bladder invasion and one patient had adrenal metastasis. In all cases with metastases three turned out to be from uterine cancer (ovarian masses in these cases were proven benign).

TABLE 2. Results of 124 ovarian masses according to their MRI features

	Malignant	Benign	Borderline
Cystic masses	5/41 (12.2%)	61/71 (85.9%)	6/12 (50%)
Solid masses	10/41 (24.4%)	4/71 (5.6%)	2/12 (16.6%)
Mixed masses	26/41 (63.4%)	6/71 (8.5%)	4/12 (33.4%)
Cases with one ovary involvement	18/30 (60%)	46/58 (79.3%)	9/10 (90%)
Cases with both ovaries' involvement	12/30 (40%)	12/58 (20.7%)	1/10 (10%)
Size of the mass (more than 4 cm)	37/41 (90.2%)	22/71 (31%)	8/12 (66.7%)
Masses with adipose tissue presence	-	5/71 (7%)	1/12 (8.3%)
Masses with high signal intensity in T2WI	5/41 (12.2%)	42/71 (59.1%)	5/12 (41.6%)
Masses with low signal intensity in T2WI	7/41 (17.1%)	18/71 (25.4%)	1/12 (8.4%)
Heterogeneous masses	29/41 (70.7%)	11/71 (15.5%)	6/12 (50%)
Diffusion restriction	39/41 (95.1%)	19/71 (26.8%)	7/12 (58.4%)
Wall thickness (more than 3 mm)	20/41 (48.8%)	12/71 (16.9%)	5/12 (41.7%)
Presence of septa	25/41 (61%)	11/71 (15.5%)	5/12 (41.7%)
Papillary projections presented	14/41 (34.1%)	-	2/12 (16.6%)
Cases with presence of ascites	16/30 (53.3%)	15/58 (25.9%)	2/10 (20%)
Lymph nodes involvement and metastases	20/30 (66.6%)	3/58* (5.2%)	1/10 (10%)

T2WI = T2 weighted imaging

Discussion

Assessing different types of adnexal lesions is important preoperatively. We find a number of reasons about the value of 3 Tesla MRI in such differentiation.

The MRI gynecological protocols we used concur the ESUR Quick Guide to Female Pelvis

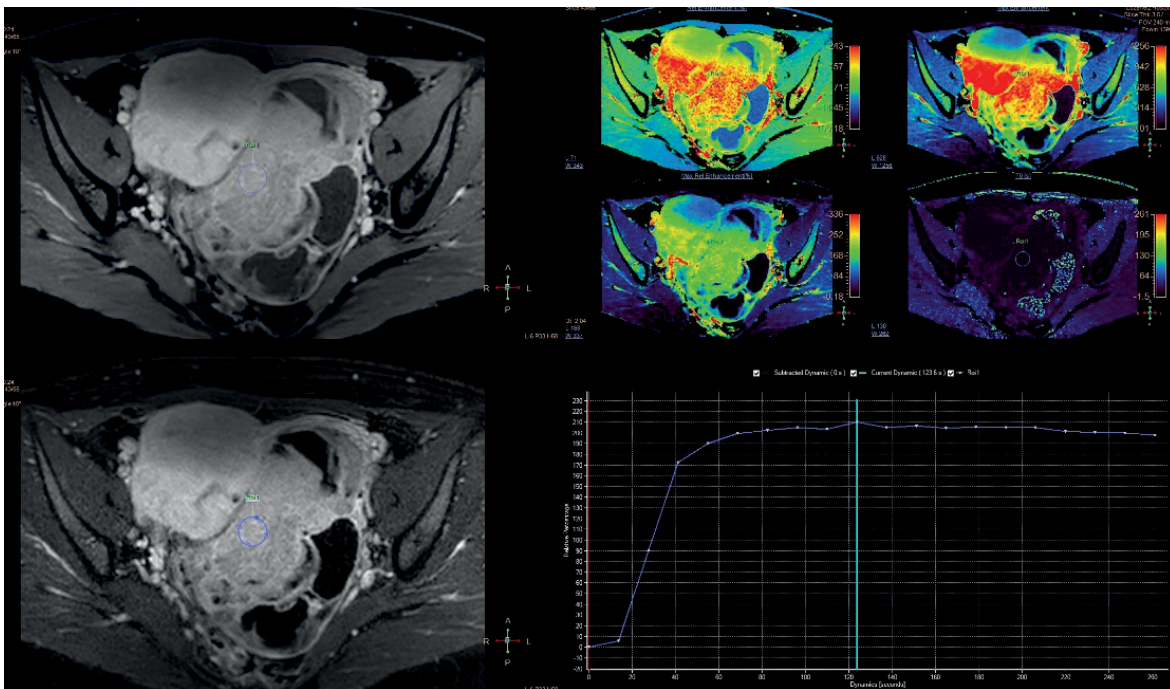


FIGURE 2. Type III time intensity curve (TIC) of a malignant adnexal mass.

Imaging, 1.0 from 2019.¹⁵ Classical sequences (T1, T2) combined with post-gadolinium sequences and diffusion techniques provide reliable information on the nature of the adnexal masses.

It is known from previous studies that dynamic contrast enhanced MRI (DCE-MRI) is helpful in characterizing adnexal tumors. It could discriminate malignant from benign masses. According to the study of Thomassin-Naggara *et al.* there are three types of TIC showing benign, borderline and malignant ovarian tumors. Figure 2 demonstrates representative Type III curve of a malignant adnexal mass.

The number of patients (98) in our study exceeds those of similar ones known from the literature (30 in El-Wakil *et al.*¹⁴ and 58 in Koc *et al.*¹⁶). The average age of patients (47.2 years) as well differs respectably by seven and four years from the cited studies.^{14,16}

The WHO histological classification (according to Foti *et al.*¹⁷) divides primary ovarian masses into three main categories: epithelial, germ cell and sex cord-stromal tumors. Metastatic tumors are classified in a separate category. In 2016 Meinhold-Heerlein *et al.* revised the WHO classification introducing seromucinous tumors as a new entity.¹⁸ Our study includes 14 histologically different groups of ovarian masses – ten benign and four

TABLE 3. Diffusion MRI appearance of histologically different groups

Histopathological findings	DWI restricted	DWI Facilitated
Simple cyst	-	5
Inclusion cyst	-	1
Abscess	1	-
Endometrioma	12	5
Teratoma	5	-
Serous cystadenoma	-	2
Mucinous cystadenoma	1	1
Serous adenofibroma	1	-
Serous cystadenofibroma	1	-
Brenner tumor	-	1
Seromucinous carcinoma	2	-
Serous papillary adenocarcinoma	2	-
Adenosarcoma	1	-
Metastases	6	-

DWI = diffusion-weighted imaging

malignant. Diffusion MRI appearance of histologically different groups is shown in Table 3. Some of the benign formations have diffusion restriction – abscess, endometrioma, mature cystic teratoma

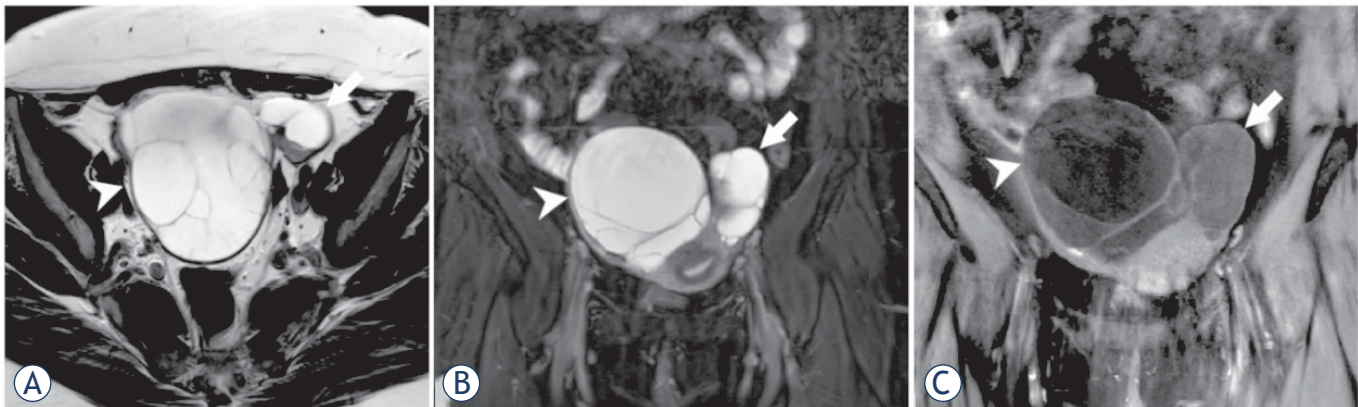


FIGURE 3. 45-year old patient with bilateral adnexal masses; serous papillary cystadenoma (arrow) and mucinous cystadenoma (arrowhead); both masses have predominantly high signal intensity on T2WI and T2WI fat sat (A), (B) and low signal intensity on T1WI fat sat (C).

and serous adenofibroma. In 88% of cases mature cystic teratomas are filled with sebaceous material and are lined with keratinized squamous epithelium¹⁹, compared to the most relevant feature – adipose tissue which is presented in only 67–75%.²⁰ Diffusion restriction is caused by the presence of keratin or Rokitansky nodule and fat globules.²¹ Endometriomas as containing blood and hemosiderin can show diffusion restriction too.^{21,22} Solid areas with similar changes can help the detection of malignant transformation. When it comes to an ovarian abscess, diffusion characteristics depend on the content – in more viscous one the signal intensity is higher on DWI and lower on ADC map.²³ Diffusion techniques could differentiate abscess from cystic or necrotic neoplasm. Neoplasms usually show diffusion restriction peripherally and abscesses centrally.^{22,24} According to cystic degeneration, some adenofibromas also could be characterized by restriction of the water molecules.^{22,25,26}

In this study adnexal masses are classified based on their morphological appearance, similar to Foti *et. al.*¹⁷ and divided into three main groups – cystic, solid and mixed (cystic and solid).

Cystic adnexal masses could be unilocular or multilocular. Some of them have a non-ovarian origin. They are usually benign, with low signal intensity on T1-weighted images and high signal intensity on T2-weighted images.

Peritoneal inclusion cysts and hydrosalpinx are the most common extra ovarian lesions. They occur almost exclusively in premenopausal women and at imaging the ovaries are clearly separated from these cystic formations.^{27,28}

Functional ovarian cysts are the most common finding in women of reproductive age. Follicles are up to 20 mm as the dominant one could be 25 mm. Follicular cysts and corpus luteum cysts are larger and tend to increase if there is internal bleeding. This manifests with an increase of the signal on

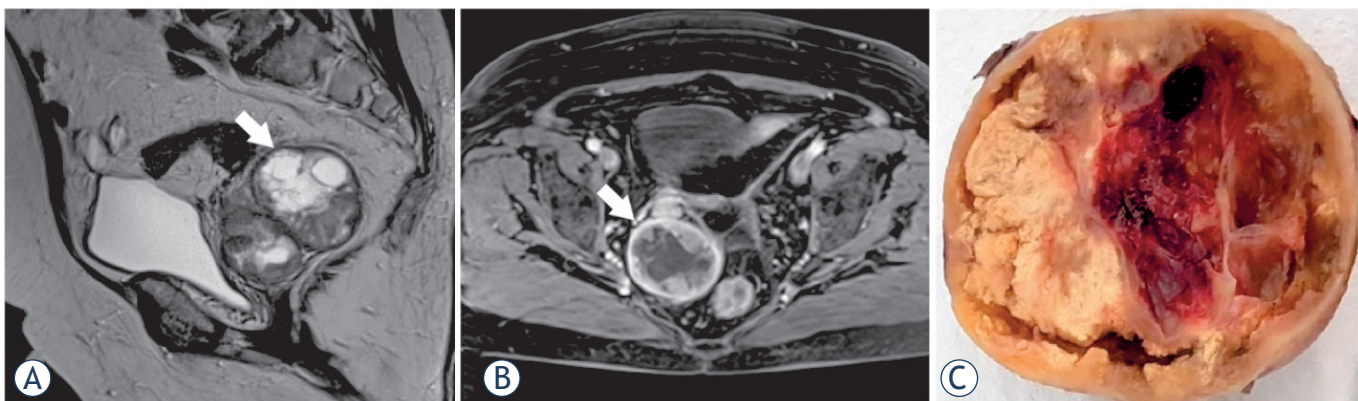


FIGURE 4. 68-year old patient with previous hysterectomy; right serous cystadenofibroma (arrow); complex mass - heterogeneous on T2WI (A) which shows peripheral enhancement on T1WI fat sat with contrast (B). (C) Macroscopic histological preparation of the tumor.

T1-weighted images.^{13,17} They do not usually have diffusion restriction and does not change after contrast administration. Although, in corpus luteum cysts intense wall enhancement may be seen.

Serous cystadenoma and mucinous cystadenoma are benign tumors with thin walls (Figure 3). Mucinous type is usually larger, septated and has variable intensity on both T1- and T2-weighted images based on different mucin concentration. Some loculi are hyperintense on T1-weighted images, forming a pattern known as “honeycomb” or “stained glass”.^{17,29,30} Serous cystadenoma is more often bilateral and its wall could contain small nodules due to fibrosis or calcification.^{31,32} Diffusion restriction could be detected in mucinous cystadenoma due to the dense mucinous material.¹²

Cystadenofibroma is usually a benign epithelial tumor that can present as a complex cystic mass with thick septa and solid component. It could present with plaques and nodules that have low signal intensity on T2-weighted images due to fibrous tissue (Figure 4).³³⁻³⁵

Endometriomas are part of the cystic lesions containing blood products. In addition to that, they characterize with hyperintensity on T1-weighted images and lower signal intensity on T2-weighted images, called “shading sign”. Sometimes these lesions could have high signal intensity on both T1- and T2-weighted images. They do not change their signal intensity on fat-suppressed sequences.^{13,31,36,37} Patients having endometriosis are at risk of developing ovarian malignancies.³⁸ Endometriomas usually do not enhance after contrast administration but could have restricted diffusion.^{11,22}

Mixed ovarian masses containing both cystic and solid parts are always suspicious for malignant – surface epithelial tumors and metastases. The benign representative of this category is mature cystic teratoma.

Mature cystic teratoma is known as the most common ovarian neoplasm that arises from ovarian germ cells.^{13,31} Usually part of this tumor has high signal intensity on T1WI and intermediate on T2WI, fat-fluid or fluid-fluid level, low signal calcification parts and floating debris. It could also have a soft-tissue protuberance called Rokitansky nodule. On fat-suppressed sequences the areas containing fat show drop in signal intensity. Malignant transformation of mature cystic teratoma is rare.^{19,37,39,40} Enhancement after contrast application is not typical. They could represent with restricted diffusion in the areas with keratin and fat globules.^{22,23}

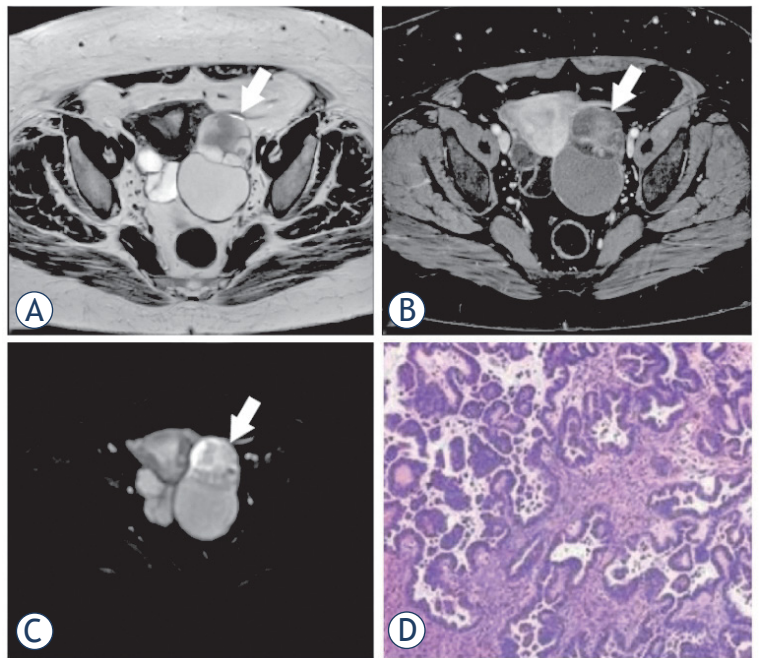


FIGURE 5. 57- year old patient with left serous papillary adenocarcinoma (arrow); predominantly cystic mass with high signal intensity on T2WI (A) and solid component which is enhanced on T1WI fat sat with contrast (B). Part of the mass characterizes with diffusion restriction (C). (D) Microscopy preparation of the tumor.

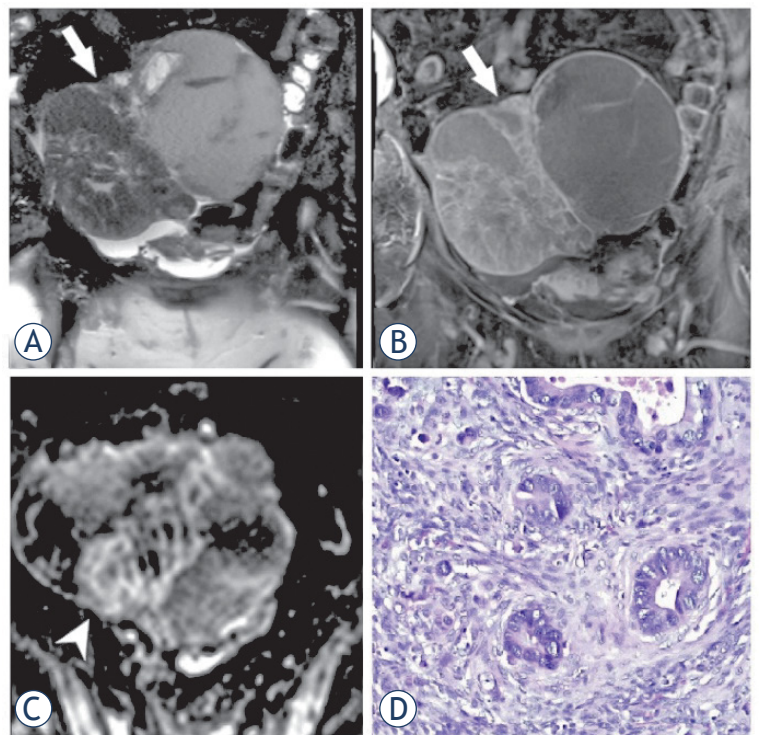


FIGURE 6. 63- year old patient with right ovarian metastasis from adenocarcinoma with intestinal phenotype; complex septated mass with heterogeneous signal intensity on T2WI (A); enhancement mostly in wall and septa on T1WI fat sat with contrast (B); part of the mass (arrowhead) has restricted diffusion; (D) Microscopy preparation of the metastasis.

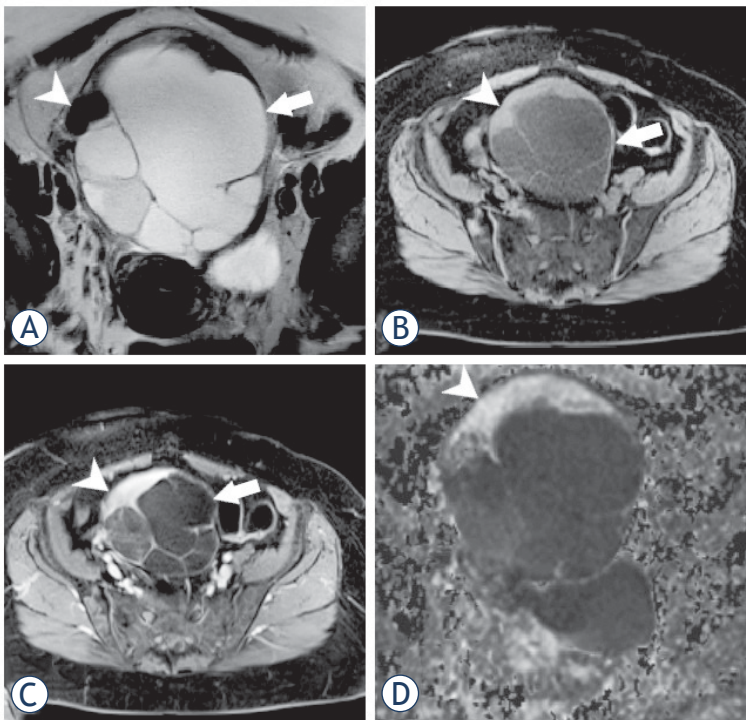


FIGURE 7. 54-year old patient with mucinous cystadenoma (arrow) coexisting with benign Brenner tumor (arrowhead); mucinous cystadenoma has high signal intensity on T2WI (A) and low on T1WI fat sat (B); compared to it Brenner tumor has low signal intensity on T2WI (A) and high on T1WI fat sat (B); on T1 fat sat with contrast (C) only Brenner tumor shows enhancement and on DWI (D) only Brenner tumor shows restricted diffusion.

Serous and mucinous cystadenocarcinoma are the most common epithelial malignancies of the ovaries – 50% and 10% of malignant lesions.⁴¹ Mucinous tumors are larger, lobulated and may be hyperintense on T1WI in addition to the high protein concentration in mucoid material.^{30,42} Cystadenocarcinomas have thick and irregular walls, septations, solid components and papillary projections that have low signal intensity on T2WI with contrast enhancement after contrast administration. Serious fluid part demonstrates with high signal intensity on T2WI (Figure 5). Peritoneal invasion is sometimes discovered.^{17,41} In connection with their malignant nature, a pronounced diffusion restriction is observed.

Ovarian metastases most frequently originate from a primary process in the female genital tract, gastrointestinal tract (Krukenberg tumor) or breast. They are more commonly bilateral and multiloculated. Their solid parts are hypointense on T2WI and enhance after gadolinium administration. Distinguishing them from a primary ovarian process is not easy.^{17,41,43} Ovarian metastases have

high signal intensity on DWI and low on ADC map (Figure 6).

Other less common representatives of mixed ovarian neoplasms are endometrioid tumors, yolk sac tumors and granulosa cell tumors.

Solid ovarian masses could have benign, borderline and malignant behavior. They include all three main histological types – epithelial, germ cell and sex cord tumors and metastases.

The Brenner tumor is a rare epithelial tumor and represents 2% of ovarian neoplasms.⁴⁴ It is usually benign and has largely homogeneous low signal intensity on T1- and T2-weighted images. Its signal intensity is similar to those of fibromas but no cysts and necrosis are found in Brenner tumor. This ovarian tumor can occur in association with mucinous cystadenoma (Figure 7). Mild enhancement is observed after contrast application. Diffusion restriction is not characteristic of benign representatives of this tumor.^{39,45}

Fibromas encounter around 4% of all ovarian tumors. They could mimic malignant neoplasm as their size can vary and may be associated with ascites and pleural effusion (Meig syndrome). Another pathology they should be defined from is pedunculated uterine leiomyoma. These tumors demonstrate low signal intensity on both T1- and T2-weighted images. Scattered areas of high signal intensity could be present on T1WI due to cystic degeneration or edema.^{13,17,35} In this case diffusion restriction may be found. After contrast administration minimal enhancement is evident.

In this study 72.7% of histologically proven malignant neoplasms were mixed cystic and solid, 18.2% were solid and only one (9.1%) was cystic. That statement disagrees with El-Wakil *et al.*¹⁴ where no solid mass was found but cystic masses were 37.5% of their case series. However, 62.5% of tumors in their study were mixed cystic and solid which roughly coincides with our findings.

All of the histologically proven malignant lesions in this study show restricted diffusion. This confirms the literature data that an adnexal mass with higher signal intensity on DWI and lower on ADC map usually is a malignant lesion. Our results confirm the findings of previous studies in the literature that benign adnexal lesions have higher ADC values than the malignant once. We also found some exceptions of this statement concerning endometrioma, mature teratoma and chronic abscess presenting with lower ADC values despite of their benign origin.

Borderline ovarian tumors are usually complex masses that have some of the MR characteristics of

the malignant one. They could show cellular proliferation and moderate nuclear atypia but without stromal invasion.^{46,47} Similar to the study of Bent *et al.*⁴⁶ we identified 11 of the cases as suspicious. All of them demonstrated one or more MRI feature suggestive for malignancy – size more than 4 cm, solid part, cystic part with vegetations and septations, wall thickness more than 3 mm; contrast enhancement. In our study only one of the 10 suspicious cases were bilateral.

CA-125 is established tumor marker for ovarian cancer.^{13,48} Limitation of this study is the small number of CA-125 tests performed before magnetic resonance imaging. Of these, elevated levels of CA-125 were found in 12 patients. Similarly, to other studies, over 60% of our patients with elevated CA-125 levels have proven malignant ovarian lesions.

Concerning unilateral or bilateral adnexal masses, we found malignant to be more often bilateral. Unilateral lesions are more often found in the right adnexa and in younger patients. This study as well as the Zhang *et al.* one⁴⁹ suggests that large sizes and atypical signal intensity may influence the correct assessment of the type of ovarian lesions. The main limitations of our study include the retrospective reviewing of patients with some clinical missing, as well as surgical missing findings in patients who underwent surgery in another hospital.

Conclusions

Classifying adnexal masses is essential for the preoperative management of the patients. 3T MRI protocols, in particular diffusion techniques, increase significantly the accuracy of the diagnostic assessment. Further studies correlated with histological validation would support the role of MRI as a mandatory part of the patients' management.

Acknowledgements

This study was partially supported by the Japanese Society for the Promotion of Science (JSPS) (Grand-in-aid "Kakenhi C" granted to R.B. and the Japanese Agency for Medical Research and Development (AMED) (Project for Cancer Research and Therapeutic Evolution, P-CREATE, no. 16 cm0106202h0001).

References

- Expert Panel on Women's Imaging, Atri M, Alabousi A, Reinhold C, Akin EA, Benson CB, Bhosale PR, et al. ACR Appropriateness Criteria[®] clinically suspected adnexal mass, no acute symptoms. *J Am Coll Radiol* 2019; **16**: S77-93. doi: 10.1016/j.jacr.2019.02.011
- Sharma A, Apostolidou S, Burnell M, Campbell S, Habib M, Gentry-Maharaj A, et al. Risk of epithelial ovarian cancer in asymptomatic women with ultrasound-detected ovarian masses: a prospective cohort study within the UK collaborative trial of ovarian cancer screening (UKCTOCS). *Ultrasound Obstet Gynecol* 2012. **40**: 338-44. doi: 10.1002/uog.12270
- Biggs WS, Marks ST. Diagnosis and management of adnexal masses. *Am Fam Physician* 2016; **93**: 676-81. PMID: 27175840
- Van Calster B, Timmerman D, Valentin L, Mclndoe A, Ghaem-Maghani S, Testa AC, et al. Triaging women with ovarian masses for surgery: observational diagnostic study to compare RCOG guidelines with an International Ovarian Tumour Analysis (IOTA) group protocol. *BJOG* 2012; **119**: 662-71. doi: 10.1111/j.1471-0528.2012.03297.x
- Thomassin-Naggara I, Poncelet E, Jalaguier-Coudray A, Guerra A, Fournier LS, Stojanovic S, et al. Ovarian-adnexal reporting data system magnetic resonance imaging (O-RADS MRI) score for risk stratification of sonographically indeterminate adnexal masses. *JAMA Netw Open* 2020; **3**: e1919896. doi: 10.1001/jamanetworkopen.2019.19896
- Valentini AL, Gui B, Miccò M, Mingote MC, De Gaetano AM, Ninivaggi V, et al. Benign and suspicious ovarian masses-MR imaging criteria for characterization: Pictorial review. *J Oncol* 2012; **2012**: 481806. doi: 10.1155/2012/481806
- Kataoka M, Kido A, Koyama T, Isoda H, Umeoka S, Tamai K, et al. MRI of the female pelvis at 3T compared to 1.5T: evaluation on high-resolution T2-weighted and HASTE images. *J Magn Reson Imaging* 2007; **25**: 527-34. doi: 10.1002/jmri.20842
- Léautaud A, Marcus C, Ben Salem D, Bouché O, Graesslin O, Hoeffel C. *Pelvic MRI at 3.0 Tesla. J Radiol* 2009; **90**: 277-86. doi: 10.1016/s0221-0363(09)72506-5
- Hussain SM, van den Bos IC, Oliveto JM, Martin DR. MR imaging of the female pelvis at 3T. *Magn Reson Imaging Clin N Am* 2006; **14**: 537-44. vii. doi: 10.1016/j.mric.2007.01.008
- Thomassin-Naggara I, Balvay D, Rockall A, Carette MF, Ballester M, Darai E, et al. Added value of assessing adnexal masses with advanced MRI techniques. *Biomed Res Int* 2015; **2015**: 785206. doi: 10.1155/2015/785206
- Davaranpanah AH, Kambadakone A, Holalkere NS, Guimaraes AR, Hahn PF, Lee SI. Diffusion MRI of uterine and ovarian masses: identifying the benign lesions. *Abdom Radiol* 2016; **41**: 2466-75. doi: 10.1007/s00261-016-0909-2
- Dhanda S, Thakur M, Kerkar R, Jagmohan P. Diffusion-weighted imaging of gynecologic tumors: diagnostic pearls and potential pitfalls. *Radiographics* 2014; **34**: 1393-416. doi: 10.1148/rg.345130131
- Jeong YY, Outwater EK, Kang HK. Imaging evaluation of ovarian masses. *Radiographics* 2000; **20**: 1445-70. doi: 10.1148/radiographics.20.5.g00se101445
- El-Wakil A, Mohammad S Abdullah MS, El-Kholy SS. The role of MRI in the differentiation between benign and malignant ovarian lesions. *Menoufia Med J* 2017; **32**: 106-11. doi: 10.4103/mmj.mmj_548_17
- Alt C, Bharwani N, Brunesch L, Danza FM, Derme M, El Sayed RF, et al. *ESUR quick guide to female pelvis imaging 1.0*. 2019: European Society of Urogenital Radiology. [cited 2020 May 15]. Available at: http://www.esur.org/fileadmin/content/2019/ESUR_2019_-_ESUR_Quick_Guide_to_Female_Pelvis_Imaging.pdf
- Koc Z, Erbay G, Ulusan S, Seydaoglu G, Aka-Bolat F. Optimization of b value in diffusion-weighted MRI for characterization of benign and malignant gynecological lesions. *J Magn Reson Imaging* 2012; **35**: 650-9. doi: 10.1002/jmri.22871
- Foti PV, Attinà G, Spadola S, Caltabiano R, Farina R, Palmucci S, et al. MR imaging of ovarian masses: classification and differential diagnosis. *Insights Imaging* 2016; **7**: 21-41. doi: 10.1007/s13244-015-0455-4
- Meinhold-Heerlein I, Fotopoulou C, Harter P, Kurzeder C, Mustea A, Wimberger P, et al. The new WHO classification of ovarian, fallopian tube, and primary peritoneal cancer and its clinical implications. *Arch Gynecol Obstet* 2016; **293**: 695-700. doi: 10.1007/s00404-016-4035-8

19. Outwater EK, Siegelman ES, Hunt JL. Ovarian teratomas: tumor types and imaging characteristics. *Radiographics* 2001; **21**: 475-90. doi: 10.1148/radiographics.21.2.g01mr09475
20. Caruso PA, Marsh MR, Minkowitz S, Karten G. An intense clinicopathologic study of 305 teratomas of the ovary. *Cancer* 1971; **27**: 343-8. doi: 10.1002/1097-0142(197102)27:2<343::aid-cnrcr2820270215>3.0.co;2-b
21. Nakayama T, Yoshimitsu K, Irie H, Aibe H, Tajima T, Nishie A, et al. Diffusion-weighted echo-planar MR imaging and ADC mapping in the differential diagnosis of ovarian cystic masses: usefulness of detecting keratinoid substances in mature cystic teratomas. *J Magn Reson Imaging* 2005; **22**: 271-8. doi: 10.1002/jmri.20369
22. Agostinho L, Horta M, Salvador JC, Cunha TM. Benign ovarian lesions with restricted diffusion. *Radiol Bras* 2019; **52**: 106-11. doi: 10.1590/0100-3984.2018.0078
23. Feuerlein S, Pauls S, Juchems MS, Stuber T, Hoffmann MH, Brambs HJ, et al. Pitfalls in abdominal diffusion-weighted imaging: how predictive is restricted water diffusion for malignancy. *AJR Am J Roentgenol* 2009; **193**: 1070-6. doi: 10.2214/AJR.08.2093
24. Dunn DP, Kelsey NR, Lee KS, Smith MP, Mortelet KJ. Non-oncologic applications of diffusion-weighted imaging (DWI) in the genitourinary system. *Abdom Imaging* 2015; **40**: 1645-54. doi: 10.1007/s00261-015-0471-3
25. Duarte AL, Dias JL, Cunha TM. Pitfalls of diffusion-weighted imaging of the female pelvis. *Radiol Bras* 2018; **51**: 37-44. doi: 10.1590/0100-3984.2016.0208
26. Takeuchi M, Matsuzaki K, Nishitani H. Diffusion-weighted magnetic resonance imaging of ovarian tumors: differentiation of benign and malignant solid components of ovarian masses. *J Comput Assist Tomogr* 2010; **34**: 173-6. doi: 10.1097/RCT.0b013e3181c2f0a2
27. Moyle PL, Kataoka MY, Nakai A, Takahata A, Reinhold C, Sala E. Nonovarian cystic lesions of the pelvis. *Radiographics* 2010; **30**: 921-38. doi: 10.1148/rg.304095706
28. Kim MY, Rha SE, Oh SN, Jung SE, Lee YJ, Kim YS, et al. MR Imaging findings of hydrosalpinx: a comprehensive review. *Radiographics* 2009; **29**: 495-507. doi: 10.1148/rg.292085070
29. Laurent PE, Thomassin-Piana J, Jalaguier-Coudray A. Mucin-producing tumors of the ovary: MR imaging appearance. *Diagn Interv Imaging* 2015; **96**: 1125-32. doi: 10.1016/j.diii.2014.11.034
30. Marko J, Marko KI, Pachigolla SL, Crothers BA, Mattu R, Wolfman DJ. Mucinous neoplasms of the ovary: radiologic-pathologic correlation. *Radiographics* 2019; **39**: 982-97. doi: 10.1148/rg.2019180221
31. Vargas HA, Barrett T, Sala E. MRI of ovarian masses. *J Magn Reson Imaging* 2013; **37**: 265-81. doi: 10.1002/jmri.23721
32. Jung SE, Lee JM, Rha SE, Byun JY, Jung JI, Hahn ST. CT and MR imaging of ovarian tumors with emphasis on differential diagnosis. *Radiographics* 2002; **22**: 1305-25. doi: 10.1148/rg.226025033
33. Cho SM, Byun JY, Rha SE, Jung SE, Park GS, Kim BK, et al. CT and MRI findings of cystadenofibromas of the ovary. *Eur Radiol* 2004; **14**: 798-804. doi: 10.1007/s00330-003-2060-z
34. Tang YZ, Liyanage S, Narayanan P, Sahdev A, Sohaib A, Singh N, et al. The MRI features of histologically proven ovarian cystadenofibromas-an assessment of the morphological and enhancement patterns. *Eur Radiol* 2013; **23**: 48-56. doi: 10.1007/s00330-012-2568-1
35. Siegelman ES, Outwater EK. Tissue characterization in the female pelvis by means of MR imaging. *Radiology* 1999; **212**: 5-18. doi: 10.1148/radiology.212.1.r99j455
36. Woodward PJ, Sohaey R, Mezzetti TP Jr. Endometriosis: radiologic-pathologic correlation. *Radiographics* 2001; **21**: 193-216; questionnaire 288-94. doi: 10.1148/radiographics.21.1.g01ja14193
37. Rockall A, Forstner R. Adnexal diseases. In: Hodler J, Kubik-Huch RA, von Schulthess GK, editors. *Diseases of the abdomen and pelvis 2018-2021: diagnostic imaging*. Cham (CH): IDK Book; 2018. p. 75-84.
38. Siegelman ES, Oliver ER. MR imaging of endometriosis: ten imaging pearls. *Radiographics* 2012; **32**: 1675-91. doi: 10.1148/rg.326125518
39. Imaoka I, Wada A, Kaji Y, Hayashi T, Hayashi M, Matsuo M, et al. Developing an MR imaging strategy for diagnosis of ovarian masses. *Radiographics* 2006; **26**: 1431-48. doi: 10.1148/rg.265045206
40. Zhang H, Zhang GF, He ZY, Li ZY, Zhang GX. Prospective evaluation of 3T MRI findings for primary adnexal lesions and comparison with the final histological diagnosis. *Arch Gynecol Obstet* 2014; **289**: 357-64. doi: 10.1007/s00404-013-2990-x
41. Funt SA, Hricak H. Ovarian malignancies. *Top Magn Reson Imaging* 2003; **14**: 329-37. doi: 10.1097/00002142-200308000-00005
42. Hussain SM, Outwater EK, Siegelman ES. MR imaging features of pelvic mucinous carcinomas. *Eur Radiol* 2000; **10**: 885-91. doi: 10.1007/s003300051029
43. Hann LE, Lui DM, Shi W, Bach AM, Selland DL, Castiel M. Adnexal masses in women with breast cancer: US findings with clinical and histopathologic correlation. *Radiology* 2000; **216**: 242-7. doi: 10.1148/radiology.216.1.r00jl15242
44. Outwater EK, Siegelman ES, Kim B, Chiowanich P, Blasbalg R, Kilger A. Ovarian Brenner tumors: MR imaging characteristics. *Magn Reson Imaging* 1998; **16**: 1147-53. doi: 10.1016/s0730-725x(98)00136-2
45. Yamashita Y, Hatanaka Y, Torashima M, Takahashi M, Miyazaki K, Okamura H. Characterization of sonographically indeterminate ovarian tumors with MR imaging. A logistic regression analysis. *Acta Radiol* 1997; **38**: 572-7. doi: 10.1080/02841859709174389
46. Bent CL, Sahdev A, Rockall AG, Singh N, Sohaib SA, Reznick RH. MRI appearances of borderline ovarian tumours. *Clin Radiol* 2009; **64**: 430-8. doi: 10.1016/j.crad.2008.09.011
47. deSouza NM, O'Neill R, McIndoe GA, Dina R, Soutter WP. Borderline tumors of the ovary: CT and MRI features and tumor markers in differentiation from stage I disease. *AJR Am J Roentgenol* 2005; **184**: 999-1003. doi: 10.2214/ajr.184.3.01840999
48. Maggino T, Gadducci A, D'Addario V, Pecorelli S, Lissoni A, Stella M, et al. Prospective multicenter study on CA 125 in postmenopausal pelvic masses. *Gynecol Oncol* 1994; **54**: 117-23. doi: 10.1006/gyno.1994.1179
49. Zhang H, Zhang GF, He ZY, Li ZY, Zhu M, Zhang GX. Evaluation of primary adnexal masses by 3T MRI: categorization with conventional MR imaging and diffusion-weighted imaging. *J Ovarian Res* 2012; **5**: 33. doi: 10.1186/1757-2215-5-33

The influence of genetic variability in *IL1B* and *MIR146A* on the risk of pleural plaques and malignant mesothelioma

Petra Piber¹, Neza Vavpetic¹, Katja Goricar², Vita Dolzan², Viljem Kovac^{1,3}, Alenka Franko^{1,4}

¹ Faculty of Medicine, University of Ljubljana, Ljubljana, Slovenia

² Pharmacogenetics Laboratory, Institute of Biochemistry, Faculty of Medicine, University of Ljubljana, Ljubljana, Slovenia

³ Institute of Oncology Ljubljana, Ljubljana, Slovenia

⁴ Clinical Institute of Occupational Medicine, University Medical Centre Ljubljana, Ljubljana, Slovenia

Radiol Oncol 2020; 54(4): 429-436.

Received 7 July 2020

Accepted 6 August 2020

Correspondence to: Assoc. Prof. Alenka Franko, M.D., Ph.D., Clinical Institute of Occupational Medicine, University Medical Centre Ljubljana, Poljanski nasip 58, SI-1000 Ljubljana, Slovenia. Email: alenka.franko@siol.net

Petra Piber and Neza Vavpetic contributed equally.

Disclosure: No potential conflict of interest were disclosed.

Background. Asbestos exposure is associated with the development of pleural plaques as well as malignant mesothelioma (MM). Asbestos fibres activate macrophages, leading to the release of inflammatory mediators including interleukin 1 beta (IL-1 β). The expression of IL-1 β may be influenced by genetic variability of *IL1B* gene or regulatory microRNAs (miRNAs). This study investigated the effect of polymorphisms in *IL1B* and *MIR146A* genes on the risk of developing pleural plaques and MM.

Subjects and methods. In total, 394 patients with pleural plaques, 277 patients with MM, and 175 healthy control subjects were genotyped for *IL1B* and *MIR146A* polymorphisms. Logistic regression was used in statistical analysis.

Results. We found no association between *MIR146A* and *IL1B* genotypes, and the risk of pleural plaques. *MIR146A* rs2910164 was significantly associated with a decreased risk of MM (OR = 0.31, 95% CI = 0.13–0.73, $p = 0.008$). Carriers of two polymorphic alleles had a lower risk of developing MM, even after adjustment for gender and age (OR = 0.34, 95% CI = 0.14–0.85, $p = 0.020$). Among patients with known asbestos exposure, carriers of at least one polymorphic *IL1B* rs1143623 allele also had a lower risk of MM in multivariable analysis (OR = 0.50, 95% CI = 0.28–0.92, $p = 0.025$). The interaction between *IL1B* rs1143623 and *IL1B* rs1071676 was significantly associated with an increased risk of MM ($p = 0.050$).

Conclusions. Our findings suggest that genetic variability of inflammatory mediator IL-1 β could contribute to the risk of developing MM, but not pleural plaques.

Key words: asbestos; genetic variation; malignant mesothelioma; miRNA; pleural plaques

Introduction

Asbestos exposure is related to several pleural diseases, such as pleural plaques, diffuse pleural thickenings, pleural effusions and malignant mesothelioma (MM). MM is an aggressive form of cancer found on the mesothelium, generally on the pleura (65%), peritoneum (30%) or other serosal membranes (1%).^{1,2}

MM is often diagnosed in its later stages, is rarely operable and can respond poorly to conventional chemotherapy.³ Clinical signs and symptoms are uncharacteristic and reminiscent of many other pulmonary diseases. Patients often experience dyspnea, chest pain, weight loss and fatigue. Only a small proportion of MM patients are asymptomatic at the time of diagnosis.^{2,4} Average life expectancy is around 7 months with support

therapy and 12 months with chemotherapy.⁵ MM most often occurs in patients older than 65 years.^{2,6} Epidemiological studies have shown that the main cause of MM is asbestos exposure, with the incidence of this cancer still increasing due to the long latent period.⁷ Genetic factors have also been suggested to influence the development of MM; patients often have mutations in tumour suppressor genes, such as *BAP1*, *CDKN2A* and *NF2*.^{8,9}

Along with MM, asbestos exposure is also related to the development of pleural plaques. Pleural plaques are white and yellow thickenings of pleura, often asymmetrical and bilateral. Histologically, they are acellular, composed of hyalinised collagen, which is covered by one layer of mesothelial cells. Half of the patients with a history of asbestos exposure develop pleural plaques, typically 20 to 30 years after exposure. The risk of pleural plaques rises with the length of asbestos exposure.¹⁰ It has been proposed that inflammation caused by asbestos is involved in the pathogenesis of both pleural plaques and MM.^{3,11} Asbestos fibres are known to trigger the release of inflammatory mediators, which leads to the downregulation of apoptosis.³

After inhalation, asbestos fibres reach pleural space and are deposited in mesothelial cells.¹² This leads to local inflammatory response and proliferation of mesothelial cells. *In vitro* studies have shown that the fibres induce inflammation and apoptosis and most of the tissue damage is related to elevated interleukin 1 beta (IL-1 β).³ Macrophages accumulate near asbestos deposits and release cytokines, such as IL-1 β and tumour necrosis factor alpha (TNF- α).⁸

In response to asbestos, an intrinsic inflammatory mechanism triggers inflammation via inflammasome NLRP3, which is NLR family pyrin domain containing 3, activated by danger-associated molecular patterns (DAMP) or pathogen-associated molecular patterns (PAMP).^{13,14} NLRP3 inflammasome is a protein complex of NLRP3, apoptosis-associated speck-like protein (ASC) and caspase-1, found in macrophages, which triggers a type of apoptosis, known as pyroptosis.^{11,13,15} The activation of NLRP3 inflammasome increases the production of IL-1 β from its precursor, mediated by caspase-1 and pro-inflammatory mediators from macrophages.^{8,15,16} IL-1 β , coded by *IL1B* gene, is an inflammatory mediator, found during chronic inflammation and a key player in carcinogenesis.^{17,18} It promotes neutrophil recruitment and transcription of NF- κ B (nuclear factor kappa B), the latter being known to influence tumour growth and response to chemo-

therapy.¹⁸ *In vitro* studies showed that IL-1 β plays an important part in increasing proliferation, leading to a malignant transformation.⁸

IL-1 β release can also be regulated by miRNAs, 21-23 nucleotides long non-coding RNAs, which inhibit translation by binding to the 3'-untranslated region (3'-UTR) of mRNA.¹⁹ miRNAs are involved in networks of gene regulation and their expression often changes in cancerous tissue, including MM.²⁰⁻²⁵ A key miRNA, influencing the expression of *IL1B*, is miRNA-146. Two human variants are found; miRNA-146a and miRNA-146b, both assumed to play a role in toll-like receptor (TLR) based signalling and cytokine response.^{21,22,26} Previous studies found that miRNA-146a has an anti-inflammatory function, with its silencing leading to an increase in IL-1 β and its induction having the opposite effect.^{22,26,27}

Genetic factors, such as single nucleotide polymorphisms (SNPs), may influence protein expression.^{17,28,29} *IL1B* rs16944 (c.-511C>T), located in 5' untranslated region (UTR), influences the binding of transcription factors.³⁰ Higher levels of IL-1 β were found in homozygotes with polymorphic allele, leading to a higher risk of developing chronic inflammation-related diseases, such as diabetes mellitus type 2 and breast cancer.^{31,32} *IL1B* rs1143623 (-1464G>C) is also located in 5' UTR and affects the binding of transcription factors.³⁰ Its polymorphic C allele was associated with a lower risk of developing lung and colorectal carcinoma, due to a lower production and release of IL-1 β .^{28,29} The relationship between *IL1B* rs1071676, located in 3'UTR, and carcinogenesis has not yet been established, but as it affects miRNA binding site, it could also influence *IL1B* expression. SNPs have also been found in genes coding for miRNAs, such as *MIR146A* rs2910164, which has been related to both higher³³ and lower risks³⁴ of malignant transformations, according to previous research.³⁵

To the best of our knowledge, the role of *IL1B* and *MIR146A* genetic variability in the development of asbestos-related diseases has not been evaluated so far. The aim of the present study was therefore to evaluate the influence of *IL1B* and *MIR146A* polymorphisms on the risk of developing pleural plaques and MM.

Subjects and methods

Subjects

The retrospective case-control study included 277 patients with histologically confirmed pleu-

ral or peritoneal MM, treated at the Institute of Oncology Ljubljana between 1 January 2001 and 30 September 2018, 394 patients with pleural plaques and 175 healthy control subjects, all of whom were previously exposed to asbestos. The control group and those with pleural plaques were occupationally exposed to asbestos by working in the factory Salonit Anhovo, Slovenia, and were presented at the State Board for the Recognition of Occupational Asbestos Diseases between January 1999 and December 2003. In 2018, the subjects from the control group were found not to have any asbestos-related disease.

The study was approved by the Slovenian Ethics Committee for Research in Medicine and was carried out according to the Declaration of Helsinki.

Clinical diagnosis

Patients with pleural plaques have been diagnosed based on X-ray and high-resolution computed tomography (HRCT), while MM diagnosis was confirmed by a pathologist based on the histopathology of samples gathered thoracoscopically in the case of the pleural and laparoscopically in the case of the peritoneal type of MM.^{2,36,37}

Asbestos exposure and smoking

A semiquantitative method was used to assess the asbestos exposure. The data on cumulative asbestos exposure expressed in fibres/cm³-years were available for all control subjects, all subjects with pleural plaques except for 6, and for 40 subjects with MM. Based on these data, the asbestos exposure in these subjects was categorised into three groups: low (< 11 fibres/cm³-years), medium (11–20 fibres/cm³-years) and high (> 20 fibres/cm³-years) asbestos exposure. For additional 49 subjects with MM who lacked the data on cumulative asbestos exposure a thorough work history was obtained by an interview performed by a single expert experienced in asbestos exposure assessment. Their exposures were compared with the exposures from the group of patients with known cumulative asbestos exposure and were categorized accordingly into three groups with presumed low, medium and high asbestos exposure.² For the remaining 188 MM patients, exact data on asbestos exposure were not available.

An interview based on a standardized questionnaire was conducted with the control group and patients with pleural plaques to collect data on smoking, while the medical documentation of the

Institute of Oncology of Ljubljana was used to obtain this piece of data for patients with MM.^{2,38}

Single nucleotide polymorphism (SNP) selection

Using LD Tag SNP Selection,³⁰ dbSNP,³⁹ Ensembl⁴⁰ and LDlink⁴¹ we identified *IL1B* SNPs, which had the minor allele frequency (MAF) greater than 0.05 in the European population, could influence the expression of *IL1B* and were located less than 5000 base pairs up- or downstream from the gene. Polymorphism rs1071676, located in 3'UTR as well as rs16944 and rs1146323, located in 5'UTR matched our criteria. Based on miRDB,⁴² miRTarBase⁴³ and Variation Viewer we identified miRNAs, that could influence *IL1B* expression and SNPs in the genes coding for these miRNAs. Based on the inclusion criteria, we selected rs2910164, a SNP in miRNA-146a.

Molecular genetic analysis

We isolated DNA from venous blood of 44 patients with MM using E.Z.N.A.[®] SQ II Blood DNA Kit (Omega Bio-tek, Inc., Norcross, Georgia, USA) following the manufacturer's instructions. DNA samples of all other subjects had been isolated during previous studies.⁴⁴ Genotyping was performed using competitive allele-specific PCR (KASP), the KASP Master mix (LGC, Middlesex, UK) and custom KASP Genotyping Assay (LGC, Middlesex, UK) according to the manufacturer's instructions.

Statistics

Median and interquartile range were used to describe continuous variables, while frequencies were used for categorical variables. To compare the distribution of categorical variables, Fisher's exact test was performed, while non-parametric Kruskal-Wallis test was used for continuous variables. Deviation from the Hardy-Weinberg equilibrium (HWE) was evaluated using chi-square test. Both additive and dominant genetic models were used in statistical analyses. Univariable and multivariable logistic regression was used to analyse the association between genotypes and asbestos-related diseases (pleural plaques and MM). For the analysis of multiplicative interactions between genotypes, logistic regression models using dummy variables were used. All statistical analyses were performed using the Statistical Package for the Social Sciences (SPSS) for Windows, version 21.0 (IBM Corporation, Armonk, NY, USA).

Results

Characteristics of patients with MM and pleural plaques as well as the control group are shown in Table 1. There was a statistically significant difference between the groups in respect to age ($p < 0.001$) and asbestos exposure ($p < 0.001$). MM patients were significantly older than the control group or patients with pleural plaques. Among the subjects with known asbestos exposure, 51.7% of patients with MM had medium or high exposure compared to 23.4% of the control group and 28.4% of patients with pleural plaques. There was no statistically significant difference between groups regarding gender ($p = 0.410$) and smoking status ($p = 0.267$) (Table 1).

A further analysis of asbestos exposure showed that medium and high levels of asbestos exposure were associated with an increased risk of MM compared both to the control group (odds ratio [OR] = 3.50; 95% confidence interval [CI] = 2.03–6.02; $p < 0.001$) and patients with pleural plaques (OR = 2.70; 95% CI = 1.69–4.33; $p < 0.001$).

Among the patients with MM, 19 (6.9 %) had stage I MM, 61 (22.1 %) were in stage II of the disease, 83 (30.1 %) had stage III and 81 (29.3 %) stage IV MM. Thirty-two patients (11.6 %) had the peritoneal subtype of MM, where stage was not determined and in one patient, the MM stage could not be determined. In our cohort, the most prevalent histological subtype of MM was the epithelioid subtype (206; 74.4 %); however some of the patients had either the biphasic (26; 9.4 %) or sarcomatoid subtype (26; 9.4 %) and in the case of a few patients (19; 6.6 %), the histological subtype was not determined.

A comparison of patients with pleural plaques and healthy controls revealed no statistically significant influence on the risk of pleural plaques for any of the selected polymorphisms, neither in univariable analysis nor after adjustments for age, gender and asbestos exposure (Supplementary Table 1).

The analysis of the association between genetic polymorphisms and MM has shown statistically significant influence of polymorphism *MIR146A* rs2910164 on the risk of developing MM. Carriers of two polymorphic alleles (genotype CC) had a lower risk of developing MM (OR = 0.31; 95% CI = 0.13–0.73; $p = 0.008$). There was no influence of other genetic polymorphisms on the development of MM (Table 2).

In multivariable analysis, polymorphism *MIR146A* rs2910164 remained associated with a decreased risk of developing MM after adjustment for age and gender (OR = 0.34; 95% CI = 0.14–0.85; $p = 0.020$). However, in the subgroup with asbestos exposure data, *MIR146A* rs2910164 polymorphism no longer showed statistically significant influence on the risk of MM after adjustment for age, gender and asbestos exposure (OR = 0.39; 95% CI = 0.11–1.38; $p = 0.144$) (Table 2). Carriers of at least one polymorphic *IL1B* rs1143623 (genotype GC or CC) showed a significantly decreased risk of MM after adjustment for age, gender and asbestos exposure (OR = 0.50; 95% CI = 0.28–0.92; $p = 0.025$) (Table 2).

A comparison of patients with MM and pleural plaques showed that polymorphism *MIR146A* rs2910164 was statistically significantly associated with the risk of the development of MM compared to pleural plaques (Table 3). Patients that had two polymorphic *MIR146A* rs2910164 alleles (geno-

TABLE 1. Characteristics of subjects included in the study

Characteristics		Control group N = 175	Pleural plaques N = 394	Malignant mesothelioma N = 277	Test	p
Gender	Male, N (%)	119 (68.0)	271 (68.8)	202 (72.9)	1.757 ^a	0.410
	Female, N (%)	56 (32.0)	123 (31.3)	75 (27.1)		
Age	Median (25%–75%)	55.3 (48.6–63.7)	54.9 (48.8–62.7)	66.0 (59.0–73.0)	151.666 ^b	< 0.001
Asbestos exposure	Low, N (%)	134 (76.6)	278 (71.6) [6]	43 (48.3) [188]	26.891 ^a	< 0.001
	Medium, N (%)	13 (7.4)	41 (10.6)	24 (27.0)		
	High, N (%)	28 (16.0)	69 (17.8)	22 (24.7)		
Smoking	No, N (%)	94 (53.7)	194 (49.4) [1]	150 (55.6) [7]	2.640 ^a	0.267
	Yes, N (%)	81 (46.3)	199 (50.6)	120 (44.4)		

^a calculated using Fisher exact test; ^b calculated using Kruskal-Wallis test; number of missing data is presented in [] brackets

TABLE 2. Association between selected polymorphisms and the risk of developing malignant mesothelioma

SNP	Genotype	Controls N (%)	MM N (%)	OR (95% CI)	p	OR (95% CI) _{adj1}	P _{adj1}	OR (95% CI) _{adj2}	P _{adj2}
IL1B rs1143623	GG	88 (50.3)	152 (54.9)	reference		reference			
	GC	67 (38.3)	97 (35.0)	0.84 (0.56–1.26)	0.396	0.82 (0.52–1.29)	0.388	0.56 (0.29–1.05)	0.072
	CC	20 (11.4)	28 (10.1)	0.81 (0.43–1.52)	0.514	0.69 (0.35–1.38)	0.294	0.34 (0.11–1.04)	0.060
	GC+CC	87 (49.7)	125 (45.1)	0.83 (0.57–1.22)	0.341	0.79 (0.52–1.20)	0.266	0.50 (0.28–0.92)	0.025
IL1B rs16944	TT	21 (12.0)	36 (13.0)	1.10 (0.60–2.02)	0.756	0.94 (0.48–1.82)	0.849	0.53 (0.20–1.43)	0.210
	TC	75 (42.9)	118 (42.6)	1.01 (0.67–1.51)	0.960	0.98 (0.63–1.52)	0.911	0.67 (0.36–1.24)	0.198
	CC	79 (45.1)	123 (44.4)	reference		reference			
	TC+TT	96 (54.9)	154 (55.6)	1.03 (0.70–1.51)	0.878	0.97 (0.64–1.47)	0.873	0.63 (0.35–1.13)	0.122
IL1B rs1071676	GG	105 (60.0)	165 (59.6)	reference		reference			
	GC	60 (34.3)	98 (35.4)	1.04 (0.69–1.56)	0.851	0.97 (0.62–1.51)	0.895	1.00 (0.53–1.89)	0.993
	CC	10 (5.7)	14 (5.1)	0.89 (0.38–2.08)	0.789	0.96 (0.38–2.41)	0.931	2.03 (0.70–5.90)	0.194
	GC+CC	70 (40.0)	112 (40.4)	1.02 (0.69–1.50)	0.927	0.97 (0.64–1.48)	0.885	1.15 (0.64–2.08)	0.632
MIR146A rs2910164	GG	94 (53.7)	158 (57.0)	reference		reference			
	GC	64 (36.6)	110 (39.7)	1.02 (0.69–1.53)	0.913	0.91 (0.59–1.41)	0.672	0.67 (0.36–1.25)	0.209
	CC	17 (9.7)	9 (3.2)	0.31 (0.13–0.73)	0.008	0.34 (0.14–0.85)	0.020	0.39 (0.11–1.38)	0.144
	GC+CC	81 (46.3)	119 (43.0)	0.87 (0.60–1.28)	0.488	0.79 (0.52–1.21)	0.278	0.62 (0.34–1.11)	0.109

adj1 = adjustment for age and gender; adj2 = adjustment for age, gender and asbestos exposure; CI = confidence interval; MM = malignant mesothelioma; OR = odds ratio; SNP = single nucleotide polymorphism

TABLE 3. Association between selected polymorphisms and the risk of developing malignant mesothelioma compared to pleural plaques

SNP	Genotype	Pleural plaques N (%)	MM N (%)	OR (95 % CI)	p	OR (95 % CI) _{adj1}	P _{adj1}	OR (95 % CI) _{adj2}	P _{adj2}
IL1B rs1143623	GG	205 (52.0)	152 (54.9)	reference		reference			
	GC	157 (39.8)	97 (35.0)	0.83 (0.60–1.16)	0.277	0.88 (0.61–1.27)	0.499	0.67 (0.39–1.15)	0.151
	CC	32 (8.1)	28 (10.1)	1.18 (0.68–2.04)	0.554	1.07 (0.58–1.99)	0.827	0.65 (0.22–1.86)	0.418
	GC+CC	189 (48.0)	125 (45.1)	0.89 (0.66–1.21)	0.467	0.92 (0.65–1.29)	0.617	0.67 (0.40–1.11)	0.123
IL1B rs16944	TT	50 (12.7)	36 (13.0)	1.02 (0.63–1.67)	0.923	0.96 (0.56–1.67)	0.897	0.54 (0.22–1.34)	0.184
	TC	169 (42.9)	118 (42.6)	0.99 (0.71–1.38)	0.969	0.98 (0.68–1.42)	0.929	0.70 (0.41–1.19)	0.186
	CC	175 (44.4)	123 (44.4)	reference		reference			
	TC+TT	219 (55.6)	154 (55.6)	1.00 (0.73–1.36)	0.998	0.98 (0.69–1.38)	0.905	0.66 (0.40–1.10)	0.110
IL1B rs1071676	GG	233 (59.1)	165 (59.6)	reference		reference			
	GC	145 (36.8)	98 (35.4)	0.95 (0.69–1.32)	0.778	0.93 (0.65–1.34)	0.708	0.92 (0.53–1.60)	0.774
	CC	16 (4.1)	14 (5.1)	1.24 (0.59–2.60)	0.578	1.29 (0.56–2.97)	0.553	2.83 (1.04–7.71)	0.042
	GC+CC	161 (40.9)	112 (40.4)	0.98 (0.72–1.34)	0.911	0.97 (0.68–1.37)	0.849	1.09 (0.66–1.82)	0.731
MIR146A rs2910164	GG	196 (49.7)	158 (57.0)	reference		reference			
	GC	163 (41.4)	110 (39.7)	0.84 (0.61–1.15)	0.276	0.84 (0.58–1.20)	0.326	0.65 (0.38–1.11)	0.118
	CC	35 (8.9)	9 (3.2)	0.32 (0.15–0.68)	0.003	0.33 (0.15–0.75)	0.008	0.34 (0.11–1.09)	0.069
	GC+CC	198 (50.3)	119 (43.0)	0.75 (0.55–1.02)	0.063	0.74 (0.53–1.05)	0.092	0.59 (0.36–0.99)	0.046

adj1 = adjustment for age and gender; adj2 = adjustment for age, gender and asbestos exposure; CI = confidence interval; MM = malignant mesothelioma; OR = odds ratio; SNP = single nucleotide polymorphism

type CC) had a significantly decreased risk of MM compared to pleural plaques (OR = 0.32; 95% CI = 0.15–0.68; $p = 0.003$). Similarly, after adjustment for gender and age, patients who were homozygotes for polymorphic *MIR146A* rs2910164 still showed a lower risk of developing MM (OR = 0.33; 95% CI = 0.15–0.75; $p = 0.008$). In the subgroup with available asbestos exposure data, *MIR146A* rs2910164 was significantly associated with a decreased MM risk only in the dominant model (OR = 0.59; 95% CI = 0.36–0.99; $p = 0.046$) (Table 3). Additionally, patients that were homozygotes for the *IL1B* rs1071676 polymorphism (CC genotype) had an increased risk of developing MM when patients with pleural plaques were used as a control group and the analysis was adjusted for age, gender and asbestos exposure (OR = 2.83; 95% CI = 1.04–7.71; $p = 0.042$) (Table 3).

In further logistic regression modelling, the interactions between polymorphisms showed no significant influence on the risk of pleural plaques (data not shown). The analysis of the influence of the interaction between *IL1B* rs1143623 and *IL1B* rs1071676 polymorphisms showed significant influence on the increased MM risk (OR = 2.24, 95% CI = 1.00–5.00, $p = 0.050$). No other interactions between polymorphisms had a statistically significant influence on the risk of MM (Supplementary Table 2).

Discussion

The association between MM and asbestos exposure has first been described in 1960 and, although very few genetic factors have been studied, multiple factors have since then been considered to influence the pathogenesis of MM.⁴⁵ In the present study, we evaluated the effect of polymorphisms of IL-1 β and miRNA-146a genes on the risk of developing MM and pleural plaques. The key finding of the present study was the association between *MIR146A* rs2910164 and lower risk of the development of MM.

Consistent with the previous studies, the average age of MM patients was found to be higher than that of the patients with pleural plaques or the control group, probably due to the long latency period between the first asbestos exposure and MM.^{2,6,44} Our study showed no significant association between smoking and MM, which is in agreement with previous findings.^{2,44,46} Subjects with high or medium exposure to asbestos had a higher risk of developing MM, compared to the group with pleu-

ral plaques or the control group. Regardless of that, almost half (48.3%) of MM patients were exposed to low levels of asbestos, which is consistent with previous studies claiming there is no threshold level for the development of MM.^{47,48}

It is not yet clear to what an extent the pleural plaques present a risk factor for MM. The studies performed so far suggested that pleural plaques are more a sign of asbestos exposure, than a carcinogenic factor.^{49,50} This hypothesis is in agreement with the findings of this study as the genotype frequency distribution of patients with pleural plaques was found to be more similar to that of the control group, rather than the genotype frequency distribution of patients with MM.

Compared to both the control group and the patients with pleural plaques, homozygotes with polymorphic *MIR146A* rs2910164 C allele were at a lower risk of developing MM, even after adjustment for age and gender. In the subgroup of patients with known asbestos exposure, carriers of at least one polymorphic *MIR146A* rs2910164 allele had a lower risk of MM in comparison to patients with pleural plaques.

According to our knowledge, the relation between *MIR146A* rs2910164 and MM has not yet been studied, but the polymorphism itself has already been associated with several other malignant diseases. Previous studies suggested that the polymorphic allele C had a protective function in the oncogenesis of melanoma⁵¹ and non-small cell lung carcinoma³³, while the same was found for the G allele in case of papillary thyroid tumour.⁵² The association of rs2910164 with the pathogenesis of MM could be explained with its influence in miRNA expression: CC genotype was previously associated with a greater production of miRNA-146a in cancerous tissue.^{53–55} Increased expression of miRNA-146a in turn leads to the suppression of inflammatory pathways, reducing the expression of proinflammatory cytokines IL-1 β , IL-6 and TNF α ,⁵⁶ while miRNA-146a inhibition has been shown to increase production of those cytokines, resulting in greater inflammatory response to asbestos, promoting carcinogenesis and increasing the risk of MM.^{17,18} The role and expression of miRNA-146a in carcinogenesis is still unclear, as some studies found the levels of miRNA-146a to be decreased in cancerous tissue of the lung⁵⁷ and stomach carcinoma,⁵⁸ while other studies found increased levels in the cases of melanoma,⁵¹ cervical cancer⁵⁹ and papillary thyroid cancer.⁵² It is possible that miRNA-146a has a tissue-specific function, so further studies are required.

Another important finding of this study has been the association between the polymorphic *IL1B* rs1143623 allele and a lower risk of developing MM. In the subgroup of subjects with known asbestos exposure, subjects with at least one polymorphic C allele had a lower risk of developing MM compared to the control group. *IL1B* rs1143623 is located at the binding site of the transcription factors and can lower the expression of *IL1B*.^{30,39} Lower levels of IL-1 β result in a less intensive inflammatory reaction caused by the asbestos fibres, which could have a protective effect. The former is in agreement with the studies that showed subjects with one polymorphic C allele having a lower risk of developing lung cancer²⁸ and homozygotes for the polymorphic C allele having a lower risk of developing colorectal cancer.²⁹

Finally, this study has shown that the interaction between *IL1B* rs1143623 and *IL1B* rs1071676 is associated with a higher risk of developing MM, even though *IL1B* rs1071676 independently had no effect on the risk of MM, while *IL1B* rs1143623 was associated with a lower risk of MM within the subgroup of subjects with known asbestos exposure. *IL1B* rs1143623 was associated with a lower risk of MM only among carriers of two wild type *IL1B* rs1071676 alleles. As *IL1B* rs1143623 can influence the binding of transcription factors and rs1071676 can influence the binding of miRNA, the interaction of both polymorphisms could result in a greater expression of IL-1 β , however this has not been studied yet.³⁰ Further studies are needed to explain the role of *IL1B* rs1143623 and its interactions with other polymorphisms and environmental factors in MM.

Lack of asbestos exposure information for all the subjects has been identified as the limitation of our study. Therefore, the subgroup for which asbestos exposure has been taken into consideration, was smaller than the overall sample. This could account for the discrepancy between the results of the analysis adjusted for asbestos exposure and the results of the analysis that did not take asbestos exposure into account. The strength of this study is its large sample size. To the best of our knowledge, this is also the first study researching the effect of *IL1B* and *MIR146A* polymorphisms on the risk of developing MM.

In conclusion, our results suggest that *IL1B* and *MIR146A* polymorphisms may contribute to the risk of MM development. Further studies, possibly evaluating serum or tissue protein expression, are needed to confirm these associations in independent patient cohorts and elucidate the role of IL-1 β

and miRNA-146a in the development of asbestos-related diseases.

Acknowledgements

This work was financially supported by the Slovenian Research Agency (ARRS Grants No. P1-0170 and L3-8203).

References

- Kovac V, Dodic-Fikfak M, Americ N, Dolzan V, Franko A. Fibulin-3 as a biomarker of response to treatment in malignant mesothelioma. *Radiol Oncol* 2015; **49**: 279-85. doi: 10.1515/raon-2015-0019
- Franko A, Kotnik N, Goricar K, Kovac V, Dodic-Fikfak M, Dolzan V. The influence of genetic variability on the risk of developing malignant mesothelioma. *Radiol Oncol* 2018; **52**: 105-11. doi: 10.2478/raon-2018-0004
- Acencio MM, Soares B, Marchi E, Silva CS, Teixeira LR, Broaddus VC. Inflammatory cytokines contribute to asbestos-induced injury of mesothelial cells. *Lung* 2015; **193**: 831-7. doi: 10.1007/s00408-015-9744-4
- Bianco A, Valente T, De Rimini ML, Sica G, Fiorelli A. Clinical diagnosis of malignant pleural mesothelioma. *J Thorac Dis* 2018; **10**: S253-61. doi: 10.21037/jtd.2017.10.09
- Kovac V, Zwitter M, Zagar T. Improved survival after introduction of chemotherapy for malignant pleural mesothelioma in Slovenia: population-based survey of 444 patients. *Radiol Oncol* 2012; **46**: 136-44. doi: 10.2478/v10019-012-0032-0
- Remon J, Lianes P, Martinez S, Velasco M, Querol R, Zanui M. Malignant mesothelioma: new insights into a rare disease. *Cancer Treat Rev* 2013; **39**: 584-91. doi: 10.1016/j.ctrv.2012.12.005
- Plato N, Martinsen JI, Sparen P, Hillerdal G, Weiderpass E. Occupation and mesothelioma in Sweden: updated incidence in men and women in the 27 years after the asbestos ban. *Epidemiol Health* 2016; **38**: e2016039. doi: 10.4178/epih.e2016039
- Kadariya Y, Menges CW, Talarchek J, Cai KQ, Klein-Szanto AJ, Pietrofesa RA, et al. Inflammation-related IL1beta/IL1R signaling promotes the development of asbestos-induced malignant mesothelioma. *Cancer Prev Res (Phila)* 2016; **9**: 406-14. doi: 10.1158/1940-6207.CAPR-15-0347
- Melaiu O, Gemignani F, Landi S. The genetic susceptibility in the development of malignant pleural mesothelioma. *J Thorac Dis* 2018; **10**: S246-52. doi: 10.21037/jtd.2017.10.41
- Chapman SJ, Cookson WO, Musk AW, Lee YC. Benign asbestos pleural diseases. *Curr Opin Pulm Med* 2003; **9**: 266-71. doi: 10.1097/00063198-200307000-00004
- Franko A, Goricar K, Kovac V, Dodic Fikfak M, Dolzan V. NLRP3 and CARD8 polymorphisms influence risk for asbestos-related diseases. *J Med Biochem* 2019; **38**: 1-10. doi: 10.2478/jomb-2019-0025
- Chew SH, Toyokuni S. Malignant mesothelioma as an oxidative stress-induced cancer: an update. *Free Radic Biol Med* 2015; **86**: 166-78. doi: 10.1016/j.freeradbiomed.2015.05.002
- Hoffman HM, Wanderer AA. Inflammasome and IL-1beta-mediated disorders. *Curr Allergy Asthma Rep* 2010; **10**: 229-35. doi: 10.1007/s11882-010-0109-z
- Kim YK, Shin JS, Nahm MH. NOD-like receptors in infection, immunity, and diseases. *Yonsei Med J* 2016; **57**: 5-14. doi: 10.3349/ymj.2016.57.1.5
- Karki R, Man SM, Kanneganti TD. Inflammasomes and cancer. *Cancer Immunol Res* 2017; **5**: 94-9. doi: 10.1158/2326-6066.CIR-16-0269
- Jenko B, Praprotnik S, Tomsic M, Dolzan V. NLRP3 and CARD8 polymorphisms influence higher disease activity in rheumatoid arthritis. *J Med Biochem* 2016; **35**: 319-23. doi: 10.1515/jomb-2016-0008
- Bhat IA, Naykoo NA, Qasim I, Ganie FA, Yousuf Q, Bhat BA, et al. Association of interleukin 1 beta (IL-1beta) polymorphism with mRNA expression and risk of non small cell lung cancer. *Meta Gene* 2014; **2**: 123-33. doi: 10.1016/j.mgene.2013.12.002

18. Hai Ping P, Feng Bo T, Li L, Nan Hui Y, Hong Z. IL-1beta/NF-kb signaling promotes colorectal cancer cell growth through miR-181a/PTEN axis. *Arch Biochem Biophys* 2016; **604**: 20-6. doi: 10.1016/j.abb.2016.06.001
19. Pillai RS. MicroRNA function: multiple mechanisms for a tiny RNA? *RNA* 2005; **11**: 1753-61. doi: 10.1261/rna.2248605
20. Williams AE, Perry MM, Moschos SA, Larner-Svensson HM, Lindsay MA. Role of miRNA-146a in the regulation of the innate immune response and cancer. *Biochem Soc Trans* 2008; **36**: 1211-5. doi: 10.1042/BST0361211
21. Wang C, Zhang W, Zhang L, Chen X, Liu F, Zhang J, et al. miR-146a-5p mediates epithelial-mesenchymal transition of oesophageal squamous cell carcinoma via targeting Notch2. *Br J Cancer* 2018; **118**: e12. doi: 10.1038/bjc.2017.471
22. Xie YF, Shu R, Jiang SY, Liu DL, Ni J, Zhang XL. MicroRNA-146 inhibits pro-inflammatory cytokine secretion through IL-1 receptor-associated kinase 1 in human gingival fibroblasts. *J Inflamm (Lond)* 2013; **10**: 20. doi: 10.1186/1476-9255-10-20
23. Xie W, Li Z, Li M, Xu N, Zhang Y. miR-181a and inflammation: miRNA homeostasis response to inflammatory stimuli in vivo. *Biochem Biophys Res Commun* 2013; **430**: 647-52. doi: 10.1016/j.bbrc.2012.11.097
24. Lo Russo G, Tessari A, Capece M, Galli G, de Braud F, Garassino MC, et al. MicroRNAs for the diagnosis and management of malignant pleural mesothelioma: a literature review. *Front Oncol* 2018; **8**: 650. doi: 10.3389/fonc.2018.00650
25. Ghaffarzadeh M, Ghaedi H, Alipoor B, Omrani MD, Kazerouni F, Shanaki M, et al. Association of MiR-149 (RS2292832) variant with the risk of coronary artery disease. *J Med Biochem* 2017; **36**: 251-8. doi: 10.1515/jomb-2017-0005
26. Comer BS, Camoretti-Mercado B, Kogut PC, Halayko AJ, Solway J, Gerthoffer WT. MicroRNA-146a and microRNA-146b expression and anti-inflammatory function in human airway smooth muscle. *Am J Physiol Lung Cell Mol Physiol* 2014; **307**: L727-34. doi: 10.1152/ajplung.00174.2014
27. Ichii O, Otsuka S, Sasaki N, Namiki Y, Hashimoto Y, Kon Y. Altered expression of microRNA miR-146a correlates with the development of chronic renal inflammation. *Kidney Int* 2012; **81**: 280-92. doi: 10.1038/ki.2011.345
28. Eaton KD, Romine PE, Goodman GE, Thornquist MD, Barnett MJ, Petersdorf EW. Inflammatory gene polymorphisms in lung cancer susceptibility. *J Thorac Oncol* 2018; **13**: 649-59. doi: 10.1016/j.jtho.2018.01.022
29. Qian H, Zhang D, Bao C. Two variants of Interleukin-1B gene are associated with the decreased risk, clinical features, and better overall survival of colorectal cancer: a two-center case-control study. *Aging (Albany NY)* 2018; **10**: 4084-92. doi: 10.18632/aging.101695
30. Willems P, Claes K, Baeyens A, Vandersickel V, Werbrouck J, De Ruyck K, et al. Polymorphisms in nonhomologous end-joining genes associated with breast cancer risk and chromosomal radiosensitivity. *Genes Chromosomes Cancer* 2008; **47**: 137-48. doi: 10.1002/gcc.20515
31. Tayel SI, Fouda EAM, Elshayeb EI, Eldakamawy ARA, El-Kousy SM. Biochemical and molecular study on interleukin-1beta gene expression and relation of single nucleotide polymorphism in promoter region with Type 2 diabetes mellitus. *J Cell Biochem* 2018; **119**: 5343-9. doi: 10.1002/jcb.26667
32. Wang J, Shi Y, Wang G, Dong S, Yang D, Zuo X. The association between interleukin-1 polymorphisms and their protein expression in Chinese Han patients with breast cancer. *Mol Genet Genomic Med* 2019; **7**: e804. doi: 10.1002/mgg3.804
33. Jia Y, Zang A, Shang Y, Yang H, Song Z, Wang Z, et al. MicroRNA-146a rs2910164 polymorphism is associated with susceptibility to non-small cell lung cancer in the Chinese population. *Med Oncol* 2014; **31**: 194. doi: 10.1007/s12032-014-0194-2
34. Svoronos AA, Engelman DM, Slack FJ. OncomiR or tumor suppressor? The duplicity of microRNAs in cancer. *Cancer Res* 2016; **76**: 3666-70. doi: 10.1158/0008-5472.CAN-16-0359
35. Wei Y, Li L, Gao J. The association between two common polymorphisms (miR-146a rs2910164 and miR-196a2 rs11614913) and susceptibility to gastric cancer: a meta-analysis. *Cancer Biomark* 2015; **15**: 235-48. doi: 10.3233/CBM-150470
36. Wolff H, Vehmas T, Oksa P, Rantanen J, Vainio H. Asbestos, asbestosis, and cancer, the Helsinki criteria for diagnosis and attribution 2014: recommendations. *Scand J Work Environ Health* 2015; **41**: 5-15. doi: 10.5271/sjweh.3462
37. American Thoracic Society. Diagnosis and initial management of nonmalignant diseases related to asbestos. *Am J Respir Crit Care Med* 2004; **170**: 691-715. doi: 10.1164/rccm.200310-1436st
38. Dodic Fikfak M, Kriebel D, Quinn MM, Eisen EA, Wegman DH. A case control study of lung cancer and exposure to chrysotile and amphibole at a Slovenian asbestos-cement plant. *Ann Occup Hyg* 2007; **51**: 261-8. doi: 10.1093/annhyg/mem003
39. Dolzan V. Genetic polymorphisms and drug metabolism. *Zdrav Vestn* 2007; **76 (Suppl II)**: 5-12.
40. Zerbini DR, Achuthan P, Akanni W, Amode MR, Barrell D, Bhai J, et al. Ensembl 2018. *Nucleic Acids Res* 2018; **46**: D754-61. doi: 10.1093/nar/gkx1098
41. Machiela MJ, Chanock SJ. LDlink: a web-based application for exploring population-specific haplotype structure and linking correlated alleles of possible functional variants. *Bioinformatics* 2015; **31**: 3555-7. doi: 10.1093/bioinformatics/btv402
42. Wong N, Wang X. miRDB: an online resource for microRNA target prediction and functional annotations. *Nucleic Acids Res* 2015; **43**: D146-52. doi: 10.1093/nar/gku1104
43. Chou CH, Shrestha S, Yang CD, Chang NW, Lin YL, Liao KW, et al. miRtarBase update 2018: a resource for experimentally validated microRNA-target interactions. *Nucleic Acids Res* 2018; **46**: D296-302. doi: 10.1093/nar/gkx1067
44. Levpuscek K, Gorcar K, Kovac V, Dolzan V, Franko A. The influence of genetic variability of DNA repair mechanisms on the risk of malignant mesothelioma. *Radiol Oncol* 2019; **53**: 206-12. doi: 10.2478/raon-2019-0016
45. Riva MA, Carnevale F, Sironi VA, De Vito G, Cesana G. Mesothelioma and asbestos, fifty years of evidence: Chris Wagner and the contribution of the Italian occupational medicine community. *Med Lav* 2010; **101**: 409-15. PMID: 21141345
46. Muscat JE, Wynder EL. Cigarette smoking, asbestos exposure, and malignant mesothelioma. *Cancer Res* 1991; **51**: 2263-7. PMID: 2015590
47. Case BW, Abraham JL, Meeker G, Pooley FD, Pinkerton KE. Applying definitions of "asbestos" to environmental and "low-dose" exposure levels and health effects, particularly malignant mesothelioma. *J Toxicol Environ Health B Crit Rev* 2011; **14**: 3-39. doi: 10.1080/10937404.2011.556045
48. Carbone M, Ly BH, Dodson RF, Pagano I, Morris PT, Dogan UA, et al. Malignant mesothelioma: facts, myths, and hypotheses. *J Cell Physiol* 2012; **227**: 44-58. doi: 10.1002/jcp.22724
49. Hillerdal G, Henderson DW. Asbestos, asbestosis, pleural plaques and lung cancer. *Scand J Work Environ Health* 1997; **23**: 93-103. doi: 10.5271/sjweh.186
50. Maxim LD, Niebo R, Utell MJ. Are pleural plaques an appropriate endpoint for risk analyses? *Inhal Toxicol* 2015; **27**: 321-34. doi: 10.3109/08958378.2015.1051640
51. Forloni M, Dogra SK, Dong Y, Conte D Jr, Ou J, Zhu LJ, et al. miR-146a promotes the initiation and progression of melanoma by activating Notch signaling. *Elife* 2014; **3**: e01460. doi: 10.7554/eLife.01460
52. Jazdzewski K, Murray EL, Franssila K, Jarzab B, Schoenberg DR, de la Chapelle A. Common SNP in pre-miR-146a decreases mature miR expression and predisposes to papillary thyroid carcinoma. *Proc Natl Acad Sci U S A* 2008; **105**: 7269-74. doi: 10.1073/pnas.0802682105
53. Shen J, Ambrosone CB, DiCioccio RA, Odunsi K, Lele SB, Zhao H. A functional polymorphism in the miR-146a gene and age of familial breast/ovarian cancer diagnosis. *Carcinogenesis* 2008; **29**: 1963-6. doi: 10.1093/carcin/bgn172
54. Kogo R, Mimori K, Tanaka F, Komune S, Mori M. Clinical significance of miR-146a in gastric cancer cases. *Clin Cancer Res* 2011; **17**: 4277-84. doi: 10.1158/1078-0432.CCR-10-2866
55. Zhang W, Yi X, Guo S, Shi Q, Wei C, Li X, et al. A single-nucleotide polymorphism of miR-146a and psoriasis: an association and functional study. *J Cell Mol Med* 2014; **18**: 2225-34. doi: 10.1111/jcmm.12359
56. Wang JH, Shih KS, Wu YW, Wang AW, Yang CR. Histone deacetylase inhibitors increase microRNA-146a expression and enhance negative regulation of interleukin-1beta signaling in osteoarthritis fibroblast-like synoviocytes. *Osteoarthritis Cartilage* 2013; **21**: 1987-96. doi: 10.1016/j.joca.2013.09.008
57. Chen G, Umelo IA, Lv S, Teugels E, Fostier K, Kronenberger P, et al. miR-146a inhibits cell growth, cell migration and induces apoptosis in non-small cell lung cancer cells. *PLoS One* 2013; **8**: e60317. doi: 10.1371/journal.pone.0060317
58. Yao Q, Cao Z, Tu C, Zhao Y, Liu H, Zhang S. MicroRNA-146a acts as a metastasis suppressor in gastric cancer by targeting WAF2. *Cancer Lett* 2013; **335**: 219-24. doi: 10.1016/j.canlet.2013.02.031
59. Wang X, Tang S, Le SY, Lu R, Rader JS, Meyers C, et al. Aberrant expression of oncogenic and tumor-suppressive microRNAs in cervical cancer is required for cancer cell growth. *PLoS One* 2008; **3**: e2557. doi: 10.1371/journal.pone.0002557

Neutrophil-to-lymphocyte ratio can predict outcome in extensive-stage small cell lung cancer

Gordana Drpa¹, Maja Sutic², Jurica Baranasic², Marko Jakopovic¹, Miroslav Samarzija¹, Suzana Kukulj¹, Jelena Knezevic²

¹ Department for Lung Diseases Jordanovac, University Hospital Center Zagreb, Zagreb, Croatia

² Laboratory for Advanced Genomics, Division of Molecular Medicine, Ruđer Bošković Institute, Zagreb, Croatia

Radiol Oncol 2020; 54(4): 437-446.

Received 18 February 2020

Accepted 22 July 2020

Correspondence to: Gordana Drpa, Jordanovac 104, 10000 Zagreb, Croatia. E-mail: gordana.drpa@kbc-zagreb.hr

Disclosure: The authors declare no conflict of interest.

Background. The neutrophil-to-lymphocyte ratio (NLR), platelet-to-lymphocyte ratio (PLR), and lymphocyte-to-monocyte ratio (LMR) were analyzed in various carcinomas and their potential prognostic significance was determined. The objective of present study was to determine the correlation between these parameters and the survival of patients with small cell lung cancer (SCLC), since very few studies have been published on this type of carcinoma.

Patients and methods. One hundred and forty patients diagnosed with SCLC at University Hospital Center Zagreb, between 2012 and 2016 were retrospectively analyzed. Extensive-stage disease (ED) was verified in 80 patients and limited-stage disease (LD) in 60 patients. We analyzed the potential prognostic significance of various laboratory parameters, including NLR, PLR, and LMR, measured before the start of treatment.

Results. Disease extension, response to therapy, chest irradiation and prophylactic cranial irradiation (PCI), as well as hemoglobin, monocyte count, C-reactive protein (CRP), and lactate dehydrogenase (LDH) showed a prognostic significance in all patients. When we analyzed the patients separately, depending on the disease extension, we found that only skin metastases as well as LDH and NLR values, regardless of the cut-off value, had a prognostic significance in ED. Meanwhile, the ECOG performance status, chest irradiation, PCI, and hemoglobin and creatinine values had a prognostic significance in LD.

Conclusions. NLR calculated before the start of the treatment had a prognostic significance for ED, while PLR and LMR had no prognostic significance in any of the analyzed groups of patients.

Key words: small cell lung cancer; hematological markers; neutrophil-to-lymphocyte ratio; platelet-to-lymphocyte ratio; lymphocyte-to-monocyte ratio

Introduction

Lung cancer is still one of the most malignant diseases nowadays. It is the most commonly occurring cancer in men and the second most commonly occurring cancer in women according to the latest data by the International Agency for Research on Cancer (IACR).¹ At the same time, lung cancer is the leading cause of cancer death among both men and women. For the purposes of comparison, breast cancer in women occurs three times more of-

ten than lung cancer, while the mortality is almost equal. Moreover, prostate cancer and lung cancer have almost the same incidence in men, but the lung cancer mortality rate is four times higher than the prostate cancer mortality rate.^{1,2}

Small cell lung cancer (SCLC) is the most aggressive subtype of lung cancer. Nowadays, small cell lung cancer makes up about 15% of all lung cancers and occurs almost only in smokers. The incidence of this lung cancer subtype has decreased in the last few decades, but primarily in developed

countries.^{3,4} There are no global data on SCLC prevalence. In Croatia, there are no separate data on SCLC either, and the available epidemiological data relate to lung cancer as an entity. In the last twenty years, a slight reduction in the share of SCLC in relation to the total number of lung cancer patients has been observed at our institution, which is the largest thoracic oncology center in the country.

According to literature there are differences in survival rates for various tumors, including small cell lung cancer, depending on ethnic origin.⁵ Therefore, the results of epidemiological and clinical studies in one geographic area are not applicable to some other geographic areas.

The main characteristics of small cell lung cancer are its rapid growth and early spread to distal body parts. This is the reason why in most cases this carcinoma is diagnosed late, when metastatic disease has already developed.⁶ Surgical treatment is therefore rarely possible, but in the last few years it has been recommended for certain patients with early-stage disease.⁷ Before the introduction of platinum-based antineoplastic drugs for the treatment of malignant disease, the median survival of patients diagnosed with small cell lung cancer was two to three months.^{8,9} The survival rate has increased four to five times with chemotherapy, but for most patients with extensive-stage disease it does not exceed ten months. In fact, this tumor is extremely chemosensitive and usually responds to chemotherapy very well. However, it recurs very rapidly and most patients die after a relapse. Despite numerous clinical trials, progress in the treatment of small cell lung cancer has been modest. However, as treatment of limited disease (LD) became more successful with the introduction of thoracic radiotherapy and prophylactic cranial irradiation (PCI), concurrent chemoradiotherapy has been a standard in the treatment of LD for a long time now.⁶ The optimal radiation therapy protocol has remained controversial until this day, although it has been established that there are no differences in either survival or toxicity between hyperfractionated and normofractionated radiotherapy.^{10,11} The application of consolidation radiotherapy in selected patients with extensive-stage disease (ED) and a good initial response to chemotherapy have partly contributed to the improved survival rate, but application has been very inconsistent.^{12,13} Immunotherapy has resulted in significant progress in the treatment of numerous malignant diseases, including non-small cell lung cancer (NSCLC). Expectations for the treatment of small cell lung cancer were high

as well. For the time being, adding checkpoint inhibitors to first-line chemotherapy in ED has resulted in a slight increase of overall survival and progression-free survival, but the results are far from expected.¹⁴⁻¹⁶

It is well known that infection and deregulated inflammatory response are associated with the occurrence and progression of almost all chronic diseases, including cancers.¹⁷ In the last few decades, a great number of researches investigating the role of different inflammatory markers in cancer development and outcome have been published.¹⁸⁻²⁰ Usually the investigated inflammatory markers include C-reactive protein (CRP), lactate dehydrogenase (LDH), erythrocyte sedimentation rate, platelet (Pc) and neutrophil counts.²¹⁻²³ In most cases, it has been found that elevated levels of these parameters are associated with poorer outcome of various cancers, including small cell lung cancer.^{24,25} On the other hand, the lymphocyte count reflects the immunological status of a host, thus a low lymphocyte count is a predictor of poorer outcome.²⁶ The prognostic value of combinations of these and other parameters has also been extensively investigated. Among them, the neutrophil-to-lymphocyte ratio in various chronic diseases, including numerous malignant diseases, has been investigated the most.²⁷⁻²⁹

In this study, we have investigated CRP, LDH, Pc, hemoglobin (Hb), creatinine, neutrophil-to-lymphocyte ratio (NLR), platelet-to-lymphocyte ratio (PLR), and lymphocyte-to-monocyte ratio (LMR) and their impact on the outcome of patients with SCLC. To the best of our knowledge, this is the first study carried out exclusively on a European population which investigated the prognostic significance of all three mentioned ratios in patients with limited-stage and extensive-stage small cell lung cancer.²⁹⁻³¹

Patients and methods

Patients

For research purposes, we analyzed the medical records of 438 patients diagnosed with small cell lung cancer admitted to the University Hospital Center, Department for Lung Diseases Jordanovac between 2012 and 2016. We included only patients whose disease was verified by histopathological analysis and who had undergone first-line chemotherapy or chemoradiotherapy. Some additional criteria needed to be met in order to be included in the research: documented laboratory test results

with the investigated parameters measured up to three weeks before the first chemotherapy, as well as data on performance status, follow up, and outcome. The following patient categories were excluded from further research: surgically treated patients, patients with combined small cell lung carcinoma, patients with one or more synchronous tumors, patients who received no therapy, patients without the required medical records, and patients lost to follow-up. After exclusion of the mentioned groups, 140 patients remained who met all the required inclusion and exclusion criteria for further investigation. Out of the total number of patients, 80 were diagnosed with extensive-stage disease and 60 with limited-stage disease. The patients' performance status was measured before the start of the treatment and defined according to the Eastern Cooperative Oncology Group Performance Status (ECOG) scale.³² Regarding the ECOG status, the patients were divided into two groups: good ECOG status (0–1) and poor ECOG status (2–3).

All patients underwent a thoracic and abdominal computed tomography (CT) scan before the start of the treatment. Skeletal scintigraphy was done only in cases with a clinical indication, because it was not routinely performed at our Department. The same applied to brain CT scanning. Disease extension was defined according to the staging system established by the International Association for the Study of Lung Cancer (IASLC) in 1989, which divides SCLC into two stages, "limited-stage disease" and "extensive-stage disease".³³ The patients underwent follow-up chest X-ray scans after every two chemotherapy cycles. A follow-up CT scan was performed after the treatment was completed, especially in cases of initial limited-stage disease. Regression of a primary tumor and metastasis or stable disease was marked as response to therapy what was in fact disease control after initial therapy, whereas progression of the disease was marked as no-response. Response to therapy was assessed radiologically and clinically (*e.g.*, if a patient had subcutaneous metastases or palpable lymph nodes in a region which had not been examined by CT).

In our institution, patients usually receive 4–6 cycles of the first-line platinum-doublet chemotherapy. Patients who received a minimum of two and a maximum of six cycles of the mentioned chemotherapy, with or without radiotherapy, were included in the study. A concomitant or sequential radiotherapy protocol was carried out, primarily in patients with limited-stage disease or as palliative treatment in patients with extensive-stage disease and a good response to chemotherapy.

Prophylactic cranial irradiation was mainly performed in patients with limited-stage disease.

Data collection and ethical consideration

Data were collected by using the electronic information database, based on good clinical practice and complying with international standards including the Helsinki Declaration on Patient Safety. We obtained approval for data collection and analysis by the Ethics Committee of our institution. Since this was a retrospective study, informed consent was not required.

Demographic, laboratory, cytological, histopathological, clinical, and treatment data were collected on the patients included in the study. Laboratory test results obtained shortly before the start of treatment, that is, a maximum of three weeks before the first chemotherapy, were included in the study. Among all the hematological results, the following parameters were analyzed: leukocyte count, lymphocyte count, neutrophil count, monocyte count, platelets, hemoglobin, CRP, creatinine, and LDH. The neutrophil-to-lymphocyte ratio was calculated by dividing the total neutrophil count by the total lymphocyte count. The platelet-to-lymphocyte and lymphocyte-to-monocyte ratios were calculated in the same way.

Overall survival (OS) was defined as the length of time from the date of diagnosis to death from any cause, or the last follow-up for patients who were still alive. Progression-free survival (PFS) was defined as the length of time from diagnosis to progression or death, depending on what happened first.

Statistical analysis

For the analysis of demographic and clinical data, we used descriptive and inferential statistical methods. Parameters are indicated as sum and percentage, arithmetic mean \pm standard deviation, or as interquartile range limits with the median as a measure of the central tendency. Differences among the ranked parameters, *i.e.*, the investigated values, were calculated by using the Mann-Whitney U test. Differences among categorical data were tested by using the Chi-square test with Fisher's exact test for smaller samples. Intercorrelation among the variables was tested by using Spearman's rank correlation coefficient varying within the closed interval $-1 \leq r \leq +1$. For survival analysis, the Kaplan-Meier estimator was used, and the Log-rank test (Mantel-Cox) was used as a test of significance. The

TABLE 1. Patient characteristics regarding the disease stage

Variable	ED-SCLC (n = 80)	LD-SCLC (n = 60)	p-values
Age (years) x̄ (SD)	63.2 (9.1)	63.0 (9.4)	0.930
Gender			
Male	55 (68.8%)	34 (56.7%)	0.159
Female	25 (31.2%)	26 (43.4%)	
Smoking			
Yes	77 (96.2%)	57 (95.0%)	1.000
No	3 (3.8%)	3 (5.0%)	
PS (ECOG)			
0–1	64 (80.0%)	52 (86.7%)	0.368
2–3	16 (20.0%)	8 (13.3%)	
Chest irradiation			
Yes	9 (11.2%)	36 (60.0%)	< 0.0001
No	71 (88.8%)	24 (40.0%)	
PCI			
Yes	2 (2.5%)	10 (16.7%)	0.004
No	78 (97.5%)	50 (83.3%)	
Disease control			
Yes	63 (78.8%)	56 (93.3%)	0.018
No	17 (21.2%)	4 (6.7%)	
PFS (weeks) x̄ (SD)	30.1 (14.5)	60.3 (57.9)	< 0.0001
OS (weeks) x̄ (SD)	48.3 (23.4)	83.3 (59.3)	< 0.0001
Outcome			
dead	79 (98.8%)	46 (76.7%)	0.013
alive	1 (1.2%)	14 (23.3%)	
WBC count (x 10 ⁹ /l) x̄ (SD)	9.1 (3.7)	9.2 (3.3)	0.686
Platelet count (x 10 ⁹ /l) x̄ (SD)	293 (119)	304 (95)	0.249
Hemoglobin (g/l) x̄ (SD)	130.9 (17.8)	133.0 (16.8)	0.540
CRP (mg/l) x̄ (SD)	34.2 (44.6)	21.2 (26.6)	0.048
Creatinine (umol/l) x̄ (SD)	81.9 (20.0)	82.3 (29.6)	0.443
LDH (U/l) x̄ (SD)	336.2 (193.5)	311.1 (607.3)	0.004
Lymphocytes (x 10 ⁹ /l) x̄ (SD)	1.6 (0.8)	1.7 (0.7)	0.202
Neutrophils (x 10 ⁹ /l) x̄ (SD)	6.6 (3.4)	6.6 (3.2)	0.812
Monocytes (x10 ⁹ /l) x̄ (SD)	0.7 (0.3)	0.7 (0.3)	0.700
NLR x̄ (SD)	5.1 (3.6)	4.6 (3.4)	0.485
PLR x̄ (SD)	217.9 (119.9)	213.4 (123.3)	0.714
LMR x̄ (SD)	2.5 (1.4)	3.0 (2.4)	0.271

CRP = C-reactive protein; ECOG = Eastern Cooperative Oncology Group; ED-SCLC = extensive-stage disease small cell lung cancer; LDH = lactate dehydrogenase; LD-SCLC = limited-stage disease small cell lung cancer; LMR = lymphocyte-to-monocyte ratio; NLR = neutrophil-to-lymphocyte ratio; OS = overall survival; SD = standard deviation; PCI = prophylactic cranial irradiation; PFS = progression-free survival; PLR = platelet-to-lymphocyte ratio; PS = performance status; WBC = white blood cells; x̄ = arithmetic mean

Cox regression was used for determining possible multiple interactions among the parameters. The Cox regression was performed in the case of $p < 0.3$

or for clinically relevant parameters. All P values were two-tailed. The level of significance was set at Alpha = 0.05. Statistical analysis was performed by using IBM SPSS Statistics for Windows, Version 21.0 (IBM SPSS Inc, Chicago, IL, USA).

Cut-off values suggested by the literature were used for testing the potential prognostic value of the investigated ratios, since the ROC curves of the investigated ratios did not have a statistical significance. All ratios were tested regarding two cut-off values. The cut-off values for NLR were 4 and 5, those for PLR were 150 and 250, and those for LMR were 2.64 and 4.19.³⁴⁻³⁹

Results

Patient characteristics

Patient characteristics regarding the disease stage are shown in Table 1. Out of 438 patients diagnosed with small cell lung cancer or mixed neuroendocrine carcinoma between 2012 and 2016, 140 met the inclusion and exclusion criteria and were included in the study. Of those 140 patients, 80 were diagnosed with extensive-stage disease and 60 with limited-stage disease. The mean patient age was 63.1 years with a mean deviation of 9.2 years (42–87 years of age). Slightly more males than females were involved in the study (89 or 63.6%). The majority of the patients were smokers (95.7%), of good performance status, 0–1 according to the ECOG scale (82.9%). Only 14 patients (10%) received less than 4 chemotherapy cycles. Forty-five patients (32%) underwent radiotherapy, most of whom were in the limited-stage disease group. Only twelve patients underwent PCI (8.6%), again significantly more in the limited-stage disease group. Disease control was observed in 119 patients (85%). After two years, 125 patients (89.2%) died. Fifteen out of the total number of patients included in the analysis (10.7%) survived for more than 2 years, and all of them belonged to the limited-stage disease group. According to the statistical analysis, disease control, PFS, OS, and outcome were significantly better in the limited-stage disease group. Of the laboratory parameters, a significant statistical difference regarding the disease stage was only observed for CRP and LDH. The mean NLR and PLR values were higher in the extensive-stage disease group of patients, while the mean LMR value was higher in the limited-stage disease group, but the difference was not statistically significant. In the extensive-stage disease group, a statistically significant difference of LMR values regarding patient

age was observed, *i.e.*, higher LMR values were observed in the younger age group.

Survival analysis

The median survival time for all patients was 52.6 weeks (95% confidence interval [CI] 47.5–57.7). The median survival time for the ED group of patients was 45.7 weeks (95% confidence interval [CI] 42.3–49.2) and for the LD patient group it was 64.1 weeks (95% confidence interval [CI] 56.70–71.6).

According to the Kaplan-Meier estimator, survival analysis of all 140 patients showed a statistically significant difference in the overall survival regarding disease extension, radiotherapy to the primary tumor, prophylactic brain irradiation and disease control. Therefore, patients with limited-stage disease, patients with disease control, irradiated patients and patients who underwent PCI had a better survival. Of the laboratory parameters, a statistically significant difference in the overall survival was observed regarding the hemoglobin, CRP, LDH, and boundary monocyte values, whereas a statistically significant difference in the overall survival regarding the ECOG status, NLR, PLR, and LMR was not observed (Table 2).

Separate testing showed a statistically significant difference in overall survival in patients with extensive-stage disease, considering the presence of skin metastases and laboratory parameters including LDH and NLR, regardless of the cut-off values. Therefore, a better overall survival was observed in the patients who did not have skin metastases and had lower LDH and NLR values (Table 3). No positive correlation between overall survival and ECOG status, number of metastatic sites, and disease control was observed in the subjects with metastatic disease.

A statistically significant difference in overall survival, regarding the ECOG status, radiotherapy of the primary tumor, prophylactic cranial irradiation, and laboratory values such as hemoglobin and creatinine levels, was determined in the limited-stage disease group of patients (Table 4).

As we have already mentioned, Cox regression was used for determining possible multiple interactions among the variables. Thus, all statistically significant parameters from the Kaplan-Meier analysis were included in the multiple regression model. In this model LDH became the most significant prognostic factor in extensive-stage disease, while the ECOG performance status became the

TABLE 2. Prognostic parameters for survival – all patients

Variable	No. of patients	Median survival (weeks) - 95% CI	p-values (log-rank test)
Extent of disease	LD	60	64.1 (56.7–71.6)
	ED	80	45.7 (42.3–49.2)
Chest irradiation	Yes	45	69.1 (63.3–75.0)
	No	95	45.3 (39.0–51.6)
PCI	Yes	12	69.0 (12.3–125.7)
	No	128	49.1 (43.4–54.9)
Disease control	Yes	119	53.4 (49.5–57.3)
	No	21	36.4 (25.3–47.5)
Hemoglobin (g/l)	M ≥ 138	78	57.1 (50.6–63.6)
	F ≥ 119	62	40.6 (28.9–52.3)
CRP (mg/l)	< 5.0	35	57.1 (48.9–65.4)
	≥ 5.0	104	47.9 (41.4–54.3)
LDH (U/l)	< 241	55	63.0 (53.0–73.0)
	≥ 241	56	37.0 (27.7–46.3)
Monocytes (x10 ⁹ /l)	≤ 0.84	99	55.0 (49.5–60.5)
	> 0.84	41	44.3 (33.2–55.4)

CRP = C-reactive protein; ED = extensive-stage disease; LD = limited-stage disease; LDH - lactate dehydrogenase; PCI = prophylactic cranial irradiation

TABLE 3. Prognostic parameters for survival – extensive-stage disease (ED)

Variable	No. of patients	Median survival (weeks) - 95% CI	p-values (log-rank test)
Skin metastases	Yes	4	15.9 (0.7–31.0)
	No	76	46.9 (42.7–51.0)
LDH (U/l)	< 241	26	54.0 (45.4–62.6)
	≥ 241	36	33.7 (22.8–44.6)
NLR	< 4	40	50.1 (43.5–56.8)
	≥ 4	40	44.7 (37.4–52.0)
NLR	< 5	50	50.1 (44.7–55.6)
	≥ 5	30	39.6 (30.7–48.5)

LDH = lactate dehydrogenase; NLR = neutrophil-to-lymphocyte ratio

most powerful one in limited-stage disease. The data are presented in Table 5.

Discussion

Numerous prognostic factors were investigated in various cancer types in order to find the factor which would most accurately define the patient groups that could benefit from a certain therapy and consequently expect a better survival.³⁹ The established fact about the important role inflammation plays in the process of carcinogenesis has led to research into the prognostic significance of various inflammatory markers. In the past decade numerous papers have been published on such research in relation to non-small cell lung cancer^{29,31}, but, very few studies of this kind have been done for small cell lung cancer. The present study

TABLE 4. Prognostic parameters for survival – limited-stage disease (LD)

Variable		No. of patients	Median survival (weeks) - 95% CI	p-values (log-rank test)
PS (ECOG)	0–1	52	66.3 (57.6–75.0)	0.007
	2–3	8	35.9 (8.3–63.4)	
Chest irradiation	Yes	36	70.7 (51.8–89.6)	0.003
	No	24	36.7 (16.1–57.3)	
PCI	Yes	10	102.0 (0.0–209.6)	0.032
	No	50	58.3 (46.7–69.8)	
Hemoglobin (g/l)	M ≥ 138 F ≥ 119	35	71.9 (57.0–86.8)	0.033
	< 138 < 119	25	54.3 (17.7–90.9)	
Creatinine (umol/l)	M < 125 F < 107	57	66.3 (58.6–74.0)	0.001
	≥ 125 ≥ 107	3	32.9 (27.8–37.9)	

ECOG = Eastern Cooperative Oncology Group; PCI = prophylactic cranial irradiation; PS = performance status

TABLE 5. Results of Cox regression analysis

Variable		HR	95.0% CI for HR		p-value
			Lower	Upper	
ED-SCLC					
Skin metastases	Yes vs No	0.034	0.006	0.192	0.000
LDH	< 241 vs. ≥ 241	1.691	1.130	2.530	0.011
Monocytes	≤ 0.84 vs. > 0.84	1.057	0.675	1.655	0.809
NLR	< 4 vs. ≥ 4	1.497	0.757	2.961	0.246
NLR	< 5 vs. ≥ 5	0.795	0.391	1.615	0.525
LD-SCLC					
ECOG	0–1 vs. 2–3	2.865	1.032	7.953	0.043
Chest irradiation	Yes vs. No	1.558	0.793	3.047	0.195
PCI	Yes vs. No	2.038	0.893	4.654	0.091
Hemoglobin	Normal vs. Anemia	1.439	0.773	2.678	0.251
Creatinine	Normal vs. Elevated	1.432	0.155	13.198	0.751

CI = confidence interval; ECOG = Eastern Cooperative Oncology Group, ED-SCLC = extensive-stage disease small cell lung cancer; HR = hazard ratio; LDH = lactate dehydrogenase; LD-SCLC = limited-stage disease small cell lung cancer; NLR = neutrophil-to-lymphocyte ratio; PCI = prophylactic cranial irradiation

was conducted with the intention to determine potential prognostic parameters of survival in a European population of patients diagnosed with SCLC. Survival parameters were identified for the whole population of patients, as well as separately for patients with extensive-stage and those with limited-stage disease, in order to determine differences between these two groups.

As disease extension and performance status are generally among the most investigated prognostic parameters, they were verified as the most important for SCLC as well.²³ Our study also showed that disease extension was a significant prognostic factor, and certainly the most significant predictor of longer survival. On the other hand, performance status showed a prognostic value only for the

limited-stage disease patient group, which can be explained by the fact that it was possibly assessed more accurately in this patient group. As a matter of fact, performance status assessment is a subjective method and in retrospective studies there is always a possibility that the criteria for certain patients varied. Unlike in other neoplasms, age did not have a prognostic significance in most of the studies regarding SCLC, which was confirmed in our study, too.²³ Neither gender nor smoking status had a prognostic significance, but, it is noteworthy that the number of non-smokers in the study was negligible. Of all the variables, radiotherapy, PCI and disease control had a survival impact in the whole research patient group. When we separated the patients with extensive-stage from those with limited-stage disease, radiotherapy and PCI retained a survival impact in the patients with limited-stage disease, as we expected. However, disease control showed prognostic value neither in LD nor in ED.

In the last few decade various laboratory parameters regarding prognostic value have been investigated. Their ratios have also been investigated recently. Some studies verified a prognostic significance of hemoglobin, leukocyte count, CRP, LDH, and serum sodium concentration in SCLC.^{23,25,40} The prognostic significance of hemoglobin and LDH was confirmed in our patients, along with a lower significance of CRP and monocyte count as prognostic factors. When we excluded disease extension from the analysis, LDH retained a prognostic significance in the ED group, while hemoglobin retained a prognostic significance in the LD group of patients. Besides, creatinine level occurred as an independent prognostic factor for survival in the LD group of patients, but again only in the extremely small number of patients with increased creatinine levels.

Although the combinations of various laboratory indicators, including NLR, PLR, and LMR, have already been examined as prognostic factors in SCLC, a relatively small number of studies have been published regarding this type of cancer. Most of the published papers investigating the predictive significance of these parameters in patients with lung cancer address non-small cell lung carcinoma.²⁹⁻³¹ Consulting the literature in English until May, 2020, we found a total of twenty studies, seven of which had been published in 2019, which investigated one or more of these three ratios in patients with small cell lung cancer. It is interesting to note that most of the studies relate to the Asian population. For example, the prog-

nostic significance of LMR in SCLC was only investigated in two studies, both conducted in the Asian population.^{38,41} Out of twelve studies which investigated the prognostic value of PLR alone or in combination with NLR, only one was done in Europe.³⁵ NLR, as the most researched ratio, was the subject of investigation in seventeen studies, of which only three were European.^{25,35,42} There are only two studies investigating the prognostic role of NLR and/or PLR exclusively in the ED group of patients.^{34,43} To our knowledge, to date neither of these two parameters have been investigated on a European population in cases of extended SCLC.

As race has been determined as a significant prognostic factor in SCLC patients, in the sense that being Caucasian represents a favorable independent prognostic factor, we were interested in whether our results would differ from the ones obtained elsewhere so far.⁵

It is important to mention that the results of the former studies are inconsistent, that is, some studies showed a statistically significant correlation between the NLR and PLR ratios and overall survival of the patients, while others did not yield a statistical significance. In fact, some studies didn't investigate these ratios in correlation with survival at all.⁴⁴⁻⁴⁶ The only prospective study conducted in the USA on more than 900 patients verified that NLR was a prognostic parameter for OS only in the extensive-stage disease group of patients, which is consistent with our results.⁴⁷ The same study established that PLR was a prognostic parameter for OS only in limited-stage disease, which was different from our results. There are no prospective studies for LMR. Most retrospective studies which investigated NLR established its prognostic value, regardless of whether it was investigated in LD, ED, or simultaneously in both patient groups. Among twelve retrospective studies investigating PLR, only three showed a prognostic significance of this parameter.⁴⁸⁻⁵⁰ Out of the two studies investigating LMR, only one showed a prognostic significance of this parameter.³⁸

In the prospective study mentioned above, among other things it was established that NLR and PLR were statistically significantly greater in patients with extended disease.⁴⁷ In our study, the mean values of NLR and PLR were also higher in ED patients, while LMR was higher in LD, although the difference was not statistically significant. On the other hand, we found statistically significant differences in LMR values in correlation with patient age in the ED group, *i.e.*, higher LMR values in the younger age group of these patients.

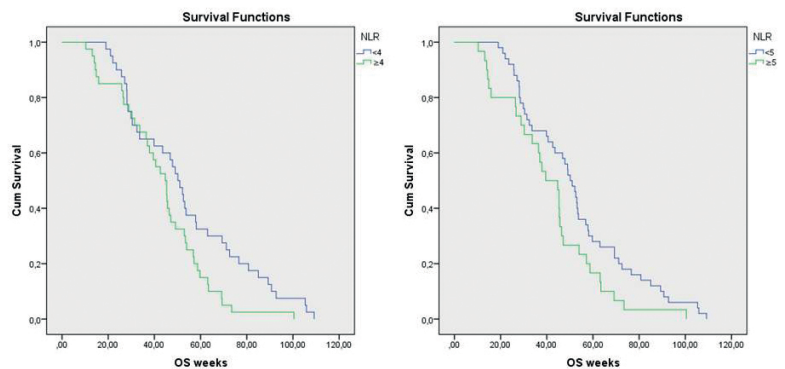


FIGURE 1. Probability of survival of all patients according to stage ($p < 0.0001$).

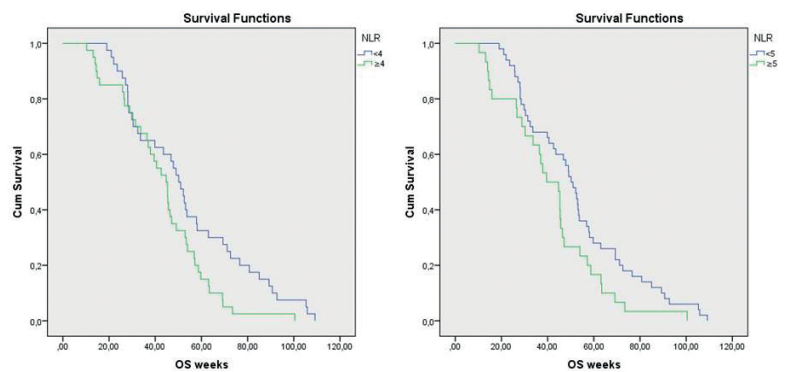


FIGURE 2. Probability of survival of extensive-stage disease small cell lung cancer patients according to neutrophil-to-lymphocyte ratio (NLR) cut-off 4 ($p = 0.026$) and NLR cut-off 5 ($p = 0.036$).

In spite of the fact that some of our results were consistent with those from the only prospective study, our study had numerous limitations. In every study where data are collected from available records, there is a possibility that some of it may not be reliable, particularly data undergoing subjective assessment. As mentioned earlier, performance status is one of such parameters, thus making it more difficult for analysis in retrospective studies. A similar situation may arise in the assessment of peripheral lymph node regression during patient follow up and evaluation of the response to treatment.

Furthermore, in the determination of disease extent, especially in concomitant chemoradiotherapy candidates, assessment based only on clinical examination, bronchoscopy, and CT is not sufficient. Since this type of carcinoma is characterized by rapid spread, complete staging should be done prior to treatment, including brain CT and bone scintigraphy. This is the standard procedure at our

institution today, but was not always possible in the past for technical reasons.

The relatively small number of subjects enrolled in the study was also a limitation. However, two published studies enrolled approximately the same number of patients.^{51,52} Also, some of the published studies were conducted in even smaller groups of participants.^{44,51,53} Although some studies had a large number of patients, they didn't analyze patients separately considering disease extension.⁵⁴

It is important to note that the number of patients enrolled in the study was probably not adequate for the analysis of certain variables. Namely, only a very small number of patients with skin metastases and increased creatinine participated in the study, as well as very few patients with a low performance status. This presents a problem for many studies, since low-performance status patients are usually not candidates for differential treatment and are rarely included in clinical studies. The same applies for kidney failure patients. On the other hand, since the skin is an uncommon metastatic site, such patients are rare. Considering the confidence interval, it is clear that according to this study skin metastases are not a favorable indicator of survival. On the contrary, creatinine can be considered a favorable indicator of survival despite the small number of patients.

As far as the investigated treatment procedures and their prognostic values are concerned, there are certain limitations as well. In the group of all patients, statistically significant differences were found for survival in relation to PCI and thoracic irradiation. However, when the patients were analyzed separately in relation to the extent of the disease, those differences disappeared in the ED group. This is due to the fact that disease extent is one of the most important prognostic factors for SCLC, which was established in 2003 in a prospective study involving 436 patients.²³ Therefore, these two patient groups should always be investigated separately, because the differences in their prognoses entail different modes and aims of treatment. In our study, PCI remained prognostically valuable in the LD patient group, but with an insufficient number of subjects for the result to be considered reliable. This treatment procedure has always been controversial, presenting an issue for confrontation and opposing research.⁵⁵ The prognostic value of PCI was certainly not the primary aim of our study. In spite of its limitations, we believe that our study will contribute to the elucidation of small cell lung cancer, as well as stimulate further research on this type of carcinoma, which

has somehow always remained in the margins of lung cancer research.

Conclusions

The objective of this study was to determine a potential prognostic value of the neutrophil-to-lymphocyte, platelet-to-lymphocyte, and lymphocyte-to-monocyte ratios in patients diagnosed with extensive-stage and limited-stage small cell lung cancer. To the best of our knowledge, this is the first study carried out on a European population which analyzed all three of the mentioned ratios. According to the study, NLR could be a good prognostic marker in patients with extensive-stage SCLC. Further prospective studies are definitely needed for this type of cancer.

Acknowledgments

This research was supported by the grant awarded to JK (Croatian Scientific Foundation; IP-06-2016-1441). This research did not receive any other specific grant from funding agencies in the public, commercial, or not-for-profit sectors.

We wish to thank the Croatian Scientific Foundation for its financial support. We would also like to thank Mario Sekerija for providing us with patient outcome data and Goran Knezevic for the statistical analysis. We are grateful to Aleksandra Zmegac Horvat for language editing of the manuscript.

References

1. Bray F, Ferlay J, Soerjomataram I, Siegel RL, Torre LA, Jemal A. Global cancer statistics 2018: GLOBOCAN estimates of incidence and mortality worldwide for 36 cancers in 185 countries. *CA Cancer J Clin* 2018; **68**: 394-424. doi: 10.3322/caac.21492
2. Ferlay J, Colombet M, Soerjomataram I, Mathers C, Parkin DM, Piñeros M, et al. Estimating the global cancer incidence and mortality in 2018: GLOBOCAN sources and methods. *Int J Cancer* 2019; **144**: 1941-53. doi: 10.1002/ijc.31937
3. Govindan R, Page N, Morgensztern D, Read W, Tierney R, Vlahiotis A, et al. Changing epidemiology of small-cell lung cancer in the United States over the last 30 years: analysis of the surveillance, epidemiologic, and end results database. *J Clin Oncol* 2006; **24**: 4539-44. doi: 10.1200/JCO.2005.04.4859
4. Riaz SP, Lichtenborg M, Coupland VH, Spicer J, Peake MD, Møller H. Trends in incidence of small cell lung cancer and all lung cancer. *Lung Cancer* 2012; **75**: 280-4. doi: 10.1016/j.lungcan.2011.08.004
5. Albain KS, Crowley JJ, LeBlanc M, Livingston RB. Determinants of improved outcome in small-cell lung cancer: an analysis of the 2,580-patient Southwest Oncology Group data base. *J Clin Oncol* 1990; **8**: 1563-74. doi: 10.1200/JCO.1990.8.9.1563

6. Lally BE, Urbanic JJ, Blackstock AW, Miller AA, Perry MC. Small cell lung cancer: have we made any progress over the last 25 years? *Oncologist* 2007; **12**: 1096-104. doi: 10.1634/theoncologist.12-9-1096
7. Yang Y, Yuan G, Zhan C, Huang Y, Zhao M, Yang X, et al. Benefits of surgery in the multimodality treatment of stage IIB-IIIC small cell lung cancer. *J Cancer* 2019; **10**: 5404-12. doi: 10.7150/jca.31202
8. Lassen U, Østerlind K, Hansen M, Dombrowski P, Bergman B, Hansen HH. Long-term survival in small-cell lung cancer: posttreatment characteristics in patients surviving 5 to 18+ years - an analysis of 1,714 consecutive patients. *J Clin Oncol* 1995; **13**: 1215-20. doi: 10.1200/JCO.1995.13.5.1215
9. Kato Y, Ferguson TB, Bennett DE, Burford TH. Oat cell carcinoma of the lung. A review of 138 cases. *Cancer* 1969; **23**: 517-24. doi: 10.1002/1097-0142(196903)23:3<517::aid-cnrcr2820230301>3.0.co;2-I
10. Faivre-Finn C, Snee M, Ashcroft L, Appel W, Barlesi F, Bhatnagar A, et al. Concurrent once-daily versus twice-daily chemoradiotherapy in patients with limited-stage small-cell lung cancer (CONVERT): an open-label, phase 3, randomised, superiority trial. *Lancet Oncol* 2017; **18**: 1116-25. doi: 10.1016/S1470-2045(17)30318-2
11. Simone CB 2nd, Bogart JA, Cabrera AR, Daly ME, DeNunzio NJ, Detterbeck F, et al. Radiation therapy for small cell lung cancer: an ASTRO clinical practice guideline. *Pract Radiat Oncol* 2020; **10**: 158-73. doi: 10.1016/j.prro.2020.02.009
12. Stanic K, Vrankar M, But-Hadzic J. Consolidation radiotherapy for patients with extended disease small cell lung cancer in a single tertiary institution: impact of dose and perspectives in the era of immunotherapy. *Radiol Oncol* 2020; **54**(4): 437-446; 29; **54**: 353-63. doi: 10.2478/raon-2020-0046
13. Tian S, Zhang X, Jiang R, Pillai RN, Owonikoko TK, Steuer CE, et al. Survival outcomes with thoracic radiotherapy in extensive-stage small-cell lung cancer: a propensity score-matched analysis of the national cancer database. *Clin Lung Cancer* 2019; **20**: 484-93.e6. doi: 10.1016/j.clc.2019.06.014
14. Tay RY, Heigener D, Reck M, Califano R. Immune checkpoint blockade in small cell lung cancer. *Lung Cancer* 2019; **137**: 31-7. doi: 10.1016/j.lungcan.2019.08.024
15. Horn L, Mansfield AS, Szczesna A, Havel L, Krzakowski M, Hochmair MJ, et al. First-line atezolizumab plus chemotherapy in extensive-stage small-cell lung cancer. *N Engl J Med* 2018; **379**: 2220-9. doi: 10.1056/NEJMoa1809064
16. Paz-Ares L, Dvorkin M, Chen Y, Reinmuth N, Hotta K, Trukhin D, et al. Durvalumab plus platinum-etoposide versus platinum-etoposide in first-line treatment of extensive-stage small-cell lung cancer (CASPIAN): a randomised, controlled, open-label, phase 3 trial. *Lancet* 2019; **394**: 1929-39. doi: 10.1016/S0140-6736(19)32222-6
17. Mantovani A, Allavena P, Sica A, Balkwill F. Cancer-related inflammation. *Nature* 2008; **454**: 436-44. doi: 10.1038/nature07205
18. Tan CSY, Read JA, Phan VH, Beale PJ, Peat JK, Clarke SJ. The relationship between nutritional status, inflammatory markers and survival in patients with advanced cancer: a prospective cohort study. *Support Care Cancer* 2015; **23**: 385-91. doi: 10.1007/s00520-014-2385-y
19. Zheng J, Seier K, Gonen M, Balachandran V, Kingham T, D'Angelica M, et al. Utility of serum inflammatory markers for predicting microvascular invasion and survival for patients with hepatocellular carcinoma. *Ann Surg Oncol* 2017; **24**: 3706-14. doi: 10.1245/s10434-017-6060-7
20. Maestu I, Pastor M, Gómez-Codina J, Aparicio J, Oltra A, Herranz C, et al. Pretreatment prognostic factors for survival in small-cell lung cancer: a new prognostic index and validation of three known prognostic indices on 341 patients. *Ann Oncol* 1997; **8**: 547-53. doi: 10.1023/a:1008212826956
21. Alexandrakis M, Passam F, Moschandreia I, Christophoridou A, Pappa C, Coulocheri S, et al. Levels of serum cytokines and acute phase proteins in patients with essential and cancer-related thrombocytosis. *Am J Clin Oncol* 2003; **26**: 135-40. doi: 10.1097/0000421-200304000-00007
22. Petekkaya I, Unlu O, Roach E, Gecmez G, Okoh A, Babacan T, et al. Prognostic role of inflammatory biomarkers in metastatic breast cancer. *J BUON* 2017; **22**: 614-22.
23. Bremnes RM, Sundstrom S, Aasebø U, Kaasa S, Hatlevoll R, Aamdal S. The value of prognostic factors in small cell lung cancer: results from a randomised multicenter study with minimum 5 year follow-up. *Lung Cancer* 2003; **39**: 303-13. doi: 10.1016/S0169-5002(02)00508-1
24. Haas M, Heinemann V, Kullmann F, Laubender R, Klose C, Bruns C, et al. Prognostic value of CA 19-9, CEA, CRP, LDH and bilirubin levels in locally advanced and metastatic pancreatic cancer: results from a multicenter, pooled analysis of patients receiving palliative chemotherapy. *J Cancer Res Clin Oncol* 2013; **139**: 681-9. doi: 10.1007/s00432-012-1371-3
25. Bernhardt D, Aufderstrasse S, König L, Adebeg S, Bozorgmehr F, Christopoulos P, et al. Impact of inflammatory markers on survival in patients with limited disease small-cell lung cancer undergoing chemoradiotherapy. *Cancer Manag Res* 2018; **10**: 6563-9. doi: 10.2147/CMAR.S180990
26. Oh SY, Heo J, Noh OK, Chun M, Cho O, Oh YT. Absolute lymphocyte count in preoperative chemoradiotherapy for rectal cancer: changes over time and prognostic significance. *Technol Cancer Res Treat* 2018; **17**: 1533033818780065. doi: 10.1177/1533033818780065
27. Ozmen S, Timur O, Calik I, Altinkaynak K, Simsek E, Gozcu H, et al. Neutrophil-lymphocyte ratio (NLR) and platelet-lymphocyte ratio (PLR) may be superior to C-reactive protein (CRP) for predicting the occurrence of differentiated thyroid cancer. *Endocr Regul* 2017; **51**: 131-6. doi: 10.1515/enr-2017-0013
28. Acartürk Tunçay E, Karakurt Z, Aksoy E, Saltürk C, Gungor S, Ciftaslan N, et al. Eosinophilic and non-eosinophilic COPD patients with chronic respiratory failure: neutrophil-to-lymphocyte ratio as an exacerbation marker. *Int J Chron Obstruct Pulmon Dis* 2017; **12**: 3361-70. doi: 10.2147/COPD.S147261
29. Zhao Q, Yang Y, Xu S, Zhang X, Wang H, Zhang H, et al. Prognostic role of neutrophil to lymphocyte ratio in lung cancers: a meta-analysis including 7,054 patients. *Onco Targets Ther* 2015; **8**: 2731-8. doi: 10.2147/OTT.S90875
30. Yu Y, Qian L, Cui J. Value of neutrophil-to-lymphocyte ratio for predicting lung cancer prognosis: a meta-analysis of 7,219 patients. *Mol Clin Oncol* 2017; **7**: 498-506. doi: 10.3892/mco.2017.1342
31. Zhao QT, Yuan Z, Zhang H, Zhang X, Wang H, Wang Z, et al. Prognostic role of platelet to lymphocyte ratio in non-small cell lung cancers: a meta-analysis including 3,720 patients. *Int J Cancer*. 2016; **139**: 164-70. doi: 10.1002/ijc.30060
32. Oken M, Creech R, Tormey D, Horton J, Davis T, McFadden E, et al. Toxicity and response criteria of the Eastern Cooperative Oncology Group. *Am J Clin Oncol* 1982; **5**: 649-55.
33. Früh M, De Ruysscher D, Popat S, Crinò L, Peters S, Felip E. Small-cell lung cancer (SCLC): ESMO Clinical Practice Guidelines for diagnosis, treatment and follow-up. *Ann Oncol* 2013; **24**(Suppl 6): vi99-105. doi: 10.1093/annonc/mdt178
34. Sakin A, Sahin S, Yasar N, Demir C, Arici S, Geredeli C, et al. The relation between hemogram parameters and survival in extensive-stage small cell lung cancer. *Oncol Res Treat* 2019; **42**: 506-15. doi: 10.1159/000501595
35. Käsmann L, Bolm L, Schild SE, Janssen S, Rades D. Neutrophil-to-lymphocyte ratio predicts outcome in limited disease small-cell lung cancer. *Lung* 2017; **195**: 217-24. doi: 10.1007/s00408-017-9976-6
36. Kang MH, Go SI, Song HN, Lee A, Kim SH, Kang JH, et al. The prognostic impact of the neutrophil-to-lymphocyte ratio in patients with small-cell lung cancer. *Br J Cancer* 2014; **111**: 452-60. doi: 10.1038/bjc.2014.317
37. Hong X, Cui B, Wang M, Yang Z, Wang L, Xu Q. Systemic immune-inflammation index, based on platelet counts and neutrophil-lymphocyte ratio, is useful for predicting prognosis in small cell lung cancer. *Tohoku J Exp Med* 2015; **236**: 297-304. doi: 10.1620/tjem.236.297
38. Go SI, Kim RB, Song HN, Kang MH, Lee US, Choi HJ. Prognostic significance of the lymphocyte-to-monocyte ratio in patients with small cell lung cancer. *Med Oncol* 2014; **31**: 323. doi: 10.1007/s12032-014-0323-y
39. Proctor MJ, Morrison DS, Talwar D, Balmer S, Fletcher C, O'reilly D, et al. A comparison of inflammation-based prognostic scores in patients with cancer: A Glasgow Inflammation Outcome Study. *Eur J Cancer* 2011; **47**: 2633-41. doi: 10.1016/j.ejca.2011.03.028
40. Rawson NS, Peto J. An overview of prognostic factors in small cell lung cancer. A report from the Subcommittee for the Management of Lung Cancer of the United Kingdom Coordinating Committee on Cancer Research. *Br J Cancer* 1990; **61**: 597-604. doi: 10.1038/bjc.1990.133

41. Cao S, Jin S, Shen J, Cao J, Zhang H, Meng Q, et al. Selected patients can benefit more from the management of etoposide and platinum-based chemotherapy and thoracic irradiation-a retrospective analysis of 707 small cell lung cancer patients. *Oncotarget* 2017; **8**: 8657-69. doi: 10.18632/oncotarget.14395
42. Lohinai Z, Bonanno L, Aksarin A, Pavan A, Megyesfalvi Z, Santa B, et al. Neutrophil-lymphocyte ratio is prognostic in early stage resected small-cell lung cancer. *Peer J* 2019; **7**: e7232. doi: 10.7717/peerj.7232
43. Suzuki R, Lin SH, Wei X, Allen PK, Welsh JW, Byers LA, et al. Prognostic significance of pretreatment total lymphocyte count and neutrophil-to-lymphocyte ratio in extensive-stage small-cell lung cancer. *Radiother Oncol* 2018; **126**: 499-505. doi: 10.1016/j.radonc.2017.12.030
44. Pan Z, Zhang L, Liu C, Huang X, Shen S, Lin X, et al. Cisplatin or carboplatin? Neutrophil to lymphocyte ratio may serve as a useful factor in small cell lung cancer therapy selection. *Oncol Lett* 2019; **18**: 1513-20. doi: 10.3892/ol.2019.10459
45. Zheng Y, Wang L, Zhao W, Dou Y, Lv W, Yang H, et al. Risk factors for brain metastasis in patients with small cell lung cancer without prophylactic cranial irradiation. *Strahlenther Onkol* 2018; **194**: 1152-62. doi: 10.1007/s00066-018-1362-7
46. Wen Q, Meng X, Xie P, Wang S, Sun X, Yu J. Evaluation of factors associated with platinum-sensitivity status and survival in limited-stage small cell lung cancer patients treated with chemoradiotherapy. *Oncotarget* 2017; **8**: 81405-18. doi: 10.18632/oncotarget.19073
47. Xie D, Marks R, Zhang M, Jiang G, Jatoi A, Garces YI, et al. Nomograms predict overall survival for patients with small-cell lung cancer incorporating pretreatment peripheral blood markers. *J Thorac Oncol* 2015; **10**: 1213-20. doi: 10.1097/JTO.0000000000000585
48. Suzuki R, Wei X, Allen PK, Cox JD, Komaki R, Lin SH. Prognostic significance of total lymphocyte count, neutrophil-to-lymphocyte ratio, and platelet-to-lymphocyte ratio in limited-stage small-cell lung cancer. *Clin Lung Cancer* 2019; **20**: 117-23. doi: 10.1016/j.clcc.2018.11.013
49. Pan H, Shi X, Xiao D, He J, Zhang Y, Liang W, et al. Nomogram prediction for the survival of the patients with small cell lung cancer. *J Thorac Dis* 2017; **9**: 507-18. doi: 10.21037/jtd.2017.03.121
50. Zhang Q, Qu Y, Liu H, Jia H, Wen F, Pei S, et al. Initial platelet-to-lymphocyte count as prognostic factor in limited-stage small cell lung cancer. *Biomark Med* 2019; **13**: 249-58. doi: 10.2217/bmm-2018-0415
51. Liu D, Huang Y, Li L, Song J, Zhang L, Li W. High neutrophil-to-lymphocyte ratios confer poor prognoses in patients with small cell lung cancer. *BMC Cancer* 2017; **17**: 882. doi: 10.1186/s12885-017-3893-1
52. Wang X, Teng F, Kong L, Yu J. Pretreatment neutrophil-to-lymphocyte ratio as a survival predictor for small-cell lung cancer. *Onco Targets Ther* 2016; **9**: 5761-70. doi: 10.2147/OTT.S106296
53. Mirili C, Guney IB, Paydas S, Seydaoglu G, Kapukaya TK, Ogul A, et al. Prognostic significance of neutrophil/lymphocyte ratio (NLR) and correlation with PET-CT metabolic parameters in small cell lung cancer (SCLC). *Int J Clin Oncol* 2019; **24**: 168-78. doi: 10.1007/s10147-018-1338-8
54. Deng M, Ma X, Liang X, Zhu C, Wang M. Are pretreatment neutrophil-lymphocyte ratio and platelet-lymphocyte ratio useful in predicting the outcomes of patients with small-cell lung cancer? *Oncotarget* 2017; **8**: 37200-7. doi: 10.18632/oncotarget.16553
55. Yin X, Yan D, Qiu M, Huang L, Yan SX. Prophylactic cranial irradiation in small cell lung cancer: a systematic review and meta-analysis. *BMC Cancer* 2019; **19**: 95. doi: 10.1186/s12885-018-5251-3

Treatment patterns and real-world evidence for stage III non-small cell lung cancer in Central and Eastern Europe

Milada Zemanova¹, Marko Jakopovic², Karmen Stanić^{3,4}, Małgorzata Łazar-Poniatowska⁵, Martina Vrankar^{3,4}, Petronela Rusu⁶, Tudor Ciuleanu⁶, Davorin Radosavljević⁷, Krisztina Bogos⁸, Sergiusz Nawrocki⁹

¹ 1st Faculty of Medicine of Charles University, Prague, Czech Republic

² Department for Respiratory Diseases Jordanovac, University Hospital Centre Zagreb, School of Medicine, University of Zagreb, Zagreb, Croatia

³ Institute of Oncology Ljubljana, Ljubljana, Slovenia

⁴ Faculty of Medicine, University of Ljubljana, Ljubljana, Slovenia

⁵ Department of Oncology and Radiotherapy, Medical University of Gdansk, Gdansk, Poland

⁶ Institute of Oncology “Prof. Dr. Ion Chiricuta”, Cluj-Napoca, Romania

⁷ Institute for Oncology and Radiology of Serbia, Belgrade, Serbia

⁸ National Koranyi Institute of TB and Pulmonology, Budapest, Hungary

⁹ Department of Oncology, University of Warmia and Mazury in Olsztyn, Olsztyn, Poland

Radiol Oncol 2020; 54(4): 447-454.

Received 9 June 2020

Accepted 10 July 2020

Correspondence to: Assist. Prof. Karmen Stanić, P.D., Ph.D., Institute of Oncology Ljubljana, Zaloška 2, 1000 Ljubljana, Slovenia. E-mail: kstanic@onko-i.si

Disclosure: Dr. Zemanova reports other from AstraZeneca, during the conduct of the study; grants from AstraZeneca, grants and personal fees from BristolMyersSquibb, personal fees from Boehringer Ingelheim, personal fees from MSD, personal fees from Roche, grants from Novartis, outside the submitted work; Dr. Jakopovic reports personal fees and non-financial support from AstraZeneca, personal fees and non-financial support from Roche, personal fees and non-financial support from MSD, personal fees and non-financial support from Pfizer, personal fees and non-financial support from Boehringer Ingelheim, outside the submitted work; Dr. Stanić reports personal fees and non-financial support from AstraZeneca, during the conduct of the study; Dr. Vrankar reports personal fees from AstraZeneca, Roche, Boehringer Ingelheim, Merck Sharp & Dohme, other from AstraZeneca, Roche, Boehringer Ingelheim, outside the submitted work; Dr. Rusu reports personal fees from AstraZeneca, personal fees from AD-pharma, outside the submitted work; Dr. Ciuleanu reports consultancy fees from Astellas, Janssen, Bristol-Myers Squibb, Merck Serono, Amgen, Roche, Pfizer, Boehringer Ingelheim, Lilly, AstraZeneca, MSD, Sanofi, Novartis, Servier, AD Pharma; Dr. Radosavljević reports personal fees and non-financial support from AstraZeneca, personal fees and non-financial support from MSD, personal fees and non-financial support from Roche, personal fees and non-financial support from Pfizer, personal fees from Boehringer Ingelheim, personal fees and non-financial support from Merck, personal fees and non-financial support from Amicus, outside the submitted work; other authors have nothing to disclose.

Background. The aim of this project was to collect real-world evidence and describe treatment patterns for stage III non-small cell lung cancer in Central and Eastern Europe. Based on real-world evidence, an expert opinion was developed, and the unmet needs and quality indicators were identified.

Patients and methods. A systematic literature search and a multidisciplinary expert panel of 10 physicians from 7 countries used a modified Delphi process to identify quality indicators and unmet needs in patients with stage III non-small cell lung cancer. The profound questionnaire was used to characterize treatment patterns used for stage III non-small cell lung cancer, and a systematic review identified patterns in Central and Eastern Europe. The first questionnaire was completed by a group of medical oncologists, radiation oncologists and pneumologists. The panel of experts attended an in-person meeting to review the results of the questionnaire and to process a second round Delphi. An additional survey was then compiled and completed by the panel.

Results. A complete consensus was reached by the panel of experts on a set of evidence-based clinical recommendations. The experience-based questionnaire generated a highly variable map of treatment patterns within the region. A list of unmet needs and barriers to quality care were developed with near-unanimous consent of the panel of experts.

Conclusions. The current landscape of diagnostic and therapeutic approaches in Central and Eastern European countries is highly variable. We identified several significant barriers, mainly related to the availability of diagnostic and imaging methods and low rates of chemoradiotherapy with curative intention as initial treatment for unresectable stage III NSCLC.

Key words: stage III non-small cell lung cancer; treatment patterns; Delphi method; quality of care; expert panel; real-world evidence

Introduction

Lung cancer is the leading cause of cancer mortality worldwide, with over 2 million newly diagnosed cases annually. Lung cancer constituted 11.6% of all cancer cases diagnosed in 2018, according to the International Agency for Research on Cancer and worldwide numbers are still rising.¹ There were over 1.8 million deaths caused by lung cancer in 2018.¹ In Central and Eastern Europe (CEE)², the lung cancer incidence was almost 150,000 newly diagnosed cases in 2018, with over 131,000 deaths caused by lung cancer in the region.³

The most common form of lung cancer is non-small cell lung cancer (NSCLC), accounting for 80%–85% of all cases.⁴ Stage III non-small cell lung cancer comprises approximately one-third of NSCLC patients and is very heterogeneous with a variable, although mostly poor, prognosis.⁴ Due to its heterogeneity, a general schematic management approach is not appropriate and is recommended that the decision about the treatment is reached through multidisciplinary tumor board. Usually, a combination of local therapy with systemic platinum-based doublet chemotherapy and, recently added, immune therapy is used.⁴

According to the TNM 8 staging system, stage III NSCLC is subclassified into stage IIIA, IIIB, and IIIC.^{5,6} Lung cancer symptoms occur mostly late in the disease, so the majority of patients with NSCLC present with advanced metastatic disease that is incurable with currently available therapy, therefore, patient prognosis is critically dependent on early diagnosis and early treatment.

European Society for Medical Oncology (ESMO) guidelines, which were updated in 2017, directs the treatment of locally advanced NSCLC as follows: concurrent chemoradiotherapy is considered the preferred treatment for patients who are in good condition in stage IIIA, IIIB and IIIC. If chemoradiotherapy is not possible, then sequential chemotherapy followed by definitive radiotherapy represents a valid and effective alternative.⁷ Results from the PACIFIC trial show improvement in overall survival (OS) and progression-free survival (PFS) using a combination of chemoradiotherapy and immunotherapy (represented by durvalumab in this case).^{8,9} In this randomized trial, the 36-month OS rate was 57.0% in the durvalumab group and 43.5% in the placebo group.¹⁰ PFS was reported as a median duration of 17.2 months in the durvalumab group and 5.6 months in the placebo group ($p < 0.001$) according to the study report from 2018.⁹

Real-world data on treatment patterns of locally advanced NSCLC in CEE are limited. Therefore, we aimed to:

1. Generate a real-world matrix on treatment patterns in CEE based on an extensive literature search.
2. Generate a summary of treatment patterns used in stage III NSCLC in CEE based on clinical practice, find the main barriers to treatments, and formulate a set of quality of care indicators.
3. Develop a consensus on evidence-based clinical recommendations for Stage III NSCLC in CEE in cooperation with a panel of experts (henceforth referred to as the expert panel [EP]) from the region.

The Delphi method was used as a technique for consensus development.

Patients and methods

Study design

The study consisted of five parts: (1) an extensive literature search with a focus on real-world evidence (RWE); (2) development of a questionnaire; (3) selection of an expert panel; (4) an online survey; and (5) analyzing and discussing the results during the expert panel meeting. This study consisted of a survey of expert opinions, and no patient data were collected, so no specific independent ethical approval was necessary.

Expert panel

The expert panel was composed of 10 members from CEE countries, including Croatia, Czech Republic, Hungary, Poland, Romania, Serbia, and Slovenia. Due to the multidisciplinary nature of NSCLC therapy, representatives from a variety of disciplines were nominated to be on the expert panel, which ultimately consisted of medical oncology, radiation oncology and pneumology. Each of the panelists was an authority in the particular area of expertise in her or his country.

Literature search

Web of Science, PubMed, and the Cochrane library were thoroughly searched. A total of ten hits was considered relevant, and from those, a map of treatment patterns in CEE was generated. The goal was to identify synthesized research evidence

TABLE 1. List of real-world evidence literature from the Central and Eastern Europe region

Authors	Type of study, country	Treatment	Stages of NSCLC	Type of cancer	Population
Zemanová et al., 2020 ¹⁸	Registry, Czechia, Austria, Latvia, Serbia, Hungary, Poland	Surgery 23%, RT 55%, CT 80%	IIIA 55%, IIIB 45%	Squamous 53%, adenoc. 38%, not specified 6%, other 3%	583 p., 78% males
Vrankar et al., 2018 ²²	Observational, Slovenia	Induction CT in 3 cycles, + CCRT, 2 cycles	IIIA 57%, IIIB 43%	Squamous 58%, adenoc. 22%, large cell 6%, other 14%	102 p., 79% males
Ramlau et al., 2017 ²³	Registry, Poland	Surgery 27%, 14% RT, 80% systemic therapy	IIIA 12%, IIIB 15%	Adenoc. 37%	696 p., 60% males
Podmaniczky et al., 2015 ²⁴	Observational, Hungary	Platinum-based neoadjuvant CT	IIIA 60%, IIIB 20%	Squamous 59%, adenoc. 41%	46 p., 63% males
Jeremic, 2015 ²⁵	Review, Serbia	Standard treatment options	NA	NA	NA
Georgieva et al., 2014 ²⁶	Observational, Bulgaria	NA	III 2.4%, IIIA 12%, IIIB 2.4%	Squamous 22%, adenoc. 55%, non-small 14%, other 10%	42 p., 57% males
Zielinski et al., 2013 ²⁷	Retrospective observational study, Poland	Staging	NA	NA	899 p.
Kolodziejczyk et al., 2011 ²⁸	Prospective study, Poland	Radical RT, neoadjuvant CT 46%	IIIA 31%, IIIB 39%	Squamous 41%, adenoc. 8%, large cell 2%, no specification 45%, no histology 4%	100 p., 78% males
Jeremic et al., 2011 ²⁹	Toxicity studies, Serbia	CCRT	NA	NA	600 p.
Kepka et al., 2011 ³⁰	Observational, Poland	Surgery, RT, CT	NA	NA	291 p.

CCRT = concurrent chemoradiotherapy; CT = chemotherapy; NA = not available; NSCLC = non-small cell lung cancer; p. = patients; RT = radiotherapy

including clinical practice, systematic reviews, meta-analyses, and conference proceedings. Articles were included in the RWE map if they were fully published in English.

Online survey

The online expert questionnaire was divided into three parts. These parts covered expert experiences in diagnosis, therapy, and organization of the care of patients with stage III NSCLC. The expert panel members entered the rates of utilization in each category or other specific counts according to clinical practice in their medical center. Some of the outcomes, e.g. the number of specialized oncology centers in the country, were determined as counts in the country of panelists.

Delphi panel

The Delphi technique is a method for collecting data from respondents within their domain of expertise.¹¹ The aim is to achieve a convergence of opinion on a specific medical issue (in this case, NSCLC stage III therapy). There have been sev-

eral published cases using the Delphi method to study lung cancer.¹²⁻¹⁷ The consensus part of the study was carried out using a modified Delphi method. The first round of the Delphi consensus was built as a set of 12 evidence-based recommendations extracted from ESMO clinical guidelines.⁷ Responses were collected on a 5-point Likert scale. In the 1st round, each panelist responded using the following answers: (1) strongly disagree; (2) basically disagree; (3) doubtful; (4) basically agree; or (5) strongly agree. A Delphi consensus was reached when the mean of all values was > 4.0. If the mean of all values was 5.0, the consensus was considered unanimous. All statements then underwent a second Delphi round. The second Delphi round was held as an in-person meeting, and all 12 statements were discussed. In the meeting, it was possible to vote for or against each statement. A consensus was defined as > 80% of the responses were in favor of the statement. The overall decision was then distributed via email for any subsequent comments by the expert panel. A total of nine panelists responded to the first round and ten panelists responded to the second round. The first round took place from November 11–23, 2019 and

was performed via an online survey. The second round took place in Prague, Czech Republic, on November 29, 2019.

Statistical analysis

Descriptive analytical methods were used to analyze continuous and categorical variables. Continuous variables were reported as mean, standard deviation, minimum, and maximum. Categorical variables were reported as count and rate. MS Excel was used for the analysis.

Manuscript preparation

Based on the input of expert panel, the draft manuscript was prepared by medical writing agency. This project began in August 2019 and ended in March 2020. During the drafting of the article, newly published literature was reviewed to analyze the clinical implications of any new data in patients with stage III NSCLC.

Results

A literature search of RWE in CEE

There was a limited number of RWE-based literature on population diagnosed with stage III NSCLC from the CEE region. Table 1 presents a list of analyzed literature from 2011–2020. This includes data on patient registries and observational and toxicity studies. The only relevant literature with the texts written completely in English related to Bulgaria, Czech Republic, Hungary, Poland, Slovenia and Serbia. Mostly, these publications presented data on treatment, diagnostic methods and staging.

Treatment patterns based on clinical experience

Table 2 presents the data collected in the area of staging and diagnosis of stage III NSCLC. Concerning the staging of NSCLC, 32% ($\pm 13\%$) of NSCLC patients in any particular medical center were diagnosed with stage III NSCLC, and most of those were in stage IIIB (45% $\pm 12\%$). Good consistency in the field of imaging was observed. The most common diagnostic procedures, i.e. X-Ray, chest computed tomography (CT) (including the CT of upper abdomen area), and bronchoscopy, were provided to at least 93% of patients with stage III NSCLC. Differences in the percentages of treated patients who received abdominal CT, brain CT, en-

TABLE 2. Patterns in stage III non-small cell lung cancer diagnosis in Central and Eastern Europe region; % of patients treated in the medical center of particular panelists

	N	Mean (\pm SD)	Min-Max
Staging			
All stage III	9	32% ($\pm 13\%$)	20%–65%
Stage IIIA	9	37% ($\pm 14\%$)	20%–60%
Stage IIIB	9	45% ($\pm 12\%$)	30%–60%
Stage IIIC	9	18% ($\pm 11\%$)	6%–40%
Imaging			
X-Ray	9	99% ($\pm 3\%$)	90%–100%
Chest CT	9	98% ($\pm 4\%$)	90%–100%
Abdominal CT	9	87% ($\pm 19\%$)	50%–100%
Brain CT	9	58% ($\pm 33\%$)	12%–100%
Bronchoscopy	9	93% ($\pm 10\%$)	75%–100%
EBUS	9	37% ($\pm 29\%$)	9%–80%
PET-CT	9	54% ($\pm 30\%$)	20%–80%
Bone scan	9	15% ($\pm 16\%$)	0%–40%
Brain MRI	9	14% ($\pm 7\%$)	2%–20%
Biomarkers			
PD-L1 reflex testing	9	50% ($\pm 40\%$)	2%–100%
PD-L1 results available*	9	56% ($\pm 31\%$)	2%–100%

* Rates of PD-L1 results available of PD-L1 tests performed; CT = computed tomography; EBUS = endobronchial ultrasound; MRI = magnetic resonance imaging; PET-CT = positron emission tomography-computed tomography; SD = standard deviation

dobronchial ultrasound (EBUS), and PET-CT were evaluated. Bone scans and brain MRIs were provided at lower rates to patients (14%–15%). Also, PD-L1 was tested at various rates within the CEE. The mean rate of patients undergoing the PD-L1 reflex testing was 50% ($\pm 40\%$). The mean rate of available PD-L1 results was 56% ($\pm 31\%$), as proportion of patients was tested on demand.

The most heterogeneous set of responses was obtained for the descriptions of initial patient therapy, which reflects high variability in treatment approaches across the region (Table 3). About two-thirds of patients initially received radical treatment, and a mean of 30% of patients were treated palliative. When looking at the initial radical treatment modalities, with the intention to cure, showed that clinical practice was heterogeneous from country to country, and even individual clinical centers within countries had their own approach. As reported, in mean, chemotherapy alone was administered in 13% and cumulatively, concurrent and sequential chemoradiotherapy was ad-

ministered in more than 50% of patients in mean. Palliative radiotherapy was provided in 60% of patients intended for palliative treatment.

Table 4 describes how the care of patients with stage III NSCLC is organized. Usually, the first contact physician is a general practitioner (54% ± 27%) or a pneumologist (35% ± 29%). Other, less common, first contact variants included other professionals such as medical oncologists and radiation oncologists. In four out of nine countries lung cancer patients are referred to specialized oncology centers, where the patient has access to innovative oncology treatment options, while in other five countries, lung cancer is treated in local hospitals. The number of specialized oncology centers per country varies from 3 to 50, according to the population size of the particular country. Most respondents (89%) reported that patients diagnosed with stage III of NSCLC were referred to a multidisciplinary team. In most cases, medical oncologist is supervising the follow-up after initial therapy for unresectable stage III patients.

Evidence-based clinical recommendations

Table 5 shows the level of consensus for the twelve evidence-based clinical recommendations relative to stage III NSCLC. There was a high level of consensus and sometimes even unanimity with many of the twelve statements.

Main barriers and quality indicators

Table 6 presents the final list of the main barriers to treatment of stage III NSCLC identified and consensually agreed on by the expert panel. Rates of chemoradiotherapy (CRT) are low due to the long waiting times for radiotherapy and especially for advanced radiotherapy techniques. The reason for the low CRT rates could also be caused by providing radiotherapy and chemotherapy in different institutions. Another barrier is a long referral process among different physician specialties. Next, awareness of lung cancer symptoms, risk factors, and treatment options among patients is affected by health literacy and the influence of social status. Finally, late access to diagnostic and imaging procedures is also combined with long waiting times and low capacity.

The list of the agreed quality of care indicators is presented in Table 7. The proportion of patients treated with chemoradiotherapeutic radical treatment intention was described as the most signifi-

TABLE 3. Patterns in stage III non-small cell lung cancer diagnosis therapy; % of patients treated in the medical center of the particular panelist

	N	Mean (±SD)	Min-Max
Initial treatment			
Radical treatment	9	70% (±20%)	30%–96%
Palliative treatment	9	30% (±20%)	4%–70%
Radical treatment			
Surgery	9	17% (±6%)	10%–25%
Chemotherapy	8	13% (±16%)	0%–48%
Radiotherapy	8	15% (±9%)	5%–25%
Concurrent chemoradiotherapy	8	21% (±12%)	0%–30%
Sequential chemoradiotherapy	8	34% (±14%)	18%–50%
Palliative treatment			
Palliative radiotherapy	8	60% (±33%)	3%–90%
Best supportive care	8	29% (±24%)	10%–80%

TABLE 4. Patterns in stage III non-small cell lung cancer diagnosis organization of care; % of patients treated in the medical centers of particular panelists

First contact physician	N	Mean (±SD)	Min-Max
General practitioner	9	54% (± 27%)	20%–90%
Pneumologist	9	35% (± 29%)	10%–95%
Medical oncologist	9	9% (± 13%)	0%–30%
Radiation oncologist	9	3% (± 5%)	0%–10%
Other	9	5% (± 5%)	0%–10%

cant indicator of quality of care, followed by the improved survival over time.

Discussion

The main scope of the project was to explore the treatment patterns in stage III NSCLC in the CEE region since the current information on this topic is very limited. Data were gathered through a systematic literature search, an online survey of leading experts, and a modified Delphi consensus. It should be noted that the abovementioned data on treatment patterns represent the particular medical centers associated with the respondents and that situations in particular countries could differ slightly.

The literature search generated a limited amount of real-world data from the CEE region and only represented a subset of the countries participating in the study. This is mainly because most of the

TABLE 5. Evidence based clinical recommendations consensus

Statement	1 st round average N = 9	Final consensus
1. All patients planned for stage III NSCLC treatment should undergo a diagnostic contrast-enhanced CT scan of the chest and upper abdomen followed by a PET or a combined PET-CT using a CT technique with adequately high resolution for initial staging purposes.	4.8	Consensus
2. All patients planned for curative stage III NSCLC treatment should receive brain imaging for initial staging.	4.8	Consensus
3. Concurrent CRT is the treatment of choice in patients evaluated as unresectable in stage IIIa, IIIb, and IIIc.	4.6	Consensus
4. If concurrent CRT is not possible - for any reason - sequential ChT followed by definitive RT represents a valid and effective alternative.	4.8	Consensus
5. An experienced multidisciplinary team is of paramount importance in any complex multimodality treatment strategy decision.	4.9	Consensus
6. In the absence of contraindications, the optimal ChT to be combined with radiation in stage III NSCLC should be platinum-based therapy.	4.3	Consensus
7. When delivered perioperatively, platinum-based combinations are considered the treatment of choice, in the absence of contraindications.	4.6	Consensus
8. In the stage III disease CRT strategy, two to four cycles of concomitant ChT should be delivered.	4.9	Consensus
9. In the perioperative setting, three to four cycles of platinum-based ChT are recommended.	4.8	Consensus
10. 60–66 Gy in 30–33 daily fractions is recommended for concurrent CRT. The maximum overall treatment time should not exceed 7 weeks.	5.0	Unanimity
11. In sequential approaches, RT delivered over a short overall treatment time is recommended.	4.3	Consensus
12. Adjuvant anti PD-L1 checkpoint inhibitor durvalumab is indicated for unresectable NSCLC with PD-L1 ≥ 1% without progression after chemoradiotherapy with a platinum-based regime.	5.0	Unanimity

ChT = chemotherapy; CRT = chemoradiotherapy; CT = computed tomography; NSCLC = non-small cell lung cancer; PET-CT = positron emission tomography-computed tomography; RT = radiotherapy

TABLE 6. Main barriers in the treatment of stage III non-small cell lung cancer found by our panel of experts

Main barriers
1. Low chemoradiotherapy rates due to long waiting times for radiotherapy, especially for advanced RT techniques and/or radiotherapy and chemotherapy performed by different institutions.
2. Long referral process among different specialities (general practitioner, pneumologist, medical oncologist, radiotherapist).
3. Poor health literacy and social status of patients influence awareness of lung cancer symptoms, risk factors and treatment.
4. Late access to imaging and diagnostic procedures, especially PET-CT – long waiting times, low capacity.
5. Barriers to implementing targeted population screening programs.

PET-CT = positron emission tomography-computed tomography; RT = radiotherapy

TABLE 7. Quality of care indicators in stage III non-small cell lung cancer found by our panel of experts

Quality of care indicators
1. The proportion of patients treated with chemoradiotherapy in radical treatment intention.
2. Improved survival (median OS, 5 years survival) over time.
3. Time from first symptoms to first contact with a lung cancer specialist, time from first contact with a lung cancer specialist to first treatment.
4. The proportion of patients with full histopathological/molecular confirmation of the diagnosis – PET-CT, brain imaging, PD-L1.
5. The proportion of treatment decisions confirmed by a multidisciplinary team.

OS = overall survival; PET-CT = positron emission tomography-computed tomography

published data were not published in English or in the indexed literature. It is worth noting that much of the literature was published in recent years, which may reflect the availability of new therapeutic modalities.

A comparison of the expert panel consensus with the ESMO guidelines and the current practice in staging, diagnosis, and treatment of stage III NSCLC revealed differences.⁷ This fact was well described in the survey of the main barriers

and quality of care indicators among the panelists. There was great agreement regarding the evidence-based recommendations extracted from ESMO clinical guidelines in the treatment of stage III NSCLC, even though the experience-based survey revealed considerable differences in current treatment patterns. The list of quality of care indicators produced by the expert panel agreed in part with the list produced in other countries (e.g., the United Kingdom and China), especially with

regard to the proportions of patients intended to various treatments or histopathological diagnostic procedures, but our list also proposed several new indicators relative to the decision making role of multidisciplinary teams.^{14,16} Expert panel agreed a new era for unresectable stage III NSCLC patients in CEE is coming and expert panel agreed to reevaluate the 1–2 year the treatment improvement based on the indicators.

Significantly, our survey found a great deal of heterogeneity in therapy organization and treatment modalities offered (available) in different medical centers within CEE. The heterogeneity was found in almost all parts of the survey, excluding consent rates of patients in long-term established diagnostic procedures such as X-Ray and CT. The more specific the procedure, e.g., histopathological diagnostic procedures, the greater the variance in rates of utilization in patients. It is agreed, that reflex PD-L1 testing and brain MRI rates should be improved. Moreover, patterns of initial radical treatment showed great variability among the panelists. This fact was also observed in a recent publication by Zemanová *et al.*, which mapped these patterns in the same region.¹⁸ It is important to focus on improving the rates of chemoradiotherapy provided to patients. Yet in 2007, the positive impact of concurrent chemoradiotherapy with vinorelbine and platinum based compounds followed by consolidation chemotherapy was proven by Rusu *et al.*¹⁹ This study reported a 15 months median OS in patients with stage III NSCLC and well tolerability of the treatment.

Importantly, the expert panel unanimously agreed that adjuvant anti PD-L1 checkpoint inhibitor durvalumab is indicated for unresectable NSCLC with PD-L1 $\geq 1\%$ without progression after chemoradiotherapy with a platinum-based regime (Table 5). Chemoradiotherapy followed by the immunotherapy is new standard of care according to the National Comprehensive Cancer Network (NCCN) guidelines and The National Institute for Health and Care Excellence (NICE) guidance.^{20,21} Improving the chemoradiotherapy rates, PD-L1 testing and gaining access to durvalumab are the next needed steps to be implemented in CEE in order to treat the stage III unresectable patients according to new standard of care.

Conclusions

The current landscape of diagnostic and therapeutic approaches in CEE countries is highly variable,

and relevant real-world data are missing. We identified several significant barriers, mainly related to the availability of diagnostic and imaging methods and low rates of chemoradiotherapy with curative intention as initial treatment for unresectable stage III NSCLC. Improving CRT rates will also enable consolidative treatment with durvalumab to further improve the OS of stage III unresectable patient population.

The way forward will involve an agreement to establish a set of quality of care indicators with routine monitoring and assessment within the clinical practice framework. The panel of experts agreed on future monitoring of improvement in the standards of care for stage III unresectable NSCLC.

Acknowledgements

This manuscript presents independent work of the expert panel. The views and opinions expressed by authors in this publication are those of the authors and do not necessarily reflect the overall situation in specific country.

The project was funded by AstraZeneca for logistical and medical writing support.

Tina Jerič, M. Pharm. and Lenka Mikasová, Ph. D. of AstraZeneca contributed to the project design and participated at the expert panel meeting.

Medical writing support, which was in accordance with good publication practice guidelines, was provided by Tomáš Doležal and Tereza Tumova, of Value outcomes (Prague, Czech Republic).

References

1. International Agency for Research on Cancer. World Health Organization. Press release N. 263. [cited 2020 Feb 13]. Available at: <https://www.who.int/cancer/PRGlobocanFinal.pdf>
2. Publications Office of the EU. Central and Eastern Europe. [cited 2020 Feb 14]. Available at: <https://op.europa.eu/en/web/eu-vocabularies/th-concept/-/resource/eurovoc/914>
3. International Agency for Research on Cancer. World Health Organization. Lung cancer. [cited 2020 Feb 15]. Available at: <https://gco.iarc.fr/today/data/factsheets/cancers/15-Lung-fact-sheet.pdf>
4. Huber RM, Ruyscher DD, Hoffmann H, Reu S, Tufman A. Interdisciplinary multimodality management of stage III nonsmall cell lung cancer. *Eur Respir Rev* 2019; **28**: 190024. doi: 10.1183/16000617.0024-2019
5. Deterbeck FC, Boffa DJ, Kim AW, Tanoue LT. The eighth edition lung cancer stage classification. *Chest* 2017; **151**: 193-203. doi: 10.1016/j.chest.2016.10.010
6. Goldstraw P, Chansky K, Crowley J, Rami-Porta R, Asamura H, Eberhardt WEE, et al. The IASLC Lung Cancer Staging Project: proposals for revision of the TNM stage groupings in the forthcoming (eighth) edition of the TNM classification for lung cancer. *J Thorac Oncol* 2016; **11**: 39-51. doi: 10.1016/j.jtho.2015.09.009

7. Postmus PE, Kerr KM, Oudkerk M, Senan S, Waller DA, Vansteenkiste J, et al. Early and locally advanced non-small-cell lung cancer (NSCLC): ESMO Clinical Practice Guidelines for diagnosis, treatment and follow-up. *Ann Oncol* 2017; **28**: iv1-21. doi: 10.1093/annonc/mdx222
8. Antonia SJ, Villegas A, Daniel D, Vicente D, Murakami S, Hui R, et al. Durvalumab after chemoradiotherapy in stage III non-small-cell lung cancer. *N Engl J Med* 2017; **377**: 1919-29. doi: 10.1056/NEJMoa1709937
9. Antonia SJ, Villegas A, Daniel D, Vicente D, Murakami S, Hui R, et al. Overall Survival with Durvalumab after Chemoradiotherapy in Stage III NSCLC. *N Engl J Med* 2018; **379**: 2342-50. doi: 10.1056/NEJMoa1809697
10. Gray JE, Villegas A, Daniel D, Vicente D, Murakami S, Hui R, et al. Three-year overall survival with durvalumab after chemoradiotherapy in Stage III NSCLC - update from PACIFIC. *J Thorac Oncol* 2020; **15**: 288-93. doi: 10.1016/j.jtho.2019.10.002
11. McMillan SS, King M, Tully MP. How to use the nominal group and Delphi techniques. *Int J Clin Pharm* 2016; **38**: 655-62. doi: 10.1007/s11096-016-0257-x
12. Isla D, de Castro J, García-Campelo R, Lianes P, Felip E, Garrido P, et al. Treatment options beyond immunotherapy in patients with wild-type lung adenocarcinoma: a Delphi consensus. *Clin Transl Oncol* 2019; **22**: 759-71. doi: 10.1007/s12094-019-02191-y
13. Isla D, González-Rojas N, Nieves D, Brosa M, Finfern HW. Treatment patterns, use of resources, and costs of advanced non-small-cell lung cancer patients in Spain: results from a Delphi panel. *Clin Transl Oncol* 2011; **13**: 460-71. doi: 10.1007/s12094-011-0683-0
14. Darling G, Malthaner R, Dickie J, McKnight L, Nhan C, Hunter A, et al. Quality indicators for non-small cell lung cancer operations with use of a modified Delphi consensus process. *Ann Thorac Surg* 2014; **98**: 183-90. doi: 10.1016/j.athoracsur.2014.03.001
15. Moldaver D, Hurry M, Evans WK, Cheema PK, Sangha R, Burkes R, et al. Development, validation and results from the impact of treatment evolution in non-small cell lung cancer (ITEN) model. *Lung Cancer* 2020; **139**: 185-94. doi: 10.1016/j.lungcan.2019.10.019
16. Wang X, Su S, Li S, Bao H, Zhang M, Liu D, et al. Development of quality indicators for non-small cell lung cancer care: a first step toward assessing and improving quality of cancer care in China. *BMC Cancer* 2017; **17**: 306. doi: 10.1186/s12885-017-3602-0
17. Provencio M, Carcereny E, Artal Á. Consensus on the use of immune-related response criteria to evaluate the efficacy of immunotherapy in non-small cell lung cancer. *Clin Transl Oncol* 2019; **21**: 1464-71. doi: 10.1007/s12094-019-02072-4
18. Milada Zemanová, Pírker R, Petruzelka L, Zbožinkova Z, Jovanovic D, Rajer M, et al. Care of patients with non-small-cell lung cancer Stage III – the Central European real-world experience. *Radiol Oncol* 2020; **54**(4): 447-454. doi: 10.2478/raon-2020-0026
19. Rusu P, Ciuleanu TE, Cernea D, Pelau D, Gaal V, Cebotaru C, et al. Concurrent chemoradiotherapy with vinorelbine and a platinum compound followed by consolidation chemotherapy for unresectable stage III non-small cell lung cancer: preliminary results of a phase II study. *J BUON* 2007; **12**: 33-9.
20. National Comprehensive Cancer Network. *NCCN Clinical Practice Guidelines in Oncology - Non-Small Cell Lung Cancer*. [Internet]. Version 5.2020. [cited 2020 May 27]. Available at: https://www.nccn.org/professionals/physician_gls/pdf/nscl.pdf
21. Durvalumab for treating locally advanced unresectable non-small-cell lung cancer after platinum-based chemoradiation | Guidance | NICE [Internet]. [cited 2020 Feb 27]. Available at: <https://www.nice.org.uk/guidance/ta578/chapter/1-Recommendations>
22. Vrankar M, Stanic K. Long-term survival of locally advanced stage III non-small cell lung cancer patients treated with chemoradiotherapy and perspectives for the treatment with immunotherapy. *Radiol Oncol* 2018; **52**: 281-8. doi: 10.2478/raon-2018-0009
23. Ramlau R, Krawczyk P, Dziadziuszko R, Chmielewska I, Milanowski J, Olszewski W, et al. Predictors of EGFR mutation and factors associated with clinical tumor stage at diagnosis: Experience of the INSIGHT study in Poland. *Oncol Lett* 2017; **14**: 5611-8. doi: 10.3892/ol.2017.6907
24. Podmaniczky E, Fábíán K, Pápay J, Puskás R, Gyulai M, Furák J, et al. Decreased ERCC1 Expression After Platinum-Based Neoadjuvant Chemotherapy in non-Small Cell Lung Cancer. *Pathol Oncol Res* 2015; **21**: 423-31. doi: 10.1007/s12253-014-9839-x
25. Jeremić B. Standard treatment option in stage III non-small-cell lung cancer: case against trimodal therapy and consolidation drug therapy. *Clin Lung Cancer* 2015; **16**: 80-5. doi: 10.1016/j.clcc.2014.08.003
26. Georgieva N, Bochev P, Dancheva Z, Chaushev B, Balev B, Klisarova A, et al. PET/CT in NSCLC with brain metastases. *Rentgenol Radiol* 2014; **53**: 204-10.
27. Zielinski M, Szlubowski A, Kołodziej M, Orzechowski S, Laczynska E, Pankowski J, et al. Comparison of endobronchial ultrasound and/or endo-esophageal ultrasound with transcervical extended mediastinal lymphadenectomy for staging and restaging of non-small-cell lung cancer. *J Thorac Oncol* 2013; **8**: 630-6. doi: 10.1097/JTO.0b013e318287c0ce
28. Kołodziejczyk M, Kepka L, Dziuk M, Zawadzka A, Szalun N, Gizewska A, et al. Impact of [18F]fluorodeoxyglucose PET-CT staging on treatment planning in radiotherapy incorporating elective nodal irradiation for non-small-cell lung cancer: a prospective study. *Int J Radiat Oncol Biol Phys* 2011; **80**: 1008-14. doi: 10.1016/j.ijrobp.2010.04.018
29. Jeremić B, Miličić B, Milisavljevic S. Toxicity of concurrent hyperfractionated radiation therapy and chemotherapy in locally advanced (stage III) non-small cell lung cancer (NSCLC): single institution experience in 600 patients. *Clin Transl Oncol* 2012; **14**: 613-8. doi: 10.1007/s12094-012-0848-5
30. Kepka L, Bujko K, Orłowski TM, Jagiello R, Salata A, Matecka-Nowak M, et al. Cardiopulmonary morbidity and quality of life in non-small cell lung cancer patients treated with or without postoperative radiotherapy. *Radiother Oncol* 2011; **98**: 238-43. doi: 10.1016/j.radonc.2010.09.020

Treatment of rhabdomyosarcoma in children and adolescent from four low health expenditures average rates countries

Maja Cesen Mazic¹, Aleksandra Bonevski², Martina Mikeskova³, Emilia Mihut⁴, Gianni Bisogno⁵, Janez Jazbec^{1,6}

¹ University Children's Hospital Ljubljana, Slovenia

² Children's Hospital Zagreb, Croatia

³ University Children's Hospital Bratislava, Slovakia

⁴ Oncology Institute Cluj-Napoca, Romania

⁵ Hematology Oncology Division, Department of Women's and Children's Health, University of Padova, Italy

⁶ Faculty of Medicine, University of Ljubljana, Ljubljana, Slovenia

Radiol Oncol 2020; 54(4): 455-460.

Received 18 June 2020

Accepted 8 September 2020

Correspondence to: Maja Česen Mazič, M.D., University Children's Hospital Ljubljana, Bohoričeva 20, 1000 Ljubljana, Slovenia. Phone: 00 386 1 522 9215; Fax: 00 386 1 522 4036; E-mail: maja.cesenmazic@kclj.si

Disclosure: No potential conflicts of interest were disclosed.

Background. Survival of children with cancer in Eastern and Central Europe is 10–20% lower than in high income European countries. We evaluated outcome of children and adolescents with rhabdomyosarcoma (RMS) in Slovenia, Croatia, Slovakia and in Romania.

Patients and methods. We retrospectively analysed event-free survival (EFS) and overall survival (OS) for all patients treated in Slovenia and Croatia. Slovakia included patients from two centers, representing half of expected cases. Romania included patients from single institution, representing only 10% of expected patients. Joint database for analysis was established.

Results. One hundred seventy-eight children and adolescent with RMS diagnosed from January 2000 to December 2015 were included. Mean patient age at diagnosis was 7.7 years, one third was older than 10 years. Twenty-five percent had alveolar histology and 72% unfavorable location. Higher than expected proportion of patients had nodal involvement (24%) or metastatic disease (27%). All patients received systemic chemotherapy, 57% had radiotherapy and 63% surgery as local control. Kaplan- Meier estimates for 5-year EFS and OS were 50.7% and 59.6%, respectively. Five-year OS for patients with localised disease was 72% compared to 24% for metastatic disease.

Conclusions. Children with RMS treated in Eastern and Central Europe have inferior outcome compared to their counterparts treated in high income European countries. Active participation of low health expenditures average rates (LHEAR) countries in international clinical trials may improve outcome of paediatric oncology patients.

Key words: rhabdomyosarcoma; low income country; outcome

Introduction

Cancer is diagnosed in more than 35.000 children and young adults across Europe each year.¹ Despite great improvement in treatment and care over last decades, cancer is still leading cause of death due to disease in this population. While 5-year survival rates are around 80% with best

available therapy², survival in Eastern and Central Europe is 10–20% lower than in high income European countries.³

European Society of Pediatric Oncology (SIOPE) study confirmed lack of health care resources to ensure minimal standards of care for children with cancer as one of the main reasons for existing inequalities.⁴

ALL IC BFM 2002 trial is a role model for international collaboration between centers with limited resources and lower level of experience. Improved management of children with acute lymphoblastic leukemia was achieved with detailed treatment agenda and supportive care guidelines.⁵

Outcome of patients with soft tissue sarcomas is improved, if patients are treated according to established guidelines and in expert centers.⁶ Quality of local control is critical point in therapy and is increased in specialized centers with high expertise.⁶ We report outcome of children and adolescent with rhabdomyosarcoma in four low health expenditure average rate (LHEAR) countries.

Patients and methods

Patients

Study presents data from 178 patients aged 0–17 years with rhabdomyosarcoma treated in four LHEAR countries (Slovenia, Slovakia, Croatia, Romania) from January 2000 to December 2015. Data from Slovenia were extracted from National Cancer Registry and are population based. Data from Croatia were collected from all pediatric oncology hospitals in Croatia (two in Zagreb, Rijeka, Split) and cover entire population. Slovakia provided data from two centers (Department of Pediatric Oncology/Hematology, Children University Hospital, Bratislava and Kosice) and Romania from single center (Oncology Institute Cluj Napoca). Data were collected by first author in joint database.

We estimated expected number of patients from WHO International Incidence of Childhood Cancer 3 report (IICC-3).⁷ In IICC-3 Slovenia has an annual average of 2.2; Croatia an annual average of 4.9; Slovakia an annual average of 5.9 and Romania an annual average of 28 children with soft-tissue sarcoma. Present study includes 25 cases from Slovenia (annual average 1.6), 73 cases from Croatia (annual average 4.5), 40 cases from Slovakia (annual average 2.5) and 39 cases from Romania (annual average 2.4). Number of cases reported in study from Croatia and Slovenia correspond to expected in population, approximately 50% of cases are reported from Slovakia and 10% from Romania. Slovenia has 2 million, Croatia 4 million, Slovakia 5,4 million and Romania 19 million inhabitants. Patients were eligible for this analysis, if diagnosis of rhabdomyosarcoma was confirmed by local pathologist. Disease staging included postsurgical tumor stage (IRS), age and size, histology, site, presence of nodal involvement or distant metastasis.

Treatment in Slovenia was based on Cooperative Weichteilsarcom Studiengruppe protocol (CWS); from 2011–2015 patients were enrolled in European Pediatric Soft Tissue Sarcoma Group protocol (5 cases) (EpSSG RMS 2005). Patients from Slovakia were treated according to International Society of Pediatric Oncology malignant Mesenchymal Tumor Group (MMT) guidelines; from 2006 patients were enrolled in EpSSG RMS 2005 protocol (16 cases). Croatia and Romania treated patients according to CWS protocols. Five patients from Croatia were treated according to RMS 2005 recommendations and 3 patients from Romania according to MMT protocols. Patients from Romania and Croatia did not participate in clinical trials.

Statistical methods

Disease staging included postsurgical tumor stage (primary complete resection (R0), microscopic residual (R1) or macroscopic residual/biopsy only (R2)), patient age and tumor size (favorable = tumor size < 5 cm and age < 10 years, unfavorable = tumor size > 5 cm and age > 10 years or < 1 year), histology (favorable = embryonal, spindle cell, botryoid, unfavorable = alveolar), primary tumor site (favorable = orbit, para-testicular, vagina/uterus, head/neck, unfavorable = para-meningeal, extremities, genitourinary bladder/prostate and other), presence of nodal involvement or distant metastases. Treatment included surgery (yes/no) and quality of resection (complete resection [R0], microscopic residual [R1] or macroscopic residual [R2]), chemotherapy (yes/no) and radiotherapy (yes/no).

Follow up was performed by pediatric oncologist at least 5 years after completed therapy or until 18 years old, whatever comes later.

Five-year overall survival (OS) and event-free survival (EFS) were estimated using Kaplan-Meier method with Pandas, Phyton data analysis library. The statistical significance of each variable was tested by log-rank test.

Results

Local pathologists classified 111 tumors (62%) as embryonal, 45 (25%) as alveolar, 10 (5%) spindle or botryoid RMS; for 12 cases histology subtype was unknown. Fusion status was determined in 21 (11%) tumors.

Mean patient age at diagnosis was 7.7 years (range 3 months to 17.9 years) (Figure 1). Fifty-

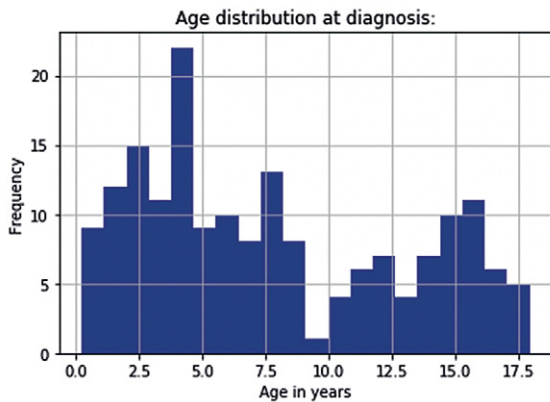


FIGURE 1. Age distribution at diagnosis.

eight patients (32%) were older than 10 years, 9 were infants.

Sixty-three patients (35%) presented with small tumors (< 5 cm) and favorable age. Nodal involvement was present in 67 patients (37%), 31 had localized disease. Metastases were diagnosed in 48 patients (27%), 9 had pulmonary metastases only.

Eleven patients had head/neck (6%), 50 parameningeal (28%), 13 orbit (7%), 21 extremity (12%), 15 thoracic (8%), 30 abdominal (16%), 14 bladder/prostate (8%), 21 para-testicular (12%) and 3 vaginal primary tumors (Figure 2).

All patients received chemotherapy.

Biopsy was only surgical procedure for 124 patients (70%) at diagnosis. Remaining 54 patients (30%) had primary surgery; 33 primary complete resection, 15 microscopic and 6 macroscopic residual disease. Secondary surgery was performed in 66 patients, 62 had biopsy at diagnosis, 4 patients had primary R1 resection. Complete resection was achieved in 24 patients, 23 had microscopic and 15 macroscopic residual disease. For 4 patients result of surgery is not known. Complete resection was most commonly achieved in patients with para-testicular, prostate/bladder, extremity and head and neck primary.

Radiotherapy was part of primary treatment in 102 patients (57%). Radiotherapy was omitted in 17/21 patients with para-testicular, 8/13 orbit, 11/14 bladder/prostate and 6/11 head/neck primary. Fourteen metastatic patients and fifteen (50%) with abdominal primary had no radiotherapy. Local control with radiotherapy was applied in 27 patients for the first time at relapse. Patient and disease characteristics are shown in Table 1.

For whole group 5-year OS was 59.6% (95% CI 51.8–66.6%) and 5-year EFS 50.7% (95% CI

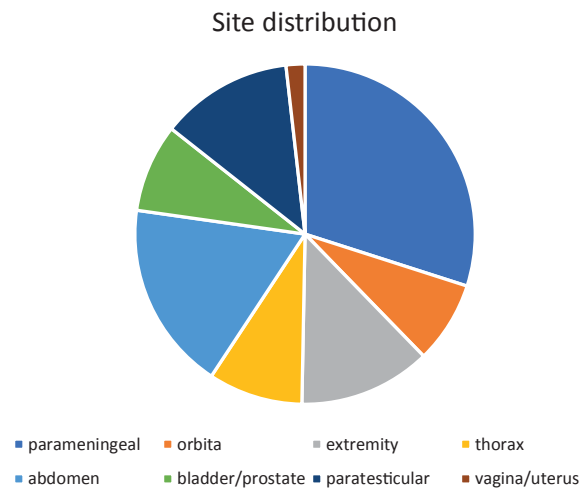


FIGURE 2. Site distribution.

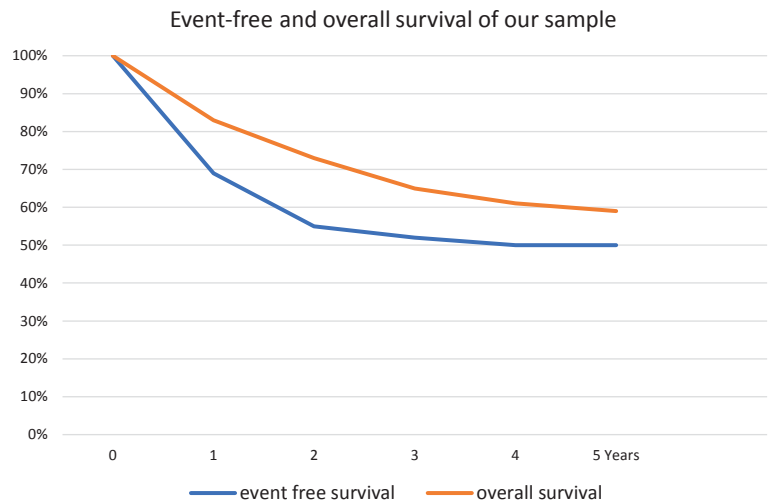


FIGURE 3. Event-free (EFS) and overall survival (OS) of investigated sample.

43.0–58.0%) (Figure 3). At median follow up of 5 years 106 patients were alive, 69 dead due to disease relapse or progression and 3 from toxic death. Patients with bladder/prostate (92%), orbit (72%) and para-testicular (81%) primary had highest OS and those with thoracic primary poorest outcome (40%). Survival in patients with head and neck (54%), para-meningeal (55%), extremity (47%), abdominal and pelvic primaries (48%) was around 50%.

In the study 15/21 of children with para-testicular rhabdomyosarcoma were older than 10 years and had additional poor prognostic signs (6 alveolar histology, 9 lymph node involvement, 4 metastatic disease). Only 6 children with para-testicular RMS fulfilled criteria for low risk group and had

TABLE 1. Patient and disease characteristics

Country	Slovenia	Croatia	Slovakia	Romania
Number (pt)	25	72	40	41
Age < 1 year	1	2	3	3
Age > 10 years	8	21	12	17
Favourable histology	19	41	31	30
Unfavourable histology	5	21	8	11
Primary surgery				
Biopsy	20	50	28	26
R0	2	19	4	8
R1	1	3	8	3
R2	2	NA	NA	4
Site				
Orbit	2	3	7	1
Paratesticular	1	6	8	6
Vagina/uterus	1	1	1	NA
Head/neck	NA	3	2	6
Parameningeal	12	22	3	13
Extremity	NA	7	9	5
Abdomen	NA	19	6	5
Thorax	7	5	1	2
Bladder/prostate	2	6	3	3
Size (> 5 cm)	13	44	32	24
Nodes +	6	31	12	18
Metastases +	6	24	13	5
RT	21 (84%)	39 (54%)	21 (52%)	21 (51%)
RTsalvage	2	13	5	7
Secondary surgery	7	29	18	12
R0	1	11	9	3
R1	5	6	4	8
R2	1	12	1	1
Primary+secondary surgery	12 (48%)	51 (70%)	26 (65%)	27 (65%)
Alive	16 (64%)	44 (61%)	23 (57%)	23 (56%)

PT = patients; RT = radiotherapy; RTsalvage = salvage radiotherapy

excellent 5-year OS (100%). Local control in parameningeal primaries was not optimal, since nobody had surgery and 10/50 had no radiotherapy. Radiotherapy was not part of primary therapy in 8/13 of patients with orbital RMS. Radiotherapy at relapse salvaged only 1/4 patient, 3 died despite further treatment with chemoradiotherapy. Outcome for patients with bladder/prostate primary was excellent, but extent of surgery and mutila-

tion was not reported. Last 3 patients in the study patients were managed in expert foreign centre with combined organ preservation surgery and brachytherapy.

Patients with embryonal histology (5-year OS 62% embryonal *vs.* 48% alveolar, $P = 0.003$) and favorable size and age (5-year OS 76% favorable *vs.* 51% unfavorable, $P = .001$) had better outcome.

5-year OS for 130 patients with localized disease was 72% compared to 24% for metastatic patients. Survival of subgroup of patients with pulmonary metastases only was better compared to other metastatic patients (33% *vs.* 21%, $P = 0.02$). All metastatic patients treated without radiotherapy died.

Twelve patients out of 27 irradiated as salvage at relapse survived; patients had either orbit, head and neck, para-meningeal, para-testicular, bladder/prostate or vaginal primary.

5-year OS of patients with localized disease treated with or without radiotherapy (77% *vs.* 72%, $P = 0.53$) was similar. Outcome of patients with surgical resection was better (5-year OS 70 *vs.* 48%, $P = 0.001$) and depended on quality of surgical resection (R0 90% *vs.* R1 66% and R2 50% 5-year OS, $P = 0.001$). Complete resection was most commonly achieved in patients with para-testicular, prostate/bladder, extremity and head/neck primary. There are no data regarding mutilation after surgery.

Discussion

Our study supports previous reports of lower survival of pediatric cancer patients in Eastern and Central Europe.³ OS for the whole group was close to 60%, with high proportion (27%) of metastatic patients and patients with advanced localized disease (24%). Nodal involvement in localized disease was almost two times higher compared to MMT 89 (13%)⁸ and RMS 2005 study (15%).⁹ In large cohorts approximately 15% of patients with rhabdomyosarcoma had metastases.^{10,11} Survival rate of patients with metastatic disease in our study was also lower from published analysis of pooled metastatic patients from Europe and United States (24% *vs.* 34% 5-year OS).¹²

Survival of patients with localised disease (72%) is almost 10% lower than in recently presented RMS 2005 study, where 5-year OS reached 80%.⁹ Patients with localized disease have comparable survival to high-risk patients treated in recent RMS 2005 study¹³ or with survival in MMT 89 study (5-year OS 71%) where 50% of survivors were treated without significant local therapy.⁸

Less than two thirds of the patients (57%) were treated with radiotherapy as part of primary treatment. Results from previous studies and recent RMS 2005 show that about 30% of children with RMS can be cured without radiotherapy.^{11,14-17} Omitting radiotherapy in patients with para-testicular, bladder/prostate, head/neck and orbital primary was in line with MMT protocols. Patients with abdominal, thoracic or para-meningeal primary and metastases were not eligible for radiotherapy due to progressive disease, unacceptable toxicity for local radiotherapist or unavailable general anesthesia for small children. Without radiotherapy adequate local control cannot be achieved in substantial proportion of children with soft tissue sarcoma.¹⁴⁻¹⁷ There is difference between participating countries in number of patients irradiated (Table 1). High percentage (84%) of irradiated patients in Slovenia is consequence of longstanding tradition of pediatric radiotherapy and site distribution. Multidisciplinary team for pediatric cancer patients in Slovenia (pediatricians, radiation oncologist, cytologist/pathologist, surgeons) was established in 1960s by founding member of SIOP, prof. B Jereb.¹⁸

Small proportion of children with orbital, head and neck, para-meningeal, testicular, bladder/prostate and vaginal primary tumor were salvaged with use of radiotherapy at relapse.

Majority of patients had biopsy only at diagnosis. Primary surgery was less common than secondary. Two thirds had surgery for local control at any point of treatment. Most patients with unfavorable site (para-meningeal and trunk location) had no surgery. Surgical resection was performed in 2/3 of patients in Croatia, Slovakia and Romania and only in half of patients in Slovenia; unfavorable site distribution precluding surgery (80% para-meningeal and thoracic primary). Quality of resection, with 84% of patients achieving R0 or R1 resection, is comparable with data in MMT 89 study.⁸ Paratesticular, prostate/bladder, extremity and head/neck primaries were most common accessible for complete excision.

Distribution according to site was as expected, with half of the patients presenting with tumor in head and neck region, majority being para-meningeal. Genitourinary region was second most frequent site (20%). Outcome of patients with paratesticular, orbit and para-meningeal primary was lower than expected. Children with paratesticular RMS in our study were older, with unfavourable histology and disseminated disease. Those in low risk group had excellent survival as expected.^{19,20}

Poor local control compromised outcome of patients with para-meningeal RMS.²¹⁻²³ In RMS 2005 study there was substantial gap between EFS (77%) and OS (94%) for patients with orbit primary, most patients were salvaged by additional chemoradiotherapy. This was not repeated in our study, since only 1/4 patients survived. Outcome for bladder/prostate primary was comparable to published results, probably more mutilating surgeries were performed without concomitant radiotherapy.²⁴

Relation of local control modality on outcome was not assessed for other variables, such as tumor site and size, nodal or metastatic disease and is thus of limited value.

This study has major limitations. Data for Slovakia and Romania are not population based and are thus source of selection bias, precluding firm conclusions. Lack of standardized diagnostic and therapeutic protocol reflects in poor quality of the data and therefore suboptimal statistical analysis.

Improved outcome for patients with rhabdomyosarcoma observed in high income European countries over the last three decades is the result of well-designed protocols based on a multidisciplinary approach and prospective data collection²⁵, which results in standardization of diagnostic procedures, chemotherapy protocols, radiotherapeutic and surgical guidelines and supportive measures. Unfortunately substantial number of children from member states of European Union are not included in academic (therapy optimization) trials. This results not only in inferior treatment outcomes, but also loss from scientific standpoint as data from this group of patients are not used for therapy optimization trials. Our retrospective analysis of data from four countries should be seen as a step towards activation and motivation of pediatric oncology centers in LHEAR European countries to more active participation and involvement in clinical research work in the field of pediatric oncology.

References

1. Bray F, Ferlay J, Soerjomataram I, Siegel RL, Torre LA, Jemal A, et al. Global cancer statistics 2018: GLOBOCAN estimates of incidence and mortality worldwide for 36 cancers in 185 countries. *CA Cancer J Clin* 2018; **68**: 394-424. doi: 10.3322/caac.21492
2. Vassal G, Fitzgerald E, Schrappe M, Arnold F, Kowalczyk J, Walker D, et al. Challenges for children and adolescents with cancer in Europe: the SIOP-Europe agenda. *Pediatr Blood Cancer* 2014; **61**: 1551-7. doi: 10.1002/pbc.25044
3. Gatta G, Botta L, Rossi S, Aareleid T, Bielska-Lasota M, Clavel J, et al. Childhood cancer survival in Europe 1999-2007: Results of EUROCARE-5-a population-based study. *Lancet Oncol* 2014; **15**: 35-47. doi: 10.1016/S1473-0454(13)70548-5

4. Kowalczyk JR, Samardakiewicz M, Fitzgerald E, Essiaf S, Ladenstein R, Vassal G, et al. Towards reducing inequalities: European standards of care for children with cancer. *Eur J Cancer* 2014; **50**: 481-5. doi: 10.1016/j.ejca.2013.11.004
5. Stary J, Zimmermann M, Campbell M, Castillo L, Dibar E, Donska S, et al. Intensive chemotherapy for childhood acute lymphoblastic leukemia: results of the randomized intercontinental trial ALL IC-BFM 2002. *J Clin Oncol* 2014; **32**: 174-84. doi: 10.1200/JCO.2013.48.6522
6. Pasquali S, Bonvalot S, Tzani D, Casali PG, Trama A, Gronchi A, et al. RARECARENet Working Group. Treatment challenges in and outside a network setting: Soft tissue Sarcomas. *Eur J Surg Oncol* 2019; **45**: 31-9. doi: 10.1016/j.ejso.2017.09.015
7. *International incidence of childhood cancer. Volume III.* Steliarova-Foucher E, Colombet M, Ries LAG, Hesselting P, Moreno F, Shin HY, et al, editors. Lyon, France: International Agency for Research on Cancer; 2017. [cited 2020 May 15]. Available at: <http://iicc.iarc.fr/results/>.
8. Stevens MC, Rey A, Bouvet N, Ellershaw C, Flamant F, Habrand JL, et al. Treatment of nonmetastatic rhabdomyosarcoma in childhood and adolescence: third study of the International Society of Paediatric Oncology - SIOP Malignant Mesenchymal Tumor 89. *J Clin Oncol* 2005; **23**: 2618-28. doi: 10.1200/JCO.2005.08.130
9. Bisogno G, De Salvo GL, Bergeron C, Gallego Melcón S, Merks JH, Kelsey A, et al; European paediatric Soft tissue sarcoma Study Group. Vinorelbine and continuous low-dose cyclophosphamide as maintenance chemotherapy in patients with high-risk rhabdomyosarcoma (RMS 2005): a multicentre, open-label, randomised, phase 3 trial. *Lancet Oncol* 2019; **20**: 1566-75. doi: 10.1016/S1470-2045(19)30617-5
10. Breneman JC, Lyden E, Pappo AS, Link MP, Anderson JR, Parham DM, et al. Prognostic factors and clinical outcomes in children and adolescents with metastatic rhabdomyosarcoma: a report from the Intergroup Rhabdomyosarcoma Study IV. *J Clin Oncol* 2003; **21**: 78-84. doi: 10.1200/JCO.2003.06.129
11. Koscielniak E, Harms D, Henze G, Jürgens H, Gadner H, Herbst M, et al. Results of treatment for soft tissue sarcoma in childhood and adolescence: a final report of the German Cooperative Soft Tissue Sarcoma Study CWS-86. *J Clin Oncol* 1999; **17**: 3706-19. doi: 10.1200/JCO.1999.17.12.3706
12. Oberlin O, Rey A, Lyden E, Bisogno G, Stevens MC, Meyer WH, et al. Prognostic factors in metastatic rhabdomyosarcomas: results of a pooled analysis from United States and European cooperative groups. *J Clin Oncol* 2008; **26**: 2384-9. doi: 10.1200/JCO.2007.14.7207
13. Bisogno G, Jenney M, Bergeron C, Gallego Melcón S, Ferrari A, Oberlin O, et al. Addition of dose-intensified doxorubicin to standard chemotherapy for rhabdomyosarcoma (EpSSG RMS 2005): a multicentre, open-label, randomised controlled, phase 3 trial. *Lancet Oncol* 2018; **19**: 1061-71. doi: 10.1016/S1470-2045(18)30337-1
14. Crist WM, Anderson JR, Meza JL, Fryer C, Raney RB, Ruymann FB, et al. Intergroup rhabdomyosarcoma study-IV: results for patients with nonmetastatic disease. *J Clin Oncol* 2001; **19**: 3091-102. doi: 10.1200/JCO.2001.19.12.309
15. Flamant F, Rodary C, Rey A, Praquin MT, Sommelet D, Quintana, et al. Treatment of non-metastatic rhabdomyosarcomas in childhood and adolescence. Results of the second study of the International Society of Paediatric Oncology MMT84. *Eur J Cancer* 1998; **34**: 1050-62. doi: 10.1016/s0959-8049(98)00024-0
16. Koscielniak E, Harms D, Henze G, Jürgens H, Gadner H, Herbst M, et al. Results of treatment for soft tissue sarcoma in childhood and adolescence: a final report of the German Cooperative Soft Tissue Sarcoma Study CWS-86. *J Clin Oncol* 1999; **17**: 3706-19. doi: 10.1200/JCO.1999.17.12.3706
17. Cecchetto G, Carli M, Sotti G, Bisogno G, Dall'Igna P, C Boglino, et al. Importance of local treatment in pediatric soft tissue sarcomas with microscopic residual after primary surgery: results of the Italian Cooperative Study RMS-88. *Med Pediatr Oncol* 2000; **34**: 97-101. doi: 10.1002/(sici)1096-911x(200002)34:2<97::aid-mpo4>3.0.co;2-8
18. Jereb B, Anžič J. Pediatric oncology in Slovenia. *Pediatric Hematol Oncol* 1996; **13**: 401-4. doi: 10.3109/08880019609030851
19. Ferrari A, Bisogno G, Casanova M, Meazza C, Piva L, Cecchetto G, et al. Paratesticular rhabdomyosarcoma: report from the Italian and German Cooperative Group. *J Clin Oncol* 2002; **20**: 449-55. doi: 10.1200/JCO.2002.20.2.449
20. Stewart RJ, Martelli H, Oberlin O, Rey A, Bouvet N, Spicer RD, et al. Treatment of children with nonmetastatic paratesticular rhabdomyosarcoma: results of the Malignant Mesenchymal Tumors studies (MMT 84 and MMT 89) of the International Society of Pediatric Oncology. *J Clin Oncol* 2003; **21**: 793-8. doi: 10.1200/JCO.2003.06.040
21. Merks JH, De Salvo GL, Bergeron C, Bisogno G, De Paoli A, Ferrari A, et al. Parameningeal rhabdomyosarcoma in pediatric age: results of a pooled analysis from North American and European cooperative groups. *Ann Oncol* 2014; **25**: 231-6. doi: 10.1093/annonc/mdt426
22. Bisogno G, De Rossi C, Gamboa Y, Sotti G, Ferrari A, Dallorso S, et al. Improved survival for children with parameningeal rhabdomyosarcoma: Results from the AIEOP soft tissue sarcoma committee. *Pediatr Blood Cancer* 2008; **50**: 1154-8. doi: 10.1002/pbc.2152
23. Minard-Colin V, Kolb F, Saint-Rose C, Fayard F, Janot F, Rey A, et al. Impact of extensive surgery in multidisciplinary approach of pterygopalatine/infratemporal fossa soft tissue sarcoma. *Pediatr Blood Cancer* 2013; **60**: 928-34. doi: 10.1002/pbc.24374
24. Chargari C, Haie-Meder C, Guérin F, Minard-Colin V, de Lambert G, Mazon R, et al. Brachytherapy combined with surgery for conservative treatment of children with bladder neck and/or prostate rhabdomyosarcoma. *Int J Rad Oncol* 2017; **98**: 352-9. doi: 10.1016/j.ijrobp.2017.02.026
25. Bisogno G, Pastore G, Perilongo G, Sotti G, Cecchetto G, Dallorso S, et al. Long-term results in childhood rhabdomyosarcoma: A report from the Italian cooperative study RMS 79. *Pediatr Blood Cancer* 2012; **58**: 872-6. doi: 10.1002/pbc.23292

Influence of concurrent capecitabine based chemoradiotherapy with bevacizumab on the survival rate, late toxicity and health-related quality of life in locally advanced rectal cancer: a prospective phase II CRAB trial

Vaneja Velenik^{1,5}, Vesna Zadnik^{2,5}, Mirko Omejc^{3,5}, Jan Grosek^{3,5}, Mojca Tuta^{4,5}

¹ Division of Radiotherapy, Institute of Oncology, Ljubljana, Slovenia

² Division of Epidemiology, Institute of Oncology, Ljubljana, Slovenia

³ Division of Surgery, University Medical Center Ljubljana, Ljubljana, Slovenia

⁴ Division of Radiology, Institute of Oncology, Ljubljana, Slovenia

⁵ Medical Faculty, University of Ljubljana, 1000 Ljubljana

Radiol Oncol 2020; 54(4): 461-469.

Received 1 March 2020

Accepted 13 June 2020

Correspondence to: Assoc. prof. Vaneja Velenik, M.D., Ph.D., Institute of Oncology Ljubljana, Zaloška cesta 2, SI-1000 Ljubljana, Slovenia.
E-mail: vvelenik@onko-i.si

Disclosure: No potential conflicts of interest were disclosed.

Background. Few studies reported early results on efficacy, toxicity of combined modality treatment for locally advanced rectal cancer (LARC) by adding bevacizumab to preoperative chemoradiotherapy, but long-term data on survival, and late complications are lacking. Further, none of the studies reported on the assessment of quality of life (QOL).

Patients and methods. After more than 5 years of follow-up, we updated the results of our previous phase II trial in 61 patients with LARC treated with neoadjuvant capecitabine, radiotherapy and bevacizumab (CRAB study) before surgery and adjuvant chemotherapy. Secondary endpoints of updated analysis were local control (LC), disease free (DFS) and overall survival (OS), late toxicity and longitudinal health related QOL (before starting the treatment and one year after the treatment) with questionnaire EORTC QLQ-C30 and EORTC QLQ-CR38.

Results. Median follow-up was 67 months. During the follow-up period, 16 patients (26.7%) died. The 5-year OS, DFS and LC rate were 72.2%, 70% and 92.4%. Patients with pathological positive nodes or pathological T3–4 tumors had significantly worse survival than patients with pathological negative nodes or T0–2 tumors. Nine patients (14.8%) developed grade ³ late complications of combined modality treatment, first event 12 months and last 87 months after operation (median time 48 months). Based on EORTC QLQ-C30 scores one year after treatment there were no significant changes in global QOL and three symptoms (pain, insomnia and diarrhea), but physical and social functioning significantly decreased. Based on QLQ-CR38 scores body image scores significantly increase, problems with weight loss significantly decrease, but sexual dysfunction in men and chemotherapy side effects significantly increase.

Conclusions. Patients with LARC and high risk factors, such as positive pathological lymph nodes and high pathological T stage, deserve more aggressive treatment in the light of improving long-term survival results. Patients after multimodality treatment should be given greater attention to the regulation of individual aspects of quality of life and the occurrence of late side effects.

Key words: rectal cancer; bevacizumab; preoperative chemoradiotherapy

Introduction

Colorectal cancer (CRC) represents a major public health problem in developed countries, especially in parts of Europe (Hungary, Slovenia, Slovakia, the Netherlands and Norway).¹ In Slovenia CRC is most frequently diagnosed among age group 50–74.² The standard treatment for LARC consists of capecitabine-based chemoradiation (CRT) followed by counseling surgery and adjuvant chemotherapy (ChT). Advances in multimodality treatments have significantly reduced 5-year local recurrence rates to less than 10% but this fact is not reflected in better survival.^{3,4} High rate of distant metastases (30% at 10 years) represents the main problem in achieving even better results of rectal cancer treatment.⁵ Thus, to achieve better control of systemic disease and consequently better survival, intensified systemic therapy is warranted.

The main guideline in developing the most optimal rectal cancer treatment regimen is elimination of subclinical micrometastases or/and interruption of the metastatic cascade. Angiogenesis plays a significant role in tumor growth, invasion and metastasis. The benefit of antiangiogenic inhibitors on better survival is already known in the treatment of metastatic colorectal cancer.⁶ Pre-clinical experiments in a variety of tumor models have shown encouraging results with the combination of antiangiogenic strategies with cytotoxic agents such as chemotherapy, ionizing radiation, or both in rectal cancer.^{7,8} Although bevacizumab, a recombinant humanized monoclonal antibody against vascular endothelial cell growth factor (VEGF), is widely tested in the preoperative treatment of LARC, there are only few studies evaluating survival benefit.^{9–11} Consequently, safety and efficacy of adding bevacizumab in the preoperative treatment of LARC remain unclear.

Significant progress in various approaches to rectal cancer treatment has led to the fact that long-term results and assessment of a patient's quality of life (QOL) has become increasingly important for offering patient optimal treatment. The European Organization for Research and Treatment of Cancer (EORTC) Quality of Life Questionnaire (QLQ-C30) and its tumor-specific 38-item questionnaire module Quality of Life Questionnaire Colorectal Cancer Module (QLQ-CR38), that later got its successor QLQ-CR29 with revised and fewer questions, were the first questionnaires introduced specifically for CRC.^{12–14} In addition to these QOL assessment tools for CRC, the Functional Assessment of Cancer Therapy-Colorectal (FACT-C) is also widely used.¹³

The FACT-C places a larger emphasis on emotional aspects of QOL while the QLQ-CR38 and QLQ-CR29 have greater dominance in the assessment of disease- and treatment-related symptoms.¹³

Our phase II trial was originally designed to determine the pathologic complete response rate of CRT and bevacizumab as a part of a combined modality approach. This report includes the long-term outcome, late complications and health related QOL of patients treated in CRAB study.

Patients and methods

The trial design, eligibility criteria, treatment and assessments have been published previously in detail.¹⁵ All patients provided signed informed consent based on international standards. The study was approved by the National Medical Ethics Committee of the Republic of Slovenia (Number 173/07/08) and was in agreement with the Declaration of Helsinki. It was registered in the ClinicalTrials.gov database (NCT 00842686).

Patient selection

In brief, patients with histologically proven stage II/III adenocarcinoma of the rectum within 15 cm of the anal verge and without contraindications for ChT or targeted agents were included. Local extend of the disease was determined by magnetic resonance imaging.

Treatment

Radiotherapy (RT) was delivered using three-dimensional conformal computed tomography (CT)-based treatment planning. Four-field box technique with all fields treated daily was used. Patients received 45 Gy to the pelvis plus 5.4 Gy as a boost to the primary tumor in 1.8 Gy over 5.5 weeks. Capecitabine 825 mg/m² twice daily was administered concomitantly continuously throughout of RT without interruptions on weekends. Patients received bevacizumab intravenously at a dose 5 mg/kg 14 days prior and on days 1, 15 and 29 during chemoradiotherapy (CRT). Resection (low anterior resection or abdominoperineal amputation with total mesorectal excision) was performed 6–8 weeks after the completion of CRT. Patients with histopathological R0 resection received 6 cycles of adjuvant chemotherapy with capecitabine, while in those with R1 additional 2 cycles were given. Pathologic response after CRT with bevacizumab

was determined according to Dworak tumor regression grade (TRG) system. The pathological complete response (pCR) was defined as TRG 4, meaning no tumor cells in surgical specimen.

Statistical methods

Results for primary endpoint of this prospective phase II study, the pCR rate, and on some secondary endpoints (pathological response rate, rate of sphincter-sparing surgical procedure, radical resection rate, acute and perioperative toxicity of combined modality treatment) have been reported previously.¹⁵ Here we report results on other secondary endpoints of this updated analysis: local control (LC), disease free (DFS) recurrence-free (RFS) and overall survival (OS), late toxicity and health related QOL. Survival rates were calculated using Kaplan-Meier technique. All time intervals were calculating from the date of inclusion. The end day for LC was the date of last follow-up or recurrence in the pelvis; for OS the date of last follow up or death from any cause; for DFS the date of relapse, secondary cancer, death for any cause or the last follow-up.

Separate analysis was performed for health related QLQ applying the questionnaires launched by the EORTC. For this study the core questionnaire EORTC QLQ-C30¹⁶ adjoined with the colorectal module EORTC QLQ-CR38¹² was delivered to the patients twice: before starting the treatment and one year after the treatment was finished. The EORTC QLQ-C30 is a questionnaire assessing individual HRQL during the previous week. The EORTC QLQ-C30 has 30 items and is divided into five function scales (physical, role, cognitive, emotional and social functions); three symptom scales (fatigue, pain, nausea or vomiting) and one global health-status/quality of life dimension. The six single items address specific symptoms: dyspnoea, appetite loss, insomnia, constipation, diarrhoea and a question addressing the financial impact of the disease. The EORTC QLQ-CR38 has 38 questions and is divided into four functional and seven scales of symptoms/problems. The answers recorded by the questionnaires were transformed into dimensions ranged 0–100 according to the EORTC scoring instructions.¹⁷ For functional scales and single items higher scores represent a higher level of functioning, but for symptom scales and single items, a higher score represents a higher level of symptoms. To examine the statistically significant changes in QLQ scores over time the Wilcoxon signed-rank test was applied.

All statistical analysis was performed using the SPSS statistical software package, version 24 (SPSS Inc, Chicago, IL, USA). Values of $p < 0.05$ were considered statistically significant.

Results

Between February 2009 and March 2010, 61 patients entered the study protocol at our institution. The detailed characteristics of the patients have been presented previously.¹⁵ Baseline assessment included complete history, physical examination, full blood count, serum biochemistry, carcinoembryonic antigen, chest radiography, ultrasonography and/or computed tomography (CT) scan of the whole abdomen. Twelve pts (19.7%) presented with stage II and all other with stage III of disease. In 28 patients (45.9%) the tumor invaded the mesorectal fascia. Radical resection was achieved in 57 pts (95%). Sixty patients were eligible for efficacy analysis. TRG 4 (pCR) was recorded in 8 pts (13.3%) and TRG 3 in 9 pts (15%). Fifty-one pts (83.6%) received capecitabine postoperatively. An intention-to-treat analysis was performed on 60/61 pts as one was misdiagnosed. Median follow-up was 67 months (range, 7 to 79 months). During the follow-up period, 16 patients (26.7%) died. A total of 13 (21.7%) of these deaths were a consequence of rectal cancer progression and the remaining 3 due to unrelated causes.

Survival analysis

The 5-year OS was 72.2% (95% CI 58.2–84). Recurrences were observed in 14 patients (23.3%) and in one secondary cancer occurred. The latest distant recurrence was observed 54 months after the operation. The 5-years recurrence-free survival and DFS were 75.6% (95% CI 64.6–81.3) and 70% (95% CI 58.5–81.5), respectively. Local recurrence as any component of first failure occurred in 4 patients (6.7%), with isolated local recurrence in 1 (1.7%). The 5-year LC rate was 92.4% (95% CI 85.4–99.4). Figure 1 illustrates OS, DFS and recurrence-free survival and LC of patients treated in CRAB trial.

Based on the Cox proportional hazards regression model, there were no significant association between OS or DFS and gender, age, performance status, cT, cN, TRG and adjuvant ChT. Patients with pathological positive nodes or pathological T3–4 tumors had significantly worse survival than

TABLE 1. Overall survival (OS) and disease free survival (DFS) according to pTumor and pNodal stage on univariate analysis

Factor	OS		DFS	
pTumor stage				
pT0-2	85%		85.7%	
pT3-4	60.9%	p=0.043	61.8%	p=0.044
pNodal stage				
pN0	81%		81%	
pN+	37.5%		41.7%	p=0.003

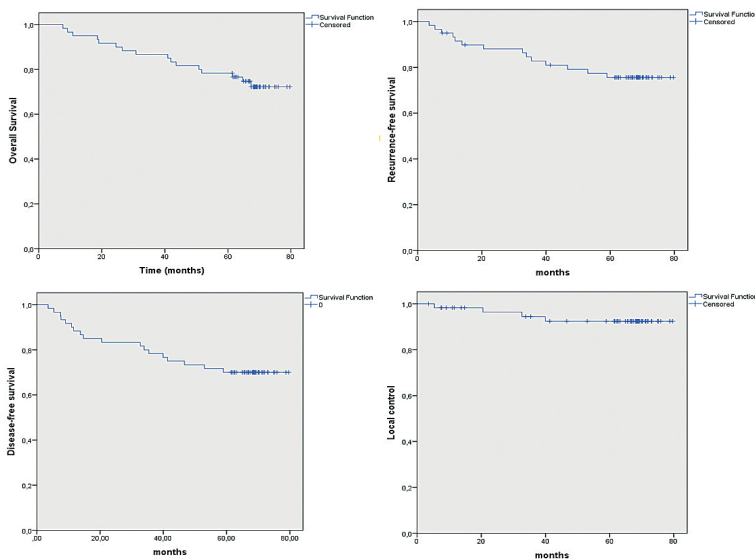


FIGURE 1. Overall survival (OS), disease free survival (DFS), recurrence-free survival and local control (LC) of patients treated in CRAB trial.

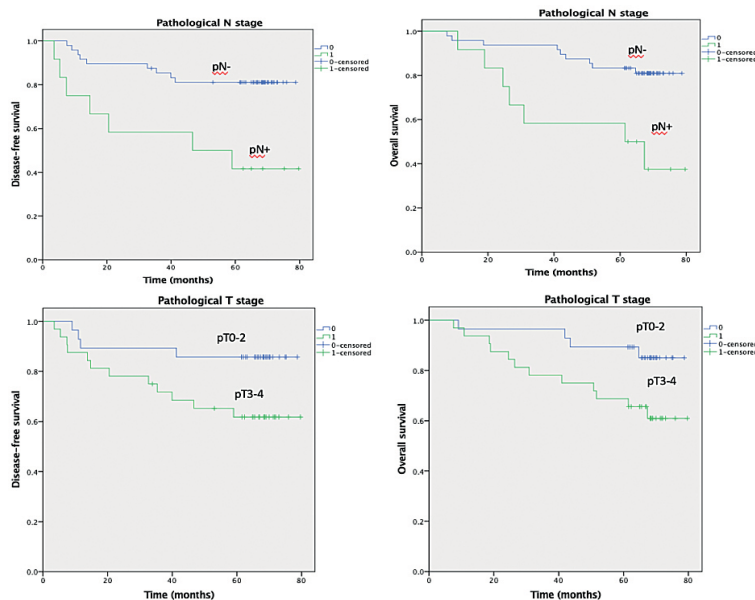


FIGURE 2. Prognostic significance of pathological nodal stage (pN) and tumor stage (pT) on 5-year disease free survival (DFS) and overall survival (OS).

patients with pathological negative nodes or T0–2 tumor (Table 1 and Figure 2).

Late complications

Nine patients (14.8%) developed grade 3 late complications of combined modality treatment (Common Terminology Criteria for Adverse Events version 4.0) for which hospitalization and/or urgent intervention was needed. We recorded the first event 12 months and the last 87 months after the operation with the median time to occurrence of 48 months. All these complications, time to occurrence after surgery of primary cancer and procedures needed are presented in Table 2. Among patients without mentioned complications, we observed permanent defecation complications in 11: constipation in 4, defecation urgency in 3 and fecal incontinence in 4 colostomy free patients. Two patients with stoma experienced permanent urinary complications: 1 incompleting bladder emptying and 1 urinary incontinence.

Health related quality of life

The results of the health related QOL analysis is summarized in Table 3. One year after treatment there were no significant changes in global quality of life, however the physical and social functioning significantly decreased. On the other hand, there was a significant decrease in three symptoms: pain, insomnia and diarrhea.

Based on QLQ-CR38 scores there were no significant change on three functional scales (i.e. future perspectives, sexual functioning and enjoyment), but the body image scores significantly increase. One year after treatment has been completed our patients reported significantly less problems with weight loss, but there was a significant increase in ChT side effects (dry mouth, thin or lifeless hair and different taste) and sexual dysfunction in men.

Discussion

The final results of CRAB study show that preoperative CRT with bevacizumab and capecitabine is feasible with good compliance and acceptable toxicity.¹⁵ The pCR rate of 13% was similar to an earlier phase II study by our group examining neoadjuvant single-agent capecitabine plus RT in LARC.¹⁸

Direct comparison of long term results could only be possible with the study from Gasparini *et*

TABLE 2. Late grade 3 adverse events in CRAB trial

Event	N	Time to appearance (after the operation)	Procedure
Fistula rectovaginalis	1	12 months	Hartman operation
	1	31 months	Abdominoperineal excision
Fistula enteroperinealis	1	74 months	No action due to local and distant progression of the disease
Fistula enteroglutealis	1	54 months	Incision, drain
Fistula uretroperinealis	1	87 months	Conservative
Fistula enteroperinealis	1	54 months	No action due to poor performance status
Abscessus perinealis	1	48 months	Incision, drain
Abscessus presacralis	1	36 months	Incision, transversostomy
Stenosis ureteri bill.	1	43 months	J splint bill

al, as they reported comparable characteristics of patients and the same treatment regimen (neoadjuvant bevacizumab 5 mg/kg on days -14, and 1, 15, 29, and concomitant CRT with capecitabine 825/mg/m²/bid with total radiation dose of 50.4 Gy), but such data were not published.¹⁹ Only one study from Willett *et al.* reported 5-years survival data for LARC, treated with concurrent bevacizumab and preoperative capecitabine-based CRT.¹⁰ In comparison to our study Willett *et al.* reported comparable pCR rate of 16%, although their study had slightly different treatment regimen (neoadjuvant bevacizumab 5–10 mg/kg on days 1,8,15,22 and concomitant CRT with 4 cycles of fluorouracil 225 mg/m²/24h with total radiation dose of 50.4 Gy). Additionally, our is the largest study on the long term efficacy and the only one evaluating late toxicity for neoadjuvant bevacizumab in LARC (Willett *et al.* vs. CRAB, 32 patients vs. 61 patients).¹⁰ To our knowledge our study is one of the first evaluating longitudinal health related QOL of rectal cancer patients after combined modality treatment and the only one with bevacizumab in this specific group of patients.²⁰

Survival

Compared to our study, Willett *et al.* reported better 5-year LC rate (92,4% vs. 100%) and OS (72.2% vs. 100%).¹⁰ However, no difference in 5-year DFS (Willett *et al.* vs. CRAB, 75% vs. 75.6%) was observed. Pathologic complete response rate and gender ratio between studies were comparable. Some differences were seen regarding pathological nodal stage and age of patients. Our results revealed that pathological positive nodes and pathological T3/4 tumors were significantly associated with worse

survival (Table 1 and Figure 2). Among patients with pathological positive nodes and pathological T3/4 tumors, the 5-year OS and DFS were 37.5% and 60.9%, 41.7% and 61.8%, respectively. These poor results for high-risk subgroup suggest that more aggressive approach is needed for such a patient. Proportion of patient included in CRAB study with pathological negative nodes was lower than in American study (19.7% vs. 28%).¹⁰ This fact could affected poorer survival results in CRAB study. Other studies have also shown that pathologic nodal status may represent a superior predictor of better survival for patients with LARC.^{21,22}

Furthermore, patient characteristics (sex and age) predict survival. In the largest analysis examining the impact of demographic characteristics on the survival of patients with rectal cancer, older age and male gender are associated with worse cancer-specific and OS.²³ One of the possible causes for our worse OS could be in the older population that was included in the CRAB study compared to American study (median age with range; 60 years [31–80] vs. 51 years [35–72]).¹⁰

A comparison between neoadjuvant single-agent capecitabine CRT and the current study revealed promising oncologic outcome with adding bevacizumab in the standard neoadjuvant treatment of LARC in Slovenia (5-year OS, DFS and LC; 61.4, 52.4% and 87.4 vs. 72.2, 75.6 and 92.4%).²⁴ Thus, this difference is not statistically significant and we cannot state with certainty that the improvement depends only on adding bevacizumab to standard neoadjuvant capecitabine-based CRT due to differences in the prescribed radiation dose. In CRAB study we used additionally concomitant radiation boost for which it is known that might have a positive effect on OS.²⁵

TABLE 3. Health related quality of life analysis: Comparisons of mean scores with standard deviations (SD) before and 1 year after completed treatment for all scales of EORTC QLQ-C30 and EORTC QLQ-CR38

Scale	Item	Number responding before and 1 year after treatment	Before treatment mean (SD)	1 year after treatment mean (SD)	p value Wilcoxon signed-rank test*
EORTC QLQ-C30					
<i>Global health status/quality of life</i>					
	29,30	50	62.5 (20.8)	68.0 (19.7)	0.087
<i>Functional scales</i>					
Physical functioning	1 to 5	50	89.9 (15.3)	84.7 (14.9)	0.008
Role functioning	6,7	50	85.3 (23.4)	81.3 (24.4)	0.557
Emotional functioning	21 to 24	50	80.6 (19.0)	83.0 (20.8)	0.259
Cognitive functioning	20,25	50	89.4 (17.1)	86.7 (20.2)	0.346
Social functioning	26,27	50	86.7 (16.2)	77.7 (21.7)	0.007
<i>Symptom scales</i>					
Fatigue	10,12,18	50	21.5 (22.0)	20.7 (18.8)	0.607
Nausea and vomiting	14,15	50	2.5 (6.0)	2.3 (6.7)	1.000
Pain	9,19	50	19.7 (27.5)	11.7 (15.9)	0.017
Dyspnoea	8	50	3.3 (11.8)	4.7 (13.5)	0.782
Insomnia	11	50	24.4 (25.9)	15.3 (22.5)	0.044
Appetite loss	13	50	7.8 (20.7)	6.7 (17.8)	0.726
Constipation	16	50	4.4 (14.3)	12.0 (23.1)	0.126
Diarrhoea	17	50	31.1 (30.6)	12.0 (18.8)	0.002
Financial difficulties	28	49	11.9 (22.1)	18.0 (24.5)	0.103
EORTC QLQ-CR38					
<i>Functional scales</i>					
Body image	13,14,15	50	8.8 (16.1)	23.1 (24.9)	0.001
Sexual functioning	17,18	47	28.7 (22.9)	29.4 (26.5)	0.859
Future perspective	16	50	54.0 (30.5)	49.7 (30.1)	0.420
Sexual enjoyment	19	22	44.4 (24.6)	48.1 (29.7)	0.527
<i>Symptom scales</i>					
Chemotherapy side effects	10,11,12	51	7.3 (11.8)	10.7 (13.7)	0.021
General gastrointestinal symptoms	4 to 8	51	22.1 (19.3)	18.0 (18.3)	0.084
Defecation problems	25 to 31	26	27.5 (21.1)	30.2 (16.4)	0.456
Stoma-related problems	32 to 38	0		28.0 (12.3)	
Sexual dysfunction of men	20,21	23	15.3 (18.0)	42.6 (35.6)	0.006
Sexual dysfunction of women	22,23	4	16.7 (18.6)	11.1 (27.2)	1.000
Radiation-induced effects micturition	1,2,3	51	21.1 (18.3)	21.4 (19.0)	0.945
Weight loss	9	50	19.9 (27.4)	8.5 (18.7)	0.016

*statistically significant values ($p < 0.050$) are bolded

Late toxicities

Bevacizumab may cause severe late side effects in metastatic setting but late side effects are relatively rare.²⁶ Most often described bevacizumab related late adverse events are spontaneous intestinal per-

foration and delayed anastomotic leak.^{27,28} The addition of bevacizumab to standard CRT could be one of the possible causes for a higher proportion of fistulas in our study.

Only few studies analyzed the incidence of the late anastomotic leakage after low anterior resection

(LAR). Delayed anastomotic leakages that develop after 30 days after surgery are not uncommon. The incidence is between 0.3% and 9.8%.²⁹⁻³⁵ It is not clear whether early and late anastomotic leakage after LAR are different entities because some patients with late anastomotic leakage may show uneventful postoperative clinical recovery.²⁹ Late leakages more frequently involve the fistula type (22–100%) than early postoperative leakage.^{29-32,34,35} Pelvic abscess and anastomotic-vaginal fistula were the most common causes of delayed complications.³⁵

In our study only one female patient developed anastomotic vaginal fistula 12 months after rectal surgery. In the two studies with higher number of female patients included, the overall rate of anastomotic-vaginal fistula after LAR was higher, 3% (11/371) and 5.1% (20/390).^{36,37} Anastomotic-vaginal fistulas in both studies were diagnosed mostly late, on median postoperative day 83 (15–766) in the first study and 25 (5–172) in the second. Despite that only 3% of the female patients in the first study were treated with preoperative ChT and no one with RT, pre-op ChT was one of the independent risk factor for anastomotic-vaginal fistula formation.³⁶ In the second study, risk factors for anastomotic-vaginal fistula were preoperative radiotherapy, anastomosis < 5 cm above the anal verge and cancer stage IV.³⁷

The incidence of the delayed anastomotic leakage in present study was high (13.1%), but it is important that only three fistulas were diagnosed before 5 years of follow up. Comparing the incidence of the delayed anastomotic leakage in our study with other studies is controversial. Follow up in our study was the longest than it was in other published studies. The longest interval between the surgery and fistula formation we found in the literature was 5.7 years and in our study 7.25 years. RT and ChT were identified as an independent risk factor for the development of the late anastomotic complications.^{32,34,35} In all published studies patients with very mixed type of neo-adjuvant and adjuvant treatment or without treatment were included. On the other side, in our study all patients were treated with neo-adjuvant CRT. According to previous facts, it is important that we pay attention to the appearance of early signs of the fistula during follow up in the patient previous treated with bevacizumab even several years after the completion of treatment.

Health related QOL

The global health status (mean 68), which refers to the general assessment of the health and qual-

ity of life of the last seven days, was similar over time, and also comparable to the Slovenian general (mean 71.1) and CRC patients (mean 68.3).^{38,39}

The values of social and physical functioning indicated by patients were significantly influenced by the time between diagnosis and 1 year after treatment indicating a high incidence of problems in this area. On the other hand, 1 year after treatment patients reported less pain, insomnia and diarrhea. These results are consistent with QLQ-C30 scores of Slovenian CRC patients after surgical treatment.³⁹ However, compared above mentioned items with the general Slovenian population, patients 1 year after treatment report more diarrhea, lower physical and social functioning, but less pain and insomnia. The population-based QOL reference values should be taken into account in the interpretation of disease progress and treatment effects. For Slovenian general population it was shown that gender, age and self-rated social class are important confounders in the QOL scores descriptions.³⁸

Our long-term trends in longitudinal QOL are in agreement with study published from Couwenberg *et al.* including rectal cancer patients treated with CRT and surgery.²⁰ They demonstrated that treatment of rectal cancer has larger impact on QOL decline within 3–6 months after the start of treatment, but still gradually improves within 1 year after treatment. Moreover, within two years all scores normalize towards pretreatment levels, although compared to general population lower functioning, more insomnia and fatigue persist for more than 2 years from diagnosis.

Based on QLQ-CR38 significantly more ChT side effects and sexual dysfunction of men were observed after 1 year of treatment. However, body image has improved and patients reported less weight loss. Male sexual dysfunction is common and remains high after multimodality treatment for rectal cancer, more precisely, surgical nerve damage remain the main cause.⁴⁰ Patients treated with well-defined and standardized technique of total mesorectal excision together with minimally invasive techniques experienced less sexual dysfunction compared to conventional surgery.⁴¹ In addition, laparoscopic resection contributes more to the maintenance of the nerves.⁴⁰

Limitations

The main limitations of this study include the single center design of the study with small number of patients, which limits statistical power. To assess

the QOL we have chosen a QLQ-CR38 and not revised successor QLQ-CR29, because the latter was published later in 2007. Consequently, our results are less comparable to others that have been used QLQ-CR29.

Conclusions

The optimal treatment strategy for patients with LARC is still controversial. Neoadjuvant bevacizumab with standard CRT in LARC is acceptable strategy. Further studies of its effect on better long-term outcome are warranted. Patients with LARC with high risk factors, such as positive pathological lymph nodes and high pathological T stage, deserve more aggressive treatment in the light of improving long-term survival results. While advances in multimodality treatment of CRC are enormous, some of the QOL aspects and long-term safety are often not published and inadequately discussed with patients. LARC treatment may no longer be standardized, but adjusted to the wishes, needs and characteristics of an individual patient.

References

- Bray F, Ferlay J, Soerjomataram I, Siegel RL, Torre LA, Jemal A. Global cancer statistics 2018 : GLOBOCAN Estimates of incidence and mortality worldwide for 36 cancers in 185 countries. *CA Cancer J Clin* 2018; **68**: 394-424. doi: 10.3322/caac.21492
- Zadnik V, Primic Zakelj M, Lokar K, Jarm K, Ivanus U, Zagar T. Cancer burden in Slovenia with the time trends analysis. *Radiol Oncol* 2017; **51**: 47-55. doi: 10.1515/raon-2017-0008
- Ludmir EB, Palta M, Willett CG, Czito BG. Total neoadjuvant therapy for rectal cancer: An emerging option. *Cancer* 2017; **123**: 1497-506. doi: 10.1002/cncr.30600
- Sauer R, Becker H, Hohenberger W, Rödel C, Wittekind C, Fietkau R, et al. Preoperative versus postoperative chemoradiotherapy for rectal cancer. *N Engl J Med* 2004; **351**: 1731-40. doi: 10.1056/NEJMoa040694
- Sauer R, Liersch T, Merkel S, Fietkau R, Hohenberger W, Hess C, et al. Preoperative versus postoperative chemoradiotherapy for locally advanced rectal cancer: results of the German CAO/ARO/AIO-94 randomized phase III trial after a median follow-up of 11 years. *J Clin Oncol* 2012; **30**: 1926-33. doi: 10.1200/JCO.2011.40.1836
- Mody K, Baldeo C, Bekaii-Saab T. Antiangiogenic therapy in colorectal cancer. *Cancer J* 2018; **24**: 165-70. doi: 10.1097/PPO.0000000000000328
- Nieder C, Wiedenmann N, Andratschke NH, Astner ST, Molls M. Radiation therapy plus angiogenesis inhibition with bevacizumab : rationale and initial experience. *Rev Recent Clin Trials* 2007; **2**: 163-8. doi: 10.2174/157488707781662733
- Willett CG, Boucher Y, Duda DG, di Tomaso E, Munn LL, Tong RT, et al. Surrogate markers for antiangiogenic therapy and dose-limiting toxicities for bevacizumab with radiation and chemotherapy: continued experience of a phase I trial in rectal cancer patients. *J Clin Oncol* 2005; **23**: 8136-9. doi: 10.1200/JCO.2005.03.5881
- Fornaro L, Capareello C, Vivaldi C, Rotella V, Musettini G, Falcone A, et al. Bevacizumab in the pre-operative treatment of locally advanced rectal cancer : a systematic review. *World J Gastroenterol* 2014; **20**: 6081-91. doi: 10.3748/wjg.v20.i20.6081
- Willett CG, Duda DG, Di Tomaso E, Boucher Y, Ancukiewicz M, Sahani D V, et al. Efficacy, safety, and biomarkers of neoadjuvant bevacizumab, radiation therapy, and fluorouracil in rectal cancer: multidisciplinary phase II study. *J Clin Oncol* 2009; **27**: 3020-6. doi: 10.1200/JCO.2008.21.1771
- García M, Martínez-Villacampa M, Santos C, Navarro V, Teule A, Losa F, et al. Phase II study of preoperative bevacizumab, capecitabine and radiotherapy for resectable locally-advanced rectal cancer. *BMC Cancer* 2015; **15**: 59. doi: 10.1186/s12885-015-1052-0
- Sprangers MA, Te Velde A, Aaronson NK. The construction and testing of the EORTC colorectal cancer-specific quality of life questionnaire module (QLQ-CR38). *Eur J Cancer* 1999; **35**: 238-47. doi: 10.1016/S0959-8049(98)00357-8
- Gujral S, Conroy T, Fleissner C, Sezer O, King PM, Avery KN, et al. Assessing quality of life in patients with colorectal cancer : an update of the EORTC quality of life questionnaire. *Eur J Cancer* 2007; **43**: 1564-73. doi: 10.1016/j.ejca.2007.04.005
- Ganesh V, Agarwal A, Popovic M, Cella D, McDonald R, Vuong S, et al. Comparison of the FACT-C , EORTC QLQ-CR38 , and QLQ-CR29 quality of life questionnaires for patients with colorectal cancer: a literature review. *Support Care Cancer* 2016; **24**: 3661-8. doi: 10.1007/s00520-016-3270-7
- Velenik V, Ocvirk J, Mušič M, Bračko M, Anderluh F, Oblak I, et al. Neoadjuvant capecitabine, radiotherapy, and bevacizumab (CRAB) in locally advanced rectal cancer: results of an open-label phase II study. *Radiat Oncol* 2011; **6**: 105. doi: 10.1186/1748-717X-6-105
- Aaronson N, Ahmedzai S, Bergman B, Bullinger M, Cull A, Duez N, et al. The European organisation for research and treatment of cancer QLQ-C30: a quality-of-life instrument for use in international clinical trials in oncology. *J Natl Cancer Inst* 1993; **85**: 365-76. doi: 10.1093/jnci/85.5.365
- Fayers P, Aaronson N, Bjordal K, Groenvold M, Curran D, Bottomley A. *EORTC QLQ-C30 scoring manual*. 3rd Edition. Brussels: European Organisation for Research and Treatment of Cancer; 2001.
- Velenik V, Anderluh F, Oblak I, Strojjan P, Zakotnik B. Capecitabine as a radiosensitizing agent in neoadjuvant treatment of locally advanced resectable rectal cancer: prospective phase II trial. *Croat Med J* 2006; **47**: 693-700. PMID: 17042060
- Gasparini G, Torino F, Ueno T, Cascinu S, Troiani T, Ballestrero A, et al. A phase II study of neoadjuvant bevacizumab plus capecitabine and concomitant radiotherapy in patients with locally advanced rectal cancer. *Angiogenesis* 2012; **15**: 141-50. doi: 10.1007/s10456-011-9250-0
- Couwenberg AM, Burbach JPM, van Grevenstein WMU, Smits AB, Consten ECJ, Schiphorst AHW, et al. Effect of neoadjuvant therapy and rectal surgery on health-related quality of life in patients with rectal cancer during the first 2 years after diagnosis. *Clin Colorectal Cancer* 2018; **17**: 499-512. doi: 10.1016/j.clcc.2018.03.009
- Kim NK, Baik SH, Seong JS, Kim H, Roh JK, Lee KY, et al. Oncologic outcomes after neoadjuvant chemoradiation followed by curative resection with tumor-specific mesorectal excision for fixed locally advanced - impact of postirradiated pathologic downstaging on local recurrence and survival. *Ann Surg* 2006; **244**: 1024-30. doi: 10.1097/01.sla.0000225360.99257.73
- Hernandez JM, Clark W, Weber J, Fulp WJ, Lange L, Shibata D. The impact of pathologic nodal status on survival following neoadjuvant chemoradiation for locally advanced rectal cancer. *Int J Color Dis* 2014; **29**: 1061-8. doi: 10.1007/s00384-014-1917-8
- Berger MD, Yang D, Sunakawa Y, Zhang W, Ning Y, Matsusaka S, et al. Impact of sex, age and ethnicity/race on the survival of patients with rectal cancer in the United States from 1988 to 2012. *Oncotarget* 2016; **7**: 53668-78. doi: 10.18632/oncotarget.10696
- Velenik V, Oblak I, Anderluh F. Long-term results from a randomized phase II trial of neoadjuvant combined-modality therapy for locally advanced rectal cancer. *Radiat Oncol* 2010; **5**: 88. doi: 10.1186/1748-717X-5-88
- Badakhshi H, Ismail M, Boskos C, Zhao K, Kaul D. The role of concomitant radiation boost in neoadjuvant chemoradiotherapy for locally advanced rectal cancer. *Anticancer Res* 2017; **37**: 3201-5. doi: 10.21873/anticancer.11681
- O'Hare T, McDermott R, Hannon R. Late anastomotic breakdown with bevacizumab in colorectal cancers, a case-based review. *Ir J Med Sci* 2018; **187**: 333-6. doi: 10.1007/s11845-017-1676-y
- Borzomati D, Nappo G. Infusion of bevacizumab increases the risk of intestinal perforation: results on a series of 143 patients consecutively treated. *Updat Surg* 2013; **65**: 121-4. doi: 10.1007/s13304-013-0207-2

28. Machida E, Miyakura Y, Takahashi J, Tamaki S, Ishikawa H, Hasegawa F, et al. Bevacizumab is associated with delayed anastomotic leak after low anterior resection with preoperative radiotherapy for rectal cancer: a case report. *Surg Case Rep* 2019; **5**: 14. doi: 10.1186/s40792-019-0573-1
29. Floodeen H, Hallböök O, Rutegård J, Sjödah R, Matthiessen P. Early and late symptomatic anastomotic leakage following low anterior resection of the rectum for cancer: are they different entities? *Color Dis* 2013; **15**: 334-40. doi: 10.1111/j.1463-1318.2012.03195.x
30. Hyman N, Manchester TL, Osler T, Burns B, Cataldo PA. Anastomotic leaks after intestinal anastomosis: it's later than you think. *Ann Surg* 2007; **245**: 254-8. doi: 10.1097/01.sla.0000225083.27182.85
31. Iwamoto M, Kawada K, Hida K, Hasegawa S, Sakai Y. Delayed anastomotic leakage following laparoscopic intersphincteric resection for lower rectal cancer: report of four cases and literature review. *World J Surg Oncol* 2017; **15**: 143. doi: 10.1186/s12957-017-1208-2
32. Lim S, Yu CS, Kim CW, Yoon YS, Park IJ, Kim JC. Late anastomotic leakage after low anterior resection in rectal cancer patients: clinical characteristics and predisposing factors. *Color Dis* 2016; **18**: 135-40. doi: 10.1111/codi.13300
33. Matthiessen P, Lindgren R, Hallböök O, Rutegård J, Sjödah R, Study GRCT on DS. Symptomatic anastomotic leakage diagnosed after hospital discharge following low anterior resection for rectal cancer. *Color Dis* 2010; **12**: 82-7. doi: 10.1111/j.1463-1318.2009.01938.x
34. Morks AN, Ploeg RJ, Sijbrand Hofker H, Wiggers T, Havenga K. Late anastomotic leakage in colorectal surgery: a significant problem. *Color Dis* 2013; **15**: 271-5. doi: 10.1111/codi.12167
35. Shin US, Kim CW, Yu CS, Kim JC. Delayed anastomotic leakage following sphincter-preserving surgery for rectal cancer. *Int J Color Dis* 2010; **25**: 843-9. doi: 10.1007/s00384-010-0938-1
36. Watanabe J, Ota M, Kawaguchi D, Shima H, Kaida S, Osada S, et al. Incidence and risk factors for rectovaginal fistula after low anterior resection for rectal cancer. *Int J Color Dis* 2015; **30**: 1659-66. doi: 10.1007/s00384-015-2340-5
37. Matthiessen P, Hansson L, Sjödah I, Rutegård J. Anastomotic-vaginal fistula (AVF) after anterior resection of the rectum for cancer - occurrence and risk factors. *Color Dis* 2010; **12**: 351-7. doi: 10.1111/j.1463-1318.2009.01798.x
38. Velenik V, Šečerov-Ermenc A, But-Hadžić J, Zadnik V. Health-related quality of life assessed by the EORTC QLQ-C30 questionnaire in the general slovenian population. *Radiol Oncol* 2017; **51**: 342-50. doi: 10.1515/raon-2017-0021
39. Grosek J, Novak J, Kitek K, Bajrič A, Majdič A, Košir JA. Health-related quality of life in Slovenian patients with colorectal cancer: a single tertiary care center study. *Radiol Oncol* 2019; **53**: 231-7. doi: 10.2478/raon-2019-0015
40. Nagpal K, Bennett N. Colorectal surgery and its impact on male sexual function. *Curr Urol Rep* 2013; **14**: 279-84. doi: 10.1007/s11934-013-0341-x
41. Chew M, Yeh Y, Lim E, Seow-Choen F. Pelvic autonomic nerve preservation in radical rectal cancer surgery: changes in the past 3 decades. *Gastroenterol Rep* 2016; **4**: 173-85. doi: 10.1093/gastro/gow023

Breast size and dose to cardiac substructures in adjuvant three-dimensional conformal radiotherapy compared to tangential intensity modulated radiotherapy

Ivica Ratoso^{1,2}, Aljasa Jenko¹, Zeljko Sljivic^{1,3}, Maja Pirnat⁴, Irena Oblak^{1,2}

¹ Department of Radiotherapy, Institute of Oncology Ljubljana, Ljubljana, Slovenia

² Faculty of Medicine, University of Ljubljana, Ljubljana, Slovenia

³ Faculty of Health Sciences, University of Ljubljana, Ljubljana, Slovenia

⁴ Department of Radiology, University Medical Centre Maribor, Maribor, Slovenia

Radiol Oncol 2020; 54(4): 470-479.

Received 18 March 2020

Accepted 10 May 2020

Correspondence to: Assist. Ivica Ratoša, M.D., Ph.D., Institute of Oncology Ljubljana, Zaloška cesta 2, SI-1000 Ljubljana, Slovenia.
E-mail: iratoso@onko-i.si

Disclosure: No potential conflicts of interest were disclosed.

Background. The aim of the study was to quantify planned doses to the heart and specific cardiac substructures in free-breathing adjuvant three-dimensional radiation therapy (3D-CRT) and tangential intensity modulated radiotherapy (t-IMRT) for left-sided node-negative breast cancer, and to assess the differences in planned doses to organs at risk according to patients' individual anatomy, including breast volume.

Patients and methods. In the study, the whole heart and cardiac substructures were delineated for 60 patients using cardiac atlas. For each patient, 3D-CRT and t-IMRT plans were generated. The prescribed dose was 42.72 Gy in 16 fractions. Patients were divided into groups with small, medium, and large clinical target volume (CTV). Calculated dose distributions were compared amongst the two techniques and the three different groups of CTV.

Results. Mean absorbed dose to the whole heart (MWH) (1.9 vs. 2.1 Gy, $P < 0.005$), left anterior descending coronary artery mean dose (8.2 vs. 8.4 Gy, $P < 0.005$) and left ventricle (LV) mean dose (3.0 vs. 3.2, $P < 0.005$) were all significantly lower with 3D-CRT technique compared to t-IMRT. Apical (8.5 vs. 9.0, $P < 0.005$) and anterior LV walls (5.0 vs. 5.4 Gy, $P < 0.005$) received the highest mean dose (D_{mean}). MWH and LV- D_{mean} increased with increasing CTV size regardless of the technique. Low MWH values (< 2.5 Gy) were achieved in 44 (73.3%) and 41 (68.3%) patients for 3D-CRT and t-IMRT techniques, correspondingly.

Conclusions. Our study confirms a considerable range of the planned doses within the heart for adjuvant 3D-CRT or t-IMRT in node-negative breast cancer. We observed differences in heart dosimetric metrics between the three groups of CTV size, regardless of the radiotherapy planning technique.

Key words: breast cancer; breast size; 3D-CRT; IMRT; heart dose; left anterior descending coronary artery

Introduction

Cardiovascular diseases are becoming the most critical competing mortality risk in women with early breast cancer treated with present-day radiotherapy (RT).^{1,2} The relative risk of radiation-induced heart failure increases with rising cardiac radiation exposure, typically reported as mean ab-

sorbed dose to the whole heart (MWH).³⁻⁵ MWH values reflect local radiation therapy practices, and with the help of modern RT approaches, now ranging from 1.7–5.4 Gy⁶⁻⁸ and 1.22–1.65 Gy⁹, for mean and median values, respectively. However, even very low cardiac exposure does not eliminate the risk of radiotherapy-mediated cardiotoxicity, which has been demonstrated in recent studies.^{3,5,10}

In many recent publications, authors favor the use of intensity modulated techniques over three-dimensional conformal radiotherapy (3D-CRT) in node negative breast cancer adjuvant RT, arguing for lower MWHD, decreased skin toxicity and more homogeneous dose distribution in the target volume.¹¹⁻¹³ Besides the RT technique used, MWHD depends on the position of the patient's heart relative to the irradiated breast and the shape of their chest wall.¹⁴ Different simple anatomical measures were evaluated to predict increased MWHD and subsequently for the need to use one of the heart-sparing techniques, namely deep inspiration breath hold technique (DIBH). Useful anatomical measures are increased chest wall separation (CWS)⁹, maximum heart distance (the distance between the anterior cardiac contour crossing over the posterior edge of the tangential fields)¹⁵, multidimensional assessment of the presence of the heart in contact with the chest wall¹⁴ and linear heart contact distance from the left sternal to the beginning of the lung parenchyma edges at the 4th costal arch in the axial axis.¹⁶ It has also been shown that the shape and size of the clinical target volume (CTV) result in increased mean and/or maximum point heart doses.^{9,17,18} If a cohort of breast cancer patients with similar breast volume is defined, specific problems and resolutions can be proposed, because breast contours according to breast size and shape may be associated with the variations in the target volume coverage and calculated dose to organs at risk.¹⁹ Three-dimensional treatment planning allows target volume to be measured and CTVs of $\leq 500\text{--}975\text{ cm}^3$, $975\text{--}1.600\text{ cm}^3$ and $\geq 1.600\text{ cm}^3$ have been typically, but not consistently, defined as small, medium and large breasts, respectively.^{20,21} Additionally, quite a few clinical studies have reported a comparison of the clinical adverse events in regard to the three groups of breast sizes.²²

Although observed average MWHD in a population of breast cancer survivors is low, smaller fragments of the heart might have received doses exceeding 25–40 Gy.^{4,10,23,24} Subclinical cardiac dysfunction was observed early after adjuvant radiotherapy for breast cancer with molecular biomarkers^{25,26}, radionuclide myocardial perfusion imaging²⁷⁻²⁹, echocardiography³⁰⁻³², and functional magnetic resonance imaging.³¹ Limited data exist regarding the range of doses received by individual heart substructures with adjuvant free-breathing 3D-CRT or tangential intensity modulated radiotherapy (t-IMRT) for left-sided breast cancer. It has been shown that MWHD does not necessarily correlate to mean radiation doses, absorbed by cardiac

chambers or coronary arteries in adjuvant breast cancer radiotherapy.³³⁻³⁶ Lately, detailed studies of the specific cardiac structures' absorbed radiation dose in thoracic radiation therapy^{24,36,37}, and the efforts to understand the specific radiation dose-volume effects in the heart have emerged.^{4,38-41} With expanding knowledge in this field, German Society of Radiation Oncology (DEGRO) recommends new stringent dose constraints for the heart and its substructures: MWHD $< 2.5\text{ Gy}$, left ventricle (LV) $D_{\text{mean}} < 3\text{ Gy}$ (LV mean dose), LV $V_5 < 17\%$ (volume of LV receiving $\leq 5\text{ Gy}$), LV $V_{23} < 5\%$ (volume of LV receiving $\leq 23\text{ Gy}$), left anterior descending coronary (LADCA) $D_{\text{mean}} < 10\text{ Gy}$ (LADCA mean dose), LADCA $V_{30} < 2\%$ (volume of LADCA receiving $\leq 30\text{ Gy}$), and LADCA $V_{40} < 1\%$ (volume of LADCA receiving $\leq 40\text{ Gy}$).⁴²

To standardize the reporting of cardiac imaging regardless of diagnostic modality, both The American Society of Echocardiography and the European Association of Cardiovascular Imaging recommend using a segmentation model of the LV to assess regional LV function.^{42,44} The LV segmentation model reflects coronary arteries' territories and permits to compare echocardiography with other imaging modalities.⁴³ Five main LV segments, defined in a cardiac atlas by Duane *et al.*²⁴ are based on a previously described 17-segmentation model.⁴⁴

In this work, we hypothesized that in the setting of the node-negative left-sided breast cancer adjuvant radiotherapy, the lowest median MWHD and doses to the cardiac substructures would be achieved with the t-IMRT, compared to 3D-CRT. In addition, we assumed that individual patient characteristics, which include chest wall separation and breast volume, would contribute to the differences in absorbed doses to the heart and cardiac substructures, regardless of the treatment planning technique. To test our hypothesis, we aimed to quantify doses to the heart and cardiac substructures in present-day free-breathing adjuvant 3D-CRT and t-IMRT and to analyze the differences in dosimetric metrics to organs at risk between three different groups of CTV according to breast size and other individual anatomical information.

Patients and methods

Patient selection and CT simulation

The study was approved by the ethics review board committee (approval number KME 78/07/15). Based on the size of the CTV, we randomly selected

TABLE 1. Target goals used in the planning process

Structure	Target goals
PTV	$D_2\% < 108\%$
PTVeval	$V_{95\%} > 95\%$
Whole Body Contour	Global $D_{max} < V110\%$
Heart	$D_{mean} < 3.2 \text{ Gy}$ $V_{17 \text{ Gy}} < 10\%$ $V_{35 \text{ Gy}} < 5\%$
Ipsilateral Lung	$D_{mean} < 10 \text{ Gy}$ $V_{17 \text{ Gy}} < 25\%$ $V_{26 \text{ Gy}} < 20\%$
Bilateral lung	$D_{mean} < 3.2 \text{ Gy}$

D_{max} = maximum dose; D_{mean} = mean dose; $D_x\%$ = absorbed dose, received by x % of the PTV; PTV = planning target volume; PTVeval = planning target volume for evaluation; $V_x\%$ = fractional volume, receiving x % of the prescribed dose; $V_x \text{ Gy}$ = fractional volume receiving x Gy

patients with early left-sided node-negative breast cancer. The definitions of the small, medium, and large breast volumes were like those made available elsewhere.²² The patients were referred to adjuvant radiotherapy between the years 2014 and 2015. All patients underwent a free-breathing non-enhanced simulation computed tomography (CT) scan with a 3 mm slice thickness. The treatment position for all women was supine, on an inclined simulation table using a breast board, with both arms positioned above the head.

Delineation, treatment planning, and data collection

Whole heart, LV with its anterior, apical, inferior, lateral, and septal walls, right ventricle (RV), left atrium (LA), right atrium (RA), LADCA with proximal, middle and distal segments, right coronary artery (RCA), left circumflex coronary artery (LCX), and left main coronary artery (LMCA) were delineated by one radiation oncologist. We followed identification of the individual structure segments by the instructions proposed by Duane *et al.*²⁴ in a recently published heart atlas. We used a 6 mm diameter for all coronary arteries' segments, as previously proposed.²³ The thickness of the LV wall was set to 10 mm. An experienced cardiac radiologist reviewed the contoured cardiac segments. We delineated CTV to include total glandular breast tissue according to published guidelines.⁴⁵ Planning target volume (PTV) was generated by adding a 5 mm uniform margin to the CTV, and the planning target volume for evaluation (PTVeval) was created similarly, with a modification that excludes 5 mm

below the skin surface. Additionally, we collected anatomically based distance metrics, such as chest wall separation (CWS) and a previously described "4th arch" metric.¹⁶

We used Monaco (Elekta AB®, Stockholm, Sweden) as a contouring and treatment planning platform. The prescribed dose was 42.72 Gy in 16 fractions, 5 days per week. For the 3D-CRT treatment planning, we used 6MV photon tangential beam arrangement with wedge filters and additional 6MV or 15MV small beams in tangential or non-tangential beam direction where needed to achieve a homogeneous dose distribution. The "Collapsed Cone" algorithm was used to calculate the dose. For t-IMRT plans we used the same isocenter position as with 3D-CRT planning and two tangential 6 MV photon beams positioned in the same direction as for 3D-CRT plans. The plans were calculated using inverse dose optimization with "Monte-Carlo" algorithm. Dynamic Multileaf Collimator (dMLC) technique was used with minimum segment size 1 cm and 30 control points, which generated 25–30 segments per beam. Although "the dose-to-water" reporting is typically used in clinical routine for the inverse optimization treatment plans and since "Collapsed Cone" algorithm does not have that option for calculation, we used "the dose-to-medium" reporting in our study for both 3D-CRT and t-IMRT planning in order to improve treatment plan comparability.

In the planning optimization procedure, we used institutional target goals for both treatment plans (Table 1). Dose constraints for the specific cardiac substructures were not incorporated into the optimization process but we strived to keep the dose to the whole heart as low as possible without compromising the target coverage for both techniques. Each plan was thoroughly evaluated for target coverage and OAR. We reported nominal median absolute doses, without EQD₂ (equivalent dose in 2 Gy per fraction) conversion. All treatment plans were created by one dosimetrist and one medical physicist.

Statistical analyses

Calculated dose distributions were compared amongst the two techniques and the three different groups of CTV. Due to mostly non-parametrically distributed data, dose distributions data between the groups were compared using the Kruskal-Wallis and Mann-Whitney tests. Friedman ANOVA and Wilcoxon signed-rank test were also used to compare values between the two techniques. All

TABLE 2. Target volumes' and organs at risk's metrics

Target volume/ Organ at risk	The whole group N = 60	Small CTV N = 22	Medium CTV N = 21	Large CTV N = 17	p value
CTV [cm ³]	800.6 (124.8–2970.9)	425.7 (124.8–545.5)	867.0 (652.1–1295.1)	1586.8 (1348.9–2970.9)	0.021
PTVeval [cm ³]	990.7 (233.5–3336.1)	583.0 (233.5–711.1)	1035.9 (834.3–1576.5)	1874.3 (1605.8–3336.1)	< 0.005
PTV [cm ³]	1163.3 (340.1–3792.2)	730.7 (340.1–856.6)	1212.3 (985.1–1805)	2134.8 (1826.4–3792.2)	< 0.005
CWS [cm]	23.1 (17.9–33.2)	19.5 (17.9–23.2)	24.0 (19.9–28.5)	27.5 (22.9–33.2)	< 0.005
4 th arch metrics [cm]	4.4 (0–11.6)	1.6 (0–9.6)	5.5 (0–11.6)	7.1 (0–10.7)	0.008
Heart [cm ³]	677.7 (432.9–1192.7)	625.2 (432.9–912.8)	671.1 (563.5–872.4)	817.9 (620.1–1192.7)	< 0.005
Left Ventricle [cm ³]	173.8 (116–277.4)	161.3 (116–251.7)	173.8 (120.8–229.8)	188.7 (147.4–277.4)	0.018
Left Lung [cm ³]	1245.1 (809.3–2127.9)	1458.9 (824.5–2127.9)	1123.8 (944.2–1619.2)	1230.6 (809.3–1541.7)	0.003
Right Lung [cm ³]	1563.4 (855–2560.1)	1721.9 (992.9–2560.1)	1466.4 (855.1–1838.2)	1493.2 (1089.6–1925.6)	0.002
Lungs [cm ³]	2879.7 (1504.6–4789.2)	3241.3 (1877.5–4789.2)	2634.4 (1504.6–3513.6)	2799.8 (1960.2–3479.2)	0.001

CTV = clinical target volume; CWS = chest wall separation distance at isocenter; PTV = planning target volume; PTVeval = planning target volume for evaluation

numbers are presented as median values with a range. Statistical analyses were performed with IBM® SPSS® version 24.0 (SPSS Inc., Armonk: NY, IBM corporation). We considered a p-value ≤ 0.05 as statistically significant.

Results

Patient population and treatment plans

Sixty patients with left-sided breast cancer were included in this analysis, divided into groups of small (N = 22, 36.6%), medium (N = 21, 35.0%) and large (N = 17, 28.4%) CTV size. Target volumes' and OAR's metrics are presented in Table 2.

There was a statistically significant difference between the three groups for all measured target volumes, OAR volumes, and anatomically based simple distance metrics. Regarding target coverage, all except two dosimetric parameters (PTVeval V₁₀₇%, PTVeval D₂%), were superior in the 3D-CRT group (Tables 3 and 4). Nevertheless, the t-IMRT approach resulted in lower high-dose areas (PTVeval V₁₀₅%) across all three CTV groups.

Whole heart

For the whole group of evaluated patients, 3D-CRT technique showed significant lower MWHD compared to t-IMRT (Table 5) with an absolute difference of 0.2 Gy.

Absolute difference in MWHD between the two techniques ranged from 0.06, 0.46 and 0.7 for the groups of medium-, large- and small-sized CTVs, respectively (Table 6). CTV size had an impact on

MWHD regardless of the RT technique, while other parameters were not statistically different except for heart-V₅ Gy in 3D-CRT technique. In 3D-CRT, MWHD correlated with increased CWS relative to 18.0 cm (0.09 Gy/1 cm, p = 0.0022) and with CTV size (0.06 Gy/100 cm³, p = 0.0015). Low MWHD values (< 2.5 Gy) were achieved in 44 (73.3%) and 41 (68.3%) patients for 3D-CRT and t-IMRT techniques, correspondingly (Figure 1).

Heart chambers

Selected dose-volume parameters for the LV are presented in Table 5 and 6. For the whole group, 3D-CRT showed lower dosimetric metrics for the

TABLE 3. Target volume dosimetric metrics

Target volume	3D-CRT	t-IMRT	p value
PTVeval D ₉₈ % [Gy]	40.6 (39.8–41.4)	40.3 (38.7–41.6)	0.002
PTVeval D ₂ % [Gy]	44.7 (44.4–45.5)	43.8 (43.8–47.1)	NS
PTVeval D ₅₀ % [Gy]	43.3 (42.7–43.7)	42.9 (42.2–43.9)	< 0.005
PTVeval V ₉₅ % [%]	98.1 (95.3–99.6)	96.8 (79.9–99.9)	0.001
PTVeval V ₁₀₅ % [%]	1.3 (0.1–10.3)	4.3 (0.01–85.9)	< 0.005
PTVeval V ₁₀₅ % [cm ³]	11.7 (0.08–656.7)	5.4 (0.06–68.0)	0.014
PTVeval V ₁₀₇ % [%]	0 (0–1.4)	0.1 (0–9.6)	< 0.005
PTVeval V ₁₀₇ % [cm ³]	0 (0–321.4)	0 (0–7.2)	NS
PTVeval V ₁₁₀ % [%]	0 (0–0)	0 (0–0)	NS
D _{max} [Gy]	45.7 (45.1–46.9)	46.9 (45.3–51)	< 0.005

3D-CRT = three-dimensional conformal radiotherapy; D₂% = near maximum dose, D₅₀% = median dose; D₉₈% = near minimum dose, D_{max} = maximal absorbed dose, NS = not significant; PTVeval = planning target volume for evaluation; t-IMRT = tangential intensity modulated radiation therapy; V_x% = fractional volume, receiving x % of the prescribed dose

TABLE 4. Target volume dosimetric metrics and CTV size

Target volume	Small CTV	Medium CTV	Large CTV	p value (S vs. M vs. L)
3D-CRT PTVeval V _{95%} [%]	97.7 (95.3–99.6)	98.3 (96.2–99.5)	98.8 (97.5–99.4)	0.022 (S vs. M, S vs. L)
t-IMRT PTVeval V _{95%} [%]	97.9 (96.3–99.2)	97.3 (95.3–99.0)	96.8 (79.9–99.9)	NS
p value (3D-CRT vs. T-IMRT)	NS	p = 0.003	p = 0.013	
3D-CRT PTVeval V _{105%} [cm ³]	8.1 (0.5–17.5)	12.5 (0.08–91.3)	87.3 (9.5–656.6)	< 0.005 (S vs. M, S vs. L, M vs. L)
t-IMRT PTVeval V _{105%} [cm ³]	7.4 (0.1–61.5)	5.9 (0.09–54)	4.2 (0.06–68.2)	NS
p value (3D-CRT vs. T-IMRT)	NS	NS	p = 0.012	

3D-CRT = three-dimensional conformal radiotherapy; L = large; M = medium; NS = not significant; PTVeval = planning target volume for evaluation; S = small; t-IMRT = tangential intensity modulated radiation therapy; V_{x%} = fractional volume, receiving x % of the prescribed dose

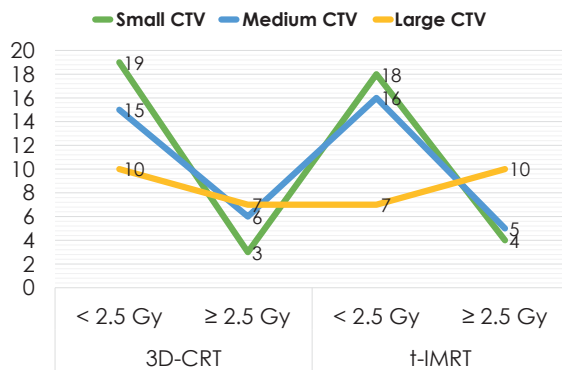


FIGURE 1. Mean whole heart dose and number of plans within each CTV groups, concerning optimal mean dose value.

3D-CRT = three-dimensional conformal radiotherapy; CTV = clinical target volume; Gy = Gray; t-IMRT = tangential intensity modulated radiation therapy

TABLE 5. Radiotherapy technique and selected dose-volume parameters for the whole heart and selected cardiac substructures

Parameter	3D-CRT	t-IMRT	p value*
MWHD [Gy]	1.90 (0.61–4.14)	2.13 (1.06–4.4)	< 0.005
LV-D _{mean} [Gy]	2.98 (0.78–8.03)	3.22 (1.31–7.25)	< 0.005
LV-V ₅ Gy [%]	8.67 (0–26.3)	9.21 (0–26.02)	0.455
LV-V ₂₃ Gy [%]	2.46 (0–14.32)	1.86 (0–10.58)	0.003
LV anterior-D _{mean} [Gy]	5.00 (1.27–20.17)	5.42 (1.94–19.18)	< 0.005
LV apical-D _{mean} [Gy]	8.97 (1.22–24.89)	8.47 (1.64–22.16)	< 0.005
LADCA-D _{mean} [Gy]	8.20 (1.23–27.92)	8.39 (1.8–27.62)	< 0.005
LADCA-V ₃₀ Gy [%]	5.39 (0–66.34)	2.01 (0–84.20)	< 0.005
LADCA-V ₄₀ Gy [%]	0 (0–37.8)	0 (0–43.09)	< 0.005
LADCA-prox-D _{mean} [Gy]	2.17 (0.62–8.68)	2.66 (1.22–12.43)	< 0.005
LADCA-mid-D _{mean} [Gy]	9.63 (1.67–40.07)	11.05 (2.26–39.63)	0.956
LADCA-dist-D _{mean} [Gy]	13.73 (1.44–41.11)	15.93 (2.03–3.89)	0.132

*Wilcoxon signed-rank test; 3D-CRT = three-dimensional conformal radiotherapy; dist = distal; D_{mean} = mean dose; Gy = Gray; LADCA = left anterior descending artery; LV = left ventricle; mid = middle; MWHD = whole heart mean dose; prox = proximal; t-IMRT = tangential intensity modulated radiation therapy; V_x Gy = fractional volume receiving x Gy

LV contour, except for LV apical-D_{mean} and LV-V₂₃ Gy. The lowest D_{mean} values of the dosimetric metrics for LV, including anterior, lateral, septal, and inferior LV wall, were obtained in the small CTV group, regardless of treatment technique.

In 3D-CRT, apical and anterior LV walls received the highest D_{mean} (Table 5), while lateral, septal, and inferior regions, received 1.9, 1.6, and only 0.6 Gy, respectively. The D_{mean} of RV, RA, and LA were 1.41 Gy (range, 0.5–4.8), 0.5 Gy (0.3–1.2), and 0.6 Gy (0.4–1.5), respectively and were not statistically significantly different among different groups of the CTV size. Likewise, with IMRT, apical and anterior LV walls received similarly high mean radiation doses. The D_{mean} varied from 8.5 Gy (range, 1.64–22.16), 5.4 Gy (1.94–19.18), 2.33 Gy (1.18–7.59), 2.18 Gy (1.01–4.46), and 1.11 Gy (0.77–1.98) for apical, anterior, lateral, septal and inferior LV walls, correspondingly. Seventeen-segmental LV models, represented as a Bull's eye diagram, with respective D_{mean} dose distributions, are presented in Figure 2. Low LV-D_{mean} (< 3 Gy), LV-V₅ (< 17%), and LV-V₂₃ (< 5%) values were achieved in 51.6%, 88.3%, and 73.3% of treatment plans in 3D-CRT and in 41.6%, 88.3%, and 85.0% of treatment plans in t-IMRT, respectively.

Coronary arteries

Planned median D_{mean} values for LADCA and its segments are presented in Table 5. Median mean doses to other coronary arteries, namely RCA, LCX, and LMCA were 0.7 Gy (range, 0.3–4.7), 0.7 Gy (0.3–2.0), and 0.8 Gy (0.5–2.0), in the 3D-CRT group and 1.14 Gy (0.77–1.86), 1.10 Gy (0.79–2.18) and 1.31 Gy (0.96–2.17) in the t-IMRT group, respectively. For the entire group, only parameter LADCA-V₃₀ Gy was found to be lower with t-IMRT compared to 3D-CRT technique, but the reduction

was seen only in the medium and large CTV-size groups.

Compared to t-IMRT, 3D-CRT technique showed advantages in terms of lower planned D_{mean} values of proximal, middle and distal LADCA segments (Table 5). However, dose to the proximal LADCA segment increased with the CTV size, regardless of the planning method. The highest D_{mean} values of the middle and distal LADCA segments were achieved in patients with the medium or large target volumes.

Low LADCA- D_{mean} (< 10 Gy), LADCA- V_{30} (< 2%), and LADCA- V_{30} Gy (< 1%) values were achieved in 55.0%, 48.3%, and 71.6% of treatment plans in 3D-CRT and in 56.6%, 51.6%, and 86.6% of treatment plans in t-IMRT, respectively. Figure 2 represents Bull's eye diagrams of the LV and segment models of the coronary arteries with reported median D_{mean} distributions for 3D-CRT technique.

Discussion

By tradition and its contouring pragmatism, MWHd is the most frequently reported surrogate for the assessment of the potential subsequent cardiotoxic effects after radiation therapy for breast cancer. In the present study, we aimed to compare doses to the individual cardiac structures in the circumstances that represent everyday practice in free-breathing node-negative left-sided breast cancer adjuvant 3D-CRT or t-IMRT. Herein, we report reasonably low median MWHd values achieved with both techniques, 1.9 Gy with 3D-CRT and 2.1 Gy with t-IMRT. In the contemporary series, measured mean or median MWHd values in free-breathing node-negative left-sided breast cancer adjuvant RT are in the range of 2.6–3.6 Gy for 3D-CRT^{6,33,35,36} and 1.8–4.8 for the intensity modulated techniques.^{11,46,47}

In both evaluated techniques, we observed statistically significant differences between the groups of small, medium, and large CTV sizes for the following dose-volume parameters: MWHd, mean doses for proximal LADCA segment, anterior, lateral, inferior, and septal LV walls. In medium and large-sized CTV, we observed reduction of LADCA- D_{mean} with t-IMRT technique, which was not statistically different. Our results are consistent with previously published studies showing increased CWS, relative to 22 cm, to be one of the predictors for a higher MWHd, in both normo- and hypofractionation.⁹ Other studies have also demonstrated the correlation between the calcu-

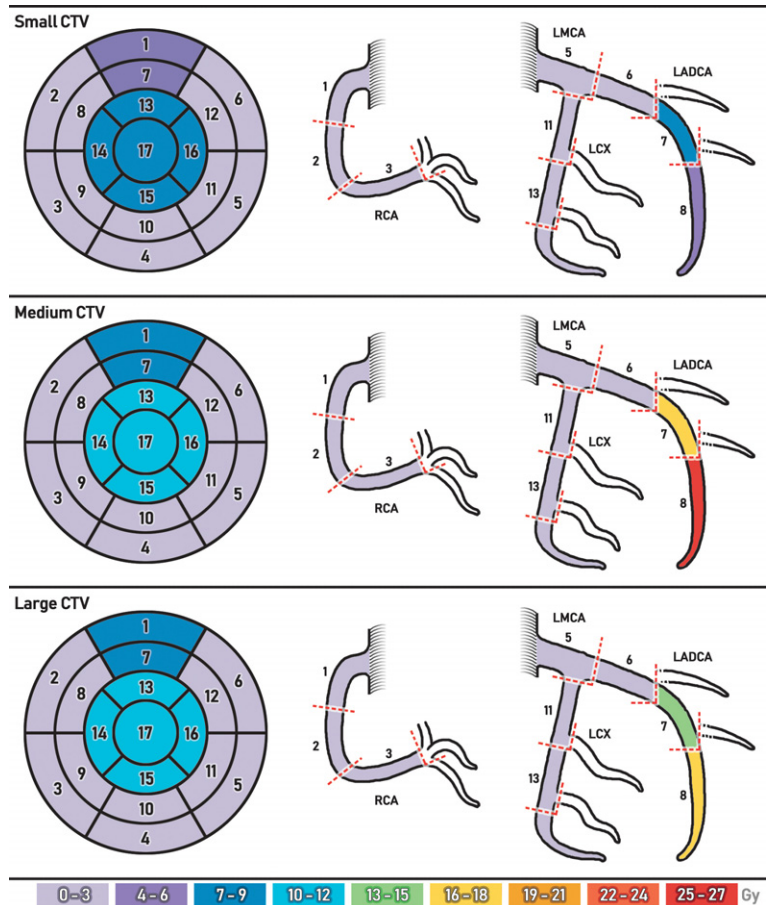


FIGURE 2. Bull's eye diagrams of the left ventricle and segment models of the coronary arteries with reported median D_{mean} distributions in three-dimensional conformal radiotherapy plans, divided in groups according to clinical target volume size. Contouring segments of left ventricle consisted of anterior (segments 1 and 7), apical (segments 13–17), inferior (segments 4 and 10), lateral (segments 5, 6, 11, 12) and septal regions (segments 2, 3, 8, 9).

CTV = clinical target volume; Gy = Gray; LADCA = left anterior descending artery; LCX = left circumflex artery; LMCA = left main coronary artery; RCA = right coronary artery

lated heart dose and increasing breast size, especially when PTV exceeds 1500 cm³.^{17,18} Compared to small-sized CTV, MWHd increased with medium- and large- sized CTVs in our study, although the absolute differences between the groups were relatively small, ranging from 0.73 Gy and 0.97 Gy for the t-IMRT and 3D-CRT, respectively. Our results imply that patients' anatomy, including CWS and/or CTV/PTV volume, should be also considered when choosing the appropriate radiotherapy technique (3D-CRT *vs.* modulated approaches), patient setup (prone or lateral *vs.* supine), and breathing adaptation techniques. As previously mentioned, breast size grouping could be useful in this context, helping to tailor whole breast irradiation.¹⁹

TABLE 6. Breast size and selected dose-volume parameters for the whole heart and cardiac substructures

Parameter	Small CTV		Medium CTV		Large CTV		p value
	3D-CRT	t-IMRT	3D-CRT	t-IMRT	3D-CRT	t-IMRT	
MWHD [Gy]	1.29 (0.61–3.75)	1.99 (1.06–3.98)	2.05 (1.06–3.84)	2.11 (1.62–3.54)	2.26 (1.04–4.14)	2.72 (1.46–4.4)	< 0.005*; 0.047†
Heart-V ₅ Gy [%]	2.56 (0.02–10.84)	3.77 (0.1–11.01)	4.99 (0.59–10.87)	4.34 (1.19–9.58)	5.29 (0–12.81)	6.19 (0.04–12.83)	0.043*
Heart-V ₁₀ Gy [%]	1.28 (0–7.91)	2.01 (0–7.59)	2.71 (0.01–7.73)	2.24 (0.12–68.14)	3.09 (0–8.24)	3.17 (0–8.54)	NS
Heart-V ₁₇ Gy [%]	0.76 (0–6.61)	1.22 (0–6.08)	2.03 (0–6.52)	1.36 (0–4.79)	2.37 (0–6.92)	3.36 (0–6.42)	NS
Heart-V ₂₀ Gy [%]	0.62 (0–6.22)	1 (0–5.63)	1.83 (0–6.16)	1.17 (0–4.38)	2.15 (0–6.51)	2.01 (0–5.81)	NS
Heart-V ₃₅ Gy [%]	0.15 (0–4.12)	0.2 (0–3.4)	0.93 (0–4.15)	0.31 (0–2.3)	1.06 (0–4.32)	0.63 (0–2.91)	NS
Heart-V ₄₀ Gy [%]	0.02 (0–1.41)	0.01 (0–1.65)	0.24 (0–1.45)	0.03 (0–0.42)	0.03 (0–1.93)	0.04 (0–1.69)	NS
LV-D _{mean} [Gy]	2.3 (0.7–5.7)	2.9 (1.31–5.84)	3.2 (1.1–6.9)	3.15 (1.78–5.97)	3.5 (1.3–8.0)	3.92 (1.83–7.25)	0.019*
LV-V ₅ Gy [%]	6.8 (0–17.4)	8.27 (0–17.39)	9.7 (0–22.0)	8.47 (0.46–19.87)	10.8 (0–26.3)	12 (0–26.02)	0.052*
LV-V ₂₅ Gy [%]	1.4 (0–9.5)	1.73 (0–8.47)	2.8 (0–12.0)	1.81 (0–8.18)	3.3 (0–14.3)	3.1 (0–10.58)	NS
LV anterior-D _{mean} [Gy]	3.6 (1.2–12.8)	4.86 (1.94–12.35)	6.8 (2.0–15.9)	5.71 (2.69–14.48)	6.8 (1.9–20.1)	6.94 (2.58–19.18)	0.017*
LV lateral-D _{mean} [Gy]	1.6 (0.7–2.8)	2.16 (1.18–3.38)	1.8 (0.9–6.3)	2.24 (1.55–5.12)	2.5 (1.2–8.7)	2.98 (1.73–7.59)	< 0.001*, < 0.001†
LV inferior-D _{mean} [Gy]	0.5 (0.3–3.3)	0.96 (0.77–1.17)	0.6 (0.5–0.9)	1.07 (0.9–1.32)	0.8 (0.6–2.0)	1.33 (0.96–1.98)	< 0.005*, < 0.005†
LV septal-D _{mean} [Gy]	1.2 (0.4–3.4)	1.8 (1.01–3.71)	1.6 (1.1–3.4)	2.19 (1.77–3.74)	1.9 (1.2–3.9)	2.56 (1.72–4.46)	< 0.005*, < 0.005†
LV apical-D _{mean} [Gy]	6.9 (1.2–19.6)	8.54 (1.64–19.79)	9.0 (1.7–21.9)	8.42 (2.46–19.68)	9.5 (1.2–24.8)	8.91 (1.76–22.16)	NS
LADCA-D _{mean} [Gy]	5.2 (1.2–27.9)	6.84 (1.8–27.62)	13.8 (2.6–25.2)	10.76 (3.01–20.73)	11.1 (2.2–21.2)	8.24 (2.84–21.22)	NS
LADCA-V ₃₀ Gy [%]	0.2 (0–66.3)	0.36 (0–63.48)	17.8 (0–59.0)	7.39 (0–84.2)	8.9 (0–43.3)	2.13 (0–46.34)	NS
LADCA-V ₄₀ Gy [%]	0 (0–37.8)	0 (0–43.09)	0.5 (0–32.9)	0 (0–3.22)	0 (0–19.2)	0 (0–7.26)	NS
LADCA-prox-D _{mean} [Gy]	1.6 (0.6–8.6)	2.22 (1.22–7.95)	2.9 (0.6–7.2)	2.96 (1.96–5.19)	2.5 (1.4–7.2)	2.84 (2.07–12.43)	< 0.001*, 0.002†
LADCA-mid-D _{mean} [Gy]	7.9 (1.6–40.0)	9.12 (2.26–39.63)	17.9 (2.0–38.7)	13.81 (4.22–30.95)	10.4 (2.5–29.8)	11.14 (3.23–36.01)	NS
LADCA-dist-D _{mean} [Gy]	5.5 (1.4–41.1)	8.58 (2.03–40.65)	26.9 (3.5–39.4)	17.46 (3.98–35.39)	14.0 (2.4–39.7)	16.32 (2.87–34.95)	NS

*intergroup comparison within 3D-CRT technique, using Kruskal-Wallis test; † intergroup comparison within t-IMRT technique using Kruskal-Wallis test; 3D-CRT = three-dimensional conformal radiotherapy; CTV = clinical target volume; D_{mean} = mean dose; dist = distal; Gy = Gray; LADCA = left anterior descending artery; LV = left ventricle; mid = middle; MWHD = whole heart mean dose; NS = not significant; prox = proximal; t-IMRT = tangential intensity modulated radiation therapy; V_x Gy = fractional volume receiving x Gy

Despite the low MWHD for the whole group, our study confirms that apical and anterior parts of LV and mid or distal LADCA segments in both 3D-CRT and t-IMRT techniques receive disproportionately higher D_{mean} radiation doses. Likewise, in the study by Tang *et al.*, segments corresponding to anterior and apical LV wall absorbed the highest doses, 9.2 Gy and 14.9 Gy, respectively. Patients were treated with tangential breast RT, with or without regional nodal irradiation and with or without DIBH.³⁶ Corresponding values in our study were lower in both evaluated techniques, 3D-CRT *vs.* t-IMRT for anterior and apical LV walls were 5.0 *vs.* 5.4 Gy and 8.5 *vs.* 8.9 Gy, respectively. Lower numbers might reflect a difference in contoured thickness of the LV wall, 6–9 mm in the study of Tang *et al.* compared to 10 mm used in our study, as suggested by Duane *et al.*²⁴

In our work, the LADCA-D_{mean} was 8.2 Gy (range, 1.2–27.9) in 3D-CRT and 8.4 Gy (range, 1.8–27.6) in t-IMRT, respectively. Drost *et al.* in their systematic review of heart doses reported varying dose-volume measurements for the LADCA. The LADCA-D_{mean} ranged from 1.9–40.8 Gy (average 12.4 Gy)⁶, which is similar to our data. In our series of treatment plans, we have demonstrated the highest D_{mean} for the middle LADCA segment in the group of women with medium-sized CTVs (17.9 Gy) but was not significantly different compared to the smallest or the largest CTV groups. With t-IMRT, it was possible to lower LADCA high-dose areas (V₃₀ Gy), but not low-dose areas or mean doses to the coronary arteries. Carosi *et al.* observed no difference in MWHD when t-IMRT was compared to 3D-CRT (2.0 *vs.* 1.9 Gy) in 24 patients with a median breast volume of 645 cm³.

However, the authors showed a statistically meaningful difference in LADCA D_{mean} (10.3 vs. 11.9 Gy, $p=0.0003$), LADCA- D_{max} and LADCA- V_{17} Gy parameters using t-IMRT compared to 3D-CRT.⁴⁸

There are many possible explanations for the dissimilar reported heart and heart substructures' absorbed doses in free-breathing left-breast only RT. The differences may arise from the discrepancy in the total dose prescription and the size of the radiation field, CTV definition and size, OAR contouring, including diameter of the coronary arteries and LV thickness, the lack of detailed heart contouring atlases, individual coronary topology, heart size, body mass index, CWS distance, and finally radiotherapy technique used.^{9,33,49-52} The use of contrast agent⁵³ or automatic substructures' segmentation without⁵⁴ or with cardiac magnetic resonance imaging⁵⁵ could improve contouring consistency, but these technical solutions are unlikely to be widely adopted in the near future. Non-automatic contouring is feasible as showed in a study by Francolini *et al.* Authors made multiple comparisons of delineated cardiac chambers and 5 left LV wall segments according to aforementioned cardiac atlas²⁴ and confirmed high interobserver delineation consistency.⁵⁶

Spatial variation in contouring has been shown to result in less than 1 Gy dose variation for most segments and in most regimens in adjuvant breast cancer RT, but higher dose variations up to 21.8 Gy were seen for segments close to the radiation field edge.²⁴ Substantial variation in the estimated dose was observed for LADCA, regardless of which particular delineation guidelines were used.⁵⁷ Except for proximal LADCA (2.6 Gy vs. 2.5 Gy), absorbed mean D_{mean} values of LADCA segments and LV were lower in our study compared to the partially wide tangential technique used in Duane and co-workers' research; 15.1 Gy vs. 25.1 Gy for middle LADCA segment, 17.6 Gy vs. 35.8 Gy for distal LADCA segment, and 3.2 vs. 6.7 Gy for LV. In the study of Wennstig *et al.*, three radiation oncologists, using the heart atlas of Feng *et al.*, achieved substantial spatial agreement in delineating coronary arteries on 32 CT study sets. The agreement was the highest for LMCA and LADCA, and less for RCA.^{23,58} In our study, the coronary vessel diameter was set to 6 mm considering both cardiac and respiratory motion, similar to Wennstig and colleagues' work.²³

Based on recent clinical reports, the DEGRO group proposed stringent dose constraints for the heart and its substructures in adjuvant breast cancer radiation treatment.⁴² We surpassed at least one

of the proposed optimal dose constraints for LV ($D_{\text{mean}} < 3$ Gy, $V_5 < 17\%$, and $V_{23} < 5\%$) or LADCA ($D_{\text{mean}} < 10$ Gy, $V_{30} < 2\%$, and $V_{40} < 1\%$) in 11.7–51.7% of all evaluated plans. In our plan optimization process, we did not use specific dose-volume constraints for cardiac substructures. However, it has been shown that additional LADCA or LV constraints in breast cancer adjuvant 3D-CRT or IMRT treatment planning might help to optimize heart dosimetric metrics further.^{23,59}

In our study, the evaluation of the planned dose to the heart and specific cardiac substructures was performed in a free-breathing simulation CT scan and in the supine position. Ideally, the dose to cardiac substructures should also be evaluated for patients treated using alternative treatment positions (lateral decubitus or prone) or with DIBH. Due to various reasons, most patients are still treated in the conventional free-breathing supine position, whereas prone positioning or DIBH is in the best-case scenario offered to only 28–83% of breast cancer patients.^{15,60} All delineations were performed on a non-enhanced CT scan, an approach that may impact the visibility of the small cardiac segments. Additional drawback of our study is not including patients receiving peri-clavicular regional nodal irradiation with or without internal mammary lymph chain irradiation. Strengths of this study include careful contouring of individual cardiac substructures and using a cardiac atlas based on individual anatomy. An experienced cardiac radiologist thoroughly evaluated the contours.

Conclusions

This is the first study to evaluate the cardiac contouring atlas for radiotherapy by Duane *et al.*²⁴ simultaneously considering different CTV size. We confirmed that regardless of very low D_{mean} values for the whole heart achieved using a 3D-CRT or t-IMRT free-breathing adjuvant RT technique for breast cancer, a small volume of the heart may receive disproportionate D_{mean} or D_{max} values exceeding 40 Gy. We observed differences in heart dosimetric metrics between the small, medium, and large CTV sizes for both evaluated techniques, which may disappear with DIBH technique. With t-IMRT technique, only few dosimetric metrics were improved compared to 3D-CRT. The observed results in our study suggest that anatomic differences, especially breast volume and CWS, should be considered in clinical practice as well as in the dosimetric studies of various treatment plan-

ning techniques. Subdividing breast target volume into similar cohorts could be helpful in this context and further research is warranted. The quantification of the radiation dose variability of individual cardiac substructures is an important first step to understand the unique cardiac structures' dose-volume predictors for cardiotoxicity in adjuvant, free-breathing breast cancer radiation therapy. In the future, reported absorbed doses may be paired with cardiac imaging and help to choose patients for whom more intense cardiac function monitoring is warranted.

References

- Abdel-Qadir H, Austin PC, Lee DS, Amir E, Tu J V, Thavendiranathan P, et al. A population-based study of cardiovascular mortality following early-stage breast cancer. *JAMA Cardiol* 2017; **2**: 88. doi: 10.1001/jamacardio.2016.3841
- Weberpals J, Jansen L, Müller OJ, Brenner H. Long-term heart-specific mortality among 347 476 breast cancer patients treated with radiotherapy or chemotherapy: a registry-based cohort study. *Eur Heart J* 2018; **39**: 3896-903. doi: 10.1093/eurheartj/ehy167
- Darby SC, Ewertz M, Hall P. Ischemic heart disease after breast cancer radiotherapy. *N Engl J Med* 2013; **368**: 2527. doi: 10.1056/NEJMc1304601
- van den Bogaard VAB, Ta BDP, van der Schaaf A, Bouma AB, Middag AMH, Bantema-Joppe EJ, et al. Validation and modification of a prediction model for acute cardiac events in patients with breast cancer treated with radiotherapy based on three-dimensional dose distributions to cardiac substructures. *J Clin Oncol* 2017; **35**: 1171-8; doi: 10.1200/JCO.2016.69.8480
- Saiki H, Petersen IA, Scott CG, Bailey KR, Dunlay SM, Finley RR, et al. Risk of heart failure with preserved ejection fraction in older women after contemporary radiotherapy for breast cancer. *Circulation* 2017; **135**: 1388-96. doi: 10.1161/CIRCULATIONAHA.116.025434
- Drost L, Yee C, Lam H, Zhang L, Wronski M, McCann C, et al. A systematic review of heart dose in breast radiotherapy. *Clin Breast Cancer* 2018; **18**: e819-24. doi: 10.1016/j.clbc.2018.05.010
- Taylor CW, Wang Z, Macaulay E, Jagi R, Duane F, Darby SC. Exposure of the heart in breast cancer radiation therapy: a systematic review of heart doses published during 2003 to 2013. *Int J Radiat Oncol Biol Phys* 2015; **93**: 845-53. doi: 10.1016/j.ijrobp.2015.07.2292
- Taylor C, Correa C, Duane FK, Aznar MC, Anderson SJ, Bergh J, et al. Estimating the risks of breast cancer radiotherapy: evidence from modern radiation doses to the lungs and heart and from previous randomized trials. *J Clin Oncol* 2017; **35**: 1641-9. doi: 10.1200/JCO.2016.72.0722
- Pierce LJ, Feng M, Griffith KA, Jagi R, Boike T, Dryden D, et al. Recent time trends and predictors of heart dose from breast radiation therapy in a large quality consortium of radiation oncology practices. *Int J Radiat Oncol* 2017; **99**: 1154-61. doi: 10.1016/j.ijrobp.2017.07.022
- Jacobse JN, Duane FK, Boekel NB, Schaapveld M, Hauptmann M, Hooning MJ, et al. Radiation dose-response for risk of myocardial infarction in breast cancer survivors. *Int J Radiat Oncol Biol Phys* 2018; **103**: 595-604. doi: 10.1016/j.ijrobp.2018.10.025
- Karpf D, Sakka M, Metzger M, Grabenbauer GG. Left breast irradiation with tangential intensity modulated radiotherapy (t-IMRT) versus tangential volumetric modulated arc therapy (t-VMAT): trade-offs between secondary cancer induction risk and optimal target coverage. *Radiat Oncol* 2019; **14**: 156. doi: 10.1186/s13014-019-1363-4
- Halasz LM, Patel SA, McDougall JA, Fedorenko C, Sun Q, Goulart BHL, et al. Intensity modulated radiation therapy following lumpectomy in early-stage breast cancer: patterns of use and cost consequences among Medicare beneficiaries. *PLoS One* 2019; **14**: e0222904. doi: 10.1371/journal.pone.0222904
- Jin G, Chen LX, Deng XW, Liu XW, Huang Y, Huang XB. A comparative dosimetric study for treating left-sided breast cancer for small breast size using five different radiotherapy techniques: conventional tangential field; filed-in-field; tangential-IMRT; multi-beam IMRT and VMAT. *Radiat Oncol* 2013; **8**: 89. doi: 10.1186/1748-717X-8-89
- Lee G, Rosewall T, Fyles A, Harnett N, Dinniwell RE. Anatomic features of interest in women at risk of cardiac exposure from whole breast radiotherapy. *Radiation Oncol* 2015; **115**: 355-60. doi: 10.1016/j.radonc.2015.05.002
- Desai N, Currey A, Kelly T, Bergom C. Nationwide trends in heart-sparing techniques utilized in radiation therapy for breast cancer. *Adv Radiat Oncol* 2019; **4**: 246-52. doi: 10.1016/j.adro.2019.01.001
- Mendez LC, Louie A V., Moreno C, Wronski M, Warner A, Leung E, et al. Evaluation of a new predictor of heart and left anterior descending artery dose in patients treated with adjuvant radiotherapy to the left breast. *Radiat Oncol* 2018; **13**: 124. doi: 10.1186/s13014-018-1069-z
- Guan H, Dong Y-L, Ding L-J, Zhang Z-C, Huang W, Liu C-X, et al. Morphological factors and cardiac doses in whole breast radiation for left-sided breast cancer. *Asian Pac J Cancer Prev* 2015; **16**: 2889-94. doi: 10.7314/ap-jcp.2015.16.7.2889
- Hannan R, Thompson RF, Chen Y, Bernstein K, Kabarriti R, Skinner W, et al. Hypofractionated whole-breast radiation therapy: does breast size matter? *Int J Radiat Oncol* 2012; **84**: 894-901. doi: 10.1016/j.ijrobp.2012.01.093
- Yang DS, Lee JA, Yoon WS, et al. Whole breast irradiation for small-sized breasts after conserving surgery: is the field-in-field technique optimal? *Breast Cancer* 2014; **21**: 162-9. doi: 10.1007/s12282-012-0365-y
- Vicini FA, Sharpe M, Kestin L, Martinez A, Mitchell CK, Wallace MF, et al. Optimizing breast cancer treatment efficacy with intensity-modulated radiotherapy. *Int J Radiat Oncol Biol Phys* 2002; **54**: 1336-44. doi: 10.1016/S0360-3016(02)03746-X
- Michalski A, Atyeo J, Cox J, Rinks M, Morgia M, Lamoury G. A dosimetric comparison of 3D-CRT, IMRT, and static tomotherapy with an SIB for large and small breast volumes. *Med Dosim* 2014; **39**: 163-8. doi: 10.1016/j.meddos.2013.12.003
- Ratosa I, Jenko A, Oblak I. Breast size impact on adjuvant radiotherapy adverse effects and dose parameters in treatment planning. *Radiol Oncol* 2018; **52**: 233-44. doi: 10.2478/raon-2018-0026
- Wennstig A-K, Garmo H, Hällström P, Nyström PW, Edlund P, Blomqvist C, et al. Inter-observer variation in delineating the coronary arteries as organs at risk. *Radiation Oncol* 2017; **122**: 72-8. doi: 10.1016/j.radonc.2016.11.007
- Duane F, Aznar MC, Bartlett F, Cutter DJ, Darby SC, Jagi R, et al. A cardiac contouring atlas for radiotherapy. *Radiation Oncol* 2017; **122**: 416-22. doi: 10.1016/j.radonc.2017.01.008
- Skyttä T, Tuohinen S, Boman E, Virtanen V, Raatikainen P, Kellokumpu-Lehtinen P-L. Troponin T-release associates with cardiac radiation doses during adjuvant left-sided breast cancer radiotherapy. *Radiat Oncol* 2015; **10**: 141. doi: 10.1186/s13014-015-0436-2
- D'Errico MP, Petruzzelli MF, Gianicolo EAL, Grimaldi L, Loliva F, Tramacere F, et al. Kinetics of B-type natriuretic peptide plasma levels in patients with left-sided breast cancer treated with radiation therapy: results after one-year follow-up. *Int J Radiat Biol* 2015; **91**: 804-9. doi: 10.3109/09553002.2015.1027421
- Kaidar-Person O, Zagar TM, Oldan JD, Matney J, Jones EL, Das S, et al. Early cardiac perfusion defects after left-sided radiation therapy for breast cancer: is there a volume response? *Breast Cancer Res Treat* 2017; **164**: 253-62. doi: 10.1007/s10549-017-4248-y
- Lind PA, Pagnanelli R, Marks LB, Borges-Neto S, Hu C, Zhou SM, et al. Myocardial perfusion changes in patients irradiated for left-sided breast cancer and correlation with coronary artery distribution. *Int J Radiat Oncol Biol Phys* 2003; **55**: 914-20. doi: 10.1016/s0360-3016(02)04156-1
- Zyromska A, Malkowski B, Wisniewski T, Majewska K, Reszke J, Makarewicz R. (15)O-H2O PET/CT as a tool for the quantitative assessment of early post-radiotherapy changes of heart perfusion in breast carcinoma patients. *Br J Radiol* 2018; **91**: 20170653. doi: 10.1259/bjr.20170653
- Tuohinen SS, Skyttä T, Virtanen V, Virtanen M, Luukkaala T, Kellokumpu-Lehtinen P-L, et al. Detection of radiotherapy-induced myocardial changes by ultrasound tissue characterisation in patients with breast cancer. *Int J Cardiovasc Imaging* 2016; **32**: 767-76. doi: 10.1007/s10554-016-0837-9

31. Heggemann F, Grotz H, Welzel G, Dösch C, Hansmann J, Kraus-Tiefenbacher U, et al. Cardiac function after multimodal breast cancer therapy assessed with functional magnetic resonance imaging and echocardiography imaging. *Int J Radiat Oncol Biol Phys* 2015; **93**: 836-44. doi: 10.1016/j.ijrobp.2015.07.2287
32. Erven K, Florian A, Slagmolen P, Sweldens C, Jurcut R, Wildiers H, et al. Subclinical cardiotoxicity detected by strain rate imaging up to 14 months after breast radiation therapy. *Int J Radiat Oncol* 2013; **85**: 1172-8. doi: 10.1016/j.ijrobp.2012.09.022
33. Jacob S, Camilleri J, Derreumaux S, Walker V, Lairez O, Lapeyre M, et al. Is mean heart dose a relevant surrogate parameter of left ventricle and coronary arteries exposure during breast cancer radiotherapy: a dosimetric evaluation based on individually-determined radiation dose (BACCARAT study). *Radiat Oncol* 2019; **14**: 29. doi: 10.1186/s13014-019-1234-z
34. Duma MN, Herr A-C, Borm KJ, Trott KR, Molls M, Oechsner M, et al. Tangential field radiotherapy for breast cancer—the dose to the heart and heart subvolumes: what structures must be contoured in future clinical trials? *Front Oncol* 2017; **7**: 130. doi: 10.3389/fonc.2017.00130
35. Becker-Schiebe M, Stockhammer M, Hoffmann W, Wetzel F, Franz H. Does mean heart dose sufficiently reflect coronary artery exposure in left-sided breast cancer radiotherapy? *Strahlenther Onkol* 2016; **192**: 624-31. doi: 10.1007/s00066-016-1011-y
36. Tang S, Otton J, Holloway L, Delaney GP, Liney G, George A, et al. Quantification of cardiac subvolume dosimetry using a 17 segment model of the left ventricle in breast cancer patients receiving tangential beam radiotherapy. *Radiother Oncol* 2019; **132**: 257-65. doi: 10.1016/j.radonc.2018.09.021
37. Tong Y, Yin Y, Cheng P, Lu J, Liu T, Chen J, et al. Quantification of variation in dose-volume parameters for the heart, pericardium and left ventricular myocardium during thoracic tumor radiotherapy. *J Radiat Res* 2018; **59**: 462-8. doi: 10.1093/jrr/rry026
38. Taylor C, McGale P, Brønnum D, Correa C, Cutter D, Duane FK, et al. Cardiac structure injury after radiotherapy for breast cancer: cross-sectional study with individual patient data. *J Clin Oncol* 2018; **36**: 2288-96. doi: 10.1200/JCO.2017.77.6351
39. Abouegylah M, Braunstein LZ, Alm El-Din MA, Niemierko A, Salama L, Elebrashi M, et al. Evaluation of radiation-induced cardiac toxicity in breast cancer patients treated with Trastuzumab-based chemotherapy. *Breast Cancer Res Treat* 2018; **174**: 179-85. doi: 10.1007/s10549-018-5053-y
40. Moignier A, Broggio D, Derreumaux S, Baudré A, Girinsky T, Paul J-F, et al. Coronary stenosis risk analysis following Hodgkin lymphoma radiotherapy: a study based on patient specific artery segments dose calculation. *Radiother Oncol* 2015; **117**: 467-72. doi: 10.1016/j.radonc.2015.07.043
41. Jacobse JN, Duane FK, Boekel NB, Schaapveld M, Hauptmann M, Hoening MJ, et al. Radiation dose-response for risk of myocardial infarction in breast cancer survivors. *Int J Radiat Oncol Biol Phys* 2019; **103**: 595-604. doi: 10.1016/j.ijrobp.2018.10.025
42. Piroth MD, Baumann R, Budach W, Dunst J, Feyrer P, Fietkau R, et al. Heart toxicity from breast cancer radiotherapy. *Strahlenther Onkol* 2019; **195**: 1-12. doi: 10.1007/s00066-018-1378-z
43. Lang RM, Badano LP, Mor-Avi V, Afialo J, Armstrong A, Ernande L, et al. Recommendations for cardiac chamber quantification by echocardiography in adults: an update from the American Society of Echocardiography and the European Association of Cardiovascular Imaging. *J Am Soc Echocardiogr* 2015; **28**: 1-39.e14. doi: 10.1016/j.echo.2014.10.003
44. Cerqueira MD, Weissman NJ, Dilsizian V, Jacobs AK, Kaul S, Laskey WK, et al. Standardized myocardial segmentation and nomenclature for tomographic imaging of the heart. A statement for healthcare professionals from the Cardiac Imaging Committee of the Council on Clinical Cardiology of the American Heart Association. *Circulation* 2002; **105**: 539-42. doi: 10.1161/hc0402.102975
45. Offersen B V, Boersma LJ, Kirkove C, Hol S, Aznar MC, Sola AB, et al. ESTRO consensus guideline on target volume delineation for elective radiation therapy of early stage breast cancer, version 1.1. *Radiother Oncol* 2015; **114**: 3-10. doi: 10.1016/j.radonc.2014.11.030
46. De Rose F, Fogliata A, Franceschini D, Iftode C, Torrissi R, Masci G, et al. Hypofractionated volumetric modulated arc therapy in ductal carcinoma in situ: toxicity and cosmetic outcome from a prospective series. *Br J Radiol* 2018; **91**: 20170634. doi: 10.1259/bjr.20170634
47. Fogliata A, De Rose F, Franceschini D, Stravato A, Seppälä J, Scorsetti M, et al. Critical appraisal of the risk of secondary cancer induction from breast radiation therapy with volumetric modulated arc therapy relative to 3D conformal therapy. *Int J Radiat Oncol Biol Phys* 2018; **100**: 785-93. doi: 10.1016/j.ijrobp.2017.10.040
48. Carosi A, Ingrosso G, Turturici I, Valeri S, Barbarino R, Di Murro L, et al. Whole breast external beam radiotherapy in elderly patients affected by left-sided early breast cancer: a dosimetric comparison between two simple free-breathing techniques. *Aging Clin Exp Res* 2020; **32**: 1335-41. doi: 10.1007/s40520-019-01312-5
49. Moignier A, Broggio D, Derreumaux S, El Baf F, Mandin A-M, Girinsky T, et al. Dependence of coronary 3-dimensional dose maps on coronary topologies and beam set in breast radiation therapy: a study based on CT angiographies. *Int J Radiat Oncol Biol Phys* 2014; **89**: 182-90. doi: 10.1016/j.ijrobp.2014.01.055
50. Mkanna A, Mohamad O, Ramia P, Thebian R, Makki M, Tamim H, et al. Predictors of cardiac sparing in deep inspiration breath-hold for patients with left sided breast cancer. *Front Oncol* 2018; **8**: 564. doi: 10.3389/fonc.2018.00564
51. Wollschläger D, Karle H, Stockinger M, Bartkowiak D, Bürhel S, Merzenich H, et al. Radiation dose distribution in functional heart regions from tangential breast cancer radiotherapy. *Radiother Oncol* 2016; **119**: 65-70. doi: 10.1016/j.radonc.2016.01.020
52. Appelt AL, Vogelius IR, Bentzen SM. Modern hypofractionation schedules for tangential whole breast irradiation decrease the fraction size-corrected dose to the heart. *Clin Oncol (R Coll Radiol)* 2013; **25**: 147-52. doi: 10.1016/j.clon.2012.07.012
53. Lee J, Hua K-L, Hsu S-M, Lin J-B, Lee C-H, Lu K-W, et al. Development of delineation for the left anterior descending coronary artery region in left breast cancer radiotherapy: an optimized organ at risk. *Radiother Oncol* 2017; **122**: 423-30. doi: 10.1016/j.radonc.2016.12.029
54. Van Dijk-Peters FB, Sijtsema NM, Kierkels RGJ, Vliegthart R, Langendijk JA, Maduro JH, et al. OC-0259: validation of a multi-atlas based auto-segmentation of the heart in breast cancer patients. *Radiother Oncol* 2015; **115**: S132-3. doi: 10.1016/S0167-8140(15)40257-9
55. Morris ED, Ghanem AI, Pantelic M V, Walker EM, Han X, Glide-Hurst CK. Cardiac substructure segmentation and dosimetry using a novel hybrid MR/CT cardiac atlas. *Int J Radiat Oncol Biol Phys* 2018; **103**: 985-93; doi: 10.1016/j.ijrobp.2018.11.025
56. Francolini G, Desideri I, Meattini I, Becherini C, Terziani F, Olmetto E, et al. Assessment of a guideline-based heart substructures delineation in left-sided breast cancer patients undergoing adjuvant radiotherapy: quality assessment within a randomized phase III trial testing a cardioprotective treatment strategy (SAFE-2014). *Strahlenther Onkol* 2019; **195**: 43-51. doi: 10.1007/s00066-018-1388-x
57. Lorenzen EL, Taylor CW, Maraldo M, Nielsen MH, Offersen B V, Andersen MR, et al. Inter-observer variation in delineation of the heart and left anterior descending coronary artery in radiotherapy for breast cancer: a multi-centre study from Denmark and the UK. *Radiother Oncol* 2013; **108**: 254-8. doi: 10.1016/j.radonc.2013.06.025
58. Feng M, Moran JM, Koelling T, Chughtai A, Chan JL, Freedman L, et al. Development and validation of a heart atlas to study cardiac exposure to radiation following treatment for breast cancer. *Int J Radiat Oncol Biol Phys* 2011; **79**: 10-8. doi: 10.1016/j.ijrobp.2009.10.058
59. Tan W, Wang X, Qiu D, Liu D, Jia S, Zeng F, et al. Dosimetric comparison of intensity-modulated radiotherapy plans, with or without anterior myocardial territory and left ventricle as organs at risk, in early-stage left-sided breast cancer patients. *Int J Radiat Oncol Biol Phys* 2011; **81**: 1544-51. doi: 10.1016/j.ijrobp.2010.09.028
60. Park HJ, Oh DH, Shin KH, Kim JH, Choi DH, Park W, et al. Patterns of practice in radiotherapy for breast cancer in Korea. *J Breast Cancer* 2018; **21**: 244-50. doi: 10.4048/jbc.2018.21.e37

Long-term toxicity and survival outcomes after stereotactic ablative radiotherapy for patients with centrally located thoracic tumors

Banu Atalar^{1,2}, Teuta Zoto Mustafayev², Terence T. Sio³, Bilgehan Sahin¹, Gorkem Gungor², Gokhan Aydın², Bulent Yapici², Enis Ozyar^{1,2}

¹ Department of Radiation Oncology, Acibadem MAA University, Istanbul, Turkey

² Department of Radiation Oncology, Acibadem Maslak Hospital, Istanbul, Turkey

³ Department of Radiation Oncology, Mayo Clinic Hospital, Phoenix, Arizona

Radiol Oncol 2020; 54(4): 480-487.

Received 2 April 2020

Accepted 30 May 2020

Correspondence to: Banu Atalar, M.D., Department of Radiation Oncology, Acibadem MAA University, Istanbul, Turkey.
E-mail: banu.atar@acibadem.edu.tr

Disclosure: Terence T. Sio, M.D., M.Sc., provides strategic and scientific recommendations as a member of the Advisory Board and speaker for Novocure, Inc. This position has no relation to this manuscript. All other authors have no additional conflict of interest to disclose.

Background. Stereotactic ablative radiotherapy (SABR) is effective for thoracic cancer and metastases; however, adverse effects are greater for central tumors. We evaluated factors affecting outcomes and toxicities after SABR for patients with primary lung and oligometastatic tumors.

Patients and methods. We retrospectively identified consecutive patients with centrally located lung tumors that were treated at our hospital from 2009-2016. The effects of patient, disease, and treatment-related parameters on local control (LC), overall survival (OS), and toxicity-free survival (TFS) were evaluated with multivariate analyses.

Results. Among 65 consecutive patients identified with 70 centrally located tumors, 20 tumors (28%) were reirradiated. Median (range) total dose for all tumors was 55 (30–60) Gy in 5 (3–10) fractions. Radiographic complete response was obtained in 43 lesions (61%). None of the analyzed factors were correlated with complete response. After a median follow-up of 57 (95% CI, 48–65) months, 10 tumors (14%) relapsed and 37 patients (57%) died; the actuarial 2- and 5-year OS rates were 52% and 28%, respectively. Median OS was significantly lower in patients with grade 3 or higher toxicity vs. lower toxicity (5 vs. 39 months; $P < 0.001$). Among 17 severe toxicities, 5 were grade 5, and 3 of them were reirradiated to the same field. Grade 3 to 5 TFS was lower with vs. without reirradiation (2-year TFS, 63% vs. 96%; $P = 0.02$).

Conclusions. Our study showed that modern SABR is effective for central lung tumors, and toxicities are acceptable. SABR for reirradiated central lung lesions and possibly for lesions abutting the tracheobronchial tree may result in higher risk of serious toxicities.

Key words: lung cancer; radiation; stereotactic ablative radiotherapy; stereotactic body radiation therapy; survival outcomes; toxicity

Introduction

Because local control (LC) and survival have shown limited improvement after conventionally fractionated radiotherapy for early inoperable lung tumors, interest in alternative, hypofractionated treatment schedules has increased. Stereotactic ablative radiotherapy (SABR) has been effective for primary lung tumors, as well as pulmonary

metastases that are associated with other primary organs.^{1,2} In early studies, biological effective doses (BEDs) to the tumor with an alpha/beta ratio of 10 (BED_{10}) greater than 100 Gy given in 3 or 4 fractions resulted in better LC and improved overall survival (OS) compared with conventional radiotherapy.³⁻⁵ However, this potential therapeutic gain can come with a risk of increased toxicities including fatal events, although they are usually rare.⁶ Proximity

to the trachea or main bronchi, within 1–2 cm of the tracheobronchial tree (TBT), is directly related to increased toxicities observed clinically.^{6–8} As a result, highly fractionated ablative schedules such as 54 Gy in 3 fractions should not be used for centrally located thoracic tumors with such proximity.

Recently, the highly anticipated NRG Oncology/Radiation Therapy Oncology Group (RTOG) 0813 trial was published.⁹ The maximally tolerated dose of 12 Gy per fraction over 5 fractions was reached in the study; however, the dose-limiting toxicity rate of 7.2% still gives certain clinicians pause for using a 5-fraction regimen, especially for “ultra-central” lesions.^{10–13} A more fractionated dosing scheme and strict adherence to the organs-at-risk constraints may still need to be defined, especially for tumors that directly invade critical structures. A phase II prospective study (LungTech) by the European Organisation for Research and Treatment of Cancer using 60 Gy in 8 fractions for central lung tumors is ongoing; another Canadian study, SUNSET, mainly focuses on ultracentral lesions using SABR techniques.^{14,15}

With the full results of these prospective trials still unavailable, we aimed to clarify the effects of current treatment regimens and predisposing factors for increased toxicities in central lung cancers. In the current study, we identified patients treated in our center and reviewed their long-term outcomes regarding LC, OS, and toxicities after SABR for centrally located primary lung and oligometastatic tumors.

Patients and methods

Patient selection and grouping

After approval by our institutional review board, we retrospectively searched our patient database for the records of all consecutive patients treated with their first SABR course to one or more centrally located lung lesions between October 2009 and April 2016 at our hospital. Primary stage I or II non-small cell lung cancers (NSCLCs), recurrent tumors after previous irradiation (regularly fractionated treatments), and oligometastatic tumors from other primary organs were included. Lesions were grouped according to distance from the tracheobronchial tree and mediastinum: 1) tumors with gross tumor volume (GTV) and/or planning target volume (PTV) very close to or abutting the tracheobronchial tree (≤ 1 cm); 2) tumors with GTV and/or PTV 1 to 2 cm away from the tracheobronchial tree; 3) tumors intersecting the mediastinum;

and 4) tumors abutting the aorta. Patients with at least 3 months of follow-up, or patients who died within 3 months after SABR completion, were included in all of the analyses.

SABR treatments

All patients were simulated in the supine position using a wing board. Patients had 1 of 3 motion management methods: 4-dimensional computed tomography (CT) using a Respiratory Gating System (Anzai Medical) or a Real-time Position Management System (Varian Medical Systems), CT performed during 3 phases (free breathing, end-expiratory phase, and inspiratory phase), or planning CT during free-breathing or during breath-hold. CT slice thickness was set at 1 to 1.5 mm. Positron emission tomography (PET)/CT fusion was used to assist delineation for some tumors. The target tumor (as GTV) was delineated on the maximum intensity projection when applicable or by using volumes from all 3 phases of breathing, which were united to form the internal target volume. No additional expansion was given to form the clinical target volume (i.e., clinical target volume equaled GTV). PTV margin was given as a 0.5 cm isotropic expansion to the internal target volume for all cases.

All patients were treated using a linear accelerator (Trilogy or TrueBeam STx; Varian Medical Systems). One patient had a tumor treated by CyberKnife (Accuray, Inc).

Organs-at-risk dose constraints and PTV coverage were done according to the RTOG study protocols. Kilovoltage portal imaging and cone beam CT were used in every fraction for every patient's treatments during the daily setup. For the patient treated by CyberKnife, the Xsight lung tracking and Synchrony systems (Accuray, Inc) were used.

Treatment dose and fractionation were determined at the discretion of the treating physician, but lower doses or more protracted schedules, in general, were used for patients undergoing reirradiation and for tumors abutting the tracheobronchial tree. BED calculations, based on alpha/beta ratios of 10 (acute) and 3 (late) evaluations, were performed conventionally on the basis of classic radiobiology principles in radiation oncology.

Statistical methods and outcomes

Toxicity-free survival (TFS) and local relapse-free survival (LRFS) were calculated as time since the end of SABR to event occurrence (death or a

TABLE 1. Patient, tumor, and treatment characteristics for 65 patients (70 tumors) receiving stereotactic ablative radiotherapy (SABR)

Characteristic	Value ^a
Age, year	64 (22–95)
Men	50 (77)
Primary cancer	
Lung	49 (70)
Colorectal	10 (14)
Other (breast, gastric, melanoma, germ cell, RCC)	11 (16)
Treatment indication	
Primary lung (medically inoperable T1–T2)	12 (17)
Relapse (primary lung and oligometastatic)	24 (34)
Oligometastatic	34 (49)
Previous radiation to chest	20 (29)
Tumor location	
≤ 1 cm from tracheobronchial tree	24 (34)
> 1 cm but ≤ 2 cm from tracheobronchial tree	12 (17)
Lesions intersecting mediastinum	22 (31)
≤ 1 cm from thoracic aorta	12 (17)
Left laterality	37 (53)
Lesion size (PTV), cc	33.4 (7.3–461.5)
Total dose, Gy	55 (30–60)
Dose per fraction, Gy	9.75 (4–18)
Fractions	5 (3–10)
BED ₁₀ , Gy	110 (48–151.2)
BED ₁₀	
< 100 Gy	16 (23)
≥ 100 Gy	54 (77)
BED ₃ , Gy	228 (90–378)
Treatment time, days	10 (5–19)
Treatment time	
< 10 days	30 (43)
≥ 10 days	40 (57)
Treatment on consecutive days	6 (9)

BED = biological effective dose; PTV = planned tumor volume; RCC = renal cell carcinoma;
^a Values are median (range) or No. of patients/tumors (%).

grade 2 or higher toxicity for TFS and death or locoregional relapse for LRFS, whichever occurred earlier). OS for patients with multiple SABR treatments was calculated as time since the end of the last SABR to death. Toxicity was graded according to the Common Terminology Criteria for Adverse Events, 4th edition.

OS, TFS, and LRFS were calculated using the Kaplan-Meier method, and log-rank tests were used for comparison between groups. *Complete response* was defined as shrinkage or radiographic disappearance of the tumor on 3-month follow-up scans, with decreasing maximum standardized uptake values (SUV). *Partial response* was defined as minimal decrease in tumor size or maximum SUV. *Progression* was defined as an increase in tumor size and also maximum SUV, concerning for residual tumor or recurrence. Multivariate hazard ratios (HRs) and corresponding 95% CIs were calculated by Cox regression analysis. Statistical analysis was performed with IBM SPSS Statistics software version 23 (IBM SPSS Statistics). All *P* values were 2-sided, and *P* < 0.05 was considered statistically significant.

Results

Our search identified 65 patients (70 lesions) with at least 3 months of follow-up or who died within 3 months after SABR completion. The type of tumor was primary lung in 49 (70%) and oligometastatic in 21 (30%). The patient, tumor, and treatment characteristics are summarized in Table 1. The treatment planning was 4-dimensional CT in 15 patients (23%), CT during 3 phases in 43 (66%), and CT during free-breathing or during breath-hold in 7 (11%). PET/CT fusion was used to assist delineation for 50 patients (77%). Volumetric modulated arc therapy was the most commonly used technique (34, 52%), followed by 3-dimensional conformal (29, 45%) and dynamic conformal arc (2, 3%) radiotherapies. Median (range) total dose was 55 Gy (30–60 Gy), fraction dose was 9.75 Gy (4–18 Gy), BED₁₀ was 110 Gy (41–151 Gy), and BED₃ was 228 Gy (90–378 Gy). The median (range) number of fractions was 5 (3–10).

Reirradiation was performed for 20 tumors (28%) (Table 1). The median dose given as reirradiation was lower than for other tumors (reirradiation BED₁₀ dose: 94.4 Gy reirradiation *vs.* 110 Gy non-reirradiation; *P* = 0.009).

After a median follow-up of 57 months (95% CI, 48–65 months), 43 (61%) of the tumors achieved complete response (Table 2). On univariate analysis, BED₁₀ (> 100 *vs.* ≤ 100 Gy), PTV size (> 33.4 *vs.* ≤ 33.4 cc), and type of tumor (colorectal metastases *vs.* other tumors) were not related to complete response radiographically by PET/CT at 3 months after the end of SABR treatments (all *P* > 0.05).

Locoregional control and survival

LRFS was lower in patients with colorectal cancer as a primary tumor (2-year LRFS: colorectal metastases, 59% *vs.* other primary tumors, 89%; $P = 0.02$) (Figure 1A). LRFS also was lower in tumors that did not have a complete response 3 months after the end of SABR (2-year LRFS: no complete response, 51% *vs.* complete response, 100%; $P < 0.001$) (Figure 1B). On multivariate analyses, tumors with less than complete response had lower LRFS (HR, 18.2; 95% CI, 2.3–145.9; $P = 0.006$). Other factors, including previous radiotherapy, BED₁₀ greater than 100 Gy, PTV size, or tumor location in relation to the tracheobronchial tree, had no effect on local relapse (all $P > 0.05$).

Overall survival

During follow-up, 10 tumors (14%) relapsed (2- and 5-year LC were 84% and 70%, respectively), and 37 patients (57%) died (2- and 5-year OS were 52% and 28%, respectively). Median OS was significantly lower in patients who had toxicity of grade 3 or higher (5 months, grade ≥ 3 toxicity *vs.* 39 months grade < 3 toxicity) (Figure 2A). Grade 3 or higher toxicity conferred a significantly increased risk of death (HR, 4.7, 95% CI, 2.0–11.2; $P < 0.001$). Median OS was slightly lower in patients with primary lung cancer than in patients with other primary cancer origins (19 months, lung cancer *vs.* 49 months, other cancers) (Figure 2B), but the risk of death was not significantly increased (HR, 2.3; 95% CI, 1.0–5.6; $P = 0.06$). Factors including previous radiotherapy, BED₁₀ higher than 100 Gy, PTV size, or position of the lesions in relation to the tracheobronchial tree had no effect on OS (all $P > 0.05$).

SABR-related toxicities

Seventeen toxicities of grade 2 or higher were observed in 13 patients, some patients have more than 1 toxicity (Table 2). Imaging examples of patients with tracheal rupture and vocal cord paralysis are shown in Figure 3. The most common toxicity was radiation-induced pneumonia. Less common toxicities, including brachial plexus injury (giving rise to Lhermitte sign) and vocal cord paralysis (due to vagus or recurrent laryngeal nerve injury), were observed in 3 patients; radiation-related esophagitis occurred in 2 patients.

Seven of the 10 toxicities of grade 3 to 5 were observed in reirradiation patients, which conferred an HR of 5.8 (95% CI, 1.7–20.3). Also, 7 of 10 grade

TABLE 2. Tumor and patient outcomes after stereotactic ablative radiotherapy (SABR) for central lung tumors

Characteristic	Value ^a
Response on 3-month PET/CT after SABR	
Complete response	43 (61)
Partial response	19 (27)
Progression	2 (3)
Unknown (patient died before 3 months or imaging not performed)	6 (9)
Locoregional control	
2-year	84%
5-year	70%
Median	Not reached
Overall survival	
2-year	52%
5-year	28%
Median	28 months
2-Year toxicity-free survival	81%
All Toxicities (grade 2 or higher)	17 (26.2%)
RT-induced pneumonitis	9 (13.8%)
Brachial and recurrent laryngeal nerve injury	3 (4.6%)
Esophagitis	2 (3%)
Tracheal perforation	1 (1.5%)
Fatal hemoptysis	1 (1.5%)
Possible RT-related death	1 (1.5%)
Toxicity, grade 5 (fatal)	5 (7.7%)
RT-induced pneumonitis	2 (3%)
Tracheal perforation	1 (1.5%)
Fatal hemoptysis	1 (1.5%)
Possible RT-related death	1 (1.5%)

PET/CT = positron emission tomography/computed tomography; RT = radiotherapy; ^a Values are No. patients/tumors (%) or No. patients unless otherwise stated.

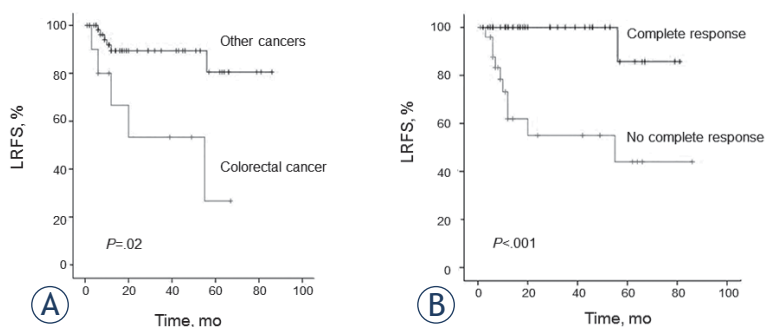


FIGURE 1. Kaplan-Meier curves for locoregional relapse-free survival (LRFS). (A) LRFS of all patients according to primary tumor type (colorectal cancer *vs.* others). (B) LRFS of all patients according to radiographic response 3 months after radiotherapy (complete response *vs.* no complete response). Tick marks on lines indicate censored patients.

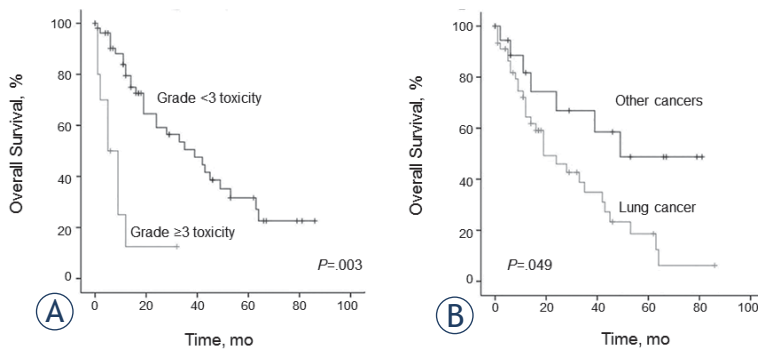


FIGURE 2. Kaplan-Meier curves for overall survival (OS). **(A)** OS of all patients according to development of a grade 3 or higher toxicity (vs. not). **(B)** OS of all patients according to primary tumor type (lung cancer vs. others). Tick marks on lines indicate censored patients.

3 to 5 toxicities were observed in lesions abutting the tracheobronchial tree, for an HR of 4.5 (95% CI, 1.3–15.8). Among the 17 toxicities, 5 were grade 5 (fatal). Three out of 5 fatal toxicity patients were reirradiated to the same RT field, and one of them was irradiated to a neighboring field. The prior and reirradiation doses of each patient were 66Gy/33 fractions and 30 Gy/5 fractions; 40 Gy/10 fractions and 59.5Gy/7 fractions; 66 Gy/33 fractions and 30 Gy/5 fractions; and 45 Gy/15 fractions with the neighboring field dose and 50 Gy/5 fractions, respectively. We were able to get the medical reports and the thoracic CT for 3 of the patients and confirmed the grade 5 toxicity; in regard to patient #4, which was reported as “possible RT-related death,” this was due to the fact that his death was unexpected, and happened only a few weeks shortly after his SABR course; this information was given to us by his relatives. To be estimating this toxicity

rate conservatively, we believe that it is reasonable to account for this in the statistics (so it did not appear that we were biased), as the death did happen within one month after SABR. The last patient who had grade 5 toxicity after 1st SABR was treated to a total dose of 59.5Gy in 7 fractions and notably he had a lesion encasing bronchus with a size of 55 mm which was considered to be a larger lesion for SABR. After a reasonable amount of effort, we could not locate his radiological images; however, the emergency medical notes noted symptoms and signs of him developing an acute pneumonia. As a result, we considered the possibility that it could be a RT-related pneumonia due to the proximity of timing to his SABR course.

Survival free of grade 3 to 5 toxicity was lower after reirradiation than in patients without reirradiation (2-year TFS: 63% after reirradiation vs. 96% without reirradiation) (Figure 4A); the HR was 5.1 (95% CI, 1.3–20.3; $P = 0.02$). TFS also was lower in tumors abutting the tracheobronchial tree (2-year TFS: 69%, tumors abutting the tracheobronchial tree vs. 93%, other cases) (Figure 4B), but the associated risk did not reach statistical significance (HR, 3.5; 95% CI, 0.9–13.9; $P = 0.08$).

Discussion

Grade 3 or higher complications of SABR for centrally located lung tumors are still a substantial concern, as reported by multiple studies, including the most recently published NRG Oncology/RTOG 0813 trial.^{5,6,8,9,12} Therefore, more studies are required to evaluate whether these findings are similar in the general population. To our knowledge, the current retrospective study is one of the

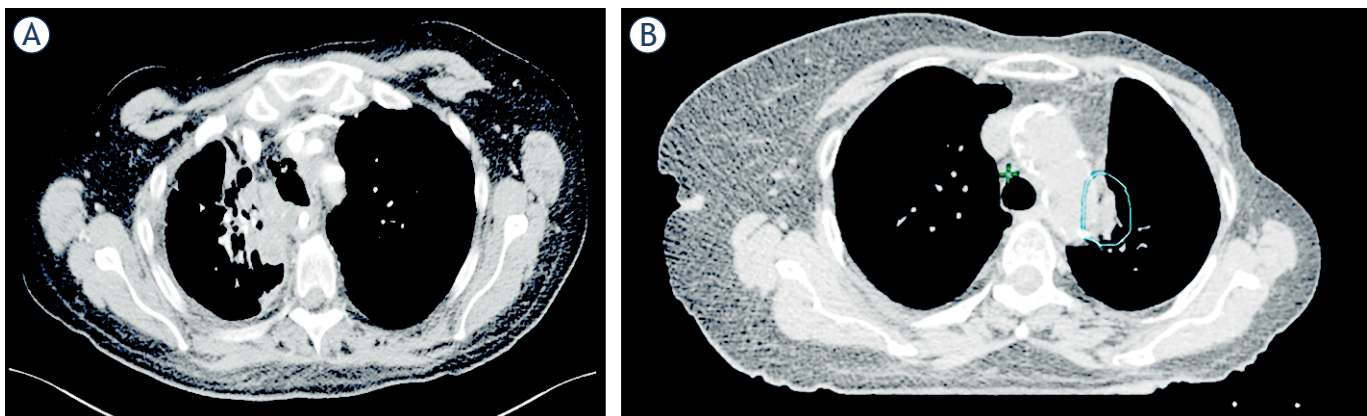


FIGURE 3. Computed tomographic imaging examples of patients with a grade 3 or higher toxicity. **(A)** Patient with a tracheal rupture after reirradiation. **(B)** Patient with vocal cord paralysis after reirradiation (previous chest wall radiotherapy). The circled portion indicates the planning target volume.

largest series to date for centrally located and ultra-central lung tumors. Favorable outcome and toxicity profiles were achieved, which supports the use of 5-fraction and also moderately hypofractionated regimens in this population.

The LC rates in our series are comparable to those of other published series which showed excellent tumor control. Although we saw no correlation of BED₁₀ doses higher than 100 Gy with better LC, previous studies indicated that BED₁₀ of 100 Gy or higher led to better local progression-free survival and OS.^{3,4} The reason for the lack of correlation in our study may be the high number of reirradiation lesions, which were prescribed lower radiotherapy doses (mean reirradiation BED₁₀ dose, 94.4 Gy). reirradiation lesions also had shorter follow-up, so their local recurrence rates may appear lower at the time of data analysis. The difference also may relate to the heterogeneity of these tumors, including colorectal oligometastatic, lung cancers with epidermal growth factor receptor or anaplastic large-cell lymphoma kinase-gene mutations, and other confounding factors such as chemotherapy before or after SABR. If only non-reirradiation primary lung lesions are considered, the LC rates in our study (2-year LC, 71%) are similar to those in the literature.² Metastatic tumors with a separate primary seemed to have higher LC rates (2-year LC, 81%) than those reported in the literature (51%–96%, with various radiotherapy doses).¹ At this time, there is no clear correlation between LC and radiotherapy doses, although LC was found to be positively correlated with favorable response radiographically 3 months after SABR by PET/CT in our study (the use of PET/CT for follow-up is a routine practice at our institution).

In our series, 2- and 5-year OS were 48% and 20%, respectively, for patients with primary lung cancer and were 60% and 44%, respectively, for patients with oligometastatic tumors. The 2-year OS rates in the literature range from 33% to 84% depending on primary tumor type, size and number of lesions, disease-free survival from primary tumor treatment to onset of metastasis, and other treatment-related factors.¹ Similarly, survival after SABR for patients with NSCLC has also varied among studies, with 2-year OS ranging from 43% to 90% depending on radiotherapy dose, tumor size, clinical performance status, and tumor location (central *vs.* not).² With 29% of our tumor cases being reirradiation and 16% of tumors being larger than 5 cm, our results are comparable to the historical controls as a result. The higher rates of toxicities

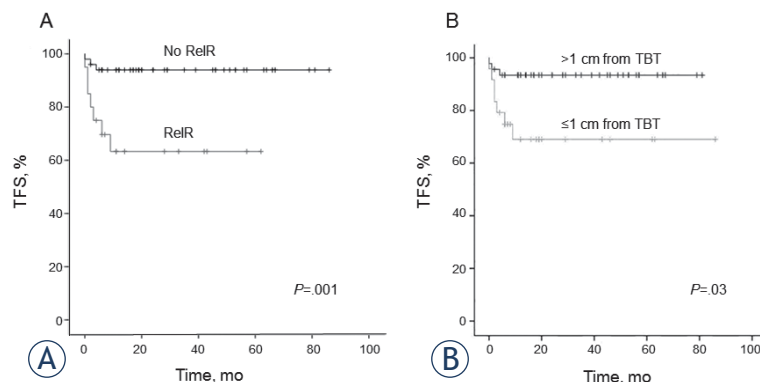


FIGURE 4. Kaplan-Meier Curves for grade 3 or higher toxicity-free survival (TFS). **(A)** TFS for all patients according to reirradiation vs. no reirradiation. **(B)** TFS for all patients according to the distance of the planning target volume from the tracheobronchial tree (> 1 cm or ≤ 1 cm). Tick marks on lines indicate censored patients.

(including grade 5 cases) also contributed to the lower OS rates in our study.

Compared with rates reported in the literature, a slightly higher rate of possible grade 5 toxicities was noted in our cohort; 5 patients who died had treatment complications that may have been causative, including pneumonitis, tracheal perforation, and hemoptysis. OS in patients with grade 3 to 5 toxicity was short, with a median of only 5 months after SABR. Reirradiation carried significant risks in these cases because it resulted in a high cumulative dose in the mediastinum. More guidance and research in the future are required for making SABR safer in these clinical scenarios, in which patients often have no other choice but reirradiation, along with proper counseling regarding potential treatment outcomes and adverse effects.

For centrally located lung tumors or nodal recurrences after previous irradiation, some authors have discouraged the use of SABR because of the perceived high risks of toxicity.^{16,17} In other studies that included central lesions without prior radiotherapy, a higher rate of grade 5 toxicities was often reported.¹⁶⁻¹⁸ In an analysis of 32 lesions (11 central) that were previously irradiated, Peulen *et al.* reported that treatment of central lung lesions and lesions with larger volumes resulted in higher toxicity; 9 of 29 patients had grade 3 or higher toxicity, including 3 cases of fatal hemoptysis.¹⁷ Another prospective trial studying salvage SABR in NSCLC did not include any central lesions in their reirradiation series.¹⁸

The GTV or PTV was within 1 cm of the tracheobronchial tree (ultracentral) in 24 (34%) of our patients. Four of these patients had grade 5 toxicity. Because 3 of those patients also had reirradiation,

we do not know conclusively whether the death was related to reirradiation, tumor proximity to the tracheobronchial tree, or both. The literature reports conflicting results regarding the importance of proximity to the tracheobronchial tree (lesions abutting the tracheobronchial tree *vs.* other central lesions), with some studies considering these lesions as harboring similar risk as other central tumors and other studies advocating for more caution in their treatment planning.^{7,8,10,13}

Vocal cord paralysis is a rarely recognized complication of SABR. To our knowledge, only 2 studies have reported its occurrence.^{19,20} Shultz *et al.* concluded that reirradiation to the vagal or recurrent laryngeal nerve in 1 case and connective tissue disorders in another case led to nerve injury and paralysis of the vocal cord.²⁰ Two of our patients had vocal cord paralysis, which was confirmed by laryngoscopy. In both patients, PET/CT was performed at the onset of voice hoarseness to exclude local recurrence or as part of follow-up: None of the patients had lesions that would otherwise explain their symptoms. One of the patients had had SABR to the same lesion previously, and the other patient had previous ipsilateral breast irradiation (the contribution from the previous breast radiotherapy was estimated to be about 15 Gy to the new GTV [by SABR]). Both lesions were located adjacent to the aortic arch and invaded the vagus nerve; they were also in close proximity to the recurrent laryngeal nerve (Figure 3).

Our study has several limitations. The study was retrospective, and the patient population was more heterogeneous than in other reported series on this topic (in terms of radiotherapy dose and also inclusion of primary lung *vs.* oligometastatic tumors). Because our institution is a tertiary referral center, some patients' follow-up was not completed in our department. The circumstances related to patients' death were derived from interviews with relatives instead of medical records, which led us to recategorize 1 of the grade 5 toxicities as SABR related instead of "unknown cause." Heterogeneity and lower patient numbers in different subgroups also may have limited our study power.

Conclusions

SABR is an effective treatment modality for centrally located lung cancers. SABR to reirradiation lesions, and possibly lesions abutting the tracheobronchial tree, appeared to carry a higher risk of higher grade toxicities developing in the long term.

More research is needed to define the optimal dose and fractionation schedule for both centrally and ultracentrally located lung tumors. We are waiting for completion of more prospective trials, which will hopefully give more information regarding suitable treatment regimens and clearer factors that may predispose patients to increased toxicities after SABR for central lung cancers.

Acknowledgment

Portions of this manuscript were presented at the International Association for the Study of Lung Cancer 19th World Conference on Lung Cancer, Toronto, Canada, September 23–26, 2018.

References

- Shultz DB, Filippi AR, Thariat J, Mornex F, Loo BW, Jr, Ricardi U. Stereotactic ablative radiotherapy for pulmonary oligometastases and oligometastatic lung cancer. *J Thorac Oncol* 2014; **9**: 1426-33. doi:10.1097/JTO.0000000000000317
- Shah JL, Loo BW, Jr. Stereotactic ablative radiotherapy for early-stage lung cancer. *Semin Radiat Oncol* 2017; **27**: 218-28. doi: 10.1016/j.semradi.2017.03.001
- Lagerwaard FJ, Haasbeek CJ, Smit EF, Slotman BJ, Senan S. Outcomes of risk-adapted fractionated stereotactic radiotherapy for stage I non-small-cell lung cancer. *Int J Radiat Oncol Biol Phys* 2008; **70**: 685-92. doi: 10.1016/j.ijrobp.2007.10.053
- Timmerman R, Paulus R, Galvin J, Michalski J, Straube W, Bradley J, et al. Stereotactic body radiation therapy for inoperable early stage lung cancer. *JAMA* 2010; **303**: 1070-6. doi: 10.1001/jama.2010.261
- Onishi H, Araki T, Shirato H, Nagata Y, Hiraoka M, Gomi K, et al. Stereotactic hypofractionated high-dose irradiation for stage I nonsmall cell lung carcinoma: clinical outcomes in 245 subjects in a Japanese multiinstitutional study. *Cancer* 2004; **101**: 1623-31. doi: 10.1002/cncr.20539
- Timmerman R, McGarry R, Yiannoutsos C, Papiez L, Tudor K, DeLuca J, et al. Excessive toxicity when treating central tumors in a phase II study of stereotactic body radiation therapy for medically inoperable early-stage lung cancer. *J Clin Oncol* 2006; **24**: 4833-9. doi: 10.1200/JCO.2006.07.5937
- Tekatli H, Haasbeek N, Dachele M, De Haan, Verbakel PW, Bongers E, et al. Outcomes of hypofractionated high-dose radiotherapy in poor-risk patients with "ultracentral" non-small cell lung cancer. *J Thorac Oncol* 2016; **11**: 1081-9. doi: 10.1016/j.jtho.2016.03.008
- Haseltine JM, Rimner A, Gelblum DY, Modh A, Rosenzweig KE, Jackson A, et al. Fatal complications after stereotactic body radiation therapy for central lung tumors abutting the proximal bronchial tree. *Pract Radiat Oncol* 2016; **6**: e27-33. doi: 10.1016/j.pro.2015.09.012
- Bezjak A, Paulus R, Gaspar LE, Timmerman RD, Straube WL, Ryan WF, et al. Safety and efficacy of a five-fraction stereotactic body radiotherapy schedule for centrally located non-small-cell lung cancer: NRG Oncology/RTOG 0813 Trial. *J Clin Oncol* 2019; **37**: 1316-25. doi: 10.1200/JCO.18.00622
- Chaudhuri AA, Tang C, Binkley MS, Jin M, Wynne JF, von Eyben R, et al. Stereotactic ablative radiotherapy (SABR) for treatment of central and ultra-central lung tumors. *Lung Cancer* 2015; **89**: 50-6. doi: 10.1016/j.lungcan.2015.04.014
- Chang JY, Li QQ, Xu QY, Allen PK, Rebuena N, Gomez DR, et al. Stereotactic ablative radiation therapy for centrally located early stage or isolated parenchymal recurrences of non-small cell lung cancer: how to fly in a "no fly zone". *Int J Radiat Oncol Biol Phys* 2014; **88**: 1120-8. doi: 10.1016/j.ijrobp.2014.01.022

12. Haasbeek CJ, Lagerwaard FJ, Slotman BJ, Senan S. Outcomes of stereotactic ablative radiotherapy for centrally located early-stage lung cancer. *J Thorac Oncol* 2011; **6**: 2036-43. 12. doi: 10.1097/JTO.0b013e31822e71d8
13. Raman S, Yau V, Pineda S, Le LW, Lau A, Bezjak A, et al. Ultracentral tumors treated with stereotactic body radiotherapy: single-institution experience. *Clin Lung Cancer* 2018; **19**: e803-e810. doi: 10.1016/j.clcc.2018.06.001
14. Adebahr S, Collette S, Shash E, Lambrecht M, Le Pechoux C, Faivre-Finn C, et al. LungTech, an EORTC Phase II trial of stereotactic body radiotherapy for centrally located lung tumours: a clinical perspective. *Br J Radiol* 2015; **88**: 20150036. doi: 10.1259/bjr.20150036
15. Giuliani M, Mathew AS, Bahig H, Bratman SV, Filion E, Glickel D, et al. SUNSET: stereotactic radiation for ultracentral non-small-cell lung cancer - a safety and efficacy trial. *Clin Lung Cancer* 2018; **19**: e529-32. doi: 10.1016/j.clcc.2018.04.001
16. Matsuo Y. A systematic literature review on salvage radiotherapy for local or regional recurrence after previous stereotactic body radiotherapy for lung cancer. *Technol Cancer Res Treat* 2018; **17**: 1533033818798633. doi: 10.1177/1533033818798633
17. Peulen H, Karlsson K, Lindberg K, Tullgren O, Baumann P, Lax I, et al. Toxicity after reirradiation of pulmonary tumours with stereotactic body radiotherapy. *Radiother Oncol* 2011; **101**: 260-6. doi: 10.1016/j.radonc.2011.09.012
18. Sun B, Brooks ED, Komaki R, Liao Z, Jeter M, McAleer M, et al. Long-term outcomes of salvage stereotactic ablative radiotherapy for isolated lung recurrence of non-small cell lung cancer: a phase II clinical trial. *J Thorac Oncol* 2017; **12**: 983-92. doi: 10.1016/j.jtho.2017.02.018
19. Binkley MS, Hiniker SM, Chaudhuri A, Maxim PG, Diehn M, Loo BW Jr, et al. Dosimetric factors and toxicity in highly conformal thoracic reirradiation. *Int J Radiat Oncol Biol Phys* 2016; **94**: 808-15. doi: 10.1016/j.ijrobp.2015.12.007
20. Shultz DB, Trakul N, Maxim PG, Diehn M, Loo BW, Jr. Vagal and recurrent laryngeal neuropathy following stereotactic ablative radiation therapy in the chest. *Pract Radiat Oncol* 2014; **4**: 272-8. doi: 10.1016/j.prro.2013.08.005

Does regular quality control improve the quality of surgery in Slovenian breast cancer screening program?

Andraz Perhavec^{1,2}, Sara Milicevic¹, Barbara Peric^{1,2}, Janez Zgajnar^{1,2}

¹ Department of Surgical Oncology, Institute of Oncology Ljubljana, Ljubljana, Slovenia

² Faculty of Medicine, University of Ljubljana, Ljubljana, Slovenia

Radiol Oncol 2020; 54(4): 488-494.

Received 4 April 2020

Accepted 26 April 2020

Correspondence to: Prof. Janez Žgajnar, M.D., Ph.D., Department of Surgical Oncology, Institute of Oncology Ljubljana, Zaloska 2, SI-1000 Ljubljana, Slovenia. E-mail: e-mail: jzgajnar@onko-i.si

Disclosure: No potential conflicts of interest were disclosed.

Background. The aim of our study was to evaluate the quality of surgery of Slovenian breast cancer screening program (DORA) using the requested EU standards. Furthermore, we investigated whether regular quality control over the 3-year period improved the quality of surgical management.

Patients and methods. Patients who required surgical management within DORA between January 1st, 2016 and December 31st, 2018 were included in the retrospective study. Quality indicators (QIs) were adjusted mainly according to European Society of Breast Cancer Specialists (EUSOMA) and European Breast Cancer Network (EBCN) recommendations. Five QIs for therapeutic and two for diagnostic surgeries were selected. Additionally, variability in achieving the requested QIs among surgeons was analysed.

Results. Between 2016 and 2018, 14 surgeons performed 1421 breast procedures in 1398 women. There were 1197 therapeutic (for proven breast cancer) and 224 diagnostic surgical interventions respectively. Overall, the minimal standard was met in two QIs for therapeutic and none for diagnostic procedures. A statistically significant improvement in three QIs for therapeutic and in one QI for diagnostic procedures was observed however, indicating that regular quality control improves the quality of surgery. A high variability in achieving the requested QIs was observed among surgeons, which remained high throughout the study period.

Conclusions. Adherence to all selected surgical QIs in patients from screening program is difficult to achieve, especially to those specifically defined for screen-detected lesions. Regular quality control may improve results over time. Reducing the number of surgeons dedicated to breast pathology may reduce variability of management inside the institution.

Key words: breast surgery; mammography screening program; quality control

Introduction

Breast cancer is the most common female cancer with an estimated incidence of 523,000 cases in Europe in 2018 and the third leading common cause of death from cancer (138,000 cases per year).¹ A 5-year survival rate in women with breast cancer ranges from 25.1% to 95.7% and depends mainly on the stage of the disease at the time of diagnosis.² Screening programs are efficient in early detection of cancer and lead to a better prognosis and less intensive treatment.^{3,4}

As the management of early breast cancer is complex, the optimal outcomes are ensured in the specialized multidisciplinary breast cancer centres.⁵ Comprehensive quality assurance is of great importance for maintaining the appropriate balance between benefits and harms.³ European Society of Breast Cancer Specialists (EUSOMA) and European Breast Cancer Network (EBCN) provided a set of quality indicators (QIs) in order to establish minimum standard of care and to improve the quality of care, patient satisfaction and outcome. QIs also allow standardised quality of care evaluation.⁵⁻⁷

Slovenian breast cancer screening program, called DORA, is a national population-based organized screening program inviting women aged 50–69 to biannual mammography and it is aimed to detect breast cancer in asymptomatic women in early stages. Quality of surgery and the impact of regular quality control on improvement of QIs within screening program is not known. In 2016, we defined and regularly monitored a set of surgical QIs mainly from EUSOMA and EBCN for women that undergo surgical procedure for a suspicious or malignant lesion detected in Slovenian Breast Cancer screening Program.

The aim of our study was to evaluate the quality of surgical treatment of patients from the DORA program and to investigate whether the surgical approach fulfils the requested EU standards. Furthermore, we investigated whether regular quality control over the 3-year period improved the quality of surgical management.

Patients and methods

A retrospective study of women who required surgical management within Slovenian Breast Cancer screening Programme between January 1st, 2016 and December 31st, 2018 was performed. The data were prospectively collected from the National screening programme registry and missing data supplemented by reviewing patient's records.

Slovenian National screening program DORA, with centrally organized invitation system, provides screening mammography every two years for women aged from 50 to 69 with residence in Slovenia. The programme was initiated in April 2008. The average participation rate in the years between 2008 and 2018 was 73%. Between 2016 and 2018, 216,717 women were screened in the DORA programme. A total of 1352 (0.6%) breast cancers were detected during that time.⁸

For the purpose of this study, patients were divided into two groups: the group in which breast cancer was preoperatively histologically or cytologically confirmed (B5 or C5 lesions) and the group in which diagnostic surgical procedure was performed due to lesions of uncertain malignant potential.

A decision on management of screen-detected breast cancer was always made within multidisciplinary tumour board. Thus, this QI was not monitored, as it was not expected to change over time. Since all patients were operated at the same institution (Institute of oncology Ljubljana), the same rationale approaches were used.

All but one QIs have been chosen according to EUSOMA recommendations from 2010 and EBCN recommendations from 2006.^{6,7} We did not include all QIs as we do not routinely collect all the required data. Furthermore, we tried to avoid becoming overwhelmed with too many indicators.

QIs that have been defined and regularly monitored in patients in which breast cancer was preoperatively histologically or cytologically confirmed are:

- (1) median waiting time (in days) from multidisciplinary tumour board to surgery and proportion of patients who waited less than 15 working days from multidisciplinary tumour board to surgery: both EUSOMA and EBCN consider waiting time as a QI; since in our study only patients with screen detected lesions were included, we decided to choose more strict EBCN recommendation;
- (2) proportion of patients (invasive and noninvasive cancers) who received a single (breast) operation for the primary tumour (excluding reconstruction): EUSOMA recommendation considers invasive and noninvasive cancers separately and the recommendation is stricter for invasive cancers (80%) compared to noninvasive cancers (70%); we decided to combine invasive and noninvasive cancers into one QI with stricter criteria to provide more robust numbers and to avoid becoming overwhelmed with too many rather similar QIs;
- (3) proportion of patients with invasive breast cancer not greater than 3 cm (total pathological size, including DCIS component) who underwent breast conserving treatment (BCT): EUSOMA QI;
- (4) proportion of patients with invasive cancer and axillary clearance performed with at least 10 lymph nodes (LN) examined: EUSOMA QI;
- (5) mean weight of the excised specimen and the proportion of specimens from the breast with weight less than 80 g when breast conserving surgery was performed: this is neither the EUSOMA nor the EBCN QI. We decided to include it as a surrogate of expected cosmetic result. The average specimen from breast conserving surgery should weigh between 20 and 40 g and as a general rule, 80 g of breast tissue is the maximum weight that can be removed from a medium-sized breast without resulting in deformity.⁹

QIs that have been regularly monitored in patients in which diagnostic surgical procedure was performed due to lesions of uncertain malignant potential are:

- (1) median waiting time (in days) from multidisciplinary tumour board to surgery and proportion of patients who waited less than 15 working days from multidisciplinary tumour board to surgery: EBCN QI;
- (2) mean weight of the excised specimen and the proportion of specimens with weight less than 30 g: EBCN QI.

Patients who received neoadjuvant chemotherapy were excluded from calculations of median waiting time.

All selected QIs have been regularly monitored each year, starting in 2016.

All statistical analyses were performed using SPSS for Windows, version 22.0. Data were summarized using frequencies and percentages for categorical variables and median or mean for continuous variables. Chi square test was used to compare categorical variables and Mann-Whitney test or ANOVA for continuous variables. P-values ≤ 0.05 were considered statistically significant.

This study was conducted according to the rules of the Ethical Committee of the Institute of oncology Ljubljana.

Results

Between 2016 and 2018, 14 surgeons performed 1421 breast procedures in 1398 women from breast cancer screening program DORA. There were 1197 procedures therapeutic because of histologically or cytologically proven invasive or *in situ* breast cancer and 224 procedures were diagnostic because of lesions of uncertain malignant potential.

To determine whether our surgical approach reaches the requested EU standards, quality of care was evaluated by predefined QIs.

Pathologic characteristics of patients that underwent therapeutic surgical procedures split by the year of treatment are shown in Table 1. Quality indicators of therapeutic surgical procedures split by the year of surgery are shown in Table 2.

Pathologic characteristics of patients that underwent diagnostic surgical procedures split by the year of surgery are shown in Table 3. Quality indicators of diagnostic surgical procedures split by the year of surgery are shown in Table 4.

Nineteen out of 224 (8.5%) patients needed reoperation after diagnostic breast surgical procedure; 5/224 (2.2%) re-excision, 4/224 (1.8%) mastectomy, 2/224 (0.9%) re-excision followed by mastectomy and 8/224 (3.6%) only sentinel lymph node biopsy.

There were 1421 breast procedures performed by 14 surgeons. The variability among surgeons in 3 years period is shown in Table 5.

Discussion

Regularly reporting and analysing outcome data is important in order to allow centres to ensure patients with breast cancer the optimal management and to recognise the particular areas, where the improvements are required. Namely, focusing on QIs shows higher compliance to recommended treatment and better outcome.¹⁰⁻¹⁴ Furthermore, by providing outcome data, the new scientific knowledge is incorporated and minimum standards are upgraded.⁵

TABLE 1. Characteristics of therapeutic procedures performed between 2016 and 2018

No. of procedures	All	2016	2017	2018	p-value
	1197	296	417	484	
Procedure type in breast					
BCT	927 (77.4%)	218 (73.6%)	312 (74.8%)	397 (82.0%)	0.007
mastectomies	270 (22.6%)	78 (26.4%)	105 (25.2%)	87 (18.0%)	
Procedure type in axilla:					
none	202 (16.9%)	34 (11.5%)	72 (17.3%)	96 (19.8%)	0.002
SNB	858 (71.7%)	211 (71.3%)	304 (72.9%)	343 (70.9%)	
ALND	87 (7.3%)	35 (11.8%)	25 (6.0%)	27 (5.6%)	
SNB + ALND	50 (4.2%)	16 (5.4%)	16 (3.8%)	18 (3.7%)	
Histologic tumour type					
Benign	64 (5.3%)	6 (2.0%)	19 (4.6%)	39 (8.1%)	0.004
<i>In situ</i>	214 (17.9%)	50 (16.9%)	84 (20.1%)	80 (16.5%)	
Microinvasive carcinoma	19 (1.6%)	2 (0.7%)	12 (2.9%)	5 (1.0%)	
Invasive carcinoma	899 (75.1%)	238 (80.4%)	302 (72.4%)	359 (74.2%)	
Other	1 (0.1%)	0 (0.0%)	0 (0.0%)	1 (0.2%)	
Mean tumour diameter \pm S.D. (mm)	17.8 \pm 13.3	18.9 \pm 14.6	18.2 \pm 13.6	16.8 \pm 12.0	0.127

ALND = axillary lymph node dissection; BCT = breast conserving treatment; S.D. = standard deviation; SNB = sentinel node biopsy

TABLE 2. Quality indicators of therapeutic surgical procedures split by the year of treatment

	Recommendation:	All	2016	2017	2018	p-value
1. QI: waiting time						
Median (days)	Not more than 15 working days	33	38	34	28	< 0.001
Proportion of patients with waiting time less than 15 working days	days ≥ 90%	4.2%	1.7%	2.9%	6.9%	
2. QI: proportion of patients (invasive and noninvasive cancers) who received a single (breast) operation for the primary tumour (excluding reconstruction)						
	Minimum standard: 80%	1088/1197 (90.9%)	266/296 (89.9%)	379/417 (90.9%)	443/484 (91.5%)	0.735
	Target: 90%					
3. QI: proportion of patients with invasive breast cancer not greater than 3 cm (total size, including DCIS component) who underwent BCT						
	Minimum standard: 70%	669/801 (83.5%)	165/211 (78.2%)	220/265 (83.0%)	284/325 (87.4%)	0.019
	Target: 80%					
4. QI: proportion of patients with invasive cancer and axillary clearance performed with at least 10 LN examined						
	Minimum standard: 95%	124/137 (90.5%)	45/51 (88.2%)	40/41 (97.6%)	39/45 (86.7%)	0.014
	Target: 98%					
5. QI: weight of the excised specimen from the breast						
Mean ± S.D. (g)	Proportion of specimen after BCT with weight less than 80g ≥ 90%	69.0 ± 42.5	75.3 ± 50.3	63.8 ± 35.9	69.7 ± 42.3	0.009
Proportion of specimens with weight ≤ 80g (%)		70.0%	61.8%	75.6%	70.0%	

BCT = breast conserving treatment; DCIS = ductal carcinoma in situ; LN = lymph nodes; QI = quality indicator; S.D.= standard deviation

In 2016, we defined a series of five surgical QIs for therapeutic and two surgical QIs for diagnostic procedures for women diagnosed with breast lesion within national screening program. Overall, the minimal standard was met in two QIs for therapeutic (proportion of patients (invasive and non-invasive cancers) who received a single (breast) operation for the primary tumour (excluding reconstruction) and proportion of patients with invasive breast cancer not greater than 3 cm (total size,

including DCIS component) who underwent BCT and none for diagnostic procedures. Furthermore, we observed a statistically significant improvement in three QIs for therapeutic (waiting time, proportion of patients with invasive breast cancer not greater than 3 cm (total size, including DCIS component) who underwent BCT and weight of the excised specimen) and in one QI for diagnostic procedures (waiting time), indicating that regular quality control may improve the quality of sur-

TABLE 3. Results of the diagnostic surgical procedures split by the year of treatment

No. of procedures	All	2016	2017	2018	p-value
	224	78	66	80	
Procedure type in axilla:					
- none	208 (92.9%)	75 (96.2%)	59 (89.4%)	74 (92.5%)	0.289
- SNB	16 (7.1%)	3 (3.8%)	7 (10.6%)	6 (7.5%)	
- ALND	0 (0.0%)	0 (0.0%)	0 (0.0%)	0 (0.0%)	
- SNB + ALND	0 (0.0%)	0 (0.0%)	0 (0.0%)	0 (0.0%)	
Histologic tumour type					
- Benign	177 (79.0%)	63 (79.5%)	52 (78.8%)	62 (77.5%)	0.610
- <i>In situ</i>	28 (12.5%)	11 (14.1%)	6 (9.1%)	11 (13.8%)	
- Microinvasive carcinoma	1 (0.4%)	1 (1.3%)	0 (0%)	0 (0.0%)	
- Invasive carcinoma	14 (6.3%)	2 (2.6%)	6 (9.1%)	6 (7.5%)	
- Other malignant	4 (1.8%)	1 (1.3%)	2 (3%)	1 (1.3%)	
Mean tumour diameter ± S.D. (mm)	15.5 ± 14.1	15.0 ± 14.1	19.0 ± 18.7	12.2 ± 5.7	0.701

ALND = axillary lymph node dissection; S.D. = standard deviation; SNB, sentinel node biopsy

TABLE 4. Quality indicators of diagnostic surgical procedures split by the year of surgery

	Recommendation	All	2016	2017	2018	p-value
1 QI: waiting time						
- Median (days)	Not more than 15	41	44.5	42	34	< 0.001
- Proportion of patients with waiting time less than 15 working days	working days \geq 90%	10.3%	2.6%	6.2%	21.5%	
2 QI: weight of the excised specimen from the breast						
- Mean \pm S.D. (g)	Proportion of specimen with weigh less than 30g \geq 90%	37.3 \pm 23.4	40.3 \pm 25.8	32.6 \pm 22.1	38.2 \pm 22.1	0.131
- Proportion of specimens with weight \leq 30g		47.8%	46.2%	60.6%	38.8%	

QI = quality indicator; S.D. = standard deviation

gery. However, the number of QIs meeting the minimum standard was the same through all three studying years.

Timely treatment is an important requisite for the quality of surgery as it maximizes the benefit of early detection and reduces anxiety of patients and their families.⁵ This is especially important in screen-detected lesions as participation rate is critically dependent on patient's satisfaction. Thus, we set a recommendation for waiting time as defined by EBCN (15 working days), which is much stricter compared to EUSOMA (6 weeks). In the first year of our quality control monitoring, only 1.7% of patients with therapeutic operation and 2.6% of patients with diagnostic operation met the EBCN recommendations on waiting time for surgery, which is far below the minimum standard (\geq 90%). Several reasons contributed to a long wait-

ing time. First, our institution has been faced with increasing number of surgical oncology patients and the screening patients had to be scheduled for surgical intervention regarding the waiting time and indications of all patients. Second, during the analysed period our institution was the only hospital in Slovenia performing the surgery of screening patients. Recently another institution, after meeting all necessary quality checks, started to operate on these patients, which will contribute to lower the waiting times. Finally, in many patients longer preoperative preparation including examinations by other physicians (i.e. cardiologist, diabetologist etc.) were required and thus the surgical intervention was postponed until it could be safely performed.

Several measures have been taken to shorten waiting time. First, patients were referred to the

TABLE 5. The variability of QIs within the institution for each studying year and altogether

	All	2016	2017	2018	
Therapeutic procedures	Number of procedures: least active surgeon - most active surgeon	1-166	1-45	6-62	1-67
	Proportion of mastectomies: surgeon with lowest proportion - surgeon with highest proportion	17.8%-100.0%	10.0%-100.0%	12.5%-44.4%	0.0%-100.0%
	Median waiting time (in days): surgeon with lowest - surgeon with highest waiting time	28.0-45.0	24.0-45.0	27.0-41.0	23.0-136.0
	Single (breast) operation for the primary tumour (excluding reconstruction): surgeon with lowest - surgeon with highest proportion	83.1%-100.0%	73.3%-100.0%	71.4%-100.0%	75.0%-100.0%
	Invasive breast cancer not greater than 3 cm who underwent BCT: surgeon with lowest - surgeon with highest proportion	0.0%-92.6%	0.0%-94.4%	40.0%-100.0%	77.8%-100.0%
	Weight (g) of the excised specimen from the breast: surgeon with lowest mean - surgeon with highest mean	35.5-89.0	33.5-104.5	28.0-94.0	37.0-81.5
	Patients with invasive cancer and axillary clearance performed with at least 10 LN examined: surgeon with lowest - surgeon with highest proportion	71.4%-100.0%	50.0%-100.0%	80.0%-100.0%	50.0%-100.0%
Diagnostic procedures	Number of procedures: least active surgeon - most active surgeon	3-30	1-12	1-11	1-12
	Median waiting time (in days): surgeon with lowest - surgeon with highest waiting time	25.5-45.0	24.0-59.0	28.5-76.0	20.0-71.0
	Weight (g) of the excised specimen from the breast: surgeon with lowest mean - surgeon with highest mean	18.0-70.0	22.0-73.0	15.0-55.0	18.0-94.0

BCT = breast conserving treatment; LN = lymph nodes

surgeon in maximum 2 weeks after the decision on operation was made within multidisciplinary meeting. Second, all other investigations needed before surgery were made on the day of appointment with surgeon. Finally, we provided additional time in operating theatre dedicated for women from screening program. Because of described measures, the waiting time had significantly improved over the next two years. Nevertheless, activities to shorten waiting time should be intensified to reach the minimum standard.

Three QIs from EUSOMA working group had been chosen to monitor the quality of surgery in women with proven breast cancer: proportion of patients (invasive and noninvasive cancers) who received a single (breast) operation for the primary tumour (excluding reconstruction), proportion of patients with invasive breast cancer not greater than 3 cm (total size, including DCIS component) who underwent BCT and proportion of patients with invasive cancer and axillary clearance performed with at least 10 LN examined. The recommended standard was met for the first two QIs every single year. Furthermore, QI proportion of patients with invasive breast cancer not greater than 3 cm (total size, including DCIS component) who underwent BCT significantly improved over the study period. On the other hand, we had not reached the minimal proportion of patients with invasive cancer and axillary clearance performed with at least 10 LN examined. However, in the majority of patients low number of examined lymph nodes was not the result of low technical skills of the surgeons, but rather the decision of the surgeons that complete axillary lymph node dissection might not be necessary, following the trends towards minimizing the axillary surgery as reviewed in an article by Henke *et al.*¹⁵ Overall, the number of these patients is very low. As more data become available that less aggressive axillary surgery does not affect survival in breast cancer patients, the inclusion of this QI in monitoring surgical quality control should be reconsidered. Indeed, in the last version of EUSOMA QIs from 2017, this QI is no longer included and was replaced by QI monitoring the ability to avoid axillary overtreatment (proportion of patients with no more than 5 SLN excised).⁵

As the breast is aesthetically sensitive organ and important for woman's self-esteem, the cosmetic results are of utmost importance in breast surgery. However, measurement of cosmetic results are difficult and subjective assessments could not be ruled out. Weight of the excised specimen is a proxy for expected final cosmetic result and preserved shape

and symmetry with the contralateral breast.¹⁶ Although far from ideal as it does not take into account the effect of oncoplastic reconstruction, it represents an objective measurement of the surgeon's ability to balance between aggressiveness and clear margins on the one hand and cosmetic issues on the other. The weight of the specimen was significantly reduced in the second and third studying year compared to the first one for therapeutic procedures and a trend towards weight reduction was observed for diagnostic procedures. However, the goal was still not met and efforts to reduce the weight of the specimens should be continued.

Besides monitoring surgical QIs at the institutional level, we also analysed the variability of management among surgeons. As all surgeons were informed about their own results each year, we would expect that the variability among surgeons becomes less pronounced over time. However, the variability remained high throughout the studying years, which is most probably the reflection of the number of surgeons involved in breast surgery at our department. As recommended by EUSOMA, any breast surgeon at the breast centre must carry out primary surgery as first operator on at least 50 newly diagnosed breast cancers a year. If the centre has surgeons in training, those responsible for supervising trainees might perform fewer than 50 primary cases as first operator. In this case documentation on their role as second operator supervising trainees must be available.¹⁷ Although surgeons involved in breast surgery at our department operate other breast lesions besides those detected in the screening program, many surgeons still do not meet the requested volume standards. To further improve the compliance with QIs and to reduce the variability of surgical management inside the institution, the importance of concentrating the breast pathology to a reduced number of surgeons meeting the requested standards could not be overemphasized. It seems that this measure may provide important step towards improved quality of breast surgery.

Although many studies addressed the compliance to QIs as defined by EUSOMA, our study is the first considering only screen-detected breast lesions and including both, diagnostic and therapeutic procedures. Since women with screen-detected lesions represent a specific population and the quality of management of those women, including the quality of surgery, is important not only for the woman in question but also for the appropriate participation rate and the operation of the screening program as a whole, we included QIs specifi-

cally recommended for screen-detected lesions as well. As a result, our results are not fully comparable to other studies considering EUSOMA QIs only. Nevertheless, the results from other studies show, similar to ours, that complete adherence to guidelines is difficult to achieve. However, continuous monitoring is of paramount importance as it results in better performance of QIs over time.¹⁸⁻²⁰

Besides being the first study addressing the topic of monitoring surgical QIs within breast cancer screening program, other strengths of our study are large number of included cases, comprehensive data collection from a prospective database and thus low number of missing data and the recent nature of the data. Furthermore, in the study period all patients with screen-detected lesions detected in the national screening program, underwent surgery at our institution, minimizing the selection bias. The limitations of our study are limited number of QIs that were monitored and inclusion of old EUSOMA QIs defined in 2010. Looking ahead, a set of our QIs should be updated according to the latest EUSOMA recommendations. Furthermore, all potential cofounders were not taken into account in our analysis. First, the results of most EUSOMA indicators improves over time independent of quality control as demonstrated by van Dam *et al.*¹⁸; these time trends were not considered in our study. Second, without multivariate analysis adjusting for differences in case mix firm conclusions are difficult to draw. In conclusion, our results showed that adherence to all surgical QIs in patients from screening program is difficult to achieve, especially to those specifically defined for screen-detected lesions. Nevertheless, regular quality control may improve results over time. Reducing the number of surgeons dedicated to breast pathology may reduce variability of management inside the institution.

Acknowledgment

The study was supported by the research program of the Slovenian research agency P3-0352.

References

1. Ferlay J, Colombet M, Soerjomataram I, Dyba T, Randi G, Bettio M, et al. Cancer incidence and mortality patterns in Europe: estimates for 40 countries and 25 major cancers in 2018. *Eur J Cancer* 2018; **103**: 356-87. doi: 10.1016/j.ejca.2018.07.005
2. Wang F, Shu X, Meszoely I, Pal T, Mayer IA, Yu Z, et al. Overall mortality after diagnosis of breast cancer in men vs women. *JAMA Oncol* 2019. [Epub ahead of print]. doi: 10.1001/jamaoncol.2019.2803
3. Lauby-Secretan B, Scoccianti C, Loomis D, Benbrahim-Tallaa L, Bouvard V, Bianchini F, et al. Breast-cancer screening-viewpoint of the IARC working group. *N Engl J Med* 2015; **372**: 2353-8. doi: 10.1056/NEJMsr1504363
4. Myers ER, Moorman P, Gierisch JM, Havrilesky LJ, Grimm LJ, Ghate S, et al. Benefits and harms of breast cancer screening: a systematic review. *JAMA - J Am Med Assoc* 2015; **314**: 1615-34. doi: 10.1001/jama.2015.13183
5. Biganzoli L, Marotti L, Hart CD, Cataliotti L, Cutuli B, Kühn T, et al. Quality indicators in breast cancer care: an update from the EUSOMA working group. *Eur J Cancer* 2017; **86**: 59-81. doi: 10.1016/j.ejca.2017.08.017
6. Rosselli Del Turco M, Ponti A, Bick U, Biganzoli L, Cserni G, Cutuli B, et al. Quality indicators in breast cancer care. *Eur J Cancer* 2010; **46**: 2344-56. doi: 10.1016/j.ejca.2010.06.119
7. Perry N, Broeders M, de Wolf C, Tornberg S, Holland R, von Karsa L. European guidelines for quality assurance in breast cancer screening and diagnosis [Internet]. *Eur Guidel* 2006 [cited 2020 Mar 30]. Available from: http://screening.iarc.fr/doc/ND7306954ENC_002.pdf
8. DORA programme colleagues. [Annual Report on the DORA Breast Cancer National Screening Program 2018]. [Slovenian]. [Internet]. Institute of Oncology Ljubljana - DORA National Breast Cancer Screening Programme 2019 [cited 2020 Mar 30]. Available from: https://dora.onko-i.si/fileadmin/user_upload/Dokumenti/DORA_letno_porocilo_2018_knjiznica.pdf
9. Cicero U, Rietjens M, Mahmoud ET, Virgilio S. *Oncoplastic and reconstructive breast surgery*. Cham: Springer; 2019.
10. Rizzo M, Bumpers H, Okoli J, Senior-Crosby D, O'Regan R, Zelnak A, et al. Improving on national quality indicators of breast cancer care in a large public hospital as a means to decrease disparities for african american women. *Ann Surg Oncol* 2011; **18**: 34-9. doi: 10.1245/s10434-010-1204-z
11. Wilcox N, McNeil JJ. Clinical quality registries have the potential to drive improvements in the appropriateness of care. *Med J Aust* 2016; **205**: S27-9. doi: 10.5694/mja15.00921
12. Cheng SH, Wang CJ, Lin JL, Horng CF, Lu MC, Asch SM, et al. Adherence to quality indicators and survival in patients with breast cancer. *Med Care* 2009; **47**: 217-25. doi: 10.1097/MLR.0b013e3181893c4a.
13. Van Dam PA, Verheyden G, Sugihara A, Trinh XB, Van Der Mussele H, Wuyts H, et al. A dynamic clinical pathway for the treatment of patients with early breast cancer is a tool for better cancer care: implementation and prospective analysis between 2002-2010. *World J Surg Oncol* 2013; **11**: 70. doi: 10.1186/1477-7819-11-70
14. Plavc G, Ratoša I, Žagar T, Zadnik V. Explaining variation in quality of breast cancer care and its impact: a nationwide population-based study from Slovenia. *Breast Cancer Res Treat* 2019; **175**: 585-94. doi: 10.1007/s10549-019-05186-z
15. Henke G, Knauer M, Ribi K, Hayoz S, Gerard MA. Tailored axillary surgery with or without axillary lymph node dissection followed by radiotherapy in patients with clinically node-positive breast cancer (TAXIS): study protocol for a multicenter, randomized phase-III trial. *Trials* 2018; **19**: 667. doi: 10.1186/s13063-018-3021-9
16. Ojala K, Meretoja TJ, Leidenius MHK. Aesthetic and functional outcome after breast conserving surgery - Comparison between conventional and oncoplastic resection. *Eur J Surg Oncol* 2017; **43**: 658-64. doi:10.1016/j.ejso.2016.11.019
17. Biganzoli L, Cardoso F, Beishon M, Cameron D, Cataliotti L, Coles CE, et al. The requirements of a specialist breast centre. *Breast* 2020; **51**: 65-84. doi: 10.1016/j.breast.2020.02.003
18. Van Dam PA, Tomatis M, Marotti L, Heil J, Mansel RE, Rosselli del Turco M, et al. Time trends (2006-2015) of quality indicators in EUSOMA-certified breast centres. *Eur J Cancer* 2017; **85**: 15-22. doi: 10.1016/j.ejca.2017.07.040
19. Van Dam PA, Tomatis M, Marotti L, Heil J, Wilson R, Rosselli Del Turco M, et al. The effect of EUSOMA certification on quality of breast cancer care. *Eur J Surg Oncol* 2015; **41**: 1423-9. doi: 10.1016/j.ejso.2015.06.006
20. Hartmann-Johnsen OJ, Kåresen R, Schlichting E, Naume B, Nygård JF. Using clinical cancer registry data for estimation of quality indicators: Results from the Norwegian breast cancer registry. *Int J Med Inform* 2019; **125**: 102-9. doi: 10.1016/j.ijmedinf.2019.03.004

Experimental validation of Monte Carlo based treatment planning system in bone density equivalent media

Djeni Smilovic Radojic^{1,3}, Bozidar Casar^{2,4}, David Rajlic¹, Manda Svabic Kolacio¹, Ignasi Mendez², Nevena Obajdin¹, Dea Dundara Debeljuh^{1,5}, Slaven Jurkovic^{1,3}

¹ Medical Physics Department, University Hospital Rijeka, Rijeka, Croatia

² Department for Dosimetry and Quality of Radiological procedures, Institute of Oncology Ljubljana, Ljubljana, Slovenia

³ Department of Medical Physics and Biophysics, Faculty of Medicine, University of Rijeka, Rijeka, Croatia

⁴ Faculty of Mathematics and Physics, University of Ljubljana, Ljubljana, Slovenia

⁵ General Hospital Pula, Radiology Department, Pula, Croatia

Radiol Oncol 2020; 54(4): 495-504.

Received 10 June 2020

Accepted 9 July 2020

Correspondence to: Assist. prof. Slaven Jurkovic, Ph.D., Medical Physics Department, University Hospital Rijeka, Kresimirova 42, HR-51000 Rijeka, Croatia. E-mail: slaven.jurkovic@medri.uniri.hr

Disclosure: No potential conflicts of interest were disclosed.

Djeni Smilovic Radojic and Bozidar Casar have equally contributed to this work.

Introduction. Advanced, Monte Carlo (MC) based dose calculation algorithms, determine absorbed dose as dose to medium-in-medium ($D_{m,m}$) or dose to water-in-medium ($D_{w,m}$). Some earlier studies identified the differences in the absorbed doses related to the calculation mode, especially in the bone density equivalent (BDE) media. Since the calculation algorithms built in the treatment planning systems (TPS) should be dosimetrically verified before their use, we analyzed dose differences between two calculation modes for the Elekta Monaco TPS. We compared them with experimentally determined values, aiming to define a supplement to the existing TPS verification methodology.

Materials and methods. In our study, we used a 6 MV photon beam from a linear accelerator. To evaluate the accuracy of the TPS calculation approaches, measurements with a Farmer type chamber in a semi-anthropomorphic phantom were compared to those obtained by two calculation options. The comparison was made for three parts of the phantom having different densities, with a focus on the BDE part.

Results. Measured and calculated doses were in agreement for water and lung equivalent density materials, regardless of the calculation mode. However, in the BDE part of the phantom, mean dose differences between the calculation options ranged from 5.7 to 8.3%, depending on the method used. In the BDE part of the phantom, neither of the two calculation options were consistent with experimentally determined absorbed doses.

Conclusions. Based on our findings, we proposed a supplement to the current methodology for the verification of commercial MC based TPS by performing additional measurements in BDE material.

Key words: treatment planning system; dose-to-medium; dose-to-water; experimental validation of dose calculation; Monte Carlo

Introduction

Implementation of advanced radiation therapy techniques into clinical practice has set high demands on the quality and accuracy of various devices used for radiation treatment planning, treatment delivery, and dose verification. Besides the required high performance of medical linear accelerators and their ancillary systems, there are also strict requirements on dose calculation and

optimization using treatment planning systems (TPS). Precise dose calculation is one of the most critical steps in the radiation therapy process since it is the basis for accurate and safe treatment delivery using high-energy photon beams. To provide necessary dosimetric accuracy, the verification of the calculated doses should be performed using a reproducible and reliable methodology. To ensure acceptable reliability of the verification results, an appropriate methodology for dose verification

should be carefully selected, while the limitations of the specific method must be fully understood. The latter is essential for an adequate interpretation of the verification results.

Comprehensive verification methodology for the evaluation of calculation algorithms built in the TPSs has been proposed by the International Atomic Energy Agency (IAEA).^{1,2} However, the rapid development of treatment delivery devices and, consequently, the utilization of the advanced radiation therapy techniques call for further development of the verification methods. In some published studies and documents³⁻⁵, methodologies for the verification of dosimetry parameters for the implementation of Intensity Modulated Radiotherapy (IMRT) have been proposed. However, neither the means of verification nor the methods were explicitly spelled out.

Presently, Monte Carlo based dose calculation algorithms built in the TPS are assumed to be the most accurate computational systems for the appropriate simulation of particle transport and dose calculation.^{6,7} Those algorithms offer two alternative options for the calculation and reporting of the absorbed dose: dose-to-medium as calculated by Monte Carlo algorithms, referred as dose to medium-in-medium, $D_{m,m}$, and dose-to-water converted from dose-to-medium using stopping power ratios water-to-medium, referred as dose to water-in-medium, $D_{w,m}$, or sometimes “biological dose to water”.⁸⁻¹⁰ The first approach calculates absorbed energy in a medium voxel divided by the mass of the medium element, while the second calculates the absorbed energy in a small cavity of water divided by the mass of that cavity. For brevity, $D_{m,m}$ and $D_{w,m}$ calculation options will be denoted as D_m (dose-to-medium) and D_w (dose-to-water) respectively in the rest of the paper.

Since it is a matter of debate whether to use D_m or D_w calculation approach for dose planning⁹⁻¹³, the American Association of Physicists in Medicine (AAPM) Task Group 105¹⁰ recommended that the material to which the dose is computed should be explicitly indicated and conversion between dose-to-medium and dose-to-water calculation modes should be available. Several previously published studies^{9,12,14-16} were dedicated to comparisons of the two mentioned calculation modes built in the contemporary TPSs. Those studies have shown that differences between dose-to-medium and dose-to-water calculation modes can be expected in bone density equivalent (BDE) material. While D_m is the quantity inherently computed by MC dose algorithms, D_w calculation approach is still indis-

pensable in clinical radiation therapy due to some practical and historical experience of prescribers.¹⁰ Because there is still no agreement regarding the calculation approach that should be used as a clinical standard and due to the absence of the appropriate verification methodology, the present work aimed to propose a supplement to the existing verification methodology to establish the validity of both approaches. For that purpose, calculated absorbed doses using D_m and D_w options were compared to those determined experimentally in the semi-anthropomorphic phantom focusing on the dose differences in the part of the phantom having density close to the bone density.

The ultimate goal of the study was to define and propose an additional verification procedure as a supplement to the set of existing preclinical commissioning tests provided in the IAEA TECDOC 1583², for the specific case where TPS uses Monte Carlo based calculation algorithms. Such additional test may well eliminate potential misinterpretations of the commissioning results for bone density material, where D_m and D_w calculation approaches lead to different conclusions.^{9,12,14-16}

We have to note that the proposed addendum to the verification methodology has no intention to be an answer to which reporting mode, D_m or D_w , should be used for radiotherapy treatment prescription or dose calculation, neither to discuss possible limitations of the conversion methodology from D_m to D_w , which is based on stopping power ratios water-to-medium.⁸

Materials and methods

In this work we used 6 MV photon beam generated by Siemens Oncor Expression (Siemens Healthineers, Erlangen, Germany) linear accelerator, Siemens Somatom Open Computerized Tomography (CT) simulator (Siemens Healthineers, Erlangen, Germany) and Elekta Monaco treatment planning system version 5.11 (Elekta, Stockholm, Sweden). Monaco TPS is a Monte Carlo based system which calculates absorbed dose using the D_m approach that can be converted to D_w mode using water-to-medium stopping power ratios to account for different energy absorption in both media.¹⁷ Linear accelerator and Elekta Monaco ver. 5.11 TPS were commissioned and prepared for the clinical implementation of Intensity Modulated Radiotherapy according to the international recommendations.^{1,2,4,18-21} All dosimetric measure-

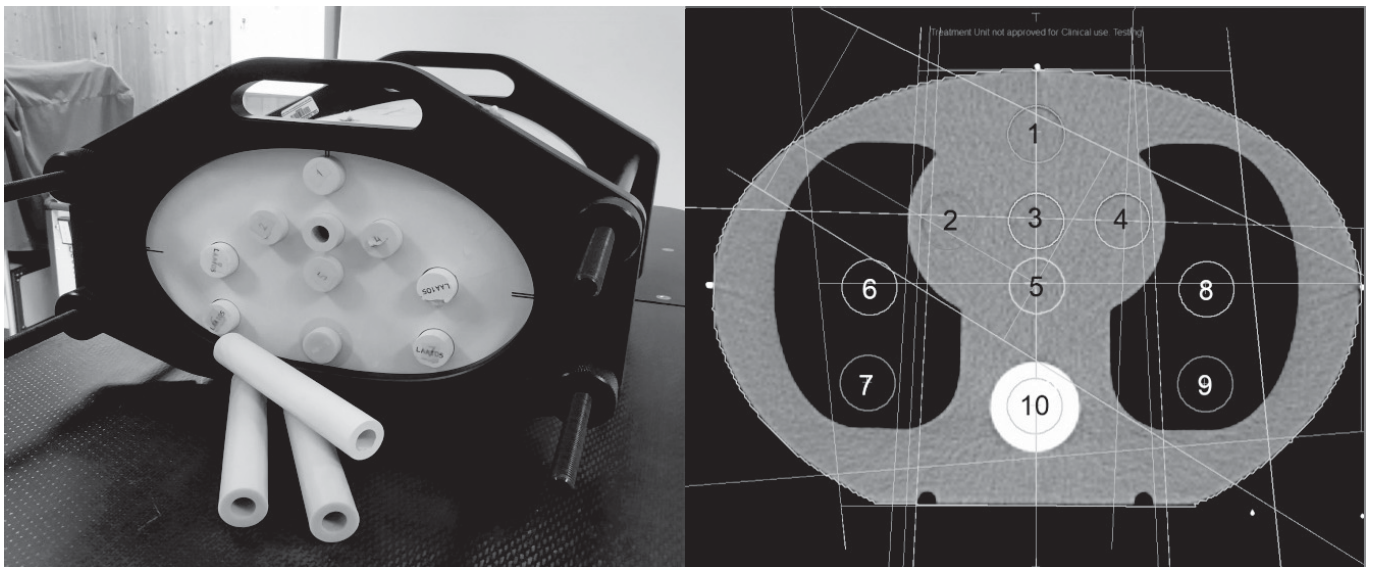


FIGURE 1. Photo of the semi-anthropomorphic CIRS Thorax phantom with interchangeable rod inserts (left) and its CT image (right). Positions of 10 interchangeable rod inserts are marked with numbers from 1 to 10. Five measuring points are in the water equivalent part of the phantom (grey area), four points are in the lung density equivalent material (black area), and one point is in the bone density equivalent part of the phantom.

ments were performed using a PTW 30013 Farmer type ionization chamber and PTW UNIDOS electrometer (PTW, Freiburg, Germany).

Standard measurements in the CIRS Thorax phantom

Accuracy of the TPS Monaco ver. 5.11 calculation algorithm was experimentally verified using a semi-anthropomorphic CIRS Thorax phantom (CIRS Inc., Norfolk, VA, USA) consisting of a body made of water equivalent material ($\rho = 1.003 \text{ g/cm}^3$), lung equivalent parts ($\rho = 0.207 \text{ g/cm}^3$), and bone equivalent part ($\rho = 1.506 \text{ g/cm}^3$) with cylindrical holes for placement of ionization chamber into interchangeable rod inserts having three different densities.² The phantom was scanned using the Somatom Open CT simulator. Acquired CT images were used for the delineation of volumes of interest and subsequent dose calculations. Measurements of absorbed dose were performed at ten measuring positions within the phantom (Figure 1) for 15 different irradiation set-ups (Table 1), using a PTW Farmer-type ionization chamber. All measurements were carried out at the central part of the selected radiation fields, excluding the regions of high dose gradients.

Measured doses were compared to the corresponding doses obtained by both calculation options, D_m and D_w . Dose differences δD_m and δD_w between measured and calculated values for

dose-to-medium and dose-to-water calculation approach, were calculated according to the IAEA methodology^{1,2} as:

$$\delta D_m = 100 \cdot \frac{D_m - D_{meas}}{D_{meas,ref}} \quad [1]$$

$$\delta D_w = 100 \cdot \frac{D_w - D_{meas}}{D_{meas,ref}} \quad [2]$$

where D_{meas} denotes measured absorbed dose at the selected measuring point, while $D_{meas,ref}$ stands for the absorbed dose measured at the reference point, which was chosen on the central axis of the beam at the isocenter (Table 1).

Dose differences δD_m and δD_w between calculated and measured doses were analysed for both calculation options through the comparison of the respective average values $\overline{\delta D_m}$ and $\overline{\delta D_w}$

$$\overline{\delta D_m} = \frac{1}{n} \sum_{i=1}^{i=n} \delta D_{m,i} \quad [3]$$

$$\overline{\delta D_w} = \frac{1}{n} \sum_{i=1}^{i=n} \delta D_{w,i} \quad [4]$$

The index i stands for a particular dose difference for i -th dose measurement and corresponding calculated dose for two different calculation modes in the selected part of the CIRS Thorax phantom (water equivalent part, lung equivalent part, or bone density equivalent part).

TABLE 1. Irradiation set-ups for measurements in 6 MV photon beam used for experimental verification of the Monaco ver. 5.11 treatment planning systems (TPS) calculation algorithm in the semi-anthropomorphic CIRS Thorax phantom. Reference and measuring points (I_1 to I_{10}) are shown in the last two columns; subscripts 1 to 10 correspond to the labelling in Figure 1

Set-up	Irradiation geometry	Field size [cm ²]	SSD/SAD	Gantry angle [°]	reference point	measuring points
1	Single square fields	10×10	SSD	0	I_5	I_1, I_3, I_{5-10}
2		10×10	SAD	0	I_5	I_1, I_3, I_{5-10}
3		4×4	SAD	0	I_5	I_{1-9}
4		10×10	SAD	90	I_3	I_{2-10}
5	Rectangular field	10× 15	SAD	300	I_1	$I_1, I_4, I_{6-8}, I_{10}$
6	Single asymmetric fields	(6+8)×15	SAD	0	I_5	I_{1-10}
7		(3+8)×15	SAD	90	I_5	I_1, I_{5-10}
8		(4+10)×15	SAD	180	I_5	I_{1-3}, I_{5-10}
9		(3+7)×15	SAD	300	I_5	I_{2-10}
10	4 fields (box)	12×10	SAD	0	I_5	I_{2-5}
		12×10	SAD	180		
		12×8	SAD	90		
		12×8	SAD	270		
11	3 fields	4×4	SAD	30	I_5	I_2, I_{5-9}
		16×4	SAD	90		
		16×4	SAD	270		
12	Diamond-shaped field	14×14	SAD	0	I_3	I_1, I_3, I_{5-10}
13	Irregular L shaped field	/	SAD	45	I_1	$I_{1-2}, I_{4-6}, I_{8-10}$
14	MLC cylinder shaped field	/	SAD	0	I_2	$I_{1,2}, I_5, I_{8,9}, I_{10}$
15	3 non-coplanar fields	16×4	SAD	90	I_5	$I_1, I_{5-6}, I_8, I_{10}$
		4×4 ^a	SAD	30		

^a Couch angle = 270°

SAD = source to axis distance; SSD = source to surface distance

Throughout the study, all calculations within Monaco TPS were performed on a 0.2 cm calculation grid, with 0.5% statistical uncertainty per control point.

Differences between D_m and D_w calculation modes in the bone density equivalent part of the CIRS Thorax phantom

In the second part of the study, we were aiming to determine differences between D_m and D_w calculation approaches in the Monaco ver. 5.11 TPS in the bone equivalent part of the CIRS Thorax phantom, following the same methodology as described in the preceding section.

Three irradiation geometries (single asymmetric rectangular fields having different gantry angles: 0°, 90°, and 180°) were selected for this part of

the study (Table 1, set-ups 6, 7, and 8). For each of those irradiation geometries, two phantom assemblies were used to analyze differences between the two calculation approaches with respect to the measurements performed by PTW 30013 Farmer type ionization chamber in the bone density equivalent (BDE) part of the CIRS Thorax phantom. In the first assembly, referred to as *non-standard*, the water equivalent insert with the ionization chamber was placed into the BDE part of the phantom (Figure 2A). In this way, the measuring point in the phantom was surrounded by water equivalent material of sufficient thickness to fulfill conditions required by the Bragg-Gray cavity theory for the determination of absorbed dose in terms of dose to water. In the second assembly, referred to as *standard*, the BDE insert was placed in the BDE part of the phantom (Figure 2B).

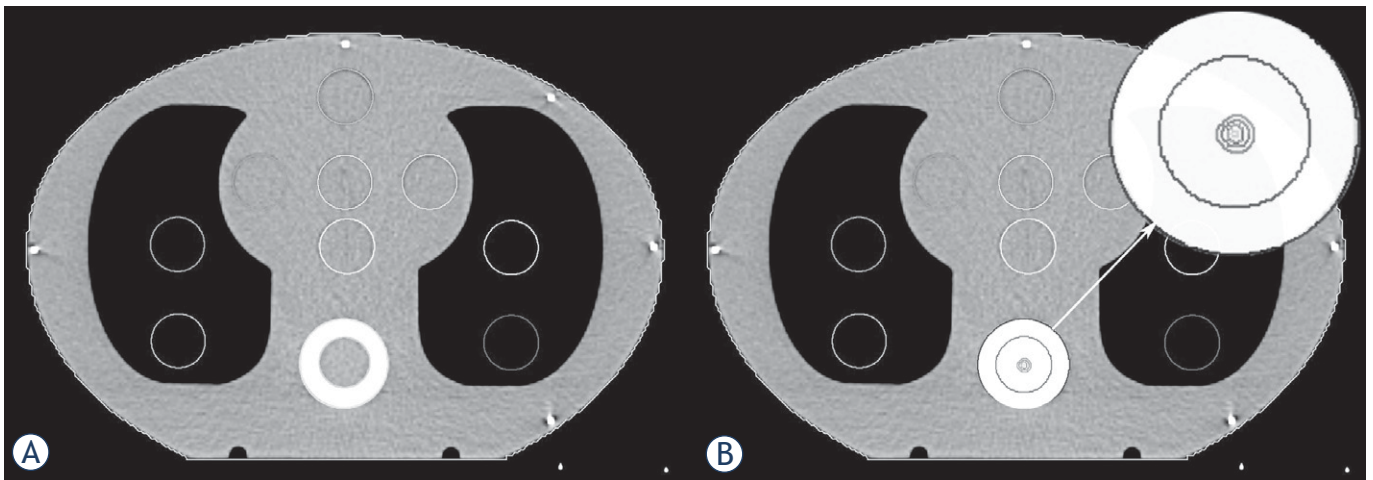


FIGURE 2. CT image of the CIRS Thorax phantom: water equivalent insert inside BDE part of the phantom (A); a BDE insert inside bone density equivalent (BDE) part of the phantom (B) and cross-section of small “water cylinders” of different dimensions delineated inside BDE part of the phantom to find limits for calculating geometry where cavity theory applies (top right).

In the last part of the study, the phantom assembly was additionally virtually modified for the calculation purposes in the Monaco TPS: cylinders of various volumes (constant length and different diameters) were delineated inside the BDE insert on the CT scans (Figure 2, top right). This approach was utilized to obtain the limits above which the differences between D_m and D_w calculation approaches become non-significant and in agreement with experimentally determined absorbed doses. The length of the cylinders was set equal to the length of the cavity volume of the PTW 30013 ionization chamber, while the electron density of such cylinders was set to be equal to the electron density of the water. According to the IAEA TRS-398 Code of practice²², the charge measured by an ionization chamber calibrated in terms of absorbed dose to water is directly proportional to the absorbed dose in water at the point of measurement in the absence of the chamber. By delineating cylinders having the electron density of water inside the BDE part of the phantom, we have tried to simulate the mentioned theoretical situation to different degrees.

To verify the accuracy of dose-to-medium and dose-to-water calculation modes, we have analyzed differences δD_m and δD_w between calculated and measured absorbed doses for both calculation modes and different volumes of “water cylinders” smaller than the volume of the PTW 30013 ionization chamber’s cavity volume (0.6 cm^3), using Eqs. [1] to [4]. We were aiming to find the volume of “water cylinder,” above which there will exist an agreement between calculated and measured doses without a statistically significant difference

between both calculation approaches. Our final challenge was to define an addendum to the existing TPS verification methodology based on the described method and experimental findings from the present work.

Evaluation of results and estimation of uncertainties

The uncertainty of $\overline{\delta D_m}$ was estimated as the combination in quadrature of the statistical uncertainty of $\overline{\delta D_m}$ and the uncertainty of Monte Carlo calculation of 0.5% (1 SD) for D_m , using a coverage factor $k = 2$ (2 SD). The uncertainty of $\overline{\delta D_w}$ was calculated in the same manner.

We considered that the D_m and D_w calculation modes differed significantly within 95% confidence limits (two standard deviations – 2 SD, *i.e.*, coverage factor $k = 2$) if the relation

$$|\overline{\delta D_m} - \overline{\delta D_w}| > u_c(k = 2) \quad [5]$$

was satisfied. u_c is a combined uncertainty which was determined as the combination in quadrature of the individual uncertainties of $\overline{\delta D_m}$ and $\overline{\delta D_w}$. This estimation was considered conservative due to the fact that the uncertainties of the terms $D_{meas}/D_{meas,ref}$ were included in the compute of the individual uncertainties $\overline{\delta D_m}$ and $\overline{\delta D_w}$.

Secondly, we considered that the dose calculations within Monaco TPS were in agreement with the experimentally determined doses if the conditions

$$|\overline{\delta D_m}| < 1\% \quad [6]$$

$$|\overline{\delta D_w}| < 1\% \quad [7]$$

were satisfied. At this point we note, that throughout the rest of the paper all combined uncertainties are stated within two standard deviations, *i.e.*, using a coverage factor $k = 2$.

Results

Standard measurements in the CIRS Thorax phantom

Differences between calculated and measured absorbed doses for two calculation modes, dose-to-medium D_m and dose-to-water D_w , were determined using Eqs. [1] and [2] for all 15 standard irradiation configurations and ten measurement points in the CIRS Thorax semi-anthropomorphic phantom (Table 1). Mean values of percentage dose differences $\overline{\delta D_m}$ and $\overline{\delta D_w}$ calculated by Eqs. [3] and [4] are presented with corresponding uncertainties in terms of two standard deviations in Figure 3, separately for the water equivalent part (five measurement points), lung density equivalent part (four measurement points), and BDE part (one measurement point) of the phantom. Statistical significance of the obtained

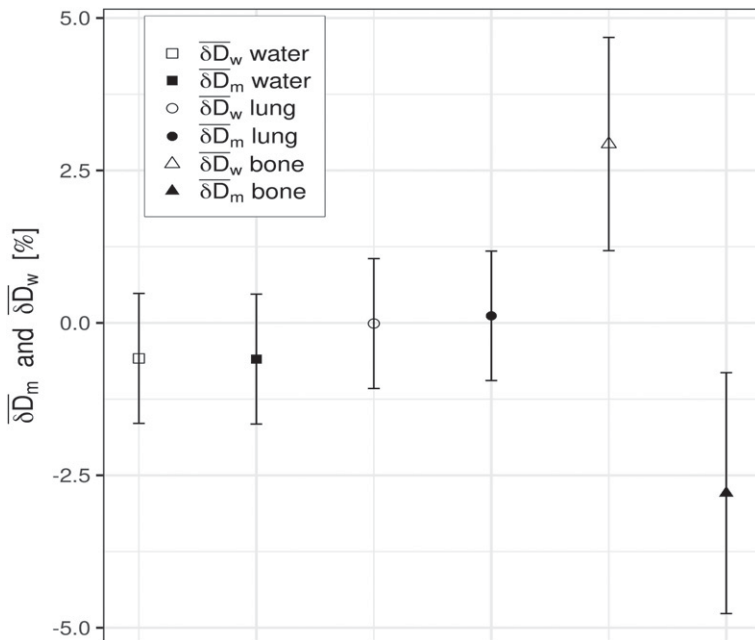


FIGURE 3. Mean percentage dose differences $\overline{\delta D_m}$ and $\overline{\delta D_w}$ between calculated and measured doses in different parts of the CIRS Thorax phantom (water, lung, and bone density equivalent materials) for both calculation options built in the Monaco TPS: dose-to-medium D_m and dose-to-water D_w . Error bars represent corresponding combined uncertainties.

differences between $\overline{\delta D_m}$ and $\overline{\delta D_w}$ was evaluated using the relations shown in Eqs. [5] to [7].

Comparison of measured and calculated doses in the water equivalent part of the phantom showed that the mean percentage dose difference for all points was -0.6% ($u_C = 1.1\%$) for the dose-to-medium calculation mode and -0.6% ($u_C = 1.1\%$) for the dose-to-water calculation mode (Figure 3). The two calculations were found not to be significantly different within 95% confidence limits since the condition from Eq. [5] was not satisfied: $|\overline{\delta D_m} - \overline{\delta D_w}| = 0.0\%$ ($u_C = 1.5\%$).

Comparison of measured and calculated doses in the lung density equivalent part of the phantom showed that $\overline{\delta D_m} = 0.1\%$ ($u_C = 1.1\%$) for the dose-to-medium calculation approach, while $\overline{\delta D_w} = 0.0\%$ ($u_C = 1.1\%$) for the dose-to-water mode (Figure 3). Also in this case, the difference between both applied calculation approaches was statistically non-significant within 95% confidence limits: $|\overline{\delta D_m} - \overline{\delta D_w}| = 0.1\%$ ($u_C = 1.5\%$).

In the bone density equivalent part of the CIRS Thorax phantom, the percentage dose differences between the two calculation options were larger than in the previous two cases (Figure 3). Mean difference $\overline{\delta D_m}$ for the dose-to-medium calculation mode was -2.8% ($u_C = 2.0\%$), while for the dose-to-water calculation approach the mean difference $\overline{\delta D_w}$ was 2.9% ($u_C = 1.8\%$). Consequently and importantly, in the BDE part of the phantom, the absolute differences between the two calculation modes were found to be statistically significant within 95% confidence limits: $|\overline{\delta D_m} - \overline{\delta D_w}| = 5.7\%$ ($u_C = 2.6\%$).

Dose calculations within Monaco TPS were in agreement with experimentally determined doses for water equivalent and lung equivalent parts of the CIRS Thorax phantom, since the conditions from Eqs. [6] and [7] were satisfied. On the contrary, for the BDE part of the phantom, conditions from Eqs. [6] and [7] were not satisfied. Therefore, we can conclude that the dose calculations in Monaco TPS ver. 5.11 were not in agreement with measured absorbed doses for the BDE part of the phantom, regardless of the calculation mode.

Differences between D_m and D_w calculation modes in the bone density equivalent part of the CIRS Thorax phantom

The second part of the study was focused on the differences between calculated and measured absorbed doses in the BDE part of the CIRS Thorax phantom. Three simple asymmetric fields with

different gantry angles were selected for that purpose utilizing two different phantom assemblies, *standard* and *non-standard*, as described in the section Materials and methods and shown in Table 1 (set-ups 6, 7, and 8) and Table 2.

For *non-standard* phantom geometry, we did not find statistically significant differences between measured and calculated absorbed doses: $\overline{\delta D}_m = -0.3\%$ ($u_C = 1.3\%$) and $\overline{\delta D}_w = 0.3\%$ ($u_C = 1.3\%$). In this case, the absolute difference $|\overline{\delta D}_m - \overline{\delta D}_w|$ between both approaches was 0.6% and was statistically non-significant within 95% confidence limits ($u_C = 1.8\%$).

In the *standard* phantom geometry, however, the differences $\overline{\delta D}_m$ and $\overline{\delta D}_w$ between measured and calculated doses were larger and statistically significant (Table 2). $\overline{\delta D}_m = -3.9\%$ ($u_C = 2.1\%$) and $\overline{\delta D}_w = 4.4\%$ ($u_C = 1.9\%$).

The absolute value of the difference between both approaches was in this case statistically significant: $|\overline{\delta D}_m - \overline{\delta D}_w| = 8.3\%$ ($u_C = 2.8\%$).

As a final point, we investigated differences between calculated and measured doses in the phantom, which was virtually modified for the calculation purposes, as described in the section Materials and methods. Results for five delineated "water cylinders," including the results for *standard* geometry ($V = 0 \text{ cm}^3$), are presented in Table 3. Differences gradually decrease as the volumes of delineated "water cylinders" become larger. The maximal difference was $|\overline{\delta D}_m - \overline{\delta D}_w| = 8.3\%$, for $V = 0 \text{ cm}^3$ (*i.e.*, BDE plug without delineated "water cylinder"). The smallest difference of 0.1% between $\overline{\delta D}_m$ and $\overline{\delta D}_w$ was found for the largest investigated "water cylinder" of volume 0.573 cm^3 . This difference was statistically non-significant within 95% confidence limits ($u_C = 1.9\%$).

Discussion

Standard measurements in the CIRS Thorax phantom

Differences between calculated and measured doses in the water equivalent part of the CIRS Thorax semi-anthropomorphic phantom were within 1% and not significantly different from zero (Eqs. [6] and [7]), regardless of the applied calculation option. The latter is in good agreement with previously published data.^{9,16} Similarly, in lung density equivalent material, the calculated mean percentage dose differences were not significantly different than zero for both calculation modes, confirming the results from previously published studies.^{3,9,13}

TABLE 2. Differences δD_m and δD_w between two different calculation options in the Monaco ver. 5.11. treatment planning systems (TPS) and measured data obtained in the bone density equivalent (BDE) part of the CIRS Thorax phantom, according to Eqs. [1] and [2]. Two phantom assemblies and three simple beam set-ups were considered for this part of the study

Irradiation geometry (field, gantry)	Phantom assembly	δD_m [%]	δD_w [%]
(6+8) x 15 cm ² Gantry = 0°	standard ^a	- 2.9	2.9
	non-standard ^b	- 0.7	- 0.2
(3+8) x 15 cm ² Gantry = 90°	standard ^a	- 3.0	5.1
	non-standard ^b	- 0.7	- 0.1
(4+10) x 15 cm ² Gantry = 180°	standard ^a	- 5.7	5.4
	non-standard ^b	0.5	1.3

^a BDE insert with the ionization chamber placed in the BDE part of the phantom

^b Water equivalent insert with the ionization chamber placed in the BDE part of the phantom

TABLE 3. Mean differences, $\overline{\delta D}_m$ and $\overline{\delta D}_w$, between calculated and measured doses in the bone density equivalent (BDE) part of the CIRS Thorax phantom for D_m and D_w calculation approaches, respectively. The absorbed doses were calculated using the Monaco ver. 5.11 treatment planning systems (TPS) in the center of delineated "water cylinders" of volume V , in the BDE part of the phantom. Corresponding combined uncertainties are denoted as $u_{C,m}$ and $u_{C,w}$ for dose-to-medium and dose-to-water calculation options, respectively

V [cm ³]	$\overline{\delta D}_m$ [%]	$u_{C,m}$ [%]	$\overline{\delta D}_w$ [%]	$u_{C,w}$ [%]
0	- 3.9	2.1	4.4	1.9
0.035	- 2.6	1.5	2.5	1.9
0.141	- 1.4	1.3	1.8	1.7
0.279	- 0.3	1.2	1.2	1.5
0.573	0.3	1.4	0.4	1.3

The differences between the two calculation approaches, dose-to-medium and dose-to-water, were, however, significant in BDE media (Table 2 and Figure 3). Andreo *et al.*⁹ have shown that a 10% difference in ICRP bone can be expected for Monaco ver. 5.0 TPS between two calculation modes after conversion of D_m to D_w . Results of the present study confirm those findings as well as the opposite signs of mean percentage dose differences for D_m and D_w reporting modes in the case when Monaco ver. 5.11 TPS has been used. Considerable differences between calculated dose distributions using D_m and D_w calculation approaches have also been reported in clinical studies.^{15,23}

Differences between D_m and D_w calculation modes in the bone density equivalent part of the CIRS Thorax phantom

In the BDE part of the CIRS Thorax semi-anthropomorphic phantom, mean percentage dose differences $\overline{\delta D}_m$ and $\overline{\delta D}_w$ were calculated by applying

Eqs. [1] and [2] for two phantom assemblies - *standard* and *non-standard* and three selected irradiation geometries, as shown in Table 2. In the case of *non-standard* geometry, both $\overline{\delta D}_m$ and $\overline{\delta D}_w$ were within 1%, demonstrating that there is a negligible difference between applied calculation modes.

However, differences between the respective mean values $\overline{\delta D}_m = -3.9\%$ and $\overline{\delta D}_w = 4.4\%$ were statistically significant if *standard* geometry was utilized. The latter case was also assumed as our first result in the part of the study where we attempted to find the volume of "water cylinder" delineated in the Monaco ver. 5.11 TPS for which the difference between $\overline{\delta D}_m$ and $\overline{\delta D}_w$ would become non-significant.

For further discussion, analysis, and graphical presentation, the exponential function was selected to fit the data from Table 3. The general form of the fitting function is given as

$$y = a + b \cdot e^{cx} \quad [8]$$

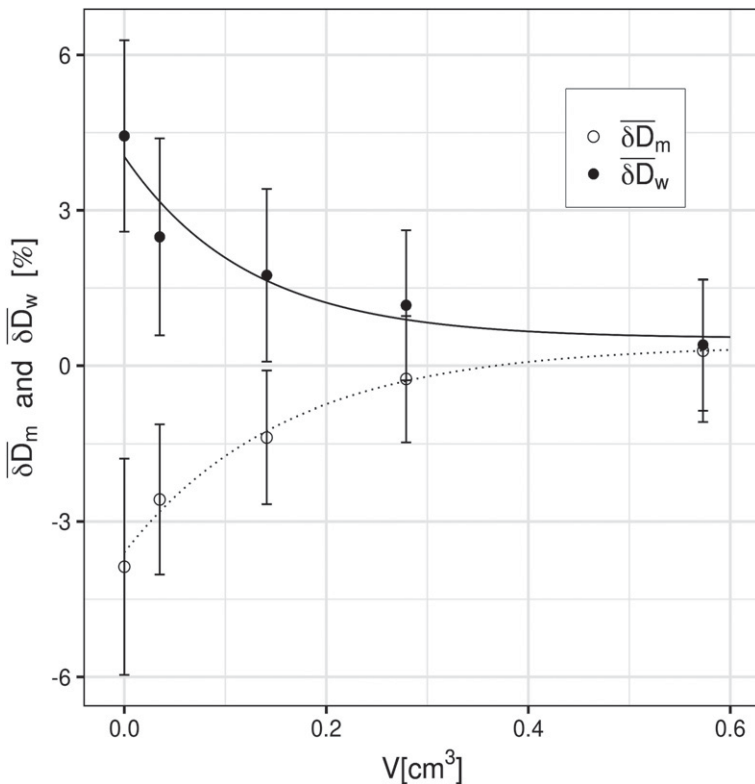


FIGURE 4. Average differences $\overline{\delta D}_m$ and $\overline{\delta D}_w$ between calculated and measured doses in the bone density equivalent (BDE) part of the CIRS Thorax phantom, as a function of the volumes of the simulated "water cylinders" (see Figure 2 and Table 3). $\overline{\delta D}_m$ and $\overline{\delta D}_w$ are presented as individual values/points calculated using Eqs. [1] to [4], and in the form of two analytical functions from Eqs. [9] and [10]. Error bars represent corresponding uncertainties within 95% confidence limits.

with fitting coefficients, a , b , and c . The dependent variable y denotes average values $\overline{\delta D}_m$ and $\overline{\delta D}_w$, while x stands for volumes of delineated "water cylinders". The explicit forms of the exponential fitting functions obtained were

$$\overline{\delta D}_m = 0.397 - 3.995 \cdot e^{-6.274 \cdot V} \quad [9]$$

$$\overline{\delta D}_w = 0.526 + 3.510 \cdot e^{-8.131 \cdot V} \quad [10]$$

for D_m and D_w reporting modes, respectively. Both functions from Eqs. [9] and [10] are graphically presented in Figure 4 having residual standard errors of the fit equal to 0.340% and 0.165% (on two degrees of freedom) for D_m and D_w calculation modes, respectively.

Applying Eqs. [9] and [10] for large volumes, we can see that $\overline{\delta D}_m$ and $\overline{\delta D}_w$ converge to the values of the free fitting coefficients a , i.e., $\overline{\delta D}_m = a_m \cong 0.397\%$ and $\overline{\delta D}_w = a_w \cong 0.526\%$. a_m and a_w denote free fitting coefficients in Eqs. [9] and [10], respectively. Those values are non-significantly different from zero, thus in agreement with experimentally determined absorbed doses. From the latter observations, we can deduct two key facts, which form a basis for the recommended additional procedure to the existing methodology for the verification of the accuracy of the Monte Carlo based TPS we were aiming at. Briefly:

- (i) Differences $|\overline{\delta D}_m - \overline{\delta D}_w|$ between dose-to-medium and dose-to-water calculation approaches gradually fade away as the volumes of "water cylinders" become larger and closer to the volume of the Farmer chamber;
- (ii) $|\overline{\delta D}_m|$ and $|\overline{\delta D}_w|$ fall below 1% for volumes of delineated "water cylinders" larger than 0.3 cm³.

Irrespective of the fact that the ionization chamber is calibrated in terms of dose to water, we propose an additional verification test of the accuracy of the Monaco TPS calculation modes for BDE regions considering the mentioned observations:

1. One can select three simple irradiation geometries (single fields, different gantry angles) and perform measurements of absorbed doses with the Farmer type ionization chamber in the BDE part of CIRS Thorax semi-anthropomorphic phantom, using a BDE insert ("standard" geometry). The ionization chamber should be positioned at the central part of the radiation field, where the measured signal is sufficiently large.

2. Measured doses are compared to the calculated ones using both calculation modes, D_m and D_w , applying Eqs. [1] to [4] for the additional four “water cylinders” delineated in the TPS.
3. Obtained mean values $\overline{\delta D_m}$ and $\overline{\delta D_w}$ of the percentage dose differences are fitted by the analytical function from Eq. [8].

Finally, the acceptability of the tested TPS algorithm is based on two conditions, which have to be fulfilled concurrently:

- i) Differences $|\overline{\delta D_m} - \overline{\delta D_w}|$ between dose-to-medium and dose-to-water calculation approaches should fall within 1% for the “water cylinder” of volume 0.6 cm^3 , i.e.,

$$|\overline{\delta D_m}(V = 0.6 \text{ cm}^3) - \overline{\delta D_w}(V = 0.6 \text{ cm}^3)| < 1\% \quad [11]$$

Fulfilment of this condition means that both calculation options yield to the same results within statistical uncertainty for large volumes, as expected. Since significant differences do exist for small volumes of delineated “water cylinders,” we have to consider this fact as well. The maximal difference $|\overline{\delta D_m} - \overline{\delta D_w}|$ can be obtained from the corresponding fitting functions for $V = 0 \text{ cm}^3$ (in our study, the maximal difference between both calculation options was 7.6%).

- ii) Obtained values $|\overline{\delta D_m}|$ and $|\overline{\delta D_w}|$ have to fall below 1% (see Eqs [6] and [7]) for large volumes of delineated “water cylinders”. If this condition is fulfilled, one can conclude that TPS dose calculations are in agreement with experimentally determined doses for both calculation modes.

It is important to note that our investigation was limited to the region of charged particle equilibrium (CPE) and for 6 MV photon beam only.

Conclusions

In the present study, a Monte Carlo based calculation algorithm built in the Elekta Monaco ver. 5.11 TPS was analyzed for 6 MV photon beam. It was confirmed that both calculation approaches, dose-to-medium and dose-to-water, yield to the similar results in the water equivalent and lung density equivalent parts of the semi-anthropomorphic phantom and are in agreement with experimentally determined absorbed doses.

In the bone density equivalent part of the phantom, significant differences were observed when calculations were compared to the measured absorbed doses. While the dose-to-medium approach yields to lower doses compared to the measured ones, calculations utilizing the dose-to-water computing approach revealed similar differences but of opposite sign. The observed differences can lead to ambiguity regarding the acceptability of the verification results before the clinical implementation of a newly commissioned TPS Monaco.

To overcome the ambiguity on the pertinence of the verification results in the bone density equivalent material, a supplement to the current TPS commissioning methodology has been proposed, having in mind inherent differences between the two calculation modes. This supplement relies on the findings from the present study. We consider it as a consistent and efficient method for the experimental verification of the absorbed dose calculation in both calculation modes D_m and D_w . A proposed supplementary test to the present verification methodology of the algorithm built in the Monaco TPS can assure higher accuracy and confidence compared to the current methodology.

While the selection of beams in this study assumes conditions of charged particle equilibrium, it would be highly interesting and worthwhile to set-up the study where CPE is violated, e.g., for small fields where lateral CPE does not exist. However, an experimental determination of absorbed doses in small fields is demanding. It requires determination of detector specific correction factors, which have to be utilized individually for the selected detector and are associated with additional uncertainties.²⁴⁻²⁶ The latter can pose a problem to conduct such a study with sufficient reliability and robustness.

Acknowledgement

Bozidar Casar acknowledges the financial support from the Slovenian Research Agency through the research Grant P1-0389.

References

1. Andreo P, Cramb J, Fraass BA, Ionescu-Farca F, Izewska J, Levin V, et al. *Technical report series No. 430: commissioning and quality assurance of computerised planning system for radiation treatment of cancer*. Vienna: International Atomic Energy Agency; 2004.
2. Brunckhorst E, Gershkevitsh E, Ibbott G, Korf G, Miller D, Schmidt R, et al. *IAEA-TECDOC-1583 Commissioning of radiotherapy treatment planning systems: testing for typical external beam treatment techniques*. Vienna: International Atomic Energy Agency; 2008.

3. Kry SF, Alvarez P, Molineu A, Amador C, Galvin J, Followill DS, et al. Algorithms used in heterogeneous dose calculations show systematic differences as measured with the radiological Physics Center's anthropomorphic thorax phantom used for RTOG credentialing. *Int J Radiat Oncol Biol Phys* 2013; **85**: 95-100. doi: 10.1016/j.ijrobp.2012.08.039
4. The Netherlands Commission of Radiation Dosimetry. *Code of practice for the quality assurance and control for intensity modulated radiotherapy*. Delft, Netherlands; 2013.
5. Smilowitz JB, Das IJ, Feygelman V, Fraass BA, Kry SF, Marshall IR, et al. AAPM Medical Physics Practice Guideline 5.a.: Commissioning and QA of treatment planning dose calculations - megavoltage photon and electron beams. *J Appl Clin Med Phys* 2015; **16**: 14-34. doi: 10.1120/jacmp.v16i5.5768
6. Van Dyk J, Battista J. Has the use of computers in radiation therapy improved the accuracy in radiation dose delivery? *J Phys Conf Ser* 2014; **489**: 012098. doi: 10.1088/1742-6596/489/1/012098
7. Fogliata A, Cozzi L. Dose calculation algorithm accuracy for small fields in non-homogeneous media: the lung SBRT case. *Phys Med* 2017; **44**: 157-62. doi: 10.1016/j.ejmp.2016.11.104
8. Reynaert N, Crop F, Sterpin E. On the conversion of dose to bone to dose to water in radiotherapy treatment planning systems. *Phys Imaging Radiat Oncol* 2018; **5**: 26-30. 2018. doi: 10.1016/j.phro.2018.01.004
9. Andreo P. Dose to 'water-like' media or dose to tissue in MV photons radiotherapy treatment planning: still a matter of debate. *Phys Med Biol* 2015; **60**: 309-37. doi: 10.1088/0031-9155/60/1/309
10. Chetty IJ, Curran B, Cygler JE, DeMarco JJ, Ezzell G, Faddegonet BA, et al. Report of the AAPM Task Group No. 105: issues associated with clinical implementation of Monte Carlo-based photon and electron external beam treatment planning. *Med Phys* 2007; **34**: 4818-53. doi: 10.1118/1.2795842
11. Liu HH, Keal P. D_m rather than D_w should be used in Monte Carlo treatment planning. (Point/Counterpoint), *Med Phys* 2002; **29**: 922-4. doi: 10.1118/1.1473137
12. Ma C-M, Li J. Dose specification for radiation therapy: dose to water or dose to medium? *Phys Med Biol* 2011; **56**: 3073-89. doi: 10.1088/0031-9155/56/10/012
13. Reynaert N, Van der Marck S, Schaart D, Van der Zee W, Van VlietVroegindeweij C, Tomsej M, et al. Monte Carlo treatment planning for photon and electron beams. *Radiat Phys Chem* 2007; **76**: 643-86. doi: 10.1016/j.radphyschem.2006.05.015
14. Dogan N, Siebers JV, Keall PJ. Clinical comparison of head and neck and prostate IMRT plans using absorbed dose to medium and absorbed dose to water. *Phys Med Biol* 2006; **51**: 4967-80. doi: 10.1088/0031-9155/51/19/015
15. Walters BRB, Kramer R, Kawrakow I. Dose to medium versus dose to water as an estimator of dose to sensitive skeletal tissue. *Phys Med Biol* 2010; **55**: 4535-46. doi: 10.1088/0031-9155/55/16/S08
16. Sterpin E. Potential pitfalls of the PTV concept in dose-to-medium planning optimization. *Phys Med* 2016; **32**: 1103-10. doi: 10.1016/j.ejmp.2016.08.009
17. Siebers JV, Keall PJ, Nahum AE. Converting absorbed dose to medium to absorbed dose to water for Monte Carlo based photon beam dose calculations. *Phys Med Biol* 2000; **45**: 983-95. doi: 10.1088/0031-9155/45/4/313
18. Abratt R, Aguirre F, Andreo P, Coffey M, Drew J, El Gueddari B, et al. IAEA *Comprehensive audits of radiotherapy practices: a tool for quality improvement quality assurance team for radiation oncology-QUATRO*. Vienna: International Atomic Energy Agency; 2007.
19. Ezzell GA, Galvin JM, Low D, Palta J, Rosen I, Sharpe MB, et al. Guidance document on delivery, treatment planning, and clinical implementation of IMRT: report of the IMRT Subcommittee of the AAPM radiation therapy committee. *Med Phys* 2003; **30**: 2089-115. doi: 10.1118/1.1591194
20. Klein EE, Hanley J, Bayouth J, Yin FF, Simon W, Dresser S, et al. Task Group 142 report: quality assurance of medical accelerators. *Med Phys* 2009; **36**: 4197-212. doi: 10.1118/1.3190392
21. Ezzell GA, Burmeister JW, Dogan N, LoSasso TJ, Mechalakos JG, Mihailidis D, IMRT commissioning: multiple institution planning and dosimetry comparisons, a report from AAPM Task Group 119. *Med Phys* 2009; **36**: 5359-73. doi: 10.1118/1.3238104
22. Andreo P, Burns DT, Hohlfield K, Huq MS, Kanai T, Laitano F, et al. *Absorbed dose determination in external beam radiotherapy: An international code of practice for dosimetry based on standards of absorbed dose to water*. IAEA TRS-398. Vienna: International Atomic Energy Agency; 2006.
23. Smilović Radojčić Đ, Švabić Kolacio M, Radojčić M, Rajlić D, Casar B, Faj D, et al. Comparison of calculated dose distributions reported as dose-to-water and dose-to-medium for intensity-modulated radiotherapy of nasopharyngeal cancer patients. *Med Dos* 2018; **43**: 363-9. doi: 10.1016/j.meddos.2017.11.008
24. Palmans H, Andreo P, Huq MS, Christaki K, Alfonso R, Izewska J, et al. Dosimetry of small static fields used in external beam radiotherapy: An International Code of Practice for reference and relative dose determination. *Technical Report Series No. 483*. IAEA TRS483. Vienna: International Atomic Energy Agency; 2017. doi: 10.1002/mp.13208
25. Casar B, Gershkevitch E, Mendez I, Jurković S, Huq MS. A novel method for the determination of field output factors and output correction factors for small static fields for six diodes and a microdiamond detector in megavoltage photon beams. *Med Phys* 2019; **46**: 944-63. doi: 10.1002/mp.13318
26. Casar B, Gershkevitch E, Mendez I, Jurković S, Huq MS. Output correction factors for small static fields in megavoltage photon beams for seven ionization chambers in two orientations - perpendicular and parallel. *Med Phys* 2020; **47**: 242-59. doi: 10.1002/mp.13894

Comparison of three film analysis softwares using EBT2 and EBT3 films in radiotherapy

Tamás Pócza^{1,2}, Zsuzsanna Zongor¹, Barbara Melles-Bencsik¹, Dóra Zita Tatai-Szabó¹, Tibor Major^{1,3}, Csilla Pesznyák^{1,2}

¹ National Institute of Oncology, Centre of Radiotherapy, Budapest, Hungary

² Budapest University of Technology and Economics, Institute of Nuclear Techniques, Budapest, Hungary

³ Department of Oncology, Semmelweis University, Budapest, Hungary

Radiol Oncol 2020; 54(4): 505-512.

Received 23 February 2020

Accepted 27 June 2020

Correspondence to: Tamás Pócza, National Institute of Oncology, Centre of Radiotherapy, Ráth György 7-9, 1122 Budapest, Hungary.
E-mail: poczatamas87@gmail.com

Disclosure: No potential conflicts of interest were disclosed.

Introduction. The purpose of the study was to compare the results of gamma value based film analysis according to the used type of self-developer film and software product.

Material and methods. The films were irradiated with different treatment techniques such as 3D conformal and intensity modulated radiotherapy with static and rotational delivery. Stereotactic plans with conformal and intensity modulated arc techniques, using coplanar and non-coplanar beam setup were also evaluated. The data of irradiated film were compared with the planned planar dose distribution exported from the treatment planning system. Three film analysis software programs were evaluated: PTW Mephysto (PTW), FilmQA Pro (FQP) and radiochromic.com (RC). Both EBT2 and EBT3 types of films were examined. The comparisons of dose distributions were performed with gamma analysis using 10% cut-off level.

Results. The results of the gamma analysis for larger fields were between 78.3% and 98.3%, 75.7% and 100%, 80.2% and 98.8% with PTW, FQP and RC, respectively. The results of evaluation in case of stereotactic measurements were 76.8%–99.2% for PTW, 95.7%–100% for FQP and 91.2%–99.9% for RC.

Conclusions. All the three software programs are suitable for calibrating and evaluating films, performing gamma analysis, and can be used for patient specific quality assurance measurements. There is no direct connection between gamma passing rate and absolute accuracy or software quality, it is just a feature of the software. The interpretation of own results has to be defined on an institutional level according to given workflow and preliminary results.

Key words: radiochromic; IMRT; gamma analysis; film analysis software

Introduction

Over the years, film dosimetry has been developed into a powerful tool for radiotherapy treatment verification and quality assurance as a two-dimensional radiation detector system. Radiochromic film technology is based on diacetylene-dye radiation-sensitive monomers, which polymerize and change colour due to radiation. These types of films are self-developers, their colour changes directly after irradiation and they do not require chemical processing or film developing equipment. The dosimetric analysis can be applied by using a photo

scanner and a special software.¹ The speed of polymerization depends on the environmental conditions, but it stabilizes after 24–48 h.² The darkening of the film is increasing with the exposed dose, and their relation is generally approximated by polynomial or rational functions. Radiochromic films are nearly tissue-equivalent, with low energy- and dose rate dependency.³ For linear accelerators with more photon energies only one film calibration is necessary, but in kV photon energy range a new calibration is needed.^{4,5} They have a high-spatial resolution suitable for dose distribution measurement in radiation fields with high dose gradients,

for example, in stereotactic irradiation or brachytherapy. Radiochromic films are water equivalent because the active layer is made up of low atomic number materials. The different types of films could have different layer arrangements, symmetric or asymmetric, and different material constructions containing C, H, O and Li. The contamination with high atomic number material (like Cl) is kept low, so the films are nearly water-equivalent.^{6,7} The radiation sensitive monomers are located between an adhesive and a polyester protection layer. Since the introduction of the EBT2 film type, a yellow marker dye has been built in the active layer of the film to provide information about the subtle differences in the thickness of the active layer, thereby making the increment of the homogeneity possible, and reducing the sensitivity to artificial light.^{6,8}

Materials and methods

Films

In this study we investigated the GafChromic EBT2 and EBT3 films (Ashland Inc., Wayne, New Jersey). The size of EBT2 film was 8" x 10". The layer arrangement of the EBT2 film is not symmetric; consequently, film orientation is important. The substrate of the film is clear polyester (175 µm) coated with an active layer (28µm) which is covered by a 25 µm pressure-sensitive adhesive wrap and the top of the film also has a polyester layer (50 µm).⁹ The size of GafChromic EBT3 was 13" x 17". The single active layer of the film is nominally 28 µm thick and contains the active component, a marker dye. The active layer is between two 125 µm transparent matte polyester substrates.¹⁰ The film is symmetric, and an anti-Newton ring feature is added by the manufacturer.

Scanner

To digitize the film EPSON Expression 10000XL (Epson, Nagano, Japan) flatbed scanner was used with A3 scanning surface. The applied scanning parameters were as follows: transmission mode, positive film, no colour correction, landscape orientation, 48-bit RGB, 72 dpi resolution and TIFF file format.¹⁰ Considerable warm up effect was not observed for our scanner, but before every scanning we waited at least fifteen minutes, and the first five scanned images were never used.¹¹ Every pixel in a colour image has three-channel (RGB) image signal. The scanned images can be evaluated by film analysis software.¹² The film-scanner response may

depend on thickness variations in the active layer coated on the film, electronic noise, scanner instability, lateral artefact, local variations produced by systemic problems of the scanner, Newton rings, dust, scratches or other damage. The orientations of the films were noted during the irradiation, and they were positioned on the same way at the scanning, always at the same distance from the borders of the sensitive area of the scanner.¹³ The uniformity of the scanner bed was defined by placing four, non-irradiated film pieces at the corners of the scanner to cover the whole scanning surface. The inhomogeneity map of our scanner was determined to find the quasi-homogeneous part of the scanner. According to this map, only the homogeneous middle part of the scanner was used for scanning. The films have also non-uniformity, but this effect was not examined or corrected. During the scanning, a glass layer was used as compressing media. The precision of the scanning method and the applied corrections affect the results of the gamma analysis, so the used methods always have to be reported.¹⁴⁻¹⁷

Calibration measurement

During the calibration a CIRS Plastic Water sheet phantom (CIRS Inc., Norfolk, VA, USA) was applied and the film was placed between the layers of the phantom (5 cm above and 10 cm under the film). The films were irradiated at the source surface distance (SSD) of 95 cm. The size of the calibration films was 2x5 cm, and the number of calibration points were 15 cGy, 30 cGy, 50 cGy, 100 cGy, 200 cGy, 300 cGy, 400 cGy, 550 cGy, 650 cGy, 750 cGy, 850 cGy, 950 cGy and the non-irradiated film (0 cGy). The waiting time between irradiation and scanning was always 24 hours. Always the same frame positions were used and lateral correction was not applied.

The scanning of one calibration series was repeated 18 and 60 months after the initial scan. The changes of the optical density values were evaluated for all three colour channels. The absolute and relative differences were also calculated.

Treatment planning and irradiation

The irradiation was performed with a Varian TrueBeam (Varian Medical Systems, Palo Alto, CA, USA) linear accelerator and Eclipse 13.6 (Varian Medical Systems, Palo Alto, CA, USA) treatment planning system with Analytical Anisotropic Algorithm (AAA) was used for dose calculation.

A pelvic case (prostate and nodal target) was planned with different treatment techniques, such as 3D conformal (3DCRT), intensity modulated radiation therapy with sliding-window (IMRT) and RapidArc (RA), and simultaneous integrated boost with arc therapy (RA-SIB). Small field, stereotactic radiotherapy plans were also created with conformal arc (CA) and RA techniques using coplanar and non-coplanar (NC) beam setup. For the pelvic plan 10 MV, for the stereotactic CA plan 6 MV, for the stereotactic RA plan 6 MV-FFF energy was used. The original patient treatment plan was copied to the CT scan of the CIRS solid water phantom. The same phantom was also used for the calibration. The depth of the film was 5 cm with 10 cm backscatter, the isocenter of the plan was positioned at the middle of the film. After the recalculation, the 2D dose distribution at the slice position of the film was exported, and the plan was delivered to the film with the given setup. The planned dose distribution was compared with the results of the film dose distribution using a film analysis software.

The gamma method

The gamma map comparison as introduced by Low *et al.* is widely used to judge agreement between treatment plan dose distribution and dose measurement.¹⁸

The gamma map function $\gamma(\mathbf{r}_{\text{test}})$ can be defined as minimum value of the following function, according to $\mathbf{r}_{\text{reference}}$:

$$\gamma(\mathbf{r}_{\text{test}}) = \sqrt{\left(\frac{\mathbf{r}_{\text{test}} - \mathbf{r}_{\text{reference}}}{\Delta_{\text{distance}}}\right)^2 + \left(\frac{d_{\text{test}}(\mathbf{r}_{\text{test}}) - d_{\text{reference}}(\mathbf{r}_{\text{reference}})}{\Delta_{\text{dose}}}\right)^2}$$

Where $d_{\text{test}}(\mathbf{r}_{\text{test}})$ is the dosemap of the test distribution and $d_{\text{reference}}(\mathbf{r}_{\text{reference}})$ is the reference distribution.

$(\Delta_{\text{dose}}, \Delta_{\text{distance}})$ also known as 'gamma criterion'. The tolerance Δ_{dose} is given in % and the distance Δ_{distance} in mm.

A point of the test distribution (\mathbf{r}_{test}) passes the test, if $\gamma \leq 1$. In our study the data were analysed using gamma evaluation with the following criteria: 2%, 2mm and 3%, 3mm, and normalization for local dose and global dose maximum with 10% threshold.¹⁸⁻²⁰

During gamma comparison automatic matching with enabled rotation correction was used, and if it decided to be necessary, manual correction was applied. The planned distributions were the refer-

ence, and the film measurements were evaluated and compared to them.²¹

Statistics of gamma analysis and comparison was applied for the three different softwares. The results were calculated with GraphPad 8.0.1 (GraphPad Software, San Diego, CA) using ANOVA and post-hoc Dunn's test, based on all evaluated scans.

Software

Several different software programs can be applied for dosimetric the evaluation of radiochromic films. Three software products were analysed for film evaluation: PTW Mephysto (PTW), FilmQA Pro (FQP) and Radiochromic.com (RC). Each of them is dedicated for film scanning, calibration, dose map creation, gamma evaluation, and for image processing.²²⁻²⁶

PTW Mephysto (PTW)

The film analysis module of PTW Mephysto 3.0 software includes film scanning (FilmScan), calibration (FilmCal), film analysing (FilmAnalyse) options, and for gamma analysis PTW Mephysto VeriSoft 6.3 was used. This software works on the basis of single channel dosimetry which only takes into consideration the red channel from the RGB channels. One pixel value on the scanned film represents one dose value. In case of a single-channel dosimetry all response artefacts convert directly to dose artefacts. Applying this method, important data can be lost. Unfortunately, we could not find more information about the mathematical method of the software.

FilmQA Pro (FQP)

The FilmQA Pro 4.0 software is based on the Mücke-Mayer method.²⁷ Different multichannel methods have been proposed in literature for film evaluation. This software is compact, tree structured with folders and files. Appropriate tutorials and training material on the handling of the software can be found on <http://www.gafchromic.com>.²⁸ In multichannel approach, three pixel values (RGB) on the scanned image represent one dose value.²⁷⁻²⁹ Multichannel dosimetry makes it possible to reduce the artefacts, for example; the thickness of active layer, fingerprints or dust from the dose image. Radiochromic films provide a different response in each of the three colour channels, that way the signals can be separated into a dose-dependent

and a dose-independent part. The latter one can be corrected, so we can use the only dose-related data for the evaluation of films. Choosing wrong multichannel model, errors of the different colour channels can be combined, because their errors correlate with each other, and the overall error can be increased. Therefore, multichannel dosimetry is can be worse than single-channel dosimetry in case of wrong model selection.³⁰ As the dose range increases, the response of radiochromic film will be increasingly nonlinear. For this reason, the fitted polynomial function can oscillate between the data points at higher dose regions, therefore, if a polynomial calibration function is used, more calibration points are needed for fitting. The FilmQA Pro uses a special rational function for fitting the calibration curve on calibration data points because the rational function is monotonic, does not oscillate between data values and appropriate to the dosimetric properties of the radiochromic film. In clinical practice, four or five calibration points are enough for a correct calibration.

The calibration data have been fit using a function:

$$X(D) = (a + bD)/(c + D),$$

when the scanner response at dose D is $X(D)$ and, a, b, c are constants.

Radiochromic.com (RC)

This is a cloud computing web application for calibration and dosimetry of radiochromic films. The version number was 2.7. The user interface has a clear layout, available in a browser. In can be used as a free software with some limitations, and its extended version is commercially available. The software also applies multichannel dosimetry as FilmQA Pro but uses another channel independent perturbation model, the truncated normal distribution model. This model is considered as a metamodel which minimizes the uncertainty in the dose inherent in the method of channel independent perturbation. This model applies the first order Taylor expansion to the dose due to small perturbation.³¹

$$\begin{cases} D(r) = D_R(r) + \dot{D}_R(r)\Delta(r) + \epsilon_R(r) \\ D(r) = D_G(r) + \dot{D}_G(r)\Delta(r) + \epsilon_G(r) \\ D(r) = D_B(r) + \dot{D}_B(r)\Delta(r) + \epsilon_B(r) \end{cases}$$

$D(r)$ represents the dose absorbed by the film at point r .
 D_k is the absolute dose measured by the channel k (R,G,B), when no disturbance is present, and it is calculated directly from the calibration model

$\dot{D}_k(r)$ is the first derivative of the dose, with respect to the NOD (net optical density), at point r .

$\epsilon_k(r)$ is an error term accounting for the difference between the dose absorbed by the film and the dose measured in the channel k after correction by the perturbation.

The calculation algorithm of the program and the method of film analysis can be found on the website of the software: <https://radiochromic.com>. In order to perform calibration, dosimetry evaluation and gamma analysis, we uploaded the calibration films, the scanned film and the dose map exported from the treatment planning system to Radiochromic.com. It is also possible to make recalibration during the film evaluation.³² From version 3.0 the application employs the Multigaussian model.²⁶

Results

Auxiliary results

Scanner homogeneity

The homogeneity map of the scanner can be seen in Figure 1. Based on these results, it can be observed that the top 8 cm and the bottom 7 cm borders of the scanner's sensitive area are inhomogeneous. There are small inhomogeneities on the right and the left part of the scanner bed. For the film evaluation, we can use an approximately 15 cm wide homogeneous area in the centre of the scanner. Inside the homogeneous area the optical density has less than 4% deviation, outside the area it reaches 13%.

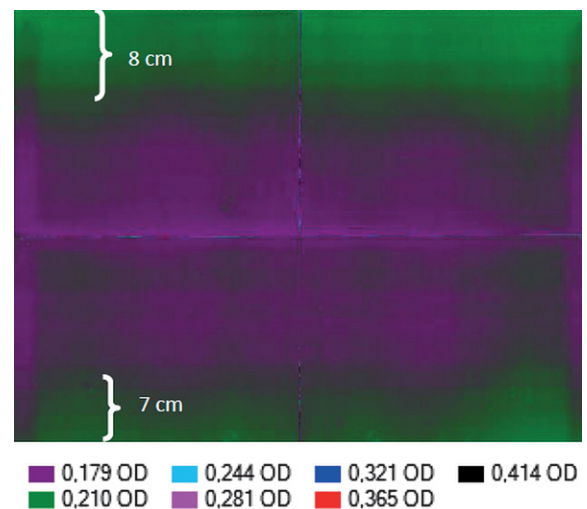


FIGURE 1. Inhomogeneity map of the full scanning surface (A) and the homogeneous area in the centre of the scanner glass (B).

Long-time darkening

18 and 60 months after the first scanning of the calibrating films, we scanned the same EBT2 films again. For films that received lower dose the relative post-irradiation colouration was higher. The difference between the channels in terms of colouration is getting wider by time. In Figure 2 the relative change of the pixel values compared to the original scan at 18 months and 60 months can be observed, according to the exposure.

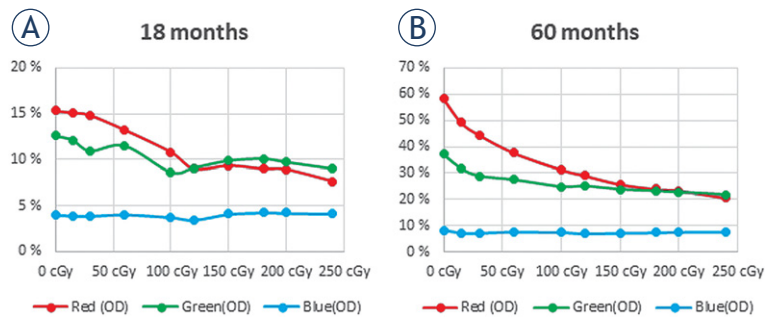


FIGURE 2. Change of optical density in % after 18 (A) and 60 (B) months of primary irradiation, in function of the primary irradiated dose (cGy).

Gamma analysis results

The results of the gamma analysis from the type of films and the three software products can be found in Table 1. The parameters of the gamma analysis were: 3%, 3 mm, and 2%, 2 mm, the negligible threshold dose was 10%, and the normalization of gamma analysis was performed on global dose maximum. A sample result - the evaluation of the RA-SIB plan with three software programs can be found in Figure 3.

The results of gamma analysis of stereotactic fields with EBT3 films can be found in Table 2. The

negligible threshold dose was 10%. The gamma analysis was calculated in two ways; in the first case, the normalization was executed for global dose maximum and in the second case, we applied a harder limit, when the normalization was performed for local plan dose.

According to statistical analysis, the passing rates for FilmQA Pro were significantly higher than PTW Mephysto and Radiochromic.com.

TABLE 1. Pass rates of the gamma analysis using three software products; the negligible threshold dose was 10% and the normalization of gamma analysis was performed on global dose maximum. (RA: RapidArc, SIB: simultaneous integrated boost)

		3DCRT		IMRT		RA		RA – SIB	
		2%,2mm	3%,3mm	2%,2mm	3%,3mm	2%,2mm	3%,3mm	2%,2mm	3%,3mm
EBT2	PTW Mephysto	87.1 %	95.5 %	89.2 %	98.2 %	83.9 %	91.5 %	86.3 %	98.3 %
	FilmQA Pro	98.9 %	100.0 %	75.7 %	93.4 %	99.9 %	100.0 %	87.3 %	92.8 %
	radiochromic.com	87.2 %	98.1 %	80.2 %	93.1 %	90.4 %	98.5 %	84.2 %	95.3 %
EBT3	PTW Mephysto	86.6 %	94.4 %	78.3 %	93.8 %	92.0 %	97.8 %	86.8 %	93.4 %
	FilmQA Pro	99.0 %	99.9 %	82.6 %	95.0 %	98.3 %	99.4 %	87.9 %	91.9 %
	radiochromic.com	91.0 %	98.8 %	80.2 %	94.4 %	95.4 %	98.7 %	87.5 %	92.1 %

TABLE 2. Pass rates of gamma analysis of small stereotactic fields; the negligible threshold dose was 10% for EBT 3 films (CA: Conformal Arc, RA: RapidArc, NC: non-coplanar)

		CA		RA		NC - CA		NC – RA	
		2%,2mm	3%,3mm	2%,2mm	3% ,3mm	2%,2mm	3%,3mm	2%,2mm	3%,3mm
global	PTW Mephysto	97.0 %	99.2 %	87.9 %	90.2 %	95.1 %	98.6 %	89.2 %	93.5 %
	FilmQA Pro	100.0 %	100.0 %	98.5 %	100.0 %	99.8 %	100.0 %	99.2 %	100.0 %
	radiochromic.com	98.2 %	99.9 %	97.2 %	99.8 %	95.0 %	99.7 %	96.4 %	99.6 %
local	PTW Mephysto	95.2 %	97.2 %	87.4 %	89.9 %	93.1 %	97.9 %	76.8 %	83.1 %
	FilmQA Pro	99.9 %	99.9 %	95.7 %	99.9 %	99.5 %	100.0 %	98.7 %	99.5 %
	radiochromic.com	96.9 %	98.5 %	93.3 %	97.5 %	91.5 %	97.3 %	91.2 %	97.8 %

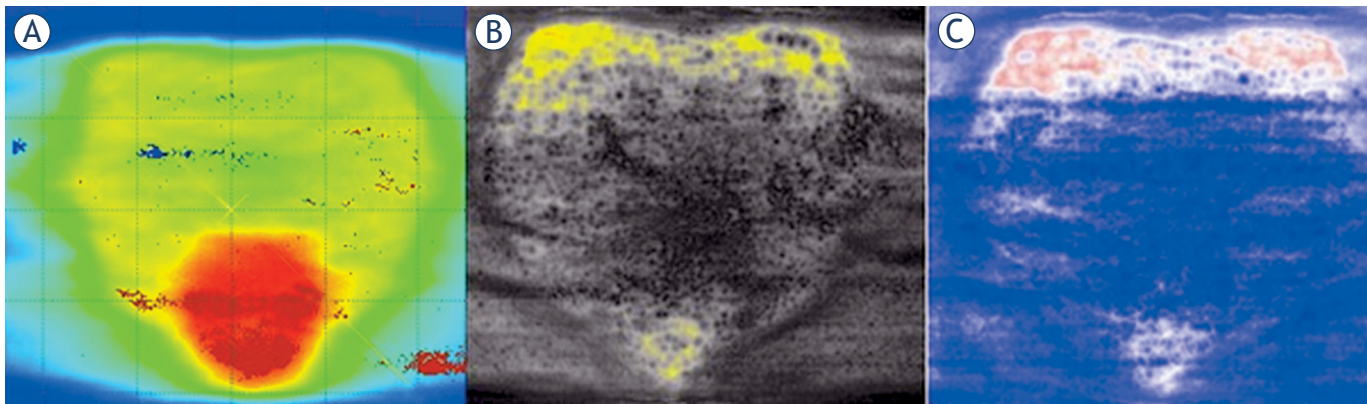
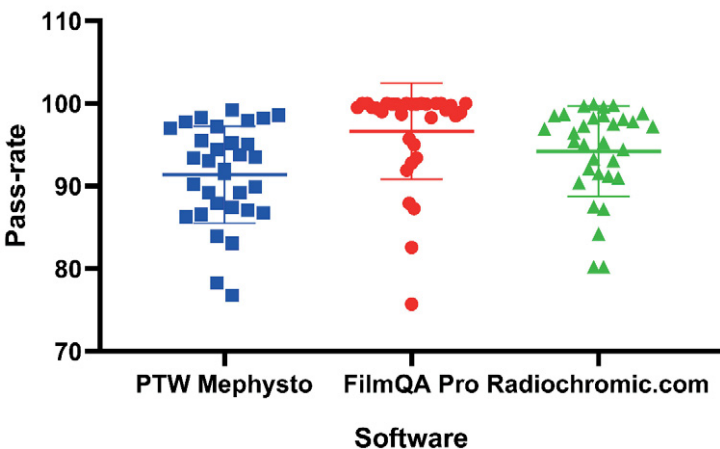


FIGURE 3. Evaluation of the simultaneous integrated boost (SIB) plan with PTW Mephysto (A), FilmQAPro (B) and radiochromic.com (C).

TABLE 3. Statistical evaluation and visualisation of the gamma passing rates for the three different softwares, according to all analysed cases

Gamma passing rate statistics (%)			
	PTW Mephysto	FilmQA Pro	Radiochromic.com
Minimum	76.8	75.7	80.2
Maximum	99.2	100.0	99.9
Median	92.6	99.5	95.9
Mean	91.4	96.6	94.2
Std. Deviation	5.9	5.8	5.5
Lower 95% CI	89.3	94.5	92.3
Upper 95% CI	93.5	98.8	96.2
Dunn's multiple comparisons test	Adjusted P Value	Significant?	
PTW Mephysto vs. FilmQA Pro	<0,0001	Yes	
PTW Mephysto vs. Radiochromic.com	0.1824	No	
FilmQA Pro vs. Radiochromic.com	0.0005	Yes	



Discussion

During the preparation of the film data, the calibration and the scanning process have to be handled very carefully. Based on the results showed in Figure 1, it is recommended to limit the scanner area to the homogeneous part, or corrections need to be applied at the border of film scanner. In case of large PTVs which cover the whole film surface, the gamma analysis showed higher deviations which were caused by the edge effects during our IMRT treatment plan evaluation.

The quality of calibration curves and the time passed since the preparation of the calibration curve can also influence the results of dosimetry analysis. More accurate results can be received with a larger number of calibration points and shorter intervals between the calibration and the film evaluation. According to our results seen in Figure 2, in case of re-evaluation of older film scans the recalibration is crucial.^{33,34} The presented changes are summation of the film ageing and the scanner characteristics changes, and both effect have to be taken into consideration during long-time usage.

Our gamma analysis results are in accordance with those found in the literature. The fact that in many cases the threshold dose and the normalization method (local dose or global maximum dose) are not published makes the comparison more difficult. Agnew *et al.* showed, that the selection and the settings of the software has a crucial effect on the gamma passing rates.³⁵ Cosumano *et al.* examined stereotactic irradiation plans (small field, large fraction dose) with EBT3 films. For the gamma criteria of 5%, 1 mm they received 94.3%.³⁶ For the stereotactic plan, Wen *et al.* applied a different criteria, for 3%, 1 mm and they found a 95±4.2% agreement during the evaluation of plans.³⁷ Hanusová *et al.*

using PTW VeriSoft v3.1 found in average 97.03% for EBT3 and 85.81% for EBT2 films agreement with for static IMRT fields with 3%, 3 mm and 5% threshold level.³⁸ Lewis *et al.* applied FQP software and achieved a correspondence ranged between 95% and 99% for all the treatment fields studied using the gamma test criterion of 2%, 2 mm to evaluate the measurements.³⁹ Also with FQP Marrazzo *et al.* found with single- and multichannel analysis for linac measurements the passing rates in average with 2%, 2mm criteria are 91% and 80%, with 3%, 3mm criteria are 98% and 94%, respectively.⁴⁰ According to Calvo-Ortega *et al.* with RC software the agreement is between 87.6% and 99.8% using fast protocol for IMRT plans with 3%, 3 mm criteria and 10% threshold.⁴¹

The software products have possibilities for automatic dose map and film fusion, but these do not always work perfectly. Manual matching is possible for all three software programs; in this case, results highly depend on the user's skills and experience. During the evaluation with FilmQA Pro and RC there is an opportunity for recalibration of sensitometric curves with the actual zero and dose maximum points. This option has a significant impact on the workflow of gamma analysis, it makes easier and faster the usage of the films from the same badge. Table 3 summarizes the statistical evaluation of our measurements. The FQP has significantly higher passing rate, than the other two softwares. As Table 1 shows, for EBT3 films the difference between the software programs is lower than for EBT2 films. In case of stereotactic plans, the agreement for the CA plans were better than for the RA plans, and for the coplanar cases were better than for the non-coplanars, as can be seen on Table 2. Using local instead of global normalization the number of passing points were decreased, but the differences between the plans were the same, independently from the used software. The advantage of self-developing film as compared to the semi-conductor or ionchamber based detector matrix is that it has a better spatial resolution, which allows us to handle the high dose-gradients in case of state-of-art ultra-conformal (stereotactic) plans. The disadvantage of films as compared to other detectors is that the usage of film is time-consuming. The film has to be prepared before the measurement and they have to be handled very carefully. The results cannot be executed immediately after the measurement, the irradiated films have to be scanned and calibrated according to strictly defined methods after the irradiation.

Based on our measurements, the EBT2 and EBT3 films are suitable for dose plan verification of 3DCRT and IMRT treatments combined with any of the 3 analysed software programs. All three evaluation programs are suitable for calibrating and evaluating films, and performing the gamma analysis. The deficiency of this paper is that some applications have been improved in the last few years, new models like Multigaussian are implemented. By using different softwares in the gamma analysis, the authors cannot exclude the influence of the implementation of the gamma calculation in the final result. Therefore, this paper is not testing which software provides more accurate film dose distributions, neither which dose distributions are more similar to the ones calculated with the treatment planning system. Based on the results, it is recommended to always use a new calibration curve during the film evaluation and the homogeneous area of the scanner should be used for scanning. Both types of films and the three software products are very sensitive to calibration, the users must pay close attention to preparation, film handling and timing. We recommend using 2%, 2 mm agreement criteria with 10% threshold for evaluating with gamma analysis. This way the results will be slightly lower, but it will be easier to identify the problematic points during the evaluation. Every institute has to define their own limit of acceptance level according to their own workflow and experience.

Acknowledgement

This work was supported by the Higher Education Excellence Program of the Ministry of Human Capacities in the frame of Biotechnology research area of Budapest University of Technology and Economics (BME FIKP-BIO).

References

1. Niroomand-Rad A, Blackwell CR, Coursey BM, Radiochromic film dosimetry: Recommendations of AAPM Radiation Therapy Committee Task Group 55. *Med Phys* 1998; **25**: 2093-115. doi: 10.1118/1.598407
2. Girard F, Bouchard H, Lacroix F. Reference dosimetry using radiochromic film. *J Appl Clin Med Phys* 2012; **13**: 339-53. doi: 10.1120/jacmp.v13i6.3994
3. Borca VC, Pasquino M, Russo G, Grosso P, Cante D, Sciacero P, et al. Dosimetric characterization and use of GAFCHROMIC EBT3 film for IMRT dose verification. *J Appl Clin Med Phys* 2013; **14**: 158-71. doi: 10.1120/jacmp.v14i2.4111
4. Soares CG. Radiochromic film dosimetry. *Radiat Meas* 2006; **41**: S100-16. doi: 10.1016/j.radmeas.2007.01.007

5. Butson MJ, Yu PKN, Cheung T, Metcalfe P. Radiochromic film for medical radiation dosimetry. *Mater Sci Eng R Reports* 2003; **41**: 61-120. doi: 10.1016/S0927-796X(03)00034-2
6. Devic S. Radiochromic film dosimetry: past, present, and future. *Phys Medica* 2011; **27**: 122-34. doi: 10.1016/j.ejmp.2010.10.001
7. Devic S, Tomic N, Lewis D. Reference radiochromic film dosimetry: review of technical aspects. *Phys Medica* 2016; **32**: 541-56. doi: 10.1016/j.ejmp.2016.02.008
8. McCaw TJ, Micka JA, Dewerd LA. Characterizing the marker-dye correction for Gafchromic EBT2 film: a comparison of three analysis methods. *Med Phys* 2011; **38**: 5771-7. doi: 10.1118/1.3639997
9. Andrés C, Del Castillo A, Tortosa R, Alonso D, Barquero R. A comprehensive study of the Gafchromic EBT2 radiochromic film. A comparison with EBT. *Med Phys* 2010; **37**: 6271-8. doi: 10.1118/1.3512792
10. Ashland Inc. GAFChromic™ EBT3 film specifications. 2014: 1-5. [cited 2020 Jan 15]. Available at : http://www.gafchromic.com/documents/EBT3_Specifications.pdf
11. Méndez I, Slijvic, Hudej R, Jenko A, Casar B. Grid patterns, spatial inter-scan variations and scanning reading repeatability in radiochromic film dosimetry. *Phys Medica* 2016; **32**: 1072-81. doi: 10.1016/j.ejmp.2016.08.003
12. Devic S, Seuntjens J, Sham E, Podgorsak EB, Schmidtlein CR, Kirov AS, et al. Precise radiochromic film dosimetry using a flat-bed document scanner. *Med Phys* 2005; **32**: 2245-53. doi: 10.1118/1.1929253
13. Ferreira BC, Lopes MC, Capela M. Evaluation of an Epson flatbed scanner to read Gafchromic EBT films for radiation dosimetry. *Phys Med Biol* 2009; **54**: 1073-85. doi: 10.1088/0031-9155/54/4/017
14. Dreindl R, Georg D, Stock M. Radiochromic film dosimetry: considerations on precision and accuracy for EBT2 and EBT3 type films. *Z Med Phys* 2014; **24**: 153-63. doi: 10.1016/j.zemedi.2013.08.002
15. Palmer AL, Bradley DA, Nisbet A. Evaluation and mitigation of potential errors in radiochromic film dosimetry due to film curvature at scanning. *J Appl Clin Med Phys* 2015; **16**: 425-31. doi: 10.1120/jacmp.v16i2.5141
16. León Marroquín EY, Herrera González JA, Camacho López MA, Villarreal Barajas JE, García-Garduño OA. Evaluation of the uncertainty in an EBT3 film dosimetry system utilizing net optical density. *J Appl Clin Med Phys* 2016; **17**: 466-81. doi: 10.1120/jacmp.v17i5
17. Aldelajjan S, Devic S, Papaconstadopoulos P, Bekerat H, Cormack RA, Seuntjens J, et al. Dose-response linearization in radiochromic film dosimetry based on multichannel normalized pixel value with an integrated spectral correction for scanner response variations. *Med Phys* 2019; **46**: 5336-49. doi: 10.1002/mp.13818
18. Low DA, Dempsey JF. Evaluation of the gamma dose distribution comparison method. *Med Phys* 2003; **30**: 2455-64. doi: 10.1118/1.1598711.
19. Winiacki J, Morgaś T, Majewska K, Drzewiecka B. The gamma evaluation method as a routine QA procedure of IMRT. *Reports Pract Oncol Radiother* 2009; **14**: 162-8. doi: 10.1016/S1507-1367(10)60031-4
20. Low DA, Harms WB, Mutic S, Purdy JA. A technique for the quantitative evaluation of dose distributions. *Med Phys* 1998; **25**: 656-61. doi: 10.1118/1.598248.
21. Clasié BM, Sharp GC, Seco J, Flanz JB, Kooy HM. Numerical solutions of the γ -index in two and three dimensions. *Phys Med Biol* 2012; **57**: 6981-97. doi: 10.1088/0031-9155/57/21/6981
22. García-Garduño OA, Lárraga-Gutiérrez JM, Rodríguez-Villafuerte M, Martínez-Dávalos A, Rivera-Montalvo T. Effect of correction methods of radiochromic EBT2 films on the accuracy of IMRT QA. *Appl Radiat Isot* 2016; **107**: 121-6. doi: 10.1016/j.apradiso.2015.09.016
23. González-López A, Vera-Sánchez JA, Ruiz-Morales C. Technical note: statistical dependences between channels in radiochromic film readings. Implications in multichannel dosimetry. *Med Phys* 2016; **43**: 2194-9. doi: 10.1118/1.4945273
24. González-López A, Vera-Sánchez JA, Ruiz-Morales C. The incidence of the different sources of noise on the uncertainty in radiochromic film dosimetry using single channel and multichannel methods. *Phys Med Biol* 2017; **62**: N525-36. doi: 10.1088/1361-6560/aa8f74
25. Li Y, Chen L, Zhu J, Liu X. The combination of the error correction methods of GAFCHROMIC EBT3 film. *PLoS One* 2017; **12**: 1-17. doi: 10.1371/journal.pone.0181958
26. Méndez I, Polšák A, Hudej R, Casar B. The Multigaussian method: a new approach to mitigating spatial heterogeneities with multichannel radiochromic film dosimetry. *Phys Med Biol* 2018; **63**: 175013. doi: 10.1088/1361-6560/aad9c1
27. Micke A, Lewis DF, Yu X. Multichannel film dosimetry with nonuniformity correction. *Med Phys* 2011; **38**: 2523-34. doi: 10.1118/1.3576105
28. Ashland Inc. Efficient protocols for accurate radiochromic film calibration and dosimetry 2016. [cited 2020 Jan 15]. Available at: <http://www.gafchromic.com/documents/Efficient%20Protocols%20for%20Calibration%20and%20Dosimetry.pdf>
29. Mayer RR, Ma F, Chen Y, Miller RI, Belard A, McDonough J, et al. Enhanced dosimetry procedures and assessment for EBT2 radiochromic film. *Med Phys* 2012; **39**: 2147-55. doi: 10.1118/1.3694100
30. Méndez I. Model selection for radiochromic film dosimetry. *Phys Med Biol* 2015; **60**: 4089-104. doi: 10.1088/0031-9155/60/10/4089
31. Méndez I, Peterlin P, Hudej R, Strojnik A, Casar B. On multichannel film dosimetry with channel-independent perturbations. *Med Phys* 2014; **41**: 011705. doi: 10.1118/1.4845095
32. Méndez I, Hartman V, Hudej R, Strojnik A, Casar B. Gafchromic EBT2 film dosimetry in reflection mode with a novel plan-based calibration method. *Med Phys* 2013; **40**: 1-9. doi: 10.1118/1.4772075.
33. Cheung T, Butson MJ, Yu PKN. Post-irradiation colouration of Gafchromic EBT radiochromic film. *Phys Med Biol* 2005; **50**: N281-5. doi: 10.1088/0031-9155/50/20/N04
34. Ruiz-Morales C, Vera-Sánchez JA, González-López A. On the re-calibration process in radiochromic film dosimetry. *Phys Medica* 2017; **42**: 67-75. doi: 10.1016/j.ejmp.2017.08.013
35. Agnew CE, McGarry CK. A tool to include gamma analysis software into a quality assurance program. *Radiation Oncol* 2016; **118**: 568-73. doi: 10.1016/j.radonc.2015.11.034
36. Cusumano D, Fumagalli ML, Marchetti M, Fariselli L, De Martin E. Dosimetric verification of stereotactic radiosurgery/stereotactic radiotherapy dose distributions using Gafchromic EBT3. *Med Dosim* 2015; **40**: 226-31. doi: 10.1016/j.meddos.2015.01.001
37. Wen N, Lu S, Kim J, Qin Y, Huang Y, Zhao B, et al. Precise film dosimetry for stereotactic radiosurgery and stereotactic body radiotherapy quality assurance using Gafchromic™ EBT3 films. *Radiat Oncol* 2016; **11**: 1-11. doi: 10.1186/s13014-016-0709-4
38. Hanušová T, Horáková I, Koniarová I. IMRT plan verification with EBT2 and EBT3 films compared to PTW 2D-ARRAY seven29. *Radiat Phys Chem* 2017; **140**: 365-9. doi: 10.1016/j.radphyschem.2017.02.041
39. Lewis D, Micke A, Yu X, Chan MF. An efficient protocol for radiochromic film dosimetry combining calibration and measurement in a single scan. *Med Phys* 2012; **39**: 6339-50. doi: 10.1118/1.4754797
40. Marrazzo L, Zani M, Pallotta S, et al. GafChromic® EBT3 films for patient specific IMRT QA using a multichannel approach. *Phys Medica* 2015; **31**: 1035-42. doi: 10.1016/j.ejmp.2015.08.010
41. Calvo-Ortega JF, Pozo M, Moragues S, Casals J. Fast protocol for radiochromic film dosimetry using a cloud computing web application. *Phys Medica* 2017; **39**: 1-8. doi: 10.1016/j.ejmp.2017.05.072

Radiol Oncol 2020; 54(4): 371-376.
doi: 10.2478/raon-2020-0053

Sodobno zdravljenje raka zunanjega spolovila

Merlo S

Izhodišča. Rak zunanjega spolovila predstavlja 3–5 % rakavih obolenj ženskega spolovila. Slovenska incidenca je 5,5 / 100.000, kar predstavlja 57 novih primerov letno. Najpogostejši histološki tip (90 %) je ploščatocelični rak. Etiološko razvrščamo rak zunanjega spolovila na dva tipa. Prvi tip je povezan z okužbo s humanim papiloma virusom in drugi tip, ki s to okužbo ni povezan. Najpogostejši in običajno dolgotrajni simptom raka zunanjega spolovila je srbenje. Glavni in najprimernejši diagnostični postopek za potrditev diagnoze raka zunanjega spolovila je *punch* oz. incizijska biopsija. Kirurgija v kombinaciji z radioterapijo predstavlja standardno zdravljenje. Biopsija varovalne bezgavke z limfoscintigrafijo pa je danes standardni del kirurškega zdravljenja, ki zmanjšuje kirurško obolevnost. Sistemskega zdravljenja se običajno poslužujemo pri paliativnih bolnicah oz. razsejani obliki bolezni.

Zaključki. Rak zunanjega spolovila je redko obolenje. Zaradi patogeneze predstavljata kirurgija in radioterapija glavni izbiri zdravljenja. Biopsija varovalne bezgavke je sodoben način zdravljenja raka zunanjega spolovila in pomenljivo zmanjša obolevnost. Napredki pri zdravljenju raka zunanjega spolovila pa so doprinesli k zmanjšanju smrtnosti med slovenskimi bolnicami.

Radiol Oncol 2020; 54(4): 377-393.
doi: 10.2478/raon-2020-0060

Primarno zdravljenje ploščatoceličnega raka v področju glave in vratu s kombinacijo radioterapije in imunoterapije. Pregled trenutnih kliničnih raziskav

Plavc G, Strojan P

Izhodišča. Ploščatocelični rak v področju glave in vratu je pri večini bolnikov že ob ugotovitvi diagnoze lokoregionalno napredovala bolezen in se kljub agresivnemu zdravljenju pogosto ponovi. Odkar so zaviralci imunskih kontrolnih točk (*angl. immune checkpoint inhibitors*) pokazali klinično dobrobit pri zdravljenju bolnikov z recidivnim ali razsejanim ploščatoceličnim rakom glave in vratu, je njihova vloga tudi v primarnem zdravljenju nemetastatske bolezni predmet številnih kliničnih raziskav. Predklinični podatki kažejo na sinergistično delovanje sočasne radioterapije in imunoterapije, zato mnoge raziskave preučujejo to kombinacijo v kontekstu definitivne, neoadjuvantne ali adjuvantne terapije nemetastatske oblike bolezni pri bolnikih s tem rakom. Zaradi zapletene interakcije med imunskim sistemom, rakom, imunoterapijo in radioterapijo ima vsak od pristopov prednosti in slabosti. Predstavljamo biološko ozadje sinergističnega delovanja sočasne imunoradioterapije, prednosti in slabosti posameznih terapevtskih pristopov in posredujemo kritičen pregled zaključenih in še potekajočih kliničnih raziskav.

Zaključki. Medtem ko je imunoterapija z zaviralci imunskih kontrolnih točk že postala standarden del zdravljenja bolnikov z recidivnim ali razsejanim ploščatoceličnim rakom glave in vratu, je učinkovitost takšne imunoterapije pri nemetastatski obliki bolezni še vedno del intenzivnega kliničnega preizkušanja. Obsevanje lahko pripomore k premagovanju številnih mehanizmov, s katerimi se rakave celice izognejo imunskemu sistemu, kar vodi v sinergistično delovanje z imunoterapijo. Glede na to, da na učinkovitost kombinacije imunoradioterapije vplivajo številni dejavniki, so podrobnosti v zasnovi kliničnih raziskav, ki preučujejo ta pristop, izjemno pomembne.

Radiol Oncol 2020; 54(4): 394-408.

doi: 10.2478/raon-2020-0055

Korelacije med kazalci difuzijskega tenzorskega slikanja in magnetnoresonančno spektroskopijo v posameznih regijah glioblastomih. Pilotna raziskava

Flores-Alvarez E, Rios-Piedra EA, Cruz-Priego GA, Durand-Muñoz C, Moreno-Jimenez S, Roldan-Valadez E

Izhodišča. Korelacije med posameznimi kazalci difuzijskega tenzorskega slikanja in z magnetnoresonančno spektroskopijo določenimi razmerji presnovkov v posameznih regijah glioblastomih še niso bili povsem raziskani.

Bolniki in metode. Pri bolnikih z glioblastomom smo retrospektivno preverili korelacije med razmerji presnovkov v možganovini (holin/N-acetil aspartat [Cho/NAA], lipidi in laktat / kreatin [LL/Cr] in mio-inositol/kreatin [ml/Cr]) in enajstimi kazalci difuzijskega tenzorskega slikanja: srednje difuzivnosti (*angl. mean diffusivity*; MD), frakcijske anizotropije (*angl. fractional anisotropy*, FA), čiste izotropne difuzije (*angl. pure isotropic diffusion*, p), čisto anizotropno difuzijo (*angl. pure anisotropic diffusion*, q), celokupno magnitudo difuzijskega tenzorja (*angl. total magnitude of the diffusion tensor*, L), linearnim tenzorjem (*angl. linear tensor*, Cl), planarnim tenzorjem (*angl. planar tensor*, Cp), sferičnim tenzorjem (*angl. spherical tensor*, Cs), relativno anizotropijo (*angl. relative anisotropy*, RA), aksialno difuzivnostjo (*angl. axial diffusivity*, AD) in radialno difuzivnostjo (*angl. radial diffusivity*, RD) v istih predelih možganovine. Opazovali smo predel robnega postkontrastnega ojačanja, predel peritumorskega edema in predel bele možganovine normalnega izgleda. Za vrednotenje korelacij skupno 546 magnetnoresonančnih spektroskopij in meritev difuzijskega tenzorskega slikanja smo uporabili Spearmanov količnik.

Rezultati. V predelu robnega postkontrastnega ojačanja smo našli štiri značilne korelacije: FA \leftrightarrow LL/Cr, $R_s = -.364$, $p = .034$; Cp \leftrightarrow LL/Cr, $R_s = .362$, $p = .035$; q \leftrightarrow LL/Cr, $R_s = -.349$, $p = .035$; RA \leftrightarrow LL/Cr, $R_s = -.357$, $p = .038$. Deset dodatnih korelacij smo odkrili v predelu peritumorskega edema: AD \leftrightarrow LL/Cr, AD \leftrightarrow ml/Cr, MD \leftrightarrow LL/Cr, MD \leftrightarrow ml/Cr, p \leftrightarrow LL/Cr, p \leftrightarrow ml/Cr, RD \leftrightarrow ml/Cr, RD \leftrightarrow ml/Cr, L \leftrightarrow LL/Cr, L \leftrightarrow ml/Cr.

Zaključki. Raziskava je pokazala, da obstajajo med kazalci magnetnoresonančne spektroskopije in difuzijskega tenzorskega slikanja pri bolnikih z glioblastomom - predvsem v predelu peritumorskega edema - značilne korelacije, kljub temu, da rezultati odsevajo različne biološke značilnosti tumorjev. Da bi opisane povezave pojasnili, so potrebne nadaljne raziskave, tako pri bolnikih z glioblastomom, kot tudi pri drugih boleznih v možganovini.

Radiol Oncol 2020; 54(4): 409-418.
doi: 10.2478/raon-2020-0052

Vzorčenje nadledvičnih ven pri primarnem aldosteronizmu. 15 let izkušenj nacionalnega referenčnega centra

Kocjan T, Jensterle M, Vidmar G, Vrčkovnik R, Berden P, Stanković M

Izhodišča. Vzorčenje nadledvičnih ven je ključni del diagnostične obravnave primarnega aldosteronizma, ki loči med enostransko in obojestransko boleznijo ter določa izbiro zdravljenja. Pregledati smo uspešnost prvih 15 let vzorčenja nadledvičnih ven pri primarnem aldosteronizmu v nacionalnem endokrinološkem referenčnem centru. Začetno obdobje smo primerjali z obdobjem po vključitvi usmerjenega radiologa v letu 2012. Dodatno smo rezultate vzorčenja nadledvičnih ven primerjali z izvidi CT in ocenili delež operiranih bolnikov z dokazano enostransko boleznijo.

Bolniki in metode. V retrospektivno presečno raziskavo smo vključili vse bolnike s primarnim aldosteronizmom, pri katerih smo naredili vzorčenje nadledvičnih ven po njegovi uvedbi v obdobju 2004 do konca 2018. Vzorčenje nadledvičnih ven smo opravili sekvenčno med neprekinjenim spodbujanjem s Synacthenom. Ko je bilo razmerje koncentracije kortizola med nadledvično veno in spodnjo votlo veno vsaj 5, smo vzorčenje nadledvičnih ven smatrali za uspešno.

Rezultati. Pregledali smo podatke 235 bolnikov (168 moških; starost 32–73, mediana 56 let; indeks telesne mase 18–48, mediana 30,4 kg/m²). Povprečno število letno opravljenih postopkov vzorčenja nadledvičnih ven se je povečalo iz 7 v obdobju 2004–2011 na 29 v obdobju med 2012–2018 ($p < 0,001$). Vzorčenje nadledvičnih ven je bilo potrebno ponoviti v 10 % primerov; uspešnih je bilo 77 % vseh postopkov in pri 86 % bolnikov. Delež bolnikov z uspešnim vzorčenjem nadledvičnih ven (92 % med 2012–2018 proti 66 % med 2004–2011, $p < 0,001$) in uspešnih postopkov vzorčenja nadledvičnih ven (82 % proti 61 %, $p < 0,001$) je bil v zadnjem obdobju statistično značilno višji.

Zaključki. Število postopkov vzorčenja nadledvičnih ven in njihova uspešnost sta se s časom povečala. Uvedba usmerjenega radiologa in tehnični napredek sta razširila in izboljšala izvedbo vzorčenja nadledvičnih ven.

Radiol Oncol 2020; 54(4): 419-428.

doi: 10.2478/raon-2020-0061

Pomen difuzijsko poudarjenih tehnik magnetnoresonančnega slikanja 3 Tesla pri adneksalnih tumorjih

Dimova J, Zlatareva D, Bakalova R, Aoki I, Hadjidekov G

Izhodišča. Namen raziskave je bil opredeliti različne vrste adneksalnih tumorjev in ugotoviti uporabnost difuzijsko poudarjenih slikovnih tehnik v primerjavi s standardnimi sekvencami ob uporabi magnetno resonančnega slikanja (MRI) 3T.

Bolniki in metode. V raziskavo smo vključili 174 žensk, starih od 13 do 87 let, pri katerih smo v obdobju treh let naredili magnetnoresonančno preiskavo medenice. Preiskave smo opravili na dveh radioloških oddelkih in dveh različnih aparatih: pri 135 bolnicah smo uporabili MRI 3 Tesla Siemens Verio in pri 39 bolnicah MRI 3 Tesla Philips Ingeina. V raziskavo smo vključili 98 preiskovank, pri katerih je bil odkrit vsaj en adneksalni tumor. Nekatere od preiskovank so bile obravnavane retrospektivno. Upoštevali smo tudi anamnestične podatke, ugotovitve kliničnih pregledov in laboratorijske podatke.

Rezultati. V skupini 98 preiskovank s povprečno starostjo 47,2 let smo odkrili 124 ovarijskih tumorjev. V skladu z magnetnoresonančnimi kriteriji je bilo 59,2 % benignih, 30,6 % malignih in 10,2 % mejnih. 58,1 % tumorjev je bilo cistične, 12,9 % trdne in 29 % mešane konsistence. Histološka analiza je potrdila 74,4 % tumorjev kot benigne in 25,6 % kot maligne. Vsi maligni tumorji so na MRI kazali omejeno difuzijo. 64 preiskovank je opravilo MRI s kontrastnim sredstvom, pri 34 je bila uporaba kontrastnega sredstva kontraindicirana. 39 % tumorjev (61 %) je kazalo ojačenje po dodatku kontrasta.

Zaključki. Opredelitev adneksalnih tumorjev je ključna v predoperativni obravnavi bolnikov. MRI 3T, še posebno difuzijsko poudarjene slikovne tehnike, pomembno izboljšajo natančnost diagnostične obravnave.

Radiol Oncol 2020; 54(4): 429-436.
doi: 10.2478/raon-2020-0057

Vpliv genetske variabilnosti v *IL1B* in *MIR146A* na tveganje za nastanek plevralnih plakov in malignega mezotelioma

Piber P, Vavpetič N, Goričar K, Dolžan V, Kovač V, Franko A

Izhodišča. Izpostavljenost azbestu je povezana s tveganjem za nastanek plevralnih plakov in malignega mezotelioma, saj njegova vlakna aktivirajo makrofage, čemur sledi sproščanje vnetnih mediatorjev, med drugim tudi interleukina 1 β (IL1 β). Na izražanje IL-1 β vpliva genetska variabilnost *IL1B* in regulatorne mikroRNA (miRNA). Ta raziskava je preučevala vpliv polimorfizmov *IL1B* in *MIR146A* na tveganje za razvoj plevralnih plakov in malignega mezotelioma.

Preiskovanci in metode. V raziskavo smo vključili 394 bolnikov s plevralnimi plaki, 277 bolnikov z malignim mezoteliomom in 175 zdravih preiskovancev, pri katerih smo določili polimorfizme *IL1B* in *MIR146A*. Za statistično analizo smo uporabili logistično regresijo.

Rezultati. Noben polimorfizem ni pokazal statistično značilnega vpliva na tveganje za razvoj plevralnih plakov. Polimorfizem *MIR146A* rs2910164 je statistično značilno zmanjšal tveganje za nastanek malignega mezotelioma (razmerje obetov [OR] = 0,31; 95 % interval zaupanja [CI] = 0,13–0,73; $p = 0,008$). Nosilci dveh polimorfni alelov so imeli manjše tveganje za nastanek malignega mezotelioma tudi po prilagoditvi po starosti in spolu (OR = 0,34; 95 % CI = 0,14–0,85; $p = 0,020$). Nosilci vsaj enega polimorfne alela *IL1B* rs1143623 v podskupini z znano izpostavljenostjo azbestu so imeli v multivariatni analizi manjše tveganje za nastanek malignega mezotelioma (OR = 0,50; 95 % CI = 0,28–0,92; $p = 0,025$). Interakcija med polimorfizmoma *IL1B* rs1143623 in *IL1B* rs1071676 je imela statistično značilen vpliv na povečanje tveganja za maligni mezoteliom ($p = 0,050$).

Zaključki. V raziskavi smo pokazali, da bi genetska variabilnost vnetnega mediatorja IL-1 β lahko vplivala na tveganje za razvoj malignega mezotelioma, ne pa plevralnih plakov.

Radiol Oncol 2020; 54(4): 437-446.

doi: 10.2478/raon-2020-0054

Razmerje med nevtrofilci in limfociti lahko napoveduje izid zdravljenja pri razširjenem drobnoceličnem raku pljuč

Drpa G, Šutić M, Baranašić J, Jakopović M, Samaržija M, Kukulj S, Knežević J

Izhodišča. Razmerje med nevtrofilci in limfociti (NLR), razmerje med trombociti in limfociti (PLR) ter razmerje med limfociti in monociti (LMR) so analizirali pri različnih rakih in opredeljevali njihov pomen pri napovedovanju poteka bolezni. Cilj pričujoče raziskave je bil ugotoviti povezavo med temi parametri in preživetjem bolnikov z drobnoceličnim rakom pljuč, saj je bilo objavljenih zelo malo raziskav pri tej vrsti raka.

Bolniki in metode. Retrospektivno smo analizirali 140 bolnikov, ki smo jim diagnosticirali drobnocelični rak pljuč na Kliničnem oddelku Jordanovac med letoma 2012 in 2016. Razširjeno bolezen smo ugotovili pri 80 bolnikih, omejeno obliko bolezni pa pri 60 bolnikih. Analizirali smo potencialni napovedni pomen različnih laboratorijskih parametrov, vključno z NLR, PLR in LMR, določenih pred začetkom zdravljenja.

Rezultati. Razširjenost bolezni, odgovor na zdravljenje, obsevanje prsnega koša in profilaktično obsevanje glave, pa tudi hemoglobin, število monocitov, C-reaktivni protein in laktatna dehidrogenaza (LDH) so bili napovedno dejavnik pri vseh bolnikih. Ko smo ločeno analizirali bolnike z ozirom na razširjenosti bolezni, smo ugotovili, da imajo napovedni pomen poteka bolezni pri razširjeni bolezni le kožne metastaze in vrednosti LDH in NLR, ne glede na mejno vrednost. Napovedni pomen pri omejeni obliki bolezni pa so imeli stanje zmogljivosti, obsevanje prsnega koša, profilaktično obsevanje glave ter vrednosti hemoglobina in kreatinina.

Zaključki. NLR, izračunan pred začetkom zdravljenja, je imel napovedni pomen poteka bolezni pri razširjeni obliki drobnoceličnega rakam pljuč, medtem ko PLR in LMR nista bila napovedno pomembna pri nobeni od analiziranih skupin bolnikov.

Radiol Oncol 2020; 54(4): 447-454.
doi: 10.2478/raon-2020-0058

Izsledki o načinih zdravljenja III. stadija nedrobnoceličnega pljučnega raka v Srednji in Vzhodni Evropi

Zemanová M, Jakopović M, Stanič K, Łazar-Poniatowska M, Vrankar M, Rusu P, Ciuleanu T, Radosavljević D, Bogos K, Nawrocki S

Izhodišča. Namen raziskave je bil zbrati izsledke o načinih zdravljenja III. stadija nedrobnoceličnega pljučnega raka v Srednji in Vzhodni Evropi. Na podlagi izsledkov o kliničnih praksah so avtorji oblikovali strokovno mnenje o pomanjkljivosti obravnave in o kazalnikih kakovosti.

Bolniki in metode. Multidisciplinarna strokovna skupina 10 zdravnikov iz 7 držav je sistematično pregledala literaturo ter uporabila modificiran postopek Delphi za določitev pomanjkljivosti obravnave in obravnavala kazalnike kakovosti pri bolnikih s III. stadijem nedrobnoceličnega pljučnega raka. Uporabili so podroben vprašalnik, s katerim so opredelili načine zdravljenja teh bolnikov in prepoznavali vzorce njihove obravnave v Srednji in Vzhodni Evropi. Najprej je vprašalnik izpolnila skupina onkologov internistov, onkologov radioterapevtov in pulmologov. Nato se je strokovna skupina osebno srečala na sestanku in pregledala rezultate vprašalnika ter pripravila drugi krog postopka Delphi, v katerem je izdelala in dopolnila dodatno anketo. Raziskavo so končali s končnim pregledom in sintezo izsledkov.

Rezultati. Strokovna skupina je dosegla popolno soglasje pri nizu kliničnih priporočil, ki temeljijo na medicinskih dokazih. Odgovori v vprašalniku so pokazali zelo različne vzorce zdravljenja v regiji. Seznam pomanjkljivosti obravnave in ovir za kakovostno oskrbo je bil pripravljen s skoraj popolnim soglasjem strokovne skupine.

Zaključki. Vzorci zdravljenja bolnikov s III. stadijem nedrobnoceličnega pljučnega raka kažejo na veliko raznolikost obravnave v Srednji in Vzhodni Evropi. Avtorji ugotavljajo, da je predvsem razpoložljivost slikovnodiagnostičnih preiskav pomanjkljiva in da je sorazmerno majhen delež bolnikov zdravljenih s kemoradioterapijo in namenom ozdravitve pri neresektabilnih tumorjih.

Radiol Oncol 2020; 54(4): 455-460.

doi: 10.2478/raon-2020-0059

Zdravljenje otrok in mladostnikov z rabdomyosarkomom v štirih evropskih državah z nizkimi izdatki za zdravstvo

Česen Mazić M, Bonevski A, Mikeškova M, Mihut E, Bisogno G, Jazbec J

Izhodišča. Preživetje otrok z rakom je v državah Vzhodne in Centralne Evrope 10–20 % nižje v primerjavi z evropskimi državami, ki za zdravstvo namenijo več denarja. Ocenili smo preživetje otrok in mladostnikov z rabdomyosarkomom, ki so bili zdravljeni v štirih evropskih državah z nizkimi izdatki za zdravstvo (Slovenija, Hrvaška, Slovaška, Romunija).

Bolniki in metode. V retrospektivni raziskavi smo ocenili preživetje za vse bolnike zdravljene v izbranem časovnem obdobju v Sloveniji in Hrvaški. Slovaška je vključila bolnike iz dveh otroških onkoloških bolnišnic, kar predstavlja polovico vseh bolnikov z rabdomyosarkomom iz te države. Romunija je posredovala podatke za bolnike zdravljene v enem samem centru, kar ustreza desetini vseh pričakovanih bolnikov.

Rezultati. Raziskava je zajela 178 otrok in mladostnikov z rabdomyosarkomom, ki so bili zdravljeni v obdobju od januarja 2000 do decembra 2015. Povprečna starost ob diagnozi je bila 7,7 let. Tretjina otrok je bila starejših od 10 let, četrtnina je imela tumor z alveolarno histologijo in 72 % neugodno lokacijo primarnega tumorja. Delež bolnikov z razširjeno boleznijo, zasevki v regionalnih bezgavkah (24 %) ali oddaljenimi zasevki (27 %), je bil večji od pričakovanega. Vsi bolniki so prejeli sistemsko kemoterapijo; 57 % bolnikov je bilo v sklopu lokalnega zdravljenja obsevanih in 63 % operiranih. Pet letno preživetje brez ponovitve in celokupno preživetje je znašalo 50,7 % oziroma 59,6 %. Pet letno preživetje bolnikov z lokalizirano boleznijo je bilo 72 %, tistih z oddaljenimi zasevki pa le 24 %.

Zaključki. Otroci in mladostniki z rabdomyosarkomom, ki so zdravljeni v državah Vzhodne in Centralne Evrope, imajo slabše preživetje kot vrstniki iz evropskih držav z velikimi izdatki za zdravstvo. Aktivno sodelovanje v mednarodnih kliničnih raziskavah na področju otroške onkologije bi lahko izboljšalo izhod bolnikov v državah z nižjimi izdatki za zdravstvo.

Radiol Oncol 2020; 54(4): 461-469.
doi: 10.2478/raon-2020-0043

Vpliv sočasne kemoradioterapije s kapecitabinom in bevacizumabom na preživetje, pozno toksičnost in z zdravjem povezano kakovostjo življenja pri bolnikih z lokalno napredovalim rakom danke. (Prospektivna raziskava faze II »CRAB«)

Velenik V, Zadnik V, Omejc M, Grosek J, Tuta M

Izhodišča. Le malo raziskav je poročalo o zgodnjih rezultatih učinkovitosti in toksičnosti kombiniranega zdravljenja lokalno napredovalnega raka danke z dodajanjem bevacizumaba k predoperativni kemoradioterapiji. Dolgoročnih podatkov o preživetju in poznih zapletih pa ni. Poleg tega nobena raziskava ni poročala o oceni z zdravjem povezane kakovosti življenja.

Bolniki in metode. Po več kot 5 letih spremljanja smo posodobili rezultate klinične raziskave II. faze pri 61 bolnikih z lokalno napredovalim rakom danke. Zdravili smo jih z neoadjuvantno s kapecitabinom, radioterapijo in bevacizumabom (raziskava CRAB) pred operacijo in adjuvantno s kemoterapijo. Sekundarni cilji posodobljene analize so bili lokalna kontrola, preživetje brez bolezni, celokupno preživetje, pozna toksičnost in kakovost življenja (pred začetkom zdravljenja in eno leto po zdravljenju) z vprašalnikom EORTC QLQ-C30 in EORTC QLQ-CR38.

Rezultati. Srednji čas spremljanja bolnikov je bil 67 mesecev. V tem obdobju je umrlo 16 bolnikov (26,7 %). 5-letna stopnja celokupnega preživetja, preživetja brez bolezni in lokalna kontrola so bila 72,2 %, 70 % in 92,4 %. Bolniki s patološkimi pozitivnimi področnimi bezgavkami ali patološkimi T3–4 tumorji so imeli znatno slabše preživetje kot bolniki s patološkimi negativnimi ali T0–2 tumorji. Devet bolnikov (14,8 %) je razvilo pozne zaplete stopnje 3 ali več kombiniranega zdravljenja. Prvi dogodek smo beležili 12 mesecev in zadnji 87 mesecev po operaciji (srednji čas 48 mesecev). Na podlagi rezultatov vprašalnika EORTC QLQ-C30 eno leto po zdravljenju ni bilo bistvenih sprememb globalne kakovosti življenja in treh simptomov (bolečina, nespečnost in diareja), fizično in socialno delovanje pa sta se znatno zmanjšala. Na podlagi rezultatov QLQ-CR38 se je telesna samopodoba bistveno izboljšala, težave z izgubo teže so se znatno zmanjšale, vendar ob povečanju spolne disfunkcije pri moških in povečanju neželenih učinkov kemoterapije.

Zaključki. Za izboljšanje dolgoročnih rezultatov preživetja potrebujejo bolniki z lokalno napredovalim rakom danke in z visokimi dejavniki tveganja, kot so pozitivne patološke bezgavke in visoki patološki stadij T, agresivnejše zdravljenje. Posebno skrb moramo nameniti uravnavanju njihovih posameznih vidikov kakovosti življenja ter pojavu in reševanju poznih sopojavov kombiniranega zdravljenja.

Radiol Oncol 2020; 54(4): 470-479.

doi: 10.2478/raon-2020-0050

Obsevalni volumni po operaciji zaradi raka leve dojke in načrtovana absorbirana doza srčnih struktur pri tridimenzionalnem konformnem obsevanju ali tangencialni obliki intenzitetno modulirajočega obsevanja

Ratoša I, Jenko A, Šljivić Ž, Pirnat M, Oblak I

Izhodišča. Namen raziskave je bila primerjava načrtovanih absorbiranih doz tridimenzionalnega konformnega obsevanja (3D-CRT) in tangencialne oblike intenzitetno modulirajočega obsevanja (t-IMRT) pri bolnicah, ki smo jih zdravili z obsevanjem po operaciji zaradi raka leve dojke. Z raziskavo smo želeli natančneje analizirati načrtovano absorbirano dozo srca, srčnih votlin in koronarnih arterij ob sočasnem upoštevanju različne anatomije oziroma velikosti obsevalnih volumnov.

Bolniki in metode. V analizo smo vključili 60 posnetkov računalniške tomografije (CT) bolnic. Na vsak set slik CT smo s pomočjo atlasa vrisali kritične zdrave organe, vključno s posameznimi strukturami srca ter tarčne volumne. Za vsak set CT smo pripravili dva obsevalna načrta: 3D-CRT in t-IMRT. Načrtovana absorbirana doza je bila 1,6-krat 2,67 Gy. Posnetke CT smo razvrstili v skupino z majhnim, srednjim in velikim kliničnim tarčnim volumnom (CTV).

Rezultati. Povprečne absorbirane doze za celotno srce (1,9 proti 2,1 Gy; $P < 0,005$), levo sprednjo koronarno arterijo (8,2 proti 8,4 Gy; $P < 0,005$) in za levi prekat (3,0 proti 3,2 Gy; $P < 0,005$) so bile nižje ob uporabi obsevalne tehnike 3D-CRT. Posamezni srčni segmenti so prejeli najvišje povprečne doze, predvsem apikalni (8,5 proti 9,0 Gy; $P < 0,005$) in sprednji predel (5,0 proti 5,4 Gy; $P < 0,005$) levega prekata. Povprečni dozi za celotno srce in levi prekat sta bili višji ob večanju CTV neodvisno od obsevalne tehnike. Nizke vrednosti povprečne obsevalne doze za srce ($< 2,5$ Gy) so bile dosežene pri 44 (73,3 %) bolnicah s tehniko 3D-CRT in pri 41 (68,3 %) bolnicah s tehniko t-IMRT.

Zaključki. Rezultati raziskave potrjujejo precejšnje razlike v povprečni absorbirani dozi srca ali levega prekata, pri bolnicah, ki se zdravijo z obsevanjem po operaciji zaradi raka leve dojke. Ugotovljene razlike so lahko posledica tako uporabljene tehnike obsevanja kakor tudi telesne konstitucije bolnice, kamor spada tudi velikost obsevalnega volumna.

Radiol Oncol 2020; 54(4): 480-487.
doi: 10.2478/raon-2020-0039

Dolgotrajni rezultati toksičnosti in preživetja po stereotaktični ablativni radioterapiji pri bolnikih s centralnimi pljučnimi tumorji

Atalar B, Mustafayev TZ, Sio TT, Sahin B, Gungor G, Aydın G, Yapici B, Ozyar E

Izhodišča. Stereotaktična ablativna radioterapija (SABR) je učinkovita pri primarnih tumorjih prsnega koša in metastazah; vendar so neželeni učinki večji pri centralnih tumorjih. Ocenili smo dejavnike, ki vplivajo na izid in toksičnost po SABR pri bolnikih s primarnimi pljučnimi in oligometastatskimi tumorji.

Bolniki in metode. Retrospektivno smo pregledali zaporedne bolnike s centralno ležečimi pljučnimi tumorji, ki smo jih v naši bolnišnici zdravili od leta 2009 do 2016. Vpliv bolnikov, bolezni in parametrov povezanih z zdravljenjem na lokalno kontrolo, celokupno preživetje in preživetje brez toksičnosti smo ocenili z multivariatno analizo.

Rezultati. Med 65 zaporednimi bolniki s 70 centralno ležečimi tumorji je bilo ponovno obsevanih 20 tumorjev (28 %). Srednja skupna doza (razpon) za vse tumorje je bila 55 Gy (30–60) v 5 (3–10) frakcijah. Radiološki popoln odgovor smo ugotovili pri 43 lezijah (61 %). Noben od analiziranih dejavnikov ni bil povezan s popolnim odgovorom. Po srednjem času spremljanja 57 (95 % interval zaupanja [CI] 48–65) mesecev se je 10 tumorjev (14 %) znova pojavilo, 37 (57 %) bolnikov je umrlo; 2- in 5-letne stopnje celokupnega preživetja so bile 52 % oziroma 28 %. Srednje celokupno preživetje je bilo bistveno nižje pri bolnikih s 3. ali višjo stopnjo toksičnosti proti nižji toksičnosti (5 v primerjavi z 39 meseci; $P < 0,001$). Med 17 primeri resne toksičnosti jih je bilo pet 5. stopnje, med njimi so bili trije ponovno obsevani na isto polje. Preživetje bolnikov brez toksičnosti stopnje 3 do 5 je bila nižja pri bolnikih, ki so bili ponovno obsevani (2-letno preživetje brez toksičnosti 63 % v primerjavi z 96 %; $P = 0,02$).

Zaključki. Raziskava je pokazala, da je sodobna SABR učinkovita pri centralnih pljučnih tumorjih, toksičnost pa je sprejemljiva. SABR pri ponovno obsevanih centralnih pljučnih lezijah in verjetno lezijah, ki se naslanjajo na traheobronhialno drevo, lahko povzroči večje tveganje za resno toksičnost.

Radiol Oncol 2020; 54(4): 488-494.

doi: 10.2478/raon-2020-0030

Ali redna kontrola kakovosti izboljšuje kirurško zdravljenje bolnic iz slovenskega presejalnega programa za raka dojk?

Perhavec A, Miličević S, Perić B, Žgajnar J

Izhodišča. Namen pričujoče raziskave je bil analizirati kakovost kirurškega zdravljenja bolnic s presejalnega programa za raka dojk (DORA) z uporabo uveljavljenih evropskih kazalnikov kakovosti. Dodatno smo analizirali ali se kakovost kirurškega zdravljenja z leti izboljšuje.

Bolnice in metode. V retrospektivno raziskavo smo vključili bolnice s programa DORA, ki so v obdobju od 1. januarja 2016 do 31. decembra 2018 potrebovale kirurški poseg. Za analizo smo uporabili kazalnike kakovosti Evropskega združenja specialistov za rak dojke (angl. *European Society of Breast Cancer Specialists*; EUSOMA) in Evropske mreže raka dojke (angl. *European Breast Cancer Network*; EBCN), pet kazalnikov za terapevtske in dva za diagnostične operacije. Dodatno smo primerjali rezultate med kirurgi.

Rezultati. V triletnem obdobju 2016–2018 je 14 kirurgov opravilo 1421 operacij dojk pri 1398 bolnicah; 1197 terapevtskih (za potrjene rake dojk) in 224 diagnostičnih. Od izbranih zahtevanih kazalcev kakovosti smo dosegali dva za terapevtske in nobenega za diagnostične operacije. Ugotovili pa smo statistično značilen napredek pri treh kazalnikih za terapevtske in enem za diagnostične operacije, kar nakazuje, da redno spremljanje kakovosti vodi k izboljšanju kirurškega zdravljenja. Med kirurgi smo opazili visoko variabilnost pri doseganju kazalcev kakovosti, ki je ostala visoka preko celotnega analiziranega obdobja.

Zaključki. Dosegati merila kazalnikov kakovosti je zahtevno, zlasti ko uporabljamo specifične kazalnike za presejalne programe. Redna kontrola kakovosti vodi k izboljševanju rezultatov. Omejitev kirurškega zdravljenja na manjše število bolj izkušenih kirurgov bi lahko vodila do manjših razlik v kakovosti kirurškega zdravljenja.

Radiol Oncol 2020; 54(4): 494-504.
doi: 10.2478/raon-2020-0051

Eksperimentalno preverjanje računskega algoritma Monte Carlo načrtovalnega sistema v snovi z gostoto kosti

Smilović Radojčić Đ, Casar B, Rajlić D, Švabić Kolacio M, Mendez I, Obajdin N, Dundara Debeljuh D, Jurković S

Izhodišča. Novejši računalniški načrtovalni sistemi, ki uporabljajo simulacijo Monte Carlo, lahko absorbirano dozo izračunavajo na dva načina: kot dozo v snovi in kot dozo v vodi. Predhodne raziskave so pokazale, da obstajajo pomembne razlike med obema načinoma, posebej v primeru, ko izračunavamo dozo v gostejših snoveh z gostoto podobno gostoti kosti. Ker moramo pred klinično uporabo računske algoritme načrtovalnih sistemov eksperimentalno preveriti, smo opravili analizo dveh načinov izračunavanja doze načrtovalnega sistema Elekta Monaco. Izračunane doze smo primerjali z eksperimentalno dobljenimi vrednostmi z namenom, da definiramo dodatni postopek k že obstoječi metodologiji preverjanja računalniških načrtovalnih sistemov.

Materiali in metode. V raziskavi smo uporabili fotonske žarke 6 MV iz linearnega pospeševalnika. Izvedli smo meritve s Farmerjevo ionizacijsko celico v semi-antropomorfnem fantomu in dobljene eksperimentalne rezultate primerjali z izračunanimi vrednostmi. Primerjali smo absorbirane doze pri treh različnih delih fantoma, ki imajo različne gostote. Osredotočili smo se na področje, kjer je gostota podobna gostoti kosti.

Rezultati. Izmerjene in izračunane doze so bile skladne za vse dele fantoma, kjer je gostota podobna gostoti vode ali gostoti pljuč. V področju, kjer je gostota podobna gostoti kosti, smo našli statistično pomembne razlike med eksperimentalnimi in izračunanimi vrednostmi absorbirane doze. Pomembne razlike smo našli tudi med obema načinoma izračunavanja doze – te so bile v razponu od 5,7 do 8,3 %, odvisno od metode, ki smo jo uporabili.

Zaključki. Na osnovi naših izsledkov smo predlagali dodatek k trenutni metodologiji za preverjanje komercialnih načrtovalnih sistemov Monte Carlo z izvedbo dodatnih meritev v snovi, ki ima podobno gostoto, kot jo imajo kosti.

Radiol Oncol 2020; 54(4): 505-512.

doi: 10.2478/raon-2020-0049

Primerjava treh programskih paketov za analizo filmov v radioterapiji ob uporabi filmov EBT2 in EBT3

Pócza T, Zongor Z, Melles-Bencsik B, Tatai-Szabó DZ, Major T, Pesznyák C

Izhodišča. Namen raziskave je bila primerjava programskih paketov za filmsko dozimetrijo z analizo vrednosti gama ob uporabi različnih tipov filmov.

Materiali in metode. Filme smo obsevali na več načinov in uporabili različne načrtovalne oziroma obsevalne tehnike. Uporabili smo tehniko 3D konformnih obsevalnih polj in intenzitetno modulirano tehniko s statičnimi in dinamičnimi obsevalnimi polji. Dodatno smo analizirali tudi obsevalne načrte pripravljene za stereotaktično ločno tehniko s konformnimi in intenzitetno moduliranimi obsevalnimi polji za koplanarna in nekoplanarna polja. Dozno porazdelitev na obsevanih filmih smo primerjali s tisto, ki smo jo dobili v računalniškem načrtovalnem sistemu. Pri analizi smo uporabili tri različne pakete programske opreme, ki jih uporabljamo za filmsko dozimetrijo, PTW Mephysto (PTW), FilmQA Pro (FQP) in Radiochromic.com (RC) ter dva tipa filmov, EBT2 in EBT3. Primerjavo doznih porazdelitev smo naredili z analizo gama kjer smo privzeli 10 % mejno stopnjo.

Rezultati. Pri večjih obsevalni poljih so bile vrednosti gama med 78,3 % in 98,3 %, 75,7 % in 100 % ter 80,2 % in 98,8 % po vrsti za programske pakete PTW, FQP in RC. V primeru, ko smo uporabili stereotaktične obsevalne tehnike, so bile vrednosti gama od 76,8 % do 99,2 % za PTW, od 95,7 % do 100 % za FQP in od 91,2 % do 99,9 % za programski paket RC.

Zaključki. Analiza vrednosti gama je pokazala, da so vsi trije testirani programski paketi ustrezni za filmsko dozimetrijo in jih lahko uporabljamo za individualno dozimetrijo pri bolnikih. Raziskava je pokazala, da ni neposredne povezave med rezultati analize gama in absolutno natančnosti ali kakovostjo programske opreme; različni rezultati so pretežno povezani z individualnimi lastnostmi posameznega programskega paketa. Izsledki pričujoče raziskave dovoljujejo vključitev dozimetričnih postopkov z radiokromskimi filmi v posamezne procese kliničnega dela.



FUNDACIJA "DOCENT DR. J. CHOLEWA"
JE NEPROFITNO, NEINSTITUCIONALNO IN NESTRANKARSKO
ZDRUŽENJE POSAMEZNIKOV, USTANOV IN ORGANIZACIJ, KI ŽELIJO
MATERIALNO SPODBUJATI IN POGLABLJATI RAZISKOVALNO
DEJAVNOST V ONKOLOGIJI.

DUNAJSKA 106
1000 LJUBLJANA

IBAN: SI56 0203 3001 7879 431



Activity of "Dr. J. Cholewa" Foundation for Cancer Research and Education - a report for the fourth quarter of 2020

Doc. Dr. Josip Cholewa Foundation for cancer research and education continues with its planned activities in the fourth quarter of 2020. Its primary focus remains the provision of grants and scholarships and other forms of financial assistance for basic, clinical and public health research in the field of oncology. In parallel, it also makes efforts to provide financial and other support for the organisation of congresses, symposia and other forms of meetings to spread the knowledge about prevention and treatment of cancer, and finally about rehabilitation for cancer patients. In Foundation's strategy, the spread of knowledge should not be restricted only to the professionals that treat cancer patients, but also to the patients themselves and to the general public.

The Foundation continues to provide support for »Radiology and Oncology«, a quarterly scientific magazine with a respectable impact factor that publishes research and review articles about all aspects of cancer. The magazine is edited and published in Ljubljana, Slovenia. »Radiology and Oncology« is an open access journal available to everyone free of charge. Its long tradition represents a guarantee for the continuity of international exchange of ideas and research results in the field of oncology for all in Slovenia that are interested and involved in helping people affected by many different aspects of cancer.

The Foundation will continue with its activities in the future, especially since the problems associated with cancer affect more and more people in Slovenia and elsewhere. Ever more treatment that is successful reflects in results with longer survival in many patients with previously incurable cancer conditions. Thus adding many new dimensions in life of cancer survivors and their families.

Borut Štabuc, M.D., Ph.D.

Andrej Plesničar, M.D., M.Sc.

Viljem Kovač M.D., Ph.D.

TANTUM VERDE®

benzidaminijev klorid

Za lajšanje bolečine in oteklin v ustni votlini in žrelu, ki so posledica radiomukozitisa



Bistvene informacije iz Povzetka glavnih značilnosti zdravila

Tantum Verde 1,5 mg/ml oralno pršilo, raztopina

Tantum Verde 3 mg/ml oralno pršilo, raztopina

Sestava 1,5 mg/ml: 1 ml raztopine vsebuje 1,5 mg benzidaminijevega klorida, kar ustreza 1,34 mg benzidamina. V enem razpršku je 0,17 ml raztopine. En razpršek vsebuje 0,255 mg benzidaminijevega klorida, kar ustreza 0,2278 mg benzidamina. **Sestava 3 mg/ml:** 1 ml raztopine vsebuje 3 mg benzidaminijevega klorida, kar ustreza 2,68 mg benzidamina. V enem razpršku je 0,17 ml raztopine. En razpršek vsebuje 0,51 mg benzidaminijevega klorida, kar ustreza 0,4556 mg benzidamina.

Terapevtske indikacije: **Samozdravljenje:** Lajšanje bolečine in oteklin pri vnetju v ustni votlini in žrelu, ki so lahko posledica okužb in stanj po operaciji. **Po nasvetu in navodilu zdravnika:** Lajšanje bolečine in oteklin v ustni votlini in žrelu, ki so posledica radiomukozitisa. **Odmerjanje in način uporabe:** Odmerjanje 1,5 mg/ml: Odrasli: 4 do 8 razprškov 2- do 6-krat na dan (vsake 1,5 do 3 ure). **Pediatrična populacija:** Mladostniki, stari od 12 do 18 let: 4-8 razprškov 2- do 6-krat na dan. Otroci od 6 do 12 let: 4 razprški 2- do 6-krat na dan. Otroci, mlajši od 6 let: 1 razpršek na 4 kg telesne mase; do največ 4 razprške 2- do 6-krat na dan. Odmerjanje 3 mg/ml: Uporaba 2- do 6-krat na dan (vsake 1,5 do 3 ure). Odrasli: 2 do 4 razprški 2- do 6-krat na dan. **Pediatrična populacija:** Mladostniki, stari od 12 do 18 let: 2 do 4 razprški 2- do 6-krat na dan. Otroci od 6 do 12 let: 2 razprška 2- do 6-krat na dan. Otroci, mlajši od 6 let: 1 razpršek na 8 kg telesne mase; do največ 2 razprška 2- do 6-krat na dan. **Starejši bolniki, bolniki z jetrno okvaro in bolniki z ledvično okvaro:** Uporabo oralnega pršila z benzidaminijevim kloridom se svetuje pod nadzorom zdravnika. **Način uporabe:** Za orofaringealno uporabo. Zdravilo se razprši v usta in žrelo. **Kontraindikacije:** Preobčutljivost na učinkovino ali katero koli pomožno snov. **Posebna opozorila in previdnostni ukrepi:** Če se simptomi v treh dneh ne izboljšajo, se mora bolnik posvetovati z zdravnikom ali zobozdravnikom, kot je primerno. Benzidamin ni priporočljiv za bolnike s preobčutljivostjo nasalicilno kislino ali druga nesteroidna protivnetna zdravila. Pri bolnikih, ki imajo ali so imeli bronhialno astmo, lahko pride do bronhospazma, zato je potrebna previdnost. To zdravilo vsebuje majhne količine etanola (alkohola), in sicer manj kot 100 mg na odmerek. To zdravilo vsebuje metilparahidroksibenzoat (E218). Lahko povzroči alergijske reakcije (lahko zapoznele). Zdravilo z jakostjo 3 mg/ml vsebuje makrogolglicerol hidroksistearat 40. Lahko povzroči želodčne težave in drisko. **Medsebojno delovanje z drugimi zdravili in druge oblike interakcij:** Študij medsebojnega delovanja niso izvedli. **Nosečnost in dojenje:** O uporabi benzidamina pri nosečnicah in doječih ženskah ni zadostnih podatkov. Uporaba zdravila med nosečnostjo in dojenjem ni priporočljiva. **Vpliv na sposobnost vožnje in upravljanja strojev:** Zdravilo v priporočenem odmerku nima vpliva na sposobnost vožnje in upravljanja strojev. **Neželeni učinki:** Neznana pogostnost (ni mogoče oceniti iz razpoložljivih podatkov): anafilaktične reakcije, preobčutljivostne reakcije, odrevenelost, laringospazem, suha usta, navzea in bruhanje, angioedem, fotosenzitivnost, pekoč občutek v ustih. Neposredno po uporabi se lahko pojavi občutek odrevenelosti v ustih in v žrelu. Ta učinek se pojavi zaradi načina delovanja zdravila in po kratkem času izgine. **Način in režim izdaje zdravila:** BRP-Izdaja zdravila je brez recepta v lekarnah in specializiranih prodajalnah.

Imetnik dovoljenja za promet: Aziende Chimiche Riunite Angelini Francesco – A.C.R.A.F. S.p.A., Viale Amelia 70, 00181 Rim, Italija **Datum zadnje revizije besedila:** 14. 10. 2019

Pred svetovanjem ali izdajo preberite celoten Povzetek glavnih značilnosti zdravila.

Samo za strokovno javnost.

Datum priprave informacije: november 2019

Odgovoren za trženje: Bonifar d.o.o.


ANGELINI

PR/BIBEN/2019/012

ONIVYDE: IZDELAN POSEBEJ ZA BOJ PROTI RAKU TREBUŠNE SLINAVKE

ONIVYDE pegylated liposomal je odobren za zdravljenje metastatskega adenokarcinoma trebušne slinavke v kombinaciji s 5-fluorouracilom (5-FU) in levkovorinom (LV) pri odraslih bolnikih, pri katerih je bolezen po zdravljenju na osnovi gemcitabina napredovala.¹

ONIVYDE JE PEGILIRANI LIPOSOM Z IRINOTEKANOM, IZDELAN POSEBEJ ZA UČINKOVITO ZDRAVLJENJE TE AGRESIVNE BOLEZNI²⁻⁵

KLINIČNI PODATKI ŠTUDIJE 3. FAZE POTRJUJEJO EDINSTVENO KLINIČNO VREDNOST ZDRAVILA ONIVYDE V KOMBINACIJI S 5-FU/LV:

- skladni podatki o učinkovitosti pri vseh opazovanih dogodkih: pomembno podaljšanje preživetja in povečana stopnja odziva⁶⁻⁸
 - ohranjena kakovost življenja^{6,9}
 - dobro poznan varnostni profil^{1,6,7}

POMEMBNA UČINKOVITOST ONIVYDE + 5-FU/LV JE POTRJENA V KLINIČNI PRAKSI¹⁰⁻¹²

ONIVYDE + 5-FU/LV PRIPOROČAJO VSE GLAVNE MEDNARODNE SMERNICE¹³⁻¹⁶

LITERATURA: 1. Povzetek glavnih značilnosti zdravila ONIVYDE. 2. Lamb YN, Scott LJ. *Drugs*. 2017;77:785-792. 3. Drummond DC et al. *Cancer Res*. 2006;66:3271-3277. 4. Kalra AV et al. *Cancer Res*. 2014;74:7003-7013. 5. Carnevale J, Ko AH. *Future Oncol*. 2016;12:453-464. 6. Wang-Gillam A et al. *Lancet*. 2016;387:545-557. 7. Wang-Gillam A et al. *Eur J Cancer*. 2019;108:78-87. 8. Chen LT et al. *Eur J Cancer*. 2018;105:71-78. 9. Hubner RA et al. *Eur J Cancer*. 2019;106:24-33. 10. Kieler M et al. *Ther Adv Med Oncol*. 2019;11:1-13. 11. Yoo C et al. *Ther Adv Med Oncol*. 2019;11:1-9. 12. Pellino A et al. *ESMO*. 2019;P660. 13. Duceux M et al. *Ann Oncol*. 2015;26:681-684. 14. Update Cancer of the Pancreas Treatment Recommendations. Published June 2019. ESMO Guidelines Committee. Available at: <https://www.esmo.org/Guidelines/Gastrointestinal-Cancers/Cancer-of-the-Pancreas/Update-Treatment-Recommendations>. Last accessed June 2020. 15. Okusaka T et al. *Pancreas*. 2020;49(3):326-335. 16. NCCN Guidelines Version 1. 2020. Pancreatic Adenocarcinoma. Available at: <https://www2.tri-kobe.org/nccn/guideline/pancreas/english/pancreatic.pdf>. Published November 26, 2019. Last accessed June 2020.

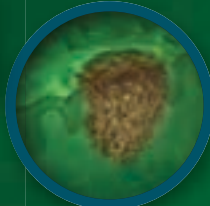


SKRAJŠAN POVZETEK GLAVNIH ZNAČILNOSTI ZDRAVILA ONIVYDE pegylated liposomal 4,3 mg/ml SESTAVA*: ONIVYDE pegylated liposomal 4,3 mg/ml koncentrat za disperzijo za infundiranje: ena viala z 10 ml koncentrata vsebuje 43 mg brezvodnega irinotekana (v obliki irinotekanijeve soli saharoznega oktasulfata v pegilirani liposomijski formulaciji). **TERAPEVTSKE INDIKACIJE***: Zdravljenje metastatskega adenokarcinoma trebušne slinavke v kombinaciji s 5-fluorouracilom (5-FU) in levkovorinom (LV) pri odraslih bolnikih, pri katerih je bolezen po zdravljenju na osnovi gemcitabina napredovala. **ODMERJANJE IN NAČIN UPORABE***: ONIVYDE pegylated liposomal (irinotekan) smejo bolnikom predpisati in dajati samo zdravstveni delavci, ki imajo izkušnje pri uporabi zdravil za zdravljenje raka. Priporočeni odmerki in režim zdravljenja zdravila ONIVYDE pegylated liposomal je 70 mg/m² intravensko 90 minut, čemur sledi LV 400 mg/m² intravensko 30 minut in nato 5-FU 2400 mg/m² intravensko 46 ur, vsaka 2 tedna. Zdravilo ONIVYDE pegylated liposomal se ne daje kot samostojno zdravilo. Pri bolnikih z znano homozigotnostjo za alel UGT1A1*28 je treba razmisлити o manjšem začetnem odmerku zdravila ONIVYDE pegylated liposomal 50 mg/m². Če zdravilo bolniki dobro prenašajo, lahko v naslednjih ciklih razmislimo o odmerku zdravila ONIVYDE pegylated liposomal 70 mg/m². Prilagajanje odmerkov se priporoča za obvladovanje toksičnosti 3. ali 4. stopnje, povezane z zdravilom ONIVYDE pegylated liposomal. **KONTRAINDIKACIJE***: Anamneza hude preobčutljivosti na irinotekan ali katero koli pomožno snov. Dojenje. **OPOMORIČILA***: Zdravilo ONIVYDE pegylated liposomal (irinotekan) ni enakovredno drugim neliposomijskim formulacijam irinotekana, zato jih ne smemo zamenjevati. **Mielosupresija/nevtropenija***: Med zdravljenjem se priporoča nadziranje celotne krvne slike. Bolniki se morajo zavedati tveganja za nevtropenijo in pomena povišane telesne temperature. Febrilno nevtropenijo je treba nujno zdraviti v bolnišnici s širokospektralnimi intravenskimi antibiotiki. Pri bolnikih, ki doživijo hude hematološke neželene učinke, se priporoča zmanjšanje odmerka ali prekinitve zdravljenja. Bolnikov s hudo odpovedjo kostnega mozga ne smemo zdraviti z zdravilom ONIVYDE pegylated liposomal. **Imunosupresivni učinki in cepiva***: Dajanje živih ali atenuiranih cepiv bolnikom s oslabilnim imunskim sistemom lahko povzroči resne ali smrtne okužbe. Bolniki azijskega porekla imajo večje tveganje za hudo in febrilno nevtropenijo. Posamezniki s homozigotnostjo 7/7 za alel UGT1A1*28 imajo povečano tveganje za nevtropenijo. **Interakcije z močnimi induktorji encima CYP3A4, močnimi zaviralci encima CYP3A4 in močnimi zaviralci encima UGT1A1***: Zdravila ONIVYDE pegylated liposomal ne smemo dajati skupaj z močnimi induktorji encima CYP3A4 (kot so antikonvulzivi, rifampicin, rifabutin in šentjanževka), močnimi zaviralci encima CYP3A4 (npr. grenivkinim sokom, klaritromicinom, indinavirjem, itrakonazolom, lopinavirjem, nefazodonom, nefinavirjem, ritonavirjem, sakvinavirjem, telaprevirjem, vorikonazolom) ali z močnimi zaviralci encima UGT1A1, razen če ni drugih terapevtskih možnosti. Zdravljenje z močnimi zaviralci encima CYP3A4 moramo prekiniti vsaj 1 teden pred začetkom zdravljenja z zdravilom ONIVYDE pegylated liposomal. **Driska***: Pri bolnikih, ki doživijo zgodnji pojav driske (v ≤ 24 urah po začetku zdravljenja z zdravilom ONIVYDE pegylated liposomal), je treba razmisлити o terapevtskem in profilaktičnem zdravljenju z atropinom, razen če je kontraindicirano. Bolnike je treba opozoriti na tveganje za zapoznelo drisko (> 24 ur), ki je izčrpavajoča in v redkih primerih tudi življenjsko nevarna. Če driska traja tudi, ko bolnik prejema loperamid več kot 24 ur, je treba razmisлити o dodatni peroralni antibiotični podpori. Zdravljenje z zdravilom ONIVYDE pegylated liposomal je treba odložiti, dokler se driska ne umiri do ≤ 1. stopnje (2-3 odvajanja/dan več kot pred zdravljenjem). Zdravila ONIVYDE pegylated liposomal ne smemo dajati bolnikom z zaporo črevesja ali kronično vnetno črevesno boleznijo, dokler se ta ne pozdravi. **Holinergične reakcije***: Zgodnji drisko lahko spremljajo rinitis, povečano slinjenje, zardevanje, diaforeza, bradikardija, mioza in hiperperistaltika. Uporabiti je treba atropin. **Akute infuzijske in povezane reakcije***: V primeru hudih preobčutljivostnih reakcij je treba zdravljenje z zdravilom ONIVYDE pegylated liposomal prekiniti. **Predhodna Whippleova operacija***: Večje tveganje za resne okužbe. Bolnike je treba spremljati glede znakov okužbe. **Zilne bolezni***: Zdravilo ONIVYDE pegylated liposomal je bilo povezano s tromboemboličnimi dogodki, kot so pljučna embolija, venska tromboza in arterijska tromboembolija. Treba je pridobiti podrobno zdravstveno anamnezo, da bi prepoznali bolnike z več dejavniki tveganja poleg osnovne neoplazme. Bolnike je treba obvestiti o znakih in simptomih tromboembolije in jim svetovati, da

se v primeru katerega od teh znakov ali simptomov takoj obrnejo na svojega zdravnika ali medicinsko sestro. **Pljučna toksičnost***: Pri bolnikih, ki so prejeli neliposomijski irinotekan, so se pojavili dogodki, podobni intersticijski pljučni bolezni (IPB), ki so vodili do smrtnih primerov. Pri bolnikih z dejavniki tveganja (obstoječa pljučna boleznijo, uporabo pnevmonotoksičnih zdravil, kolonije stimulirajočimi dejavniki ali predhodnim zdravljenjem z obsevanjem) je treba pred zdravljenjem z zdravilom ONIVYDE pegylated liposomal in po njem skrbno nadzirati respiratorne simptome. Dokler ni opravljena diagnostična ocena, je treba ob pojavu nove ali napredovale dispneje, kašlja in povišane telesne temperature zdravljenje z zdravilom ONIVYDE pegylated liposomal začasno prekiniti. Pri bolnikih s potrjeno diagnozo IPB moramo zdravljenje z zdravilom ONIVYDE pegylated liposomal dokončno prekiniti. **Jetno okvaro***: Bolniki s hiperbilirubinemijo so imeli povišane koncentracije skupnega SN-38, zato je tveganje za nevtropenijo povečano. Pri bolnikih z vrednostjo skupnega bilirubina 1,0-2,0 mg/dl je treba redno nadzirati celotno krvno sliko. Previdnost je potrebna pri bolnikih z jetno okvaro (bilirubin > 2-kratna zgoraj meja normalnih vrednosti [ULN]; aminotransferaze > 5-kratna ULN). **Ledvična okvara***: Uporaba zdravila pri bolnikih s pomembno ledvično okvaro ni bila ocenjena. **Bolniki s premajhno telesno maso (indeks telesne mase < 18,5 kg/m²)**: Potrebna je previdnost. **Pomožne snovi***: En mililiter zdravila ONIVYDE pegylated liposomal vsebuje 0,144 mmol (3,31 mg) natrija. **INTERAKCIJE***: **Previdnostni ukrepi**: Sočasno dajanje z induktorji encima CYP3A4 lahko zmanjša sistemsko izpostavljenost zdravilu ONIVYDE pegylated liposomal. Sočasno dajanje z zaviralci encima CYP3A4 ali encima UGT1A1 (npr. atazanavira, gemfibrozila, indinavira, regorafeniba) lahko poveča sistemsko izpostavljenost zdravilu ONIVYDE pegylated liposomal. **PLODNOST* NOSEČNOST***: Uporaba ni priporočljiva. **DOJENJE***: Zdravilo je kontraindicirano. **KONTRACIJA***: Ženske v rodni dobi morajo med zdravljenjem in še 1 mesec po zdravljenju uporabljati učinkovito kontracepcijo. Moški morajo med zdravljenjem in 4 mesece po zdravljenju uporabljati kondome. **VPLIV NA SPOSOBNOST VOZNIJE IN UPRAVLJANJA STROJEV***: Bolniki morajo biti med zdravljenjem pri vožnji in upravljanju strojev previdni. **NEŽELENI UČINKI***: **Zelo pogosti**: nevtropenija, levkopenija, anemija, trombocitopenija, hipokaliemija, hipomagnezija, dehidracija, zmanjšan apetit, omotica, driska, bruhanje, navzea, bolečine v trebuhu, stomatitis, alopecija, pireksija, periferni edem, vnetje sluznic, utrujenost, astenija, zmanjšana telesna masa. **Pogosti**: septični šok, sepsa, pljučnica, febrilna nevtropenija, gastroenteritis, oralna kandidoza, limfopenija, hipoglikemija, hiponatremija, hipofosfatemija, nespečnost, holinergični sindrom, dizgezija, hipotenzija, pljučna embolija, embolija, globoka venska tromboza, dispneja, disonija, kolitis, hemoroidi, hipoaalbuminija, akutna ledvična odpoved, z infuzijo povezana reakcija, edem, zvišana raven bilirubina, zvišana raven alanin-aminotransferaze, zvišana raven aspartat-aminotransferaze, zvišano mednarodno umerjeno razmerje. **Občasni**: biliarna sepsa, preobčutljivost, tromboza, hipoksija, ezofagitis, proktitis, makulopapulozni izpuščaj, obarvanje nohtov. **PREVELIKO ODMERJANJE***: Za preveliko odmerjanje zdravila ni znanega antidota. Treba je uvesti maksimalno podporno nego, s katero preprečimo dehidracijo zaradi driske in zdravimo zaplete zaradi okužb. **FARMAKODINAMIČNE LASTNOSTI***: Učinkovina zdravila ONIVYDE pegylated liposomal je irinotekan (zaviralec topoisomerase II), inkapsuliran v vezikel z lipidnim dvojelem oziroma liposom. Irinotekan je derivat kamptotecina. Kamptotecini delujejo kot specifični zaviralci encima DNA-topoisomerase I. Irinotekan in njegov aktivni presnovek SN-38 se reverzibilno vezeta na kompleks topoisomerase I in DNA ter sprožita poškodbe v enoverzijski DNA, kar zaustavi replikacijske vilice pri podvajanju DNA in povzroča citotoksičnost. Irinotekan se presnavlja s karboksilesterazo do SN-38. SN-38 je približno 1.000-krat močnejši zaviralec topoisomerase I, očiščene iz tumorskih celičnih linij človeka in glodavcev, kot irinotekan. **PAKIRANJE***: Pakiranje vsebuje eno vialo z 10 ml koncentrata. **NAČIN PREDPISOVANJA IN IZDAJE ZDRAVILA**: Rp/Spec. **DATUM ZADNJE REVIZIJE BESEDILA**: avgust 2020. **Imetnik dovoljenja za promet**: Les Laboratoires Servier, 50, rue Carnot, 92284 Suresnes cedex, Francija. **Številka dovoljenja za promet z zdravilom**: EU/1/16/1130/001. *Pred predpisovanjem preberite celoten povzetek glavnih značilnosti zdravila. Celoten povzetek glavnih značilnosti zdravila in podrobnejše informacije so na voljo pri: Servier Pharma d.o.o., Podmilščakova ulica 24, 1000 Ljubljana, tel: 01 563 48 11, www.serviersi.



Nedrobnocelični
pljučni rak¹



Melanom¹



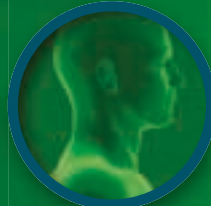
Rak ledvičnih
celic¹



Hodgkinov
limfom¹



Urotelijski
karcinom¹



Ploščatocelični
karcinom
glave in vratu¹

References: 1. Keytruda EU SmPC

SKRAJŠAN POVZETEK GLAVNIH ZNAČILNOSTI ZDRAVILA

Predpisovanjem, prosimo, preberite celoten Povzetek glavnih značilnosti zdravila!

Ime zdravila: KEYTRUDA 25 mg/ml koncentrat za raztopino za infundiranje vsebuje pembrolizumab.

Terapevtske indikacije: Zdravilo KEYTRUDA je kot samostojno zdravljenje indicirano za zdravljenje: napredovalega (neoperabilnega ali metastatskega) melanoma pri odraslih; za adjuvantno zdravljenje odraslih z melanomom v stadiju III, ki se je razširil na bezgavke, po popolni kirurški odstranitvi; metastatskega nedrobnoceličnega pljučnega raka (NSCLC) v prvi liniji zdravljenja pri odraslih, ki imajo tumorje z $\geq 50\%$ izraženostjo PD-L1 (TPS) in brez pozitivnih tumorskih mutacij EGFR ali ALK; lokalno napredovalega ali metastatskega NSCLC pri odraslih, ki imajo tumorje z $\geq 1\%$ izraženostjo PD-L1 (TPS) in so bili predhodno zdravljeni z vsaj eno shemo kemoterapije, bolniki s pozitivnimi tumorskimi mutacijami EGFR ali ALK so pred prejemom zdravila KEYTRUDA morali prejeti tudi tarčno zdravljenje; odraslih bolnikov s ponovljenim ali neodzivnim klasičnim Hodgkinovim limfomom (cHL), pri katerih avtologna presaditev matičnih celic (ASCT) in zdravljenje z brentuksimabom vedotinom (BV) nista bila uspešna, in odraslih bolnikov, ki za presaditev niso primerni, zdravljenje z BV pa pri njih ni bilo uspešno; lokalno napredovalega ali metastatskega urotelijskega raka pri odraslih, predhodno zdravljenih s kemoterapijo, ki je vključevala platino; lokalno napredovalega ali metastatskega urotelijskega raka pri odraslih, ki imajo tumorje z izraženostjo PD-L1 ≥ 10 , ocenjeno s kombinirano pozitivno oceno (CPS); ponovljenega ali metastatskega ploščatoceličnega raka glave in vratu (HNSCC) pri odraslih, ki imajo tumorje z $\geq 50\%$ izraženostjo PD-L1 (TPS), in pri katerih je bolezen napredovala med zdravljenjem ali po zdravljenju s kemoterapijo, ki je vključevala platino. Zdravilo KEYTRUDA je kot samostojno zdravljenje ali v kombinaciji s kemoterapijo s platino in 5-fluorouracilom (5-FU) indicirano za prvo linijo zdravljenja metastatskega ali neoperabilnega ponovljenega ploščatoceličnega raka glave in vratu pri odraslih, ki imajo tumorje z izraženostjo PD-L1 s CPS ≥ 1 . Zdravilo KEYTRUDA je v kombinaciji s pemetreksedom in kemoterapijo na osnovi platine indicirano za prvo linijo zdravljenja metastatskega neploščatoceličnega NSCLC pri odraslih, pri katerih tumorji nimajo pozitivnih mutacij EGFR ali ALK; v kombinaciji s karboplatinom in bodisi paklitakselom bodisi nab-paklitakselom je indicirano za prvo linijo zdravljenja metastatskega ploščatoceličnega NSCLC pri odraslih; v kombinaciji z aksamitinom je indicirano za prvo linijo zdravljenja napredovalega raka ledvičnih celic (RCC) pri odraslih. **Odmerjanje in način uporabe:** Testiranje PD-L1 pri bolnikih z NSCLC, urotelijskim rakom ali HNSCC: Za samostojno zdravljenje z zdravilom KEYTRUDA je priporočljivo opraviti testiranje izraženosti PD-L1 tumorja z validirano preiskavo, da izberemo bolnike z NSCLC ali predhodno nezdravljenim urotelijskim rakom. Bolnike s HNSCC je treba za samostojno zdravljenje z zdravilom KEYTRUDA ali v kombinaciji s kemoterapijo s platino in 5-fluorouracilom (5-FU) izbrati na podlagi izraženosti PD-L1, potrjene z validirano preiskavo. **Odmerjanje:** Priporočeni odmerek zdravila KEYTRUDA za samostojno zdravljenje je bodisi 200 mg na 3 tedne ali 400 mg na 6 tednov, apliciran z intravensko infuzijo v 30 minutah. Priporočeni odmerek za kombinirano zdravljenje je 200 mg na 3 tedne, apliciran z intravensko infuzijo v 30 minutah. Za uporabo v kombinaciji glejte povzetke glavnih značilnosti sočasno uporabljenih zdravil. Če se uporablja kot del kombiniranega zdravljenja skupaj z intravensko kemoterapijo, je treba zdravilo KEYTRUDA aplicirati prvo. Bolnike je treba zdraviti do napredovanja bolezni ali nesprejemljivih toksičnih učinkov. Pri adjuvantnem zdravljenju melanoma je treba zdravilo uporabljati do ponovitve bolezni, pojava nesprejemljivih toksičnih učinkov oziroma mora zdravljenje trajati do enega leta. Če je aksamitin uporabljen v kombinaciji s pembrolizumabom, se lahko razmisli o povečanju odmerka aksamitina nad začetnih 5 mg v presledkih šest tednov ali več. Pri bolnikih starih ≥ 65 let, bolnikih z blago do zmerno okvaro ledvic, bolnikih z blago okvaro jeter prilagoditev odmerka ni potrebna. **Odložitev odmerka ali ukinitve zdravljenja:** Zmanjšanje odmerka zdravila KEYTRUDA ni priporočljivo. Za obvladovanje neželenih učinkov je treba uporabo zdravila KEYTRUDA zadržati ali ukiniti, prosimo, glejte celoten Povzetek glavnih značilnosti zdravila. **Kontraindikacije:** Preobčutljivost na učinkovino ali katero koli pomožno snov. **Povzetek posebnih opozoril, previdnostnih ukrepov, interakcij in neželenih učinkov:** Imunsko pogojeni neželeni učinki (pnevmonitis, kolitis, hepatitis, nefritis, endokrinopatske, neželeni učinki na kožo in drugi): Pri bolnikih, ki so prejeli pembrolizumab, so se pojavili imunsko pogojeni neželeni učinki, vključno s hudimi in smrtnimi primeri. Večina imunsko pogojenih neželenih učinkov, ki so se pojavili med zdravljenjem s pembrolizumabom, je bila reverzibilnih in so jih obvladali s prekinitvami uporabe pembrolizumaba, uporabo kortikosteroidov in/ali podporno oskrbo. Pojavijo se lahko tudi po

zadnjem odmerku pembrolizumaba in hkrati prizadanejo več organskih sistemov. V primeru suma na imunsko pogojene neželeni učinke je treba poskrbeti za ustrezno oceno za potrditev etiologije oziroma izključitev drugih vzrokov. Glede na izrazitost neželenega učinka je treba zadržati uporabo pembrolizumaba in uporabiti kortikosteroide – za natančna navodila, prosimo, glejte Povzetek glavnih značilnosti zdravila Keytruda. Zdravljenje s pembrolizumabom lahko poveča tveganje za zavrnitev pri prejemnikih presadkov čvrstih organov. Pri bolnikih, ki so prejeli pembrolizumab, so poročali o hudih z infuzijo povezanih reakcijah, vključno s preobčutljivostjo in anafilaksijo. Pembrolizumab se iz obtoka odstrani s katabolizmom, zato presnovnih medsebojnih delovanj zdravil ni pričakovati. Uporabi sistemskih kortikosteroidov ali imunosupresivov pred uvedbo pembrolizumaba se je treba izogibati, ker lahko vplivajo na farmakodinamično aktivnost in učinkovitost pembrolizumaba. Vendar pa je kortikosteroide ali druge imunosupresive mogoče uporabiti za zdravljenje imunsko pogojenih neželenih učinkov. Kortikosteroide je mogoče uporabiti tudi kot premedikacijo, če je pembrolizumab uporabljen v kombinaciji s kemoterapijo, kot antiemetično profilakso in/ali za ublažitev neželenih učinkov, povezanih s kemoterapijo. Ženske v rodni dobi morajo med zdravljenjem s pembrolizumabom in vsaj še 4 mesece po zadnjem odmerku pembrolizumaba uporabljati učinkovito kontracepcijo, med nosečnostjo in dojenjem se ga ne sme uporabljati.

Varnost pembrolizumaba pri samostojnem zdravljenju so v kliničnih študijah ocenili pri 5.884 bolnikih z napredovalim melanomom, kirurško odstranjenim melanomom v stadiju III (adjuvantno zdravljenje), NSCLC, cHL, urotelijskim rakom ali HNSCC s štiri odmerki (2 mg/kg na 3 tedne, 200 mg na 3 tedne in 10 mg/kg na 2 ali 3 tedne). V tej populaciji bolnikov je mediana čas opazovanja znašal 7,3 mesece (v razponu od 1 dneva do 31 mesecev), najpogostejši neželeni učinki zdravljenja s pembrolizumabom so bili utrujenost (32 %), navzea (20 %) in diareja (20 %). Večina poročanih neželenih učinkov pri samostojnem zdravljenju je bila po izrazitosti 1. ali 2. stopnje. Najresnejši neželeni učinki so bili imunsko pogojeni neželeni učinki in hude z infuzijo povezane reakcije. Varnost pembrolizumaba pri kombiniranem zdravljenju s kemoterapijo so ocenili pri 1.067 bolnikih NSCLC ali HNSCC, ki so v kliničnih študijah prejeli pembrolizumab v odmerkih 200 mg, 2 mg/kg ali 10 mg/kg na vsake 3 tedne. V tej populaciji bolnikov so bili najpogostejši neželeni učinki naslednji: anemija (50 %), navzea (50 %), utrujenost (37 %), zaprtost (35 %), diareja (30 %), nevtropenija (30 %), zmanjšanje apetita (28 %) in bruhanje (25 %). Pri kombiniranem zdravljenju s pembrolizumabom je pri bolnikih z NSCLC pojavnost neželenih učinkov 3. do 5. stopnje znašala 67 %, pri zdravljenju samo s kemoterapijo pa 66 %, pri kombiniranem zdravljenju s pembrolizumabom pri bolnikih s HNSCC 85 % in pri zdravljenju s kemoterapijo v kombinaciji s cetuksimabom 84 %. Varnost pembrolizumaba v kombinaciji z aksamitinom so ocenili v klinični študiji pri 429 bolnikih z napredovalim rakom ledvičnih celic, ki so prejeli 200 mg pembrolizumaba na 3 tedne in 5 mg aksamitina dvakrat na dan. V tej populaciji bolnikov so bili najpogostejši neželeni učinki diareja (54 %), hipertenzija (45 %), utrujenost (38 %), hipotiroidizem (35 %), zmanjšana apetit (30 %), sindrom palmarno-plantarne eritrodisestezije (28 %), navzea (28 %), zvišanje vrednosti ALT (27 %), zvišanje vrednosti AST (26 %), disonija (25 %), kašelj (21 %) in zaprtost (21 %). Pojavnost neželenih učinkov 3. do 5. stopnje je bila med kombiniranim zdravljenjem s pembrolizumabom 76 % in pri zdravljenju s sunitinibom samim 71 %. Za celoten seznam neželenih učinkov, prosimo, glejte celoten Povzetek glavnih značilnosti zdravila

Način in režim izdaje zdravila: H – Predpisovanje in izdaja zdravila je le na recept, zdravilo se uporablja samo v bolnišnicah.

Imetnik dovoljenja za promet z zdravilom: Merck Sharp & Dohme B.V., Waarderweg 39, 2031 BN Haarlem, Nizozemska.



Merck Sharp & Dohme inovativna zdravila d.o.o.,
Šmartinska cesta 140, 1000 Ljubljana, tel: +386 1/ 520 42 01, fax: +386 1/ 520 43 50
Pripravljeno v Sloveniji, September 2020; SI-KEY-00145 EXP: 09/2022

Samo za strokovno javnost.

H - Predpisovanje in izdaja zdravila je le na recept, zdravilo pa se uporablja samo v bolnišnicah. Pred predpisovanjem, prosimo, preberite celoten Povzetek glavnih značilnosti zdravila Keytruda, ki je na voljo pri naših strokovnih sodelavcih ali na lokalnem sedežu družbe.



NOVO

Agencija FDA
je 26.8.2020 odobrila
FoundationOne® Liquid CDx
za določitev več kot 300
z rakom povezanih
genov iz vzorca
krvi.¹

OBŠIREN VPOGLED ZA NAČRTOVANJE BOLNIKU PRILAGOJENEGA ZDRAVLJENJA²⁻⁷

Odkrijte možnosti visoko kakovostnih storitev obširnega genomskega profiliranja
FoundationOne®, ki olajšajo odločitev o najustreznejšem zdravljenju za
posameznega bolnika z rakom, v različnih kliničnih stanjih.⁵⁻⁷

 **FOUNDATIONONE® CDx**

 **FOUNDATIONONE® LIQUID CDx**

 **FOUNDATIONONE® HEME**

M-SI-000001141 (v1.0)
Viri: 1. FDA Approves Liquid Biopsy Next-Generation Sequencing Companion Diagnostic Test; dostopano oktober 2020 na: <https://www.fda.gov/drugs/drug-approvals-and-databases/fda-approves-liquid-biopsy-next-generation-sequencing-companion-diagnostic-test>. 2. Frampton GM s sod. Nat Biotechnol 2013; 31:1023-1031. 3. Clark TA s sod. J Mol Diagn 2018; 20:686-702. 4. He J s sod. Blood 2016; 127:3004-3014. 5. FoundationOne® CDx Technical Specifications; dostopano oktober 2020 na: https://assets.ctfassets.net/w98cd481qyp0/YqqKHaqQmFegc5ueQk48w/0a34fcdaa3a71dbe460cdbc01cebe8ad/F1CDx_Technical_Specifications_072020.pdf. 6. FoundationOne® Liquid Technical Specifications; dostopano oktober 2020 na: https://assets.ctfassets.net/w98cd481qyp0/wVEm7VtICYR0sT5C1VbU7/cc6ac2109785d70fe6d91903b241006f/FoundationOne_Liquid_CDx_Technical_Specifications.pdf. 7. FoundationOne® Heme Technical Specifications; dostopano oktober 2020 na: https://assets.ctfassets.net/w98cd481qyp0/42r1cTE8VR4137CaHrsaen/baf91080cb3d78a52ada10c6358fa130/FoundationOne_Heme_Technical_Specifications.pdf

CDx - spremljevalna diagnostika, FDA - Uprava ZDA za hrano in zdravila (Food and Drug Administration)

Informacija pripravljena: oktober 2020. Samo za strokovno javnost.
DODATNE INFORMACIJE SO NA VOLJO PRI:
Roche farmacevtska družba d.o.o., Stegne 13g, 1000 Ljubljana
rocheprotiraku.si



**FOUNDATION
MEDICINE®**



Instructions for authors

The editorial policy

Radiology and Oncology is a multidisciplinary journal devoted to the publishing original and high quality scientific papers and review articles, pertinent to diagnostic and interventional radiology, computerized tomography, magnetic resonance, ultrasound, nuclear medicine, radiotherapy, clinical and experimental oncology, radiobiology, medical physics and radiation protection. Therefore, the scope of the journal is to cover beside radiology the diagnostic and therapeutic aspects in oncology, which distinguishes it from other journals in the field.

The Editorial Board requires that the paper has not been published or submitted for publication elsewhere; the authors are responsible for all statements in their papers. Accepted articles become the property of the journal and, therefore cannot be published elsewhere without the written permission of the editors.

Submission of the manuscript

The manuscript written in English should be submitted to the journal via online submission system Editorial Manager available for this journal at: www.radioloncol.com.

In case of problems, please contact Sašo Trupej at saso.trupej@computing.si or the Editor of this journal at gsera@onko-i.si

All articles are subjected to the editorial review and when the articles are appropriated they are reviewed by independent referees. In the cover letter, which must accompany the article, the authors are requested to suggest 3-4 researchers, competent to review their manuscript. However, please note that this will be treated only as a suggestion; the final selection of reviewers is exclusively the Editor's decision. The authors' names are revealed to the referees, but not vice versa.

Manuscripts which do not comply with the technical requirements stated herein will be returned to the authors for the correction before peer-review. The editorial board reserves the right to ask authors to make appropriate changes of the contents as well as grammatical and stylistic corrections when necessary. Page charges will be charged for manuscripts exceeding the recommended length, as well as additional editorial work and requests for printed reprints.

Articles are published printed and on-line as the open access (<https://content.sciendo.com/raon>).

All articles are subject to 900 EUR + VAT publication fee. Exceptionally, waiver of payment may be negotiated with editorial office, upon lack of funds.

Manuscripts submitted under multiple authorship are reviewed on the assumption that all listed authors concur in the submission and are responsible for its content; they must have agreed to its publication and have given the corresponding author the authority to act on their behalf in all matters pertaining to publication. The corresponding author is responsible for informing the coauthors of the manuscript status throughout the submission, review, and production process.

Preparation of manuscripts

Radiology and Oncology will consider manuscripts prepared according to the Uniform Requirements for Manuscripts Submitted to Biomedical Journals by International Committee of Medical Journal Editors (www.icmje.org). The manuscript should be written in grammatically and stylistically correct language. Abbreviations should be avoided. If their use is necessary, they should be explained at the first time mentioned. The technical data should conform to the SI system. The manuscript, excluding the references, tables, figures and figure legends, must not exceed 5000 words, and the number of figures and tables is limited to 8. Organize the text so that it includes: Introduction, Materials and methods, Results and Discussion. Exceptionally, the results and discussion can be combined in a single section. Start each section on a new page, and number each page consecutively with Arabic numerals. For ease of review, manuscripts should be submitted as a single column, double-spaced text, and must have continuous line numbering.

The Title page should include a concise and informative title, followed by the full name(s) of the author(s); the institutional affiliation of each author; the name and address of the corresponding author (including telephone, fax and E-mail), and an abbreviated title (not exceeding 60 characters). This should be followed by the abstract page, summarizing in less than 250 words the reasons for the study, experimental approach, the major findings (with specific data if possible), and the principal conclusions, and providing 3-6 key words for indexing purposes. Structured abstracts are required. Slovene authors are requested to provide title and the abstract in Slovene language in a separate file. The text of the research article should then proceed as follows:

Introduction should summarize the rationale for the study or observation, citing only the essential references and stating the aim of the study.

Materials and methods should provide enough information to enable experiments to be repeated. New methods should be described in details.

Results should be presented clearly and concisely without repeating the data in the figures and tables. Emphasis should be on clear and precise presentation of results and their significance in relation to the aim of the investigation.

Discussion should explain the results rather than simply repeating them and interpret their significance and draw conclusions. It should discuss the results of the study in the light of previously published work.

Charts, Illustrations, Images and Tables

Charts, Illustrations, Images and Tables must be numbered and referred to in the text, with the appropriate location indicated. Charts, Illustrations and Images, provided electronically, should be of appropriate quality for good reproduction. Illustrations and charts must be vector image, created in CMYK color space, preferred font "Century Gothic", and saved as .AI, .EPS or .PDF format. Color charts, illustrations and Images are encouraged, and are published without additional charge. Image size must be 2.000 pixels on the longer side and saved as .JPG (maximum quality) format. In Images, mask the identities of the patients. Tables should be typed double-spaced, with a descriptive title and, if appropriate, units of numerical measurements included in the column heading. The files with the figures and tables can be uploaded as separate files.

References

References must be numbered in the order in which they appear in the text and their corresponding numbers quoted in the text. Authors are responsible for the accuracy of their references. References to the Abstracts and Letters to the Editor must be identified as such. Citation of papers in preparation or submitted for publication, unpublished observations, and personal communications should not be included in the reference list. If essential, such material may be incorporated in the appropriate place in the text. References follow the style of Index Medicus, DOI number (if exists) should be included.

All authors should be listed when their number does not exceed six; when there are seven or more authors, the first six listed are followed by "et al.". The following are some examples of references from articles, books and book chapters:

Dent RAG, Cole P. In vitro maturation of monocytes in squamous carcinoma of the lung. *Br J Cancer* 1981; **43**: 486-95. doi: 10.1038/bjc.1981.71

Chapman S, Nakielny R. *A guide to radiological procedures*. London: Bailliere Tindall; 1986.

Evans R, Alexander P. Mechanisms of extracellular killing of nucleated mammalian cells by macrophages. In: Nelson DS, editor. *Immunobiology of macrophage*. New York: Academic Press; 1976. p. 45-74.

Authorization for the use of human subjects or experimental animals

When reporting experiments on human subjects, authors should state whether the procedures followed the Helsinki Declaration. Patients have the right to privacy; therefore the identifying information (patient's names, hospital unit numbers) should not be published unless it is essential. In such cases the patient's informed consent for publication is needed, and should appear as an appropriate statement in the article. Institutional approval and Clinical Trial registration number is required. Retrospective clinical studies must be approved by the accredited Institutional Review Board/Committee for Medical Ethics or other equivalent body. These statements should appear in the Materials and methods section.

The research using animal subjects should be conducted according to the EU Directive 2010/63/EU and following the Guidelines for the welfare and use of animals in cancer research (*Br J Cancer* 2010; 102: 1555 – 77). Authors must state the committee approving the experiments, and must confirm that all experiments were performed in accordance with relevant regulations.

These statements should appear in the Materials and methods section (or for contributions without this section, within the main text or in the captions of relevant figures or tables).

Transfer of copyright agreement

For the publication of accepted articles, authors are required to send the License to Publish to the publisher on the address of the editorial office. A properly completed License to Publish, signed by the Corresponding Author on behalf of all the authors, must be provided for each submitted manuscript.

The non-commercial use of each article will be governed by the Creative Commons Attribution-NonCommercial-NoDerivs license.

Conflict of interest

When the manuscript is submitted for publication, the authors are expected to disclose any relationship that might pose real, apparent or potential conflict of interest with respect to the results reported in that manuscript. Potential conflicts of interest include not only financial relationships but also other, non-financial relationships. In the Acknowledgement section the source of funding support should be mentioned. The Editors will make effort to ensure that conflicts of interest will not compromise the evaluation process of the submitted manuscripts; potential editors and reviewers will exempt themselves from review process when such conflict of interest exists. The statement of disclosure must be in the Cover letter accompanying the manuscript or submitted on the form available on www.icmje.org/coi_disclosure.pdf

Page proofs

Page proofs will be sent by E-mail to the corresponding author. It is their responsibility to check the proofs carefully and return a list of essential corrections to the editorial office within three days of receipt. Only grammatical corrections are acceptable at that time.

Open access

Papers are published electronically as open access on <https://content.sciendo.com/raon>, also papers accepted for publication as E-ahead of print.

